

PHYSICAL AND GEOMETRIC CONTROLS ON THE
DISTRIBUTION OF MAGMATIC AND SULPHIDE-
BEARING PHASES WITHIN THE VOISEY'S BAY
NICKEL-COPPER-COBALT DEPOSIT,
VOISEY'S BAY, LABRADOR

CENTRE FOR NEWFOUNDLAND STUDIES

**TOTAL OF 10 PAGES ONLY
MAY BE XEROXED**

(Without Author's Permission)

DAWN EVANS-LAMSWOOD

INFORMATION TO USERS

This manuscript has been reproduced from the microfilm master. UMI films the text directly from the original or copy submitted. Thus, some thesis and dissertation copies are in typewriter face, while others may be from any type of computer printer.

The quality of this reproduction is dependent upon the quality of the copy submitted. Broken or indistinct print, colored or poor quality illustrations and photographs, print bleedthrough, substandard margins, and improper alignment can adversely affect reproduction.

In the unlikely event that the author did not send UMI a complete manuscript and there are missing pages, these will be noted. Also, if unauthorized copyright material had to be removed, a note will indicate the deletion.

Oversize materials (e.g., maps, drawings, charts) are reproduced by sectioning the original, beginning at the upper left-hand corner and continuing from left to right in equal sections with small overlaps.

ProQuest Information and Learning
300 North Zeeb Road, Ann Arbor, MI 48106-1346 USA
800-521-0600

UMI[®]

NOTE TO USERS

This reproduction is the best copy available.

UMI



**National Library
of Canada**

**Acquisitions and
Bibliographic Services**

395 Wellington Street
Ottawa ON K1A 0N4
Canada

**Bibliothèque nationale
du Canada**

**Acquisitions et
services bibliographiques**

395, rue Wellington
Ottawa ON K1A 0N4
Canada

Your file Votre référence

Our file Notre référence

The author has granted a non-exclusive licence allowing the National Library of Canada to reproduce, loan, distribute or sell copies of this thesis in microform, paper or electronic formats.

The author retains ownership of the copyright in this thesis. Neither the thesis nor substantial extracts from it may be printed or otherwise reproduced without the author's permission.

L'auteur a accordé une licence non exclusive permettant à la Bibliothèque nationale du Canada de reproduire, prêter, distribuer ou vendre des copies de cette thèse sous la forme de microfiche/film, de reproduction sur papier ou sur format électronique.

L'auteur conserve la propriété du droit d'auteur qui protège cette thèse. Ni la thèse ni des extraits substantiels de celle-ci ne doivent être imprimés ou autrement reproduits sans son autorisation.

0-612-73661-X



Memorial

University of Newfoundland

This is to authorize the Dean of Graduate Studies to deposit two copies of my thesis/report entitled

Physical and Geometric Controls on the Distribution of Magmatic and Sulphide Bearing
Phases Within the Voisey's Bay Nickel-Copper-Colbalt Deposit, Voisey's Bay Labrador

in the University Library, on the following conditions. I understand that I may choose only ONE of the Options here listed, and may not afterwards apply for any additional restriction. I further understand that the University will not grant any restriction on the publication of thesis/report abstracts.

(After reading the explanatory notes at the foot of this form, delete TWO of (a), (b) and (c), whichever are inapplicable.)

The conditions of deposit are:

- (a) that two copies are to be made available to users at the discretion of their custodians,

OR

- (b) that access to, and quotation from, this thesis/report is to be granted only with my written permission for a period of one year from the date on which the thesis/report, after the approval of the award of a degree, is entrusted to the care of the University, namely, _____
19 ____, after which time the two copies are to be made available to users at the discretion of their custodians,

OR

- (c) that access to, and quotation from, this thesis/report is to be granted only with my written permission for a period of three years from the date on which the thesis/report, after approval for the award of a degree, is entrusted to the care of the University; namely, December 31, 2001 after which time two copies are to be made available to users at the discretion of their custodians.

Date Oct. 20/98
G. Kilian
Dean of Graduate Studies

Signed Dawn Evans - Lamswood
Witnessed by Dawn Evans - Lamswood

NOTES

1. Restriction (b) will be granted on application, without reason given.

However, applications for restriction (c) must be accompanied with a detailed explanation, indicating why the restriction is thought to be necessary, and justifying the length of time requested. Restrictions required on the grounds that the thesis is being prepared for publication, or that patents are awaited, will not be permitted to exceed three years.

Restriction (c) can be permitted only by a Committee entrusted by the University with the task of examining such applications, and will be granted only in exceptional circumstances.

2. Thesis writers are reminded that, if they have been engaged in contractual research, they may have already agreed to restrict access to their thesis until the terms of the contract have been fulfilled.

PHYSICAL AND GEOMETRIC CONTROLS ON THE DISTRIBUTION OF
MAGMATIC AND SULPHIDE-BEARING PHASES
WITHIN THE VOISEY'S BAY NICKEL-COPPER-COBALT DEPOSIT,
VOISEY'S BAY, LABRADOR.

By

Dawn Evans-Lamswood

A thesis submitted to the
School of Graduate Studies
in partial fulfillment of the
requirements for the degree of
Master of Science

Department of Earth Sciences/Faculty of Science
Memorial University of Newfoundland

June 1999

ABSTRACT

Physical and Geometric controls on the and Distribution of Magmatic and Sulphide-Bearing Phases within the Voisey's Bay Nickel-Copper-Cobalt Deposit, Voisey's Bay, Labrador.

The Voisey's Bay Ni-Cu-Co deposit occurs within fragment-bearing troctolites and olivine gabbros of the 1.34 Ga. Reid Brook Intrusive Complex, an early member of the predominantly anorthositic Nain Plutonic Suite (NPS). The NPS straddles the 1.85 Ga. Cratonic suture between Archean orthogneiss and the Nain Province to the east and Paleoproterozoic paragneiss of the Churchill Province to the west.

The Reid Brook, Discovery Hill, Mini-Ovoid and Ovoid are mineralized zones within a sub-vertical conduit system, the Ovoid dyke. The Reid Brook zone is the most western mineralized zone of the Voisey's Bay deposit, it contains disseminated and massive sulphide hosted within the dyke and veins in the adjacent country rocks. Mineralization of the Discovery Hill zone, unlike the Reid Brook zone to the west, is confined to the dyke and does not penetrate the country rocks. The Mini-Ovoid is west, but is geologically continuous with the Ovoid. Mineralization consists of massive to semi massive and disseminated sulphides. The Ovoid is a cauldron-shaped body of massive to semi massive sulphides with less extensive parcels of disseminated sulphides.

Striking east-west, the Ovoid dyke appears to post-date, but physically link two large troctolite intrusions, the Eastern Deeps chamber and the Western Deeps chamber. In the west, the conduit extends from the top of the Western Deeps chamber to the north margin of the Eastern Deeps chamber. Rather than being within the sub-vertical Ovoid dyke, mineralization of the Eastern Deeps zone is located within a sub-horizontal splay from the main conduit where it is connected to the base of the Eastern Deeps chamber.

All the mineralized zones in the Voisey's Bay deposit comprise magmatic-textured sulphides within fragment-bearing troctolites and olivine gabbros. Sulphides within the system are preferentially concentrated in physical traps where topographic irregularities and variations in conduit morphology favour the capture, containment and precipitation of sulphides through physiochemical changes in the magma. For example, the Eastern Deeps sulphide zone is associated with the line of entry for a feeder conduit close to a structural low in the base of the Eastern Deeps chamber; the Ovoid mineralized appears to fill a bulge in the conduit, and the Reid Brook zone is located close to an axis of inflection along the strike of the conduit. Sulphide deposition is therefore, is ultimately related to a complex interplay of dyke geometry (i.e. changes in dyke trajectory and thickness) and the fluid dynamics of the fragment-bearing magma in a constantly changing and dynamic magma conduit system.

Dyke geometry is a direct reflection of structural controls. Primary emplacement of the Ovoid dyke and gabbro-troctolite chambers was controlled by east-west lineaments which were established during the Torngat orogeny in response to the Nain/Churchill collision. Syn-magmatic crustal uplift exploited these pre-existing structures, producing local extension in a graben-like system. The extensional faults that resulted provided a media for which magma could easily intrude and be constrained. With the tectonomagmatic evolution of the system, a sub-horizontal fracture system developed, providing an alternative passage for magmatic transgression, producing the Eastern Deeps feeder. Post emplacement deformation invoked oblique stresses on the pre-existing east-

west lineaments and extensional faults, resulting in sinistral translation and the development of Reidel brittle shears.

The Voisey's Bay deposit does not conform to traditional models, where sulphide accumulations are controlled largely by gravitational settling within a magmatic chamber. In contrast, sulphide distribution is controlled by magma emplacement through multiple braids in a dynamic channel-like conduit system.

ACKNOWLEDGMENTS

This study would not have been possible without the technical and financial support provided by Voisey's Bay Nickel Company Limited and Inco Exploration, particularly the individual assistance provided by Colin McKenzie and Cameron Bell. The efforts of Kerry Sparkes and Harvey Keats are also recognized for their roles in the initiation of this program through Archean Resources and Diamond Fields Resources.

Derek Wilton is gratefully acknowledged for his technical assistance and academic guidance. Derek proved to be a major driving force behind the completion and development of this project. In addition, technical discussions with Tony Naldrett, Peter Lightfoot and Bruce Ryan were invaluable to the evolution of the geological models presented in this work. Collaborations with the geological staff, both past and present, were essential to the progress and development of this research; John Hayes, Wayne Mitchelmore, Mike Muggridge and Darrell Butt are gratefully recognized. Appreciation is also due to the geotechnical and geophysical staff who provided countless hours assisting in the collection of data for this analysis. Thanks; Theresa, Brian, Collis, Brad, Ashley, Steve, Averell, Gary, Francis, Rolanda, Dougald, and Loder.

Lastly, it is difficult to express the gratitude I feel toward Dan Lee and Robert Wheeler for their personal encouragement and professional assistance provided throughout the course of this research. Most of all, however, I am indebted to Paul for his patience and confidence in my ability to complete this program, especially when work, school, and life collided, as it frequently did.

TABLE of CONTENTS	Page
LIST of DIGITAL FILES (APPENDIX F):	ix
LIST of TABLES:	x
LIST of FIGURES:	x
LIST of PLATES:.....	xiii
LIST of ABBREVIATIONS for FIGURES.....	xiv
CHAPTER 1: Introduction.....	1
1.1 Exploration History	1
1.2 Access.....	3
1.3 Methods.....	3
1.4 Regional Geology.....	4
1.5 Main Block.....	5
1.6 Deposit.....	10
1.7 Purpose.....	11
1.8 Significance.....	12
CHAPTER 2: Methodology	13
2.1 The Collection and Manipulation of Data.....	13
2.2 Lithologies and the Identification of Textures in Drill Core.....	17
2.2.1 Paragneisses.....	18
2.2.2 Orthogneisses.....	18
2.2.3. RBIC Deposit Rocks	18
2.2.3.1 Chamber Gabbros-Troctolites	
2.2.3.1.1 Composition	18
2.2.3.1.2 Sulphide and Silicate Textures.....	19
2.2.3.2 Conduit Gabbros-Troctolites	
2.2.3.2.1 Composition.....	19
2.2.3.2.2 Sulphide and Silicate Textures.....	20
2.2.3.2.2.1 Chilled Textures (<i>CT</i>)	26
2.2.3.2.2.2 Leopard Textures (<i>LTT</i>)	26
2.2.3.2.2.3 Breccia Textures (<i>BX</i>)	37
2.2.3.2.2.4 Vein Breccia Textures (<i>Vn Bx</i>).....	38
CHAPTER 3: An Idealized Geometric Model for a Macroscopic Magmatic Feeder with Multiple Sulphide Traps that may be Analogous to the Voisey's Bay Ni, Cu, Co Deposit.....	40
3.0 Introduction.....	40
3.1 Geometric Attributes	40
3.1.1 Dilatancy.....	42
3.1.2 Dyke Necking.....	45
3.1.3 Dyke Expansion.....	50
3.2 Formation of Sulphide Traps	53

CHAPTER 4: Geological and Environmental Characteristics of the Ovoid.....	57
4.0 Introduction	57
4.1 Geometry	57
4.2 Lithostratigraphy	65
4.3 The Geological Significance of the Ovoid	
4.3.1 Introduction to Past and Present Geological Models	74
4.3.2 Physical Evidence Supporting the Existence of a Magmatic	
Feeder Conduit	76
4.3.3 Lithostratigraphic Evidence Supporting the Existence	
of an Open Magmatic System	76
4.3.4 Plunge.....	80
4.4 Multiple Feeders.....	81
CHAPTER 5: The Effect of Geometric Processes on Lithostratigraphy;	
the Mini-Ovoid.	86
5.0 Introduction.....	86
5.1 Geometric Changes to the Trap Environment.....	86
5.1.1 Transition from L13+00E through L12+50E.....	86
5.1.2. Transition from L12+50E through L12+00E.....	91
5.1.3 Transition from L12+00E through L11+50E.....	94
5.1.4 Transition from L11+50E through L11+00E-L10+50E.....	96
5.1.5 Transition from L11+00E-L10+50E through 10+00E.....	99
5.1.6 Transition from L10+00E through L9+50E.....	99
5.1.7 Transition from L9+50E through L9+00E.....	102
5.1.8 Transition from L9+00E through L8+50E,	
L8+00E and L7+50E.....	104
5.1.9 Transition from L7+50E through L7+00E.....	108
5.2 Geometric Metric Changes to the Feeder in the Formation of a	
Sub-Trap... ..	110
5.2.1 Transition from L13+00E through L12+50E and	
12+00E.....	111
5.2.2 Transition from L12+00E through L11+50E.....	113
5.2.3 Transition from L11+50E through L11+00E and	
L10+50E.....	114
5.2.4 Transition from L11+00E and 10+50E through L10+00E and	
L9+50E.....	114
5.2.5 Transition from L9+50E through L9+00E,	
L8+50E and L8+00E.....	115
5.2.6 Transition from L9+00E, L8+50E and L8+00E through L7+50E	
and L7+00E.....	116
CHAPTER 6: Investigation of Geological Environments and Flow Kinematics; The	
Western Extension.....	119
6.0 Introduction.....	119
6.1 The Reid Brook Zone.....	120

6.1.1 Relationship to Magmatic Sub-Chamber.....	120
6.1.2 Plunging Massive Sulphides (Hanging/Footwall Mineralization)...	122
6.1.3 Conjugate NNE/NNW Faults	126
6.2 Discovery Hill Zone.....	129
6.2.1 Lithology.....	129
6.2.1.1 Feeder Sequences.....	129
6.2.1.2 Noisy Sequences.....	144
6.2.1.3 Quiet Sequences.....	146
6.2.2 Flow Kinematics	147
6.2.2.1 Intrusive Relationships.....	148
6.2.2.1.1. Massive to Semi-Massive Sulphides	148
6.2.2.1.2 Leopard Textured Troctolite and Leopard Textured Breccia.....	149
6.2.2.1.3 Original Fragmental Breccia.....	149
6.2.2.1.4 Marginal and Transitional Sequences.....	150
6.2.2.2 Stratigraphic Relationships.....	150
6.2.2.2.1 Gabbro Phases.....	150
6.2.2.2.2 Gabbroic-Troctolitic Phases.....	153
6.2.2.2.3 Massive and Semi-Massive Sulphide Phases...	155

CHAPTER 7: Geological and Environmental Parameters Associated with the Eastern

Deeps Mineralization.	158
7.0 Introduction.....	158
7.1 Past and Present Geological Models	158
7.2 Stratigraphy.....	160
7.3 Feeder Melange.....	169
7.4 Geological Significance for the Stratigraphic Position of the Mineralized Zone	269
7.4.1 Terminology.....	170
7.4.2 Ore Domains.....	171
7.5 Ambiguity in locating the Entry Line in Extreme Eastern Regimes	176
7.6 Anomalous Disseminated Sulphides within Upper Stratigraphic Horizons	182
7.7 Ambiguity in Defining the upper contact of the Feeder South of the Entry Line	184
7.8 The Significance of the Conduit (Feeder) Position.....	185

CHAPTER 8: Structure; Ovoid, Mini Ovoid, Western Extension and Eastern Deeps....

8.1 Structural Model	187
8.1.1 Structural Control.....	187
8.1.2 Structural Style.....	192
8.2 Structural Controls Associated with Lithostratigraphy.....	196
8.2.1 Specific Structural Attributes of the Eastern Deeps.....	196
8.2.1.1 Primary East/West Lineaments (Normal Faults).....	199
8.2.1.2 Conjugate Normal Faults (Formation of the	

Graben-Like Structure).....	201
8.2.1.3 Syntectonic Horizontal Fractures.....	202
8.2.2 Structural Controls on the Ovoid Feeder Conduit.....	203
8.2.2.1 Normal Conjugate Faults (Formation of the Graben).....	205
8.3. Sinistral Strike-Slip Faulting.....	210
8.3.1 Deformation Effects.....	211
8.3.2 Grenvillian Deformation.....	213
8.4 Scale of the Structural Events	216
8.5 Summary of the Tectonomagmatic History of the Voisey's Bay Deposit	220
CHAPTER 9: Conclusions and Discussion.....	221
9.1 Conclusions	221
9.2 Discussions.....	227
9.2.1 Timing and Genesis.....	227
9.2.2 Comparison to Other Ni Sulphide Deposits.....	235
9.2.3 Exploration Significance, Expanding Current Resources within the Voisey's Bay Deposit.....	243
9.2.4 Finding a new high grade Voisey's Bay type of Ni sulphide deposit.....	251
BIBLIOGRAPHY.....	254
APPENDIX A.....	A-1
QUICK LOGS AND BORIS LOGS	
Abbreviation Legends Used For Quick Logs.....	A-2
An Example Of The Revised Quick Logs: VB-98-433c.....	A-3
An Example Of The Early Version Of Quick Logs: VB-95-106.....	A-5
Rock Codes Used For Boris Logs.....	A-6
An Example (VB-95-018) Of A Boris Log Which Includes: Lithology; And Recorded Assays.....	A-11
An Example (VB-95-186) Of A Boris Log Which Includes: Lithology; And Magnetic Susceptibility.....	A-22
An Example (VB-96-321) Of A Boris Log Which Includes: Lithology; Percent Mineralization; Core Axis Angles; Recovery; and RQD.....	A-30
APPENDIX B.....	B-1
DIGITIZED SECTIONS	
An Example (L13+00E) Of An Interpreted (Digitized) Section With Lithology/Rock Codes Displayed On The Drill Hole Trace (1:5000).....	B-2
An Example (L13+00E) Of An Interpreted (Digitized) Section With Lithology/Rock Codes Displayed On The Drill Hole Trace (1:1000).....	B-3
An Example (L13+00E) Of An Interpreted (Digitized) Section With Lithology/ Rock Codes Displayed On The Drill Hole Trace And Color Added (1:5000).....	B-4
An Example (040E) Of A Non-Interpreted Long Section With Lithology/Rock Codes Displayed On The Drill Hole Trace (1:5000).....	B-5

An Example (012E) Of An Interpreted (Digitized) Long Section With Lithology/Rock Codes Displayed On The Drill Hole Trace (1:2000).....	B-6
---	-----

APPENDIX C..... C-1

DATA DISPLAY

An Example Of Lithology Data From Boris Displayed On A West Facing Drill Hole Section.....	C-2
An Example Of Ni(%) Grades From Boris Assay Samples Displayed On A West Facing Drill Hole Section.....	C-3
An Example Of Ni(5) Grade Cut-Off Displayed On A West Facing Drill Hole Section, Based On Assays From Boris.....	C-4
An Example Of The Display Of Multiple Data Sets; Ni(%) Grades and Lithology On A West Facing Drill Hole Section.....	C-5
An Example Of The Display Of Lithogeochemical Sample Taken and Analyzed.....	C-6
An Example Of The Data Summary Available For Each Point On A Drill Hole Trace With A Lithogeochemical Sample Taken And Analyzed.....	C-7
An Example Of Structural Data Displayed On Drill Hole Traces With Symbols And Colors Representing Specific Structural Groups.....	C-8
An Example Of The Data Summary Available For Each Point On A Drill Hole Trace With A Recorded Structural Element.....	C-9

APPENDIX D..... D-1

RELOG DATA

An Example (VB-95-120) Of The Original Lithology Codes And The Relog Codes.....	D-2
An Example (VB-95-134) Of The Original Lithology Codes And The Relog Codes.....	D-3
An Example (VB-95-117) Of The Original Lithology Codes And The Relog Codes.....	D-4
An Example (VB-95-079) Of The Original Lithology Codes And The Fault Relog Codes.....	D-5
An Example Of An Original Drill Log (VB-95-120) Before Being Relogged For Specific Lithological Relationships.....	D-12
An Example Of An Original Drill Log (VB-95-134) Before Being Relogged For Specific Lithological Relationships.....	D-17
An Example Of A Relog (VB-95-134) For Specific Lithological Relationships....	D-23
An Example Of An Original Drill Log (VB-95-117) Before Being Relogged For Specific Lithological Relationships.....	D-27
An Example Of A Relog (VB-95-117) For Specific Lithological Relationships...	D-31
An Example Of An Original Drill Log (VB-95-079) Before Being Relogged For Specific Lithological Relationships.....	D-35
An Example Of A Relog (VB-95-117) For Structural Information.....	D-39

An Example (L5+50E) Of A Non-Interpreted Section With Old Lithology Codes Displayed On The Left Side Of The Drill Hole Trace And The New Relog Codes Displayed To The Right Side Of The Drill Hole Trace.....	D-41
An Example (L5+50E) Of An Interpreted Section With New Relog Codes Displayed On The Left Side Of The Drill Hole Trace And The Grades (%Ni) Displayed To The Right Side Of The Drill Hole Trace.....	D-42
An Example (L5+50E) Of An Interpreted Section With New Relog Codes: Codes Displayed On The Left Side Of The Drill Hole Trace And The Grades (%Ni) Displayed To The Right Side Of The Drill Hole Trace And Color Added To Enhance The Lithologies.....	D-42

APPENDIX E.....	E-1
-----------------	-----

MODEL GENERATION

An Example Of Points Snapped To A Contact On Drill Hole Traces.....	E-2
An Example (Plan View) Of A Wire Frame (DTM Surface) Model Generated Points Snapped To Drill Hole Traces.....	E-3
An Example (Plan View) Of A Wire Frame (DTM Surface) Model Sliced With Slices Converted To Strings.....	E-4
An Example (West Facing) Of A Wire Frame (DTM Surface) Model Sliced With Slices Converted To Strings.....	E-5

APPENDIX F

3-DIMENSIONAL MODELS PRESENTED IN DIGITAL FORMAT

Please not, a CD has been prepared which includes a series of .AVI files, as listed below. The .AVI files are digital video captures of the 3-dimensional models used to produce the 2 dimension figures contained in this document. It is necessary to render these models in their true 3-dimensional character to clearly display and establish their attributes as discussed in the text. The .AVI drivers are standard application in Windows 95. To initiate and view a desired file, it is only necessary to double click on the required folder with the left mouse button.

(The following file names correspond numerically and alphanumerically to the figures contained in the text, for example; Fig 4.4.AVI corresponds to Figure 4.4 contained in the text.)

Fig 4.4.AVI.....	Pocket 2 (rear)
Fig 7.7.AVI.....	Pocket 2 (rear)
Fig 7.8.AVI.....	Pocket 2 (rear)
Fig 7.9.AVI.....	Pocket 2 (rear)
Fig 7.10.AVI.....	Pocket 2 (rear)
Fig 7.11.AVI.....	Pocket 2 (rear)
Fig 8.5.a.AVI.....	Pocket 2 (rear)
Fig 8.5.b.AVI.....	Pocket 2 (rear)
Fig 8.5.c.AVI.....	Pocket 2 (rear)

Fig 8.6.a.AVI.....	Pocket 2 (rear)
Fig 8.6.b.AVI.....	Pocket 2 (rear)
Fig 8.6.c.AVI.....	Pocket 2 (rear)
Fig 8.7.a.AVI.....	Pocket 2 (rear)
Fig 8.7.c.AVI.....	Pocket 2 (rear)
Fig 8.9.a.AVI.....	Pocket 2 (rear)
Fig 8.9.b.AVI.....	Pocket 2 (rear)
Fig 9.4.a.AVI.....	Pocket 2 (rear)
Fig 9.4.b.AVI.....	Pocket 2 (rear)
Fig 9.4.c.AVI.....	Pocket 2 (rear)
Fig 9.5.AVI.....	Pocket 2 (rear)
Fig 9.6.a.AVI.....	Pocket 2 (rear)
Fig 9.6.b.AVI.....	Pocket 2 (rear)
Fig 9.7.a.AVI.....	Pocket 2 (rear)
Fig 9.7.b.AVI.....	Pocket 2 (rear)

LIST OF TABLES

1.1 HOLES COMPLETELY OR PARTIALLY LOGGED BY AUTHOR.....	6
1.2 HOLES RELOGGED FOR LITHOLOGY.....	7
1.3 HOLES RELOGGED FOR STRUCTURE.....	7

LIST OF FIGURES

1.1 LABRADOR, VOISEY'S BAY PROJECT	
<i>Location Of Voisey's Bay</i>	2
1.2 MAIN BLOCK GEOLOGY MAP (COMPILATION)	
<i>Voisey's Bay, Labrador</i>	Pocket 1A
1.3 LABRADOR, VOISEY'S BAY PROJECT	
<i>Regional Geology Of Labrador</i>	8
1.4 EXPLORATION PROGRAM	
<i>Geology Overview</i>	9
3.1 CONCEPTUALIZED MAGMATIC FEEDER SYSTEM.....	41
3.2 THERMAL PROCESSES ASSOCIATED WITH CONTINUOUS MAGMATIC FLOW.....	44
3.3 CHANGES IN GEOMETRIC PARAMETERS.....	47
3.4 CHOKING OF THE SYSTEM AS THE CONDUIT NARROWS.....	48
3.5 FLOW TRAJECTORY IN RELATION TO FRAGMENT ORIENTATION..	49
3.6 MEANDER DYNAMICS ASSOCIATED WITH GEOMETRIC CHANGES TO THE CONDUIT.....	51
4.1 DEPOSIT GEOLOGY MAP (COMPILATION)	
<i>Voisey's Bay, Labrador</i>	Pocket 1B
4.2 SECTION 14+00E.....	59
4.3 SECTION 15+00E.....	60

4.4	3D IMAGE OF OVOID/MINI-OVOID (<i>Massive Sulphides Only</i>).....	61
4.5	SECTION 15+50E.....	63
4.6	SECTION 13+50E.....	64
4.7	IDEALIZED STRATIGRAPHY OF THE OVOID.....	66
4.8	LONGITUDINAL SECTION (STRIKING 112°) 12+00E TO 15+50E.....	77
4.9	SECTION 13+00E.....	82
4.10	“OCTOPUS MODEL” FOR THE COELENC OF MULTIPLE FEEDERS.....	83
5.1	SECTION 12+50E.....	90
5.2	SECTION 12+00E.....	92
5.3	SECTION 11+50E.....	95
5.4	SECTION 11+00E.....	97
5.5	SECTION 10+50E.....	98
5.6	SECTION 10+00E.....	100
5.7	SECTION 9+50E.....	101
5.8	SECTION 9+00E.....	103
5.9	SECTION 8+50E.....	105
5.10	SECTION 8+00E.....	106
5.11	SECTION 7+50E.....	107
5.12	SECTION 7+00E.....	109
5.13	LITHOLOGICAL AND GEOMETRIC PARASITIC RELATIONSHIPS TO MACROSCOPIC FEATURES.....	117
6.1	SECTION 9+00W.....	121
6.2	SECTION 4+00W.....	123
6.3	SECTION 7+00W.....	124
6.4	2+00W TO 2+00E FAULT SYSTEM.....	128
6.5	REVIEW OF OLD TERMINOLOGIES AND THEIR STRATIGRAPHIC AFFINITIES.....	130
6.6	LITHOSTRATIGRAPHY.....	132
6.7.1	SECTION 3+00E.....	133
6.7.2	SECTION 3+50E.....	134
6.7.3	SECTION 4+00E.....	135
6.7.4	SECTION 4+50E.....	136
6.7.5	SECTION 5+00E.....	137
6.7.6	SECTION 5+50E.....	138
6.7.7	SECTION 6+00E.....	139
6.7.8	SECTION 6+50E.....	140
6.7.9	SECTION 7+00E.....	141
6.7.10	SECTION 7+50E.....	142
7.1	EASTERN DEEPS CHAMBER AND FEEDER LITHOSTRATIGRAPHY.....	161

7.2	SECTION 26+00E.....	164
7.3	SECTION 28+00E.....	165
7.4	SECTION 31+00E.....	166
7.5	SECTION 32+00E.....	167
7.6	SECTION 34+00E.....	168
7.7	FOOTWALL CONTOURS (SLICED VERTICALLY AT 25M).....	173
7.8	FOOTWALL CONTOURS (AT 25M) WITH THE WIREFRAME FOR CONTINUOUS MASSIVE SULPHIDES.....	174
7.9.	CONTOURS (25M VERTICAL SLICES) OF TOP SURFACE OF EASTERN DEEPS FEEDER WITH 0.7% Ni WIREFRAME.....	177
7.10.	FOOTWALL AND HANGING WALL WITH 0.7% Ni WIREFRAME...	178
7.11.	FOOTWALL CONTOURS WITH 0.7% Ni WIREFRAME.....	180
7.12.	SULPHIDES RANDOMLY DISPERSED IN ABSENCE OF A MICRO-TRAP.....	181
7.13.	LIP GNEISS FRACTURED AND SEPARATED FROM NORTH MARGIN.....	183
8.1	ANALYSIS OF THE DEVELOPMENT OF REGIONAL EXTENSIONAL TECTONICS.....	189
8.2	DEVELOPMENT OF REGIONAL EXTENSIONAL TECTONICS THROUGH CRUSTAL DOMING.....	190
8.3	CONCEPTUALIZED 3-D MODEL OF A GRABEN STRUCTURE.....	191
8.4	EMPLACEMENT OF THE EASTERN DEEPS FEEDER WITHIN THE GRABEN STRUCTURE.....	197
8.5.a	EMPLACEMENT OF THE EASTERN DEEPS CHAMBER WITHIN THE GRABEN STRUCTURE.....	198
8.5.b	SKELETON FOR THE CONCEPTUALIZED GRABEN STRUCTURE AND THE EMPLACEMENT OF THE EASTERN DEEPS CHAMBER.....	198
8.6.a	REIDEL BRITTLE SHEARS.....	204
8.6.b	OVOID DYKE AND EASTERN DEEPS CHAMER FAULT BOUNDED BY NORTH AND SOUTH FAULTS	204
8.6.c	EASTERN DEEPS CHAMBER AND THE OVOID DYKE.....	204
8.7.a	CONCEPTUALIZED MODEL OF THE OVOID DYKE, THE EASTERN DEEPS CHAMBER AND THE EASTERN DEEPS FEEDER.....	206
8.7.b	CONCEPTUALIZED EAST FACING MODEL FOR THE OVOID DYKE IN THE REID BROOK ZONE.....	206
8.7.c	CONCEPTUALIZED MODEL FOR THE OVOID/MINI-OVOID AND EASTERN DEEPS CHAMBER AND FEEDER.....	206
8.8	SPATIAL RELATIONSHIPS OF THE VOISEY'S BAY CHAMBERS, DYKES/CONDUITS AND TRAPS.....	207
8.9.a	THE OVOID DYKE HOSTING THE "OVOID" MASSIVE SULPHIDES.....	209
8.9.b	SCHEMATIC MODEL FOR CURRENT EROSIONAL LEVELS WITHIN THE GRABEN SYSTEM.....	209
8.10	REGIONAL STAIN ELLIPSE FOR SINISTRAL STRIKE-SLIP	

	FAULTING AND THE DEVELOPMENT OF SECONDARY BRITTLE REIDEL SHEARS.....	215
8.11	SECTION 37+00E (RED DOG).....	217
8.12	CONCEPTUALIZED MODEL FOR THE VOISEY'S BAY DEPOSIT	218
8.13	SCHEMATIC PROFILE THROUGH THE VOISEY'S BAY DEPOSIT.....	219
9.1	SCHEMATIC PROFILE CORRELATING THE CONTRACTION OF THE WESTERN DEEPS CHAMBER WITH A POSSIBLE EXPANSION IN THE OVOID DYKE.....	230
9.2	IDEALIZED LONG-SECTION THROUGH THE REID BROOK ZONE AND THE WESTERN EXTENSION.....	231
9.3	IDEALIZED LONG-SECTION THROUGH THE VOISEY'S BAY DEPOSIT.....	233
9.4.a	THE OVOID DYKE AND THE EASTERN DEEPS FEEDER.....	244
9.4.b	THE OVOID DYKE EXTRAPOLATED TO THE EAST AND THE EASTERN DEEPS FEEDER.....	244
9.4.c	EXTRAPOLATIONS OF THE OVOID DYKE AND EASTERN DEEPS FEEDER.....	244
9.5	SYMETRICAL GEOMETRY OF THE MACROSCOPIC SYSTEM.....	245
9.6.a	STRUCTURAL CONTOURS FOR THE OVOID DYKE.....	247
9.6.b	OVOID DYKE WITH MULTIPLE PLUNGING ORE ZONES (SULPHIDE TRAPS).....	247
9.7.a	STRUCTURAL CONTOURS IN RELATIONSHIP TO THE PLUNGING ORE ZONES.....	248
9.7.b	STRUCTURAL CONTOURS OF THE OVOID DYKE AND THE PLUNGE AZIMUTH OF THE ORE ZONES.....	248
9.8	CONCEPTUAL MODEL FOR THE VOISEY'S BAY DEPOSIT.....	250

LIST OF PLATES

Plate 2A	FRAGMENT AND SULPHIDE-RICH CONDUIT GABBRO-TROCTOLITE.....	21
Plate 2B	FRAGMENT-RICH AND SULPHIDE-POOR CONDUIT GABBRO-TROCTOLITE.....	22
Plate 2C	ULTRAMAFIC FRAGMENT WITH SEMI-MASSIVE SULPHIDES.....	23
Plate 2D	A PREFERRED ORIENTATION OF FRAGMENTS IN A CONDUIT GABBRO-TROCTOLITE	24
Plate 2E	FRAGMENT-RICH AND SULPHIDE-POOR CONDUIT GABBRO-TROCTOLITE WITH NO PREFERRED ORIENTATION OF FRAGMENTS.....	25
Plate 2F	FRAGMENT AND SULPHIDE-POOR CONDUIT GABBRO...	27
Plate 2G	LEOPARD TEXTURED GABBRO-TROCTOLITE.....	28
Plate 2H	LEOPARD TEXTURED GABBRO-TROCTOLITE WITH	

	SULPHIDES CONCENTRATED AT THE OIKOCRYST BOUNDARIES.....	29
Plate 2I	LEOPARD TEXTURED GABBRO-TROCTOLITE WITH SEMI- MASSIVE SULPHIDES.....	30
Plate 2J	LEOPARD TEXTURED GABBRO-TROCTOLITE WITH SULPHIDES CONCENTRATED AT THE OIKOCRYST BOUNDARIES FORMING A WAVY TEXTURE.....	31
Plate 2K	LEOPARD TEXTURED GABBRO-TROCTOLITE CONTAINING FRAGMENTS	32
Plate 2L	LEOPARD TEXTURED GABBRO-TROCTOLITE CONTAINING GNEISSIC FRAGMENTS	34
Plate 2M	LEOPARD TEXTURED GABBRO-TROCTOLITE MIXING WITH EARLY MAGMA.....	35
Plate 2N	LEOPARD TEXTURED GABBRO-TROCTOLITE CONTAINING GNEISSIC AND TROCTOLITE FRAGMENTS	36
Plate 2O	FRAGMENT-RICH AND SULPHIDE-POOR CONDUIT GABBRO- TROCTOLITE INTRUDED BY A MASSIVE SULPHIDE VEIN.....	39
Plate 4P	CHILLED GABBRO.....	67
Plate 4Q	CHILLED GABBRO BARREN OF SULPHIDE.....	68
Plate 4R	MASSIVE SULPHIDE WITH LOOP TEXTURES.....	71
Plate 4S	MASSIVE SULPHIDE WITH ALIGNED MAGNETITE.....	72
Plate 4T	MASSIVE SULPHIDE WITH A FRACTURE CLEAVAGE.....	73

LIST OF FIGURE ABBREVIATIONS

Drawn and Interpreted by DEL.....Geological interpretation by Dawn Evans-
Lamswood, geological section digitized by Dawn
Evans-Lamswood

Drawn and/or Interpreted by DEL/RW...Geological interpretation by Dawn Evans-
Lamswood and Robert Wheeler, geological
section digitized by Dawn Evans-Lamswood and
Robert Wheeler

Modified by DEL.....Original geological interpretation revised by
Dawn Evans-Lamswood, geological section
updated by Dawn Evans-Lamswood

Modified by RW.....Geological section updated by Robert Wheeler

Drawn by VBNC.....Sketch is a geological compilation from the
staff of Voisey's Bay Nickel Company Ltd.

3-DIMENSIONAL MODELS PRESENTED IN DIGITAL FORMAT

Please note, a CD has been prepared which includes a series of .AVI files, as listed below. The .AVI files are digital video captures of the 3-dimensional models used to produce the 2 dimension figures contained in this document. It is necessary to render these models in their true 3-dimensional character to clearly display and establish their attributes as discussed in the text. The .AVI drivers are standard application in Windows 95. To initiate and view a desired file, it is only necessary to double click on the required folder with the left mouse button. *See APPENDIX F*

Chapter 1: Introduction

1.1 Exploration History

The Voisey's Bay Ni-Cu-Co deposit is situated 30 km southeast of the community of Nain, along the northeastern coast of Labrador (Figure 1.1). It has been referred to as "possibly the most important mineral discovery in Canadian history" (Diamond Fields Resources, Report from Voisey's Bay, 04/1995). The distinctive gossanous appearance of what is now known as the Discovery Hill outcrop (Figure 1.2), was previously documented and the lithology sampled by a field crew from the Department of Natural Resources/Mines and Energy (Ryan and Lee, 1985). Their samples, however, did not produce significant assay results.

Eight years later, the true significance of this outcrop was brought to light by two prospectors, Albert Chislett and Chris Verbiski, who had been sampling for diamond indicator minerals for a reconnaissance program funded by Diamond Fields Resources. While completing their exploration program in the fall of 1993, they sampled the large "Discovery Hill" gossan zone. Assay results from their grab samples ran as high as 6% Cu and 3% Ni (Lee *et al*, 1995). This initial reconnaissance or "spot check" evaluation was followed up in the summer of 1994 by a grass roots exploration project. The follow-up program included a HLEM ground geophysical survey and the drilling of four diamond drill holes (Diamond Fields Resources, Report from Voisey's Bay, 04/1995). The ground geophysical surveys documented extensive and continuous conductivity, and all four drill holes intersected significant sulphide mineralization (Diamond Fields Resources, Report from Voisey's Bay, 04/1995). Based on the favorable results from the



Figure 1 1 Location of the Voisey's Bay project with reference to the major communities within Newfoundland and Labrador.

1994 program, exploration was extended into January, 1995, when diamond drill hole VB-94-007 intersected 104 m of massive sulphides in the so-called Ovoid deposit (Diamond Fields Resources, Report from Voisey's Bay, 04/1995) (Figure 1.1).

1.2 Access

Although, remote and without any established road systems, the study area is relatively accessible throughout the year. From mid-June to late October, Voisey's Bay can be entered by boat or float planes. Throughout the late fall, winter and early spring, access can be gained over the frozen waterways by snowmobile or other tracked vehicles. Furthermore, with substantial accumulations of ice, fixed winged aircraft can land on frozen bays or on inland water bodies. Helicopter transport provides access to and from the area throughout the year, but most especially during spring breakup, when thaw conditions prevent landing or transport along the waterways.

1.3 Methods

Data were generated to document the physical and lithological controls on the Voisey's Bay system through the analysis of drill hole and surface outcrops (see chapter 2). These data were then used to create three-dimensional computer-rendered models (GEMCOM and Datamine) for various aspects of the deposit (see Chapter 2) including: ore bodies, faults, magmatic chambers, and conduits.

During this study, all of the core drilled at the Voisey's Bay deposit was examined by the author (in excess of 400 diamond drill holes), with the exception of holes VB95001-VB95005 and VB95007. Approximately 150 drill holes were logged completely or

partially by the author (Table 1). An additional 75 holes were relogged for lithological and structural detail specific to this study (Tables 2 and 3). Approximately 250 core samples were collected and classified into lithological and textural groups to document distinct textural, structural and intrusive relationships that are important to the tectonomagmatic history of the deposit. Representative samples from each group were then polished and photographed.

1.4 Regional Geology

Five lithotectonic provinces comprise the fundamentals of Labrador geology: the Nain, Churchill, Superior, Makkovik and Grenville provinces (cf. Wilton, 1996) (Figure 1.3). Extensive anorthosite-monzogranite-granite massifs intruded through these provinces during the Proterozoic (Ryan *et al.*, 1995). The oldest known rocks of Labrador are found in the Nain Province (Bridgwater *et al.*, 1973). This province is separated from the Archean Superior craton to the west, by the Churchill Province. In northwestern Labrador, the Churchill Province also encloses the remnants of the Archean Rae Province (Hoffman, 1988; Wardle and Wilton, 1995). To the southeast, the Makkovik Province is a metasedimentary sequence developed on the flanks of the Nain Province (Gower *et al.*, 1982; Ryan, 1984). Lastly, the Grenville Province consists of orogenic suites and juvenile Labradorian crust which were structurally superimposed (i.e. thrust) over basement rocks ca. 1000 Ma (Gower *et al.*, 1995; Rivers, 1995).

The study area and deposit straddle the suture between the Churchill province to the west and the Nain province to the east (Figure 1.4) (Ryan, 1996). The Nain Province rocks are Archean amphibolite to granulite facies gneisses. The Churchill province consists

of predominately Proterozoic granulite facies gneisses (Wardle and Wilton, 1995; Hoffman, 1988). In the area surrounding Voisey's Bay, however, the eastern margin of the Churchill Province is marked by a distinct metasedimentary package, the Tasiuyak gneisses (Figures 1.2, 1.3 and 1.4). The Tasiuyak gneisses are interpreted to have been a clastic sequence of rocks deposited as an accretionary wedge on the Churchill Province (Wardle *et al.*, 1995).

The ca. 1.86 collision between the Nain and Rae/Churchill Provinces constitutes the Torngat Orogen, which in the north is exposed as a foreland fold and thrust belt. The central core to the orogen is the ca. 1.82 Ga Abloviak shear zone which is a transcurrent structure (Jamison and Calon, 1994; Wardle *et al.*, 1990; Korstgard *et al.*, 1987) (Figure 1.4). The suture zone between the Nain and Churchill Provinces was also the locus for the intrusion of the 1.32-1.29 Ga Nain Plutonic Suite (NPS) (Ryan, 1996) (Figure 1.3). The Voisey's Bay main block (Figure 1.4) covers the suture and the NPS.

1.5 Main Block

The NPS comprises several anorthositic, ferrodioritic, troctolitic and granitoid intrusions of which the Reid Brook Complex (RBC) is a troctolite to gabbro member (Ryan, 1996). The Voisey's Bay deposit is hosted by 1333-1338 Ma (Farrow, 1997) olivine gabbro to troctolite rocks which are part of a sheet or dyke complex within the RBC (Figure 1.2). The dyke complex is intruded by several younger members of the NPS (Figure 1.2) which have been documented by Morse (1983), Ryan (1991), Xue and Morse (1993), and Hamilton *et al.* (1994) to include episodic granitic to anorthositic plutonism as

HOLES COMPLETELY OR PARTIALLY LOGGED BY
DAWN EVANS-LAMSWOOD

VB-95-06	VB-95-145	VB-95-202	VB-97-414A
VB-95-09	VB-95-146	VB-95-203	VB-97-415
VB-95-10	VB-95-147	VB-95-205	VB-97-418
VB-95-11	VB-95-148	VB-95-209	VB-97-426
VB-95-12	VB-95-150	VB-95-211	VB-97-427
VB-95-13	VB-95-151	VB-95-213	VB-98-431
VB-95-14	VB-95-153	VB-95-220	VB-98-433
VB-95-15	VB-95-155	VB-96-273	VB-98-436
VB-95-16	VB-95-156	VB-96-276	VB-98-438
VB-95-17	VB-95-157	VB-96-285	VB-98-455
VB-95-18	VB-95-158	VB-96-299	VB-98-455a
VB-95-19	VB-95-159	VB-96-300	VB-98-458
VB-95-25	VB-95-160	VB-96-303	VB-98-461B
VB-95-26	VB-95-166	VB-96-309	VB-98-461C
VB-95-27	VB-95-166A	VB-96-310	VB-98-461D
VB-95-28	VB-95-168	VB-96-313	VB-98-462
VB-95-29	VB-95-170	VB-96-314	VB-98-463
VB-95-30	VB-95-171	VB-96-318	VB-98-466
VB-95-31	VB-95-172	VB-96-320	VB-98-467
VB-95-32	VB-95-178	VB-96-321	VB-98-470
VB-95-33	VB-95-179	VB-96-330	VB-98-474
VB-95-34	VB-95-180	VB-96-334	VB-98-476
VB-95-35	VB-95-181	VB-96-340	VB-98-477
VB-95-36	VB-95-182	VB-96-354A	VB-98-478
VB-95-37	VB-95-183	VB-96-355	VB-98-479
VB-95-38	VB-95-185	VB-96-355A	VB-98-480
VB-95-39	VB-95-186	VB-96-361	VB-98-481
VB-95-41	VB-95-187	VB-96-363	VB-98-482
VB-95-42	VB-95-188	VB-96-365	VB-98-483
VB-95-44	VB-95-189	VB-97-368	VB-98-484
VB-95-46	VB-95-190	VB-97-375	VB-98-485
VB-95-69	VB-95-191	VB-97-378	PT-97-01
VB-95-82	VB-95-192	VB-97-383	PT-97-10
VB-95-100	VB-95-196	VB-97-385	OV-97-16
VB-95-140	VB-95-198	VB-97-390	
VB-95-142	VB-95-199	VB-97-400	
VB-95-143	VB-95-200	VB-97-402	
VB-95-144	VB-95-201	VB-97-414	

Total = 149
Holes

TABLE 1

HOLES RELOGGED
FOR LITHOLOGY

VB-95- 93
VB-95- 98
VB-95- 104
VB-95- 106
VB-95- 107
VB-95- 108
VB-95- 110
VB-95- 112
VB-95- 114
VB-95- 117
VB-95- 119
VB-95- 120
VB-95- 123
VB-95- 124
VB-95- 125
VB-95- 126
VB-95- 127
VB-95- 128
VB-95- 129
VB-95- 130
VB-95- 131
VB-95- 132
VB-95- 133
VB-95- 134
VB-95- 135
VB-95- 136
VB-95- 140
VB-95- 144
VB-95- 146
VB-95- 146
VB-95- 152
VB-95- 153
VB-95- 154
VB-95- 155
VB-95- 157
VB-95- 159
VB-95- 160
VB-95- 162
VB-95- 167
VB-95- 168
VB-95- 175
VB-95- 191
VB-95- 192
VB-95- 195
VB-95- 197
VB-95- 222
VB-95- 232
VB-95- 234

TABLE 2

HOLES RELOGGED
FOR STRUCTURE

VB-95- 6
VB-95- 12
VB-95- 14
VB-95- 16
VB-95- 18
VB-95- 21
VB-95- 22
VB-95- 51
VB-95- 55
VB-95- 56
VB-95- 60
VB-95- 65
VB-95- 74
VB-95- 75
VB-95- 79
VB-95- 205
VB-95- 368
PT-97- 2
PT-97- 3
PT-97- 5
MET-95- 4
MET-95- 7
MET-95- 11
MET-95- 13
MET-95- 13
MET-95- 15
MET-95- 16
MET-95- 17
MET-95- 21
MET-95- 25
MET-95- 27

TABLE 3

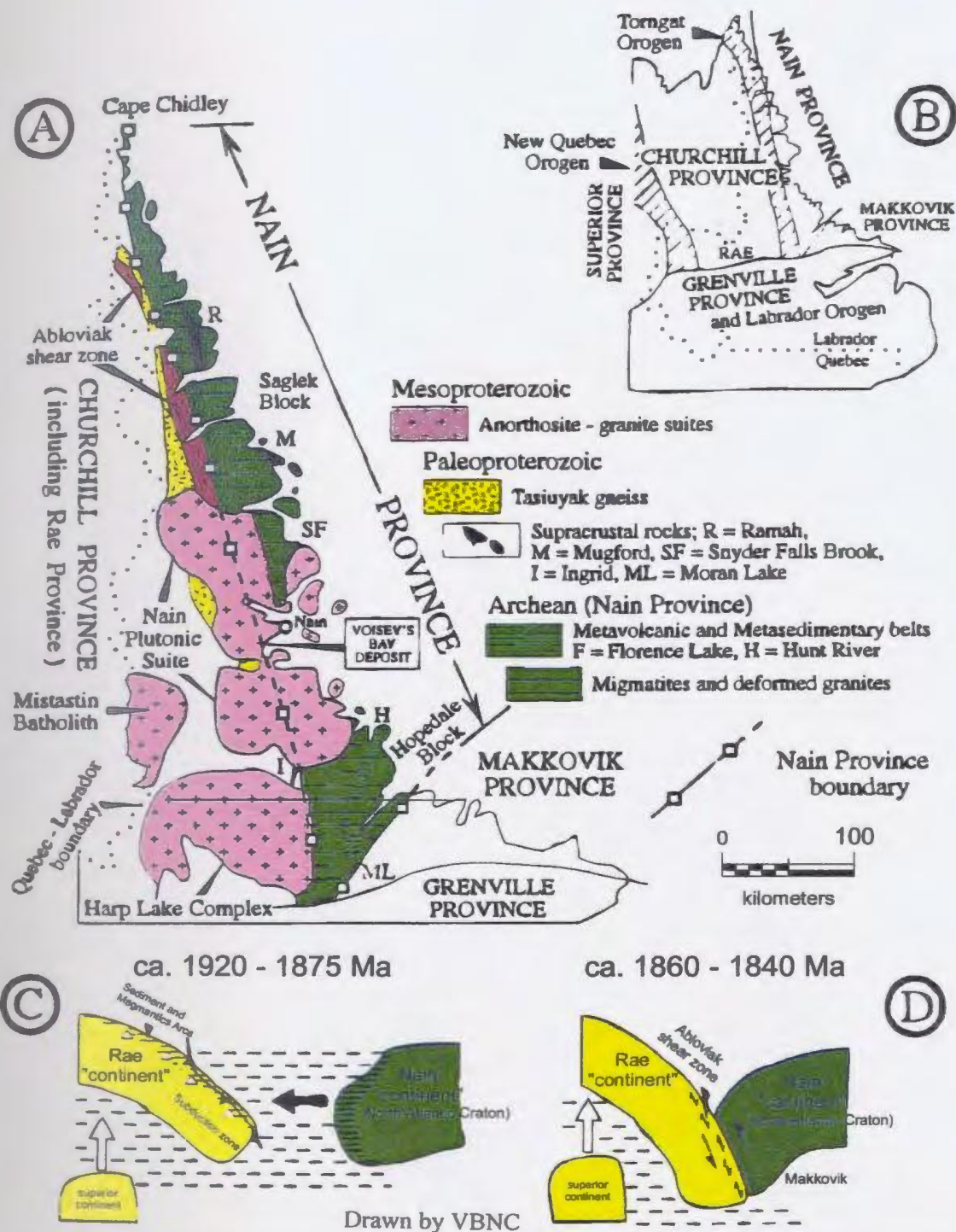
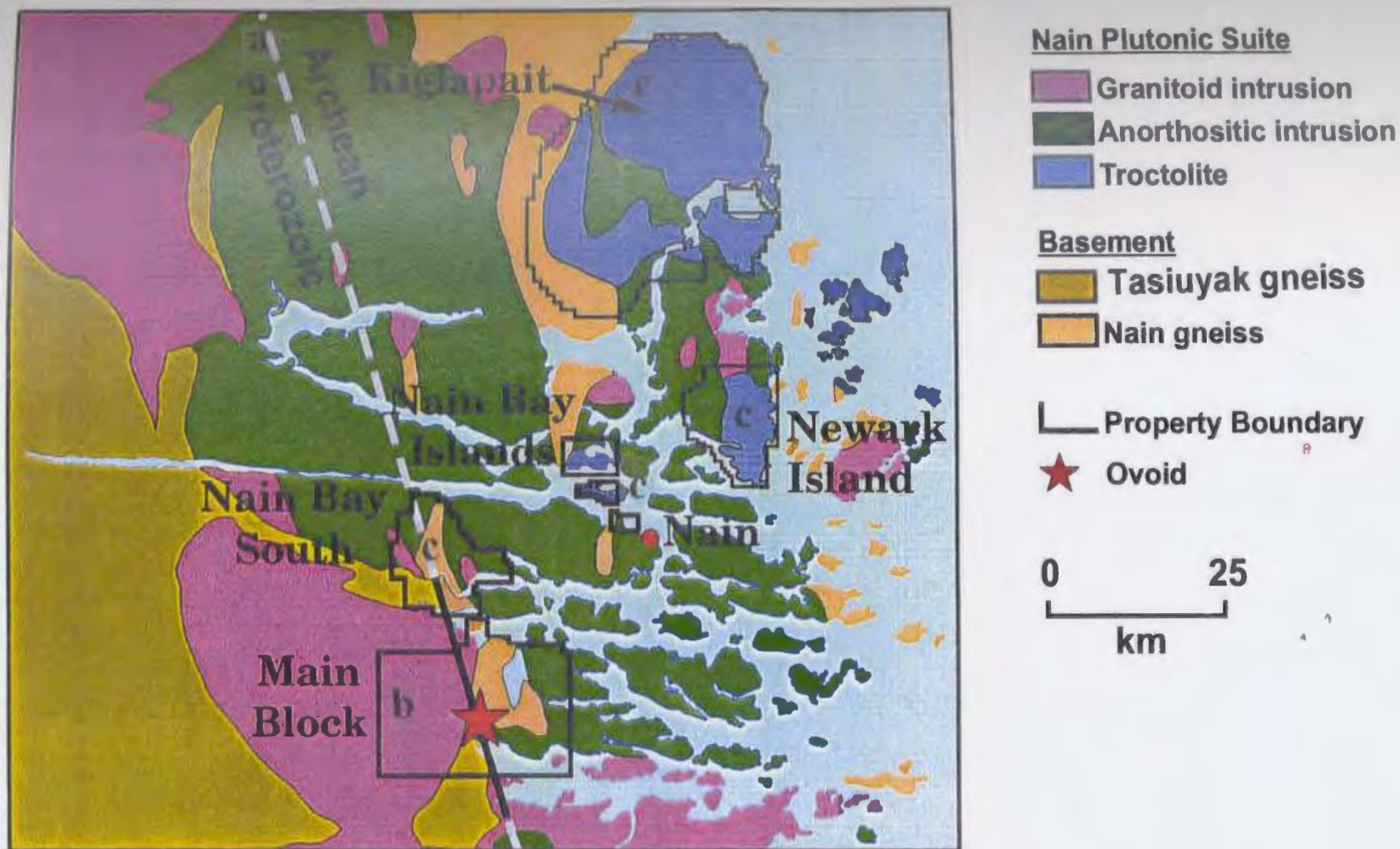


Figure 1.3 Regional geology of Northern Labrador (after Correlation programme Projects No. 290 and No. 315, 1994). (A) Major lithotectonic elements in relation to the Mesoproterozoic Nain Pluton Suite (including the Reid Brook Complex which hosts the Voisey's Bay deposit) and other similar intrusions. (B) Regional framework of Labrador showing the Paleoproterozoic Torngat orogen along the collisional boundary of the Nain Province and the Rae Province, and the New Quebec orogen at the Superior-Rae boundary. (C,D) The postulated plate tectonic setting for the Archean continents relevant to the Paleoproterozoic evolution of Northern Labrador.



Drawn by VBNC

Figure 1.4 A geological overview of the Nain Plutonic Suite (NPS). a= the tectonic suture separating orthogneisses of the Nain Province from the paragneisses (i.e. Tasiuyak gneiss) of the Churchill Province: b= the VBNC Main Block claims which host the Voisey's Bay deposit: c= VBNC claim groups within troctolite members of the NPS.

young as 1290 Ma. These members include: the Voisey's Bay granite, the Makhavinekh Lake granites (or Kangeklualuk granitoids), the Bird Lake Massif also known as the Ikadlivik granitoids, the Lister Massif, and the Mushuau Intrusion or as commonly referred to as the Sarah prospect. As exposed to the southeast, the Voisey's Bay granite consists of sub-horizontal granite to syenite sheets. The western portions of the study area are rivened by flatlying sheets of 1317 ± 2 Ma rapakivi textured granites and 1309 ± 2 Ma monazites (Farrow, 1997). These rapakivi intrusions were originally thought to be affiliated with the Makhavinekh Lake intrusion, however, it now appears that they represent younger plutonism (Farrow, 1997) (Figure 1.2). The 1318 Ma Lister massif borders the extreme eastern margin of the Reid Brook dyke and intrudes foliated layered anorthosites. The 1314 ± 2 Ma (Farrow, 1997) Mushuau intrusion lies to the north of the study area and is comprised of leucogabbro-norite and melatroctolites.

1.6 Deposit

According to Lightfoot (1998), 150 million tonnes of inferred Ni-Cu-Co resources are hosted within the dyke sheet which comprises the oldest gabbro-troctolitic rocks of the RBC. The deposit contains five distinct ore zones (Figure 1.2), the Ovoid, Mini-Ovoid, Discovery Hill zone, Reid Brook zone (Western Deeps), and the Eastern Deeps. The Ovoid and Mini-Ovoid ore dominantly consist of massive sulphides trapped within sub-vertical domains in the dyke. In comparison, the Discovery Hill zone is comprised of disseminated and veined semi-massive sulphides in a similar near vertical domain. In the Reid Brook zone, mineralization occurs as semi-massive to massive sulphides within a south dipping dyke regime. The Eastern Deeps mineralization is different from the other

mineralized zones in that it contains massive, semi-massive and disseminated sulphides in a flatlying feeder/dyke distal to the main sub-vertical sheet system.

1.7 Purpose

The purpose of this study was to document the nature and the form of the multiple ore zones within the Voisey's Bay deposit and to establish what were the physical linkages between them. To achieve these goals, the study addresses tectonic setting, geometric controls on the shape of the parental magmatic system and, as well, the physical and environmental parameters that proved favorable to sulphide capture and concentrate.

Traditionally, models for the formation of magmatic Ni sulphide deposits have been broad and generic. Most models typically involve immiscible sulphides settling out of silicate magmas within large magmatic reservoirs or intrusions. Where recognized, proximal dykes and sills are generally thought to have been uninvolved with the distribution and collection of sulphides. These features are characterized as either: channels feeding overlying ultramafic intrusions, or as later secondary structures, whereby, magma is tapped or siphoned from the magmatic chamber.

This study suggests that at the Voisey's Bay deposit, proximal dykes and sills may have had very important implications for the ultimate distribution of sulphides. Magmatic sulphide deposits have usually been studied in detail using geochemical and isotopic methods. This line of analysis has provided in-depth knowledge into the chemical genesis of these systems, however, it has provided little insight into the physical processes that progressively alter the physical dynamics of these systems. The Voisey's Bay deposit provide some clues as to the controls on these processes.

It is fundamental in the investigation of these systems to appreciate the macroscopic and mesoscopic structural history of the constituent regimes. Progressively developed structures can provide a complex network of conduits for the redistribution or redirection of sulphide and non-sulphide bearing magmas, even as the primary chambers are developing. Subsequently, geometric irregularities formed within a conduit system can provide obstructions that encourage the capture of propagating magmatic fluids.

1.8 Significance

Currently, over 500 drill holes penetrate the Voisey's Bay Deposit (Figure 1.2), including those drilled for geotechnical, metallurgic, delineation and exploration purposes. Even though a tremendous amount of data have been generated on this system, the physical and structural nature of the deposit is not known. Preliminary genetic models for the deposit have concentrated on the petrology of the ore and host rocks, along with cursory isotopic and geochemical interpretations. This study will document the overall physical shape and structural controls on the deposit. It will also investigate the spatial and temporal relationships of various mineralizing events including, local environmental parameters that contributed to sulphide distribution and containment.

Chapter 2: Methodology

2.1 The Collection and Manipulation of Data

As the accepted standard for the Voisey's Bay project, core was drilled with NQ sized (47.6 mm in diameter) rods and coring bits. Exceptions to this coring size included metallurgic and geotechnical holes which were drilled with HQ (63.5 mm in diameter) and PQ (85.0 in diameter) gear. Infrequently, BQ rods (36.5 mm in diameter) were used to bypass NQ equipment which had become welded or stuck within the hole. Drill holes were drilled along selected lines orientated north-south (355-360°) within a cut grid. These grid lines were used to reference data stations for the initial ground geophysical surveys conducted over the deposit. Holes were orientated at various dips in order to achieve the best intersection of the target. Most typically these were perpendicular to geological structures in order to obtain true and not apparent thicknesses. Distances between the grid lines used for the drilling varied from 25 to 100 meters, depending on the complexity and the footprint available for the geological target.

The drill cores were logged on the scale of meters for primary lithology and from meter to millimeter scales for texture, mineralogy, structure, alteration and mineralization. A geology summary log, or "Quick Log", (Appendix A) was recorded in an "Excel" spread sheet. These summary reports contained information pertaining to all meter scaled geological features and specific characteristics of the documented interval (i.e. type and aspect ratios of fragments, sulphide textures, alteration type and intensity).

The detailed geology was recorded within "Boris" (Appendix A), a standard logging program used by INCO Exploration for digitally storing geological data. Data

were entered directly into “Boris” while the geological logging of the drill core was conducted in the core shed. These detailed logs recorded (when applicable) whole rock lithogeochemistry and assay sample numbers and locations, rock quality data (*RQD*), point load data, magnetic susceptibility, and structural information which included measurements, descriptions and groupings (Appendix A). This information was then entered into “Boris” as point or interval data. The geology was grouped on lithology (lithogeochemical and textural affinities) and sulphide content, then recorded with a matching interval. The specific geological characteristics were then described in detail. The detailed descriptions included: lithology, geological interpretations, anomalous features, alteration, textures, fluctuations in sulphide content, contact relationships, and structural elements (Appendix A).

With final UTMs and the down-hole directional surveys (gyro or single shot) added, the log was then extracted in csv/text format to be imported into the geological modeling packages, “GEMCOM” or “Datamine”. “Boris” was used as the main database ensuring identical data were always imported into the modeling packages, whether the software was “GEMCOM” or “Datamine.” Once the geological data were stored in the modeling packages, the geological sections were created (Appendix B). When digitized, these sections reflected the geological interpretation for each area (Appendix B).

In order to accurately digitize the sections, several procedures and levels of interpretations were used. A slab width was defined for each section based on the drill hole spacing between sections. If the holes were drilled on 100 meter spaced grid lines, then the created sections used data contained 50 meters on each side of the center line of the section, and 25 meter on each side when lines are drilled with a 50 meter spacing. When a

specific section was being digitized, information from adjacent sections was “toggled” on or off, to produce an overlapping light table effect. This method of multiple display enabled use of all derived geological data, hence, allowing the final interpretation to be consistent and geologically sound (Appendix B). Once multiple sections were created and digitized, the sections were checked for “validity”. This procedure involved creating long-sections perpendicular, or skewed, to the original north-south sections (Appendix B). By changing the view, or orientation of the sections, the geological interpretation, as digitized, could be checked for spatial continuity or three dimensional legitimacy. Furthermore, to ensure spatial continuity, the digitized points and lines were “wobbled”, meaning that the digitized points and line were anchored in X, Y and Z space to the specified point in the drill hole trace. This procedure resulted in a true three-dimensional interpretation and not a two-dimensional/flat model.

Several levels of interpretation were used for the geological interpretations. Multiple data were expressed on the drill hole traces, including, lithology, individual or composite assays, RQD, raw lithogeochemistry, specific structural and relog data (Appendix C). To address specific geological problems or ambiguous relationships, the core was revisited and or relogged (Appendix D) in order to resolve the specific problem and its geological implications. Sections effected by these studies were then redigitized to reflect the new data and revised geological interpretation (Appendix D).

Several steps were required to produce accurate three dimensional geological models in both “Datamine” and “GEMCOM”. Models were created as either wireframe surfaces (*DTMs*) or as geometric solids. Evolution of the models started with review and interpretation of the geology, as explained above for the creation of cross sections. Points

were then inserted for the particular contact by snapping to the drill hole (i.e. as above. the point is anchored in true space to the specified point on the drill hole trace - see Appendix E). When the contact was defined and the accompanying points were inserted for the relevant drill holes, a preliminary DTM surface was created digitally by the modeling program using the points that were manually inserted. Next, the DTM surface was sliced vertically over narrow intervals (Appendix E). For example, if the line spacing for the drilled sections was 100 meter then the surface was sliced every 25 meters. The lines formed by the surface DTM slices were then converted to "strings". This digital transformation allowed the program/software to recognize these lines as individual digitized "strings". Simply, this allowed each individual "string" to be modified in order that it could accurately reflect the detailed geology. This process followed the same procedures performed when creating cross-sections (i.e. use of the light table effect, refinement of contacts and correction of abrupt changes in trajectory or geometry) (Appendix E).

Once the individual "strings" were modified such that they were geologically valid (as above with section creation), they were "tagged". The tagging process involved indication to the software as to which "strings" were to be joined and at which point. When the final DTMs were created, the "strings" remained open, and therefore, not true closed polygons. Alternatively, with the creation of solids the "strings" were required to be closed, to form complete polygons. Finally, with the strings appropriately "tagged" and left opened or closed, the corresponding surface or solid was rendered by the software. The software when cued, then searched for errors or invalid model generation, in example, "string cross-overs" or highly irregular changes to the geometry. If such an error was

found the model was “unrendered” (removal of solid surfaces). The interpretation and the process for “string” creation were then reviewed and modified until the model was validated and contained no errors.

2.2 Lithologies and the Identification of Textures in Drill Core

Lithologies were categorized in accordance to Streckeisen’s rock classification (1976) with modifications as defined by numerous lithogeochemical studies. These analyses included the study of isotopic systematics, whole rock REE and trace element data, and Ni/Fo abundance in olivine. This vast array of geochemical research has been conducted by Lightfoot (1998), Naldrett *et al.* (1998), Naldrett *et al.*(1996), Li and Naldrett (1997 and 1998), Lambert *et al.* (1998) and Ripley *et al.* (1998). The grouping scheme was followed during the core logging process. Identification was based upon silicate and sulphide textures, and bulk compositions (as visible to the naked eye). To ensure consistency in these lithological groupings when logging core, whole rock and thin section samples were taken where: 1) the lithology appeared ambiguous, 2) the hole was drilled in a previously unexplored domain, or 3) in locations where the lithogeochemical data from adjacent holes were sparse. The lithological and sulphide textures used to characterize the lithological groupings in the Voisey’s Bay Deposit are summarized below. The origin of these textures is summarized from observations in drill core. More intricate, site-specific, rock descriptions are described later in the text (Chapter 6) where they can be applied in direct geological context.

2.2.1 Paragneisses

The Tassuiyak paragneisses are thinly banded (1-3 cm.) garnetiferous to quartzofeldspathic-rich sequences with thinly intercalated graphite horizons. The garnets are diverse in size and range from 0.5 cm to 4 cm in diameter. The fabric is developed as a gneissosity defined by a compositional layering, however, locally can reflect intense strain and appear mylonitic.

2.2.2 Orthogneisses

The Nain gneisses occur as feldspathic, biotite- rich, granite-granodioritic orthogneisses. The gneissosity is developed as strong compositional banding. Early mafic dykes are recognized within the orthogneiss and appear slightly discordant to the fabric. Significantly, the occurrences of dykes within the orthogneisses increase to the east.

2.2.3. RBIC Deposit Rocks

The Voisey's Bay deposit is hosted within gabbro to troctolitic rocks (Naldrett *et al.*, 1996; Lightfoot, 1998). Based on the silicate and sulphide textures these rocks are divided into two groups: 1) chamber and, 2) conduit.

2.2.3.1 Chamber Gabbros-Troctolites

2.2.3.1.1 Composition

The chamber gabbros-troctolites are weakly mineralized, fragment-poor, normal (*NT*) to variable (*VT*) textured rocks (Naldrett *et al.*, 1996; Lightfoot, 1998). Where situated proximal to the wall rocks, weak to moderate biotitic alteration can be observed

within the gabbroic-troctolitic rocks. The fragments are sub-rounded, 1-3 cm in size and derived from paragneiss and orthogneiss protoliths (op cit.). The fragment content is less than 2% of the bulk composition within the NT gabbro-troctolites, but can locally reach as high as 10% within the VT sequences. The NT rocks contain only trace mineralization, however, sulphides within the VT rocks can locally account for up to 15% of the bulk composition.

2.2.3.1.2 Sulphide and Silicate Textures

The NT gabbro-troctolites are a monotonous sequence of medium grained, crystalline to rare stellate textured rocks which are weakly layered with the VT rocks. The VT rocks are found below the NT rocks and are medium to coarse grained, but can be pegmatitic. At sites where the VT has in contact with the wall rock, a mottled or patchy texture is created by the presence of weak to moderate biotite alteration and by a high concentration of bleached feldspathic-rich material (i.e. assimilated wall rock). Mineralization occurs as fine grained disseminated sulphides.

2.2.3.2 Conduit Gabbros-Troctolites

2.2.3.2.1 Composition

The conduit rocks consist of fragment-laden, sulphide-rich, gabbros-troctolites. The fragment content is diverse and consists of the following populations: ultramafic, orthogneiss, paragneiss, and gabbro-troctolite. Mineralization occurs as fine to coarse grained, disseminated to semi-massive and massive sulphides.

2.2.3.2.2 Sulphide and Silicate Textures

When multiple sequences are grouped within the conduit gabbro-troctolite rocks, the composite fragment content exceeds 10% of the bulk composition and can locally be up to 35% (Plates 2A and 2B). The ultramafic fragments occur as large elongate blocks that often exceed a meter in thickness and ten's of meters in length (Plate 2C). The gneiss fragments (Plates 2A and 2B) are generally between 1-8 cm in size, sub-rounded to sub-angular, and can express extreme aspect ratios (i.e. up to 10:1) (Plates 2A , 2B, and 2D). The highly absorbed fragments are completely pseudomorphed by spinel (Naldrett *et al.*, 1996), and therefore, appear aphyric and dark gray in color. Alternatively, the weakly absorbed fragments display a compositional zonation which is defined by dark grey, aphyric spinel-rich rims and buff colored, feldspar phyrlic cores (Plate 2E). The latter, will frequently retain a relict gneissosity preserved from its protolith (Plate 2E). Gabbro-troctolite fragments are sub-rounded and poorly absorbed, they are associated with sequences that host moderate to intense mineralization and generally, do not exceed 6 cm in size (Plates 2A , 2B, and 2D).

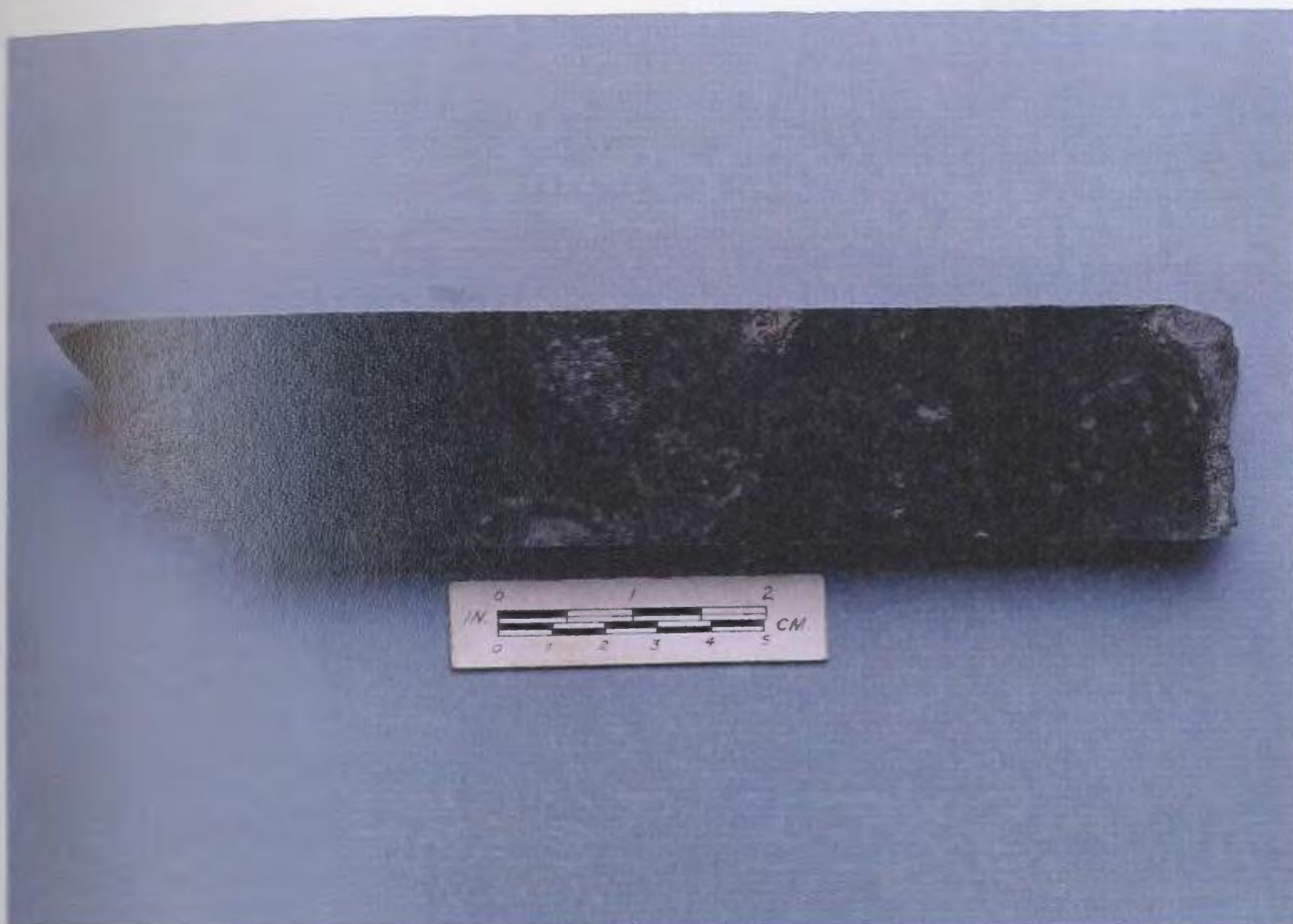
The conduit gabbroic-troctolitic rocks can be weakly mineralized (Plate 2D), however, in general contain significant nickel sulphides (Plate 2A). Distinct sulphide and silicate textures are developed within the conduit rocks and are identified as the following: Chilled, Leopard, Breccia, and Vein Breccia.



Key to Legend



Plate 2A. DDH-191 at 250 m. A sulphide-rich (35%) conduit gabbro-troctolite containing a dense concentration of fragments that form approximately 35% of the bulk composition. The sub-angular fragments display a weak alignment. Coarse, blotchy sulphide textures develop within the fragment-laden matrix. The fragment types include: a = ultramafic, b = gabbro-troctolite, c = gneiss.



Key to Legend



Plate 2B. DDH-127 at 70.1 m. A conduit gabbro-troctolite containing a dense concentration of fragments that form approximately 35% of the bulk composition. The sub-rounded fragments do not display a preferred orientation. This interval is sulphide-poor, however it is part of a sulphide-rich sequence. The fragment types include: a = mineralized gabbro-troctolite, b = aphyric gneiss fragments, c = gneiss fragment with a feldspar phyric core enclosed by spinel.



Plate 2C. DDH-134 at 183.0 m. An ultramafic block/fragment with semi-massive sulphides intruding along brittle fractures. The ultramafic fragments are found within the conduit gabbro-troctolites.



Key to Legend



Plate 2D. DDH-133 80.1 m. A fragment-laden conduit gabbro-troctolite containing a dense concentration of fragments that form 25-30% of the bulk composition. The fragments are sub-angular with extreme aspect ratios (8:1) and define a preferred orientation. Sulphides are observed to be concentrated at the margins of the fragments. Legend: a = gneiss fragments completely or partially pseudomorphed by spinel, b = mineralized gabbro-troctolite fragments, c = sulphides concentrated at the margins of the fragments.



Key to Legend



Plate 2E. DDH-134 at 216.6 m. A weakly mineralized (less than 10% sulphides) conduit gabbro-troctolite with 15-20% of the bulk composition composed of sub-angular fragments. The fragments are not preferentially aligned. Medium-coarse grained, blotchy, net-textured sulphides develop within the matrix, interstitial to the fragments. Legend: a = a gneiss fragment with a feldspar phyrlic core preserving the relict gneissosity, b = a mineralized gabbro-troctolite fragment, c = an aphyric gneiss fragment.

2.2.3.2.2.1 Chilled Textures (CT)

The CT (Plate 2F) defines a sharp reduction in crystal grain size within the conduit gabbro-troctolite rocks. These textures only occur in weakly mineralized sequences with less than 5% disseminated sulphides.

2.2.3.2.2.2 Leopard Textures (LTT)

A leopard texture (Naldrett *et al.*, 1996) is defined as a zone of uniform, interstitial disseminated sulphides with dark silicate spots (Plates 2G and 2H). The silicate spots are composed of three populations: post-sulphide augite oikocrysts (op.cit), syn-sulphide gabbro-troctolite inclusions, and pre-sulphide fragments (i.e. gneiss and gabbro-troctolite).

The oikocrystic spots contain no mineralization and consist of sub-rounded to rounded intergrowths of augite (op.cit.) (Plates 2G and 2H). The mineralized matrix may contain 10–45% net textured sulphides, however, the Leopard texture is best developed when mineralization is greater than 25% (Plates 2H, and 2I) and the spots are well contrasted against the dense sulphides-rich matrix (Plates 2G). When mineralization is 35% or greater, the sulphides can develop into a wavy texture adjacent to the oikocryst margins (Plate 2J). This texture suggests that the oikocryst growth was an event which post-dates sulphide formation. This texture is developed as the growing oikocryst expands, and therefore, pushes sulphides back into the matrix. The process will produce local increases in sulphide concentrations proximal to the rims of the oikocrysts.

The LTT can also host silicate spots that developed through crystallization during, or close to, the timing of sulphide precipitation (Plates 2K). Compositionally these spots are not monomineralic like the oikocrysts (i.e. augite), but alternatively mirror the bulk



Key to Legend

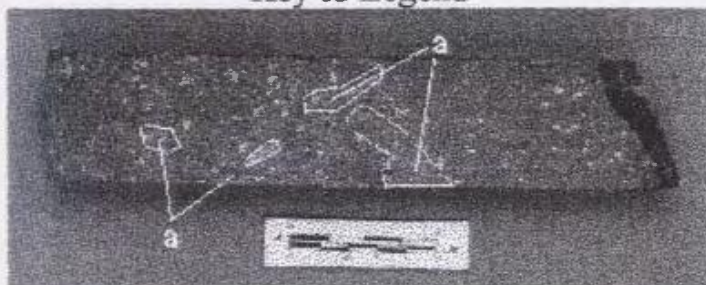


Plate 2F. DDH-141 at 192.0 m. A weakly mineralized (trace-1%) conduit gabbro-troctolite containing no fragments. This sequence is found chilled against the conduit walls or against early (pre-sulphide) gabbros. It displays a homogenous, fine-grained to chilled texture. Zones containing assimilated wall rock are defined by the buff colours, feldspathic-rich patches: a = assimilated wall rock.



Key to Legend

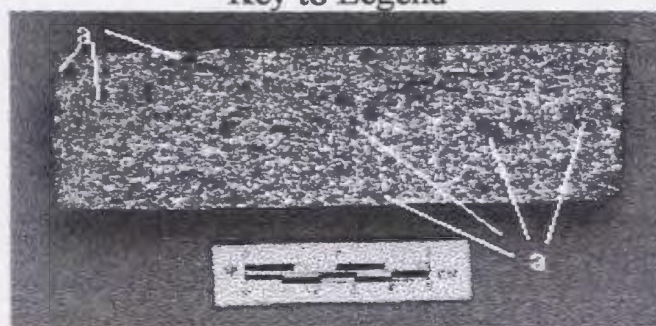


Plate 2G. DDH-117 at 149.4 m. Leopard textured gabbro-troctolite with 40% sulphides found within the conduit environment. Intergrowth of augite (Naldrett et al., 1997) formed within a thick sulphide mat produce dark spots or a Leopard texture. The formation of intergrowths or oikocrysts post-dates sulphide formation and, therefore, they do not contain sulphides. Legend: a = augite intergrowths (oikocrysts).



Key to Legend



Plate 2H. DDH-154 at 166.3 m. A Leopard textured conduit gabbro-troctolite containing 25-30% sulphides. The Leopard texture is produced by augite oikocrysts (Naldrett *et al.*, 1996) intergrown in a sulphide matrix. Oikocryst growth post-dates sulphide formation and, therefore, as the oikocrysts continue to grow they will push sulphides away with their expanding margins. Sulphides will then become more concentrated at the margins of the oikocrysts. Legend: a = oikocrysts, b = sulphides weakly concentrated along the margins of oikocrysts.

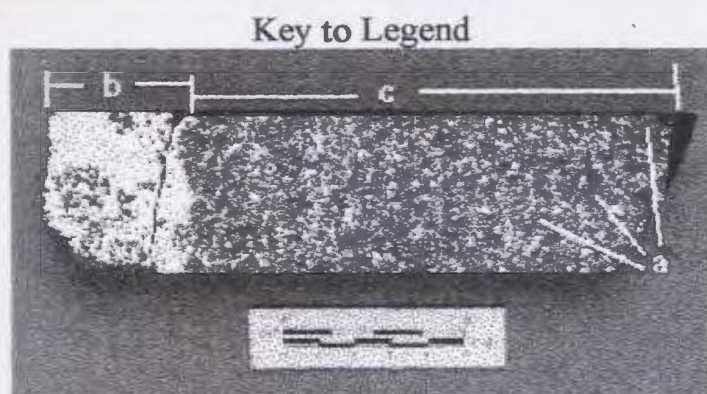


Plate 2I. DDH-140 at 269.8 m. A Leopard textured conduit gabbro-troctolite containing 20% sulphides co-existing (in equilibrium) with semi-massive sulphides. The oikocrysts (dark spots composed of augite, as defined by Naldrett et al., 1997) are not significantly contrasted against the moderate mineralization. Generally, the Leopard texture is best developed where sulphides are greater than 25% of the bulk composition. Legend: a = oikocrysts, b = semi-massive sulphides, and c = Leopard textured sulphides.



Key to Legend

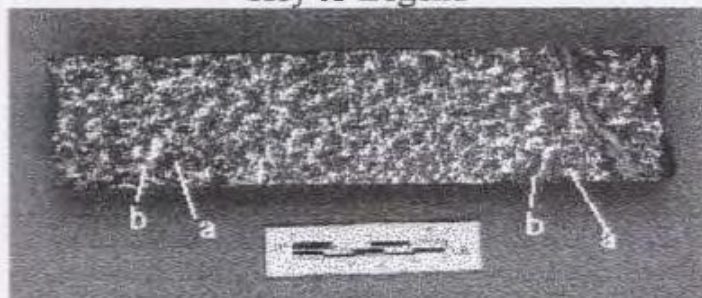


Plate 2J. DDH-191 at 212.4 m. Leopard textured, conduit gabbro-troctolite with 35% sulphides. The oikocrysts or augite intergrowths (Naldrett et al., 1997) will push sulphides aside as they expand. As a result of this process sulphides become concentrated at the margins of the oikocrysts and when multiple margins intersect, a thin (mm scale) wavy lens of sulphide develops. This relationship establishes that the oikocryst growth post-dates sulphide formation. Legend: a = oikocryst, b = wavy lens of concentrated sulphides formed along the margin of the oikocryst.



Key to Legend

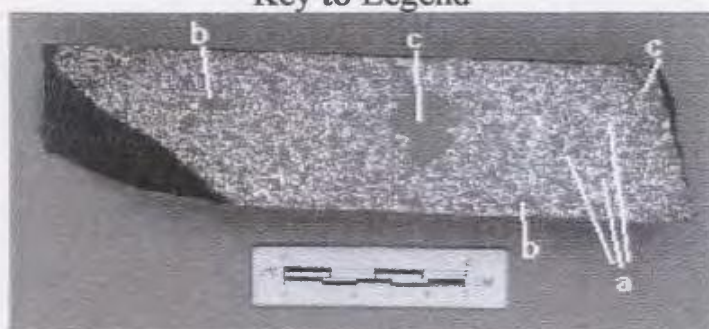


Plate 2K. DDH-199 at 105.2 m. A Leopard textured conduit gabbro-troctolite containing 30% sulphides. The dark spots which produce the Leopard texture are composed of three groups: a = oikocrysts which post-date sulphide formation, b = magmatic crystallization which occurs during sulphide (syn-sulphide) formation, c = mineralized (trace sulphides) gabbro-troctolite fragments.

composition of the magmatic host (i.e. gabbro-troctolite). These spots are diverse in shape. They appear weakly prismatic to globular with irregular margins. Unlike the oikocrysts, these margins do not display elevated sulphide concentrations. Several characteristics separate the oikocrystic spots from those spots formed during early crystallization, these include:

- 1) Oikocrysts developed within the same sequence are generally uniform in size and shape, however the syn-sulphide crystalline spots show extreme diversity in their sizes and shapes.
- 2) The rims of the crystalline spots display a splintery texture (Plate 2K) created by the sulphides as they outline the edges of euhedral crystals. Alternatively, the rims of the oikocrysts appear smoothed, an effect that is produced by the high concentration of sulphides at this site. The oikocrysts contain no mineralization, however, the crystalline spots can host trace sulphides.
- 3) Lastly, the LTT can be produced as sulphides precipitate and enclose fragments (Plates 2A, 2B, 2L, and 2M). The fragmental material can be composed of gneiss or gabbro-troctolite (Plates 2L and 2M), the latter which is interpreted to represent the earliest magmatic phases to be emplaced within the conduit.

The gneiss fragments in general are highly absorbed, and therefore, appear as dark aphyric spots which can easily be mistaken for oikocrysts (Plate 2N). The spotty textures formed by the gneiss fragments can be distinguished from the LTT produced by the original silicate mineralogy by the recognition of two characteristics:



Key to Legend

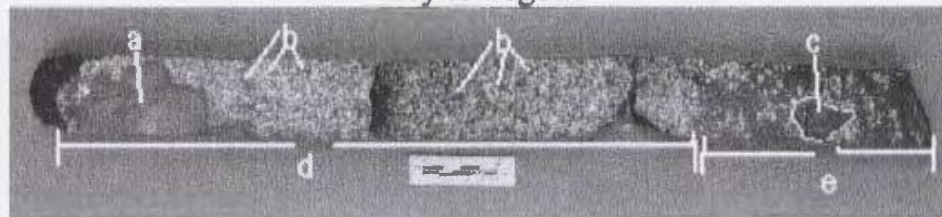


Plate 2L. DDH-191 at 250.0 m. A Leopard textured conduit gabbro-troctolite containing 35-40% sulphides. The Leopard textured sequence contains gneissic fragments and appears to be mingling with early gabbroic-troctolitic magma. The early magmatic material is enclosed by the later sulphide-rich magma (Leopard textured troctolite). Legend: a = gneiss fragment with a feldspar pyritic core and spinel replacement at the rim, b = oikocryst, c = a fragment of early sulphide-poor magma, d = Leopard textured troctolite, e = zone of magma mingling.



Key to Legend

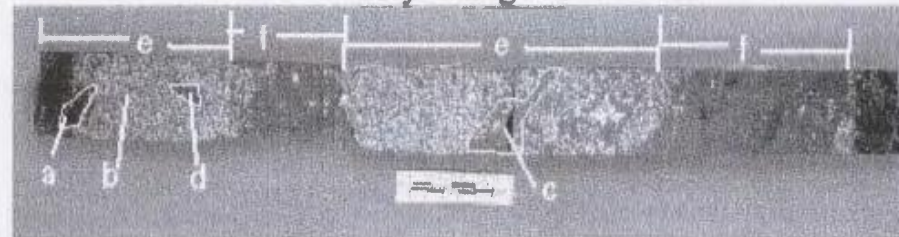


Plate 2M. DDH-155 at 99.7 m. A Leopard textured conduit gabbro-troctolite containing 30% sulphides. The Leopard textured sequence contains gneissic fragments and appears to be mingling with early gabbroic-troctolitic magma. The Leopard textured troctolite inter-fingers the early magmatic material, possibly as a result of the density contrast between the two sequences: a = sub-angular gneiss fragment, b = oikocryst, c = a patch of early sulphide magma, d = a gabbro-troctolite inclusion, e = Leopard textured troctolite, f = zone of magma mingling.



Key to Legend



Plate 2N. DDH-154 at 116.9 m. A Leopard textured conduit gabbro-troctolite containing 35-40% sulphides. The Leopard textured sequence contains gneissic and gabbro-troctolite fragments. a = gneiss fragment with a feldspar pyritic core, b = gabbro-troctolite fragments.

- 1) Uncharacteristic of the true silicate LTT, the fragments are sub-angular in shape and reflect this when outlined by sulphides (plate 2N). Similarly, the gabbro-troctolite fragments are distinguished by their angular margins which are defined by the surrounding mineralization (Plate 2L).
- 2) The fragments are typically aphyric in appearance, however, infrequently, a phyrlic feldspathic core will be preserved (Plates 2L and 2N).

2.2.3.2.3 Breccia Textures (BX)

The expression “Breccia Texture” does not imply structural deformation, but alternatively, is used to describe the processes whereby fragmental material from either gneiss or gabbro-troctolite protoliths was incorporated and transported within conduit magmas (Plates 2A, 2B, 2D, and 2E). A BX textured rock is composed of fragment populations which account for greater than 10% of the bulk composition. Previously these sequences have been termed the Basal Breccia sequence (*BBS*) (Naldrett *et al.*, 1996).

Fragments which have been only recently partitioned in the system will exhibit angular to sub-angular shapes and will not show a large degree of absorption (Plate 2B). Alternatively, those fragments which have been assimilated into the system for a prolonged period will have sub-angular to sub-rounded shapes and will display a high degree of absorption (Plates 2A, 2D, and 2E). Locally, the fragments can develop a preferred orientation (Plates 2A and 2D), in general, however, they sustain random orientations (Plate 2E). The distribution patterns for the fragments are diverse. The fragments can be uniformly dispersed within a broad belt, such that the individual fragments are isolated with no physical contact with adjacent fragments (Plates 2E).

Alternatively, the fragments can be found in dense clusters within narrow horizons (less than 1 m). In this situation fragments can maintain random orientations and be juxtaposed against or in close proximity to each other (Plate 2B and 2D).

BX textured gabbro-troctolites can host 25% sulphides (Plates 2A). The sulphides will be coarse and blotchy when found within the zones that contain a dense population of randomly orientated fragments (Plates 2A and 2E). However, elsewhere in the BX sequence mineralization will occur as fine to medium grained, net textured sulphides (Plates 2D).

2.2.3.2.2.4 Vein Breccia Textures (*Vn Bx*)

The *Vn Bx* reflects textures produced by intrusive and cross-cutting relationships (Plate 2O). The vein material is gabbro-troctolite and is extremely variant in sulphide content (i.e. 25-100% sulphides). The breccia component of this texture indicates the incorporation of fragments which can be of gneiss or gabbro-troctolite compositions, however, no ultramafic fragments are recognized within these sequences. Similar to a dyke, the *Vn Bx* intrudes along geological incompetencies, such as: fractures (Plate 2C), lithological contacts, or along density contrasts (Plate 2M). Frequently, thicker sequences (greater than 5 m) of the *Vn Bx* will intrude and fragment early magmatic material (i.e. gabbro-troctolite) (Plate 2L). The *Vn Bx* sequences will display sharp, vein-like contacts against adjacent media (Plates 2O), however, chill zones are not recognized (Plates 2M). This texture is best developed when the vein material contains semi massive to massive sulphides and it is found intruding weakly mineralized sequences, such as those associated with the CT (Plates 2M), and BX rocks (Plates 2O).

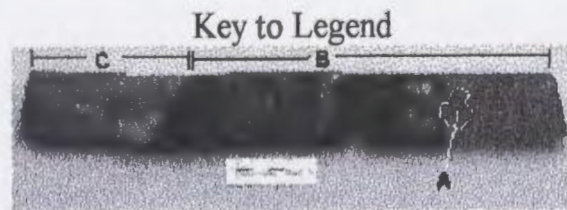
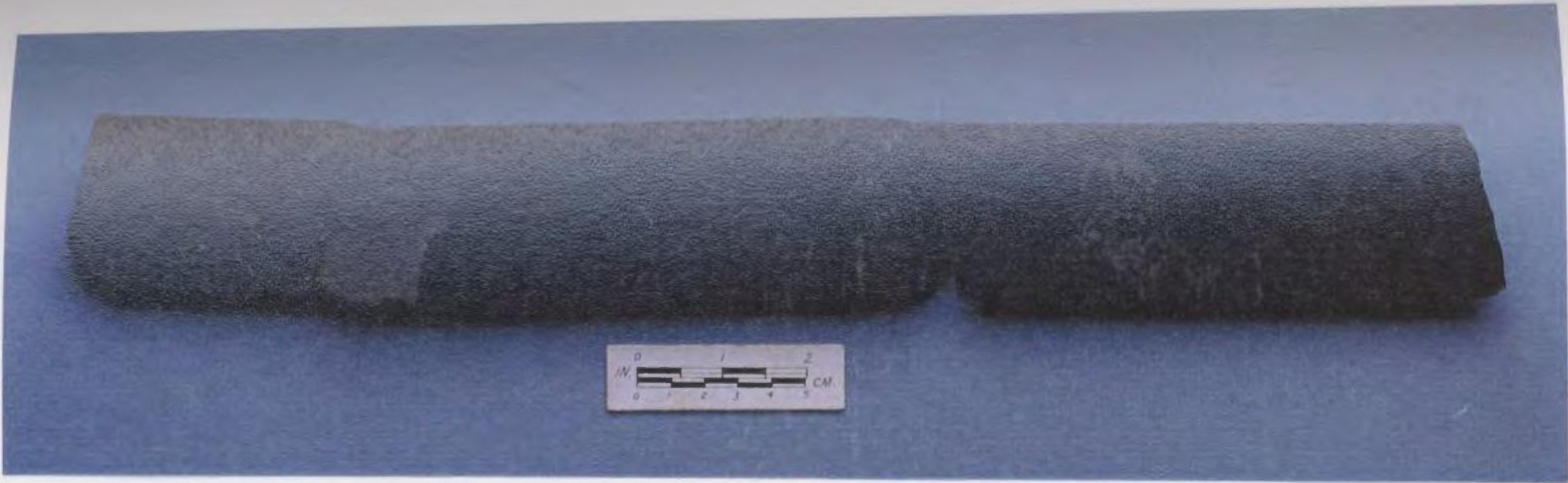


Plate 20. DDH-106 at 24.7 m. A weakly mineralized fragment-poor gabbro-troctolite (breccia) intruded by a massive sulphide vein (Vein Breccia). A = gneiss fragment, b= breccia (BBS), c = massive sulphides.

Chapter 3: An Idealized Geometric Model for a Macroscopic Magmatic Feeder with Multiple Sulphide Traps that may be Analogous to the Voisey's Bay Ni, Cu, Co Deposit.

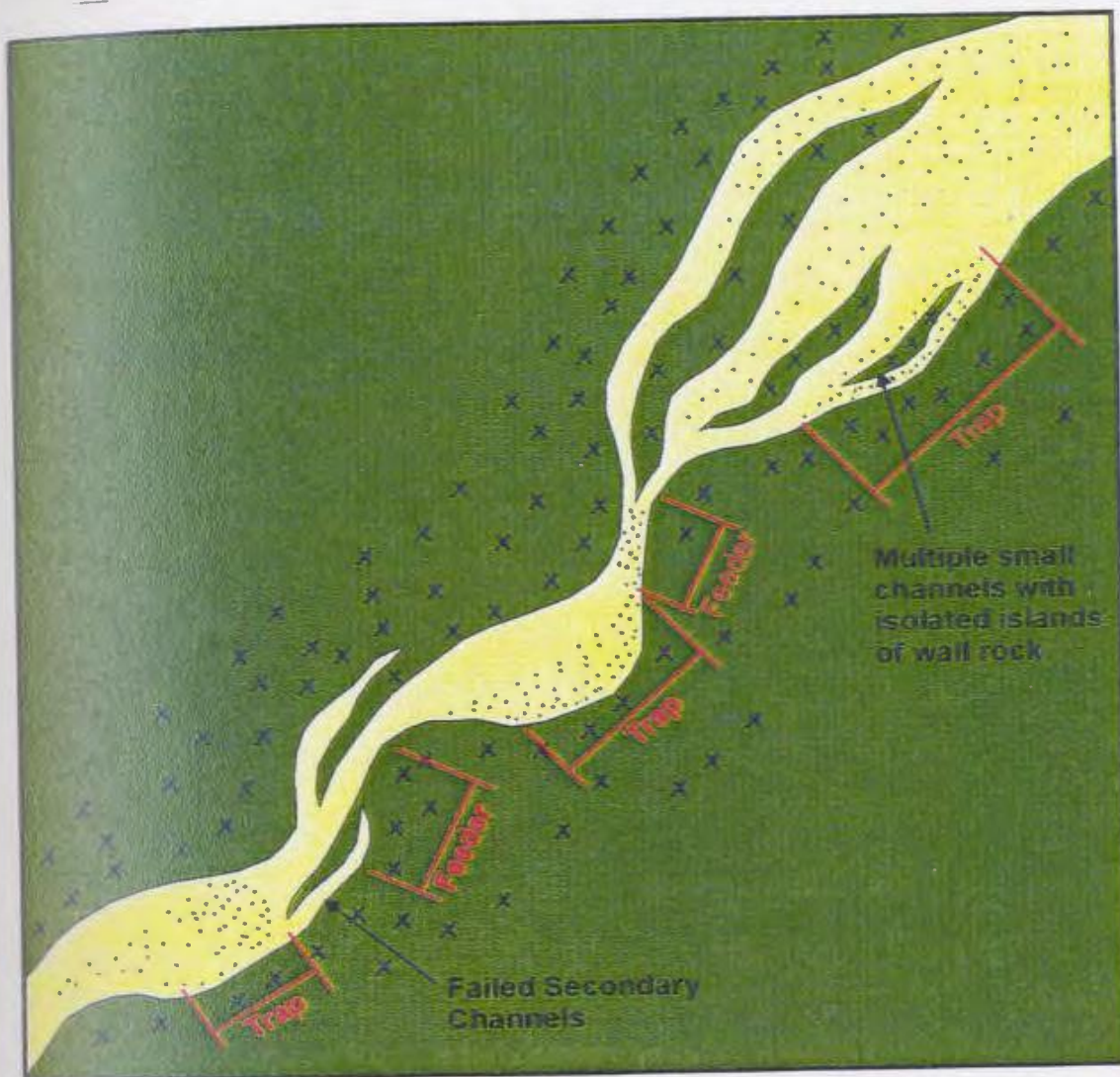
3.0 Introduction:

Geologically the Voisey's Bay deposit does not display simple geometrical relationships nor does it appear to represent a single homogenous, magmatic environment. The Voisey's Bay deposit is a complex magmatic assemblage with distinct geometric and physical characteristics. To understand the unusual distribution of mineralization within the deposit an idealized macroscopic model must be developed that can explain the numerous changes in the local controls on magmatic and sulphide distribution unique to the Voisey's Bay deposit.

3.1 Geometric Attributes

Figure 3.1 is a conceptualized geometric and stratigraphic model for an intrusive magmatic feeder conduit that can be directly applied to the Voisey's Bay system. The proposed paradigm must account for the voluminous accumulation of sulphides and their association with changes in the local magmatic environments as seen at Voisey's Bay.

Where magmatic material is manifested in either a plastic or liquid state, it can contort and conform to nearly endless geometric patterns. Restrictions on the distribution of magma appear to be controlled by the original physiochemical makeup (i.e. silicate rich-wet or silicate poor-dry magmas) of the system, and/ or by changes made to this system. Within a non-stagnant magmatic system, these changes will ultimately be reflected by alterations made to viscosity and velocity of the magma.



Interpreted by DEL

- Magmatic fluid**
- Sulphide Distribution**
- Country Rock**

Figure 3.1 A conceptualized model for an intrusive magmatic feeder. Sites where the conduit expands (i.e. lobe) generally produce effective sulphide traps because they precede or succeed sites where the conduit is narrower. Where the lobe precedes a narrowing of the conduit, viscous sulphide liquid can collect, concentrate and upgrade at the constriction, while the flow of the less viscous silicate liquid will continue since it is not significantly affected by this change in geometry. When a lobe succeeds a constriction, a drop in the confining pressure will aid in the collection, concentration and upgrade of viscous sulphide liquid at the mouth, however, the less viscous silicate liquid will continue to propagate the conduit without significant effects from the change in geometry. Alternatively, sulphides can be collected, concentrated, and upgraded within narrow segments (i.e. feeder domains) in the conduit when changes to the physical or geometric parameters are encountered, these changes can include: a change to the conduit gradient, or choking of the conduit as a dense mesh of fragmental material is collected at a particular site.

3.1.1 Dilatency

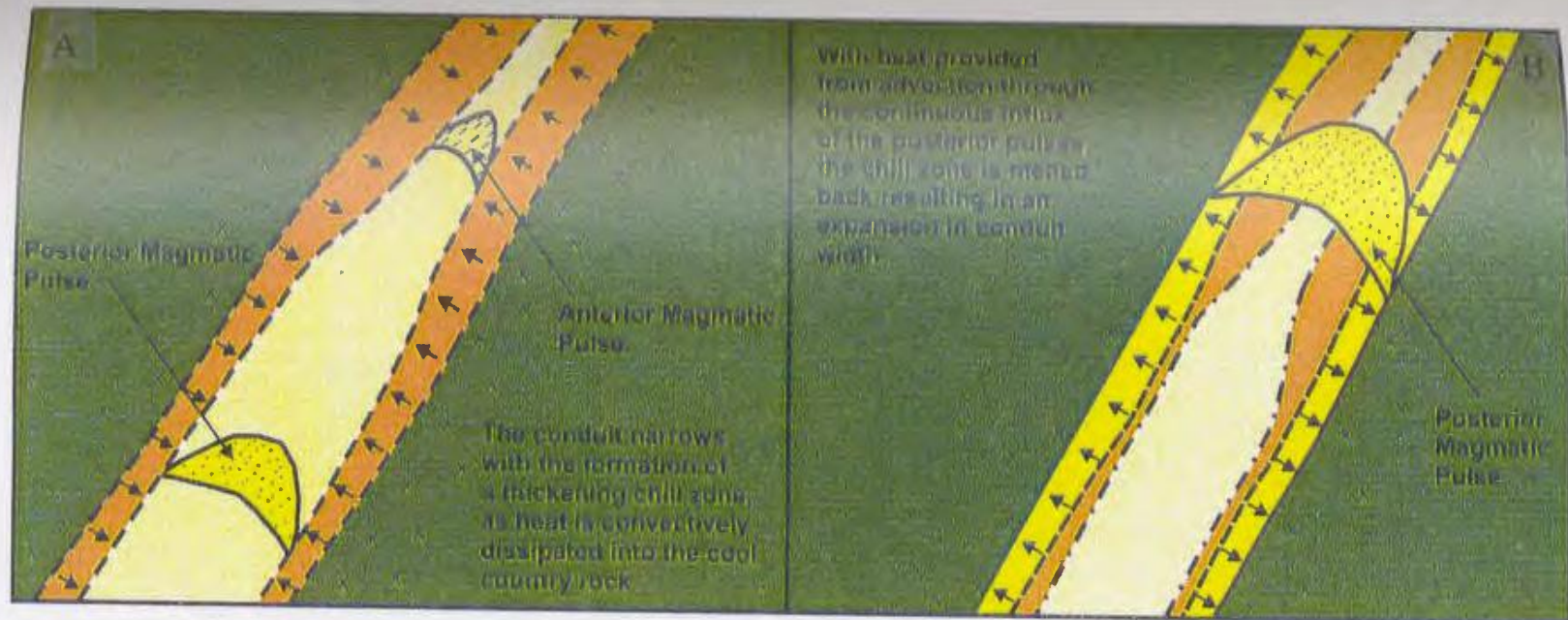
Based on the drill core distributions, the geometry of the magmatic feeder system at Voisey's Bay can be described as a narrow, moderate to steeply inclined, undulating to anastomosing surface with frequent bulbous lobes; these geological domains are termed the feeder and trap (Figure 3.1), respectively. The collective system can be envisioned as being similar to that of a meandering fluid stream. Although this analogy is relevant, it is important to realize that the magmatic fluids ascend up through the system in accordance to the nascent topographic inclination (see below Chapters 5, 8), as opposed to descending in a standard fluvial system

The feeder would operate as a conduit for the migration of magmatic fluids and, with buoyancy as the dominant driving mechanism, the magma will warp, flex and traverse in accordance to the path of least resistance. Such processes have been documented by Bruce and Huppert (1990), Riley and Kohlstedt (1990), and Spence (1990) in fluid experiments evaluating magma flow dynamics. Likewise, Turcotte (1987) indicated that magmatic flows can bifurcate (Figure 3.1) or unite where multiple passages or structural weaknesses separate or coalesce. Once branched, the magma will ordinarily ambulate and conform to the geometric properties, as dictated by each individual path. The magmatic channels or conduits are created by host rock incompetencies. These incompetencies can be manifested as joint, fracture, or fault systems and to a broader extent, regional dominant fabrics, such as gneissosities (cf. Nicolas and Ildéfonse, 1996; Riley and Kohlstedt, 1990). Often, the implicit interaction of multiple weak planes can be recognized within the channelized system and are displayed through frequent and abrupt deviations displayed in the normal trajectory (geometric patterns) of the flow system.

As stated by Turcotte (1990), physical structures such as joints, fractures or faults can cause laminar flow of the magma stream. The fluids at the leading edge of a magmatic surge rapidly transgress through the system with only minimal stoping and assimilation of the wall rock material. The rapid and constant flux of magma will reduce the effects of convective heat loss to the country rock, as documented by Turcotte (1990), Bruce and Huppert (1990), and Spence and Turcotte (1990). Solidification processes will be counteracted by thermal advection and subsequent melt back, produced by the voluminous and continuous discharge of magma through the system (e.g. Bruce and Huppert, 1990; Turcotte, 1990) (Figure 3.2). With the constant exchange of heat, no substantial alterations in viscosity, and hence velocity, of the magma will result. With only minimal disruption to flow, vast volumes of magma can pump through dilational networks over relatively short periods of time.

Alternatively, in the study of non-dilational systems, such as those produced by gneissosity, Turcotte (1990), and Spence and Turcotte (1990) speculate that a plasmic material (i.e. magma) can ascend through the development of propagation or hydraulic fractures. In such a model the magmatic fluid will inject and traverse the wall rock along the less resistant fabric plane. The country rock will be assimilated or stoped, resulting in the detachment and inclusion of wall rock blocks into the magma. An analogy can be made with a corrosive fluid introduced into a plumbing system, whereby the liquid will penetrate, partition, enclave or assimilate foreign material as it is encountered.

Without a continued influx of new magmatic fluid, the system can quickly reach limits to wall rock assimilation. Heat can convectively dissipate through the cooler wall rock as shown by Turcotte (1990), Bruce and Huppert (1990), and Spence and Turcotte



Modified by DEL

- - - Conduit width after the formation of chill zones
- Original conduit margins
- Melt back margins



Convection



Advection



Country Rock



Anterior, Sulphide Poor Magma



Posterior, Sulphide Rich Magma



Intermediate Magma within Pulse

Figure 3.2 Adapted from Bruce and Huppert, 1990.

Within a dilational system a single continuous surge of magma can be divided into two or more pulses, in example: the anterior pulse, and the posterior pulse. The rate at which these pulses are dispatched through the conduit will effect the growth or collapse of the conduit. (A) The anterior or first pulse expelled through the system will actively dissipate heat (i.e. convection) to the wall rocks. With a continuous loss of heat the chill zone will expand inwards. If the posterior or second pulse is not provided fast enough or lacks the volume to provide an adequate replenishment of heat to the system, it will also lose heat to the wall rock, until there is no further transfer of magma (i.e. the conduit is totally solidified). (B) Alternatively, if the surge provides a rapid transfer of magma the posterior pulse can provide the heat (i.e. advection) required sustain effective flow rates (i.e. heat transfer) to melt-back the chill zones and increase the conduit width. The increased width will permit the transfer of larger volumes of magma which will contribute more heat to the system and expand, once again, the conduit width.

(1990), or be absorbed by the trapped fragments as suggested by Maury and Dider (1991). Furthermore, if the viscosity of the magma is increased through heat dissipation, Riley and Kohlstedt (1990) predict that a correlative reduction to the current velocity will occur. If the magma is sufficiently slowed and cooled, it can then begin to nucleate and crystallize.

In comparison to a dilational system, a non-dilational system will result in the slower transgression of magma, since the digestion of peripheral material is a continuous process. The affects of assimilation, however, can be reduced if fresh, co-genetic magma is introduced into the system. The persistent introduction of fresh magma will replenish the system thermally, reducing the affects of heat loss due to both assimilation and formation of chill margins against the country rock (Figure 3.2). Once established, a chill zone may assist in reducing heat loss to the surrounding wall rock. For instance, Bruce and Huppert (1990) suggest that a chill margin can provide an intermediate thermal barrier between the cool country rock and the hot magma, whereby the hot magma is focused into the high velocity core of the conduit where advection processes can dominate. Furthermore, by lining the conduit walls, the chill margins smooth surface irregularities and assist in the establishment of laminar flow. In contrast, if the surface irregularities are not removed, the flow will remain turbulent and the processes of assimilation can be favored where heat can be dissipated through convection (c.f. Bruce and Huppert, 1990).

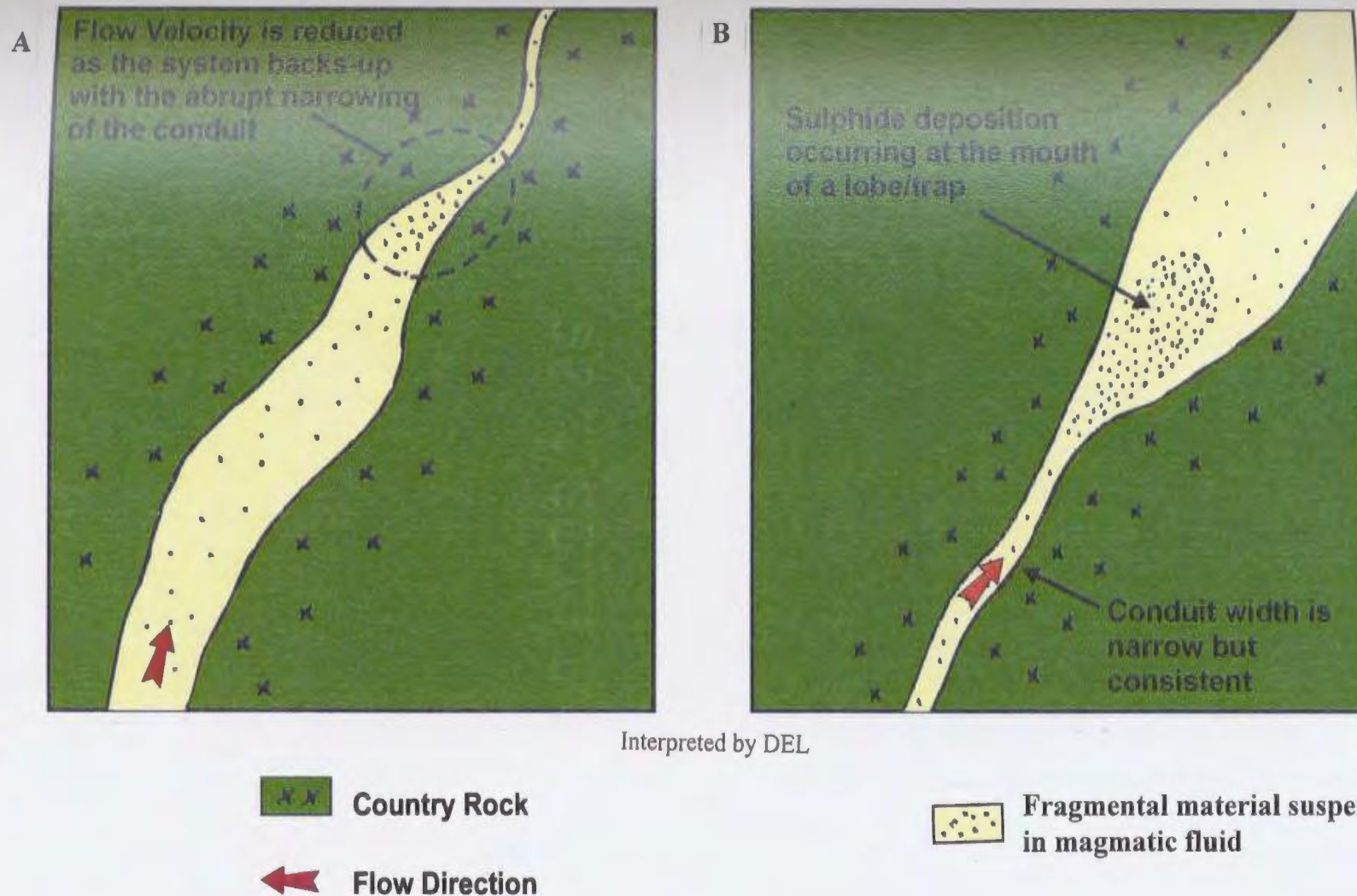
3.1.2 Dyke Necking

Experiments by Bruce and Huppert (1990) indicate that if a conduit abruptly narrows, the rate of magma transfer (i.e. velocity) would be decreased (Figure 3.3). This

process would result in the congestion of viscous magma near the tapered zone and permit a longer contact time for which the magma and wall rock can interact. In addition, wall rock interaction can be favored if the magmatic flow is turbulent upon encountering a constriction (Figure 3.1) (cf. Whitehead and Helfrich, 1990), and furthermore, as stated by Bruce and Huppert (1990), the magmatic fluid can begin to meander (i.e. cross flow) and bifurcate along subordinate passages. These processes can result in the solidification of the magma as substantial changes to the viscosity and the velocity of the magma are made.

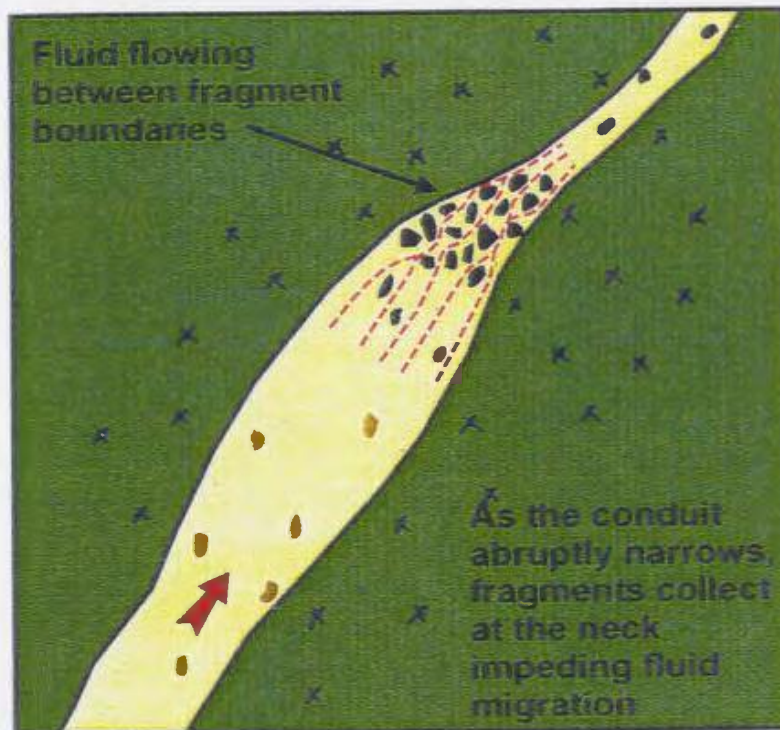
Furthermore, Maury and Dider (1991), and Nicolas and Ildefonse (1996) speculate that when a large bulk volume of wall rock material has been fragmented into the magmatic liquid, the mobility/viscosity of the magma and subsequent intrusive geometry will be greatly affected in zones where the conduit tapers. If the fragments have been completely assimilated, physiochemical changes, such as becoming water-rich, reduce the viscosity of the magma and aid in the dynamics of fluid flow. Alternatively if not completely assimilated, the dense concentration of enclosed fragments can clog and encumber the progression of the magma as it tries to navigate through a constricted conduit (Figure 3.4). In the latter case, immediate magmatic solutions can become stagnant and begin to solidification, or alternatively, resume flow if the fragments become aligned with the magmatic flow (e.g. Arbaret *et al.*, 1996; Nicolas and Ildefonse, 1996) (Figure 3.5).

Similar processes are documented within the studies of porous flow in magmatic systems by Riley and Kohlstedt (1990). Riley and Kohlstedt suggest that magmatic fluids must flow with force sufficient enough to either initiate melting at fragment boundaries and allow magma to successfully squeeze through the solidified magma-fragment mesh or,



Interpreted by DEL

Figure 3.3 The effects of geometric changes to the conduit on the sulphide-bearing silicate magma. (A) Narrowing of the conduit: the sulphide liquid is more viscous than the silicate liquid, therefore, when the magma encounters a region where the conduit is pinched, the sulphide liquid can collect at the constriction. As the silicate magma continues to flow past this site, the sulphide liquid can become concentrated and scavenge more chalcophile elements upgrading its Ni tenor. (B) An expansion in conduit width: with a reduction to the confining pressure on the magma, the viscous sulphide liquid will collect at the mouth of the opening while the silicate liquid continues to navigate the conduit. As magma continues to pump through this site, the sulphide liquid can become concentrated and up-graded in chalcophile elements.



Drawn by VBNC





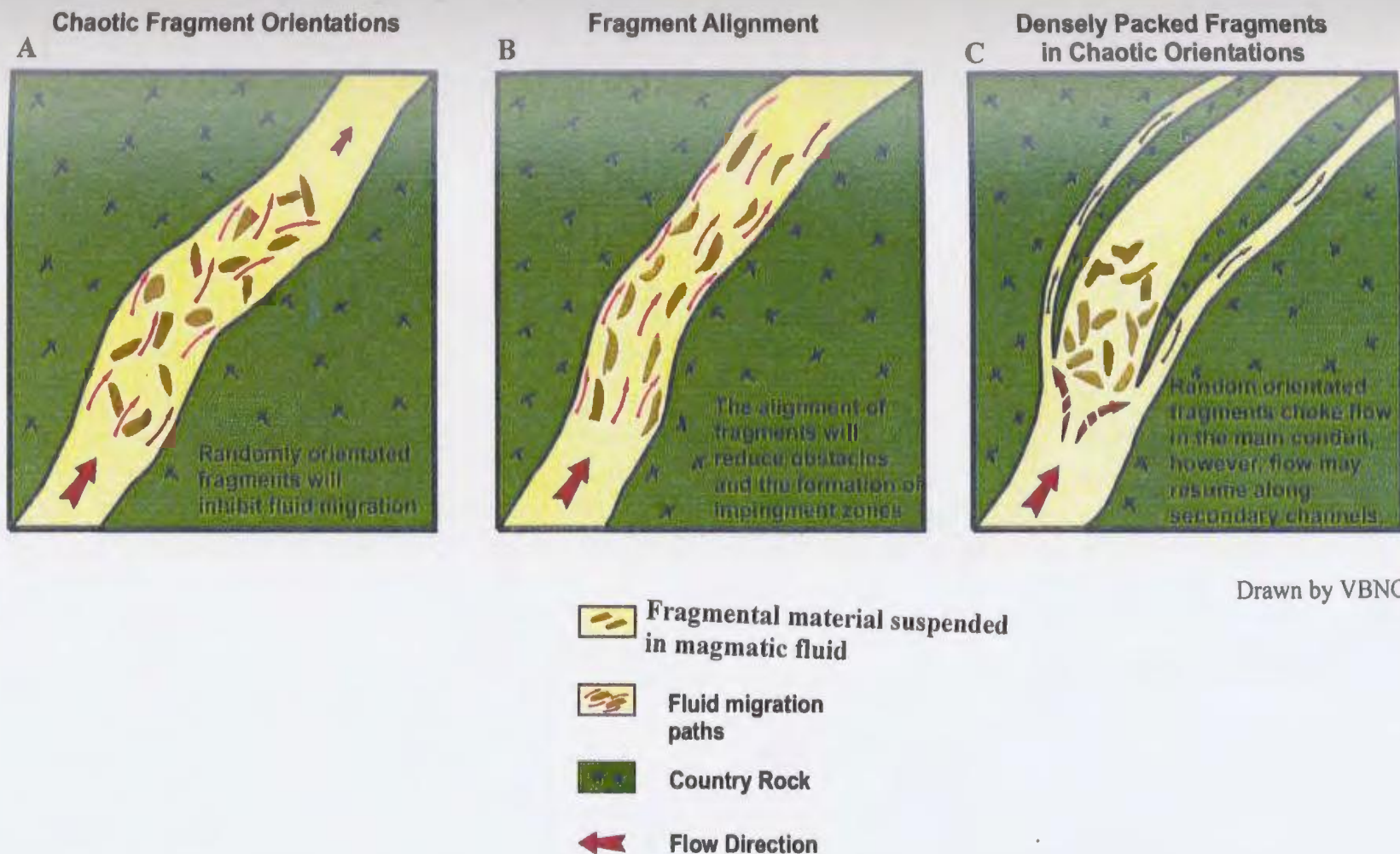
-  Fragmental material suspended in magmatic fluid
-  Fluid migration through pore spaces between fragments
-  Country Rock
-  Flow Direction

Figure 3.4 If the conduit abruptly narrows, fragmental material within the magma can form a blockage at the constriction and collect more fragmental material as it tries to navigate through this site. As a further consequence, viscous sulphide liquid can plate and concentrate against the fragmental mesh while the less viscous silicate liquid can squeeze through the fragmental matrix and continue to propagate through the conduit. With the continued transfer of silicate magma, the sulphide liquid can scavenge chalcophile elements, and therefore, upgrade its Ni tenor.



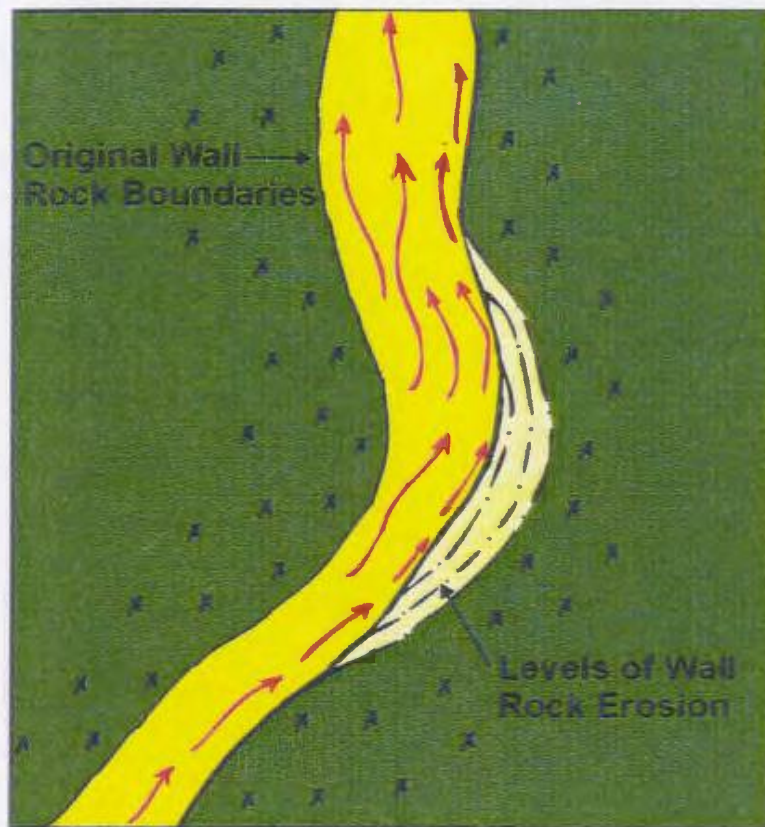
Drawn by VBNC

Figure 3.5 The flow of magma will be affected by the distribution of fragmental material within the magma. (A) When fragmental material is not preferentially aligned within the magmatic flow, the rate of magma transfer is reduced. Fragments will form a complex mesh that will collect and concentrate sulphide liquid, and as well, impede the flow of the silicate magma. (B) If the fragments are preferentially aligned with the magmatic flow (i.e. streamlined), then the magmatic transfer will continue with little disruption. (C) If the fragments are not aligned (see A) and fragment-bearing magma continues to flow through the conduit, the fragments can collect and become concentrated forming an dense, impermeable mesh. This blockage can act as a trap for the collection, concentration and upgrade of the sulphide liquid while, alternatively, the less viscous silicate magma can exploit narrow discontinuities in the wall rock and continue with the magmatic transfer/flow.

If the magma does not reestablish mobility and solidification begins, the complete package (magma and fragments) may not remain in situ, but can be enclaved and redistributed through the transgression of later magmatic pulses. For example, when subjected to a later pulse of high velocity and low viscosity magma, the earlier material in a semi-solid to solid state can be brecciated and enclaved into the new pulse. Whitehead and Helfrich (1990) suggest that if the first magma pulse remains in a liquid state, mixing will occur as the two fluids engage. The composition of the new, mixed magma can result in velocity and viscosity changes favorable to the continued propagation of both the early and later magmatic pulses, or alternatively, produce changes which can impede the propagation of both magmas.

3.1.3 Dyke Expansion

Rapid expansion of a conduit can be caused by three physical parameters; flexuring, primary dilation, and inclination. Flexures encountered along the flow channel can result in the accumulation of viscous fluid, subsequently this can cause a prolonged period of contact between the hot magma fluids and the wall rock. This interaction can result in extensive assimilation of the wall rock, and therefore, can produce an expansion of the conduit width (Figure 3.6). The fluid dynamics involved with such a process can be compared to those established within a meandering river system. The inner arc will act as an obstacle, reducing magmatic transfer through this zone and concentrating the most viscous fluids. Turbulence within the magmatic flow and the rate at which it is transferred increases proximal to the outer arc, this activity will, therefore, favor the injection (i.e. stoping) and fragmentation of the adjacent country rock. The erosion (i.e. assimilation) of



Interpreted by DEL




-  **Assimilation of the Outer Arc**
-  **Fluid Trajectory**
-  **Country Rock**

Figure 3.6 A change in the gradient or an inflection in the conduit can affect magmatic flow. Flow adjacent to the outer arc will be of a higher velocity than that which flows next to the inner arc. As a result of this flow segregation, viscous sulphide liquid will preferentially collect along the inner arc. With continued magmatic transfer the sulphide liquid can become concentrated at this site, and as well, can potentially scavenge chalcophile elements causing an upgrade to its Ni tenor. The outer arc will have the fastest magma transfer, and hence, the most heat transfer; therefore, the conduit width can be expanded through assimilation of the wall rock along this margin. In addition, if magma transfer is sufficient enough to result in the totally assimilation of the wall rock fragments the silicate magma can become wet; the resulting decrease in the viscosity of the silicate magma can assist in increasing the magmatic transfer.

the outer margin will result in an overall expansion in conduit width (Figure 3.6). However, as documented by Bruce and Huppert, (1990) and Turcotte (1990), a continuous and rapid influx of new magma (i.e. high transfer rates) is required for the initiation of these processes. If there is not a sufficient rate of magma transfer, substantial heat will be diverted to the wall rock by the initial assimilation activity, as consequence. the transgression of the system will slow and possibly reach the state of static solidification.

Dilational features encountered in the path of the developing conduit will result in a natural bloating or swelling of the system. These features can be enlarged and amplified as the system continues to develop. Dilational structures encountered in course, can produce a drop in hydraulic pressure (cf. Scarfe *et al.*, 1987). This process will result in the accumulation of the most viscous fluids near the mouth of the lobe. With the progressive influx of new magma into this site, the viscous fluids can continue to collect and concentrate. In addition, the volumous accumulation of magma and the replenishment from the influx of new magma will result in the intense assimilation of the wall rock Turcotte (1990).

A final scenario for the abrupt expansion in conduit width involves a change in topographic gradient. If the conduit evolves from a shallow dipping to a steeply dipping system, there will be an intermediate zone where the magmatic flow is disrupted and slowed along its ascent. As the most viscous magmas collect at this impediment, assimilation processes can be initiated, and with the continuous influx of magmatic fluids (i.e. magmatic transfer) the system can continue to further assimilate and erode the conduit walls, as broadly suggested by Turcotte (op. cit. 1990), and Bruce and Huppert (1990).

Also in this situation, a fraction of the magma can deviate and inject along subordinate microstructures resulting in a wide braided channel with isolated islands of wall rock (Figure 3.1).

3.2 Formation of Sulphide Traps

A sulphide trap can be described as any particular zone in which physical changes in the local or surrounding environments cause the collection and retention of sulphides. The catalyst for such events can be highly variable, ranging from changes in the physical environment hosting the magma, to internal physiochemical changes within the magmatic fluid. Often a change initiated by a single parameter can trigger a chain of multiple reactions among the remaining parameters. This evolved network of dependent parameters can be of a complex and ephemeral nature.

Although sulphide traps are dominantly coincident with regions of conduit expansion (i.e. trap), this is not a pre-requisite for sulphide deposition (Figures 3.1 and 3.3). In other words, the physical properties that regulate conduit swelling, can prove advantageous to the accumulation and collection of sulphides, but do not always guarantee their success. Conversely, the change in geometric parameters may favor sulphide accumulation, but may not contribute to conduit expansion (i.e. feeder).

The physical parameters that contribute to the deposition of sulphides in conduit lobes include flexuring, dilation and inclination. When the magmatic fluid encounters a flexure or an inflection point, flow can be segregated into high and low velocity zones. The highest velocities occur along the outer arc of the flexure, therefore, magmatic transfer will be rapid in this zone. Lower flow velocities occurring adjacent to the inner arc of the

flexure, will assist in the collection of viscous sulphide liquid. With the continued transfer of silicate magma, from both the high and low velocity zones, the sulphide liquid can become concentrated and significantly upgraded as it scavenges chalcophile elements from the passing magma. This process of Ni upgrading can be enhanced if there is wall rock assimilation along the outer arc. If the wall rock fragments are totally absorbed the silicate magma will become wet, the subsequent decrease in viscosity will permit faster magmatic transfer. This process can increase the volume of silicate magma which can come in contact with the sulphide liquid, and therefore, can potentially increase the amount of chalcophile elements scavenged from the magma. Also, the shallow limb of the conduit can contribute to sulphide capture; this structure can provide a ledge on which sulphides can collect and concentrate once they begin to precipitate and gravity settle from the liquid (Figure 3.1).

Dilational structures can provide a mechanism which lobes are built in the conduit, and as well, provide a medium for sulphide deposition. When the magmatic fluid is expelled from a narrow laterally constrained feeder into a dilational cavity, a drop in hydraulic pressure will occur (Scarf *et al.*, 1987), and as a result, viscous sulphide liquid can preferential collect at this site. As the magmatic transfer continues, the sulphide liquid can be concentrated and upgraded as it interacts with more silicate magma as it propagates pass this site (Figure 3.3).

Conversely, sulphides can also be preferentially concentrated at sites where the conduit pinches. If fragmental debris chokes the conduit at the constriction, the viscous sulphide liquid can collect and plate against the dense mesh formed by the fragments. The less viscous silicate liquid, however, may be able to navigate the fragmental mesh allowing

for continued magmatic transfer. Once again, the sulphide liquid can be exposed to large volumes of silicate magma from which more sulphide liquid can be collected and from which greater concentrations of chalcophile elements can be scavenged (Figure 3.4). Furthermore, if there is no fragmental material to choke the constricted conduit, sulphide liquid can still preferentially concentrate at this site if the constriction is great enough to disrupt its continued propagation (Figure 3.3).

A sulphide trap can also develop at a site where an increase in topographic inclination is encountered. The magmatic flow will be disrupted through a momentary stagnation, or a reduction in the flow velocity. Viscous sulphide liquid can preferentially linger at this site and with a continuous transfer of silicate magma through this site, the sulphide liquid can potentially become concentrated and upgraded in its Ni tenor.

Modifications to the local environment will contribute substantially to the amalgamation and distribution of sulphides. The above mentioned geometric controls may result in the collection and concentration of sulphide liquid or precipitated sulphides, however, subsequent secondary environmental properties can affect their final distribution. Sulphides in the leading magmatic fluid can accumulate in numerous favorable geometrical zones, but can later be redistributed by trailing/late magmatic pulses. When an obstacle traps an early sulphide-bearing magma pulse, the pulse can be brecciated and enclaved by a later magmatic pulse. The secondary/late pulse may conquer the obstacle that initially trapped the early pulse, but may itself encounter a later barrier. Under such circumstances, sulphides at this site may be distributed through two separate magmatic pulses.

In other circumstances, inflections and changes in the conduit gradient may not be intense enough to initiate changes in conduit width, but may be significant enough to

hamper the transportation and propagation of heavy sulphide liquids. If the flow is momentarily delayed by such features, a small fraction of the sulphide liquid can accumulate at this site. This small, but viscous body can act as a sieve, capturing and accumulating more sulphide liquid as silicate magma continues to flow past this zone (Figure 3.4).

Numerous physiochemical changes influence the collection and concentration of sulphides within magmatic feeder conduit. However, these physiochemical changes are induced through physical and geometric change made to the conduit. When interpreting or predicting the occurrence of sulphide traps it is, therefore, essential to obtain thorough knowledge of the conduit morphology.

Chapter 4: Geological and Environmental Characteristics of the Ovoid

4.0 Introduction

In terms of mining, the geological properties of the Ovoid ore body provide an ideally perfect model for the extraction of base metal wealth. For exploration the Ovoid is an unique and complex geological structure that if resolved, can lead to further discoveries of mineral resources, both locally and globally. Based on initial examination, the simplistic relationships displayed between the geometry and the lithologies of the Ovoid are deceiving. Masked are the complex and intricate genetic linkages that existed between the Ovoid and the macroscopic magmatic system. It is one of the numerous geological and structural elements that comprise the Voisey's Bay magnetic Ni sulphide system and therefore conforms to larger scale geometric and magmatic constraints. The Ovoid appears to be a focal point within the magmatic sulphide system, as can be interpreted from its central location and vast accumulation of massive sulphides. The Ovoid is contained within a magmatic conduit system that is continuous from west to east, and at depth (see below). The Ovoid is, therefore, produced within a complex magmatic network with intricate geological relationships. New sulphide traps have the potential to be discovered within the Voisey's Bay magmatic system, if the geological relationships documented at the Ovoid can be interpreted and extrapolated to the larger scale system.

4.1 Geometry

In a crude but accurate analogy, the Ovoid was compared in shape to that of a wine glass tilted on its side (Diamond Fields Resources, Report from Voisey's Bay,

04/1995). As defined by over 100 drill holes (Figure 4.1), the Ovoid is an oval body with oblate to weakly tapered poles in the x, y and z directions. Although confined in spatial terms, the Ovoid is actually part of an open magmatic system and specifically acts as a continuum between adjacent sulphide-bearing domains (see below). The Ovoid has frequently been characterized as a closed magmatic system which represents the base of a large magmatic chamber (i.e. Eastern Deeps chamber, see Chapter 2) (Naldrett *et al.*, 1996). Interpretations have even stretched to compare the Ovoid to Naldrett's (1997) Noril'sk model, suggesting that the Ovoid system was closed prior to the deposition and concentration of sulphides (i.e. gravitational settling of sulphides), with little to no external magmatic influences after this event.

In UTM coordinates, the Ovoid extends laterally from 555650E to 556120E (Figure 4.1). The long axis of this oval body trends obliquely at 129°. The northern margin extends to 6243420N, while the most southern edge is situated at 6242610N (Figure 4.1). Perpendicular to the axial trend, the widest part of the body reaches 260m, as is displayed by the west facing, geological cross-sections through L14+00E and L15+00E (Figures 4.2 and 4.3). The depth of the Ovoid, below the bedrock interface, varies from a minimum of 20 meters at the margins (Figure 4.3) to a maximum of 120 meters at the center (Figure 4.3).

Grossly, the Ovoid appears geometrically symmetrical, but distinct asymmetrical features can be documented on a mesoscopic scale. The eastern margin of the Ovoid is oblate and sharply tapered, to the west this tapering is less explicit and is recognized only through a weak reduction in the width of the body (Figure 4.4). The designation of the

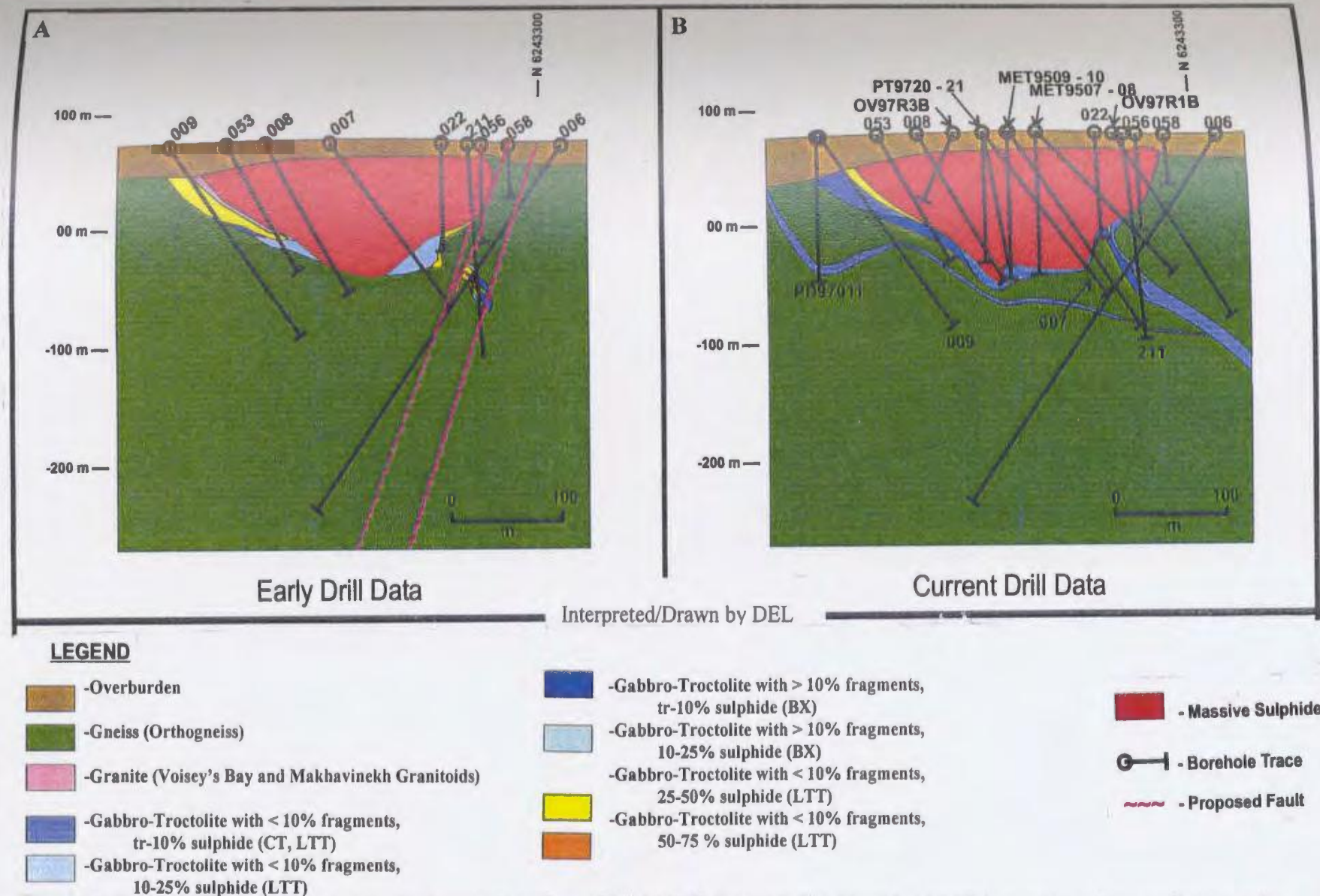


Figure 4.2 A West-facing geological cross-section of L14+00E through the Ovoid. (A) This cross-section reflects early interpretations whereby, mineralized troctolite intersected below the north margin of the Ovoid were thought to be down-faulted blocks from the north margin of the Ovoid. (B) Currently, the mineralized troctolite intersected beneath the north margin of the Ovoid is interpreted to be part of the feeder conduit which hosts the Discovery Hill and Western Extension mineralized zones to the West. In addition, narrow intersections of weakly mineralized gabbro-troctolite that form a horizon coplanar with the footwall are thought to be a secondary splay from the feeder conduit. This splay could have intersected the Ovoid above the current levels of erosion.

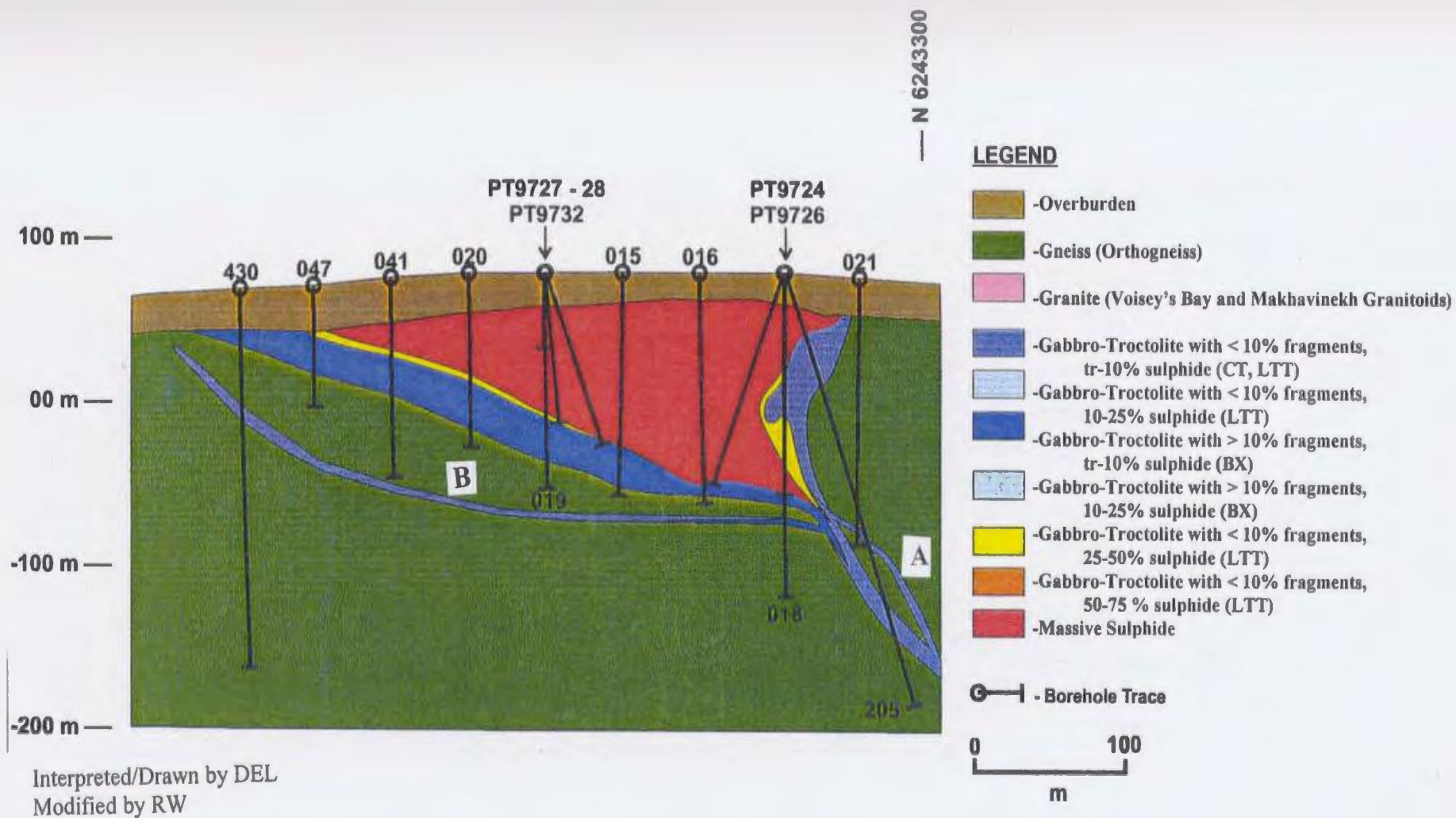
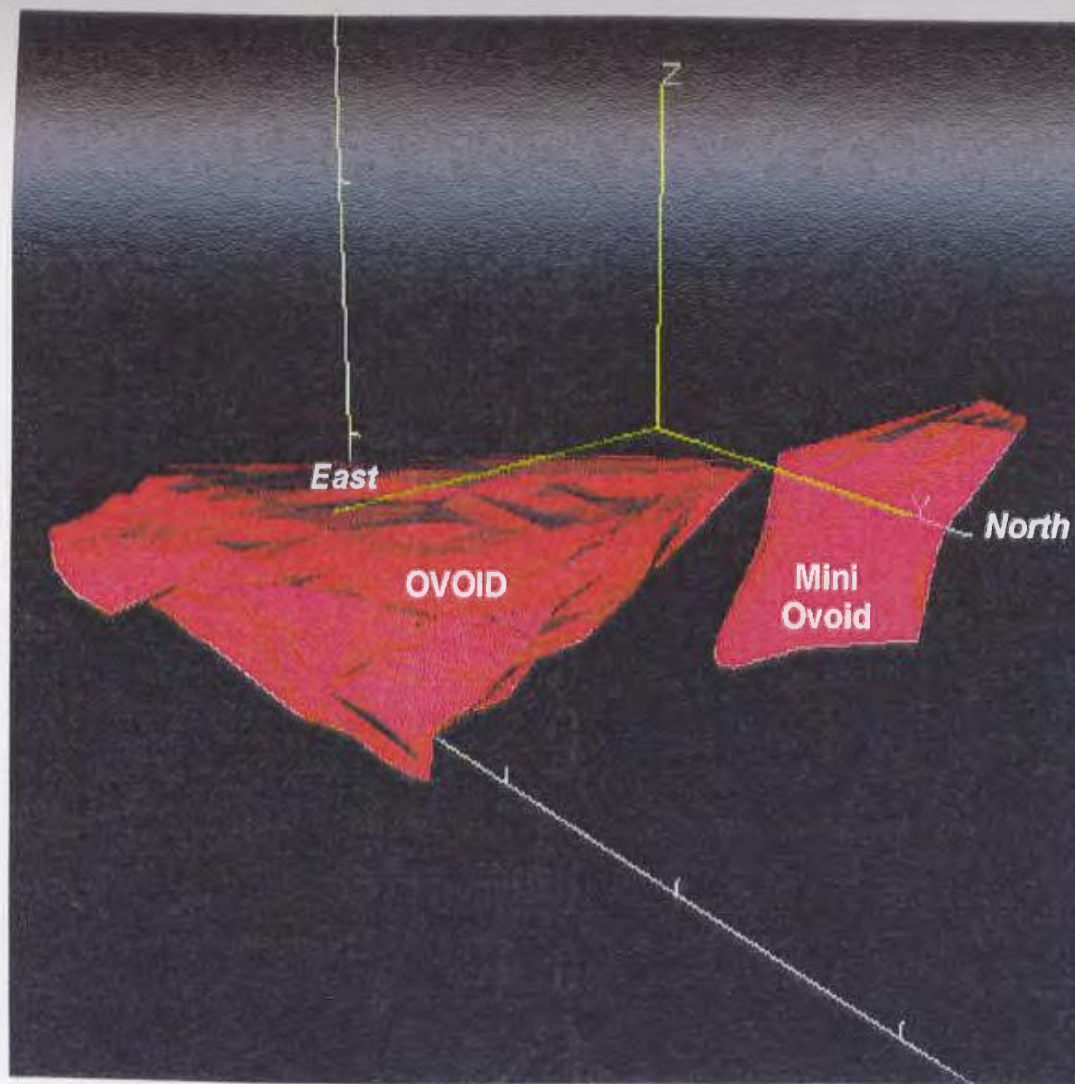


Figure 4.3 A west-facing geological cross-section of L15+00E through the Ovoid. (A) The feeder conduit beneath the north margin of the Ovoid. (B) A splay from the feeder conduit which mimics the geometry of the south margin of the Ovoid.



Interpreted/Drawn by DEL/RW

Figure 4.4 A three-dimensional model for the massive sulphide in the Ovoid and Mini-Ovoid. The massive sulphides contained within the Mini-Ovoid are not continuous with those found in the Ovoid and, furthermore, appear to plunge beneath the Ovoid. Although both mineralized zones appear to be at the same topographic level, the Ovoid is interpreted to be stratigraphically higher than the Mini-Ovoid.

southern margin of the Ovoid is not exact and is based upon geophysical and limited drill data, therefore, it is an approximation and by no means a defined or delineated surface. As it is interpreted, the boundary is a sharp, gently inclined, concave surface with the plane of best fit dipping at approximately 25° to the northeast (Figures 4.2 and 4.3). The north edge of the Ovoid is more abrupt and is represented by a steep, sub-vertical wall (Figures 4.3 and 4.5). The Ovoid tapers to both the east and west, at these sites the south walls dip shallowly to the northeast (Figures 4.2 and 4.6), while the north walls dip moderately at 45 ° to the south.

The original surface geometry of the Ovoid is idealized since physical documentation is restricted by the present level of erosion. Locally, however, narrow chill sequences remain preserved at this interface which are thought to represent the upper margin (i.e. cover sequence) of the Ovoid (Figure 4.5). Here the data are limited, but do reflect an original domed-shaped surface for the upper margin of the Ovoid. The footwall contact is interpreted from drilling data obtained at 50 m spacings as a gently undulating surface. Geometric detail provided by the metallurgic drilling program (25 m drill centers), however, establish these surface irregularities as significant features with large amplitudes (i.e. up to 30 m) (Figure 4.6). It is apparent that the footwall interface expresses microscopic to mesoscopic irregularities which become smoothed and negligible on the macroscopic scale.

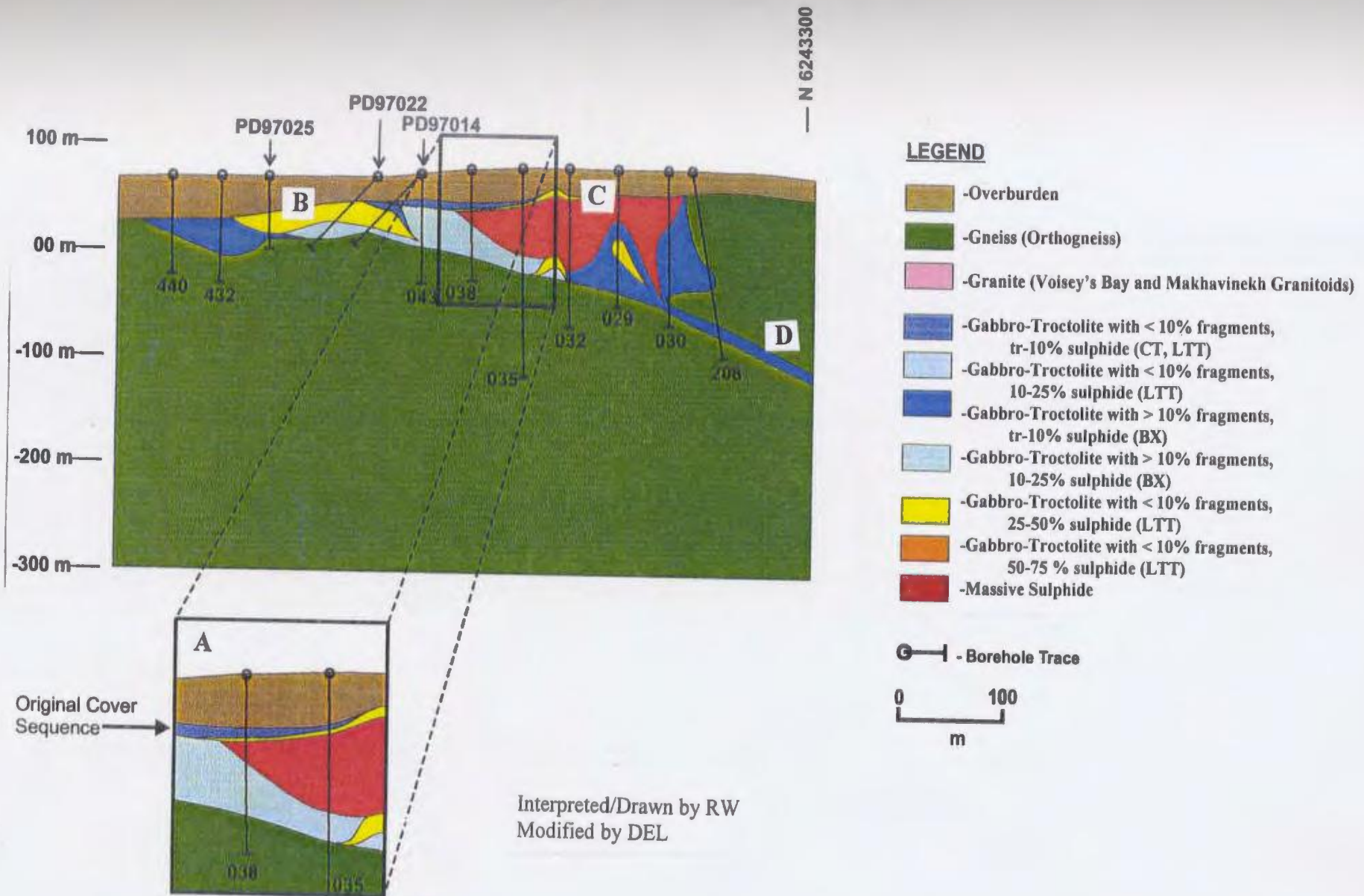


Figure 4.5 A west-facing geological cross-section of L15+50E through the Ovoid. (A) This inset shows a stratified horizon of CT gabbro above LTT gabbros-troctolites and massive sulphides. The CT rocks are interpreted to represent the cover or top of the Ovoid. (B) The Eastern Deeps chamber. (C) The Ovoid. (D) A feeder conduit.

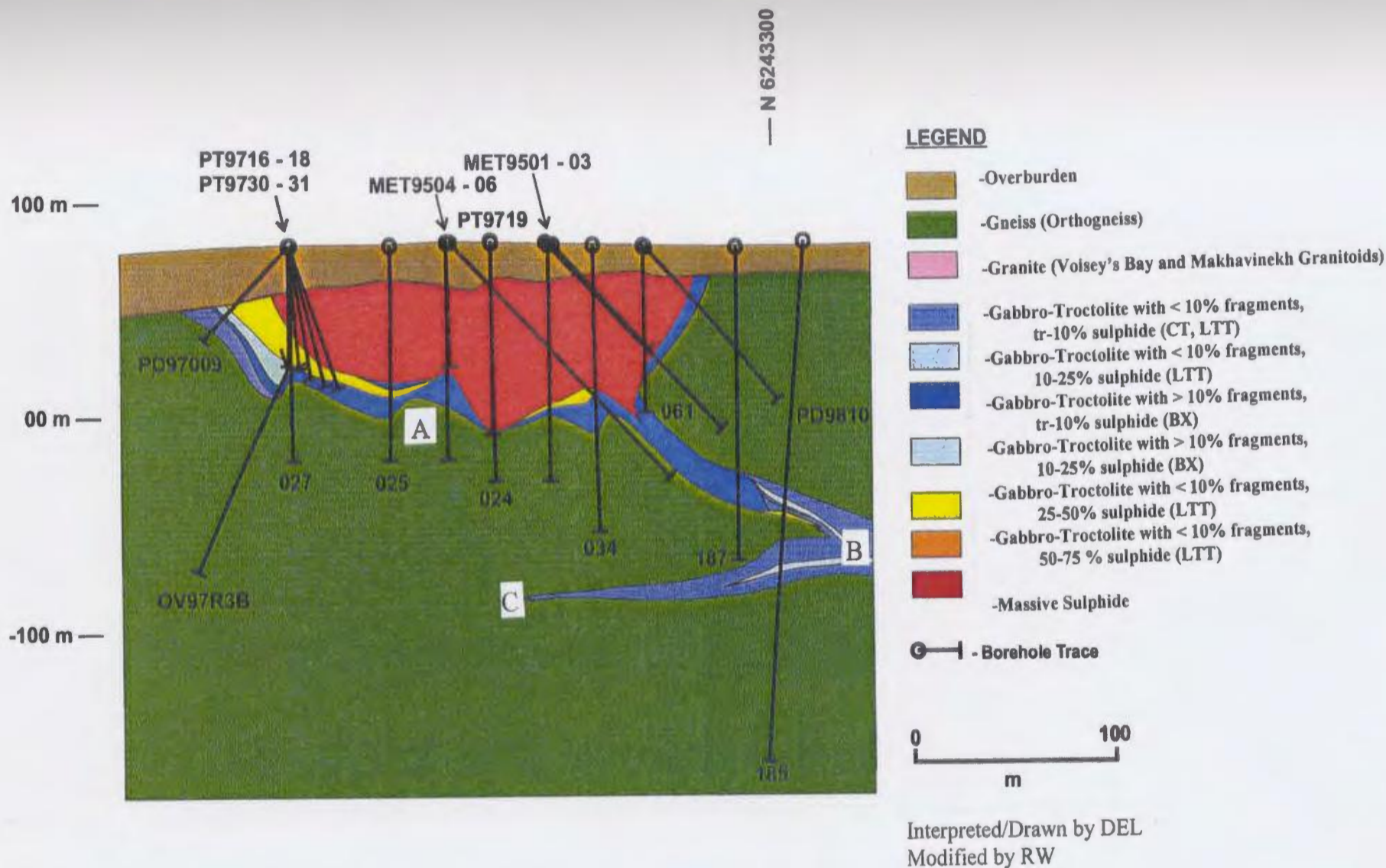
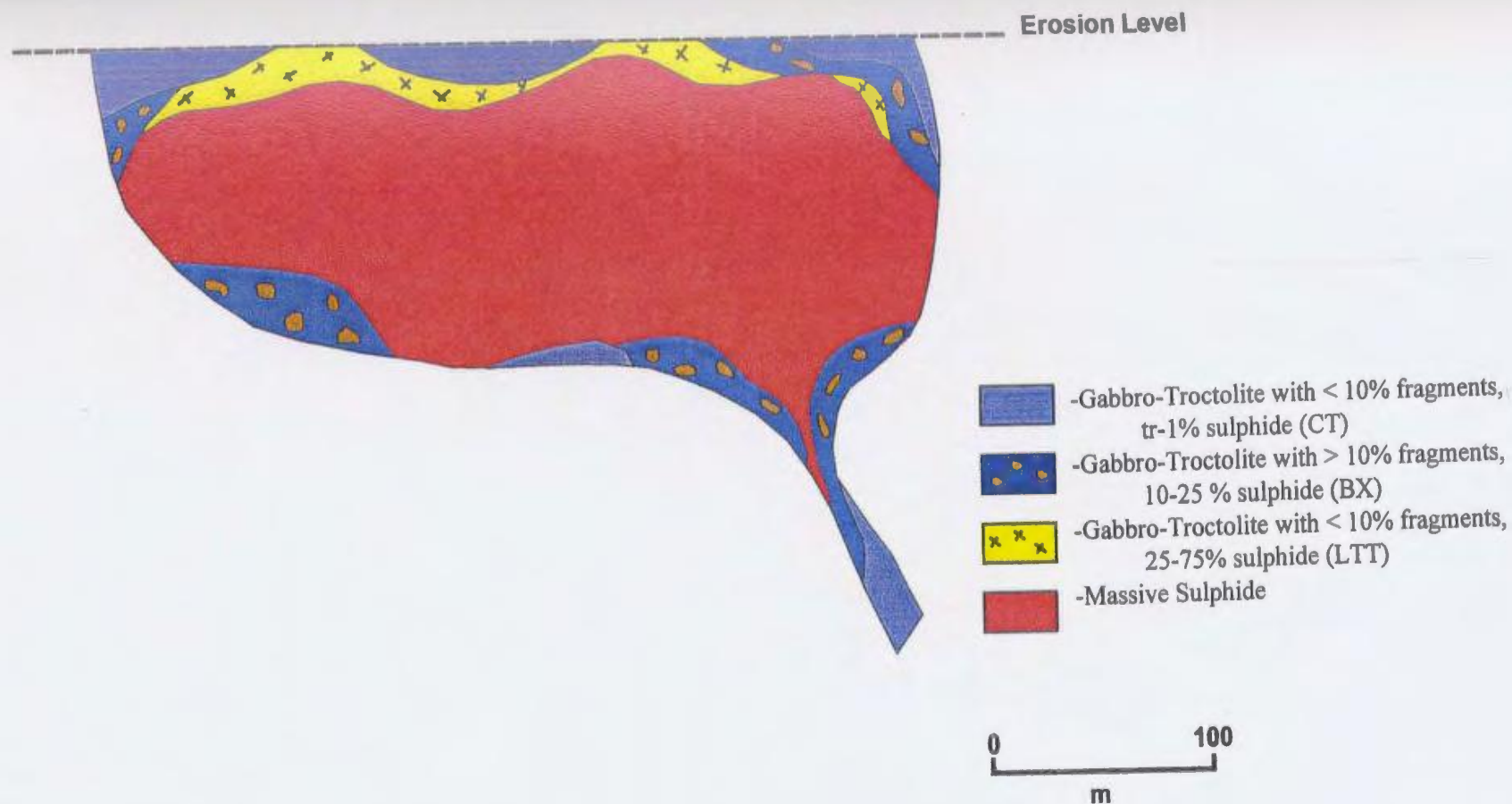


Figure 4.6 A west-facing geological cross-section of L13+50E through the Ovoid. Data from the close drill spacing (25 m) allows the footwall of the Ovoid to be delineated in detail. The footwall contact has numerous irregularities which can be recognized as intense undulations. (A) Footwall irregularities. (B) Feeder conduit. (C) A secondary splay from the feeder conduit.

4.2 Lithostratigraphy

Geologically the Ovoid provides a detailed geological transect through the most important stratigraphy in the Voisey's Bay deposit as is currently known. The rocks not only host the richest sulphide mineralization, but also document the intrusive relationships fundamental to the entire geological system. The intrusive history of the Ovoid is defined by the well preserved lithostratigraphy. Elsewhere in the study area, these original genetic and textural attributes have been masked by hybridization or progressive geological overprinting. The size of the Ovoid body has insured that its elemental geological characteristics are sufficiently preserved with only minimal overprinting by secondary geological events. Significantly, the lithologies and textures displayed by the sulphide and silicate sequences within the Ovoid body appear to be characteristic of those found within a conduit environment of a magmatic system (see Chapter 2). The geology and geometries expressed by the Ovoid are not comparable with, nor do they reflect, those which are produced within a chamber-type of environment (see Chapter 2). The lithostratigraphy, as defined within the Ovoid (Figure 4.7), is comprised of CT (Chilled gabbro-troctolite), LTT (Leopard Textured troctolite), BX (Breccia) textured gabbros to troctolites, and semi-massive to massive sulphides.

The highest sequence within the Ovoid is composed of CT gabbros; these are interpreted to be the cap or cover to the complex (Figure 4.5). Only a relic of the CT sequence remains preserved at this site, since the majority of this sequence would have been present above the current level of erosion. Texturally this unit exhibits a sharp explicit chill margin (Plates 4P and 4Q) proximal to the hanging wall. There is a gradual



Interpreted/Drawn by DEL

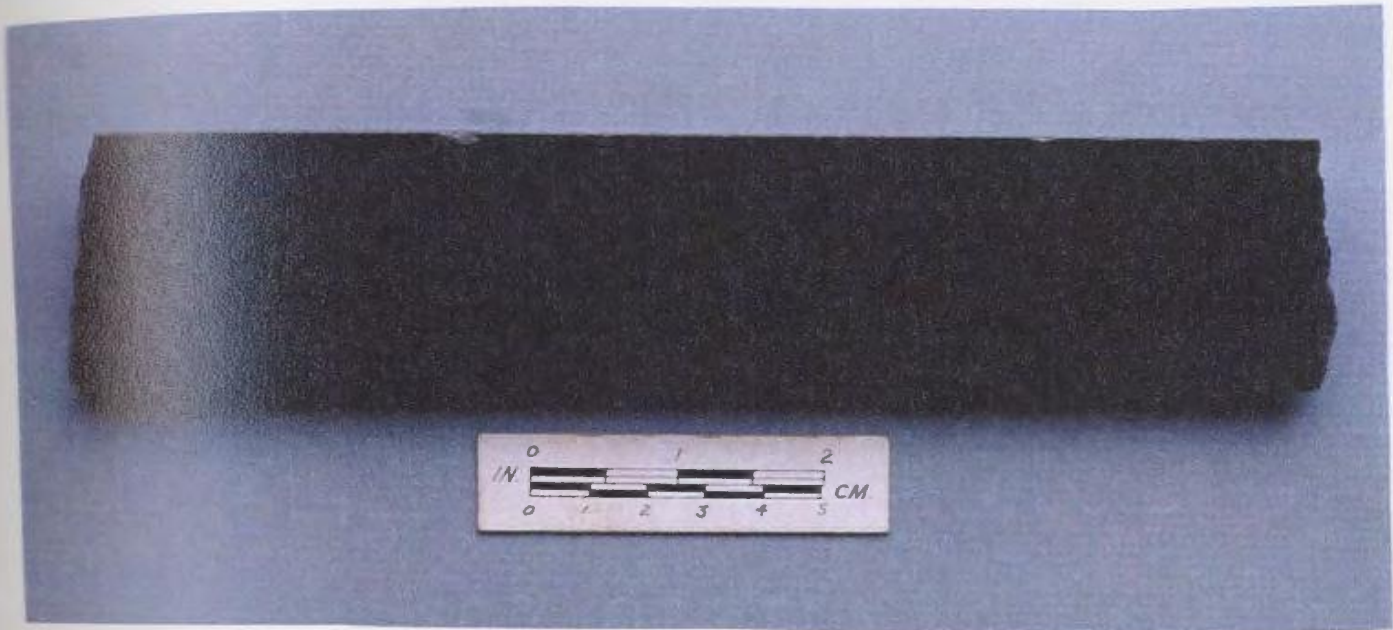
Figure 4.7 The idealized stratigraphy through the Ovoid whereby the intrusive earlier sequences to intrude are preserved at the margins of the body. For example, the CT gabbroic rocks lined the walls of the Ovoid, and then were intruded by the BX and LTT gabbros-troctolites and lastly, the massive to semi-massive sulphides.



Key to Legend



Plate 4P. DDH-PD09 (L13+50E) at 97.5 m. This is a chilled (CT) gabbro associated with the conduit environment. This sequence is the highest sequence within the Ovoid, but is also found to line the margins of the Ovoid adjacent to the gneiss contact.



Key to Legend



Plate 4Q. DDH-038 (L15+50E) at 32.0 m. This is a chilled (CT) gabbro associated with the conduit environment. The sequence is found to line the margins of the Ovoid adjacent to the gneiss contact.

increase in grain size away from the hanging wall as the sequence grades into an overall fine to medium grained gabbro. The most distinct characteristic of this sequence is the homogeneity of composition and texture. The CT gabbros are not only exposed within the highest stratigraphy, but they can also be observed to sporadically line the margins of the Ovoid (Figures 4.2 and 4.6; Plate Q). In these zones the CT gabbros are frequently thermally eroded or dislodged by the later intrusion of sulphide-bearing magma (i.e. BX or LTT gabbros-troctolites), leaving only thin and discontinuous horizons of the CT sequences preserved. This unit is conspicuously devoid of substantial mineralization, displaying on average only trace to 1% finely disseminated sulphides (Plate 2E), but locally can contain 3% sulphides (Plate 4P).

The LTT (Figure 4.7) occurs directly below the chilled zone. As described in Chapter 2, this sequence consists of gabbro-troctolite rocks with augite oikocrysts enclosed within a sulphide rich matrix (op cit. Naldrett *et al.*, 1996) (Plate 2G). The sulphide content is variable, but appears to increase down section, possibly as a function of local gravity settling. The LTT sequence is best described as containing 20 % sulphides. In the core of the Ovoid, massive to semi-massive sulphides are found beneath the LTT sequences and are observed to be in direct contact with the footwall gneisses (Figures 4.2 and 4.6). Elsewhere, however, (i.e. marginal zones) the massive to semi-massive sulphides are separated from the gneiss contact by thin sequences of either the CT or the BX gabbroic-troctolitic rocks (Figures 4.2 and 4.6). The massive sulphides are the thickest along L14+00E and L14+50E (Figure 4.2), with individual intersections of up to 120 meters. The massive sulphides are composed of pyrrhotite (Po), pentlandite (Pn) and

chalcopyrite (Cpy) (Plate 4R). Visually the Pn is euhedral, coarse grained and constrained to the massive Po matrix (Plate 4R). The Cpy is also euhedral to subhedral and forms interlocking chains called “Loop Textures” (Naldrett *et al.*, 1996) proximal to Pn crystal margins (Plate 4R).

There is a significant concentration, trace to 15%, of magnetite in the semi-massive to massive sulphide sequences. The magnetite is diverse in shape ranging from euhedral to anhedral. The euhedral crystals (<1 cm in diameter) can form globular groups with no specific orientation (Plate 4S), otherwise the individual crystals are randomly dispersed. The anhedral magnetite is blebby and exhibits a distinct alignment. This crude fabric is a prominent feature in the lower successions, wherein the magnetite develops distinct oblate shapes with a defined long axis crystal alignment (Plate 4T.).

BX textured gabbros occupy the lowest position within the Ovoid succession. These rocks occur along the lower margins of the Ovoid and are thickest to the north (Figures 4.5 and 4.6). The fragments appear to have a gneiss protolith (Naldrett *et al.*, 1996), as is indicated by a relict gneissosity preserved within their cores (Plates 2B and 2E). Petrological studies characterize these fragments as remnants of the Tasiuyak gneiss from the Churchill province (Li *et al.*, 1997, 1998; Lightfoot, 1998). There is no ubiquitous alignment of fragments, however, local consistencies in orientation can be detected (Plate 2A and 2D). The fragments are generally sub-rounded and range from 1 to 3 cm in length. The aspect ratios of the fragments vary between 1:1 to 1:6. The most intensely altered fragments appear totally pseudomorphed by hercynitic spinel (Naldrett *et al.*, 1996) (Plates 2B, 2D, and 2E), while the less digested fragments exhibit a strong

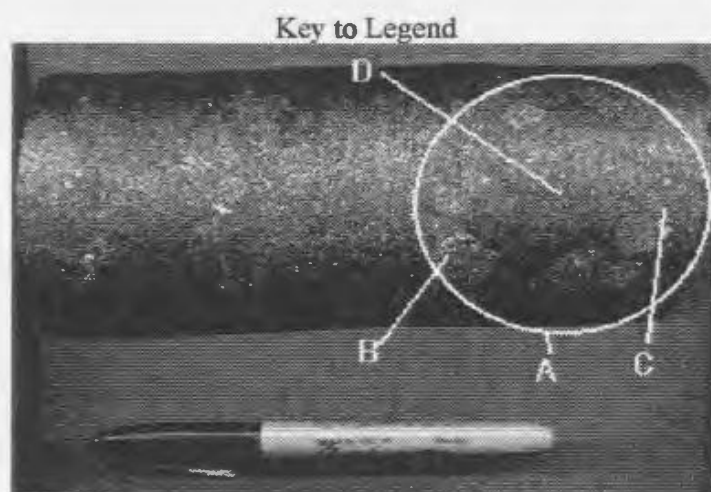
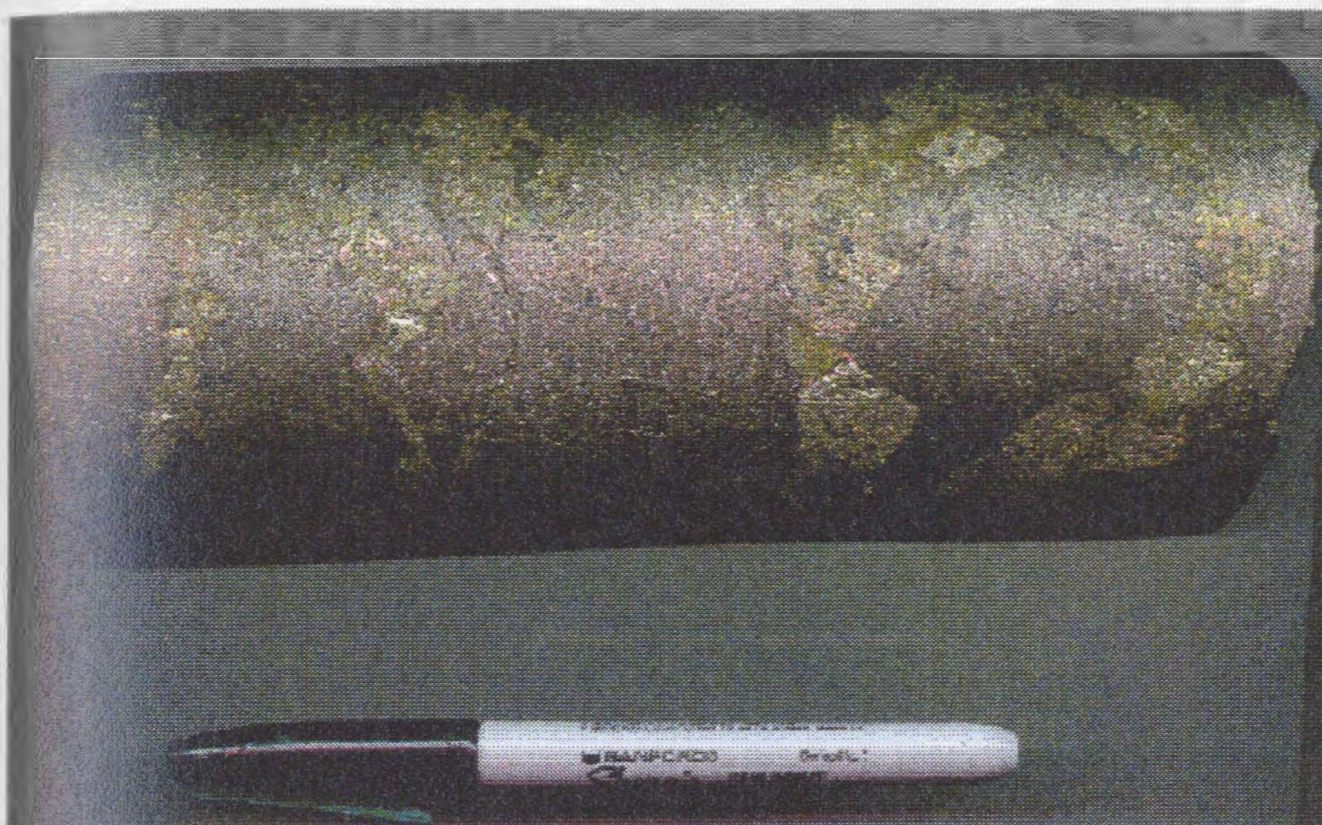


Plate 4R. DDH-PT020 (L14+00E) at 56.2 m. Massive sulphides from the Ovoid displaying vivid Loop Textures (Naldrett et al., 1996): A=Loop Texture, B= Pentlandite, C= Chalcopyrite, D= Pyrrhotite.

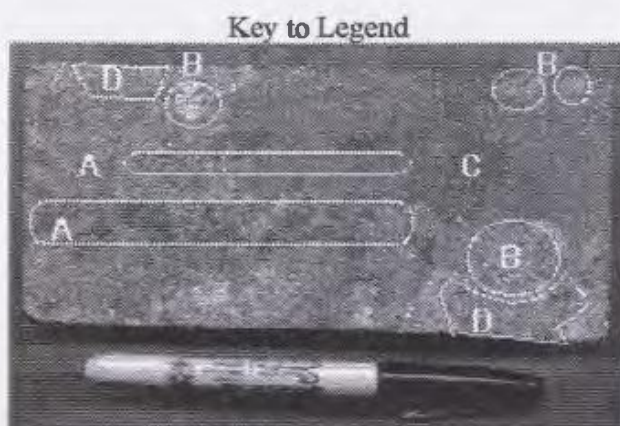


Plate 4S. DDH-PT026 (L15+00E) at 79.9 m. Massive sulphides from the Ovoid: A= flow aligned magnetite, B=Pentlandite, C=Pyrrhotite, D=Chalcopyrite.

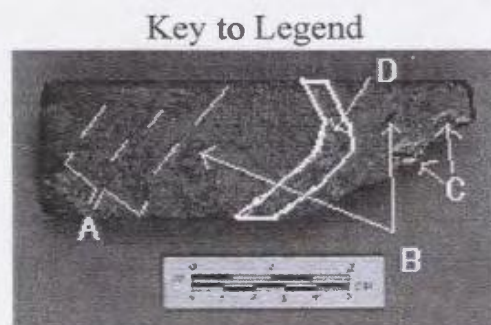


Plate 4T. DDH-018 at 35.0 m. Massive sulphides from the Ovoid showing a fracture cleavage: A= fracture cleavage, B= magnetite, C= pentlandite, D= pentlandite and chalcopyrite.

contrast in alteration between the interior regions, which were buffered from absorption processes, and the rim domains, which are subjected to the most intense alteration (Plate 2E).

Theoretically, the amount of fragment digestion should be a function of the length to width ratio, with the fragments having the highest ratios being more easily digested (c.f. Maury and Didier, 1991). The higher ratios result in more surface area per volume for direct contact with the surrounding magma where absorption processes are maximized throughout the complete fragment and are not constrained to just the edges (op cit.).

Sulphides hosted within this unit are texturally diverse; ranging from fine-grained disseminations to coarse, clotty textures. The coarser sulphides appear preferentially concentrated in zones proximal to the fragmental material (Plates 2A, 2E, and 2E), while the fine grained disseminations are ubiquitously dispersed through the matrix. As a visual estimate, the sulphides range between 1 and 40 %, and predominantly average 25%. The sulphides are comprised of Po, Pn and Cpy.

4.3 The Geological Significance of the Ovoid

4.3.1 Introduction to Past and Present Geological Models

The uniform demeanor displayed by the Ovoid lithostratigraphy was initially deceiving as the simple stratigraphic relationships overshadowed the intricate geology of the succession, as related to emplacement and the genesis of the system. Preliminary interpretations proposed a simple stratigraphic model for a top to bottom, gravity-settled system (Naldrett *et al.*, 1996). The Ovoid was modeled as a rootless chamber with semi-

massive and massive sulphides collected and concentrated through gravity settling. Simply, this model can be described as the elbow in a plumbing network, where the Ovoid served as a shelf or trap for the collection of sulphides (cf. Naldrett *et al.*, 1996). The sulphide-rich magma was subsequently captured as it slumped from an unseen, now eroded reservoir or chamber, above the Ovoid.

Within the confines of the Ovoid there is little doubt that magmatic settling was important to the current distribution of sulphides. It does not, however, appear to be the primary process for the bulk accumulation of sulphides, nor is it believed that the Ovoid is physically unrelated to a feeder network. Current geological interpretations do not only focus on sulphide distribution within the Ovoid, but also include sulphide and silicate textures. As well, recent interpretations incorporate all geological features proximal to the Ovoid which include, mineralized tails of troctolite extending from the north and following the base of the Ovoid to the south (Figures 4.2, 4.3, and 4.6) (see below). It is now thought that the sulphide stratification of the Ovoid mineralization does not reflect gravity-settling within a closed magmatic chamber, but alternatively, represents a sill-like layering created as multiple magmatic pulses interacted within an open magmatic system. Interpretations now accommodate the concept of an Ovoid magmatic trap, supplied upwards from a stratigraphically lower, but continuous feeder network. Furthermore, the Ovoid is thought to have been a bulge in the macroscopic conduit system, which at one time continued and ascended beyond current erosion levels (Figure 4.7).

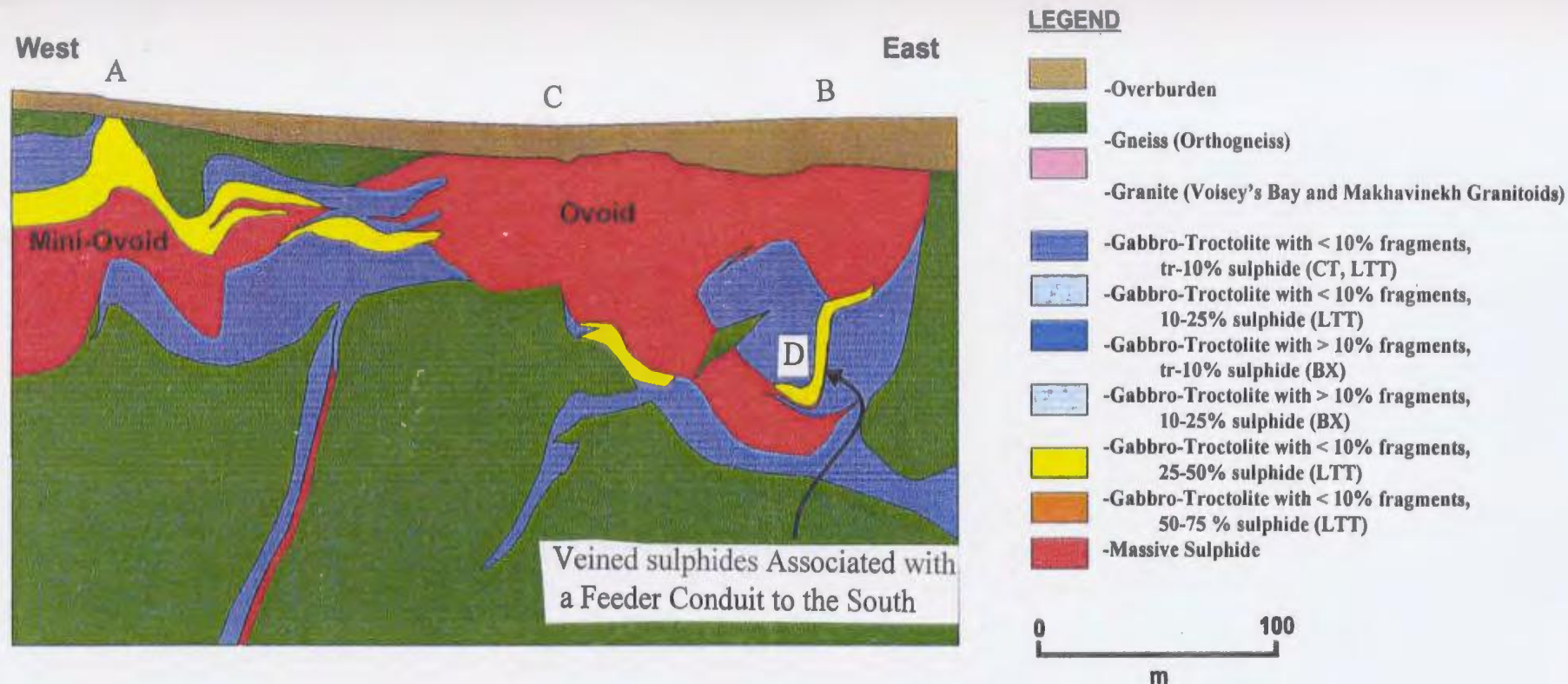
4.3.2 Physical Evidence Supporting the Existence of a Magmatic Feeder Conduit

Lithostratigraphic evidence supporting the presence of a magmatic feeder conduit is provided from numerous diamond drill holes including, VB95006, VB96205, VB96208, VB96211, and others (Figures 4.2, 4.3, and 4.6). These drill holes intersected small isolated, horizons of mineralized troctolite below the footwall, proximal to the north margin of the Ovoid (Figures 4.2, 4.3, and 4.6). Initially these troctolite tails were conceptualized as down faulted relicts of the northern lip of the Ovoid (Naldrett *et al.*, 1996) (Figure 4.2), however, with multiple intersections this zone was soon characterized as a narrow feeder conduit that was continuous with the Ovoid (Evans-Lamswood, 1997b) (Figures 4.2, 4.3, 4.5 and 4.6).

To examine the nature of the feeder at depth and to complete its documentation, two drill holes (VB273 and VB419) were targeted to intersect the conduit at depth beneath the Ovoid (Figure 4.8). These holes successfully intersected the conduit and established its geometric and geological continuity with its western counterparts (i.e. Mini Ovoid and Western Extension). This new drill hole data provided the evidence required to clearly establish the Ovoid, Mini-Ovoid, Western Extension and Reid Brook zones, as domains within a single continuous magmatic feeder conduit.

4.3.3 Lithostratigraphic Evidence Supporting the Existence of an Open Magmatic System

The discovery of the magmatic conduit at depth provides a physical link between the Ovoid and a magmatic feeder, however, this alone cannot provide documentation as to



Interpreted/Drawn by DEL

Figure 4.8 A north-facing longitudinal section from L12+00E to L15+50E and striking at 112 degrees. The massive sulphides are not continuous between the Mini-Ovoid and Ovoid and appear to mark two distinct mineralized zones. (A) The feeder conduit as seen at lower stratigraphic levels within the Mini-Ovoid. (B) The feeder conduit as seen within higher stratigraphic levels such as the Ovoid. (C) The feeder conduit as seen at intermediate stratigraphic levels in more central and western regions of the Ovoid. (D) An anomalous occurrence of veined sulphides which do not appear to be distributed from the north feeder conduit. This anomalous horizon may represent a sulphide sequence which was expelled from a second feeder conduit that entered the Ovoid from the south.

whether the Ovoid system was open or closed during sulphide formation. Distinct lithostratigraphic and textural relationships exhibited within the Ovoid, however, do appear to provide evidence supporting the presence of an open magmatic system which was continuously supplied with sulphide-bearing magma by the lower feeder conduit.

For example, the BX textured rocks infrequently exhibit an alignment of fragments (Plates 2A and 2D); this feature is thought to be produced through the segregation and rotation of fragments within a turbulent magmatic flow (cf. Arbaret *et al.*, 1996). In agreement with these observations, a consistent and pervasive alignment of fragments would not be expected to be developed in a magmatic environment influenced by local convective currents or turbulent flows, such as those which could be present in an open magmatic system. A ubiquitous alignment of the fragments would only be expected to develop through gravity settling within a stagnant, non-disruptive environment, or ideally, within a domain of homogeneous, laminar flow.

Like the fragments in the BX sequences, the magnetite within the massive sulphide sequences do not always share a common or consistent orientation (Plate 4S and 4T). The defined fabrics appear to be products of both primary and secondary (within the macroscopic system) deformation processes. Where the alignment appears to be a direct product of the magmatic flow environment, the defined fabric can be observed to meander as if circulating within an open cell (Plate 4T). To form this inconsistently orientated fabric, it is thought that stress induced upon the crystals as they approached the rigid margins of the Ovoid caused the crystals to form an oblate array perpendicular to the principal stress vector, as predicted to occur in similar situations by Arbaret *et al.* (1996).

If this alignment was a mere effect of gravity settling, as in the situation of homogeneous simple shear, a fabric developed consistently at a low angle to the vertical core axis (i.e. 75° - 90°) would be expected to be preserved (op. cit.). Where magnetite-defined fabrics are thought to be a product of secondary deformation, the alignment appears coincidental with a weak to moderately developed fracture cleavage and is not related to the processes of emplacement (Plate 4T).

Furthermore, proximal to the mouth of the feeder, the Ovoid lithologies are chaotically intercalated and, therefore, document what was once a turbulent magmatic environment (Figures 4.3 and 4.5). For example, mounds of the BX sequences are stacked along the sides of the Ovoid proximal to the conduit entrance (i.e. mouth) (Figures 4.5 and 4.6). These mounds could have formed as the heavy fragment-laden magma was expelled from the constricted feeder environment into the wide Ovoid body. As interpreted in this study, with a reduction to the confining pressure the fragment-laden magma could lose velocity upon entering the Ovoid and subsequently, heavy material would settle-out proximal to this site (i.e. entrance). In addition, convective and eddy/turbidity currents created by the continuous expulsion of magma into the Ovoid could have assisted in the restricted and proximal distribution of the early BX sequences. The cyclic or churning effect created by these processes could also result in a portion of the BX sequence being re-circulated back through the funnel shaped entrance of the Ovoid and possibly, slumping back into the feeder conduit. This process provides rationale for the occurrence of chaotically intercalated BX sequences found below the Ovoid, back within the feeder conduit (Figures 4.2 and 4.5).

Another significant observation is that the massive sulphides not only appear to have been deposited as thick, cohesive sequences, but also appear to have been emplaced as massive to semi-massive veins ($\ll 1.0$ m) which intruded other lithologies (Plates 2C and 2O). The veins are not restricted to a particular stratigraphic horizon, however, most frequently intersect the LTT and the BX sequences. This indicates the Ovoid was an open and dynamic magmatic system during sulphide formation.

The documentation of the above characteristics do not eliminate the possible influence of gravity processes on the formation of crystalline fabrics, or on the distribution of lithologies within the Ovoid. Gravity processes may in fact have acted in conjunction with the flow attributes to develop the localized, intermittent fabrics and distribution patterns of the rocks, however, the concept that the Ovoid was a closed magmatic system whereby, gravity-settling completely controlled the distribution of lithologies and sulphides does not appear to be valid for the Voisey's Bay magmatic system.

4.3.4 Plunge

The Ovoid has been modeled in both two dimensional and three dimensional space. From these schematic images the true shape of the Ovoid body is established. From this exercise, it becomes apparent that changes to the Ovoid geometry (pinching and swelling) occur not only in two dimensions (x and y directions), but as well, takes place within a third dimension (z direction) (see Chapter 5) (Figure 4.4).

This occurrence provides evidence to support the Voisey's Bay system as a plunging conduit, whereby, geological comparisons should only be made between zones at

similar stratigraphic levels, and not incorrectly through their common topographic levels. For example, slices through the most easterly margins of the Mini-Ovoid, appear geologically comparative to the adjacent transect through the Ovoid (Figure 4.9), however, upon the examination of the three dimensional model for the Ovoid and Mini-Ovoid (Figure 4.4), it becomes apparent that the two zones are discontinuous, and that the Mini-Ovoid appears to plunge beneath the Ovoid. There is little doubt that the fluctuations in the volumes and positions of the massive and disseminated sulphides between these two bodies result from each sulphide zone being emplaced by a separate magmatic pulse. The two magma pulses are trapped within different stratigraphic levels in the feeder conduit, however, due to the plunge of the conduit system, they appear at the same topographic level.

4.4 Multiple Feeders

As defined by the current geological data, a north dipping feeder permeates the lower, north wall of the Ovoid structure. This model has now been expanded to include the idea that multiple feeders coexisted and collectively nourished the Voisey's Bay magmatic system (Evans-Lamswood, 1997b). This protolith for multiple conduits (cf. Condie, 1997), is referred to as the Octopus Model (Horn, 1997 Pers. Comm.), in analogy to the postulated existence of tentacular protrusions from the Ovoid, or simply, the occurrence of multiple dykes that appear to branch and coalesce proximal to the Ovoid (Figure 4.10).

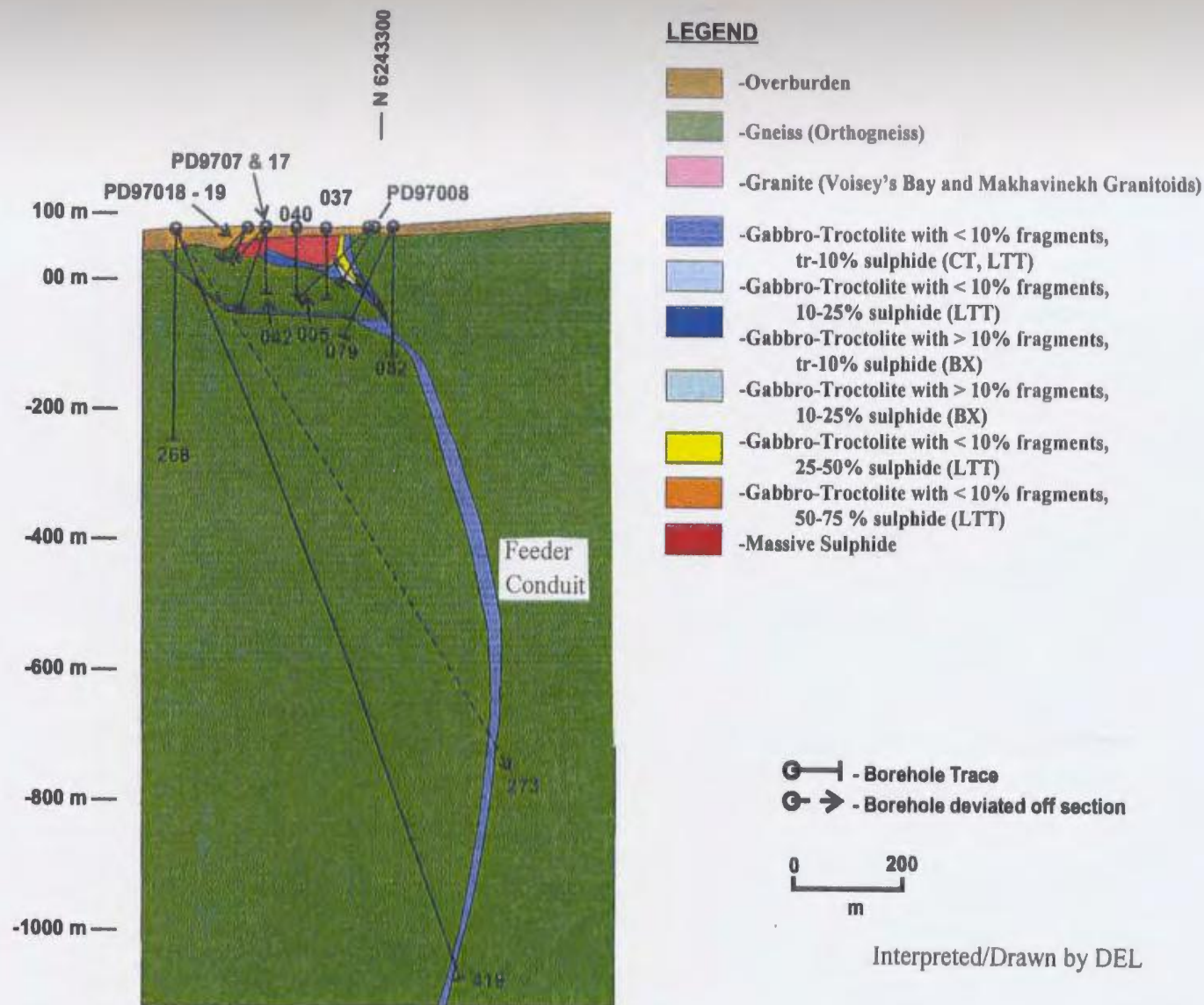


Figure 4.9 A west-facing geological cross-section of L13+00E through the Ovoid. Drill holes VB273 and VB419 intersect the feeder conduit at over a kilometer below the Ovoid. The feeder conduit appears to be continuous with the Ovoid. A second conduit is intersected beneath the Ovoid. This conduit is thought to be a secondary splay from the main feeder conduit found below the north margin of the Ovoid.

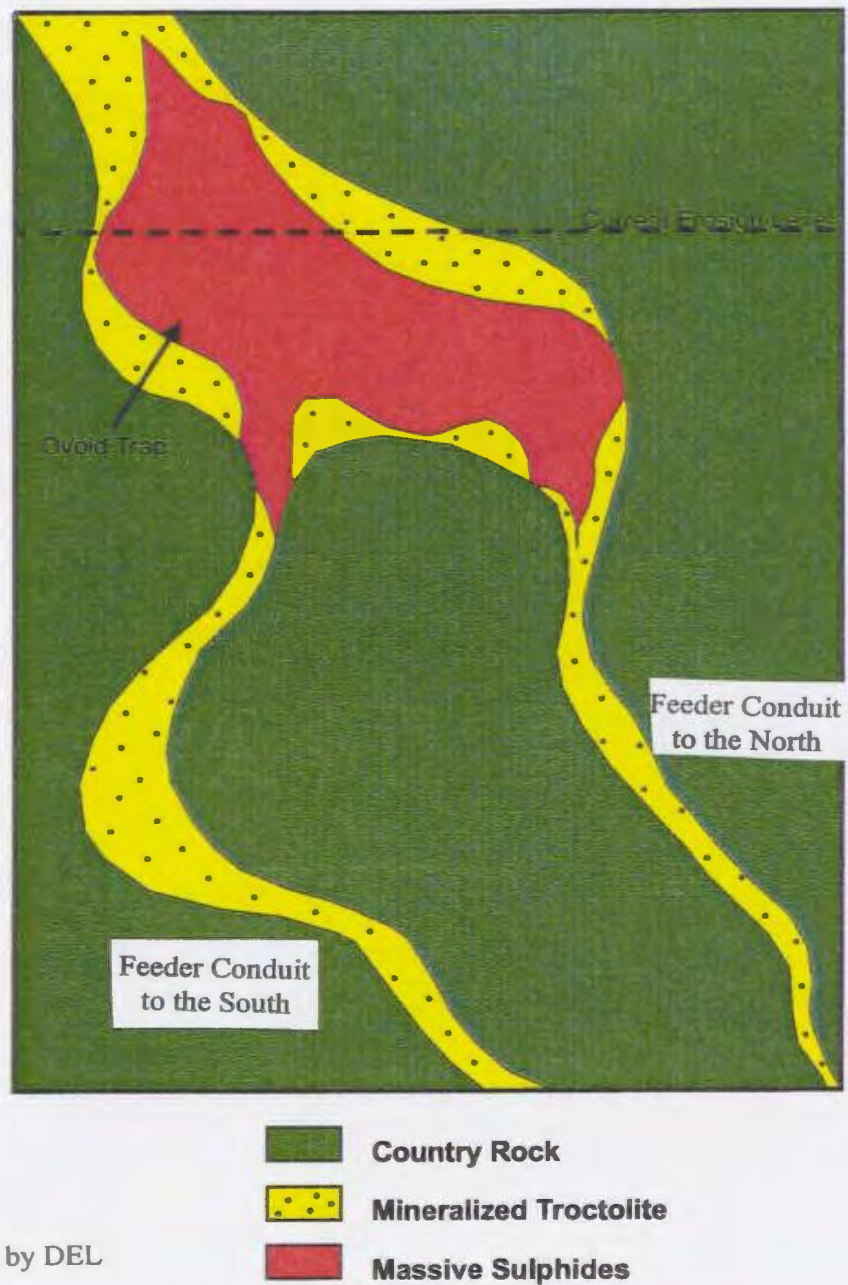


Figure 4.10 The "Octopus Model" shows the concept wherein two or more magmatic feeder conduits intersect at the Ovoid. As a result of the multiple conduits, anomalous quantities of sulphide were supplied to this site. This model also schematically depicts the continuation of the conduit system above the Ovoid.

Direct evidence for multiple conduits is inferred from drill hole data (i.e. VB96268, VB96273, VB97419, and others) (Figures 4.2, 4.3, 4.6 and 4.8), where secondary occurrences of weakly mineralized troctolite were intersected below and adjacent to the footwall of the Ovoid. When geologically modeled, these troctolite occurrences form a sill-like body parallel to the footwall of the Ovoid, and appear to originate or splay from the feeder conduit found below the north margin (Figures 4.2, 4.3, 4.6 and 4.8).

Other evidence supporting the existence of a multiple conduit network is obtained from lithostratigraphic relationships observed within Ovoid; one such example is displayed in Figure 4.9. In this situation, an intensely mineralized troctolite horizon crosscuts the surrounding sub-horizontal Ovoid stratigraphy. This horizon appears to postdate emplacement of the dominant Ovoid sequences in the southern part of the Ovoid. It is interpreted that this anomalous horizon was injected into the Ovoid from the south, where the early magma was crystallizing and forming a viscous magma mush. The magma intruding from the south would have been warmer and less viscous than the Ovoid magma, and therefore, it would not freely mix with the earlier sequences. Subsequently, this late magma would remain as a cohesive sequence or vein intruding the early Ovoid stratigraphy.

From these observations, it appears that the Ovoid is a loci where multiple conduits could have coexisted. The anomalous accumulations of sulphides within the Ovoid may not be a product of a single magmatic feeder conduit, but alternatively, the result of multiple conduits coalescing at this site. Furthermore, the presence of the sill-like conduit beneath the Ovoid, suggests that physical changes to the local geological

environment (see Chapter 3) could have triggered the formation of bifurcations or splays from an established conduit.

Chapter 5: The Effect of Geometric Processes on Lithostratigraphy; the Mini-Ovoid.

5.0 Introduction

The Mini-Ovoid provides an opportunity to examine multiple lithostratigraphic transects through the throat of the plunging magmatic feeder conduit. As documented in Chapter 4, the Mini-Ovoid is interpreted to be stratigraphically lower than the Ovoid, however, the plunge of the feeder conduit places both sulphide-bearing bodies at the same topographic level. The Mini-Ovoid documents significant physical changes in the shape of the feeder conduit. It represents a transitional zone between the Ovoid, where the conduit swelled into a bulbous trap with extreme widths, and lower sites, where the conduit was a narrow dyke-like structure. The vertical slices, depicted by the west facing geological sections presented in this chapter, will characterize the dramatic environmental changes that developed with subtle adjustments in the geometry of the dyke. This text will establish the intricate and dependent relationships maintained between physical environmental controls and the lithostratigraphy as theorized in Chapter 3. Furthermore, and of greatest importance to modeling the Voisey's Bay deposit, is documentation of the ascent of mineralization through the magmatic conduit system, as opposed to its descent through settling processes.

5.1 Geometric Changes to the Trap Environment

5.1.1 Transition from L13+00E through L12+50E

Figures 4.9 (L13+00E) and 5.1 explore the geological transition from the Ovoid to the Mini-Ovoid. This is a significant transect, documenting the changes to mineralization

with the contraction of a bulbous sulphide trap (Figure 3.1). Differing from the bowl shape of the Ovoid, as established on L13+00E, the section through L12+50E shows the conduit as a tulip-shaped body, hosting two massive sulphide sequences; the Ovoid and Mini-Ovoid. The inclination of the south and north walls of the dyke have been amplified to geometric extremes, such that both interfaces now dip moderate-steeply to the north. The volume of massive sulphides supplied by the two massive sulphide lenses is far less than that which was provided by the Ovoid alone.

Based upon examinations of the core, it is speculated that the rapid changes incurred in the volume and shape of the mineralized zones are the direct consequences of modifications in the dyke geometry (see above, Chapter 3). Within the domain of the Mini-Ovoid, the width of the dyke proved advantageous for the collection of sulphides (Figure 3.3). This mechanism, however, was restricted in effectiveness due to the steep orientation maintained by the enclosing north and south walls (cf. Bruce and Huppert, 1990).

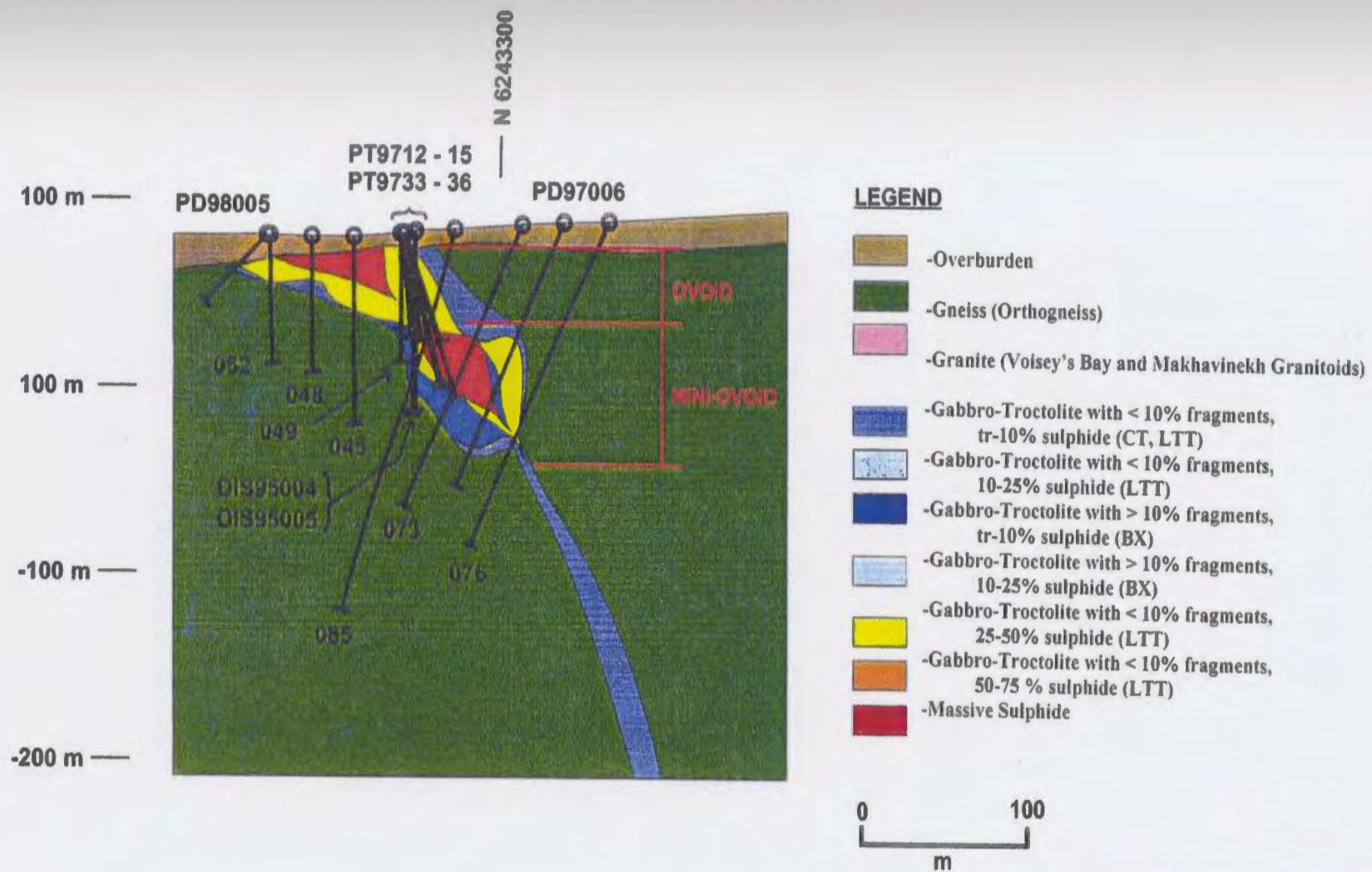
The massive sulphides at the Mini-Ovoid occur in two oblate, ellipsoidal lenses that are joined at their apexes. The upper massive sulphide horizon is truncated by the current level of erosion, but it is interpreted to have been the west margin of the Ovoid, while the lower massive sulphide body is thought to represent the eastern edge of the Mini-Ovoid. Simply, this section slices through two separate mineralized bodies, the Ovoid and Mini-Ovoid (Figure 4.4). This vertical section captures the western edge of the Ovoid before it plunges above the erosional surface, and the eastern edge of the Mini-Ovoid as it ascends up-plunge from below the Ovoid.

The steep orientation of the dyke at the Mini-Ovoid suggests that significant quantities of sulphide may have been moved through the top of this sulphide trap, since large volumes of sulphides are not present in this trap and have not slumped down into the system. The width of the dyke in this domain would slow the upward flow of the magmatic fluids (i.e. magmatic transfer) and hence, would be advantageous for sulphide capture, as documented elsewhere by Bruce and Huppert (1990) and Naldrett *et al.*, (1996) (Figure 3.3). The effectiveness of this geometric feature on sulphide capture, however, would be restricted by the steep orientation of the conduit walls. The steep inclination of the walls, would have prevented the development of a shelf for the effective collection of sulphides. Furthermore, there is no apparent change in the orientation of the conduit between the site where it expands (i.e. the trap where sulphides collect), and the site below where it narrows. Between these two sites the feeder conduit expands, however, without further disruptions to magmatic flow through a change in conduit geometry (i.e. inflection), the rate at which magma was transferred through the system would not be considerably affected. Subsequently, large volumes of magma escaped through the top of the trap (i.e. were not effectively captured and concentrated).

Furthermore, within the domain of the Mini-Ovoid, the steep inclination of the conduit will affect the distribution of lithologies throughout this zone. For example, unlike the Ovoid, the BX sequences within the Mini-Ovoid did not form mounds at the feeder entrance, but alternatively, were preserved at upper stratigraphic levels proximal to the highest massive sulphide lens (i.e. sulphides from the western margin of the Ovoid). This distribution pattern indicates that the earliest pulse of dense, fragment-laden magma was

expelled into the Mini-Ovoid rapidly, pushing it away from the conduit entrance (i.e. mouth) before thermal and gravity processes could disrupt its course. The influences from the steep attitude of the Mini-Ovoid are also reflected in the distribution of the CT gabbros. The CT sequence is continuous and remains intact proximal to the hanging wall (i.e. north wall), however, appears dislodged along the footwall contact (i.e. south wall). This observation may reflect gravity processes, whereby, heavy, fragmental or sulphide-bearing successions begin to nucleate and settle towards the lower margin and in course, thermally erode or displace the less dense CT.

The vertical cross-section L12+50E (Fig. 5.1) through the Mini-Ovoid, documents geometric changes incurred to the x and y components of the sulphide trap as it moves west from L13+00E. The changes to the z component of this domain are yet to be discussed, but appear to establish a moderate southeast plunge to the trap and the enclosed mineralization. The azimuth of the plunge (southeast) may be an apparent feature induced by late brittle-ductile deformation. The Mini-Ovoid is riddled with sub-vertical fractures, possibly associated with jointing. These fractures form conjugate systems ($310^{\circ}/030^{\circ}$) which accommodate microscopic displacements (Figure 4.1). Sinistral strike slip displacement occurs along the 310° trending system and dextral translation along the 030° conjugate planes (Evans-Lamswood, 1996b) (Figure 4.1). Without primary marker horizons it is not possible to isolate the discrete displacement associated with each individual fracture, however, the southeast plunge imposed on this zone appears to be induced by a mesoscopic right lateral translation.



Interpreted/Drawn by DEL

Figure 5.1 A west-facing geological cross-section through L12+50E in the Mini-Ovoid. This section exhibits massive sulphides from the eastern margin of the Mini-Ovoid plunging beneath massive sulphides from the western margin of the Ovoid. Sulphides were collected in a trap, a site where the conduit expanded.

5.1.2 Transition from L12+50 through L12+00E

Figures 5.1 and 5.2, are geometrically similar, but section 12+00E indicates subtle changes to the lithostratigraphy in the lower portions of the Mini-Ovoid trap. The upper stratigraphic horizons that displayed the Ovoid massive sulphides in section L12+50E, are above the erosion level on this section. At this location, the Ovoid stratigraphy would plunge above the Mini-Ovoid and, therefore, leave only one massive sulphide horizon preserved which is that of the Mini-Ovoid.

The homogenous appearance and consistent width of the massive sulphides preserved within this section reflect the geometric controls on this zone. Geometrically, this body has two physical irregularities that could have substantially controlled the distribution and collection of lithologies and sulphides. These two features include, a concave protrusion or embayment in the footwall (i.e. south) interface, and a widening of the conduit entrance (i.e. throat). The stratigraphy in this regime is more stratiform and can be directly compared to that of the Ovoid. The previous section, L12+50E, showed intense intercalation of the lithologies which can be a product of turbulent flow, as similarly documented in fluid dynamic studies by Cruden (1990), Koyaguchi and Blake (1991), and Turcotte (1990). For example, the widening of the conduit at the feeder entrance could have permitted the rapid transfer of magma into the trap (i.e. Mini-Ovoid), as is similarly recorded by the experimental studies of Bruce and Huppert (1990). The gradual change in width from the conduit to the trap would not cause significant disruptions in the flow of magma, such as those which could occur with a sharp and rapid change in conduit width (i.e. reduced confining pressure). As a product of this

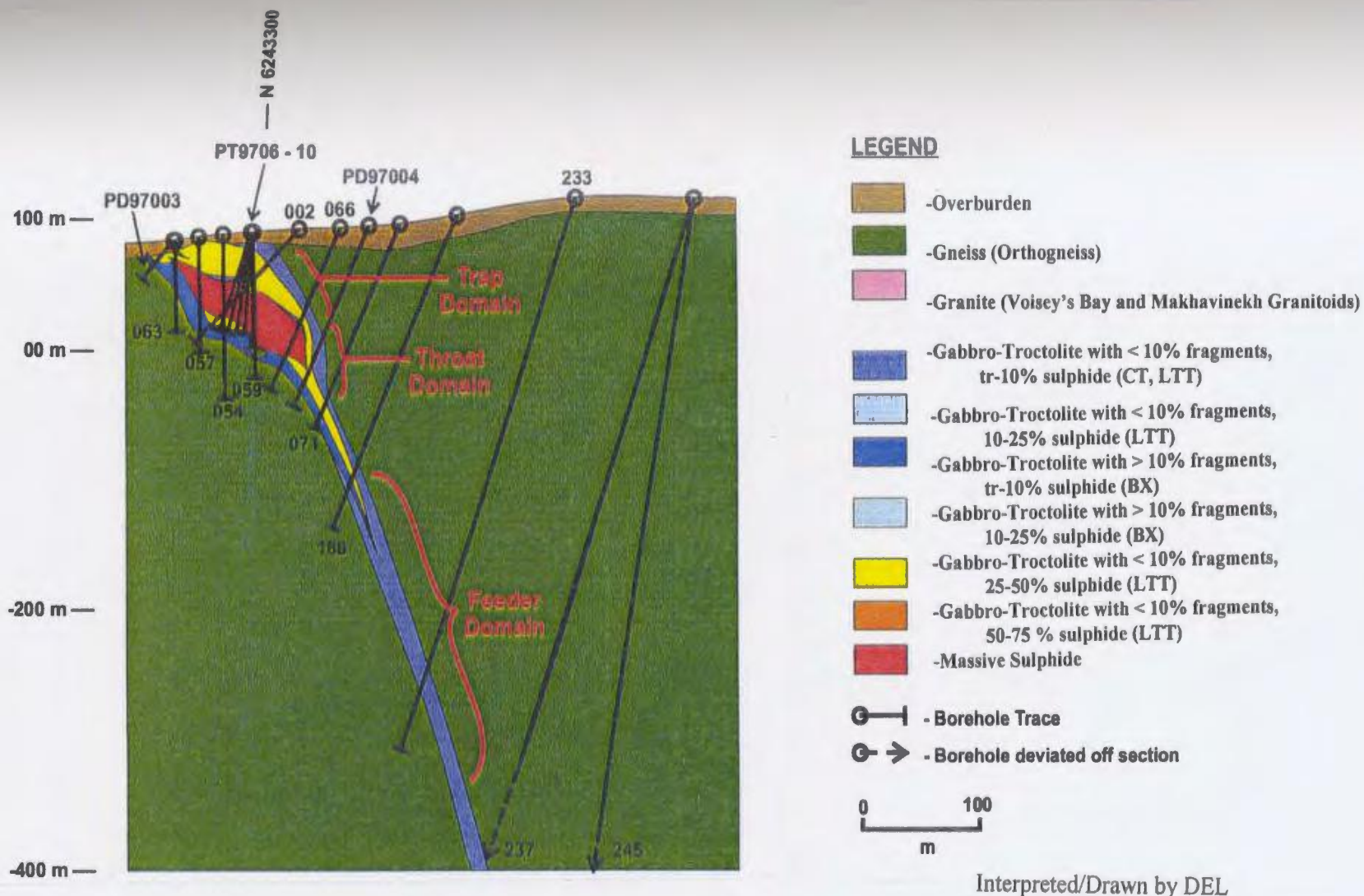


Figure 5.2 A west-facing geological cross-section through L12+00E in the Mini-Ovoid. This section shows sulphides collected at a site where the conduit expands (i.e. trap domain). The expansion to the conduit width is not sharp, but develops gradually from the narrow conduit (feeder domain) to form a throat domain or a mouth to the sulphide trap. Along this section, the Ovoid is not seen, as it is stratigraphically higher than the Mini-Ovoid and, therefore, would have been present above this level of erosion. An embayment or footwall irregularity along the south contact of the Mini-Ovoid trap assisted sulphide capture at this site.

environment the original lithologies are preserved as continuous horizons (figure 5.2). The footwall depression expressed by figure 5.2, appears to create a flexure along the south margin of the Mini-Ovoid which could have acted as a shelf for the collection of sulphides (Figure 3.1). This flattening of the conduit walls could have reduced the gravitational drag imposed on the massive sulphides at the far edge of this mineralized sequence, as can be observed to occur with this same horizon on L12+50E. Therefore, if not dominated by the effects of drag, gravity forces uniformly distributed throughout the zone could have provoked the ubiquitous settling of all the lithologies towards the shelf, as cohesive, stratified horizons (Figure 5.2).

The width and geometric attitude of this trap may have reduced the volume of sulphides escaping to upper stratigraphic levels, since establishment of the shelf could enhance its performance as a sulphide trap. Section 12+00E displays a narrow neck protruding from the upper apex of the massive sulphide sequence, indicating that the upper exit from the Mini-Ovoid trap to the conduit was narrow. While some sulphides would inevitably be expelled through this exit, the remainder would clog the exit and collect in the trap (Figures 3.3 and 3.4).

The stratigraphic position of the massive sulphides within the Mini-Ovoid (second pulse) are comparable between sections L12+50 E and L12+00E, however, the higher stratigraphic position of the early massive sulphide pulse is above the erosion level of L12+00E and therefore, is not preserved. By comparing the positions of massive sulphides from the same stratigraphic level between sections, a weak southeastern plunge can be detected in the system. Correlated with the speculated translation between L13+00E and

L12+50E, this transition also displays a dextral off-set along the 030° fracture system (Figure 4.1).

5.1.3 Transition from L12+00E through L11+50E

The transition from L12+00E to L11+50E, is depicted by figures 5.2 and 5.3. Both of these sections host comparable geometry and stratigraphy with only subtle changes detected. Unlike the previous section, the upper stratigraphic levels of L11+50E have been eroded, leaving only a partial transect through the trap. The footwall depression detected on L12+00E is not observed on L11+50E, but this may just be a reflection of the drill hole spacing used for delineation on this section. The other notable change in dyke geometry is the shift in the alignment that had previously been maintained between the feeder conduit and the Mini-Ovoid trap. In the previously viewed sections, both the trap and the conduit were congruently askewed and dipping to the north, however, this section shows an inflection between the orientation of these two conduit domains. The attitude of the feeder on L11+50E appears shifted, now being repositioned directly beneath the trap in a near vertical orientation. The repositioning of this conduit increases the inclination of the collective, feeder-trap system, thus reducing the efficiency of the sulphide capture. In the upper horizons of this succession, evidence for this interpretation has been destroyed through sub-surface erosion, but alternative documentation is provided by the slumped appearance of the massive sulphides. The massive sulphides appear to have been subjected to gravity drag, as they occur in an irregular mass at the feeder entrance. With no shelf established to catch or support the sulphides, the succession could collapse and settle

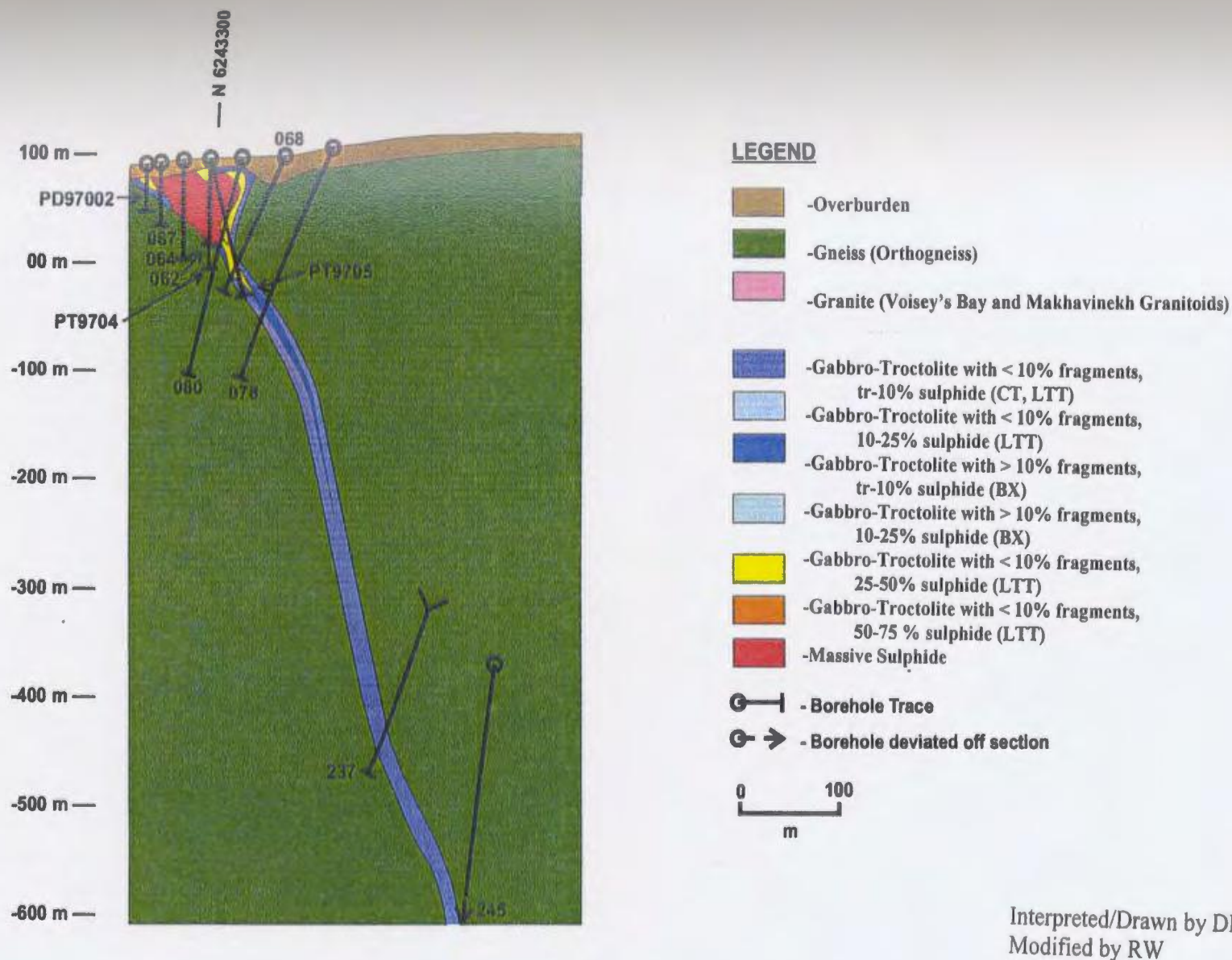


Figure 5.3 A west-facing geological cross-section through L11+50E in the Mini-Ovoid. The plunge of the conduit results in the top of the Mini-Ovoid being topographically above the level of erosion at this location. The massive sulphides appear to be preferentially concentrated along the south margin (footwall) of the conduit and, therefore, result in the earlier sequences being dislodged.

through the Mini-Ovoid (i.e. trap), until coming to rest at the base in a contorted mound. Furthermore, through the process of slumping, the massive sulphides are juxtaposed against the footwall contact, dislodging any sequence collected along this interface.

5.1.4 Transition from L11+50E through L11+00E-L10+50E

Figures 5.4 and 5.5 are transects through L11+00E and L10+50E, respectively. It is apparent that with westwards progression the Mini-Ovoid trap is migrating through higher topographic levels due to the plunge of the system. Within the present topographic level the cross-sectional slice through the Mini-Ovoid becomes limited, with only the lowest stratigraphy preserved. These limitations are compounded by a lack of deep sub-surface drilling in this zone. The lack of geological data restrict the geological contributions of these sections to the macroscopic analysis, but do, however, contribute to broad correlations made with the adjacent sections.

As observed with L11+50E, the feeder conduit is positioned directly under the Mini-Ovoid trap, establishing a steep network for the transportation and collection of sulphides. On section L11+00E, the massive sulphides are once again in apparent contact with the footwall gneiss and the northeast plunge established on L11+50E is retained. On L10+50E the contact between the massive sulphides and the gneiss is not observed, however, this is probably a function of the depth of erosion where at upper stratigraphic levels, the massive sulphides may actually abut against the gneiss wall rock. This section also presents a shift in the plunge of the ore zone. A southeastern plunge is recognized and may be a product

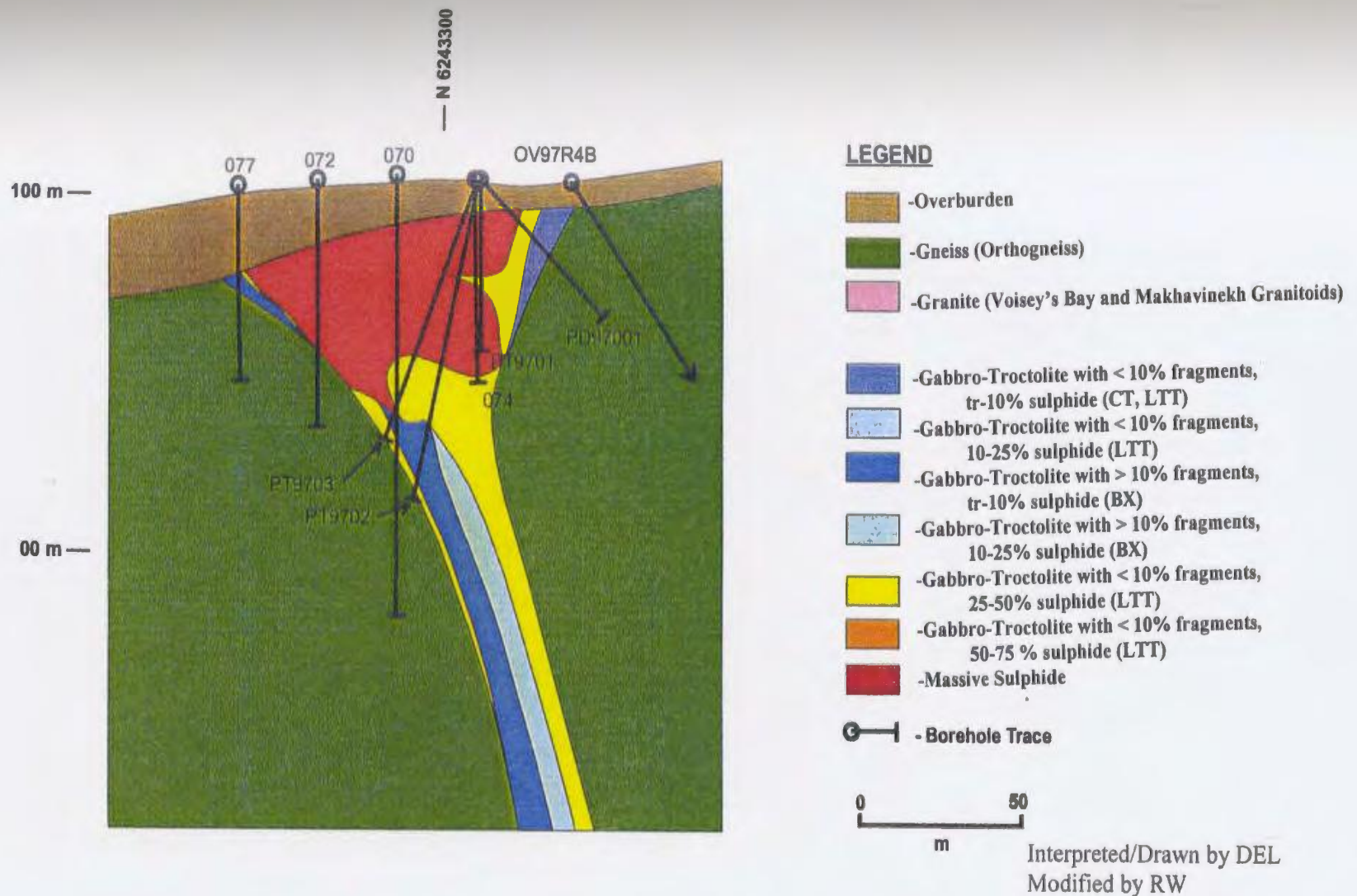


Figure 5.4 A west-facing geological cross-section through L11+00E in the Mini-Ovoid. Along this section only the base of the Mini-Ovoid is preserved; progressively to the west, the plunge of the conduit places the Mini-Ovoid at higher topographic levels and above the surface of erosion. This site, however, does express a gradational change from a narrow conduit domain (i.e. feeder) into a wide conduit domain (i.e. trap). This results in the development of an intermediate regime or transitional zone (i.e. mouth or throat) which joins the wide and narrow conduit domains.

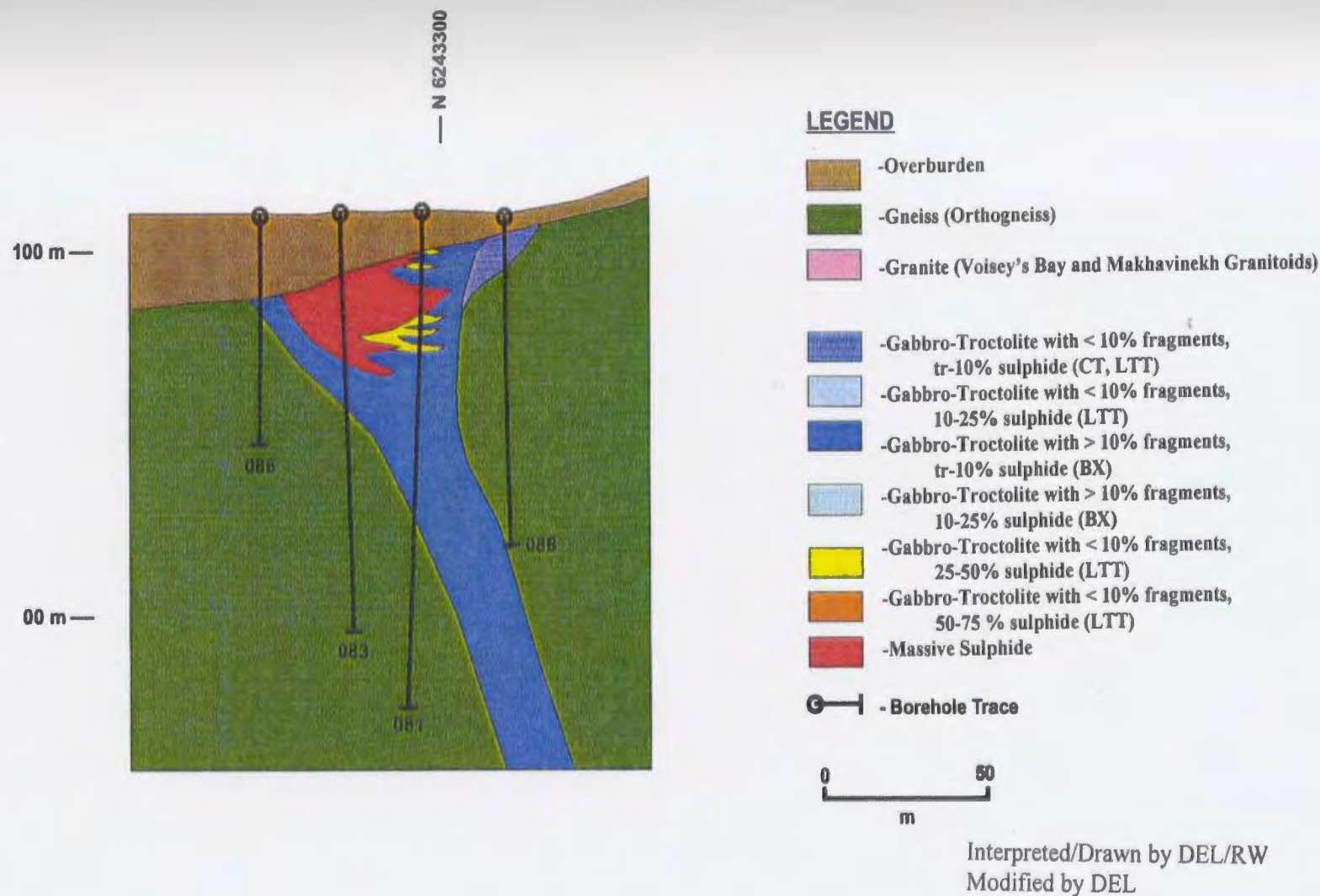


Figure 5.5 A west-facing geological cross-section through L10+50E in the Mini-Ovoid. Along this section only the base of the Mini-Ovoid is preserved; progressively to the west, the plunge of the conduit places the Mini-Ovoid at higher topographic levels and above the surface of erosion. This site, however, does express a gradational change from a narrow conduit domain (i.e. feeder) into a wide conduit domain (i.e. trap). This results in the development of an intermediate regime or transitional zone (i.e. mouth or throat) which joins the wide and narrow conduit domains.

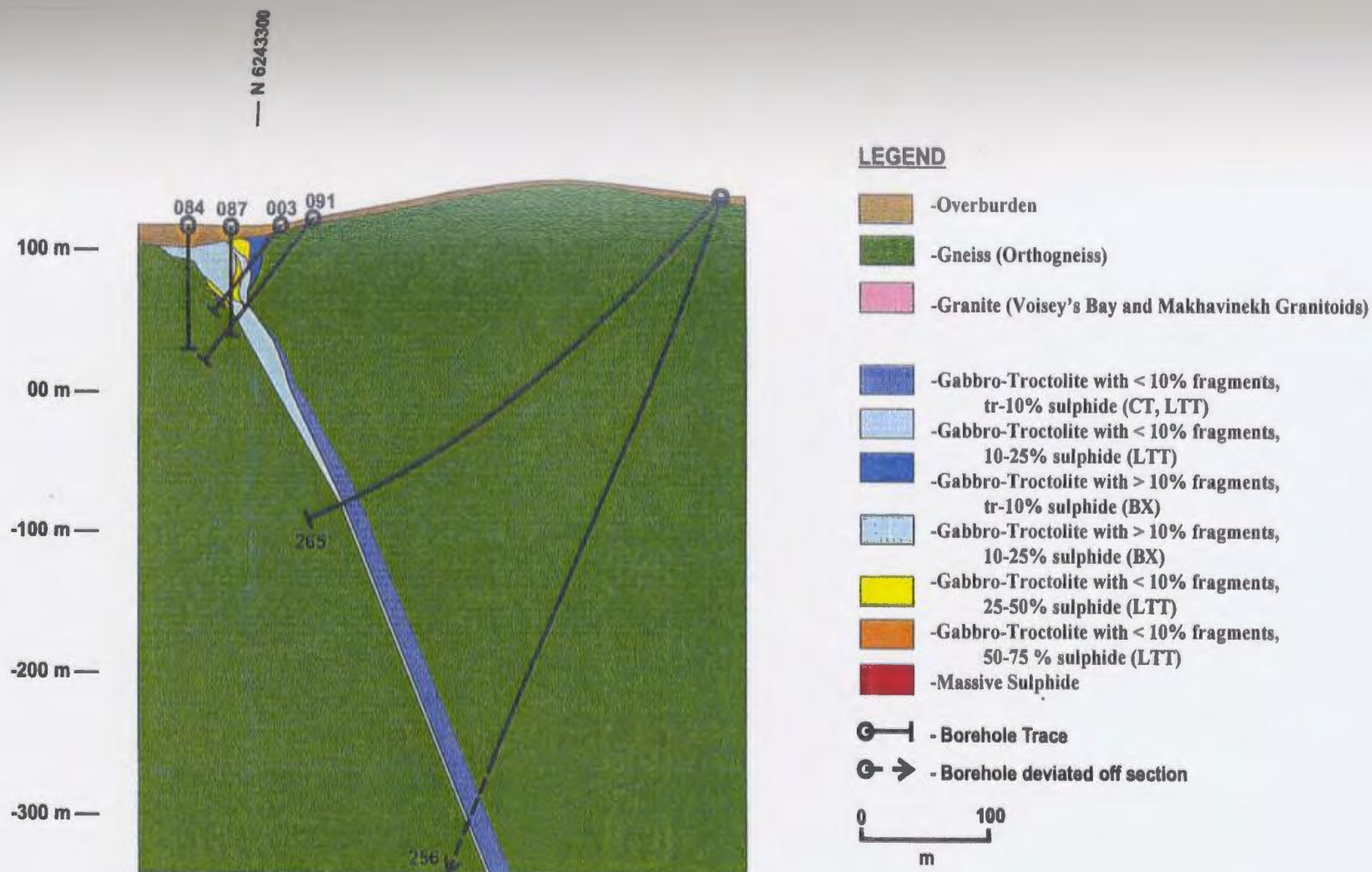
of dextral translation along late 030 ° joint planes (Evans-Lamswood, 1996b) as is speculated to occur with L12+50E (Figure 4.1).

5.1.5 Transition from L11+00E-L10+50E through L10+00E

Upon reaching L10+00E (Figure 5.6), it is apparent that the bulbous Mini-Ovoid trap has been eroded with only remnants of the funneled shaped entrance (i.e. mouth) to the conduit are preserved. With the conduit remaining intact, the skewed contact between the conduit and trap is once again present, as previously established by L12+50E - L11+50E (Figures 5.1, 5.2 and 5.3). Geometrically it is evident that the dominant northeast plunge of the trap and its captured mineralization is retained, as in sections L10+00E and L11+00E (Figures 5.6 and 5.4). Section L10+50E displays evidence for a discontinuity in the dyke between the adjacent sections, as on this section the dyke occurs far north of its interpolated projection. It is speculated that this slab has been translated to the north along the NNE conjugate strike/slip fault system, as speculated to occur between L12+00E-L12+50E (Figure 5.1) (Evans-Lamswood, 1996b). The apparent translation is dextral, indicating movement was induced by the 030 ° fracture system.

5.1.6 Transition from L10+00E through L9+50E

Continuing west, section L9+50E (Figure 5.7) exhibits a notable shift in geometry. The Mini-Ovoid trap has resumed the cylindrical styled symmetry, previously referred to as a tulip shape, in contrast to the cauldron shape displayed by the Ovoid and sections



Interpreted/Drawn by DEL/RW
Modified by DEL

Figure 5.6 A west-facing geological cross-section through L10+00E in the Mini-Ovoid. Along this section only the lowest part of the Mini-Ovoid is preserved; progressing to the west, the plunge of the conduit places the Mini-Ovoid at higher topographic levels and above the surface of erosion at this site.

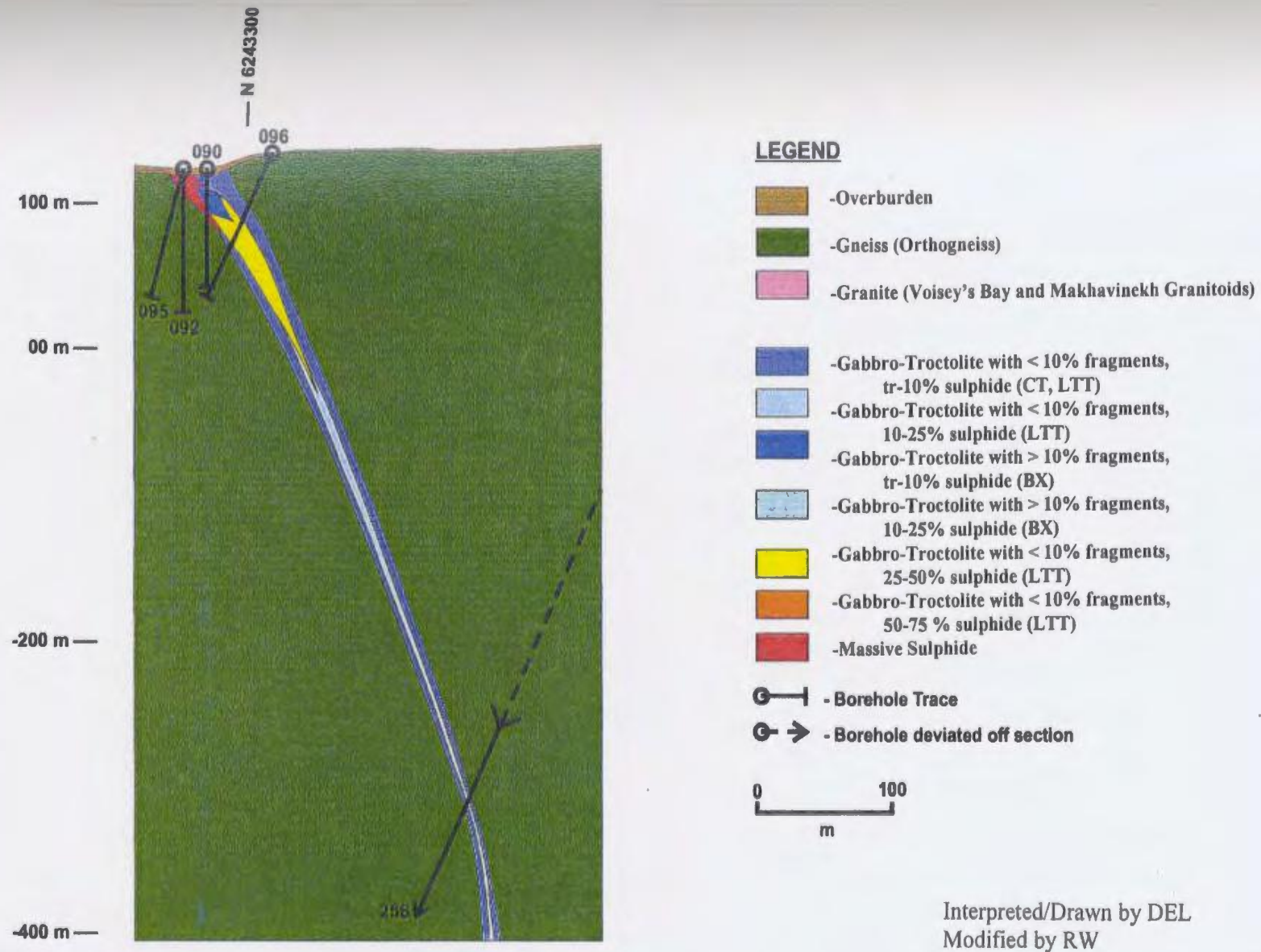


Figure 5.7 A west-facing geological cross-section through L9+50E in the Mini-Ovoid. At this location, the plunge of the conduit places the Mini-Ovoid above the level of erosion. Therefore, at this site only the narrow domain of the conduit is preserved.

L11+50E-L10+00E (Figures 5.3, 5.4, 5.5. and 5.6). Correlative with the geometric changes, the thick massive sulphide lens reappears in direct contact with the footwall gneiss. As previously viewed on sections L12+00E-L11+00E, the geometry has resulted in the formation of a shelf for the effective collection of sulphides. The shallow walls provided a favorable environment for sulphide capture and retention. Generally upon entering a trap regime, magmatic transfer is reduced, however, at this site, the feeder and trap domains do not differ greatly in width and, as well, the shallow inclination of the footwall interface could have provided a medium for the collection of sulphides. The sulphides could gravity settle onto this surface where the conservative dip of the medium provided an effective shelf for collection. As well, the moderate inclination prevented the bulk of the sulphides from slumping down, back into the feeder and, therefore, allowed for the capture and retention of significant sulphides.

The plunge of the mineralization is ambiguous since the previous sections are devoid of substantial mineralization (probably a result of erosive levels) with which to compare and define accurate plunges. The dyke itself, however, appears to adopt a prominent east-west trend with a weak northeast trend to the mineralization with no apparent structural displacement (Figure 4.1).

5.1.7 Transition from L9+50E through L9+00E

Section L9+00E displays weak mineralization in a chaotic intercalated array (Figure 5.8). The sequences dominantly consist of veined massive sulphides and sequences of BX gabbros-troctolite. The conduit and Mini-Ovoid trap have the same geometry.

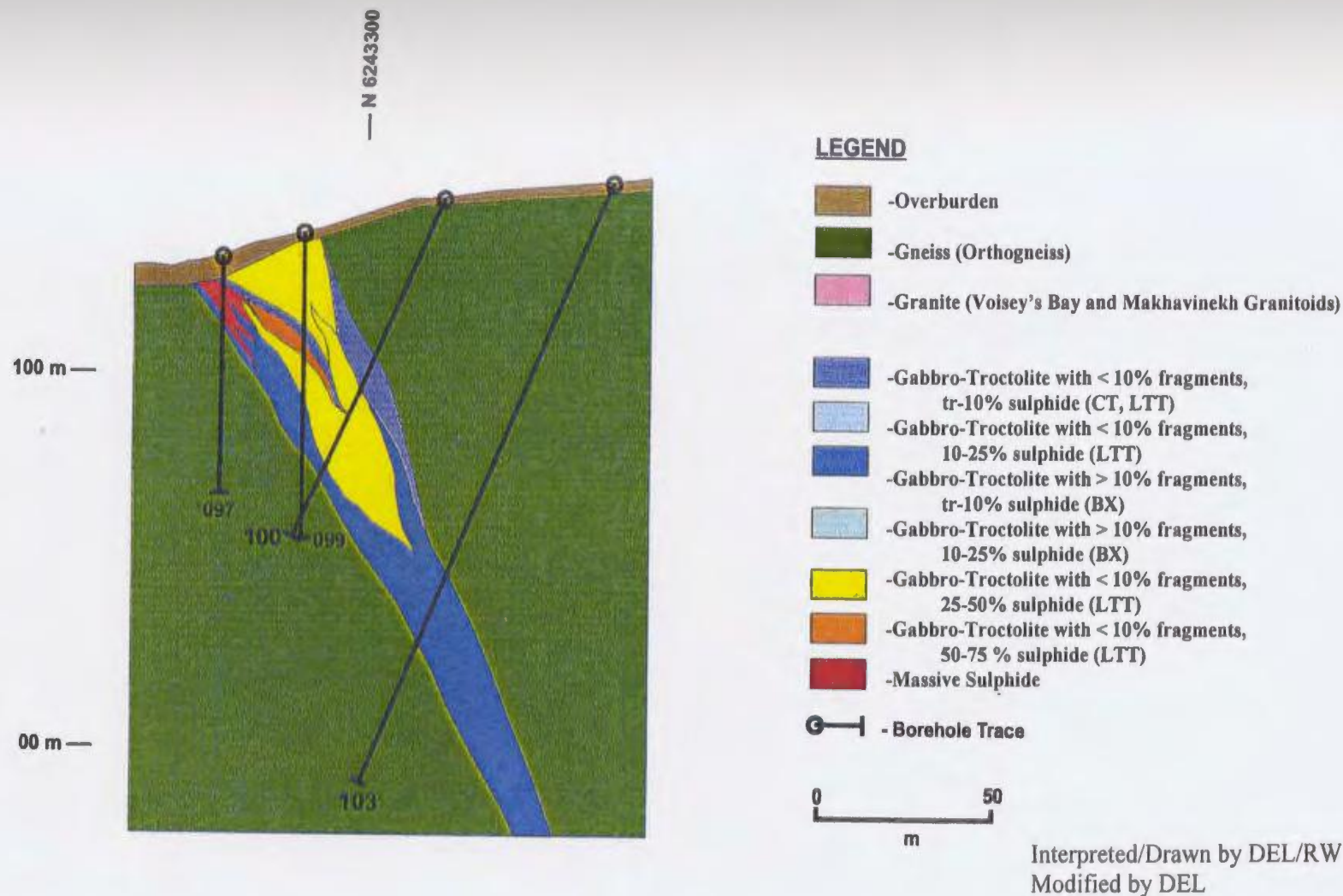


Figure 5.8 A west-facing geological cross-section through L9+00E in the Mini-Ovoid. At this location the plunge of the conduit places the Mini-Ovoid above the level of erosion. Subsequently, at this site only the narrow domain of the conduit is preserved. The mineralization appears stratified, and is preserved as continuous sequences indicating this was not a turbulent environment where mixing processes were favoured.

Significantly, the domain for sulphide capture along this section is not a trap in the true sense. The dimensions and orientation of this sulphide host are consistent with that of the lower conduit and not with that within the upper part of the conduit (i.e. trap). It is realistic to assume the true bulbous trap, represented by the Mini-Ovoid, was initially present at upper stratigraphic levels. It is also speculated that at this locality the feeder-trap conduit system had a steep attitude, hence sulphides could have accumulated at this site as they slumped down from the trap domain or, alternatively, were unable to be expelled through the throat of the conduit into the trap.

As in the previous section (Figure 5.7), the dyke appears to maintain a homogeneous east-west trend and a primary northeast plunge to the mineralization.

5.1.8 Transition from L9+00E through L8+50E, L8+00E and L7+50E

Continuing the traverse west through the conduit system, sections L8+50E, L8+00E and L7+50E (Figures 5.9, 5.10 and 5.11) show vertical transects through the conduit with the obvious absence of trap geometry. If geometric continuity is retained with the preceding sections, the trap and feeder entrance (i.e. throat) would occur up-plunge of this transect, prior to erosion, leaving only the conduit intact. The dyke continues to maintain homogeneity in strike with an east-west trend, as established by sections L10+50E - L9+50E.

Although exposure of the mineralized zones is limited, the conduit system appears to adhere to a primary northeast plunge, inferring that it has not been structurally displaced. Only limited geology is preserved along these transects showing the chaotic

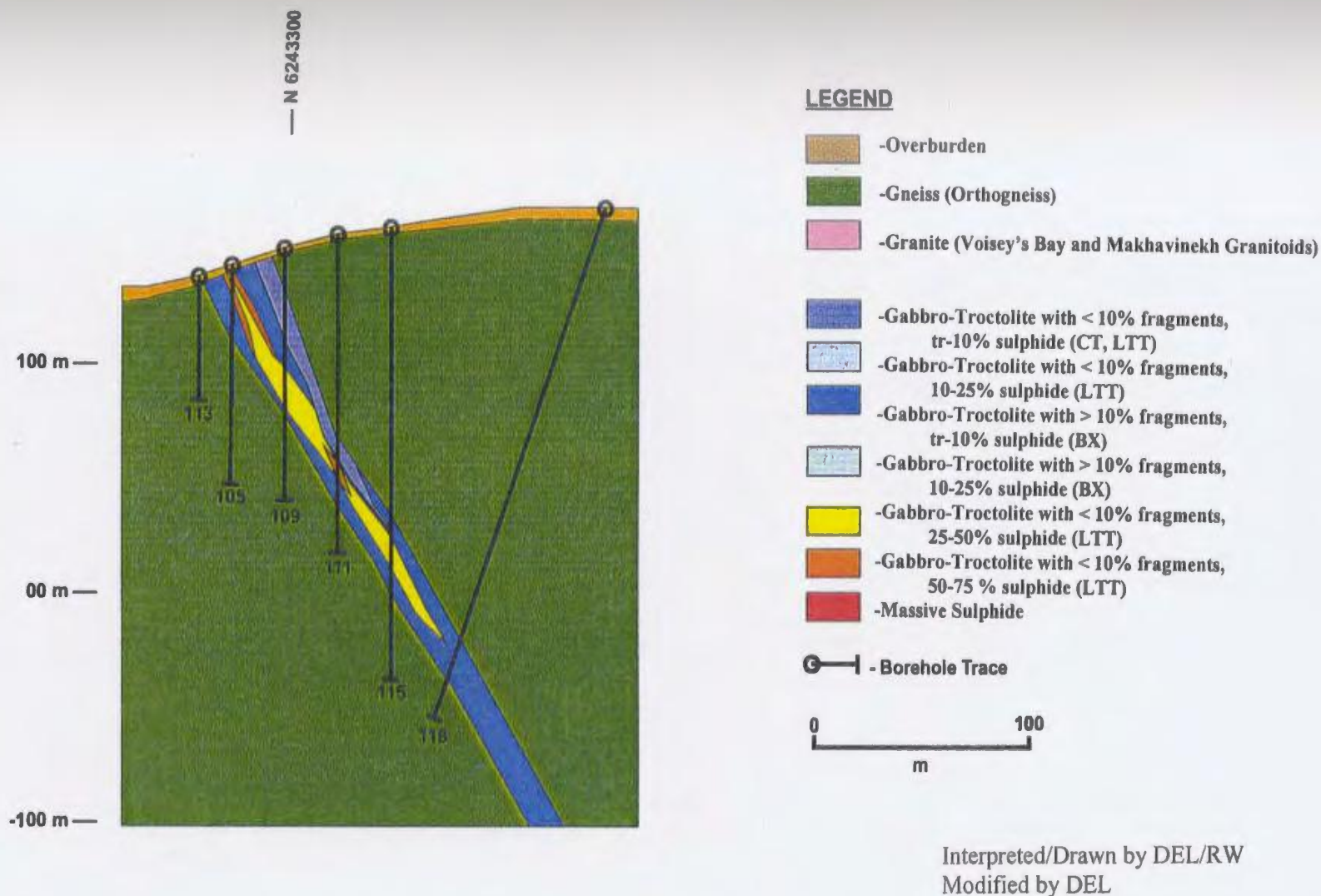


Figure 5.9 A west-facing geological cross-section through L8+50E in the Mini-Ovoid. At this location the plunge of the conduit places the Mini-Ovoid above the level of erosion. Subsequently, at this site, only the narrow domain of the conduit is preserved. The mineralization appears stratified, and is preserved as continuous sequences indicating this was not a turbulent environment where mixing processes were favoured.

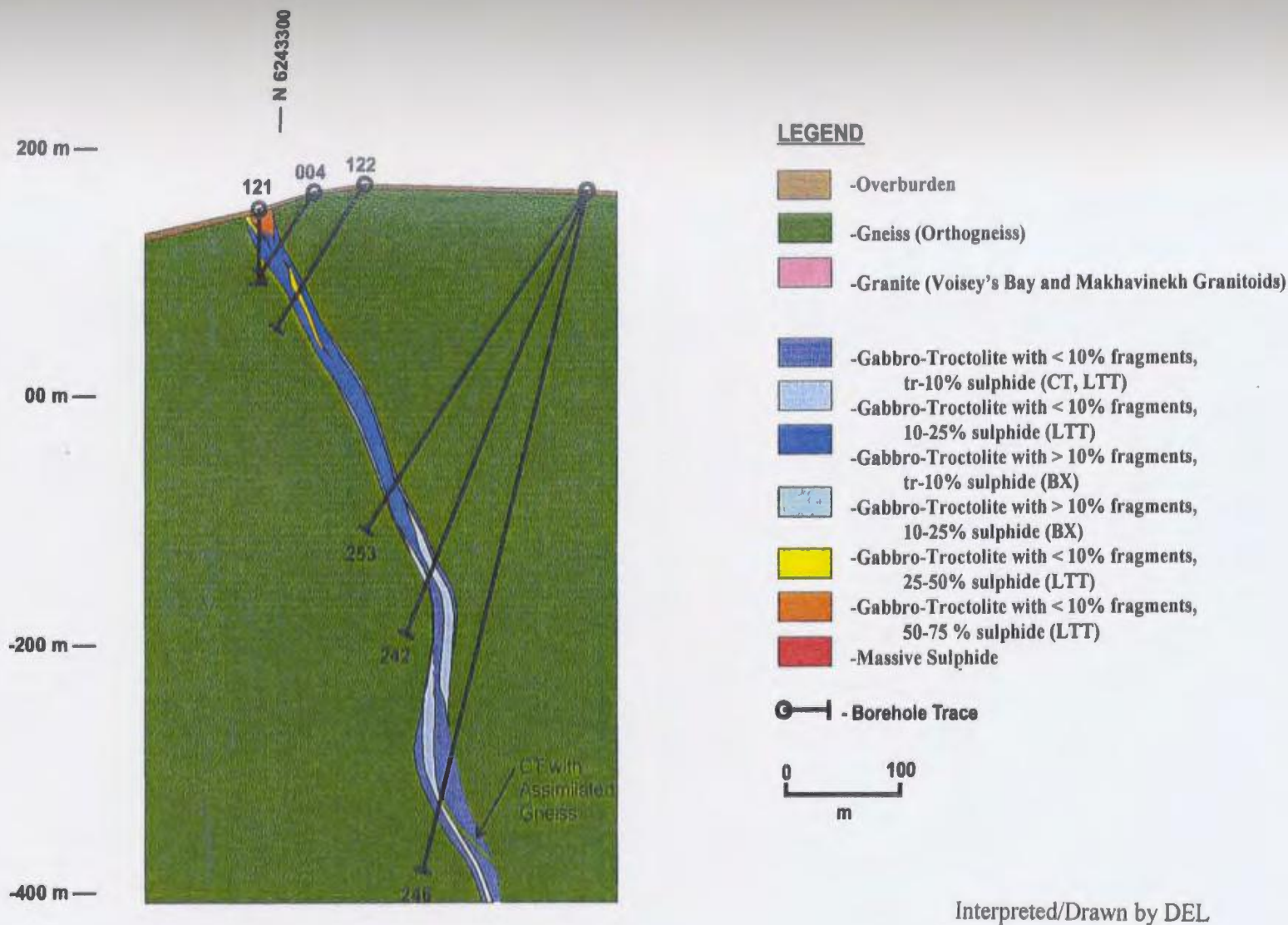
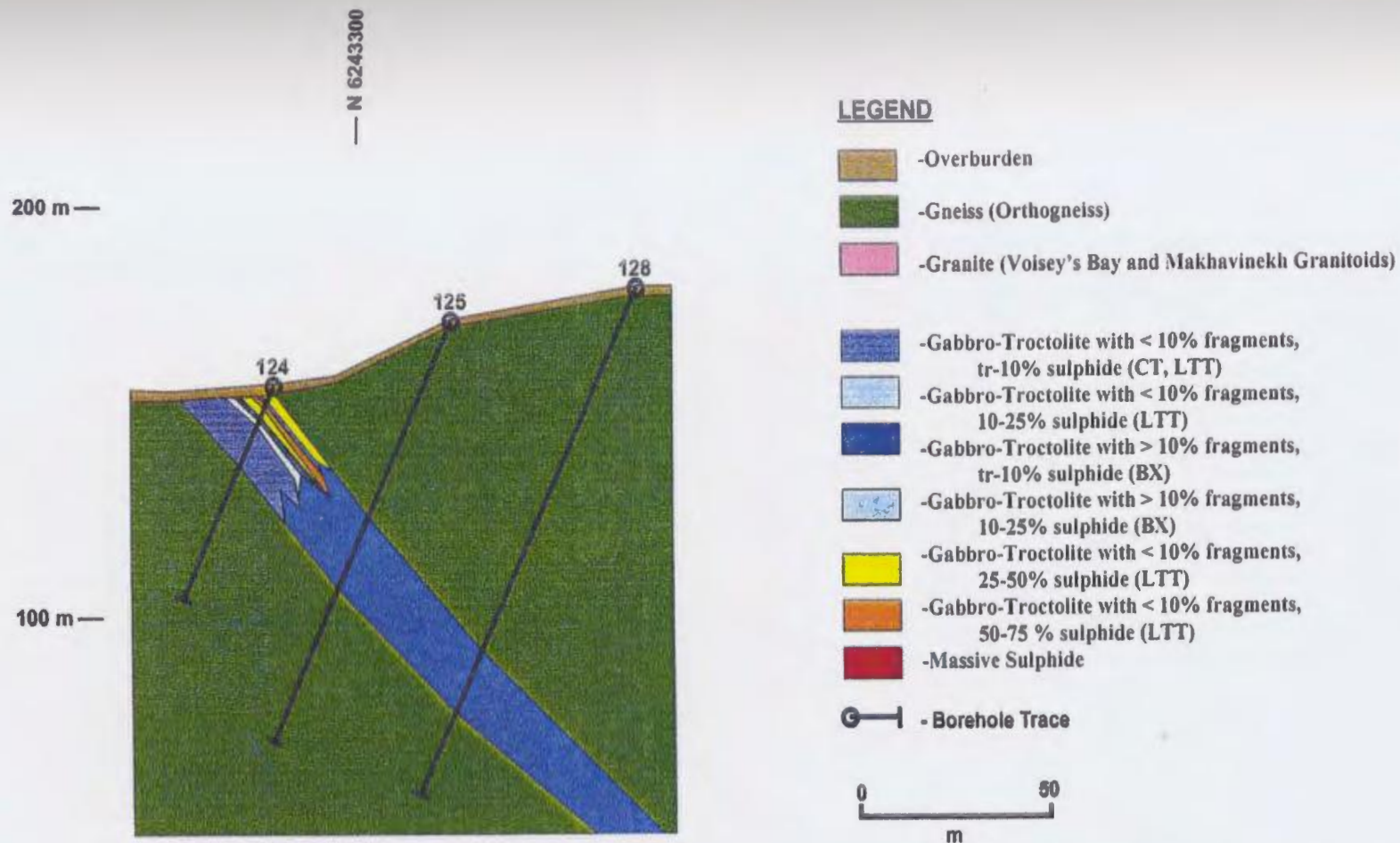


Figure 5.10 A west-facing geological cross-section through L8+00E in the Mini-Ovoid. At this location, the Mini-Ovoid trap plunges above the level of erosion and, therefore, is not preserved at this site. At depth, the conduit appears to bend and flex. These changes to the geometry of the conduit result in the segregation of magmatic material through their density contrasts.



Interpreted/Drawn by DEL/RW
Modified by DEL

Figure 5.11 A west-facing geological cross-section through L7+50E in the Mini-Ovoid. At this location, the plunge of the conduit places the Mini-Ovoid above the level of erosion. Subsequently, at this site, only the narrow domain of the conduit is preserved.

intercalation of BX gabbros-troctolites and semi-massive sulphides, morphologically typical of the environment within the lower, narrow conduit environment, and not of the wider trap environment. With the absence of the weakly mineralized and chilled sequences, as are present on L8+50E, section L8+00E appears to be stratigraphically higher. It is inconclusive as to the relative stratigraphic position of L7+50, due to the limited geological exposure.

5.1.9 Transition from L8+50E, L8+00E, L7+50E through L7+00E

Figure 5.12 characterizes the geological interpretations at L7+00E and represents the transition from the Mini-Ovoid into the Western Extension. Originally, due to the lack of drill data, the position of this domain change was arbitrarily assigned as being proximal to the Mini-Ovoid. It has subsequently been realized that at this site, the geometry of the conduit is significantly altered, resulting in the development of a new trap environment within the conduit system (Evans-Lamswood, 1997b).

This section documents an expansion to the conduit width in association with a weak accumulation of disseminated sulphides. It is interpreted that a new trap is developing at this site which was not detected in the previous sections. Conversely, it could be argued that this anomalous accumulation of sulphides is just a continuation of mineralization from the Ovoid trap, however, this interpretation would not agree with evidence supporting a northeast plunge to the conduit. In order to maintain geological continuity with the sections documented to the east, this domain (i.e. L7+00E) would have to have been subjected to a mesoscopic or macroscopic deformational event, resulting in a

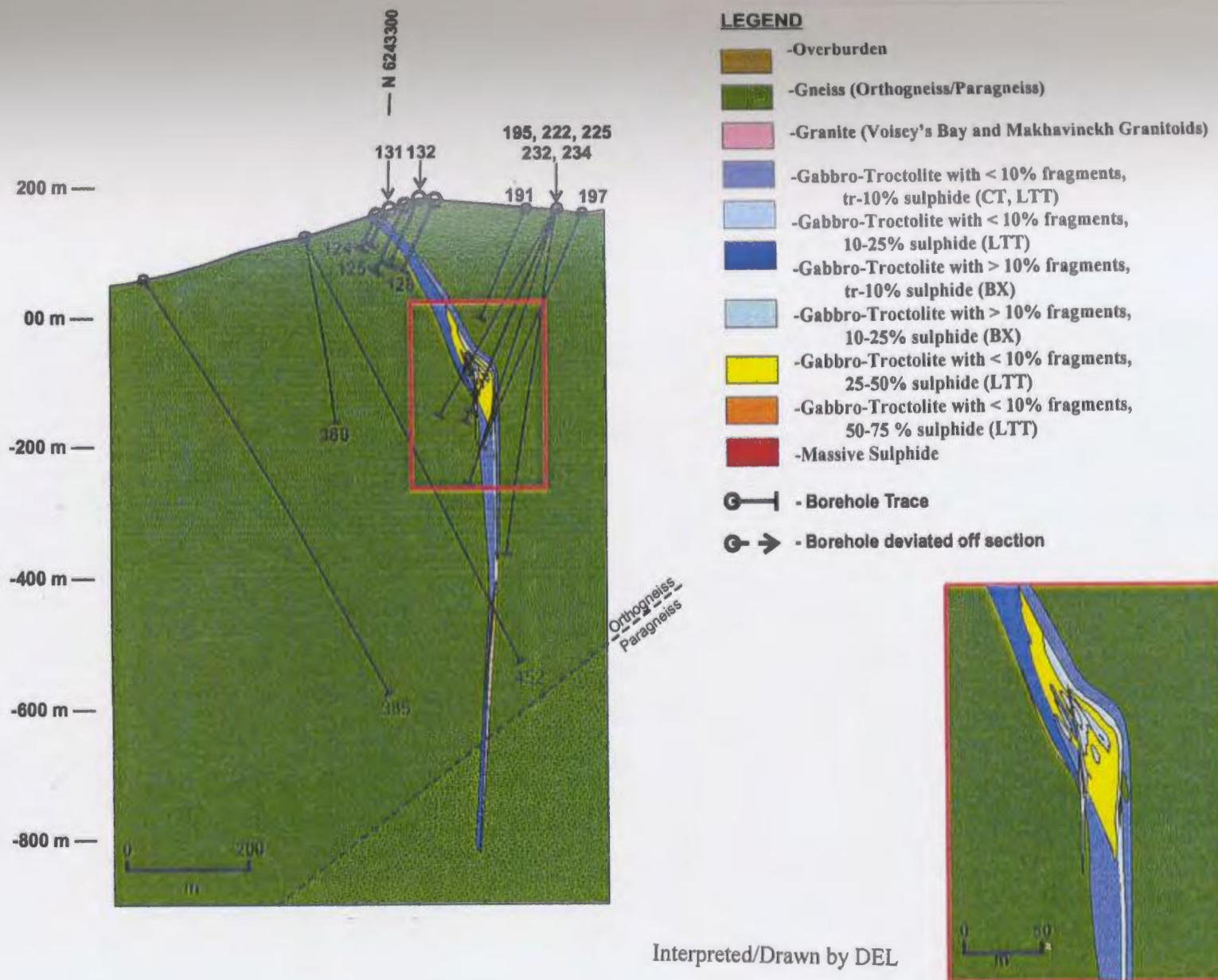


Figure 5.12 A west-facing geological cross-section through L7+00E in the Mini-Ovoid. An anomalous accumulation of sulphides are found at a site where the geometry of the conduit changes. At this site, the conduit changes from a north dipping to a sub-vertical to a south dipping structure.

150 m dip/slip displacement in the lithostratigraphy. Evidence for such an intense episode of deformation is not expressed in the area and contradicts the consistent dextral strike/slip events documented proximal to this zone.

5.2 Geometric Metric Changes to the Feeder in the Formation of a Sub-Trap

Sections from L12+50E to L7+00E documented geometric changes to the magmatic feeder conduit, and the effects of these changes on the capture of sulphides between the trap and the feeder domains. It is now important to the overall analysis of the conduit system to discuss the occurrence of other plunging mineralized zones besides the separate zones interpreted to be present within the Ovoid and Mini-Ovoid domains. By understanding and recognizing subtle geometric changes within the lower stratigraphic levels in the conduit, it may be possible to predict the occurrence of other potentially mineralized zones.

Pervasive through all the sections, inclusive of L12+50E and L7+00E, the feeder conduit is expressed as a moderate to steeply dipping, north channel. The continuity of this structure is only obviously disrupted upon reaching section L7+00E, as approached from the east. Subtle geometric changes are observed through the sectional slices, however, their significance is not truly appreciable until studied as a continuous geological structure incorporating smaller, parasitic geological domains.

5.2.1 Transition from L13+00E through L12+50E and L12+00E

The data expressed by L12+50E are limited, with the conduit viewed to only 95 m vertically below the trap. This geological section does, however, display the dramatic reduction to conduit thickness that occurs between the trap and feeder domains (Figures 3.1). L12+00E exhibits a deeper cut through the conduit, extending down to 225 m below the trap (Figures 5.2). Although drill data are sparse, environmental changes within the conduit can be recognized. The most significant change is displayed by the fluctuation in conduit thickness. At the trap entrance the conduit is wide, relative to L12+50E (Figure 5.1, see VB71), it shows a 50% increase in thickness for a true intersection of 20 m. Conversely, at depth the conduit appears more constricted as compared to its counterpart at the trap entrance, with a narrow width of only 10 m. This establishes a change in volume between the feeder conduit at lower stratigraphic levels and the conduit trap at higher stratigraphic levels.

Alterations made to the width (i.e. volume) of the conduit at depth result in significant changes to the local conduit environment. The most pronounced change is the absence of the sharp transition between the trap and feeder domains which is ambiguous on section L12+00E (Figure 5.2). The widening of the conduit at this site is gradational and, therefore, results in the development of a transitional zone where a new sub-domain or micro-trap is created. This domain will provide an intermediate zone where magmatic fluids will be segregated and partitioned before being chaotically expelled into the trap represented by the Mini-Ovoid.

At depth, the geological changes resulting from the thinning of the conduit are less obvious. however, there are three distinct features are developed; the first two being of a geometric nature and the third being lithological in nature: (1) between the upper and lower intersections, the conduit geometry narrows (constricts) by approximately 50%, (2) there is a weak flexuring of the conduit with a northward arching of the walls between these drill transects, and (3) at an intermediate depth (Figure 5.2, see VB188), the dyke displays a crude lithostratigraphy with the denser BX sequences adjacent to the south wall and the less dense CT rocks positioned tight against the north wall.

The segregation of dense magmatic material substantiates the evidence for flexuring in the conduit. As discussed in Chapter 3, when a local, but abrupt change is incurred in the trajectory of flow, the magmatic fluids can behave in a manner similar to that of a meandering stream system (Figure 3.6). When such a change in the trajectory occurs, fluids adhering to the outer walls of the arc will have faster velocities and will eventually erode the outer wall of the dyke through assimilation. This process can eventually gradually result in an expansion of the conduit width. Alternatively, magma flowing within the lower velocity zones, such as the inner arc of this flexure, will deposit fragmental debris and or segregate dense, fragment-laden fluids. Inevitably, a crude magmatic segregation will occur between these opposite sides of the conduit, as is apparent in this domain with the presence of a distinct lithostratigraphy.

At this location flexuring of the dyke is not explicit. It is reasonable, however, to conclude from the geological data presented that it may have had an active influence on the conduit widening, as is observed to occur at higher stratigraphic levels on this section.

5.2.2 Transition from L12+00E through L11+50E

The transect through L11+50E (Figure 5.3) displays geometric continuity with the lower stratigraphic intersection expressed by L12+00E. The transect extends to a vertical depth of 450 m below the trap. From L12+00E (Figure 5.2, see VB96233), an increase in the true thickness is observed in the dyke at depth (Figure 5.3, see VB96237).

Subsequently, it can be suggested that at this depth with the presence of a wide channel, magmatic fluids flowed at a rapid velocity unhampered by geometric constraints. This resulted in an integrated geological sequence without large, distinguishable stratigraphic horizons. As applied to section L12+00E, it can be speculated that at some position intermediate to L11+50E, the magmatic fluids flowed with high velocity and low viscosity. Similar correlations were noted in experimental fluid studies by Bruce and Huppert (1990), and Riley and Kohlstedt (1990). Once encountering a constriction in the channel (Figure 5.3, see VB96245), the fluids would begin to slow and cool, possibly resulting in some degree of choking in the system. In agreement with this interpretation, this change in width may not have been significant enough to hamper the overall flow of this system, but alternatively, may have initiated the segregation of the magmatic fluids. As a direct result, the denser fluids would begin to separate from the lighter less dense magma (Figures 5.2 and 5.3, see VB96188 and VB9678). With this segregation of magmatic material based on density contrasts, and with only insignificant loss to velocity in the respective media, it can be assumed that intermediate of VB233 and 237 (Figures 5.2 and 5.3), a forced expansion in the dyke occurred as a flexure was encountered. The distribution of lithologies at the

constriction (Figure 5.2, VB233) will not display distinct patterns of segregation. This only occurs through the processes invoked by constriction and, therefore, will not be present in the system until the magma has passed through this structure.

5.2.3 Transition from L11+50E through L11+00E and L10+50E

Sections through L11+00E and L10+50E (Figures 5.4 and 5.5) add little to the geological interpretations of the deep feeder morphology at depth due to the lack of drill data at level. Each section does, however, concur with the geometry of section L12+00E (Figure 5.2) in that the feeder expresses a wide throat domain. Furthermore, if drilled at depth, evidence may prove that each section is imitating the bending and contraction of the conduit at depth, as expressed by L12+00E and L11+50E. It might be geologically accurate to suggest that each transect would probably exhibit an increase in the degree of flexuring from that observed in the more eastern section.

5.2.4 Transition from L11+00E and L10+50E through L10+0E and L9+50E

The transects through L10+00E and L9+50E (Figures 5.6 and 5.7) appear to repeat geometric changes previously viewed. At a vertical depth of 375 m below the sulphide trap, the feeder conduit is observed again to be constricted to a width 8 m (Figure 5.7, see VB96256). Although thin, the conduit hosts an apparent and distinguishable stratigraphy. It is proposed that at this position, the necking of the conduit may have effected the transfer rate (i.e. flow velocity) of the magmatic fluids (cf. Bruce and Huppert, 1990; and Naldrett *et al.*, 1996), in that, as the fluids tried to funnel through the constriction, flow was obstructed. Once flow was restricted the transfer of magma

decreased, favouring the segregation of the magma into horizons of contrasting densities, as documented elsewhere by Koyaguchi and Blake (1991) and Turcotte (1990).

5.2.5 Transition from L9+50E through L9+00E, L8+50E and L8+00E

Sections through L9+00E (Figure 5.8) and L8+50E (Figure 5.9) lack drill data at depth and consequently cannot provide geological information on the lower stratigraphic horizons of the feeder. Each section does, however, appear to agree with the development of a large throat domain, as observed on section L12+00E.

The geological cross section through L8+00E (Figure 5.10) provides the most complete view through the conduit at depth. The three drill holes (VB96253, VB96242 and VB96246) intersect the dyke, respectively, at the approximate vertical depths of 235 m, 300 m and 460 m, respectively, below the trap. VB96246 portrays an increase in the width of the conduit, approximately 35 m in true thickness. Significantly it also displays two distinct stratigraphic horizons, namely the weakly mineralized troctolite and a mixed troctolite-gneiss package. The troctolite horizon is displayed adjacent to the south wall of the conduit with the mixed sequence close to the north wall. Although evidence for the conduit geometry below this stratigraphic position is not present, the geometry is inferred by the presence of stratified geological sequences and by an increase in the respective width of the conduit. This geological interpretation is in agreement with the north dip interpreted in previous sections (see above). The partitioning of the specific lithologies and the expansion in width consequentially, indicate that this intersection is the apex of a mesoscopic flexure with the troctolite segregated into the outer arc (south wall) and the

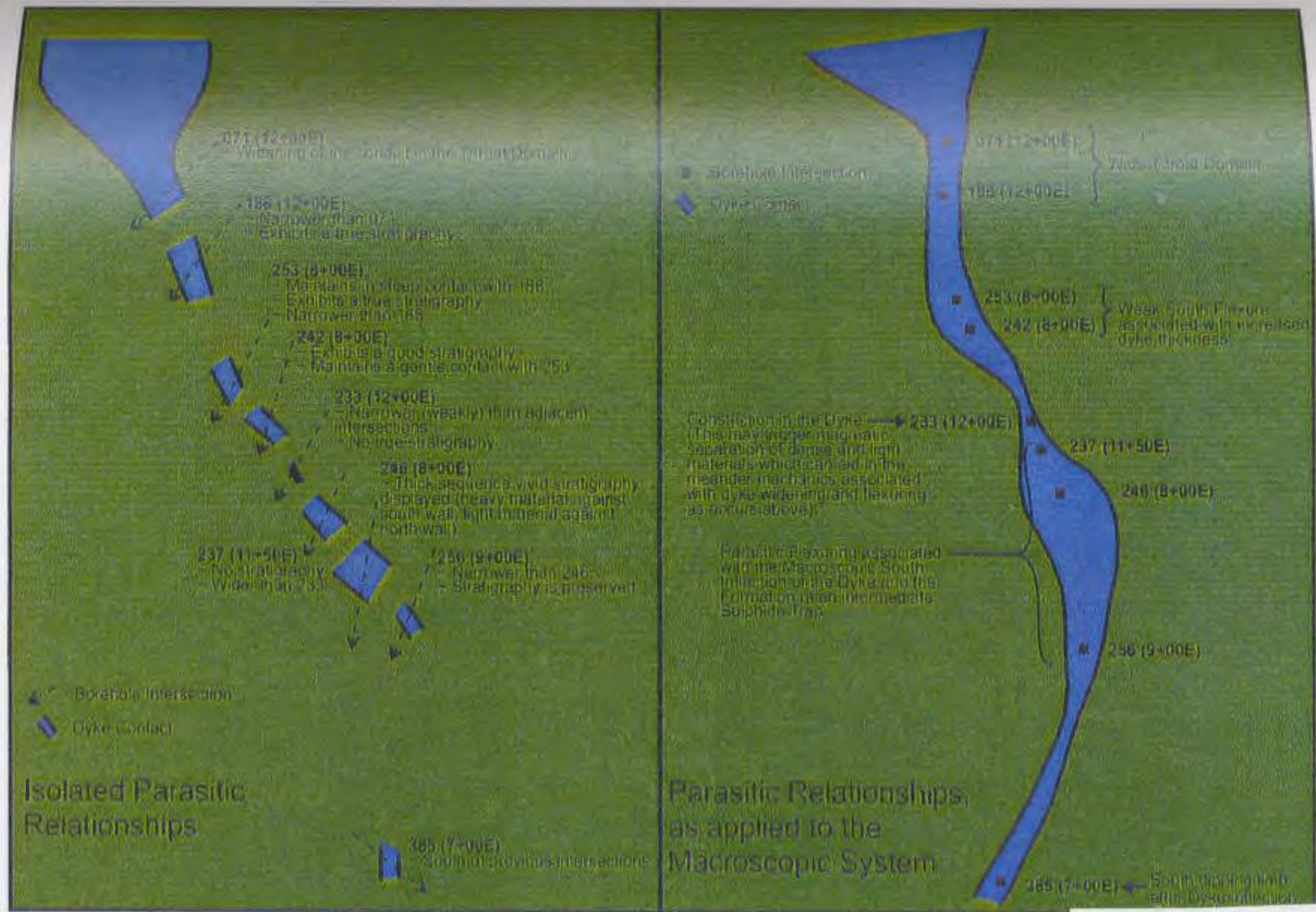
mixed sequence flushed to the inner arc (north wall) (Figure 3.6) of the conduit flexure. This interpretation, however, does not agree with the positions of the stratigraphic units as they are documented. The concept of a major flexure at this location is geologically significant, however, the direction of this flexure must be reconsidered.

Continuing with this geological cross section, drill holes VB96253 and VB96242 display 30 m and 25 m intersections through the conduit; there are no in-fill data intermediate of these intersects, thus interpretations are ambiguous. VB96242 does, however, display a crude stratigraphy inferring that some unobserved geometric changes may have occurred to the conduit.

5.2.6 Transition from L9+00E, L8+50E and L8+00E through L7+50E and L7+00E

The slice through L7+50E (Figure 5.11) restricts geological information to the upper stratigraphic levels of the conduit, but the adjacent section through L7+00E provides exposure at depth. This transect through the conduit is probably the most significant to date in terms of geometric and geological relationships. Changes in the conduit geometry are clearly evident in VB385 and 452 (Figure 5.12), substantiating geological interpretations indicated by L8+00E. This transect illustrates a significant change to the dip of the feeder, from a north to a south dipping structure. Also, quite apparent is the association of a new sulphide trap at this site, as documented by the conduit intersections in VB253, VB242, and VB246 (Figures 5.10 and 5.13).

The micro flexuring and overall undulation of the dyke from L12+50E through to the present section were essential in the development of a new sulphide trap. Individually each change to the conduit geometry appears insignificant, but when integrated they



Interpreted/Drawn by DEL

Figure 5.13 A profile documenting evidence for parasitic changes within the conduit. When analyzed together, these features will predict the macroscopic geometry of the conduit. This process can locate sites in the conduit where changes in the geometry could have lead to the potential capture of sulphides.

indicate the slow, but progressive development of a new trap domain within the conduit (Figure 5.13). These are parasitic, mesoscopic geometric features and if not for the analysis of the small subtle changes, geometric structures such as the micro-tap formed on L7+000E and the deflection of the dyke to the south, could not have been predicted and could have been misinterpreted as a deformational translations (i.e. structural off-sets). If a significant sulphide trap can be created within a radius of 25-50 m of a thin, barren domain in the conduit, the potential applications to the search for other traps in a regional context are encouraging. The most significant aspect of this analysis is verification that the conduit is continuous with the Ovoid. This establishes the Ovoid as a macroscopic trap within the one continuous magmatic system with other (multiple) plunging sulphide traps such as the Mini-Ovoid.

Chapter 6: Investigation of Geological Environments and Flow Kinematics: The Western Extension.

6.0 Introduction

The Western Extension is comprised of two distinct lithostratigraphic sub-domains, the Reid Brook (*RBZ*) and the Discovery Hill zones (*DHZ*). The *RBZ* traces the conduit (i.e. dyke) at surface for 1.6 km (L15+00W to L1+00E) (Figure 4.1.), and at depth to over 1200 m. The *DHZ* is continuous with the *RBZ*, but follows the dyke as it is expressed from L1+00E to the western edge of the Mini-Ovoid at L7+50E (Figure 4.1.). The geology of the Western Extension reflects magmatic processes that occurred at depth within the conduit and provides an opportunity to examine the plumbing network to the magmatic system. Similar to the environments investigated in the Mini-Ovoid, the Western Extension displays the formation of sulphide traps within the conduit. These traps adhere to similar environmental and lithological parameters as those in the more eastern domains of the conduit (i.e. Ovoid and Mini-Ovoid), however, they cannot compare in scale.

As examples of deep magmatic processes, the *RBZ* and *DHZ*, provide valuable information on the controls for sulphide distribution within the system and, as well, supply evidence to support the geological models introduced within the previous chapters. For example, the *RBZ* and the *DHZ* document splays or bifurcations in the magmatic conduit; the L7+00W zone in the Reid Brook domain, and the Bifurcation zone in the Discovery Hill zone. Such evidence supports the Octopus Model, where multiple feeders are thought to branch from a parental conduit.

The *RBZ* is geologically distinct from the *DHZ* in that it is at a lower position in the conduit stratigraphy and, therefore, plunges beneath the *DHZ*. The *RBZ* is contained

within a south dipping segment of the conduit below a major geometric inflection point. The DHZ plunges beneath the Mini-Ovoid and is constrained to the vertical, north dipping, segment of the conduit. Within the Western Extension, neither the Mini-Ovoid, nor the Ovoid are preserved, as these traps are positioned high within the conduit stratigraphy, plunging above the level of erosion in this area.

6.1 The Reid Brook Zone

6.1.1 Relationship to Magmatic Sub-Chamber

The Reid Brook zone profiles geology at the lowest stratigraphic levels as yet exposed in the Voisey's Bay system. Cross-sections through L15+00W - L7+00W illustrate a significant geological relationship in that the south dipping conduit is in contact with the upper margin of the Western Deeps chamber (*WDC*) (Figure 6.1). The silicate and sulphide textures expressed in the WDC are strikingly different from those which are documented by the lithologies within the conduit (see Chapter 2). In this chamber, the geology consists of barren to weakly mineralized, variable to normal textured gabbroic to troctolitic rocks, with a small quantity of fragments (less than 10%). The distinction between the conduit and the chamber is not only made with reference to the textural attributes of each body, but by a physical break separating the two magmatic structures. This break is documented by the preferential intrusion of granitic veins along the conduit/chamber contact. The conduit and chamber, to date, have not been observed to be in direct contact within this zone, but have always been observed separated by the

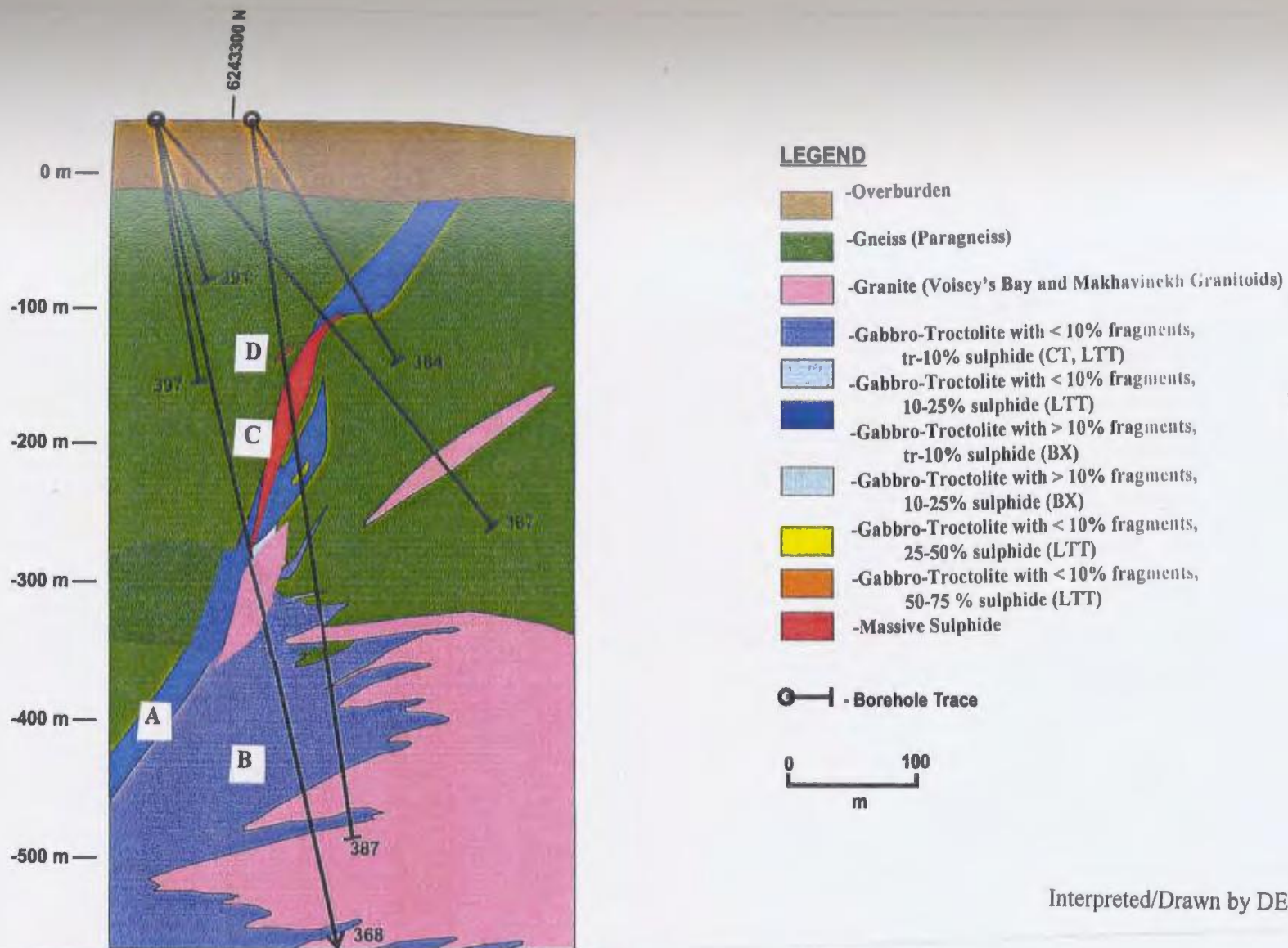


Figure 6.1 A west-facing geological cross-section of L9+00W in the Reid Brook Zone. Only the south-dipping limb of the feeder conduit is preserved. The sub-vertical and north-dipping limbs which host the Ovoid and Mini-Ovoid, plunge above the level of erosion. Furthermore, in this area, the feeder conduit is found at the top of the Western Deeps chamber: (A) Feeder conduit, (B) Western Deeps chamber, (C) Massive sulphides contained within the feeder conduit, (D) Massive sulphides splayed into the country rock.

granites. Furthermore, in the RBZ, the conduit not only follows the upper contact of WDC, but continues to focus along its southern, moderately dipping, margin. It is speculated, that the WDC was established prior to the intrusion of the conduit and, therefore, provided a structurally weak margin for which the conduit could preferentially propagate along. As well, this incompetent interface (i.e. chamber margin) would be a favourable site to accommodate dilation (see Chapter 8) and the subsequent intrusion of granite veins.

6.1.2 Plunging Massive Sulphides (Hanging/Footwall Mineralization)

Another significant geological relationship documented within the RBZ, is the presence of late veined mineralization in both the footwall and hangingwall country rocks (Evans-Lamswood, 1997c) (Figure 6.2). The mineralization occurs as massive to semi-massive sulphides lenses, ranging in individual thickness from less than 1 m to greater than 30 m. Laterally the sulphide lenses have a 60-150 m extent (op cit.).

Between L15+00W and L7+00W, the sulphides appear to be generally constrained to the conduit, however, narrow splays intrude the hangingwall. Within this zone, the axial trend of the mineralization deviates; to the east the axis has a sub-horizontal, east-west trend, however, to the west, the axis appears to flex or arch establishing a shallow, west-southwest plunge. Significantly, two massive sulphide horizons are documented on L7+00W (Figure 6.3), which are interpreted to represent separate, but genetically related, sulphide bodies. As with its counterparts to the west, the upper massive sulphide member penetrates wall rock, preferentially in the footwall. As well, this horizon maintains

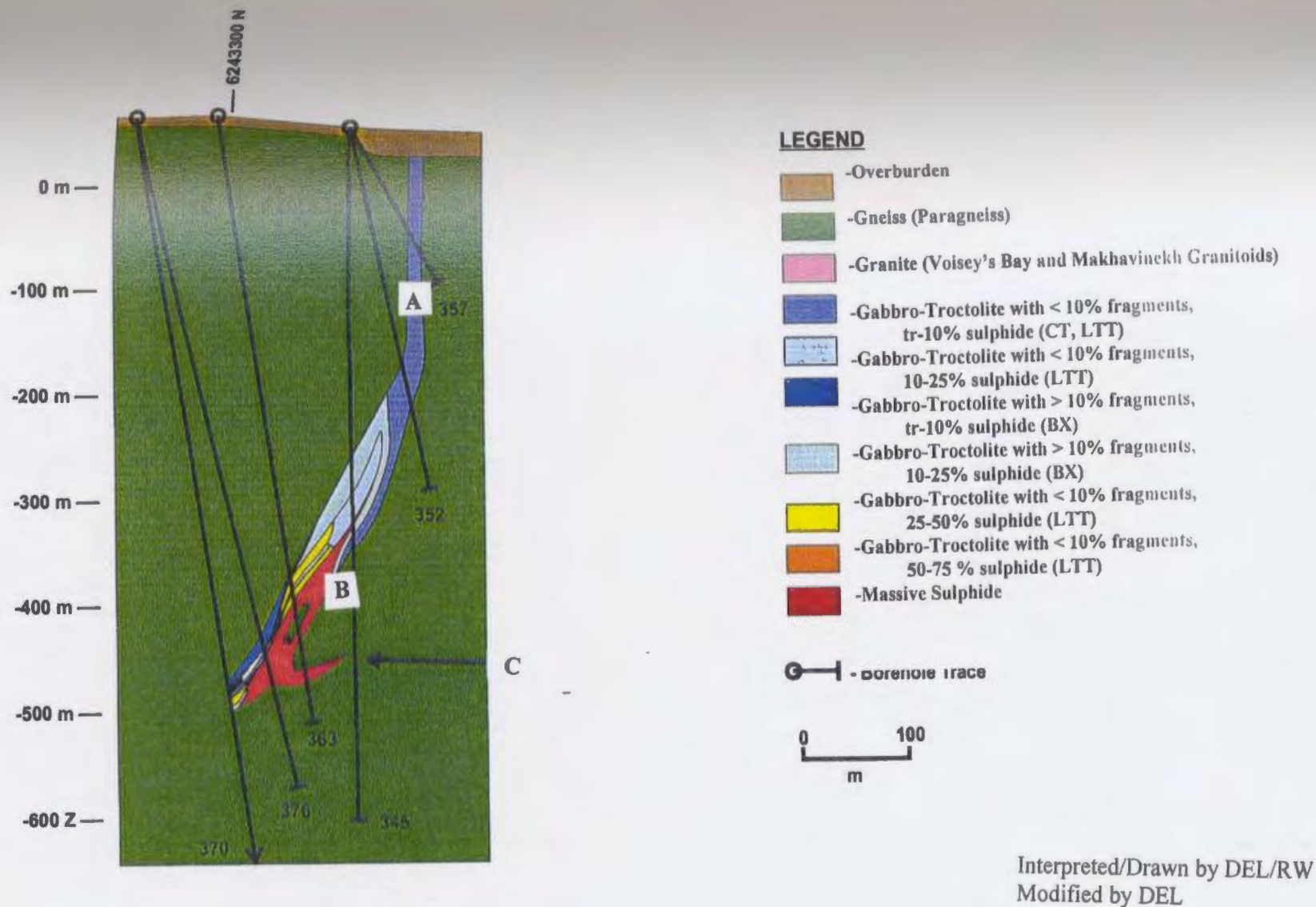


Figure 6.2 A west-facing geological cross-section through L4+00W in the Reid Brook zone. Only the south-dipping limb of the feeder conduit is preserved. The sub-vertical and north-dipping limbs which host the Ovoid and Mini-Ovoid plunge above the level of erosion. Massive sulphides are found within the feeder conduit and, as well, splayed into the country rock: (A) Feeder conduit, (B) Massive sulphides contained within the feeder conduit, (C) Massive sulphides splayed into the country rock.

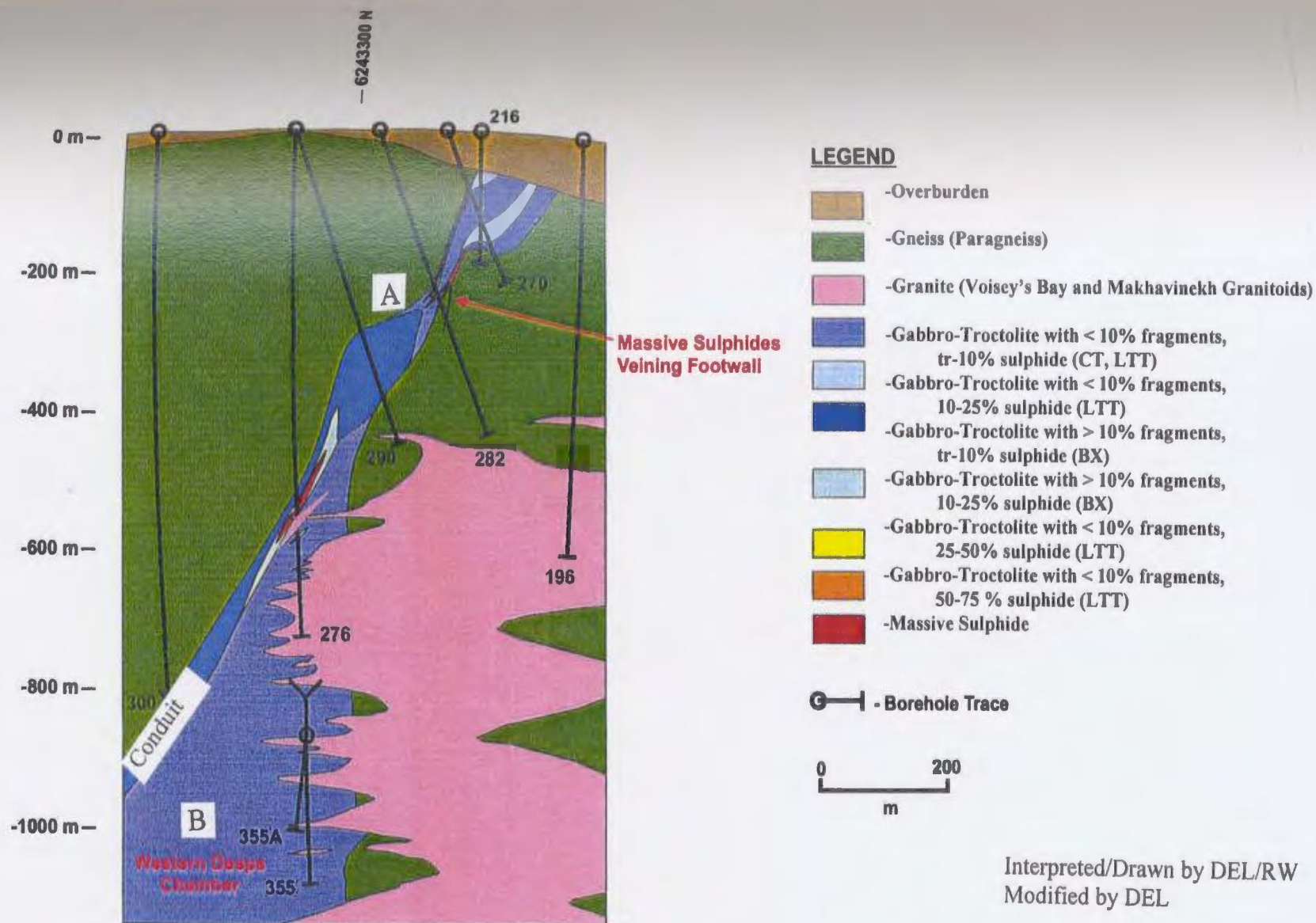


Figure 6.3 A west-facing geological cross-section through L7+00W in the Reid Brook zone. Only the south-dipping limb of the feeder conduit is preserved. The sub-vertical and north-dipping limbs which host the Ovoid and Mini-Ovoid plunge above the level of erosion. Furthermore, in this area, the feeder conduit is found at the top of the Western Deeps chamber. (A) Feeder conduit, (B) Western Deeps chamber.

geometric continuity with the more western massive sulphide horizons. Conversely, the lower massive sulphide horizon appears to be a primary, in situ constituent of the original feeder/conduit system, as it is totally constrained to the interior of the dyke and does not penetrate into the country rock. The appearance of two adjacent massive sulphide lenses that adhere to opposing physical parameters is of great geological significance. These features may represent the branching or bifurcation of a primary massive sulphide lens, produced by secondary deformation events, specifically the redistribution of sulphides (i.e. upper massive sulphide lens) along late conjugate faults (310°) (Figure 4.1.). It also suggests that post-emplacement structures may be potential sulphide hosts, and thus, establishes new exploration targets.

From L7+00W and through to L2+00W, the massive sulphides display a change in their plunge or axial trend from that which was previously established from L15+00W to L7+00W (i.e. gently inclined to the east). The massive sulphides continue to be splayed into the country as is documented between L15+00W to L7+00W, however, they are found within the footwall and not within the hangingwall. The thickest massive sulphides remain associated with the conduit/dyke like their western counterparts (i.e. L15+00W to L7+00W), but their orientation changes from a gentle easterly trend to a moderate to steep, southeasterly plunge (Evans-Lamswood, 1997c). Within this interval, the massive sulphide lens anastomoses and flexes, while migrating (east lateral) down to lower stratigraphic levels opposing the northeast plunge of the original in situ mineralization of the conduit found elsewhere in the deposit (Ovoid and Mini-Ovoid; see Chapters 4 and 5). Geological transects through this zone document the peculiar geometry of this mineralized

horizon and establish the presence of an anomalous southeast plunge to the body, and the formation of mineralized splays into the country rock (op cit.). This massive sulphide sequence does not conform to normal geometric patterns documented elsewhere in the conduit, but alternatively, establish it as a later cross-cutting geological feature.

The continuation of this massive sulphide horizon is recognized from L2+00W to L1+00E, however, there are two distinct changes to its expression. The sulphide body once again shifts its plunge axis and is observed to follow a west-east, sub-horizontal trend. Of further geological significance, the sulphide mineralization occurs in isolation, separate from the conduit. Stratigraphic positions established through the interpolation of known dyke intersections would normally be reliable for predicting stratigraphic horizons, however, unlike the previously areas discussed, this zone exhibits gaps in the continuity of the conduit. Where the massive sulphide lenses occur, the conduit can be observed stratigraphically up and down dip of the intersection, but rarely as a continuum. It is speculated the changes in the trend of the massive sulphides and the discontinuity with the adjacent conduit, are the products of structural influences that may be similar to those at the Sudbury Off-Sets (Naldrett *et al.*, 1984a, 1984b).

6.1.3 Conjugate NNE/NNW Faults

Later discussions (see below, chapter 7) will address the primary processes responsible for the initiation of these structures. These fractures are moderately dipping and maintain NNE/NNW trends (Figure 4.1.). In the Reid Brook zone, overburden prevents clear surface expression of these structures, however, their presence can be

clearly recognized in drill core. This structural style is also frequently observed in surface outcrop throughout the Main block (see Chapter 1, Figure 1.2.). Specific to this zone, the NNW fracture system appears to be the medium for the redistribution of early mineralization or the conduit for late phase mineralization. Evidence in support of this process has been gained through drill core examination which documents the coincidence of these structures with the mineralization.

The most prominent structures to transect this regime are the brittle-ductile, NNE faults. With respect to the dyke, the mid-point for the intersection of these structures aligns with L2+00W and L1+00E. Broad drill hole spacing in this domain does not allow for the specific delineation of these mesoscopic structures, however, it does allow for the extrapolation of broad, yet dominant structural trends. The NNE fault margins are preferentially recognized due to the drilling attitudes and with in-fill drilling the NNW conjugate faults should be more readily recognized.

With stratigraphic markers (massive sulphides and the conduit margins) used for the investigation of fault kinematics, a translation can be defined between L2+00W and L1+00E. An 150 m (approximate) sinistral, strike-slip movement is interpreted to occur along the NNE fracture system (Figure 6.4), but when isolated, the speculated sense of movement seems contradictory. As observed elsewhere, the NNE fracture system would initiate dextral translation with its NNW conjugate partner accommodating the sinistral movement (Evans-Lamswood, 1996b). It appears that the conjugate pairs acted coincidentally to define the cumulative dislocation (Figure 6.4).

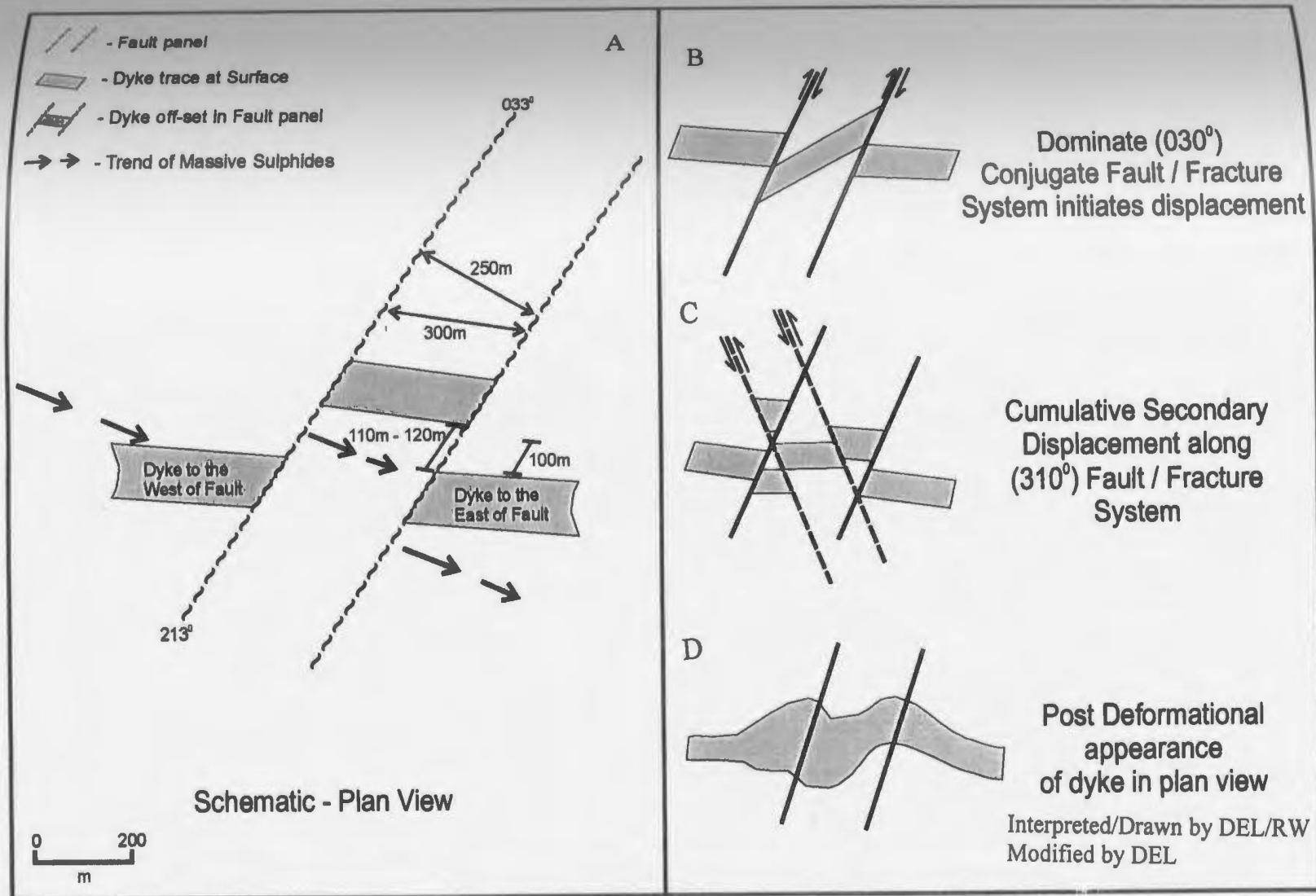


Figure 6.4 An idealized model (plan view) for structural displacement within the L2+00W to L2+00E fault zone in the Reid Brook zone. (A) A display of the current (post-deformation) position of the feeder conduit/dyke at surface and in relation to the axial trend of the massive sulphides. At surface, only the 030° structures, which are thought to represent Reidel brittle shears, are apparent. (B) The interpreted translation accommodated by the feeder conduit during early deformation as the 030° structures are developing. (C) With progressive deformational events, a 310° set of brittle shears are formed conjugate to the 030° set. (D) This figure displays zones where the conduit appears over thickened. This featured is created as sections of the conduit are translated and juxtaposed together through the 310° and 030° deformational events.

6.2 Discovery Hill Zone

6.2.1 Lithology

A relogging program in the Discovery Hill zone was initiated to establish a nomenclature that helps to explain and describe the relationships within the geological sequences of this domain. Previously this zone was characterized by terminology used to describe the simple lithostratigraphy present in the Ovoid. When nomenclature from the Ovoid was applied to the DHZ, the stratigraphic successions were grouped into broad, generic rock classifications. Such classifications could not provide the consistency required for detailed geological correlations between sections. The stratigraphy in the Western Extension is most accurately characterized when subdivided into the three environmental domains known as, the Feeder, the Noisy, and the Quiet domains (Figure 6.5 after Evans-Lamswood, 1997e).

6.2.1.1 Feeder Sequences

The Feeder sequence incorporates the earliest magmatic fluids that initially traversed and lined the conduit. There are three primary units comprising this succession, each maintaining a relative and consistent stratigraphic position within the conduit. These units are; the Marginal sequence (*MRS*), the Transitional sequence (*TNS*), and the Feeder Melange (*FM*) (op cit.).

Lithogeochemical analysis identification the MRS as a medium-grained, ferrogabbro (Lightfoot, 1997a, 1997b) (Figure 6.5). Mineralization is rare, but when

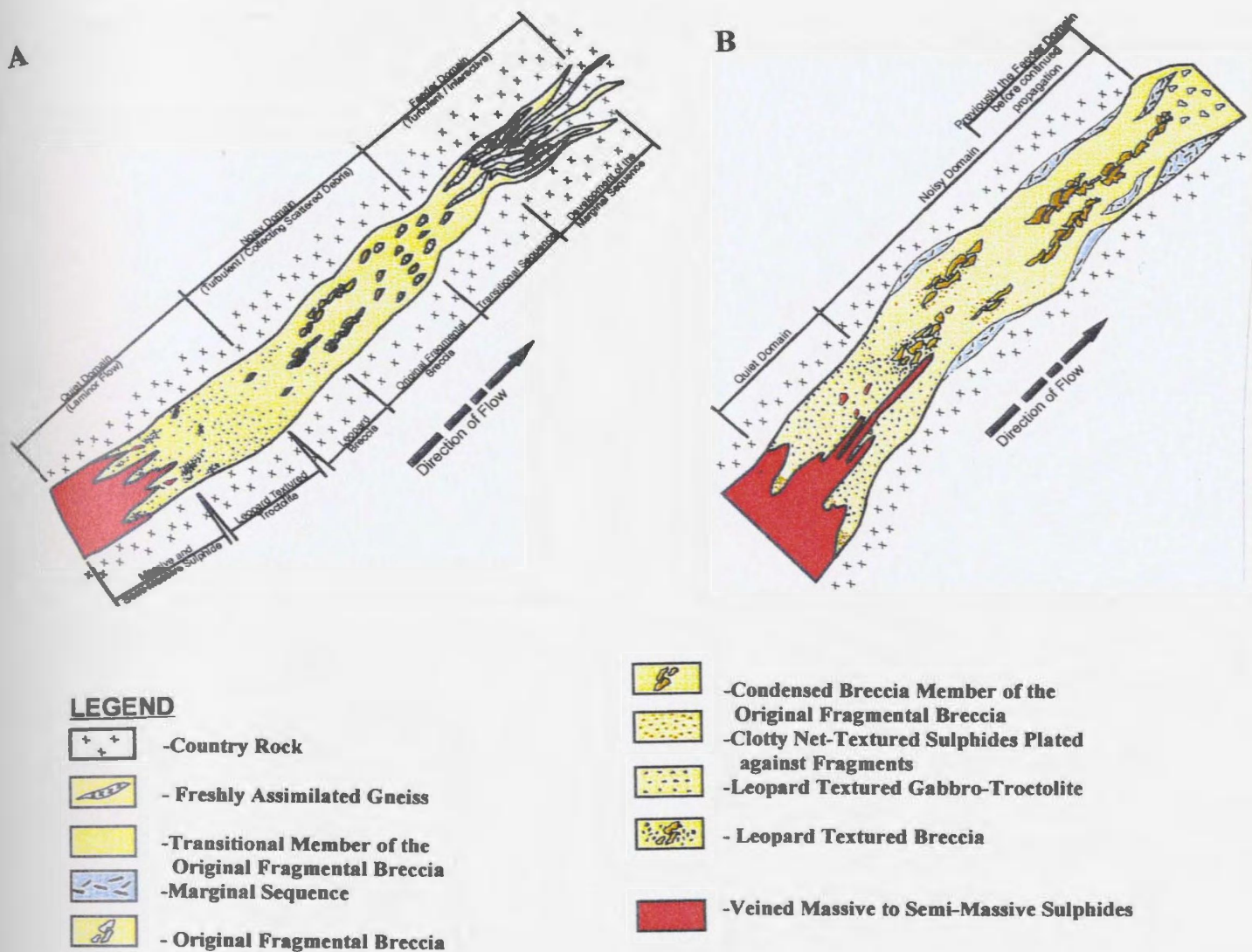
Environmental Domains in the Feeder Conduit	Lithology	Sulphide and Silicate Textures
<i>Feeder Sequence</i>	Olivine Gabbro - Ferrugabbro	Marginal Sequence
		Transitional Member
		Feeder Melange
<i>Noisy Sequence</i>	Gabbro-Troctolite with Disseminated Sulphides and Veined Massive to Semi-Massive Sulphides	Vein Breccia
		Leopard Textured Breccia
		Original Fragmental Breccia (Condensed Breccia Member and Transitional Member)
<i>Quiet Sequence</i>	Troctolite	Leopard Textured Troctolite
	Massive Sulphides	Massive Sulphides

Interpreted/Drawn by DEL

Figure 6.5 Lithologies and the sulphide and silicate textures associated with the three environmental domains (i.e. Feeder, Noisy, and Quiet domains) developed within the feeder conduit of the Discovery Hill zone (after Evans-Lamswood, 1997e).

present is observed in trace quantities as fine-grained disseminations. The MRS rocks occur as narrow, discontinuous horizons adjacent to the conduit walls. It is speculated that the discontinuous nature of this sequence is a consequence of dislocation and erosion by succeeding magmatic successions (Evans-Larnswood, 1997e). This horizon is irregularly associated with a narrow chilled margin adjacent to the gneiss contact, but otherwise, has been in a mixed, diffuse contact with the gneiss (Figures 6.6 and 6.7.1-10-j). Where a diffuse contact is present, this horizon clearly hosts various degrees of gneissic contamination. In this discrete stratigraphic position (Figures 3.2 and 3.6), it is thought that stoping and possible melt back processes resulted in the absorption of the wall rock (cf. Turcotte, 1990).

The texture of the MRS is inhomogeneous ranging from honeycombed to mottled. The honeycomb texture is defined by the relict patches of absorbed gneiss (Plate 2.F) which are frequently observed within the sequence. The boundaries of the gneissic inclusions are not always distinguishable since the magma not only streamed along their margins, but also penetrated their interiors along internal weaknesses. This pattern is to be expected when wall rock assimilation occurs through stoping and small splays of magmatic fluids weave through the wall rock interface in a net-like pattern (Figure 3.1.). In the mottled zones within the MRS, biotite alteration is prominent with subordinate chloritization of the mafic matrix. The appearance of biotite is thought to be either: (1) the consequence of a pre to syn-mineralization hydrous episode (D. Lee 1997, Pers. Comm.) or, (2) the product of alteration through further interaction with the country rock by later



Interpreted/Drawn by DEL

Figure 6.6 A and B show the development of the lithostratigraphy and textures as multiple magmatic pulses flow through the feeder conduit. (A) Lithological stratification developed within the feeder conduit during the early stages of magmatic injection and flow. The sulphide-poor, fragment-free ferrogabbros were the first magmatic pulse to enter the conduit and form the Feeder domain. The fragment-bearing gabbroic pulse was the next sequence injected into the conduit and initially did not develop a distribution pattern for the fragments. This magmatic pulse defined the Noisy domain. Finally, the significant sulphide-bearing sequences were expelled into the system and developed the Quiet domain. (B) As the feeder conduit evolves, the multiple magma pulses began to separate dense and non-dense material through flow segregation, therefore, some magmatic horizons propagated more rapidly through the conduit than others. Furthermore, when the separate magma pulses came into contact with each other, a density instability was produced. This process resulted in the mingling of magmas whereby, magma from the trailing pulses interfingered or veined magma from the earlier pulses.

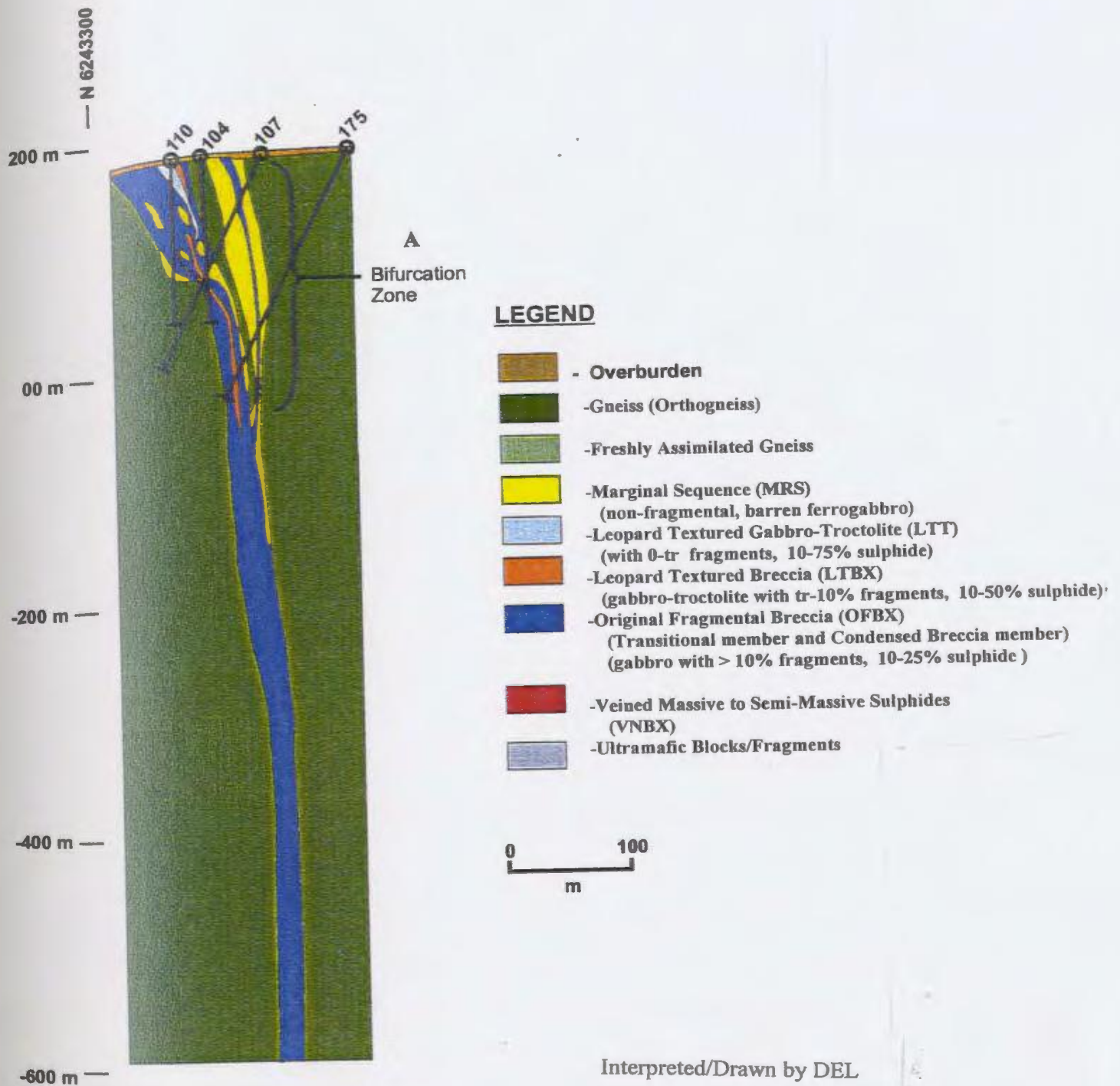


Figure 6.7.1 A west-facing geological cross-section through L3+00E in the Discovery Hill zone. The geological contacts are not only based on lithology, but also on silicate and sulphide textures present: (A) A bifurcation zone where a splay in the conduit is developed.

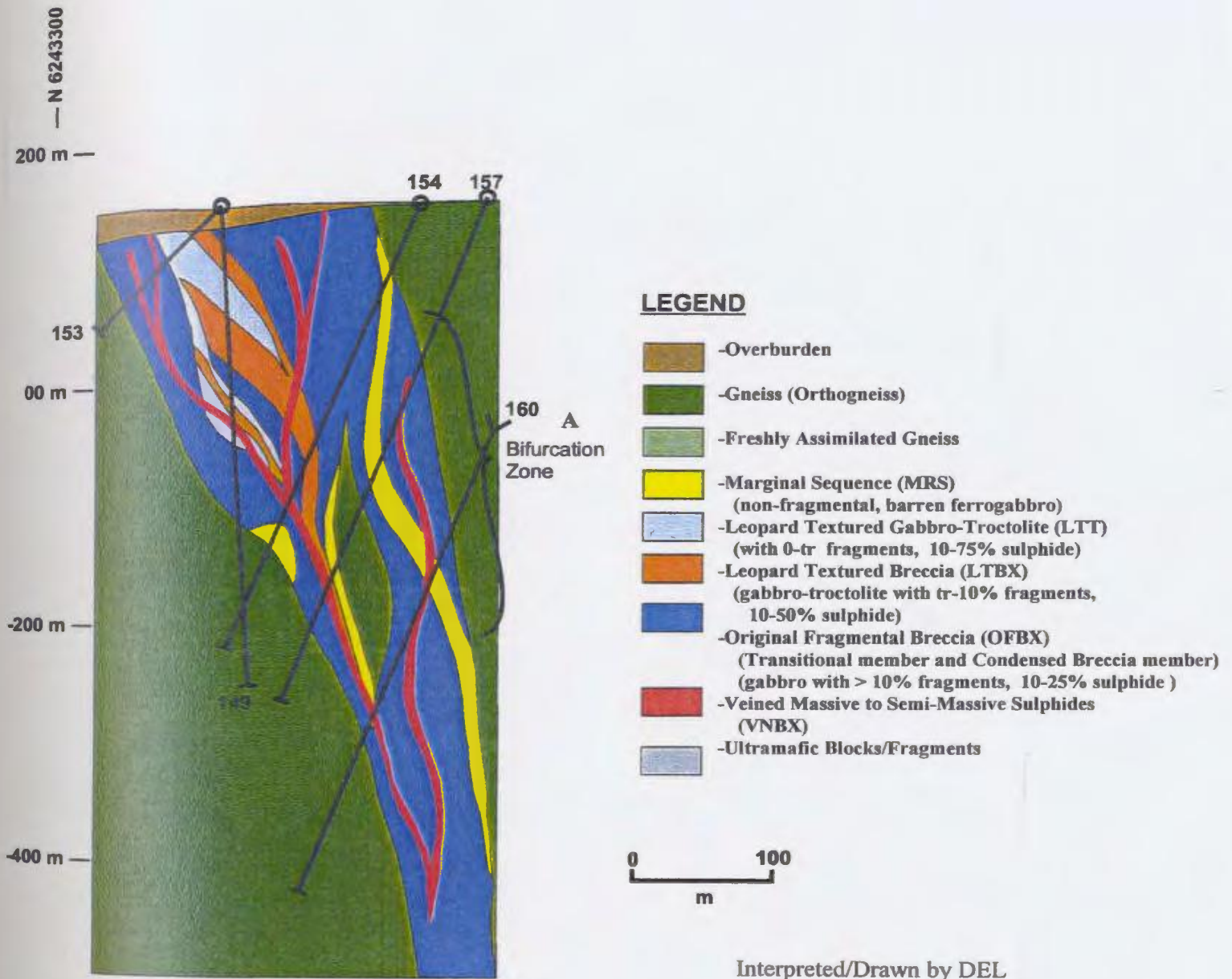


Figure 6.7.2 A west-facing geological cross-section through L3+50E in the Discovery Hill zone. The geological contacts are not only based on lithology, but also on silicate and sulphide textures present: (A) A bifurcation zone where a splay in the conduit is developed.

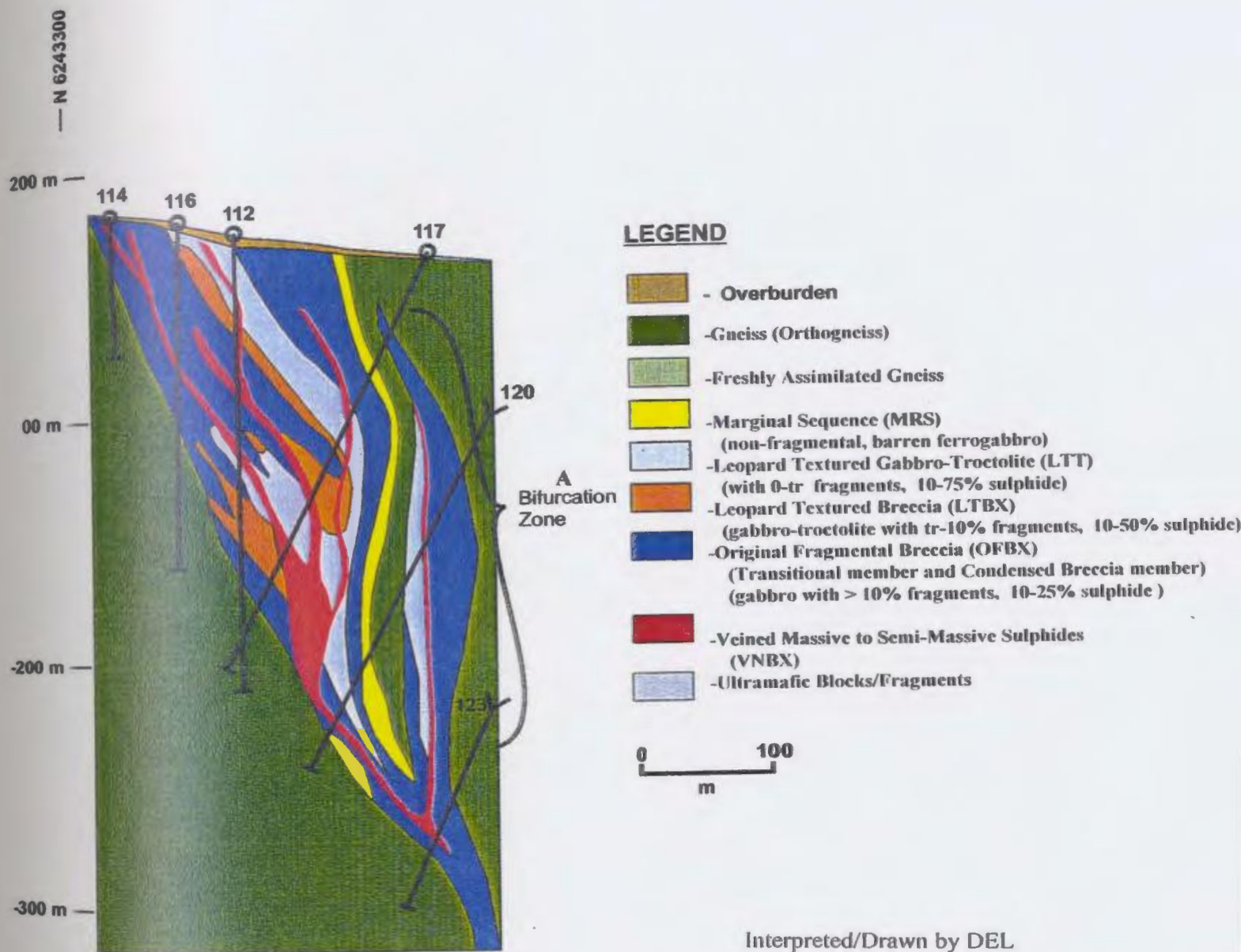


Figure 6.7.3 A west-facing geological cross-section through L4+00E in the Discovery Hill zone. The geological contacts are not only based on lithology, but also on silicate and sulphide textures present: (A) A bifurcation zone where a splay in the conduit is developed.

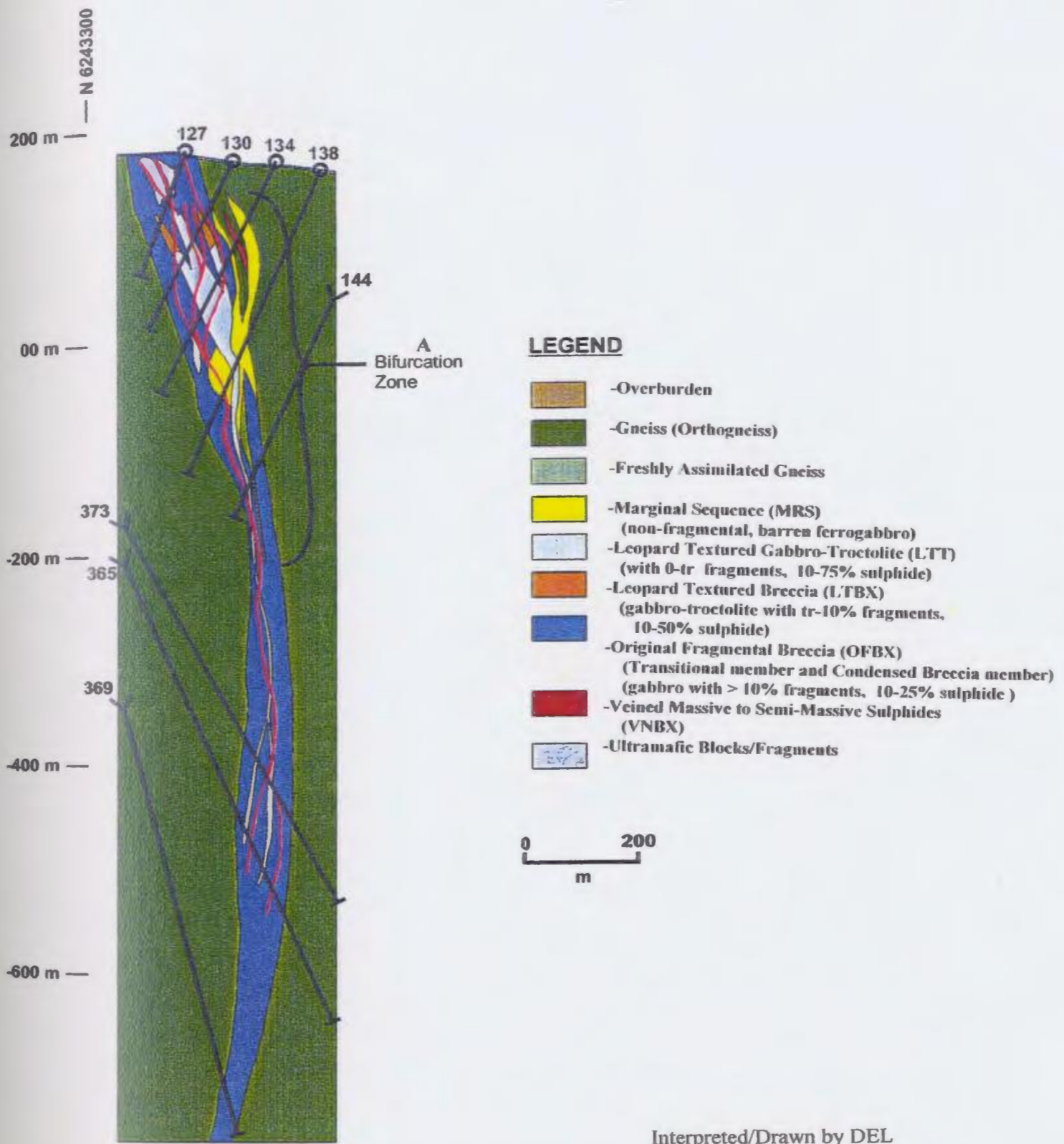


Figure 6.7.4 A west-facing geological cross-section through L4+50E in the Discovery Hill zone. The geological contacts are not only based on lithology, but also on silicate and sulphide textures present: (A) A bifurcation zone where a splay in the conduit is developed.

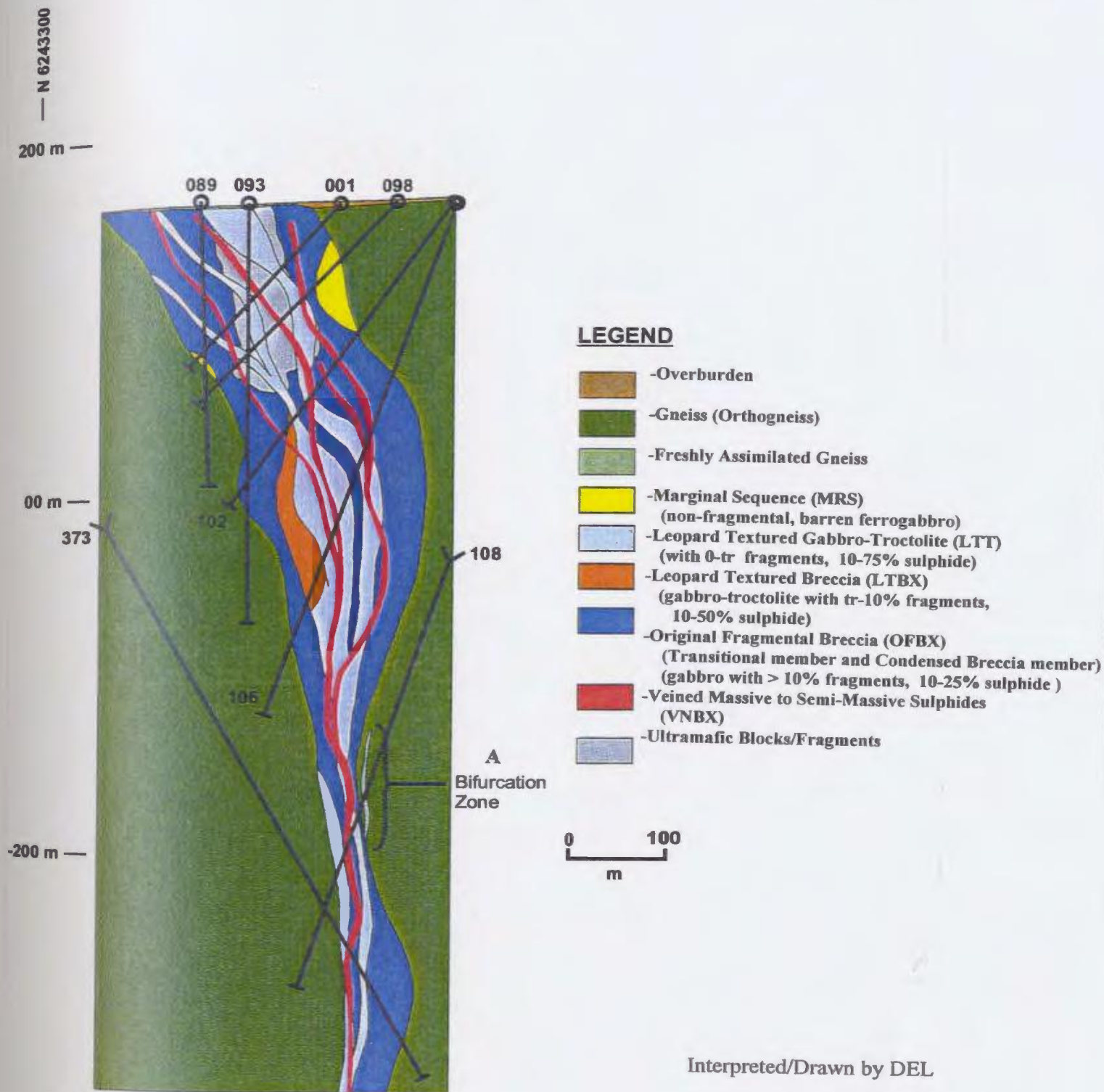


Figure 6.7.5 A west-facing geological cross-section through L5+00E in the Discovery Hill zone. The geological contacts are not only based on lithology, but also on the silicate and sulphide textures present: (A) A bifurcation zone where a splay in the conduit is developed.

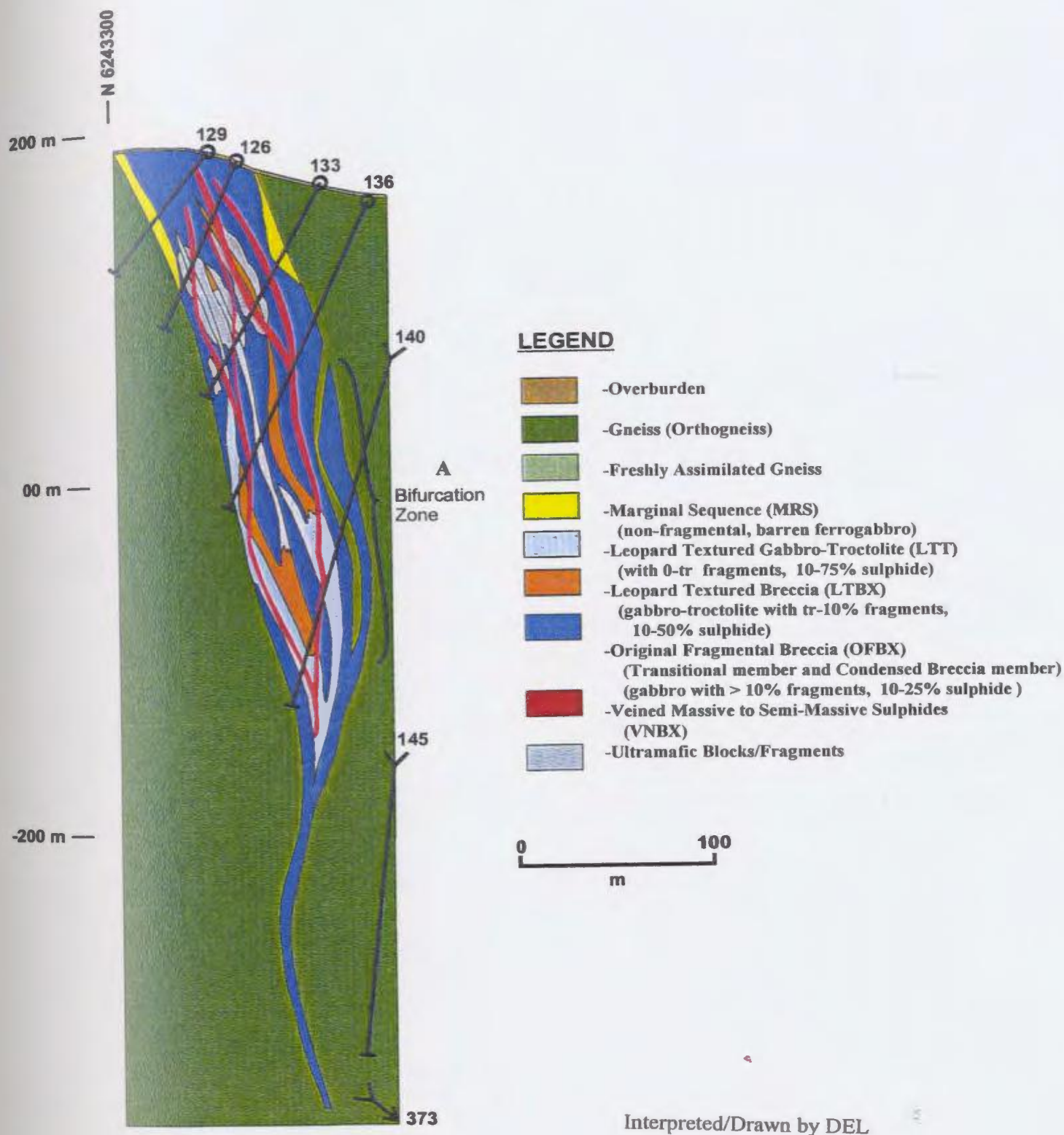


Figure 6.7.6 A west-facing geological cross-section through L5+50E in the Discovery Hill zone. The geological contacts are not only based on lithology, but also on silicate and sulphide textures present: (A) A bifurcation zone where a splay in the conduit is developed.

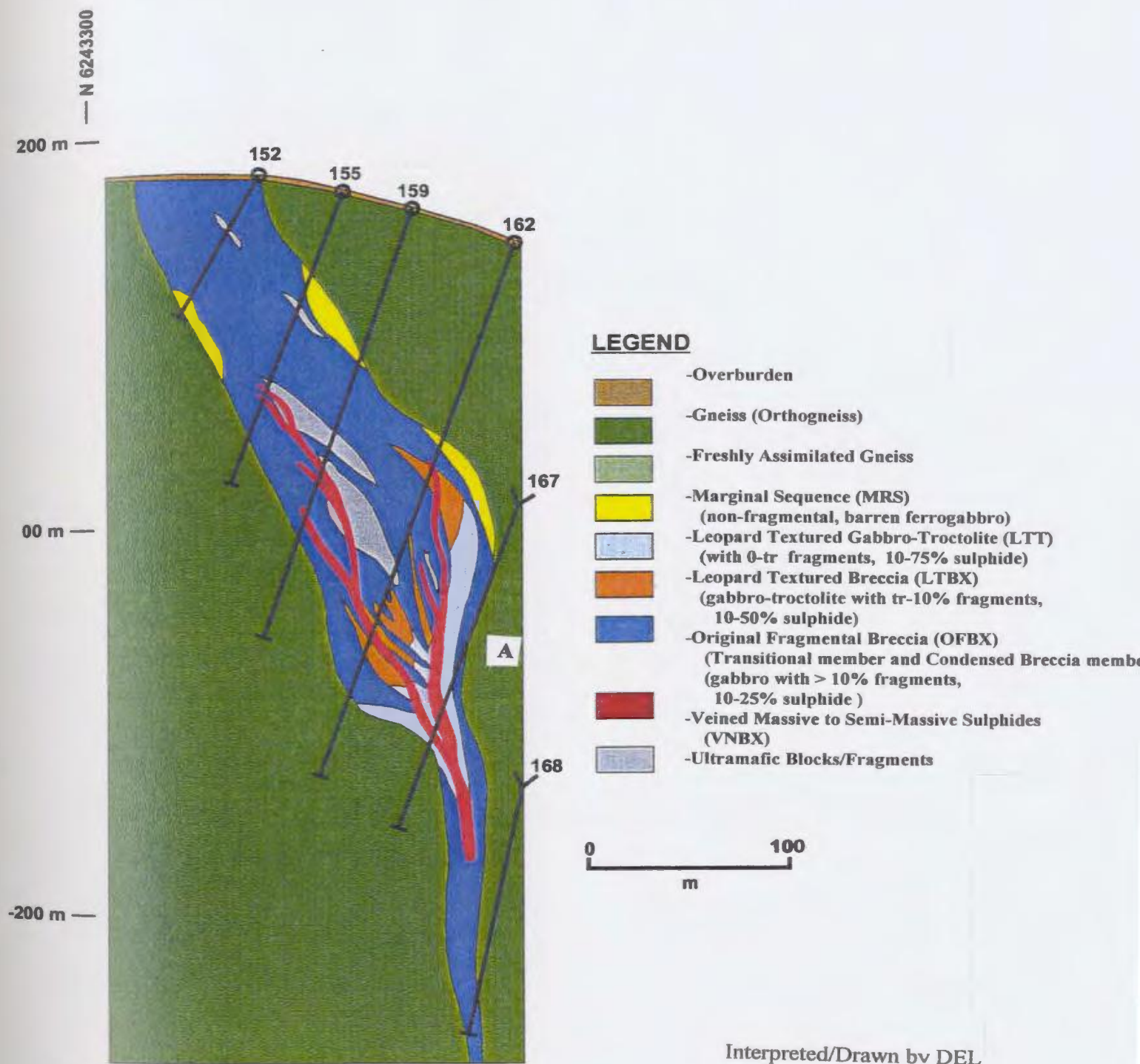


Figure 6.7.7 A west-facing geological cross-section through L6+00E in the Discovery Hill zone. The geological contacts are not only based on lithology, but also on silicate and sulphide textures present: (A) A bifurcation zone where a splay in the conduit is not recognized.

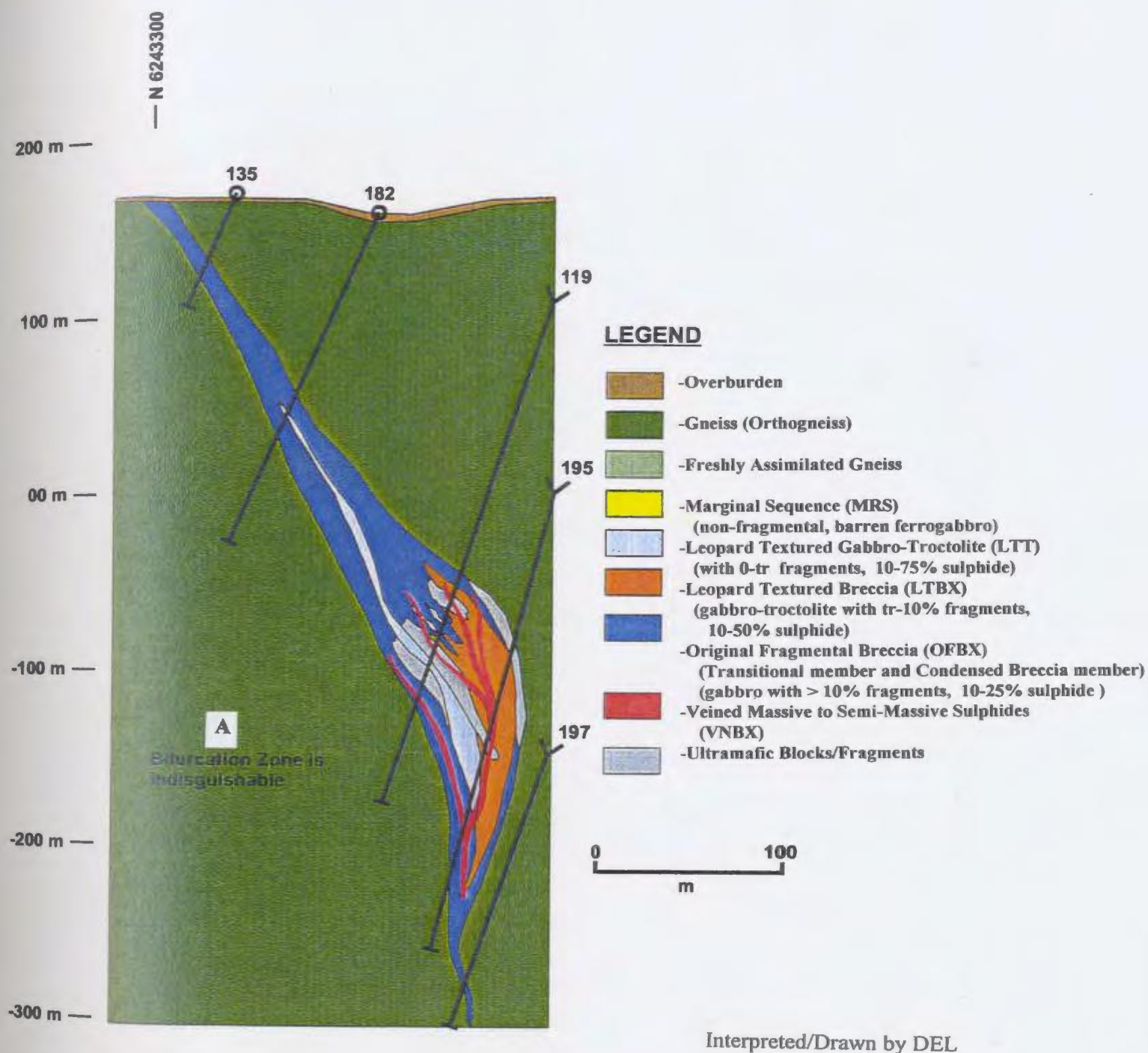
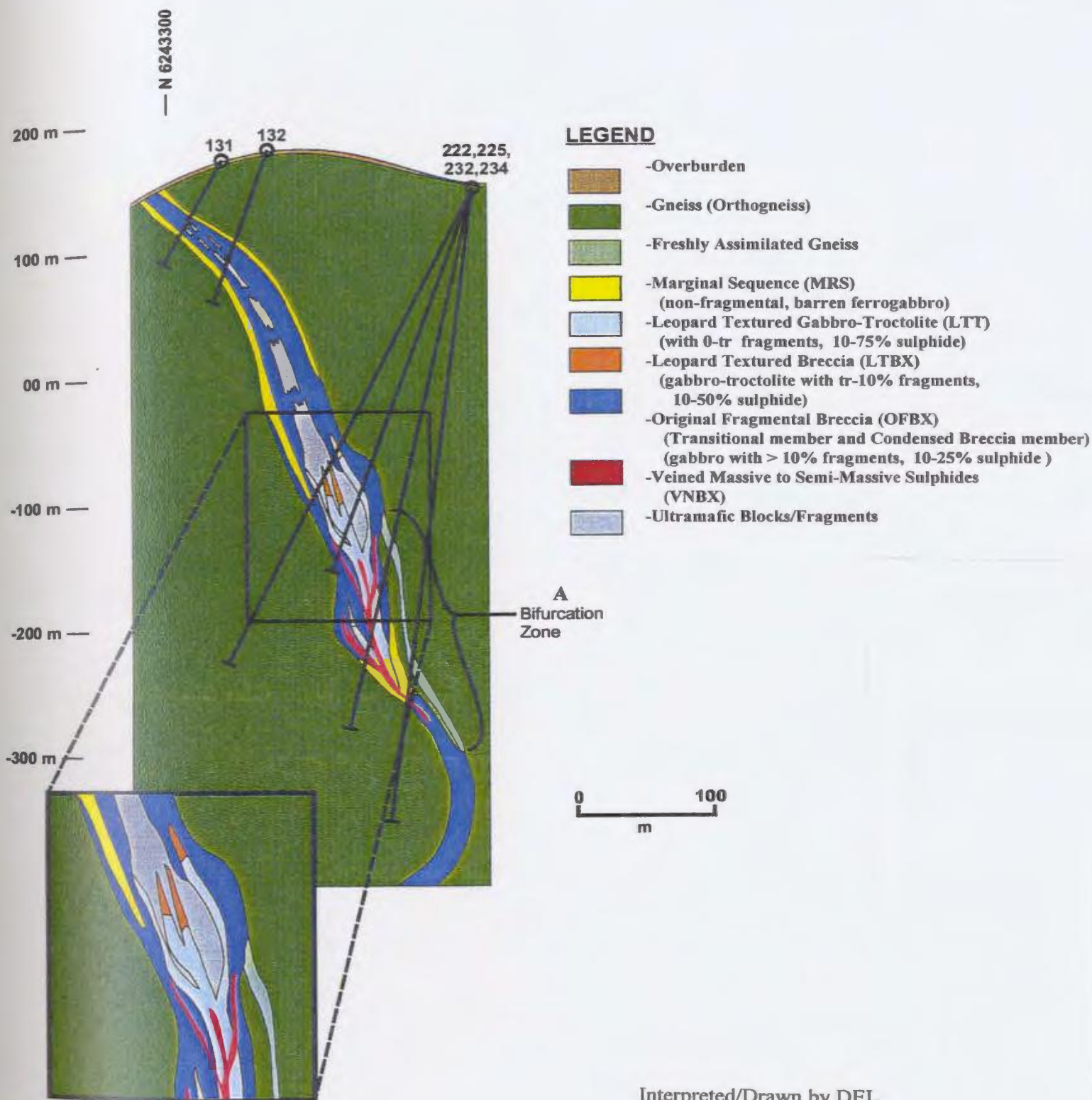


Figure 6.7.8 A west-facing geological cross-section through L6+50E in the Discovery Hill zone. The geological contacts are not only based on lithology, but also on silicate and sulphide textures present: (A) A splay in the conduit is not recognized along this section.



Interpreted/Drawn by DEL

Figure 6.7.9 A west-facing geological cross-section through L7+00E in the Discovery Hill zone. The geological contacts are not only based on lithology, but also on silicate and sulphide textures present: (A) A bifurcation zone where a splay in the conduit is developed.

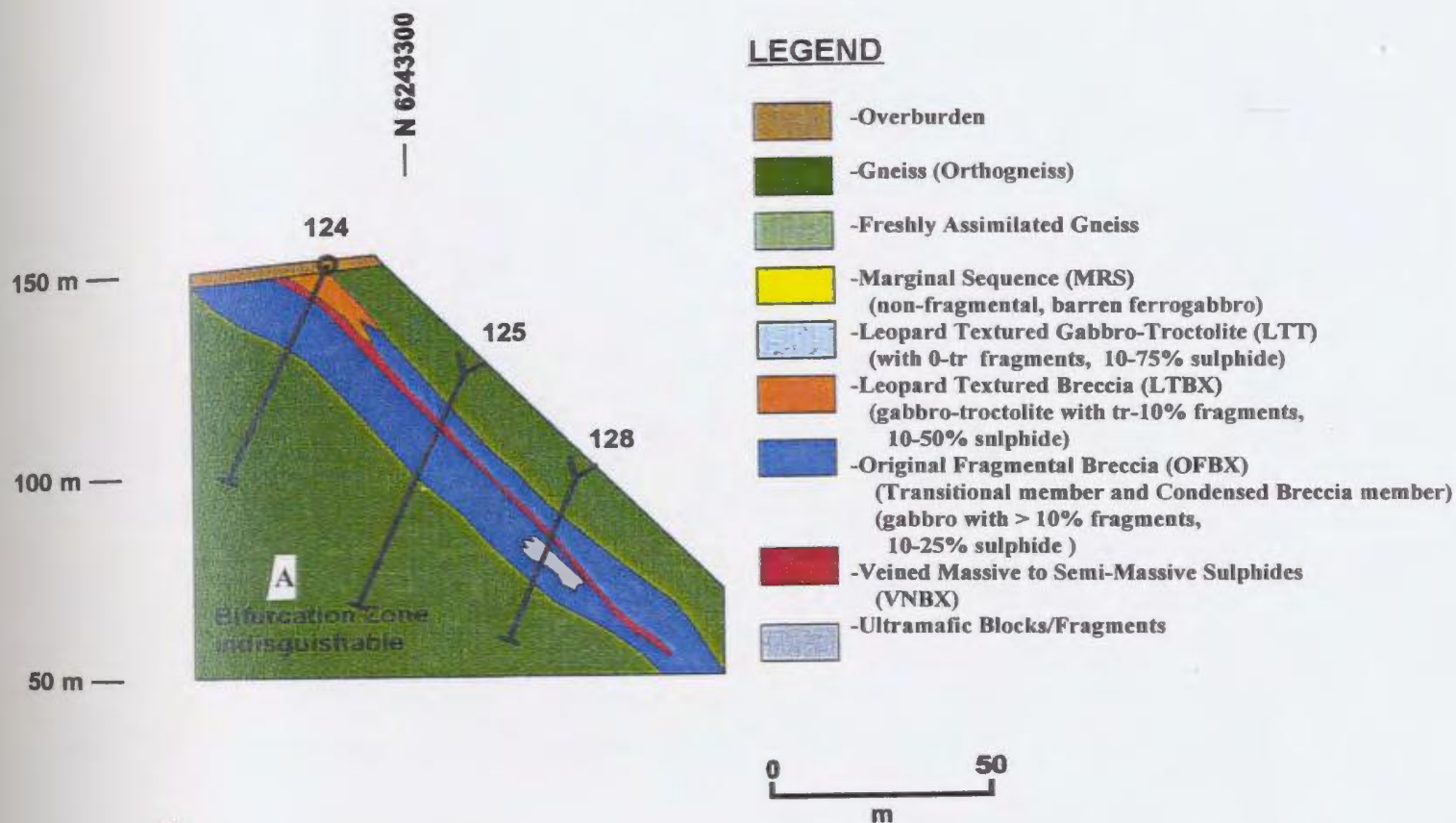


Figure 6.7.10 A west-facing geological cross-section through L7+50E in the Discovery Hill zone. The geological contacts are not only based on lithology, but also on silicate and sulphide textures present: (A) A splay in the conduit is not recognized along this section.

arriving magmatic pulses. The feldspathic material can be coarse grained to pegmatitic and is frequently bleached to a dull white color. The lower contact of this horizon is not consistent in character and can exhibit either a chilled or gradational contact with the adjacent lithologies.

The TNS (Transitional sequence) is found adjacent to the MRS, at both the upper and lower contacts (Evans-Lamswood, 1997e) (Figures 6.5, 6.6 and 6.7.1-10). The TNS has been interpreted to be compositionally a gabbroic rock (Lightfoot, 1998 and 1997b). This sequence appears to be compositionally and texturally homogeneous (Plates 2.O). The contacts exhibit distinct grain size reductions and are interpreted to be part of a crude chilled zone, however, as a whole, it is a monotonous, medium-grained sequence. Less than 5% sulphide mineralization is recognized, with trace to 1% on average. Sulphides are fine to medium-grained and occur as loose, but homogenous disseminations. Apart from the presence of a homogeneous texture and lack of accessory hydrous minerals, this sequence differs from the MRS, in that it contains a small quantity (i.e. less than 5%) of highly digested, aphyric fragments which can be totally pseudomorphed by spinel (Naldret *et al.*, 1996).

The next sequence depicted in the Feeder succession is the FM (Feeder Melange) (see Plate 2.D and Figure 6.5). This is a hydrous, intensely biotite-rich, fragmental sequence. Lithogeochemical analysis indicates that the lithology is a gabbro to ferrogabbro (Lightfoot, 1997b). Internally it hosts an array of intensely absorbed gneiss fragments characterized by a distinct alignment parallel and slightly oblique to the conduit walls. The FM is typically the lone constituent in-filling the conduit and to a lesser extent, in contact

with the MRS and BX sequences (see below.) This sequence is usually coincident with flat lying to sub-horizontal domains within the dyke, but rarely (documented only twice) can be found in steeper domains where it is thought to reflect splays in the conduit. Mineralization consists of finely disseminated to coarse blotchy sulphides, ranging in bulk composition from trace to 15%. This horizon displays a strong mineral alignment particularly near the central regions of the conduit. This alignment is probably a result of primary flow being coeval with secondary deformational events developed when a fragment laden magma is squeezed through a conduit that is continuing to develop through progressive deformation (see Chapters 7 and 8).

6.2.1.2 Noisy Sequences

The Noisy Sequence constitutes an interactive environment with multiple interrelated geological relationships (Evans-Lamswood, 1997e) (Figure 6.6). It includes intercalated sequences that are associated with the mineralizing event. The most prominent sequence is the Original Fragmental Breccia (OFBX) sequence (op cit.) (Figures 6.7.1-10). The OFBX is texturally and compositionally similar to the BX, however, it exhibits textures that developed within narrow domains of the conduit, as opposed to those which formed in wide regions such as the Ovoid. The matrix of the OFBX is geochemically comparative to the gabbros in the TNS (Evans-Lamswood, 1997e, Lightfoot, 1997a, 1997b). Within the OFBX, the quantity of fragments is extremely variable, ranging from trace to a approximately 45%. The variance in the bulk fragment content can be attributed

to the segregation of fragment-laden material through stratification processes initiated by velocity and viscosity contrasts, as described in experiments by Koyaguchi and Blake (1991) and Nicolas and Ildefonse (1996). Fragment size, shape and intensity of alteration are extremely diverse, but appear related to their aspect ratios. Rounded fragments with a low ratio appear less altered than those of the high aspect ratios with oblate. The repetitious sequences where dense populations of fragments occur in bands, are referred to as the Condensed Breccia sequences (*CBX*) (Evans-Lamswood, 1997e) (Figures 6.5 and 6.6), (Plates 2.A and 2.B.). The *CBX* occur between thin horizons of TNS (Plate 2.O). Combined, these two horizons (i.e. TNS and *CBX*) are grouped as the *OFBX* (Plate 2.O), as are the unsegregated version of this sequences which display a uniform dispersion (non dense populations) of fragments.

The sulphide content hosted by this unit is generally between 3 and 25%. Sulphides appear as fine to medium-grained disseminations or as coarse blotchy sulphides. The coarse sulphides are observed clotting around fragment boundaries within the *CBX* zones (PlateA2.A and 2.B). The fragments are of diverse populations consisting of ultramafic, gabbroic, and gneissic protoliths. There are no ubiquitous chilled or sharp contacts between the *OFBX* and the Feeder sequences, however, typically there is a distinct reduction in grain size proximal to the Feeder sequences.

Another sequence apparent in the Noisy domain, is the Leopard Textured Breccia (*LTBX*) (Evans-Lamswood, 1997e) (Figures 6.5 and 6.7.1-10). This is a transitional sequence linking opposing environments, it has attributes characteristic of both the chaotically textured Noisy Sequence and the subdued Quiet domain (Figure 6.6). It has a

semi-homogenous, spotty texture which is defined by numerous components such as, oikocrysts, gneissic fragments, gabbroic-troctolitic inclusions, and gabbroic-troctolitic fragments (Plates 2.G-2.N). The inclusions are speculated to be the earliest signs of crystal nucleation or solidification, prior to the mineralizing event. These crystals grow in regular amalgamated groups characterizing a quiet, non-turbulent regime. The fragments are diverse and range from aphyric gabbro-troctolite material to feldspar phyric gneiss fragments. The LTBX is observed as veins injecting into the more anterior sequences, such as, the OFBX, the MRS and the TNS (Evans-Lamswood, 1997e) (Plate 2.L and 2.M.). This sequence is associated with the first significant sulphide mineralization and can contain from 10 to 50% leopard textured mineralization.

The next sequence documented within the Noisy environment, is the Vein Breccia (VNBX) (op cit.) (Figures 6.5 and 6.6). This member is observed crosscutting all aforementioned sequences and occurs in the form of semi-massive to massive sulphide veins ranging in thickness from 3 cm to 1.0 m (Figures 6.7.1-10) (Plate 2O).

6.2.1.3 Quiet Sequences

The Quiet sequences formed in a subdued, non-turbulent environment where consistent intergrowth textures were favoured. The characteristic sequence of this domain is the LTT (Naldrett, *et al*, 1996) (see Chapter 2)(Figures 6.5 and 6.6), where a distinct oikocrystic texture developed and is visually enhanced by the contrasting sulphides (Plates 2.G-2.N). The sulphide content ranges from 10 to 75%, but generally the presence of at

least 15-20% sulphides is required to define this texture. Locally, inclusions of gabbro-troctolite (early nucleation) are apparent in this sequence.

Significantly the last sequence within this Quiet domain is comprised of semi-massive to massive sulphides (Figures.6.7.1-10), (Plates 4.R, 4.S, and 4.T). These sequences dominate the geology at specific stratigraphic levels and are interpreted to be the source from which the VNBX material branches and intrudes the earlier lithologies (Figures 6.5 and 6.6).

6.2.2 Flow Kinematics

To date, models for the formation of the Voisey's Bay deposit have been based on the dynamics of the magmatic system, whereby, the distribution of magmatic sulphides are thought to be controlled through settling processes (i.e. closed system) or alternatively, through fluid dynamics within an active, interconnected conduit network (i.e. open system). In the early gravitational settling models, sulphides are interpreted to flow and settle downwards from upper stratigraphic levels (Ryan *et al.*, 1995), while present models now suggest that a continuous conduit system existed where sulphide-bearing magma ascended through the system from lower stratigraphic traps (Evans-Lamswood, 1997e). Evidence for this model was directly obtained through the re-logging of the core from the Discovery Hill zone (L7+50E-L3+00E), however, support for this model was also provided from the other geological domains investigated for this study (i.e. Ovoid and

Mini-Ovoid). To effectively validate this model, the lithostratigraphy must be interpreted in two components, order of intrusion and stratigraphic position.

6.2.2.1 Intrusive Relationships

6.2.2.1.1. Massive to Semi-Massive Sulphides

The intrusive relationships observed between the conduit lithologies has been described in the preceding section, however, will be summarized in the following discussion. The massive and semi-massive sulphide sequences have been observed to crosscut all other sequences found within the conduit (Evans-Lamswood, 1997e) (Figures 6.7.1-10). At intermediate stratigraphic levels they most typically intersect the LTT and display irregular to embayed margins, however, at higher stratigraphic levels the contacts of this intrusive sequence become sharper and the sequence is observed as thin veins intruding the OFBX (Plate 2.O). Within the OFBX, the massive to semi-massive sulphide veins are ubiquitously dispersed throughout the TNS member, however, within the CBX, the veins appear to preferentially intrude along the contacts of the sequence. In the latter occurrences, the veins carry gabbroic-troctolitic fragments near their margins which are speculated to be rip-up clasts associated with the late intrusion of this sulphide-rich fluid.

The occurrence of the massive and semi-massive veins is less frequent in the highest stratigraphic sequences than in the more intermediate stratigraphic successions. When massive sulphide veins are observed, they appear to have intruded the OFBX proximal to large, fragmented blocks of ultramafic material (Evans-Lamswood, 1997e).

Only in rare instances can this sequence be observed to intrude the MRS substrate. This observation may be a reflection of the small and localized amounts of the MRS that remain intact (i.e. were not overprinted or thermally eroded).

6.2.2.1.2 Leopard Textured Troctolite and Leopard Textured Breccia

Both the LTT and the LTBX, have intrusive relationships with the OFBX (Plates 2.L, 2.M, and 2.N) and on rare occasion with the MRS (Evans-Lamswood, 1997e) (Figures 6.7.1-10). When in contact with the MRS, the LTT or LTBX are proximal to the margins which face the center of the conduit. This can be a product of velocity and viscosity contrasts, where the LTT and the LTBX preferentially segregate into the fast flow regimes situated within the core of the conduit, and also, at the margins of these sequences where a density contrast is established. These factors can establish the margins of the MRS as an incompetency where an intrusive phase could be preferentially accommodated.

6.2.2.1.3. Original Fragmental Breccia

The OFBX is intruded by the massive, semi-massive, LTT and LTBX sequences (mineralizing events). The vein-like intrusions preferentially intrude the incompetent zones within the OFBX such as the TSN member, and are rarely significant in the more rigid CBX domains (Evans-Lamswood, 1997e).

6.2.2.1.4 Marginal and Transitional Sequences

The MRS does not intrude any lithologies within the conduit. It is preserved as a contact phase against the walls of the conduit, or alternatively, as inclusions within the TSN sequences. Like the TSN package, the MRS can host LTT, LTBX, massive and semi-massive mineralization as intrusive phases (op cit.), however, due to the limited preservation of the MRS these relationships are only rarely observed.

6.2.2.2.0 Stratigraphic Relationships

The intrusive relationships, as discussed above, establish a relative timing for lithological and mineralizing events within the conduit, however, to fully establish the kinematics between these phases, analysis and documentation of the relative stratigraphic positions of these sequences is also required. Within such a analysis, the magmatic environment of the conduit can be most effectively compared to that of a prograding deltaic system (Figure 6.6), except that it is flowing against the topographic gradient (ascending) as opposed to flowing in coincidence with it (descending).

6.2.2.2.1 Gabbro Phases

The sectional diagrams indicate that relicts of the MRS are preserved at the highest stratigraphic levels within the conduit (Figures 6.7.1-10). This sequence represents relicts

of an earlier anterior sequence that was eroded and overprinted at depth. The MRS are typically preserved at the margins of the dyke/conduit and in isolated embayments, or on occasion, they are present as isolated islands contained within the TNS. At depth, where late changes to the dyke geometry induced secondary stoping, the TSN can be easily mistaken for the MRS due to the presence of weakly digested, freshly absorbed gneissic fragments. The key factor for distinguishing these two sequences, however, is the presence of a hydrous phase in the true MRS that is not present in the TSN phase.

The TSN member is found in two geological domains. High in the conduit stratigraphy, the TSN sequence is preserved along the margins of the conduit, where the MRS has been eroded. Within more intermediate stratigraphic levels, the TNS is observed as a dominant member of the OFBX (Figure 6.6). Within the higher stratigraphy, the TSN phase shows a progressive increase in the concentrations of highly digested gneiss fragments towards the central regions of the conduit. At this stratigraphic level, where the TSN sequence is found proximal to the conduit margins, the fragments are present, but are ubiquitously dispersed. Towards the conduit core, the fragments are distinctly segregated into dense populations or clusters, as is reflected by the nomenclature of CBX. At more intermediate stratigraphic levels the CBX member appears to be developed regularly as a cyclic pattern. It also becomes apparent that the ultramafic fragments occur as larger and more cohesive blocks within the upper stratigraphic levels of the conduit (Figures 6.7.1-10). These ultramafic blocks are preferentially concentrated and aligned along the low side of the conduit (i.e. footwall) (Figures 6.7.1-10). Conversely, within the lower stratigraphy

the ultramafic material appears highly fragmented, and occurs as an array of small segmented debris generally concentrated within central regions of the conduit.

Stratigraphic relationships, textures and compositions indicate that the MRS was the first sequence to intrude the conduit and was followed by the OFBX magma pulse. The MRS magmas are geochemically the most primitive magmatic phases observed within the conduit and are Ni-depleted (Lightfoot, 1997b), indicating that prior to intrusion at current stratigraphic positions they were stripped of some Ni content. It is speculated that this Ni depletion occurred through partitioning processes (cf. Rajanani and Naldrett, 1978) in a magmatic chamber or sub-chamber at depth. Once expelled from this parental chamber, the magmatic material ascended upwards along the least resistant path. As this anterior/leading magmatic pulse migrated up through the system, it peeled and stopped wall rock material from the sides of the conduit.

The OFBX is interpreted to have been the second magmatic pulse to intrude the feeder conduit, since it intrudes the MRS, and itself is intruded by the LTBX, LTT, and massive to semi-massive sulphides. Furthermore, unlike the MRS, the OFBX documents the first appearance of fragments and sulphides material within the conduit (Plate 2E and 2O). With the leading magmatic pulse (i.e. MRS) plated against the conduit walls, the second magma pulse (i.e. OFBX) would preferentially propagate through the faster, central regime of the conduit (Figure 6.6). Some fragments would stray (i.e. local eddy currents, surface irregularities) and become segregated into dense clusters. This could, therefore, provide a mechanism to form fragment-rich (i.e. CBX) (Plate 2A) and fragment-poor (i.e. TSN) (Plate 2O) horizons within the same magmatic pulse. Furthermore, the

separation of the fragmental material would allow the fragment-poor (i.e. TSN) members of this sequence to ascend more efficiently through the conduit. The fragment-rich members (i.e. CBX) could have caused further impedance of the magmatic flow, if it was engaged by more fragment-bearing magma. The CBX could act as a mesh and prevent the progression of the later fragment-bearing magma, possibly resulting in the choking of the conduit (Figure 3.4.). In some locations the fragments can become flow aligned (Figure 3.5 and Plate 2A) and, therefore, with such streamlining the magmatic transfer should not have been significantly effected (cf. Nicolas and Ildefonse, 1996). Progressively, however, these flow regimes would become more segregated, as less viscous fluids (i.e. TSN) would tend to navigate and bifurcate around the denser, fragment-rich material (i.e. CBX).

6.2.2.2.2 Gabbroic-Troctolitic Phases

The third pulse to intrude the conduit system introduced the gabbroic-troctolitic phases which contained significant mineralization and is represented by the LTBX and LTT sequences. The intrusion and intercalation of the LTBX and LTT sequences (cf. Evans-Lamswood, 1997e) with the earlier OFBX pulse is documented by either the presence clotty, coarse grained sulphides within the matrix supporting the fragments in the CBX sequence, or as vein-like horizons intruding the TSN member (Plates 2A and 2O). The intrusive relationships between the LTT and OFBX members are most typically observed near the upper limits of intermediate stratigraphic levels, however, lower in this domain, LTT-style mineralization dominates with only an insignificant presence of OFBX.

It is interpreted that when the LTT pulse intruded the conduit, it first engaged and mingled with the trailing edge of the OFBX pulse (Figure 6.6) (Plates 2L and 2M). Density contrasts maintained between the two compositionally and thermally different fluids, resulted in the inter-fingering of the later LTT magma with the earlier OFBX magma (Synder, *et al.*, 1997). When the LTT pulse encountered the CBX member of the OFBX sequence, it would not be able to successfully navigate the dense network of fragments (Figure 3.4., cf. Nicolas and Ildefonse, 1996). Sulphides would, therefore, preferentially collect and plate against the fragment boundaries, explaining the occurrences of coarse grained sulphides within the OFBX sequence (Plate 2A and 2E). Alternatively, portions of the LTT pulse would preferentially flow successfully along the less competent TSN member of the OFBX and reach higher levels within the conduit (Figure 3.4.).

Where the LTT did follow the central regions of the TSN, but flowed along the contact between the TSN and CBX, a hybrid zone (i.e. LTBX) was developed. This zone would have characteristics common to both the OFBX and the LTT (op.cf. Evans-Lamswood, 1997e). Unlike its protolith (i.e. LTT), the LTBX contains gneiss and early gabbro-troctolite fragments which can be difficult to distinguish from the spotty oikocrysts (see Chapter 2) (Plates 2K, 2L, and 2M). The LTBX sequence is speculated to represent a zone where the OFBX magma mixed with the LTT magma (Figure 6.6). This mixed zone does not appear to be constrained to local regimes since the fingers of LTBX are not recognized to end at a common elevation (Figure 6.6). Some fingers are thought to have flowed further than others, due to rock incompetencies and local density and velocity contrasts (Synder, *et al.*, 1997).

At depth, stratigraphically below but continuous with the LTBX, the true homogenous LTT sequences are recognized (Plates 2H, 2I, and 2J). As displayed within the geological sections, the LTT is associated with a trap environment within the conduit. It is speculated that if not for the physical controls directly associated with a trap environment, the velocity and viscosity conditions (i.e. non-turbulent) would not favor the development of such regular pattern of intergrowth textures. If the trap environment did not exist, this sulphide-bearing magmatic material may have developed more chaotic net textures, as opposed to the observed leopard textures. Furthermore, the varying thicknesses of the LTT sequences at depth, appear to be related and proportional to changes in the width of the conduit (i.e. size of the trap).

6.2.2.2.3 Massive and Semi-Massive Sulphide Phases

The last, but most significant, pulse to ascend through the conduit in this environment are the massive to semi-massive sulphides. As previously documented, this phase exhibits clear and intense crosscutting relationships with all other lithologies preserved in the conduit (Evans-Lamswood, 1997e) (Figures 6.7.1-10) (Plates 2C and 2O). This succession may have been subjected to similar sulphide scavenging processes at depth as the LTT sequences. The sulphide grade of this sequence suggests two possible processes for such a significant concentration of sulphides; 1) accumulation through gravity settling in a deeper parental magma chamber with discharge occurring late, 2) early discharge from the chamber and residence in a lower trap (below the Voisey's Bay system)

where the sulphide and nickel contents were upgraded by contact with magma that was constantly replenished.

Thicknesses of the massive sulphides increase with depth within the conduit domain. Like the LTT, the frequency and size of their occurrence can be related to the degree to which the trap is developed. Massive sulphide veins intruded high into the conduit stratigraphy where blocks of the ultramafic material were encountered (Plate 2O). At such sites, the intrusive relationships provide evidence for the kinematics of flow, whereby, the model for the upward flow of magmatic fluids is supported. For example, within intermediate stratigraphic levels the ultramafic fragments appear intensely brecciated by the intruding sulphide veins, however, at higher stratigraphic levels the veins are observed to passively navigate through dilational fractures within the blocks, or to alternatively, meander around the fragments. This is interpreted to be a function of the viscosity of the massive-semi-massive sulphide liquids when they encountered the ultramafic fragments. Since the lower ultramafic fragments are brecciated by the veins, it is speculated that it was at this point that the massive sulphide pulses first encountered the competent ultramafic blocks. Flowing with lower viscosity and higher velocity within lower levels of the conduit, the massive sulphide pulse could have penetrated the cooler, competent blocks causing them to splinter or brecciate (Plate 2.C). Alternatively, the ultramafic fragments at higher stratigraphic levels, do not display this explosive style of intrusion. It is, therefore, interpreted that after ascending to higher stratigraphic levels, the massive sulphide pulse had cooled resulting in a velocity reduction and a viscosity increase. Subsequently, the ascending pulses would not have the momentum to

aggressively penetrate the ultramafic fragments that lay in their path, therefore, they passively navigated around obstacles or intruded along incompetencies (i.e. fractures).

The preceding observations shape a model for the ascent of multiple magmatic pulses through a geometrically constrained conduit system. The sequence and relationships of the magmatic events are documented by the lithostratigraphy and are firmly established within this domain, however, at depth geological processes remain ambiguous. The mixing and separation of sulphide and silicate phases could have been an extensive, progressive task, performed through magmatic segregation within a single parental chamber or alternatively, within numerous traps at depth (far below the Voisey's Bay system). The sequence of magmatic events and the composition of the geological phases, therefore, may change at depth, due to local physical and environmental controls.

Chapter 7: Geological and Environmental Parameters Associated with the Eastern Deeps Mineralization.

7.0 Introduction

The Eastern Deeps consists of a large troctolite intrusion with semi-massive, massive and disseminated sulphides constrained to the base (Figure 4.1). The erosional cut-off combined with the presence of an inclined floor, gives this chamber a wedge-shaped appearance. In the deepest hollows, the gabbroic-troctolitic chamber can exceed over a kilometer of vertical thickness, while at the apparent taper the chamber is less than 400 m deep. To the north, the chamber is defined by a sharp, vertical to sub-vertical intrusive contact with the surrounding orthogneiss. The southern margin of this chamber, however, has not been totally resolved and delineation is restricted to areas proximal to the western contact. To the east, this margin has been dislocated and overprinted by an intense, post-emplacement, sinistral strike-slip fault. When the chamber is viewed on a large scale, the footwall which moderately dips to the southeast, appears to have a smooth and regular geometry, however, with more focused examination, prominent geometric irregularities can be documented. These irregularities consist of two distinct types: (1) those developed during or prior to the mineralization events, and (2) those related to post-mineralizing deformation, such as the fault marking the southern contact.

7.1 Past and Present Geological Models

To date, the Eastern Deeps is the enigma at the forefront of geological controversy concerning the formation of the Voisey's Bay deposit. The observable similarities in sulphide textures and the lateral proximity to the Ovoid, have lead to oversimplified

geological interpretations and correlations. One such widely described model, interprets the Eastern Deeps chamber and Ovoid as being a single continuous magmatic body. In this scenario (Naldrett *et al.*, 1996, Figure 11), the original emplacement geometry defined the Ovoid as being stratigraphically below the Eastern Deeps chamber. Furthermore, it was suggested that the Ovoid was once a continuation of the Eastern Deeps chamber with over a kilometer of gabbro-troctolite (op cit., Figure 11) that was subsequently removed by erosion.

In greater detail, these authors speculate that a late deformational event juxtaposed the relative positions of the Ovoid trap and Eastern Deeps chamber (op cit., Figure 3). This structural event is essential to this model as it explains why the Ovoid was preserved at a higher topographic level than the base of the chamber. The down-dip displacement required for such a dislocation of the Eastern Deeps would be in the excess of 500 m relative to the current position of the Ovoid. This model obscures the genetic relationships and the geological significance of the Ovoid and as a consequence, the role of the Ovoid in establishing a continuum for the transport of sulphur saturated magmas is lost. Instead of the Ovoid being recognized as part of a dynamic feeder conduit, this published concept is an oversimplification which makes the Ovoid the base of a stagnant magmatic intrusion.

The discussions to follow will describe and document in detail the geometric parameters that controlled sulphide distribution and capture within the Eastern Deeps regime. In addition, they will address the contribution and significance of these geological attributes to the macroscopic conduit system. Evidence will also be provided for a geological model that establishes the mineralized feeder conduit as a geological element

separate from the overlying magma chamber. With the detailed examination of these characteristics and recognition of these relationships, a more reliable and sound geological model will be developed for the complete macroscopic system.

7.2 Stratigraphy

Three stratigraphic units are recognized in the Eastern Deeps chamber (Figure 7.1). The top of the chamber, where intermittently preserved, is represented by a shallow, north-east dipping sheet of Ni-depleted olivine gabbro (Lightfoot, 1997b), the chamber Gabbro. This sheet is underlain by a thick accumulation of gabbroic-troctolitic material. Immediately below the gabbro-troctolite, the chamber hosts mineralized sequences within feeder stratigraphy. The feeder lies at the footwall contact of the chamber, and is texturally and chemically comparable to the ore-bearing sequences exhibited by the Ovoid and the Western Extension conduit environments (Naldrett *et al*, 1996).

The Ni-depleted gabbro overlying the Eastern Deeps chamber (Figure 7.1), is geochemically comparable with the Ni-depleted gabbros capping the Ovoid and lining the conduit walls in the western domains of the deposit (Western Extension and Mini-Ovoid) (Lightfoot, 1997a, 1997b). Furthermore, as found elsewhere, this gabbroic unit is fragment and sulphide-poor.

The remaining gabbroic-troctolitic sequences comprise the bulk volume of the Eastern Deeps and can be divided into two distinct sequences based upon their mineralization and bulk fragmental content: NT and VT (see Chapter 2). The NT sequence (Figure 7.1) hosts trace to 1% finely disseminated sulphides and only locally

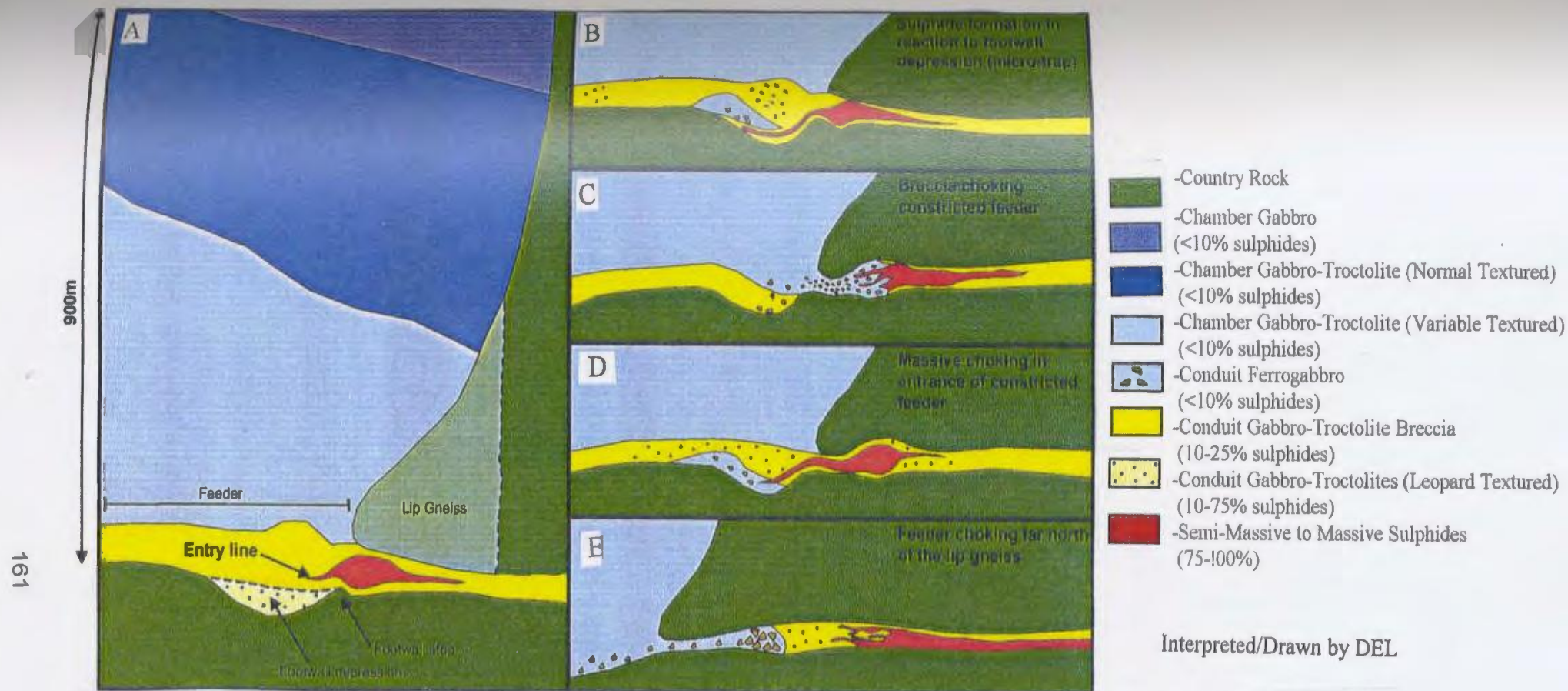


Figure 7.1 An idealized west-facing vertical cross section through the Eastern Deeps chamber and feeder conduit. The chamber consists of sulphide and fragment poor gabbro-troctolite (i.e. NT and VT). The conduit contains fragment and sulphide-rich gabbro-troctolite (i.e. BX and LTT). (A) This figure displays: the Footwall Depression which is a trough at the base of the chamber where disseminated sulphides were trapped, the Entry Line defining the entry point of massive sulphides into the chamber, the Lip Gneiss which is a wedge-shaped protrusion of orthogneiss into the chamber, the footwall step which is a structural rise marking the north margin of the Footwall Depression, and the feeder which is a sub-horizontal conduit found at the base of the chamber and extending into the orthogneiss to the north. (B) This inset displays the massive sulphides focused along the footwall step which defines the north margin of the Footwall Depression. (C) This diagram shows the massive sulphides collected under the Lip Gneiss further back in the conduit, as the conduit entrance was choked by the accumulation of BX material. (D) This figure is similar to (C), except that the narrow conduit entrance is choked by a large volume of massive sulphides, as opposed to BX material. (E) This diagram portrays the mineralization (massive and disseminated) trapped far from the mouth of the conduit back to the north within the conduit. The processes controlling the distribution of the sulphides in this area are similar to those purposed in (B), and (C), except that they occur in regions distal to the chamber.

accommodates less than 2% fragments. The texture of this sequence is extremely homogenous and rarely deviates from a fine to medium grain size.

The VT (Figure 7.1) is continuous and has gradational contacts with the NT, it is only grossly separated from the NT by the infrequent appearance of fragments and an increase in the quantity of sulphide mineralization. The texture as depicted by its name is variable, ranging from fine-grained to pegmatitic. The fragments appear aphyric, mesocratic, well rounded and appear to be derived from an gneiss protolith. Neither ultramafic, gabbroic or troctolitic fragments are recognized in this sequence and there is no substantial variation in fragment size which typically ranges between 1-3 cm. The abundance of fragments in the VT never exceeds 10% of the bulk composition. Mineralization is present as fine-grained disseminations in quantities between trace-15% and displays a definite increase in abundance towards the lower contact.

The VT and NT appear to have been influenced by gravity settling processes as stated by Naldrett *et al.*, (1996), thus fit the widely accepted models of magmatic sulphides settling in situ within a magmatic chamber. Consistent with such models, the VT displays an explicit increase in the accumulation of fragments and mineralization with depth, whereas the NT does not display such features. This broadly indicates that the fragments and dense sulphides gravity-settled from the NT and then continued to spatially segregate through the Variable sequence. It must be emphasized, however, that the controls on mineralization in this domain do not appear to be related to the occurrence, distribution or texture of sulphides within mineralized zones situated elsewhere in the Eastern Deeps system, particularly those found along the base of the chamber (see below).

For example, sulphides contained within the VT sequences do not exhibit well developed textures such as the LTT which are documented within all other significant mineralized zones within the Voisey's Bay deposit (i.e. Ovoid, Mini-Ovoid, and Western Extension). The lowest sequences within the Eastern Deeps chamber are comprised of mineralized conduit rocks identical to those found elsewhere within the conduit environment (i.e. Ovoid, Mini-Ovoid, and Western Extension). As with their western counterparts, these sequences host significant sulphides and are thought to intrude NT and VT gabbro-troctolites emplaced earlier into the chamber (Figures 7.2, 7.3, 7.4, 7.5 and 7.6). The sulphides display textures comparable to those documented elsewhere in the conduit and include FM, TNS, CBX, LTBX, LTT, and VNBX massive to semi-massive sulphides. The breccias (CBX and TNS) contain a diverse range of fragments which consist of gneiss, gabbro-troctolite and ultramafic populations. Fragment sizes and shapes are variable and are thought to be reflective of local environmental conditions. Similar to the upper stratigraphic horizon, the silicate matrix supporting the mineralization is documented as a gabbro (Lightfoot, 1997a, 1997b), however, troctolite intercalation is recognized within the LTT sequences. Contacts with the overlying VT can be locally sharp, but overall appear gradational. Where gradational contacts exist, it is speculated that localized mixing has occurred between the two discrete magmas (i.e. chamber and conduit). If the chamber magma had not been solidified when the sulphide-bearing conduit magma intruded, mixing could have been induced through several variables including, turbulence, density and viscosity (see below).

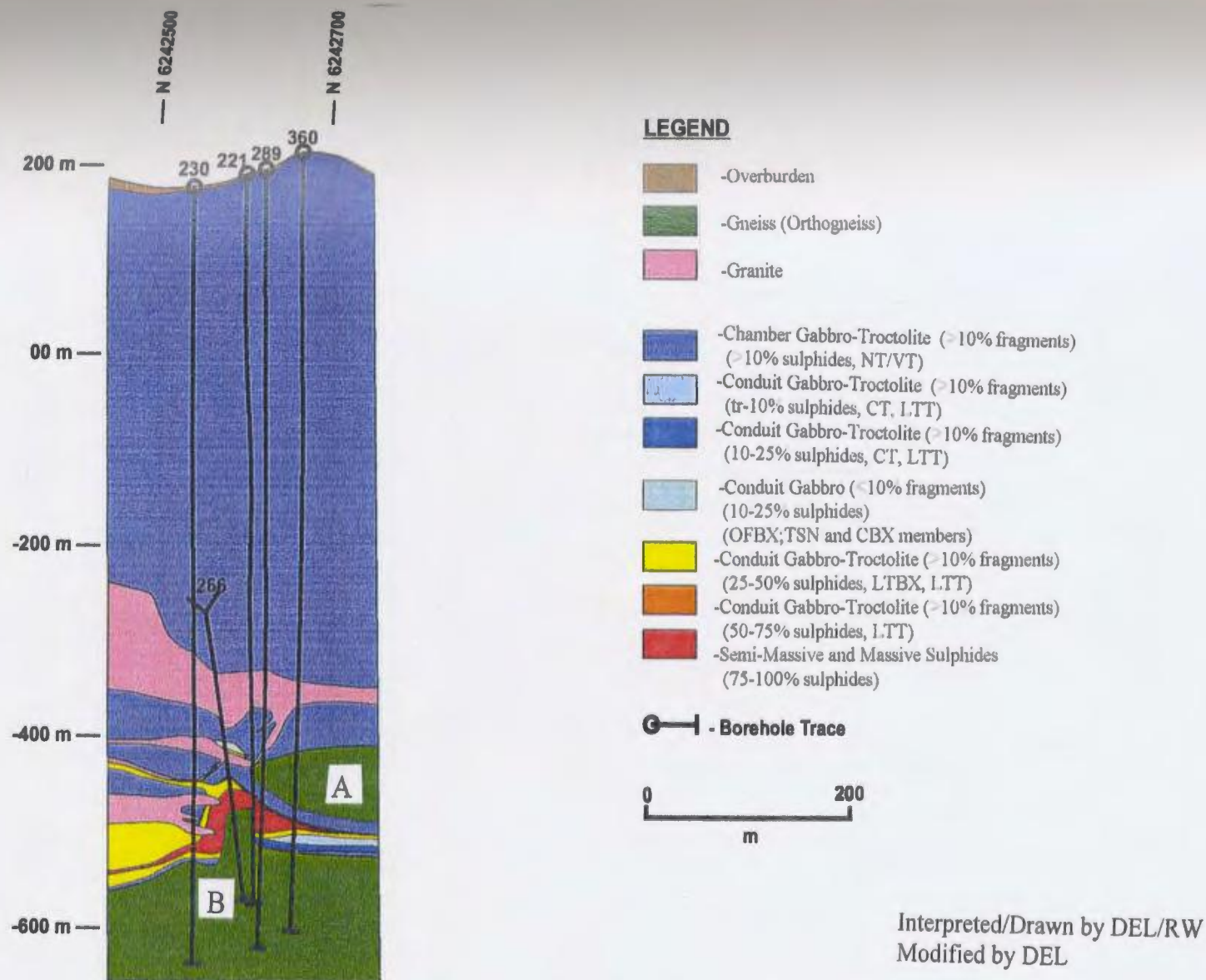


Figure 7.2 A west-facing vertical cross section through L26+00E in the Eastern Deeps. Mineralization occurs within the conduit beneath the orthogneiss wedge extending into the chamber (i.e. Lip Gneiss) and is focused at the step-like structure defining the north edge of a trough within the footwall (i.e. Footwall Depression): (A) Lip Gneiss, (B) Footwall Depression which is least developed in this most western Eastern Deeps section.

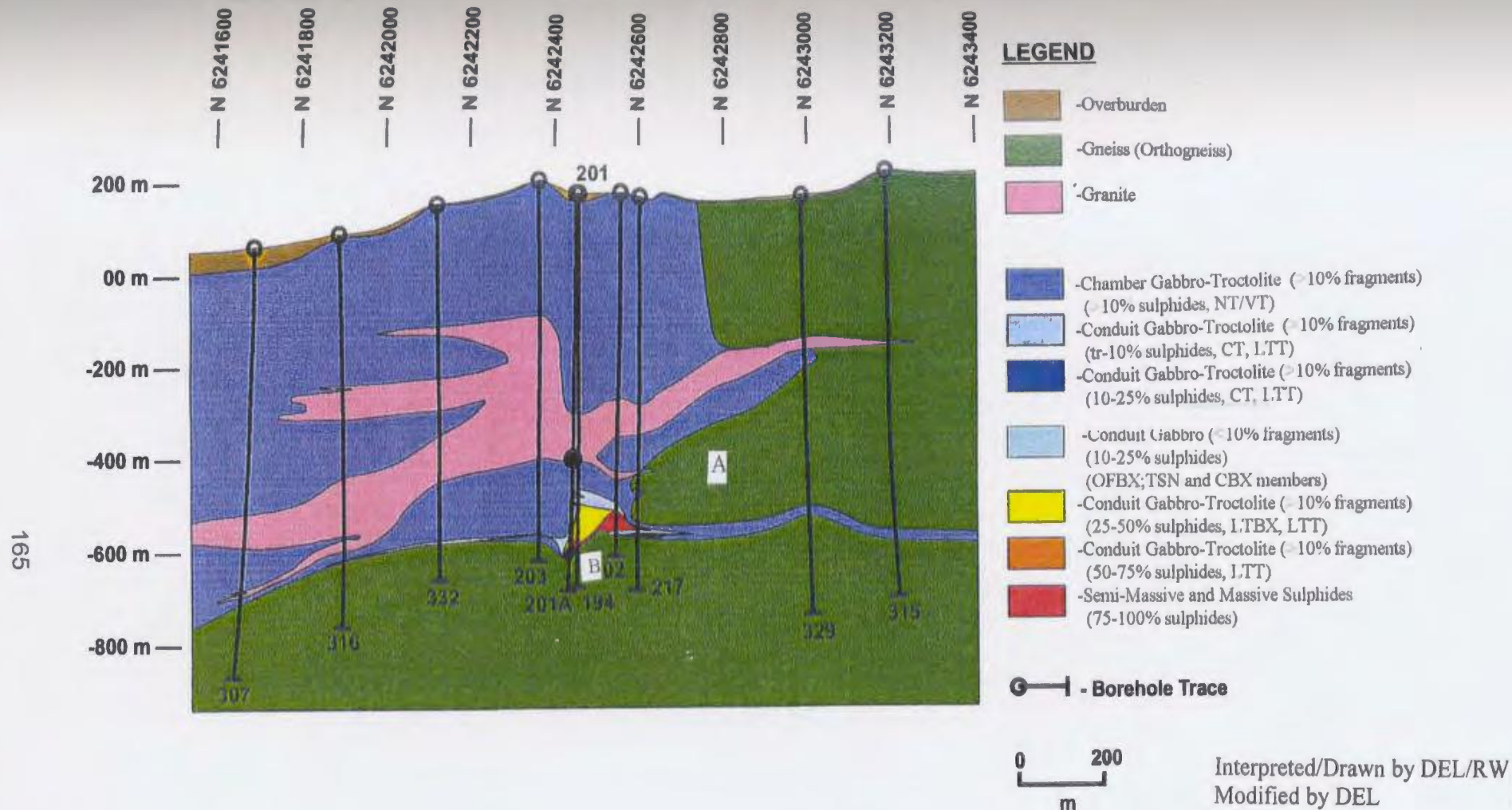


Figure 7.3 A west-facing vertical cross section through L28+00E in the Eastern Deeps. Massive sulphides occur south of the orthogneiss wedge which extends into the chamber (i.e. Lip Gneiss) and are focused at the step-like structure defining the north edge of a trough within the footwall (i.e. Footwall Depression), while the disseminated sulphides are collected within this trough: (A) Lip Gneiss, (B) Footwall Depression.

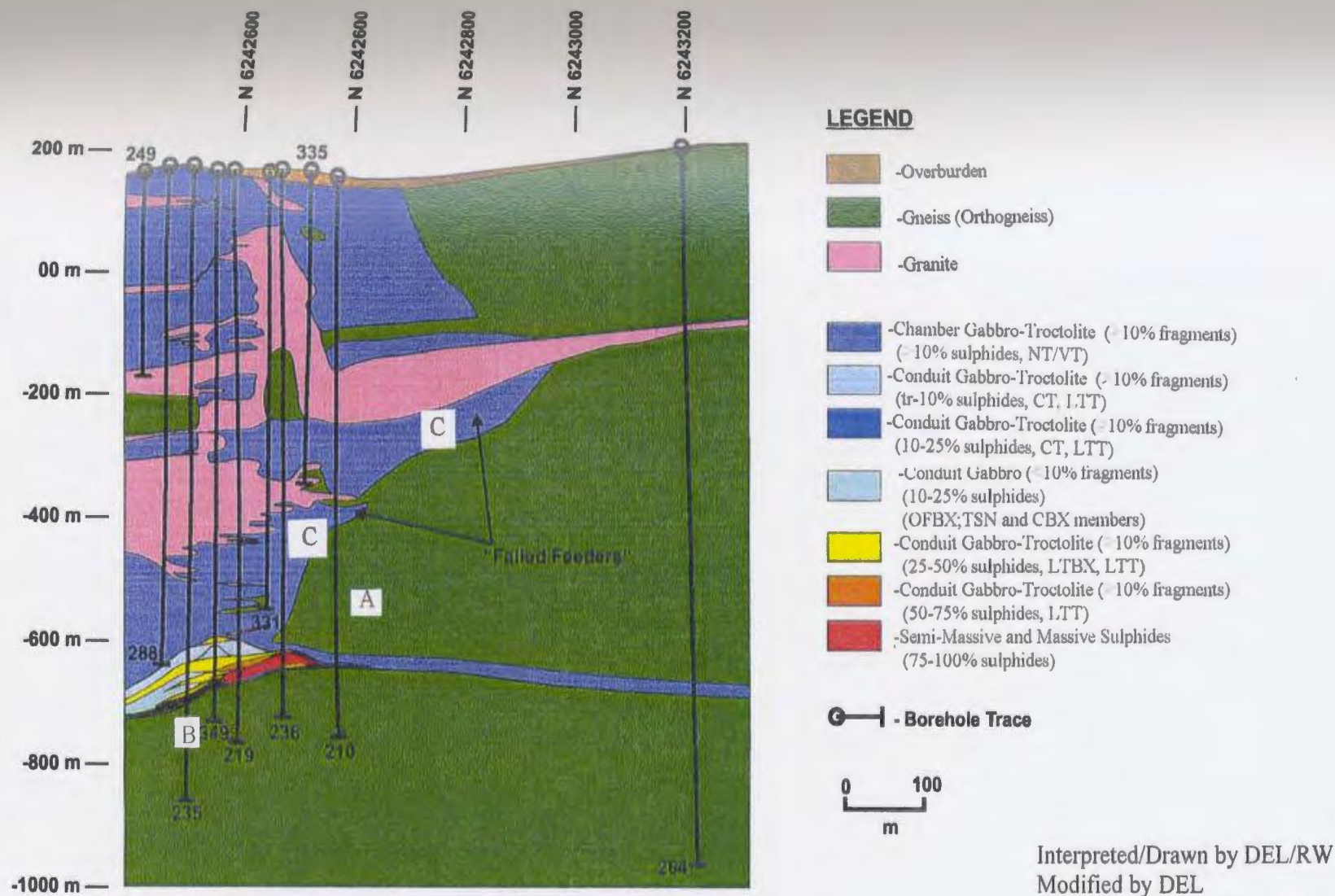


Figure 7.4 A west-facing vertical cross section through L31+00E in the Eastern Deeps. Massive sulphides occur beneath and south of the orthogneiss wedge which extends into the chamber (i.e. Lip Gneiss) and are constrained to the northern parts of the disseminated package collected within the footwall trough (i.e. Footwall Depression). At higher levels within the chamber other conduits (i.e. Failed Feeders) are speculated to intrude the north margin: (A) Lip Gneiss, (B) Footwall Depression, (C) Failed Feeders.

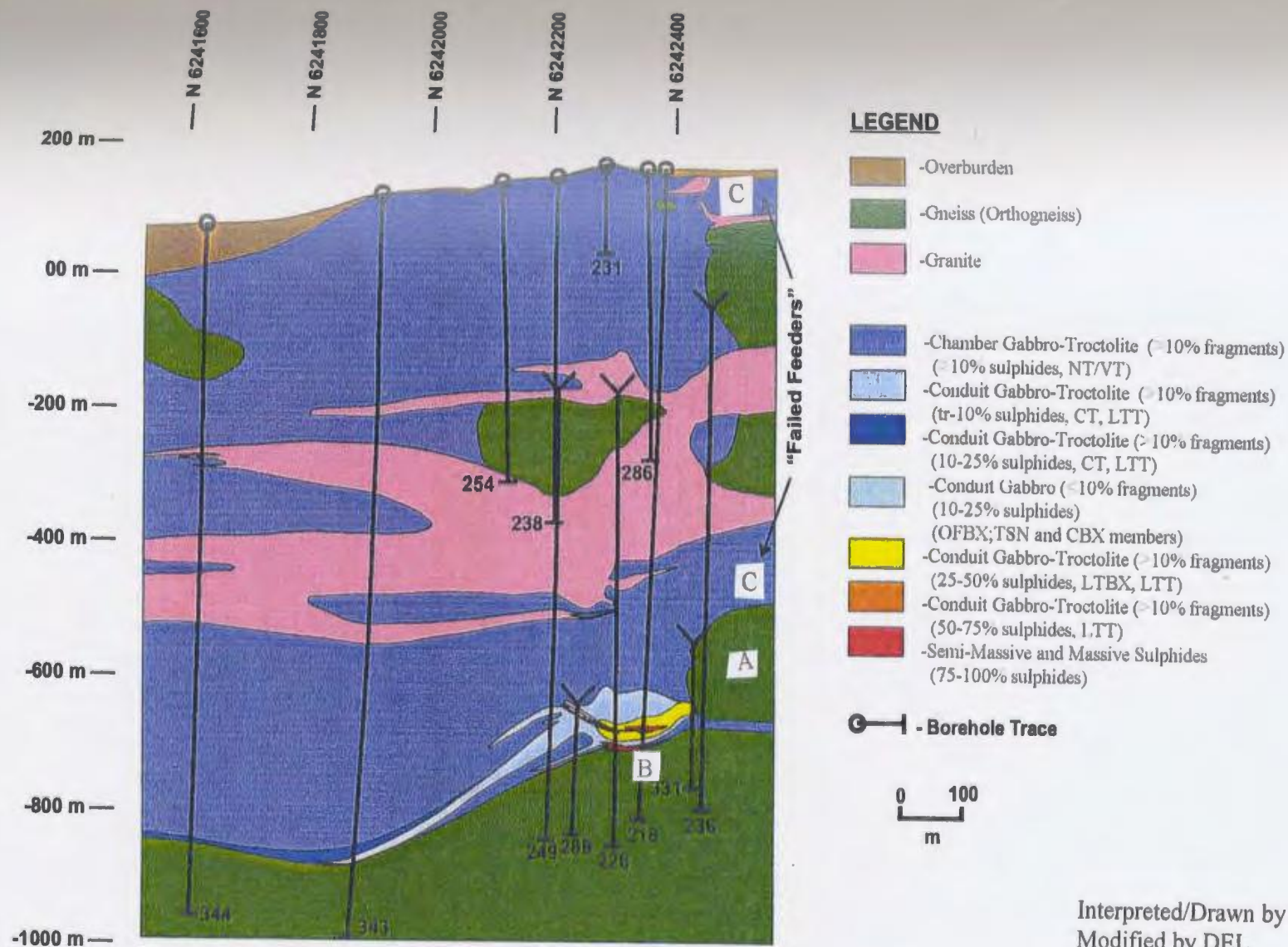


Figure 7.5 A west-facing vertical cross section through L32+00E in the Eastern Deeps. Mineralization is found concentrated within a footwall trough (i.e. Footwall Depression) south of the orthogneiss wedge which extends into the chamber (i.e. Lip Gneiss) and also deposited along the footwall in more southern areas of the chamber. Thick massive sulphide sequences are not displayed along this section, and are speculated to be trapped within the conduit back to the north. At higher levels within the chamber other conduits (i.e. Failed Feeders) are speculated to intrude the north margin: (A) Lip Gneiss, (B) Footwall Depression, (C) Failed Feeders.

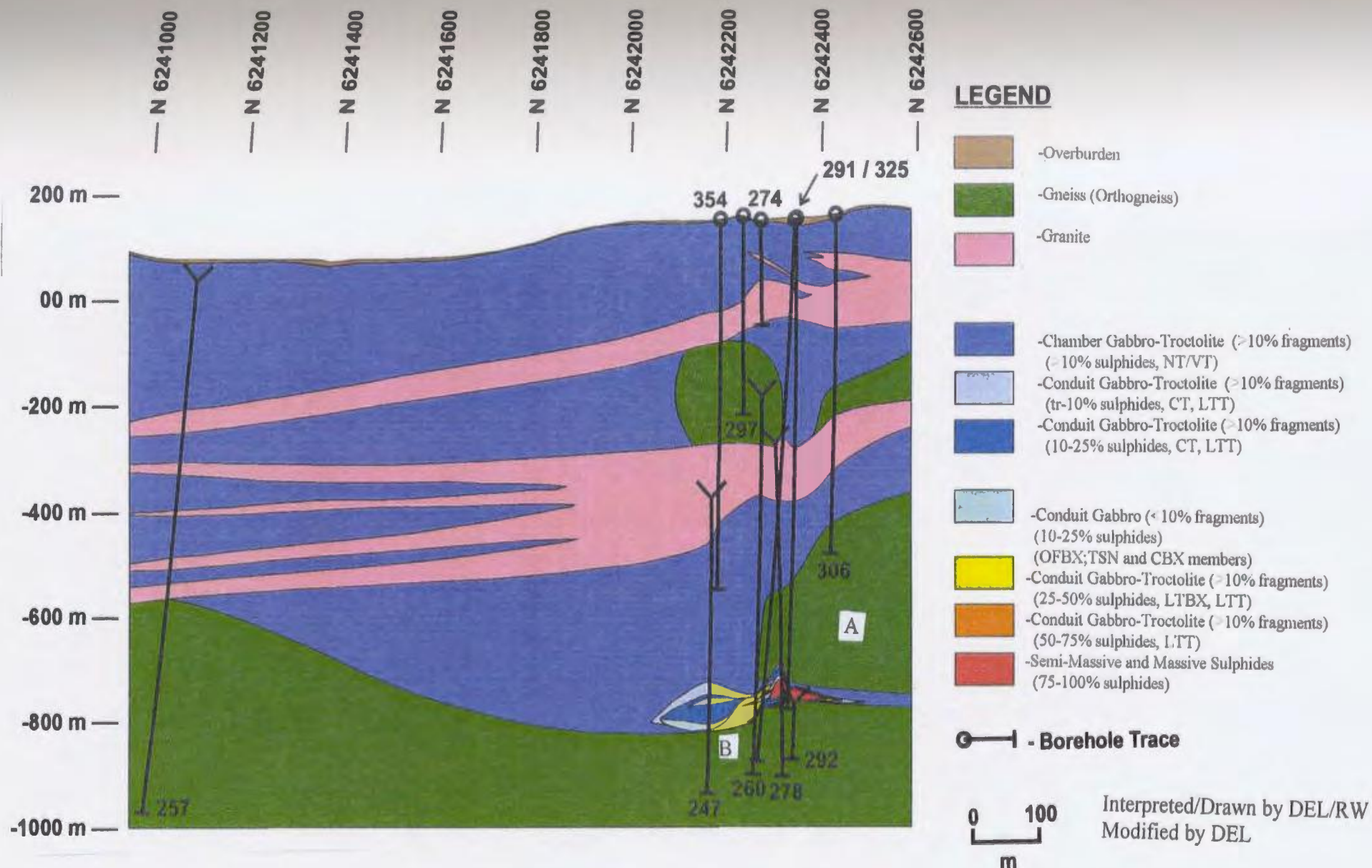


Figure 7.6 A west-facing vertical cross section through L34+00E in the Eastern Deeps. Massive sulphides are found beneath the orthogneiss wedge which extends into the chamber (i.e. Lip Gneiss) and are focused at the step-like structure defining the north edge of a trough within the footwall (i.e. Footwall Depression), while the disseminated sulphides are collected within this trough: (A) Lip Gneiss, (B) Footwall Depression.

7.3 Feeder Melange

There is one discrete horizon within the Eastern Deeps feeder stratigraphy that is not typical of the sequences found elsewhere in the conduit to the west, this is the Feeder Melange (*FM*) (Plate 2D). The FM has a high fragment to matrix ratio with extreme aspect ratios where the long axis of fragment flattening parallels the conduit walls. Since this sequence is only displayed in regions such as the Eastern Deeps where the feeder conduit has a flat lying orientation, it has been suggested that the defining texture of this sequence formed through the collapse of the conduit. Under the weight of the voluminous, overlying country rock, the conduit constricted producing a flattening and a preferential alignment of the fragments (Peter Lightfoot, 1997c, Pers. Comm.). Alternatively, this study suggests these patterns represent primary flow fabrics where the attitude and shape of the fragments were augmented by ductile deformation during the initial emplacement of the conduit (see Chapters 8). Regardless of the exact mechanism, the FM is developed through local environmental controls that appear specific to the Eastern Deeps.

7.4 Geological Significance for the Stratigraphic Position of the Mineralized Zone

Within the ore successions as broadly observed at the bottom of the Eastern Deeps chamber, there appears to be no immediate rationale for modification of accepted models of sulphide emplacement and subsequent settling within a co-genetic magmatic host (i.e. closed system). Although, with detailed examination of the textures, lithologies and geometric parameters, it is apparent these sequences are similar, if not identical in character to those of the sulphides present in the conduit to the west (Ovoid, Mini-Ovoid

and Western Extension). The occurrences and physical character of these sequences are not random or coincidental. Alternatively, these mineralized successions maintain ubiquitous, predictable geological relationships that can be explained geologically, but require complex interpretations. As documented, the physical and geometric controls over these environments deviate from the accepted norm in Ni sulphide models and, therefore, require modifications to the manner in which magmatic Ni sulphide systems such as Voisey's Bay are currently and broadly rationalized.

7.4.1 Terminology

The phrase Lip Gneiss is used to depict a surface irregularity established along the north margin of the chamber. As described above, the north margin of the chamber is vertical to sub-vertical, however, at depth a wedge shaped discontinuity exists. The orthogneiss defining the north margin protrudes inwardly into the interior of the chamber forming a canopy or, a so-called lip (Figure 7.1). Before geological continuity is resumed and contact established with the footwall, the lip gneiss is under-plated by the ore-bearing sequences. The thickest and highest grades of mineralization lie within or are proximal to this feature.

The Entry Line is a linear feature that represents the southern extent of the massive sulphides in the mineralized zone (Figure 7.1). It documents the leading edge of the massive sulphide pulse or more broadly, the trailing edge of the complete magmatic succession. As documented by the geological cross-sections, the congruence of grade and

thickness makes this an economically superior domain, in contrast to that which is expressed in the disseminated outliers.

The Footwall Depression is a topographic irregularity developed within the footwall to the Eastern Deeps chamber (Figure 7.1). This depression or trough is clearly defined through geometric analysis of the footwall substrate and occurs proximal to the north wall of the magmatic chamber, but south of the Lip Gneiss. It is thought that this discontinuity was established prior to both the magmatic and mineralizing events, and was reactivated by deformation associated with post-mineralization events (see below).

The Eastern Deeps Feeder is speculated to be the feeder conduit which controlled the geometry, transport and distribution of sulphide-bearing magma within the Eastern Deeps. This feeder is documented as a gently southeast dipping, lenticular body. The feeder transects the orthogneiss north of the chamber and extends out below the lip gneiss (Figure 7.1) along this trend. Within the limits of the chamber and proximal to the north wall, the feeder can be quite variable in thickness. North of the chamber, in the orthogneiss terrane, the conduit is constrained by the wall rock and to date has not been observed to exceed 30 m in true vertical thickness. Furthermore, in this location, the FM sequences dominate the geology within the conduit.

7.4.2 Ore Domains

It is apparent from the west-facing geological sections through the Eastern Deeps, that sulphide deposition was controlled by geometric and environmental parameters. Specifically, the Entry Line for the massive sulphides is documented to occur within two

domains and where not apparent, is speculated to exist within a third domain. These domains are: (1) the south margin of the Lip Gneiss, (2) beneath the Lip Gneiss, and (3) north of the gneiss lip, backed-up within the feeder (Figures 7.1, 7.2, 7.3, 7.4, 7.5 and 7.6).

The thickest packages of disseminated sulphides correlate directly with the Footwall Depression south of the Lip Gneiss (Figures 7.2, 7.3, 7.4, 7.5, and 7.6). Conversely, the thickest massive sulphide intersections are always found north of the Footwall Depression beneath the Lip Gneiss and are constrained along the step-like structure produced by its north margin (Figures 7.2, 7.3, 7.4, 7.6, 7.7 and 7.8).

The Entry Line for the massive sulphides can be observed to deviate from north of the Footwall Depression and into total coincidence with this surface irregularity (Figures 7.7 and 7.8). It is interpreted that once the early pulses, which carried the dense mass of disseminated sulphides, were exhaled from the constricted feeder into the open chamber, they encountered a reduction to the confining pressure. This control could have decreased magma transfer through this zone and increased magma viscosity, as documented to occur in similar processes by Riley and Kohlstedt (1990). Subsequently the dense magmatic package would not be able to propagate a great distance and settled into a trap, defined by the Footwall Depression (Figure 7.1). The trailing massive sulphides would subsequently be restricted from distribution south, past the trough, due to the barricade erected by the accumulated disseminated sulphides (Figure 7.1). This constrains the Entry Line to localities north of the Footwall Depression.

Similarly, where the Entry Line coincides with the Footwall Depression, the

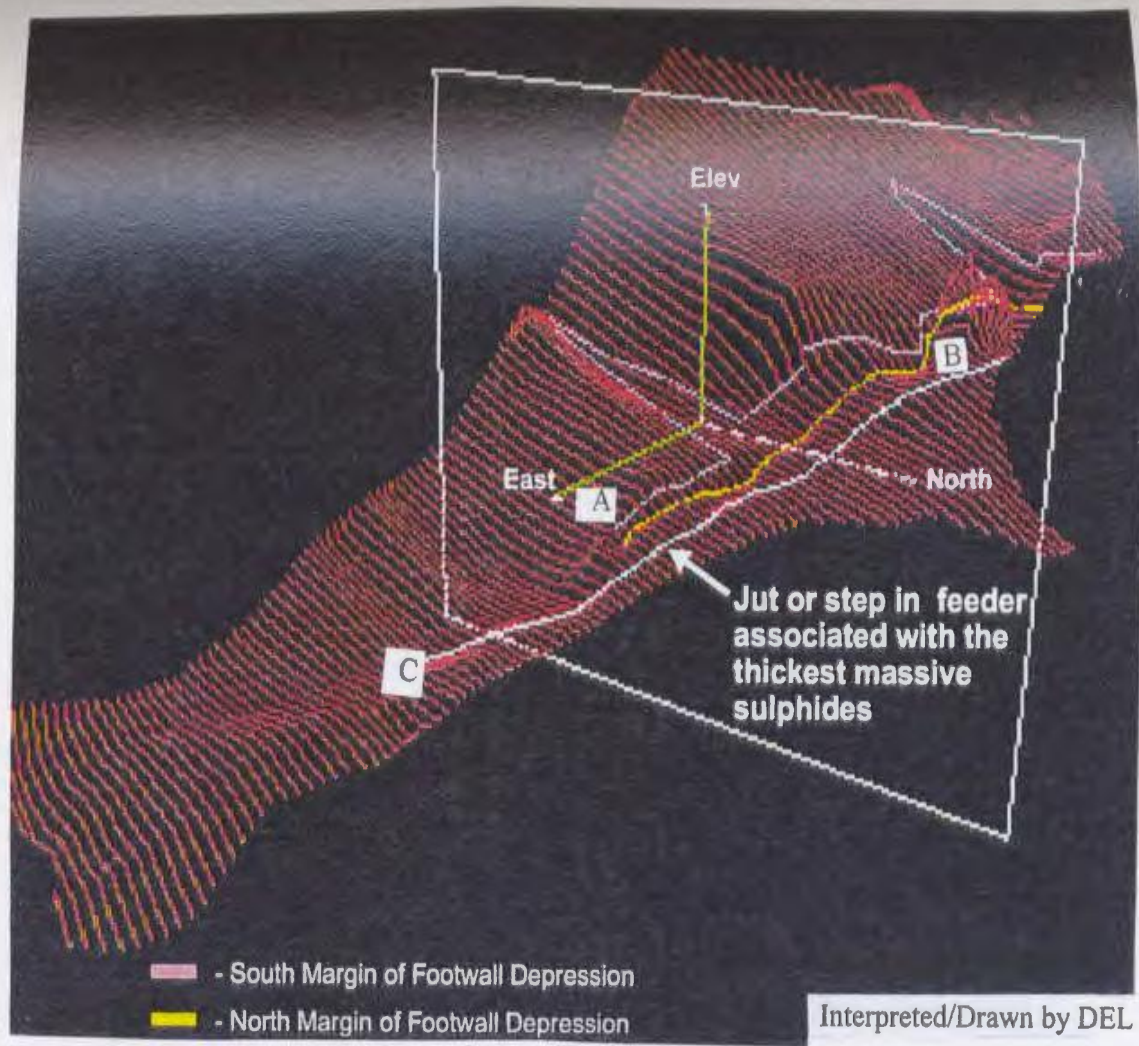


Figure 7.7 A three dimensional model showing the footwall to the Eastern Deeps chamber vertically sliced at 25 m intervals. The model defines a trough in the footwall (i.e. Footwall Depression) adjacent to a step or rise in the footwall geometry. The south margin of the trough is marked by the pink line, while the north margin of the trough is represented by the yellow line, which is coincidental with the south margin of the footwall step. The north margin of the step is defined by the white line: (A) South margin of the footwall trough, (B) North margin of the footwall trough and south margin of footwall step, (C) North margin of the footwall step.

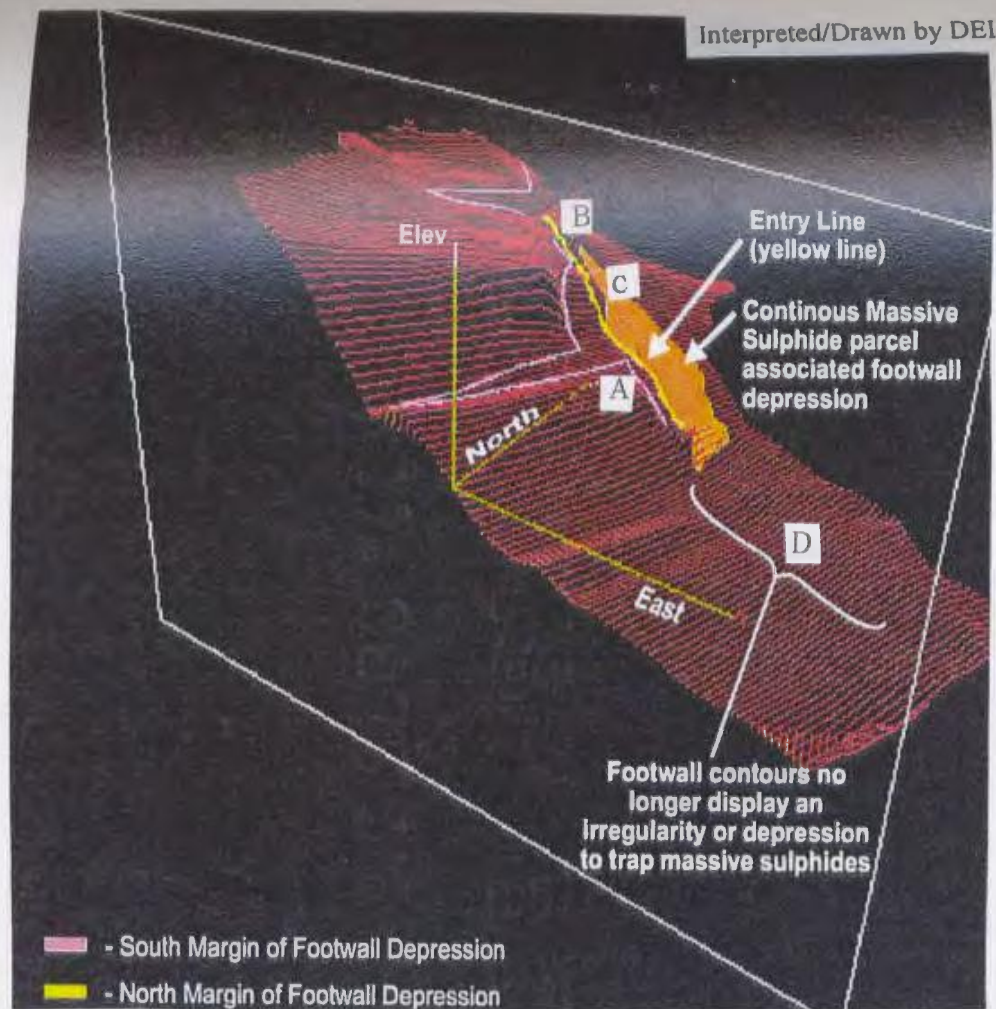


Figure 7.8 A three dimensional model showing the footwall to the Eastern Deeps chamber vertically sliced at 25 m intervals. The model defines a trough in the footwall (i.e. Footwall Depression) where massive sulphides are collected along the north margin or found adjacent to this structural irregularity along the north margin of a step or rise in the footwall geometry. The south margin of the trough is marked by the pink line, while the north margin of the trough is represented by the yellow line, which is coincidental with the south margin of the footwall step. The north margin of the step is defined by the white line: (A) South margin of the footwall trough, (B) North margin of the footwall trough and south margin of footwall step where massive sulphides enter the system (i.e. Entry Line), (C) North margin of the footwall step which the Entry Line follows to the east, (D) In western regions of the Eastern Deeps, the disappearance of the massive sulphides (i.e. Entry Line) can be related to the absence of the Footwall Depression.

massive sulphides are interpreted to have abutted against the disseminated mound where they were not able to penetrate through the dense disseminated mass. Also at this site, the geometry of the trough may not have provided the conditions favourable for the escape of these sulphides to the south (Figure 7.1). For example, it is interpreted that gravity and thermodynamic effects hampered the flow of the massive sulphide lenses up and over the south margin of the footwall depression and, therefore, restricted further transport of the system to the south. Likewise, the north margin of the footwall depression is marked by a small off-set or step (Figures 7.1 and 7.6) and in a similar fashion, this wall could have restricted the massive sulphides from further distribution. This structure is not readily expressed in two dimensional sectional view (Figures 7.2, 7.3, 7.4, 7.5 and 7.6), however, it is a prominent feature when displayed with three dimensional models (Figure 7.7).

Where the Entry Line is not apparent (Figures 7.5, 7.7 and 7.8) and no thick sequences of disseminated sulphides are intersected, it is speculated the mineralization was trapped back in the conduit, well north of the Lip Gneiss. Interpretations suggest that the constriction provided by the Lip Gneiss and the wall rock to the north, could have caused the conduit system to have become choked. If the narrow width of the conduit mouth did not provide conditions that would favor the rapid expulsion of fragment-laden magma (Figures 3.2 and 7.1), the early BX textured magmas could accumulate in a voluminous packages proximal to the feeder mouth (Figure 7.1). Under such circumstances the earliest expelled breccias could continue to restrict the exhalation of the trailing fragment-bearing magma until the feeder was completely blocked (Figures 3.4 and 7.1). As consequence,

when the trailing massive sulphides encountered this obstruction, the magmatic system could continue to back-up into more northern regimes of the conduit (Figure 7.1).

Alternatively, if were not expelled from the conduit at an appreciable rate, the massive sulphides alone could have blocked the conduit (Figure 7.1). Evidence supporting this process is provided by documentation of an increase in conduit width (Figures 7.9 and 7.10) north of the Lip Gneiss. This geometric change indicates the magmatic fluids were traversing a system of uniform width, then encountered a trap or a site where the conduit swelled. Under such circumstances, the heavy sulphides would be expected to flood the trap before continuing with flow (Figure 3.3). The continuation of flow after the trap was filled would be marked by local massive sulphide horizons found past the south margin of the trap, as is documented in the Eastern Deeps by the presence of multiple, discontinuous lenses of massive sulphides south of the Lip Gneiss (Figure 7.5). The irregular occurrence of these horizons does not allow for the confident establishment of the true Entry Line in these locations, however, as a consequence of these environmental and geometric controls, it would be expected that accumulations of massive sulphides would be found back within the conduit, to the north of the Lip Gneiss (Figure 7.1).

7.5 Ambiguity in locating the Entry Line in Extreme Eastern Regimes

To the east it becomes apparent that the Entry Line is ambiguous (Figures 7.4, 7.5, 7.6, 7.8 and 7.11). Exploration in this regime is limited, but three explanations have been arrived at for this uncertainty.

- (1) The most obvious feature is the disappearance of a distinct trough or Footwall

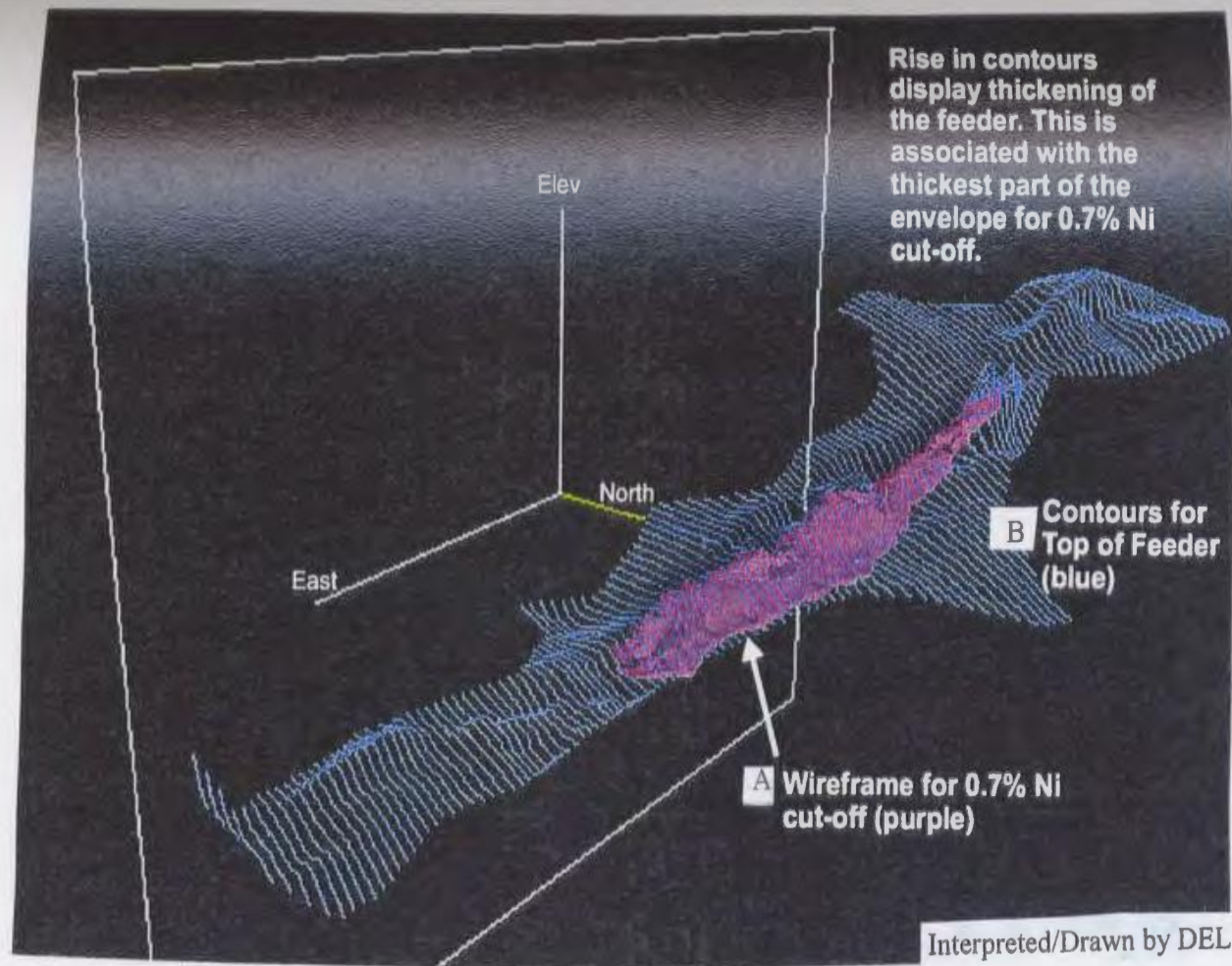


Figure 7.9 A three dimensional model showing the top of the Eastern Deeps feeder vertically sliced at 25 m intervals. The model establishes that the thickest sequences of mineralization occur within the widest portions of the feeder conduit. Physical and geometric changes within the system (see Figures 7.7 and 7.8) produce this trap environment and control the distribution of sulphides within the Eastern Deeps: (A) Wireframe model for mineralization above 0.7% Ni, (B) Contours for the top of the feeder conduit.

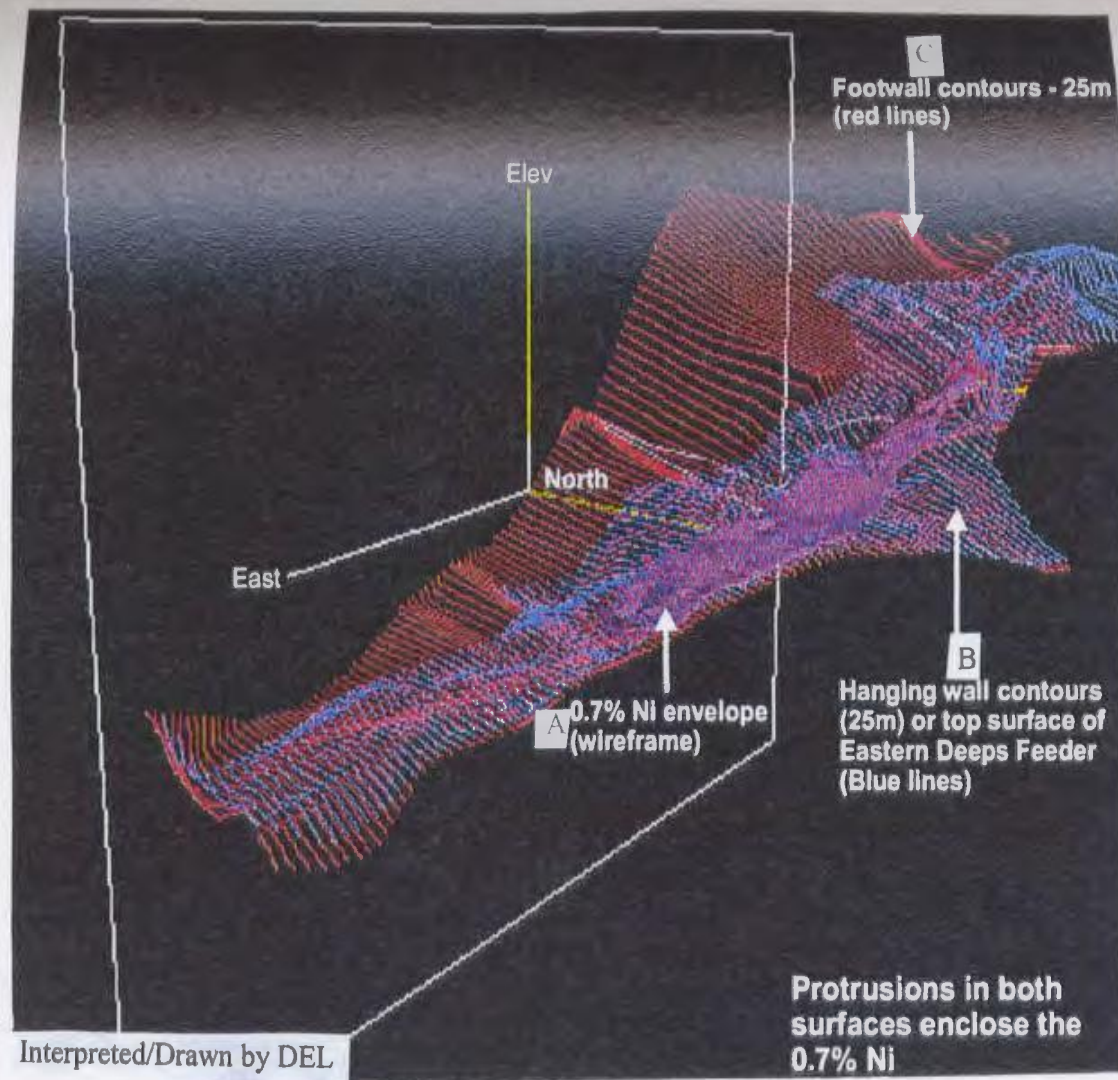


Figure 7.10 A three dimensional model showing the top (blue lines) and bottom (red lines) of the Eastern Deeps feeder vertically sliced at 25 m intervals. The model indicates that the thickest sequences of mineralization occur within the widest portions of the feeder conduit. Physical and geometric changes within the system (see Figures 7.7 and 7.8) produced this trap environment and controlled the distribution of sulphides within the Eastern Deeps: (A) Wireframe model for mineralization above 0.7% Ni, (B) Contours for the top of the feeder conduit, (C) Contours for the bottom of the feeder conduit

Depression (Figures 7.4, 7.5, 7.6, 7.8, 7.9, 7.10 and 7.11). If the massive sulphides escaped the conduit and ebbed through the feeder mouth, there may have been no distinct geometric features (i.e. embayments) to constrain their distribution (Evans-Lamswood, 1996a; 1997a). As previously described, the massive sulphides can be compared to the dense sludge in a deltaic system. With no Footwall Depression to act as a trap for the dense material, it would not accumulate but would extend outwards from the feeder mouth in a wedge or as discrete fingers (Figure 7.12). Such processes have been documented in density contrast experiments by Synder *et al.* (1997). Laterally, the thicknesses of the disseminated packages are not as extensive as those displayed to the west where the Footwall Depression is a prominent feature. With no trap established, the earliest pulses may have flowed, unhampered to the south. This subsequently could result in the formation of an apron of diluted disseminated and massive sulphides, mixed with barren chamber material (Figure 7.12).

(2) The second scenario for the undefined Entry Line can be related to choking of the system as mentioned above (Figure 7.1). In this domain there are notable accumulations of BX sequences in the conduit (Figure 3.4) and it may be that this system was choked, not proximal to the chamber margin, but further to the north, well back in the feeder plumbing (Figure 7.1).

(3) The final and most plausible scenario incorporates both previously mentioned situations. With the limited northward exploration in this geological domain, the continuity and position of the Lip Gneiss may actually be incorrect. If exploration continues to the north, it may be possible that the Lip Gneiss will no longer appear to exist as a wedge of

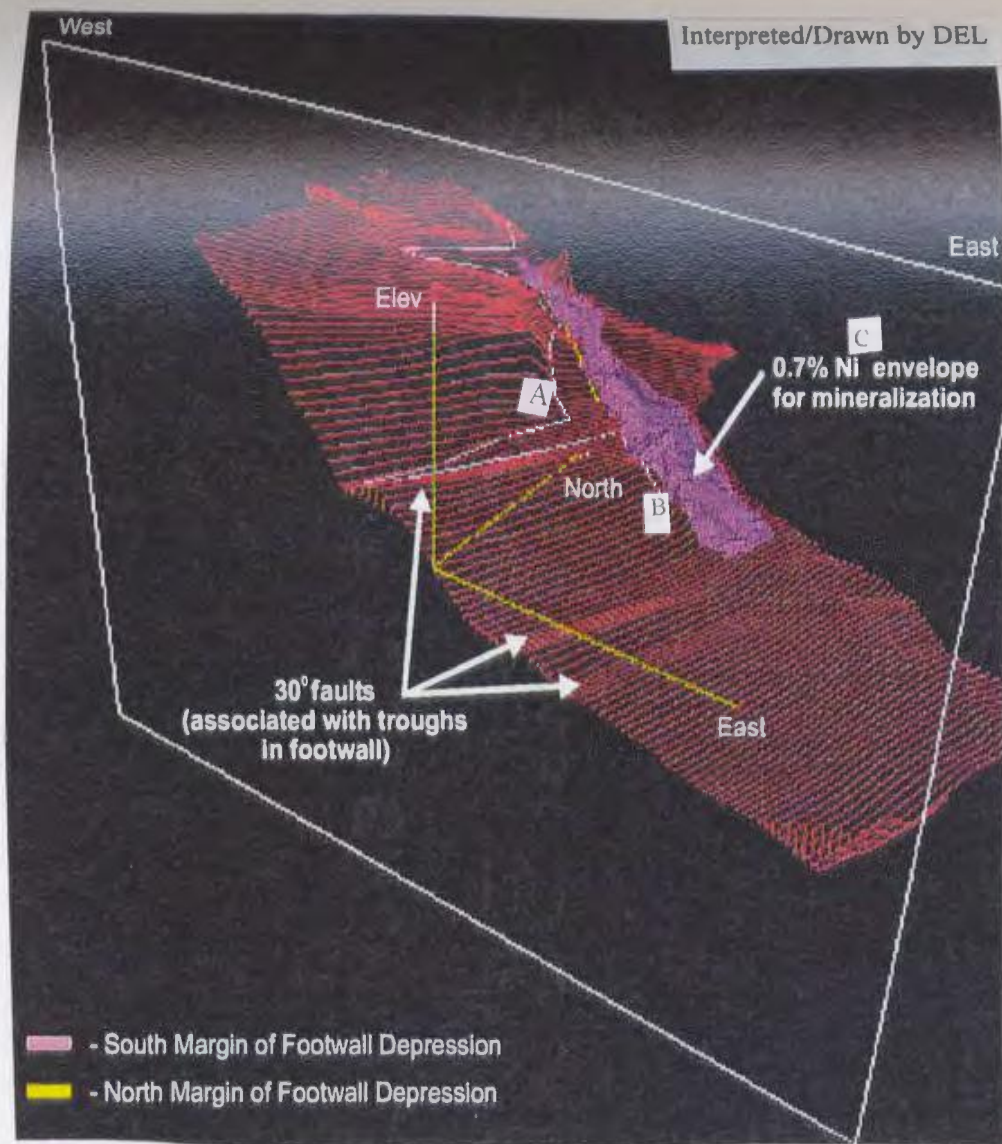


Figure 7.11 A three dimensional model showing the footwall to the Eastern Deeps chamber vertically sliced at 25 m intervals. The model defines a trough in the footwall (i.e. Footwall Depression) where all significant mineralization (i.e. greater than 0.7% Ni) is focused. The south margin of the trough is marked by the pink line, while the north margin of the trough is represented by the yellow line: (A) South margin of the footwall trough, (B) North margin of the footwall trough, (C) Wireframe for mineralization greater than 0.7% Ni.

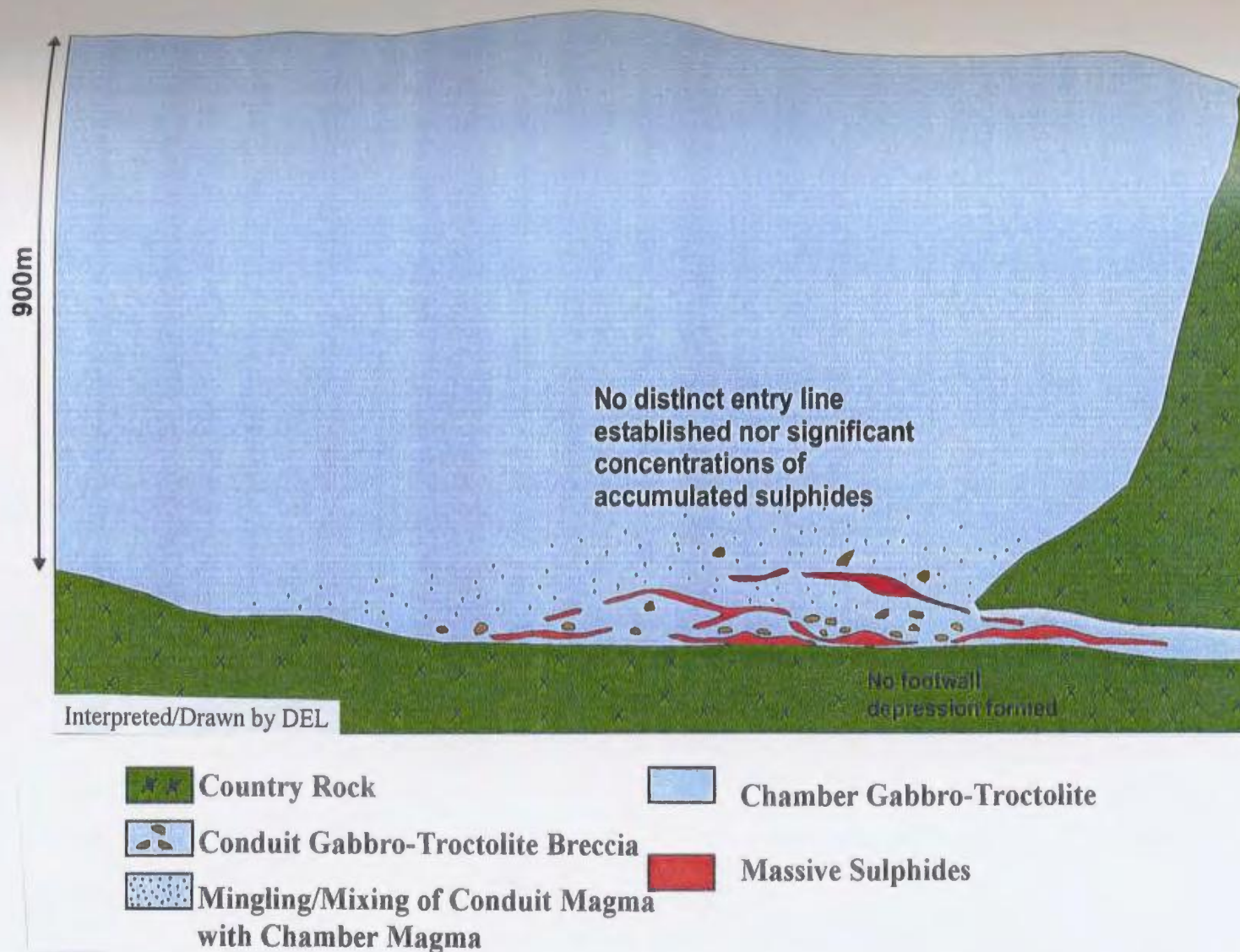


Figure 7.12 An idealized west-facing vertical cross section through the most eastern regions of the Eastern Deeps chamber and feeder conduit. This figure shows mineralization expelled from the conduit and mingling with the chamber magma. Without a trap (i.e. Footwall Depression) to constrain and collect the discharged sulphide-bearing magma, it is distributed as a broad diluted cloud of mineralization or locally occurs as a discrete interfingering pattern.

wall rock, but alternatively, as an island of orthogneiss (Figure 7.13) (Evans-Lamswood, 1996c). If the lip has been detached and actually represents a mesoscopic fragment within the chamber, as can be observed to occur in sections L3200E-L3800E, the actual location for the mouth of the feeder conduit has been misinterpreted. Consequently, the true feeder mouth and anticipated Entry Line will be located further north (Figure 7.13) beyond the extent of the current diamond drill program. It is also intriguing that this scenario suggests the existence of mesoscopic and macroscopic bifurcation zones where multiple conduits or splays (Figure 3.1) may co-exist and interact through repetitious convergence or divergence.

7.6 Anomalous Disseminated Sulphides within Upper Stratigraphic Horizons

The north wall of the Eastern Deeps is riddled with abrupt irregularities that have generally been most definable in more eastern regimes. These breaks in the orthogneissic interface are associated with increased disseminated mineralization in specific stratigraphic horizons (Figures 7.3, 7.4 and 7.5). These isolated and sharp horizons can be correlated with an anomalous increase in fragment content and alteration mineralogy (i.e. biotite). These features suggest that a second, stratigraphically higher feeder conduit system may exist in the Eastern Deeps. In some of these disconformities there is no hard evidence to suggest a feeder actually existed at this stratigraphic level, as there are no true horizons of breccia recognized nor are there any significant accumulations of sulphides. These features have been crudely referenced by the deposit geology staff as “failed feeders”, however, a broader and more significant issue arises; if a viable propagating feeder does exist

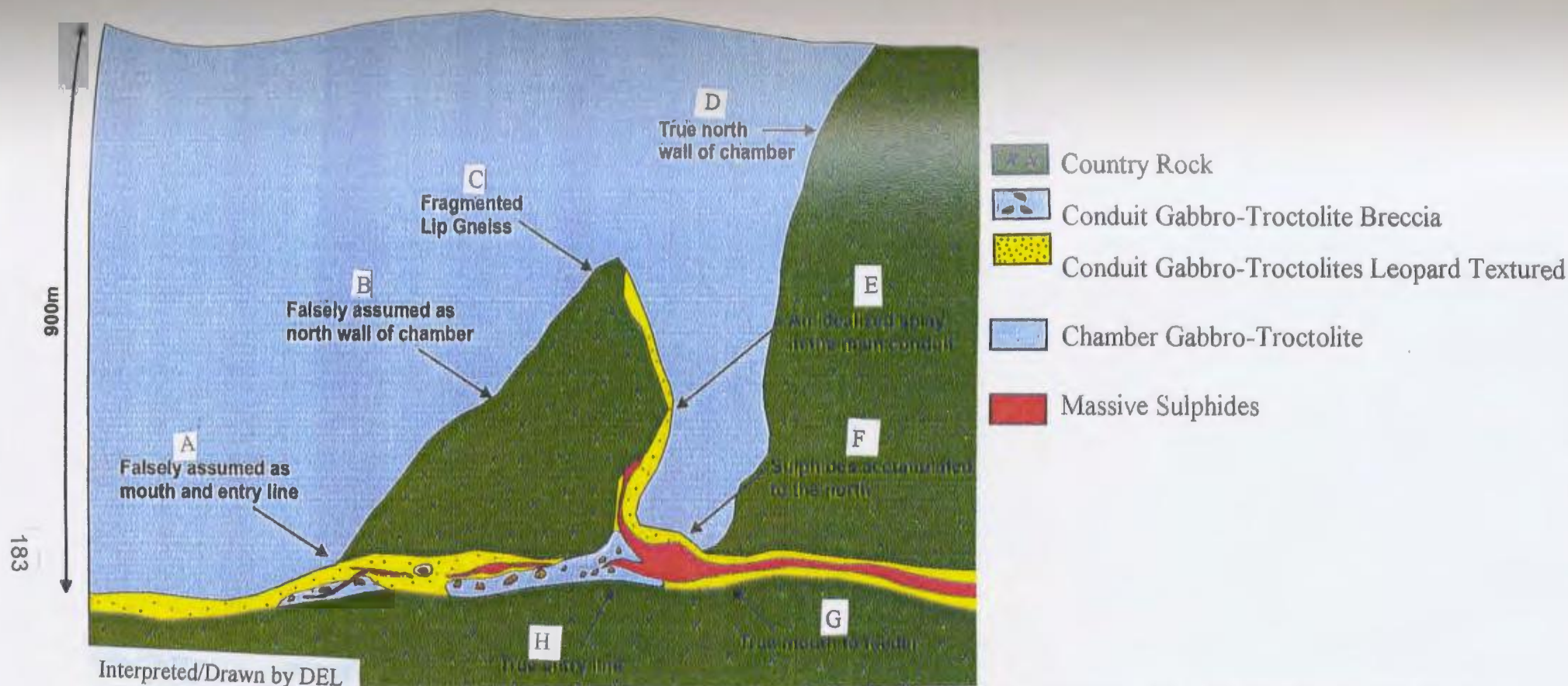


Figure 7.13 An idealized west-facing vertical cross section through the most eastern regions of the Eastern Deeps chamber and feeder conduit. This figure shows mineralization trapped within the conduit back to the north. In this northern region, the wedge of orthogneiss (i.e. Lip Gneiss) which protrudes into the chamber may actually be detached from the north wall of the chamber. At this site, a second or earlier point of entry for the conduit (i.e. Entry Line) into the chamber could be present and where sulphides would be preferentially concentrated. The conduit could splay or bifurcate in this location with one branch following the north margin of the gneiss block and the second branch continuing to follow the base of this structure: (A) Second Entry Line which can be mistaken for the only entrance into the chamber, (B) The south margin of the Lip Gneiss which can also be mistaken for the north wall of the chamber, (C) Lip Gneiss detached from the north wall of the chamber, (D) The actual north wall of the chamber where the gneiss block is detached, (E) A bifurcation or splay in the main feeder conduit. (F) Sulphides collected at the break between the Lip Gneiss and north wall of the chamber, (G) The real mouth to the chamber, (H) The first Entry Line.

elsewhere (i.e. north of the Eastern Deeps), then these “failed feeders” may represent offshoots or bifurcation channels that can lead to new discoveries of significant mineralization (Figures 3.1 and 7.13). Furthermore, this concept can also be linked (see above) to the possible existence of multiple sulphide zones in the eastern regions of the Eastern Deeps, where a second Entry Line could exist if the Lip Gneiss is broken or detached from the country rock (Figure 7.13).

7.7 Ambiguity in Defining the upper contact of the Feeder South of the Entry Line

As observed in the geological cross-sections (Figures 7.4, 7.5 and 7.6), the typical feeder morphology as recognized in the Ovoid and in more western domains is not regular, sharp or reliable in the Eastern Deeps. As with the deltaic system it is speculated that lighter, less dense magmatic sulphides will propagate to more southern extremes than their massive ore counterparts. As mentioned previously, the velocity and viscosity controls of these sequences will be less extensive. Subsequently, as this less dense (relative to the massive sulphides) material exits the feeder, it will travel greater lateral distances and mix with the hosting magmatic fluids. Mixing through density contrasts in magmatic systems has been documented elsewhere by Koyaguchi and Blake (1991), and Synder *et al.* (1997). The subsequent sulphide mineralization will be diluted and dispersed. It is obvious that mixing due to density and interface geometry could have played a major role in sulphide distribution south of the feeder mouth (Figure 7.12). In zones where both the sulphide-bearing conduit and chamber magmas mix, but do not settle prior to solidification, the upper contact will be a gradational, diffuse interface. However, where

sulphide settling does occur, sulphide distribution will be concentrated. This subsequently, limits and sharpens the position of the upper contact.

7.8 The Significance of the Conduit (Feeder) Position

The most significant feature expressed by the Eastern Deeps feeder conduit is its stratigraphic position. If it represents the base to the Eastern Deeps chamber, it totally opposes the position of the conduit relative to the Western Deeps chamber (Evans-Lamswood, 1997d, Figure 9), where it is located at the upper margin of the chamber. The significance of the opposing stratigraphic positions of the two feeders is of utmost importance geologically. They suggest a timing for mineralizing events relative to the emplacement of the chamber, and as well, establish the strict adherence to structural controls. The feeders/conduits are postulated to postdate the main magmatic events within the chamber, but not beyond the time extents that would have allowed for the complete solidification of the magmatic material in the chamber. The feeders appear to intrude during the early solidification process since the gabbro-troctolites hosted by the chambers were not substantially brecciated by the later mineralizing events. The feeder does, however, flow along a discontinuity or zone of weaker competence.

In the case of the Eastern Deeps, the rheologically incompetent environment would be established along the footwall interface where the old, competent orthogneisses are separated from the less competent gabbros-troctolites. Similarly in the Western Extension, the conduit adheres to the upper, structurally weak margin of the chamber. Within both the Eastern Deeps and the Western Extension, identical stratigraphic relationships are displayed within the respective sulphide-bearing conduit sequences. The gabbroic

magmatic phases were the initial pulses to traverse the conduit and are most frequently preserved in the marginal domains. Subsequent trailing successions consist of gabbroic OFBX, LLT gabbros-troctolites, and finally massive sulphides (Figure 6.6), respectively.

If settling processes dominantly controlled sulphide deposition and subsequent bulk accumulations, then the stratigraphy as observed in the Western Extension is totally anomalous. It would, in fact represent a reversely graded sequence, whereby, the coarse, heavy sulphides and fragment-laden material resided at the top of a less dense body of magma. With the application of environmental and geometric controls a distinct and reliable model arises for the post-chamber intrusion of the sulphide-bearing feeder conduits along media of structural incompetencies (Evans-Lamswood, 1997d, Figure 9).

Chapter 8: Structure; Ovoid, Mini Ovoid, Western Extension and Eastern Deep.

8.1 Structural Model

Throughout the recent, but extremely active, exploration program at the Voisey's Bay deposit there has been much controversy concerning emplacement mechanisms for the Reid Brook Intrusive Suite. Discussions in this study have focused on flow kinematics of sulphide-laden magma, sulphide traps, and the physical controls governing these processes. Models have been developed for magmatic behavior within the conduit network, but do not address the macroscopic tectonomagmatic evolution of the system. For example, models of magma behavior in the conduits rely heavily on the perceived nature of formation and interaction of multiple incompetencies within the host rock, yet there has been no documentation of structural deformation within the host gneiss-magma conduit system. Do such structures exist and how do they provide geometric control over such a dynamic magmatic system? There is also much debate as to whether the formation of the Voisey's Bay system was controlled by orogenic or anorogenic events. The following documentation will try to establish the importance of both processes to the development of the Voisey's Bay system: (1) pre-magmatic structures formed during the ca.1.8 Ga. orogenesis, and (2) anorogenic magmatism (ca.1.3 Ga.) which exploited these pre-existing structures.

8.1.1 Structural Control

On the scale of this study, the Voisey's Bay deposit appears to follow distinct structural trends. Five structural systems are recognized which were the locus for anorogenic magmatic emplacement and conduit distribution. These systems include: (1)

prominent east/west lineaments, (2) steeply dipping, north and south-facing conjugate faults, (3) sub-horizontal brittle fractures, (4) an east/west-trending sinistral strike-slip system, and (5) 310°/030° Reidel brittle shears (Evans-Lamswood, 1996b) (Figure 5.1).

The east/west lineaments predate the magmatic events and, hence, deposit emplacement. These structures transect the boundary between the Nain and Churchill provinces and appear most prominent within the Nain Plutonic suite where these intrusive rocks straddle the tectonic suture. These are interpreted to be brittle crustal faults (i.e. extensional joints) formed as secondary structures (i.e. primary contractional structures are thought to be in coincidence with the suture) in rheological response to primary σ_1 and σ_3 stresses applied east-west and north-south, respectively (Figure 8.1). The stress regime is interpreted to be a function of the 1.86 Ga. (Ryan, 1996) collision between the Nain and Churchill/Rae provinces which is dominated by compressional events within the Torngat Orogen (Jamison and Calon, 1994). Transpressional stresses associated with Abloviak Shear Zone (1.84-1.82 Ga.) (Korstgard, 1987) do not appear to overprint this area, thus it is speculated that the Voisey's Bay magmatic system is contained in the foreland of this orogen, beyond the eastern limits of the later transpressional event.

The steeply dipping, north and south-facing conjugate faults (Figure 8.1) are syn-magmatic structures which would, therefore, be coeval with the ca. 1.35-1.29 Ga Nain Plutonic suite (Ryan, 1996). These faults exploited planes of weakness defined by the primary east/west lineaments. Collectively, this system of faults represents an episode of juvenile extension where a graben-like structure was produced through stresses induced by crustal uplift (Figures 8.2 and 8.3).

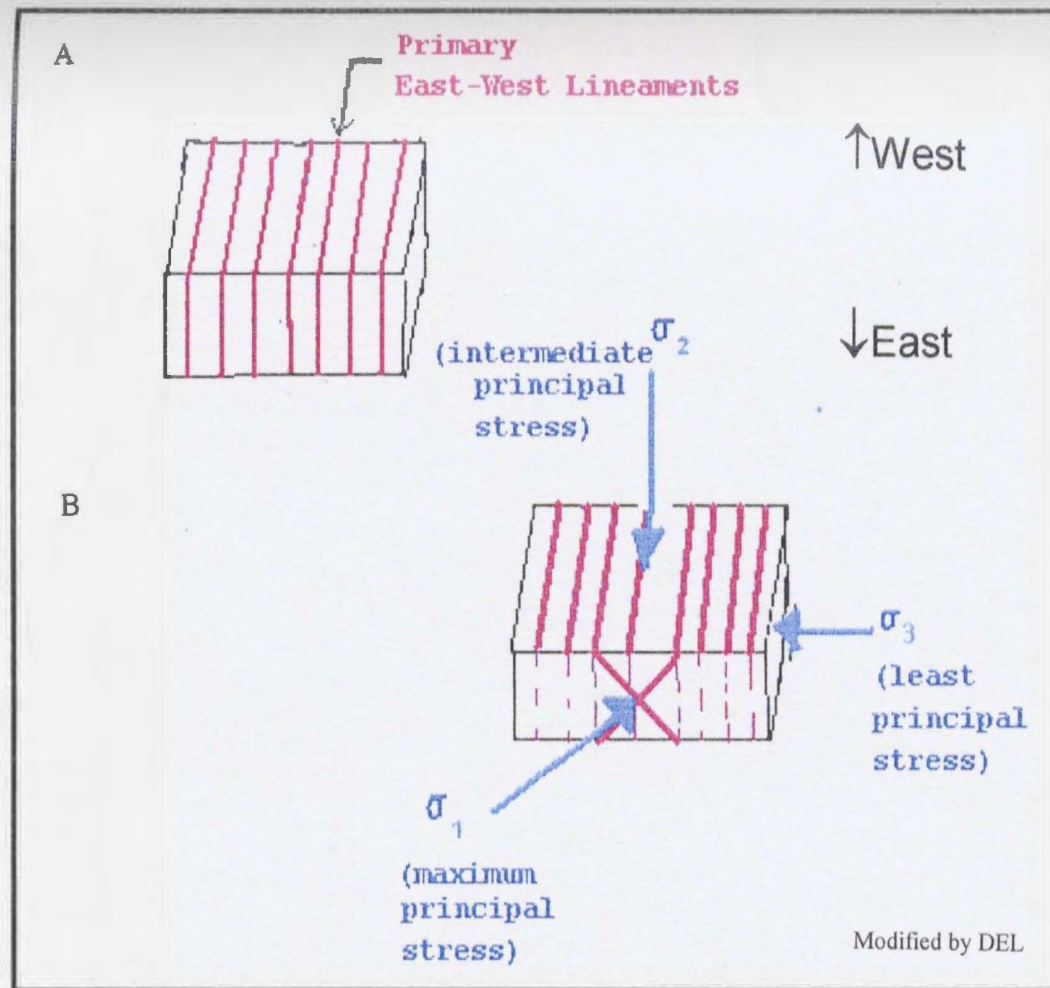


Figure 8.1 The development of extension along pre-existing east-west structures (Modified from McClay, 1987, p.118): (A) This figure shows the presence of east-west lineaments prior to the emplacement of the Voisey's Bay intrusion, (B) The principal stress axes produced within a syn-magmatic strain regime.

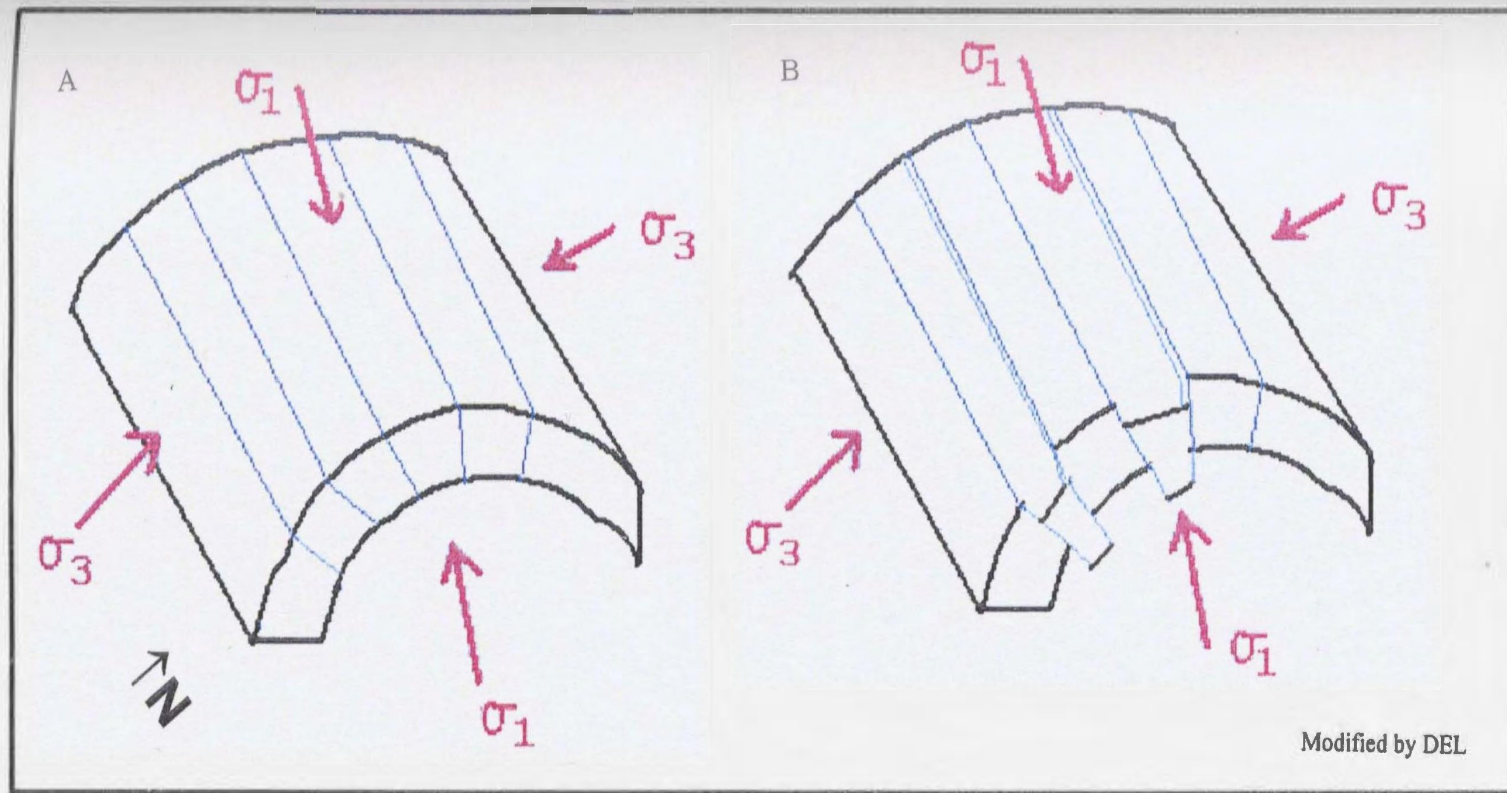


Figure 8.2 The development of extension along pre-existing east-west structures in rheologic response to stresses produced during crustal doming associated with the emplacement of the Reid Brook Intrusive suite (Modified from McClay, 1987, p.120): (A) Principal stresses produced through crustal doming, (B) Extension accommodated along the pre-existing east-west structures as the magmatic activity continues.

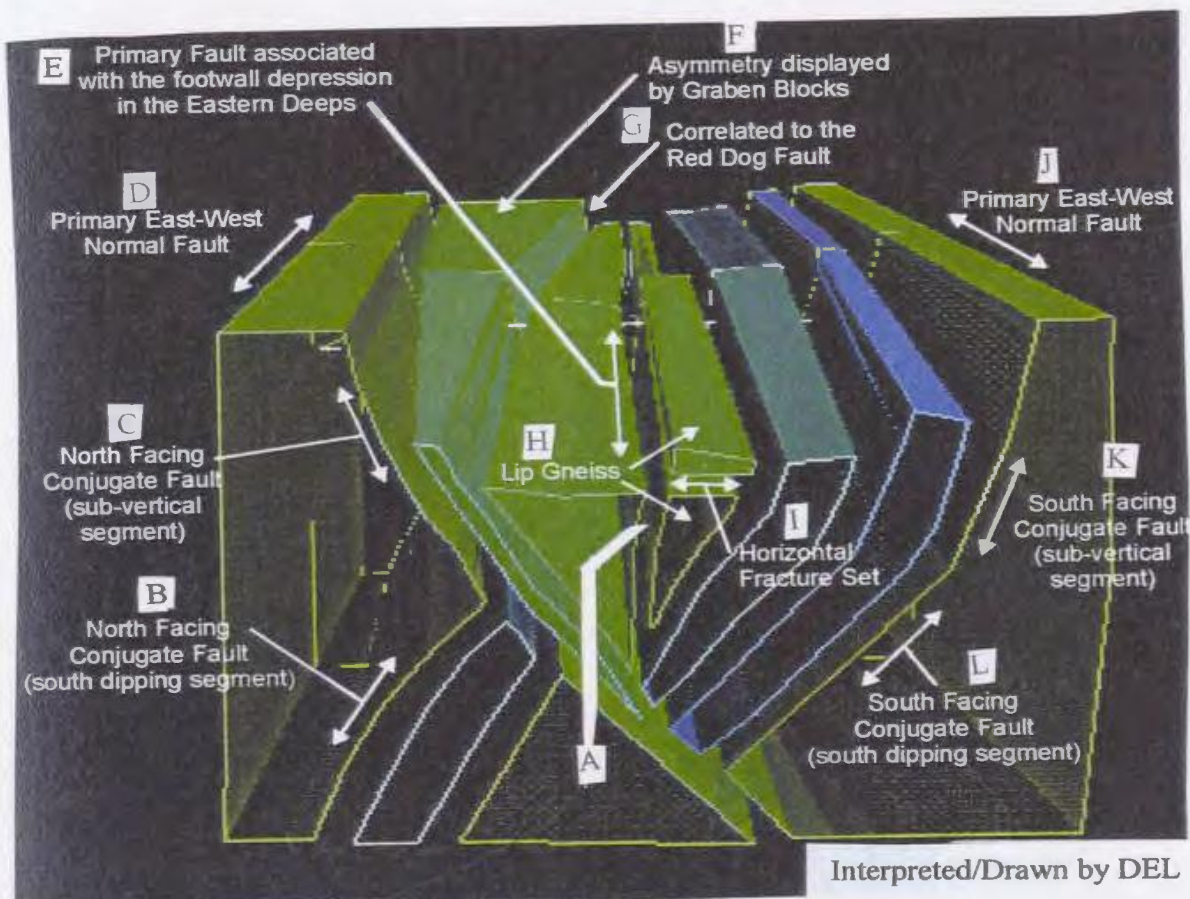


Figure 8.3 A conceptual three dimensional model for the structures which controlled the emplacement and defined the geometry of the Voisey's Bay deposit. Extension was accommodated along pre-existing east-west lineaments and resulted in the system developing a structural style that is comparable to a basin or a graben structure: (A) The Footwall Depression or trough found at the base of the Eastern Deeps chamber that is thought to mark a primary east-west fault through which the Eastern Deeps magma was emplaced, (B) A south dipping limb of a north-facing conjugate fault, (C) A sub-vertical limb of a north-facing conjugate fault, (D) A primary east-west fault or lineament which is interpreted to have developed in response to the collision of the Nain and Churchill/Rae Provinces before the intrusion of the Reid Brook Complex, (E) A primary east-west fault or lineament that is interpreted to have developed in response to the collision of the Nain and Churchill/Rae Provinces and which is thought to have been the structure along which the Eastern Deeps magma was emplaced, (F) The wedge-shaped asymmetry displayed by the graben blocks is speculated to be a result of the strain axes being tilted, (G) A north-facing conjugate fault (Red Dog fault) which defines the discontinuity at the south margin of the Eastern Deeps chamber, (H) The Lip Gneiss at the north margin of the Eastern Deeps chamber in geometric coincidence with the Footwall Depression, (I) Horizontal fractures controlling the emplacement of the Eastern Deeps feeder. (J) A primary east-west fault or lineament which is interpreted to have developed in response to the collision of the Nain and Churchill/Rae Provinces before the intrusion of the Reid Brook Complex, (K) A sub-vertical limb of a south-facing conjugate fault, (L) A south dipping limb of a south-facing conjugate fault.

The sub-horizontal brittle fractures (Figure 8.3) are thought to be secondary structures produced during the final surge of deposit-related mafic magmatism. Uplift and geothermal gradients would subside with a reduction in magmatism, and subsequently the crust would begin to relax, destroying crustal welts. The initiation of collapse would result in sub-horizontal propagation or compression fractures. These fractures would remain as prominent structural weaknesses, even after the subsidence of mafic magmatism, as they can be observed to preferentially host late granitic magmatism.

The sinistral strike-slip displacement overprints and post-dates the magmatic events in Voisey's Bay. This translation is accommodated along the pre-existing east/west lineaments and the conjugate, north and south-facing conjugate faults (Figure 8.3). This event is speculated to be related to distal compressional tectonics associated with the Grenville orogeny between ca. 1290 Ma (Krogh and Davis, 1973) and 977 Ma (Wiebe, 1995).

The 310°/030° conjugate faults were the latest structures to overprint the Voisey's Bay deposit. These features appear to be Reidel brittle shears formed in structural response to the oblique stresses applied by the sinistral strike-slip faulting.

8.1.2 Structural Style

The progressive nature of magma-induced structures and styles in the study area such as, the steeply dipping, north and south-facing conjugate faults and the sub-horizontal brittle fractures, have considerable similarity to the tectonomagmatic events documented within convergent orogenic regimes. The attributes common to both regimes

can be summarized after the works of Corrigan (1997), Warren and Ellis (1996) and Doglioni (1995), as follows:

1. Uplift enhanced by the presence of an over thickened crust, as is documented by Rivers and Mengel (1994) within more northern regions of the Torngat Orogeny proximal to the Nain-Churchill/Rae collisional suture.
2. Lithosphere displaced by asthenosphere. In the study area this is documented by the presence of crustal contamination within the Reid Brook Intrusive suite and the crustal derived granitic melts which intrude the area.
3. Uplift driven by a thermal pulse or increase in geothermal gradient. Geothermometry and geobarometry results reported by Lee (1987) indicate symplectic reactions (cordierite + orthopyroxene, cordierite + spinel) within the Tasiuyak gneisses west of the study could be the result of local contact metamorphism (i.e. late granites of the NPS) or alternatively, could be interpreted as a record for regional decompressional events (i.e. change in P-conditions).
4. Crustal uplift resulting in extension. This process is reflected by the development of syn-magmatic north and south-facing conjugate extensional faults within the study area.
5. Crustal collapse (compression in interior regimes) as thermal stability is restored. This event is thought to be represented by the sub-horizontal compressional fractures associated with the latest magmatic events documented within the Voisey's Bay deposit.

6. The uplift-extension and collapse cycle is repeated with the continued surge of thermal pulses. Similar north and south facing extensional faults and sub-horizontal brittle fractures are recognized with separate late magmatic events proximal to the study area (i.e. Mushua Intrusion, see Chapter 1 and Figure 1.2).

The Voisey's Bay system is thought to be a product of anorogenic magmatism (Ryan, 1996), however, as documented above, it displays structures similar to those which develop within orogenic systems. Although, there are geological characteristics common to these two systems, the catalytic event and subsequent driving forces for orogenic and anorogenic magmatism, are very dissimilar and only have minimal genetic linkage. For example, anorogenic magmatism is associated with local thermal disturbances in the mantle, while conversely the orogenic magmatic systems are characterized by subduction-driven mantle melting. Deviations in the genetic character of these two systems, can be condensed as follows from the works of Doglioni (1995) and Olson (1990):

- 1.A. Uplift in orogenic systems is generally a post- subduction event, generated by the advance of the asthenospheric wedge;
- B. Alternatively, in anorogenic systems, uplift is induced by the presence of a non-subduction related thermal pulse, such as that produced through an ascending mantle plume.
- 2.A. In convergent or subduction related systems, the production of an over thickened crust is innately related to magmatism;
- B. Conversely, in anorogenic systems, crustal thickening is not required to induce magmatic events, although its presence may assist in the evolution of magmatic events.

3.A. Orogenic systems can exhibit subduction, rifting and magmatism as contemporaneous events;

B. Magmatism in anorogenic terranes, however, is not dependent upon convergent tectonics.

Magmatic events, such as the Reid Brook complex (NPS), can represent anorogenic episodes (ca. 1.3), however, these magmatic systems appear to have exploited pre-existing structures formed through earlier, unrelated orogenesis (ca. 1.8 Ga.). In the case of the Voisey's Bay deposit, the syn-magmatic structures (i.e. north and south-facing conjugate faults) formed in response to progressive stresses applied to the area through the evolution of the magmatic events and are not the products of regional tectonism. Similar processes are documented by Cruden (1998) with respect to the emplacement of tabular bodies of granite. The presence of a structural system containing brittle failure will provide magmatic fluids with an incompetent media through which they can preferentially navigate (Olson, 1990). Magma focused through these systems can form complex conduit networks and the conduits can eventually channel magmatic fluids into dilational zones within the structural system. Most obviously in such a regime, dilatency occurs at the core of the system where extension is rooted. Secondary dilational structures are also present where multiple structures intersect (i.e. triple junctions) (Figure 8.3). Of greatest geological significance, these vacancies provide the space for the emplacement and constraint of large magmatic bodies (chambers), and for the establishment of secondary traps (sub-chambers) for the capture of sulphides.

8.2 Structural Controls Associated with Lithostratigraphy

The original spatial relationship between the Ovoid (trap and feeder conduit) and the Eastern Deeps (chamber and feeder) is a topic of continuing debate (Naldrett *et al.*, 1996). Older models postulate that the disparity between the current topographic levels of the Ovoid and the base of the Eastern Deeps chamber was not a product of primary geometry, but was induced through late brittle, deformational events (*op. cit.*). To date, there is no structural evidence to indicate that a disconformity (i.e. north-south fault) exists between these two systems east of the Ovoid. No such data were obtained in the geophysical surveys, nor in the more recent analysis of orientated core in this domain (Golder Associates, 1997). Furthermore, this model contradicts evidence which defines the Ovoid as part of a continuous conduit system which ascended above current topographic levels of erosion (see Chapter 4).

8.2.1 Specific Structural Attributes of the Eastern Deeps

As shown in figures 8.3, 8.4 and 8.5, the flat, stratigraphically low interface defined by the floor of the Eastern Deeps chamber suggests that it lies in the core, at the root of the extensional regime. Broadly, this structure would resemble a structural basin or graben-like system. The feeder hosting and providing the mineralization to this system is equally controlled by the geometry of this system. It is documented as a gentle, southeast dipping, sub-horizontal body following the floor or basal contact of this chamber (Figure 8.5.b).

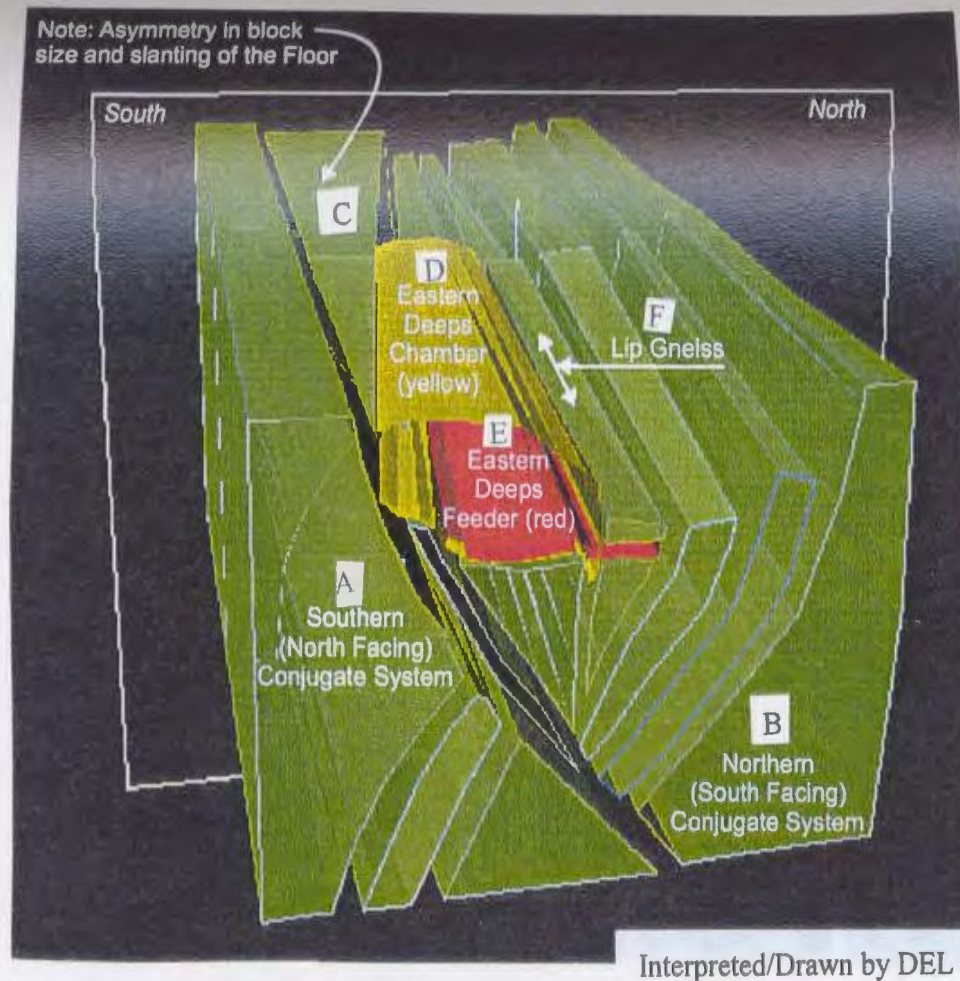
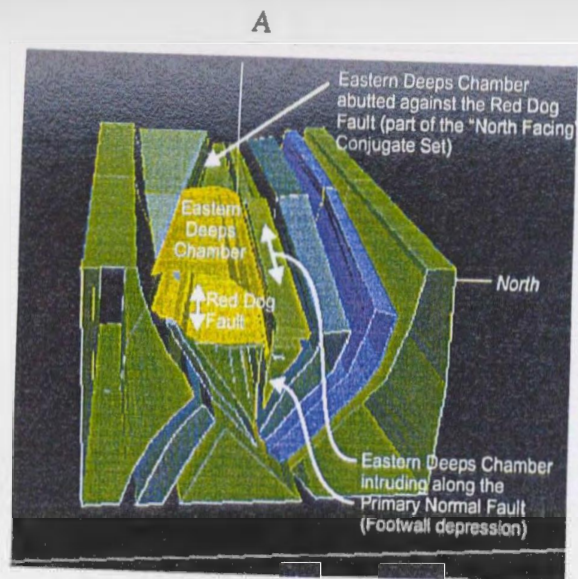
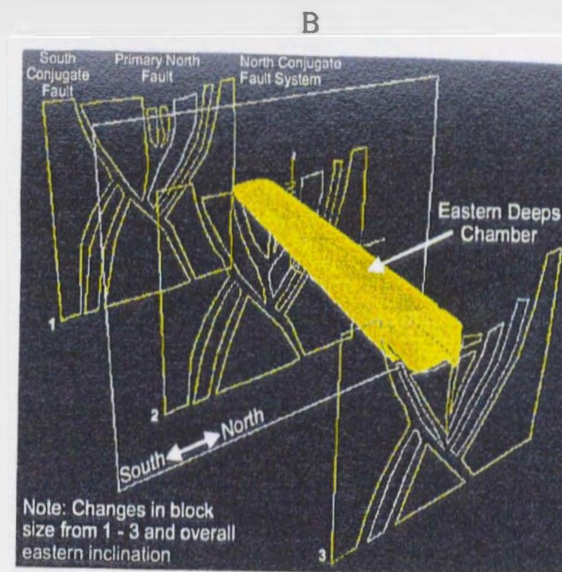


Figure 8.4 A conceptual three dimensional model for the structures which controlled the emplacement and defined the geometry of the Voisey's Bay deposit. The Eastern Deeps chamber is constrained to the core of the system and is interpreted to have been emplaced through the vertical structure (Footwall Depression) found at the base near the north margin of the chamber. The Eastern Deeps feeder is thought to have been emplaced along horizontal fractures found at the lower contact of the Lip Gneiss: (A) North-facing conjugate faults developed south of the core of the graben, (B) South-facing conjugate faults developed north of the core of the graben, (C) The wedge-shaped asymmetry displayed by the graben blocks is speculated to be a result of the strain axes being tilted, (D) The Eastern Deeps chamber, (E) The Eastern Deeps feeder, (F) The Lip Gneiss at the north margin of the Eastern Deeps chamber in geometric coincidence with the Eastern Deeps feeder.



Interpreted/Drawn by DEL



Interpreted/Drawn by DEL

Figure 8.5 Conceptual three dimensional models for the structures which controlled the emplacement and defined the geometry of the Voisey's Bay deposit. (A) The Eastern Deeps chamber is constrained to the core of the system and is interpreted to have been emplaced through the vertical structure (Footwall Depression) found at the base near the north margin of the chamber. The Eastern Deeps is thought to be constrained to the south at lower stratigraphic levels by a north-facing conjugate fault (i.e. Red Dog fault) to the south. However, at higher stratigraphic levels (above present levels of erosion) the chamber flowed over this structural rise and was constrained by a more southern north-facing conjugate fault. (B) The fill patterns for the graben system have been removed to display the plunge of the Eastern Deeps chamber and to show the asymmetry of the graben blocks.

8.2.1.1 Primary East/West Lineaments (Normal Faults)

As displayed by figures 8.3, 8.4 and 8.5, the Eastern Deeps magmatic chamber is interpreted to have been fed by a magma that ascended through the weakness provided by a primary, normal fault at the core of the graben. This linear structure is marked by the Footwall Depression (see Chapter 7). This irregularity displays a unique, but predictable geometry that can be related to the primary structural controls existing at the time the chamber was created. The Eastern deeps feeder is discounted as the conduit for the emplacement of the Eastern Deeps magma, since there are no fragments of either the NT or VT chamber rocks preserved within the conduit lithologies. Furthermore, the conduits are thought to have propagated along late structures which were not developed at the time of the chamber emplacements (see Chapters 4 and 7).

The Footwall Depression is a prominent, geometrically consistent structure transecting the footwall of the Eastern Deeps chamber. This feature consistently trends east-southeast and is documented as controlling sulphide distribution (see Chapter 7). The trend of this structural discontinuity is mimicked by other geological features which lie in proximity. For example, the south edge of the Lip Gneiss follows this trend (Figure 8.3.a), as do the thickest disseminated packages, and likewise the leading edge of the massive sulphide sequences (i.e. Entry Line) (Figures 7.8 and 7.9). If the Footwall Depression post-dated either chamber emplacement or mineralizing events, the correlations of sulphide distribution with the lip gneiss would not be displayed. Similarly, if this structure remained dormant throughout the history of the deposit, why would sulphide sequences appear dislodged in the extreme western regions, proximal to this feature (Figures 7.2 and 7.11)?

These relationships support the interpretation that this feature was established through an early episode of deformation and remained dormant until reactivated by late strain induced by the magmatic events/intrusion. It is thought that this footwall discontinuity was one of many east/west lineaments established through the ca. 1.8 Ga. (Ryan, 1996) collision of the Nain and Churchill/Rae provinces. Furthermore, it is speculated that the Voisey's Bay area may mark the southern limits for the structural expression of the Torngat Orogeny. Structural studies to the north within the Ramah Group, have documented similar styled structures associated with compressional events during the Torngat Orogeny. According to Jamison and Calon (1994), east-west trending, moderate to steep dipping faults straddle two foreland structural subprovinces; the Inner Borderland Geisses and Ramah Deformed Belt. These structures are interpreted to represent the transition between two structural styles, that of thrust and tear faulting (op. cit.). The similarity between the east-west structures within the Voisey's Bay system and those of the Ramah group, indicate that the Torngat Orogeny may have had a structural expression in the Voisey's Bay area. It can therefore, be speculated the Nain/Churchill collision in this domain, may not have been as tectonically dormant as is generally accepted. The absence of other pre-magmatic structures further suggests, that these east-west structures remained dormant until the initiation of magmatic events ca. 1.3 Ga. (op. cit.).

The late deformation thought to displace the mineralization within the Eastern Deeps and hence postdate the magmatic events, can be linked to the reactivation of the pre-existing east-west structures through the accommodation of late strike-slip

displacement along these features (Figure 8.3.a). This provides an explanation for the displacement of mineralized sequences near the western margin of the Eastern Deeps and the skewed trend followed by the Footwall Depression (i.e. east-south-east as opposed to east) (Figures 7.7 and 7.8).

8.2.1.2 Conjugate Normal faults (Formation of the Graben-Like structure)

As documented in Chapter 7, the Eastern Deeps chamber is observed to have a wedge-like shape. This tapered geometry gives the base of the chamber a skewed attitude. This peculiar geometry (Figures 8.4 and 8.5) appears to document significant tectonomagmatic events that occurred during the formation of the Voisey's Bay deposit. The irregular orientation of the Eastern Deeps chamber floor indicates that the strain axes forming this structure did not define a system with true vertical or horizontal stresses that could have correlated with the east-west, north-south stresses established during the original collisional event. Alternatively, this late syn-magmatic deformation is thought to result from σ_1 stresses developed along sub-vertical axis and σ_3 stresses accommodated along sub-horizontal strain axis (Figure 8.2) such that extension/dilation (i.e. σ_3) occurred broadly north-south along the pre-existing east-west lineaments. The tilting of the primary strain axes may have also controlled volume distribution, such that the open cell or dilatency produced in the center of the extensional system would conform to this primary asymmetry decreasing in size to the west. This effect is displayed by the blocks that represent the specific conjugate faults which are observed to thicken in a wedge-like shape from east to west (Figures 8.3, 8.4 and 8.5).

As discussed, the sub-planar orientation of the implied stresses created asymmetry in rock volumes between the east and west domains. The asymmetry of this system can be misleading, however, as the opposing domains are currently observed at similar topographic levels, but not at similar stratigraphic levels. The inclination of the strain axes established an easterly dip to the complete block faulted (graben-like structure) assemblage and induced an easterly plunge upon planar features, including the primary and secondary faults. Typically the plunge of the system is not explicit and is, therefore, often not taken into account. Consequently the system is misperceived as horizontally and vertically symmetrical. It is therefore not enough to just compare similar structural vestiges, but becomes essential to collate these features within similar stratigraphic levels.

8.2.1.3 Syntectonic Horizontal Fractures

The intrusion of the Eastern Deeps feeder in congruence with the geometry provided by the Lip Gneiss, is interpreted to have resulted from structural controls. Geotechnical analysis performed on orientated core samples (by Golder Associates, 1997) established the presence of a prominent horizontal fracture set, found dominantly within the wall rocks. This data set can be extrapolated to the Eastern Deeps to where it can be correlated to similar structures observed in the core samples. These structures are recognized as: (1) low angle fractures marked by quartzofeldspathic veins and local brecciation in the gneisses, (2) the presence of a locally developed schistosity or ductile shears in the troctolites, and (3) by a consistent flat-lying orientation maintained by the intrusion of granite veins and sheets. These sub-horizontal structures provide a structural

medium for the emplacement and regular geometry displayed by the feeder and Lip Gneiss.

This fracture network is interpreted to have developed at the end of the initial episode of extension. As a result of vertical compression during crustal relaxation (Doglioni, 1995), a sub-horizontal zone of incompetence is created. During the last surge of mineralizing events, this weak medium could be exploited for magmatic propagation and overall containment. The exploitation of rock incompetencies for magmatic flow is not a unique concept, and this process has been documented to occur elsewhere in the experimental studies of Barnes *et al.* (1997) and Cruden (1998).

8.2.2 Structural Controls on the Ovoid Feeder Conduit

If the Eastern Deeps feeder ascended along primary faults (i.e. an east/west lineament such as the Footwall Depression) in the core of the extensional network, it becomes apparent that the Ovoid feeder conduit must have also exploited similar structures. The primary geometry of the Ovoid feeder conduit at depth is regular and is thought to be fault/fracture controlled. Near surface, the conduit dips steeply to the north, only to deflect at depth to a moderate-steep, south dip. This trajectory, as interpreted for the Ovoid feeder conduit, is in complete coincidence with the geometry predicted by the south-facing, conjugate fault system, comprising the northern domain of the graben-like structure (Figure 8.6). It should, however, be recognized that the extensional system may not have originally developed as a series of listric-styled, north and south dipping, normal faults that remained continuous at depth. It appears more likely that, the graben-like

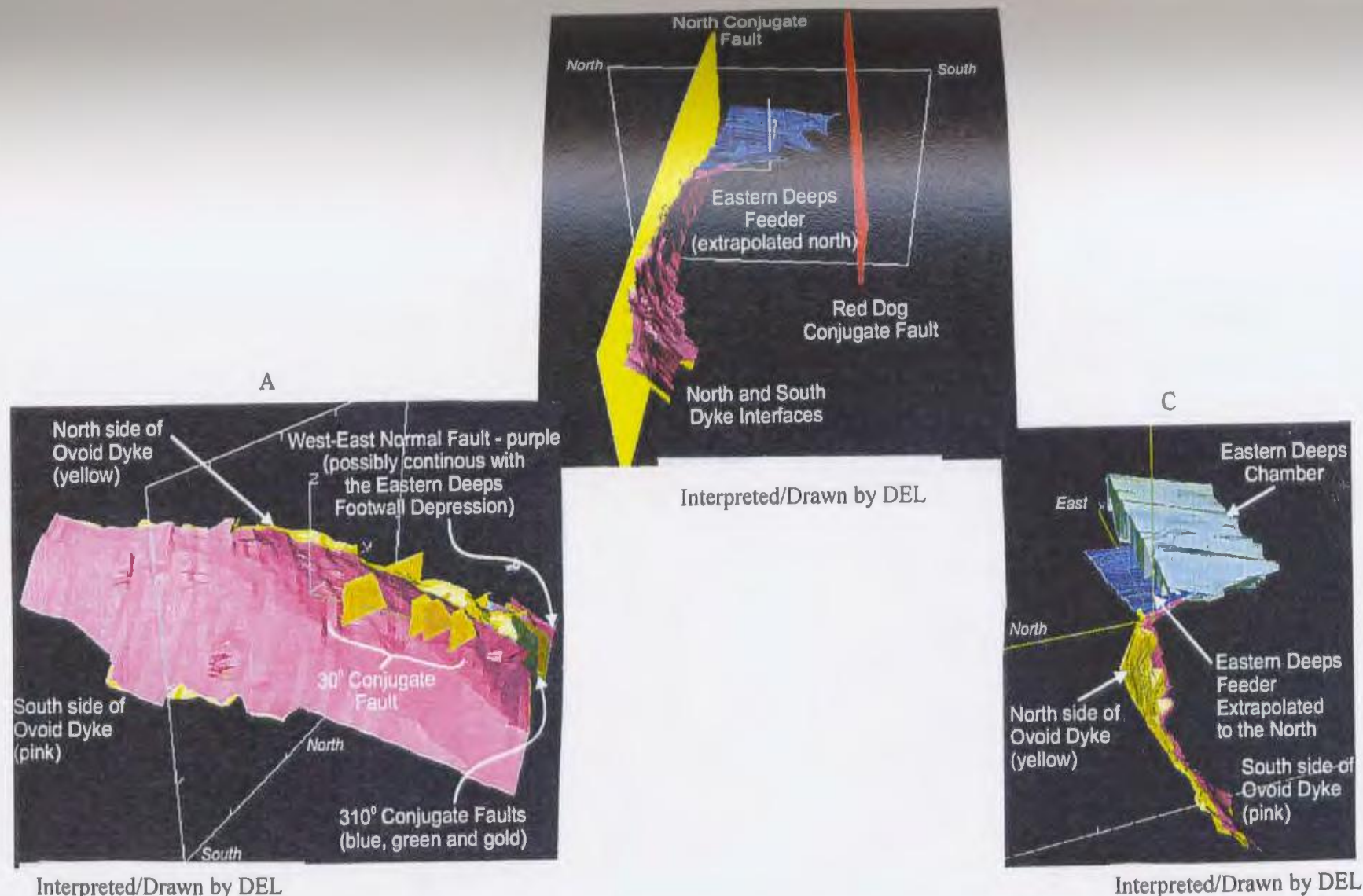


Figure 8.6 Three dimensional models for the Voisey's Bay deposit created from surface mapping and drill data. (A) This model displays the Ovoid feeder conduit constrained to the north by a primary east-west fault and transected by Reidel brittle shears at 030° and 310° orientations. (B) This model displays the geometry of the Ovoid feeder conduit/dyke and its position with respect to the Eastern Deeps chamber and the Eastern Deeps feeder conduit. (C) This model shows the Ovoid feeder conduit constrained to the north by a primary east-west lineament/fault and the Eastern Deeps feeder extending south to a similar east-west structure (i.e. Red Dog fault).

system may have been produced through extension and deflection along numerous micro to mesoscopic, east-west normal faults (lineaments), producing an overall listric-like appearance in the geometry of the macroscopic structure.

8.2.2.1 Normal Conjugate Faults (Formation of the Graben)

If the Ovoid feeder conduit exploited the south dipping, conjugate fault system, it would propagate close to the northern edge of the Eastern Deeps chamber (Figures 8.6.b and 8.7). Upon reaching the north margin of the Eastern Deeps intrusion, the magma would continue to flow along the path that provided the least resistance. It is thought that this medium would most readily develop along a density contrast between cool country rocks and hot magma. Such an incompetent medium would be produced along any margin of the intrusion at the country rock contact. Specific to this case, the conduit appears to exploit the northwest margin of the Eastern Deeps chamber. Throughout the anorogenic events, progressive deformation induced by the magmatic activity continued to exploit the lineaments and establish the extensional network. If the magmatic pulse which filled the Eastern Deeps chamber ended before the completion of the magmatic events, the core of the graben would have continued to develop (dilate) through progressive deformation along the steep east-west lineaments. When the Ovoid feeder conduit reached the north western edge of the chamber, it would have encountered a fresh dilatency developing in the core of the graben-like system. This dilatency would not be filled by the magma from Eastern Deeps chamber (Figure 8.8) since the peak of magmatic activities associated with the emplacement of the chamber would have passed. In reaction to encountering this

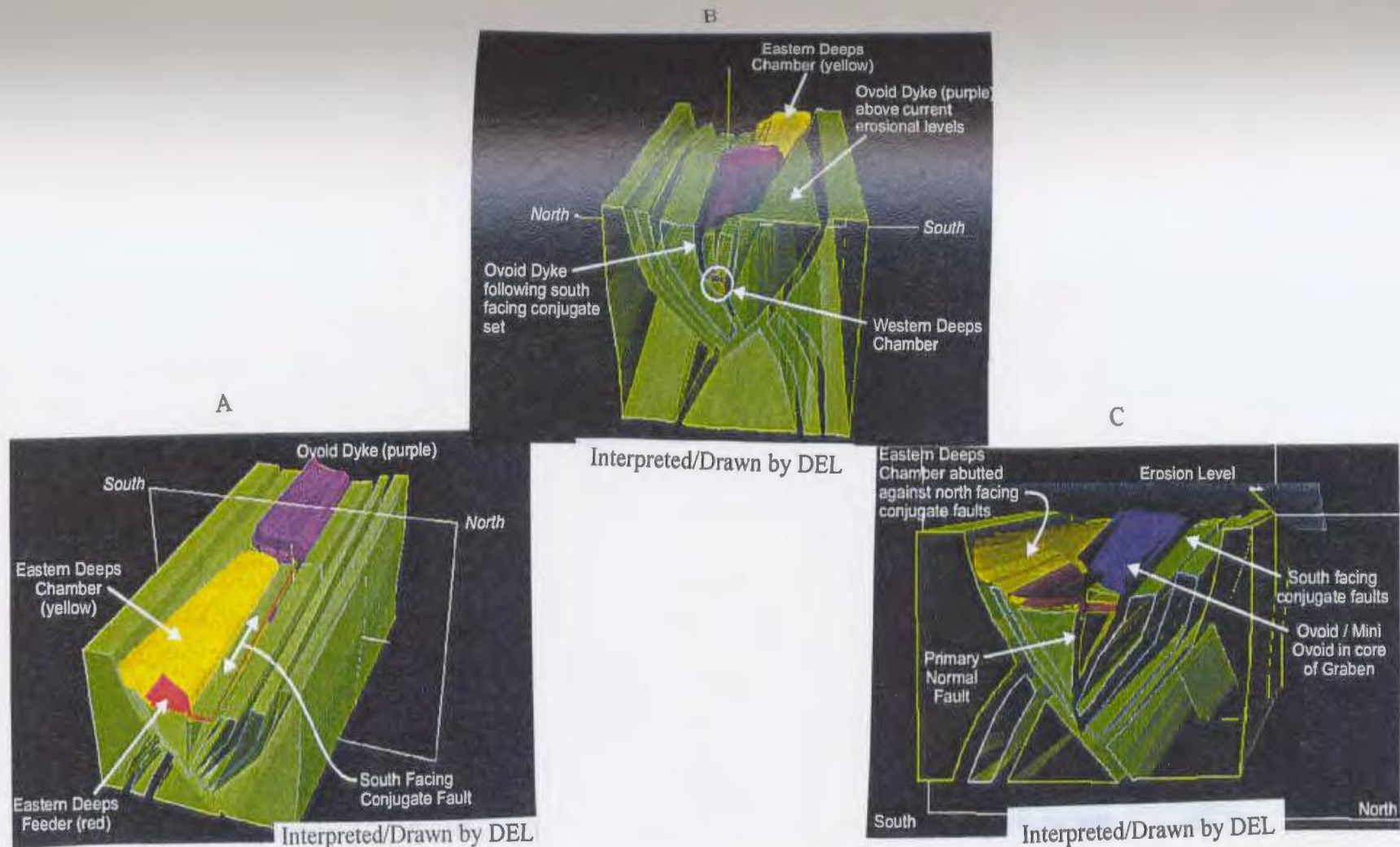
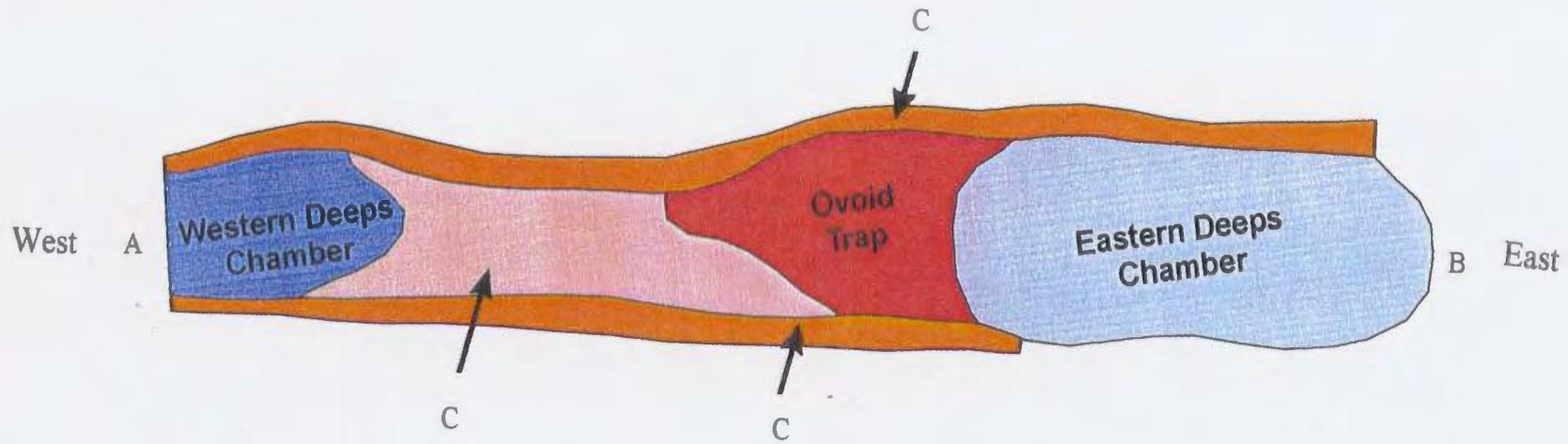


Figure 8.7 Conceptual three dimensional models for the structures which controlled the emplacement and defined the geometry of the Voisey's Bay deposit. (A) This model displays the emplacement of the Ovoid feeder conduit/dyke along the south-facing conjugate fault found closest to the core of the graben and the formation of the Ovoid trap in the dilatency developed adjacent to the Eastern Deeps chamber. (B) This model displays the Ovoid feeder conduit along the south dipping limb of the south-facing conjugate fault as it is documented to occur in the Reid Brook zone. The Western Deeps chamber is also displayed in the dilatency (triple junction) formed at the intersection of the primary east-west fault (Footwall Depression) with the conjugate north and south-facing faults. (C) This model displays the formation of the Ovoid and Mini-Ovoid in the dilatency formed adjacent to the Eastern Deeps chamber within the core of the graben.



Interpreted/Drawn by DEL

Figure 8.8 A plan-view schematic figure displaying the structural controls of the primary east-west lineaments and the north and south conjugate faults over the distribution/geometry of the Western Deeps chamber, the Eastern Deeps chamber, and the Ovoid feeder conduit: (A) Western Deeps chamber, (B) The Eastern Deeps chamber, (C) The Ovoid feeder conduit.

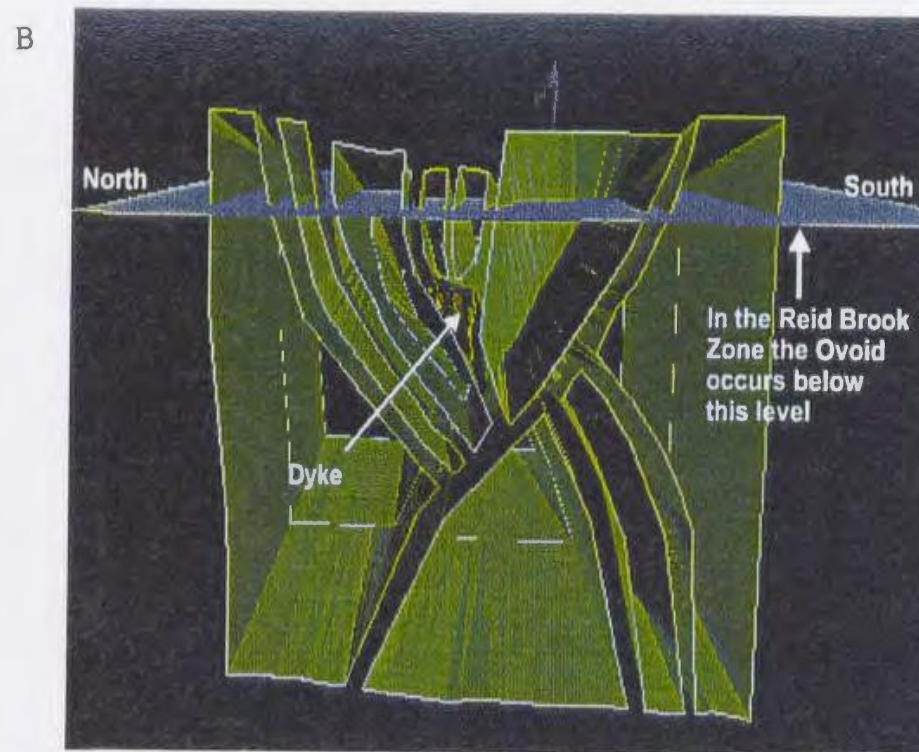
structural void, the conduit infiltrated and filled the unoccupied/open space, forming what is now recognized as the Ovoid trap (Figures 8.7, 8.8 and 8.9.a).

Continuing to the west, the Ovoid feeder conduit propagated in accordance to the geometry applied by the south facing, conjugate fault. The inclination or plunge of the graben-like structure (see above) places the Ovoid trap above present erosional levels (Figure 8.7). In more western domains (Reid Brook zone and Discovery Hill zone), erosion levels restrict the view of the Ovoid conduit to stratigraphic levels which appear below the floor of the graben. At these sites the Ovoid feeder conduit is observed along the south dipping limb of the south facing conjugate fault (Figure 8.9.b). It is possible that even if not destroyed through erosion, the Ovoid trap would not have continued to the west. Documentation has shown that near the Mini-Ovoid, the Ovoid trap pinches (Figures 8.4 and 8.5). Dilatencies in this area may have been filled by another large magmatic body (sub-chamber) prior to the intrusion of the Ovoid, thus space for collecting magma from the Ovoid feeder conduit may not have been available. Alternatively, with this style of progressive deformation, as induced by the intrusion of large magmatic bodies, the development of a trap domain (dilatency) may have ceased with the end of peak magmatism. Subsequently, full dilatency may not have been achieved at the time of the Ovoid intrusion, therefore, a significant trap would not have been developed.

As postulated, this structural model provides a mechanism for providing space needed for the voluminous accumulation of magmas. Without formation of dilational cells (i.e. Ovoid, Western and Eastern Deeps chambers), the evolution of this system would have included complex and extensive stoping events which are not evident in this area.



Interpreted/Drawn by DEL



Interpreted/Drawn by DEL

Figure 8.9 Three dimensional models for the Voisey's Bay deposit. (A) A model created from surface mapping and drill data displaying the Ovoid trap hosted at upper levels within the stratigraphy of the Ovoid feeder conduit. (B) A conceptual model showing the Ovoid feeder conduit below the level of erosion as it is preserved in the Reid Brook zone.

The open cell model for dilatency created within the core of a graben-like system, explains the positioning and containment of the Eastern Deeps gabbros-troctolites and, in addition, provides a valid explanation for the stratigraphic position of the Eastern Deeps feeder and the occurrence of the Ovoid trap. Furthermore, this tectonomagmatic model establishes geometric constraints that govern the geometry of Ovoid feeder conduit.

8.3 Sinistral Strike-Slip Faulting

The previous discussion documented the primary geometric constraints on the macroscopic system, however, it did not explain secondary dislocational events. The $310^{\circ}/030^{\circ}$ conjugate fracture/fault systems are quite dominant on the regional scale (D. Butt and J. Hayes, Pers. Comm., 07/1997) (Figure 4.1). On the macroscopic scale, these features are observed to contribute to late, brittle deformational events, along with the structurally intense east-west lineaments.

In the higher orders of scale, the east-west lineaments frequently accommodate late sinistral strike-slip dislocation. Similarly, strike-slip events are observed to have been focused along the secondary 310° and 030° conjugate fracture systems (Figures 4.1, 6.4, 8.6.a and 8.6.b), however, it is difficult to isolate the individual structures which accommodate these dislocations for two reasons: (1) the lack of mesoscopic marker horizons, and (2) the distribution of strain through parasitic microstructures.

8.3.1 Deformational Effects

The margins of the Ovoid feeder conduit not only exhibit broad east-west constraints, but locally appear weakly sheared. This suggests the pre-existing east-west lineaments were subject to reactivation and are interpreted to be the media which accommodated the later sinistral strike-slip displacement.

Other evidence supporting this transcurrent event is documented by the presence of the conjugate 310/030 ° Reidel fracture system. Locally, these structures have been interpreted by INCO and VBNC geologists to be cooling fractures accommodating no movement. With analysis of non-orientated and orientated core samples, however, kinematic indicators for movement along these substrates are recognized as chloritic coatings that maintain well developed slick-en-sides. Though it is tedious and not possible for inclined holes (unless orientated), core angle azimuth data from slick-en-sides in vertical holes can be determined using reference system such as the gneissosity of the wall rocks. It is difficult to correlate the numerous fractures displayed in the core due to their small scale and multiplicity. It becomes obvious, however, from all scales of this analysis that no one particular structure is responsible for all the observed dislocations. The deformation is cumulative whereby strain is accommodated along a multitude of microstructures, for example within a narrow interval (generally within a meter) the fracture count can reach multiples of tens. Individually each fracture can only accommodate insignificant dislocation, generally in the order of a centimeter or less. If, however, the deformation retained by these microstructures are combined, their collective dislocation (on the regional scale) is substantial, on the order of hundreds of meters.

Although the development of these structures post-dates magmatic emplacement they can provide an alternative channel for the distribution or remobilization of late magmatic fluids (see below). At depth in the Reid Brook zone, a lower massive sulphide horizon has been recognized (i.e. L7+00W) which crosscuts the stratigraphy of the Ovoid feeder conduit (Evans-Lamswood, 1997b). These sulphides are rarely associated with a gabbro-troctolite host and are observed to crosscut mineralization constrained within the conduit. To date this is an ambiguous zone for which the true geometry remains undocumented. Preliminary analyses, however, using known structural parameters, suggest that this zone moderately plunges along a south-southeast structure (Evans-Lamswood, 1997b) which resemble the Reidel shears.

It is now apparent that the post-emplacement Reidel shears can provide an alternative network through which sulphide phases can be redistributed. This study suggests that this fracture system applies geometric controls to ore distribution, in a similar manner, to those implied by the Sudbury Off-sets (Naldrett, 1984a, 1984b). These structures are not restricted to the western parts of the deposit (i.e. Western Extension, Mini-Ovoid, and Ovoid), but can also be observed occurring in the Eastern Deeps. The geometry of the footwall to the Eastern Deeps documents several channel-like features (Figures 7.8 and 7.11) that trend 030° in coincidence with the Reidel brittle shears. Similar to the western regions of the Voisey's Bay deposit, sinistral translation along pre-existing, east-west lineaments are thought to produce secondary Reidel brittle shears. The documentation of these structures through all areas of the deposit supports the structural models for the emplacement and geometries of the magmatic bodies.

8.3.2 Grenvillian Deformation

This study suggests that intra-plate mafic magmatism during Grenvillian deformation (Gower, Rivers and Ryan, 1990) could have implied the stresses required to initiate transcurrent deformation within the Voisey's Bay deposit. Speculation on the evidence for Grenvillian overprinting is not new for this area. Upton (1974) identified a series of mafic dykes (Nain dykes) intruding the Nain Plutonic suite which are of two populations: (1) LP, and (2) HP. The LP dykes trend east-northeast, while the HP dykes strike northeast through to northwest (Gower, Rivers and Brewer, 1990). Wiebe (1985) has defined an age of 977 Ma for the LP dykes and an age range of between 1042-1385 Ma. (op. cit.) for the HP dykes. The intrusion of both the LP and HP dykes post-date the emplacement of the deposit, however, the age and structural regime of the HP dykes appear to be related to the occurrence of sinistral strike-slip faults within the study area.

The age ranges of the HP dykes correlate well with Re-Os isotopic data obtained from low Os deposit troctolites and Tasiuyak gneisses by Lambert *et al.* (1998). These authors report an 1100 Ma age for the isotopic resetting of radiogenic Os in the Tasiuyak gneisses and the deposit troctolites. This 1100 Ma overprint falls within the range of the Nain HP dykes and falls within the age of Grenville deformation.

Grenville overprinting is not rare and nor constrained to regions adjacent to the Grenville Front. Aillik dykes in the Makkovik Province (south of the Nain Province), are interpreted to be related to the 1.0 Ga. Grenvillian Abitibi dykes (Gower, Rivers and

Ryan, 1990). Ermanovics *et al.* (1989) even go as far as to speculate, that dykes 75 km north of the Kiglapait mafic to ultramafic layered intrusion (Figure 2.5) are related to Grenville events. These varied magmatic suites establish that Grenville deformation was not restricted to regions south of the Grenville Front, nor was its signature within rocks from as far north as the Voisey's Bay deposit, an anomalous, isolated occurrence.

The extensional structures can form in response to primary contractional stresses such those which were established during Grenvillian deformation. The question remains, however, as to how do the contractional tectonics produce sinistral transcurrent faulting on pre-existing east/west structures within the Voisey's Bay deposit. The Nain dykes, which are most proximal to the study area, characteristically have a north to northeast trend (Gower, Rivers and Brewer, 1990). Within the stress regime of these northeast trending dykes, extension was perpendicular to the trend of the dykes, therefore, σ_3 was applied along a northwest reference axis while σ_1 was parallel the northeast trend defined by the dykes. When these stresses are extrapolated and applied to the pre-existing, east/west structures, a left-lateral dislocation could develop along these east/west planes (Figure 8.10). This interpretation provides an explanation for the presence of late sinistral, east/west strike-slip faults and $310^\circ / 030^\circ$ Reidel shears developed through the deposit area.

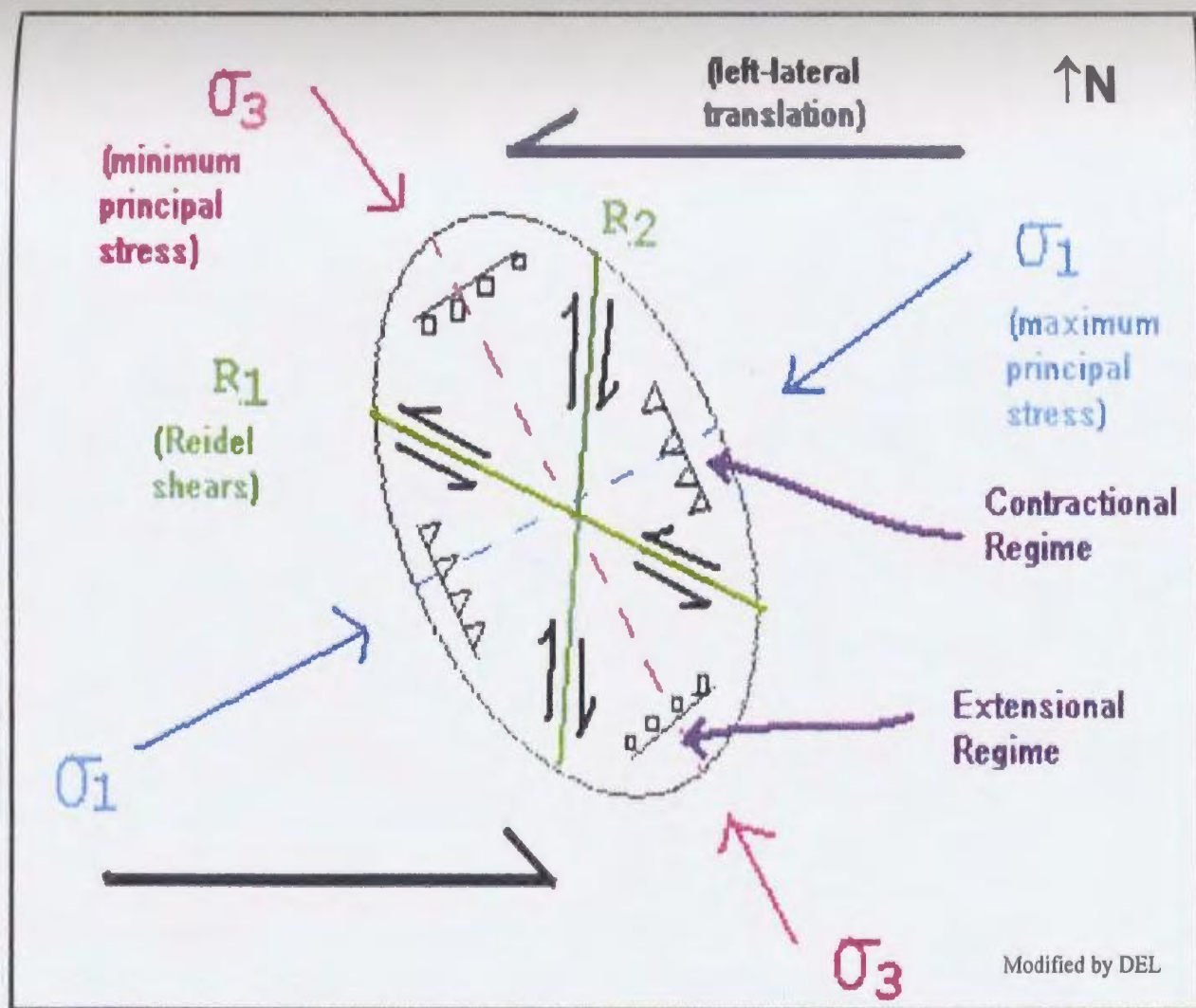


Figure 8.10 A strain ellipse displaying the orientation of the principal strain axes associated with the left-lateral (sinistral strike-slip) displacement that was accommodated along the primary east-west lineaments/faults (Modified from McClay, 1987, p.120).

8.4 Scale of the Structural Events

Most structural ambiguity lies in the scale or size of the graben-like systems. For instance, are the margins of this system defined by the normal faults (pre-existing east/west lineaments) which mark the north and south margins of the Eastern Deeps chamber (Figures 2.1, 8.4.a, 8.5.a, 8.6.b, 4.1, and 8.11)? Alternatively, do these structures represent conjugate, north and south facing, extensional faults. In the latter case, the study area would by definition be constrained to the core of the system (Figures 8.4, 8.5 and 8.7). Through schematic reconstruction of the known structural and lithological assemblages, it becomes apparent that this region represents a deep transect through the center of the graben-like structure and that the size of the basin may extend beyond the scale of the deposit, to possibly incorporate most of the main block.

To the south, the Eastern Deeps is disrupted by the Red Dog fault (Figure 4.1). This fault appears to have accommodated approximately 1.2 kilometers of sinistral, east-west strike-slip dislocation associated with the reactivation of the pre-existing, east/west structures (Evans-Lamswood, 1997a; King, 1996-4)). With removal of this late structural event, the reconstruction defines a macroscopic model that accommodates the geology and structure of the whole main block (see below) (Figures 8.12 and 8.13). The Red Dog fault appears to represent a north facing conjugate fault, proximal to the core of the extensional system. When the Eastern Deeps chamber was emplaced it could have been constrained to the south by this conjugate fault or graben step. At higher topographic levels, the upper portions of this chamber may have flowed over this step and been constrained to the south by an adjacent structural rise in the graben.

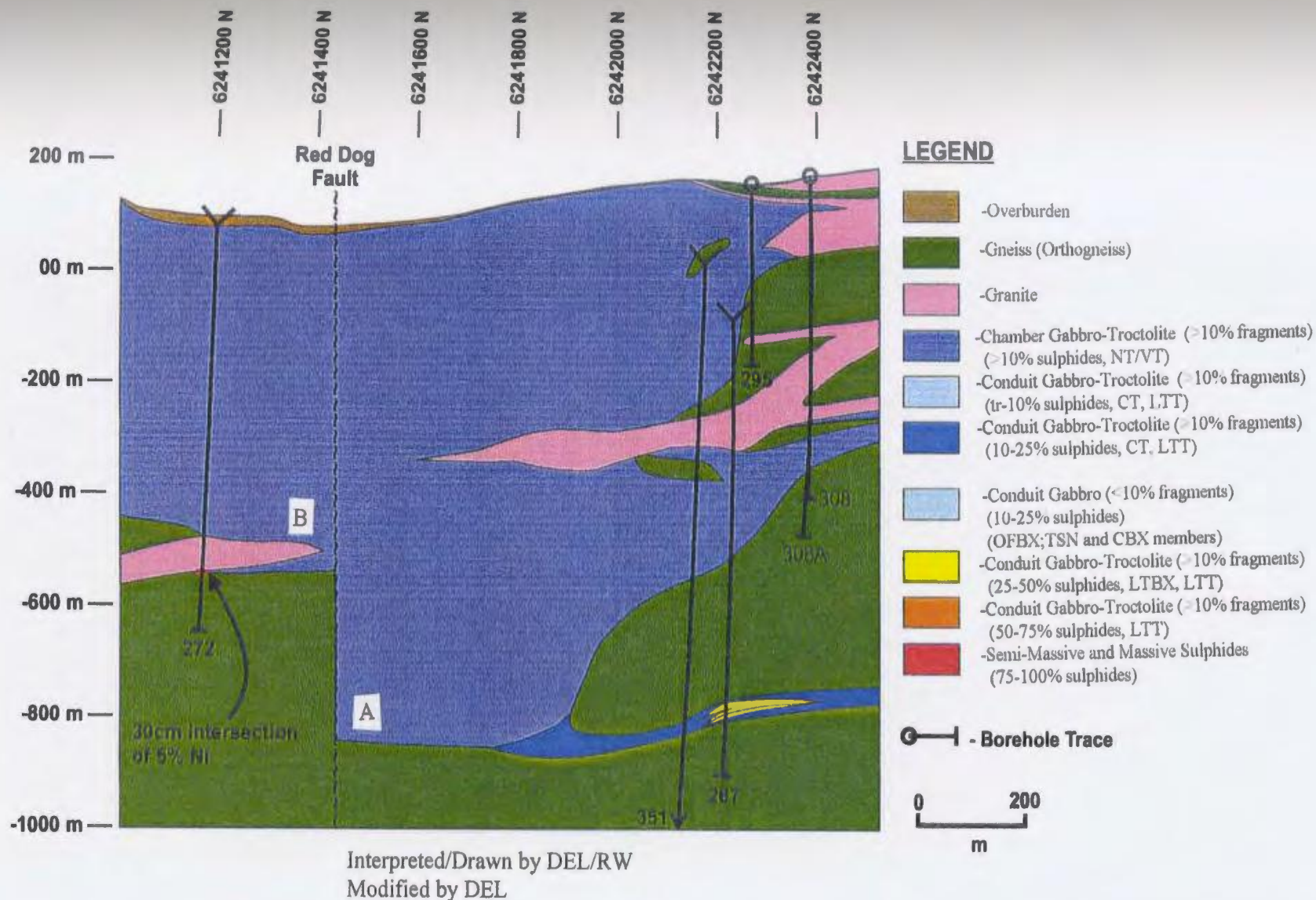
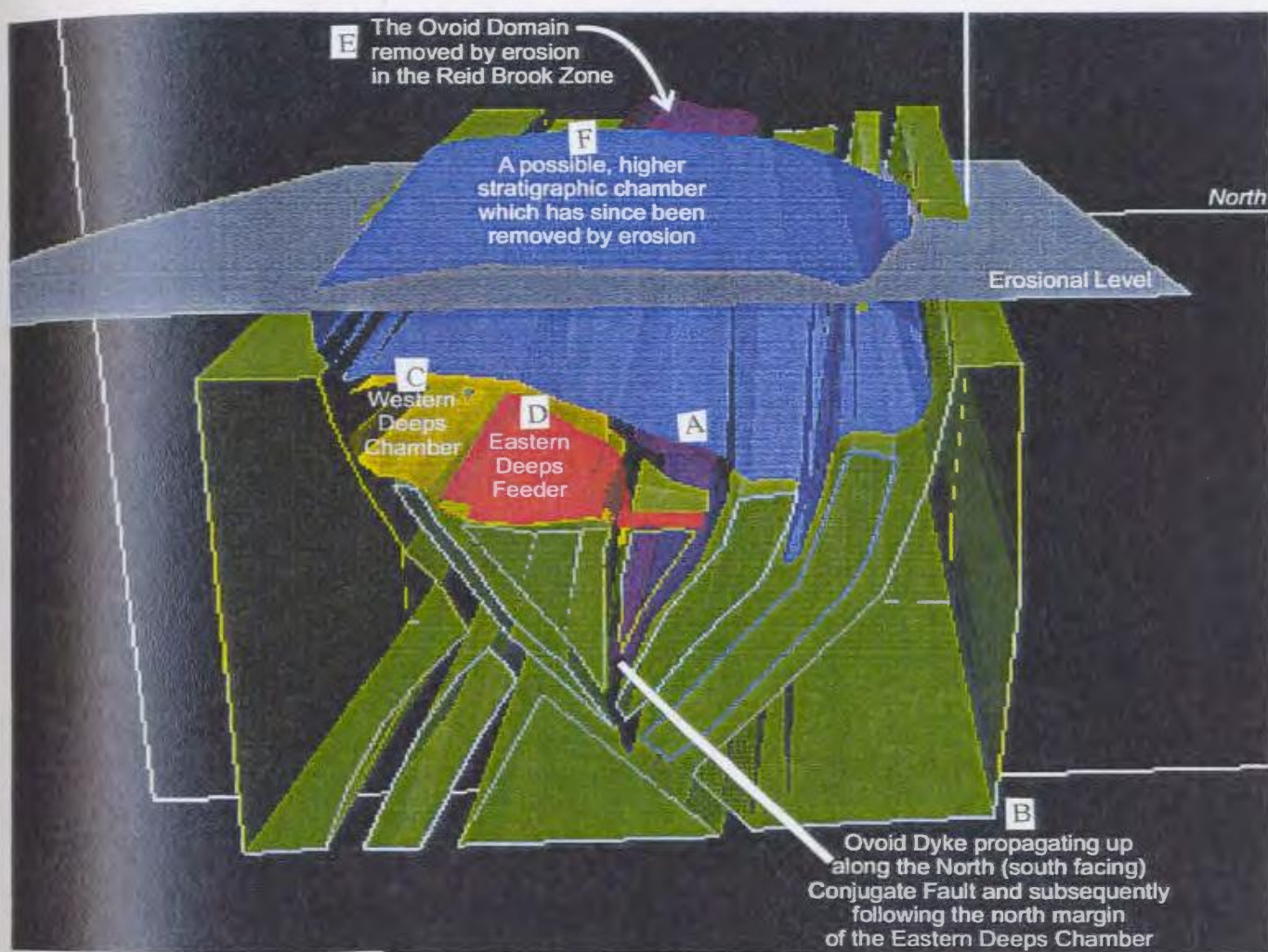
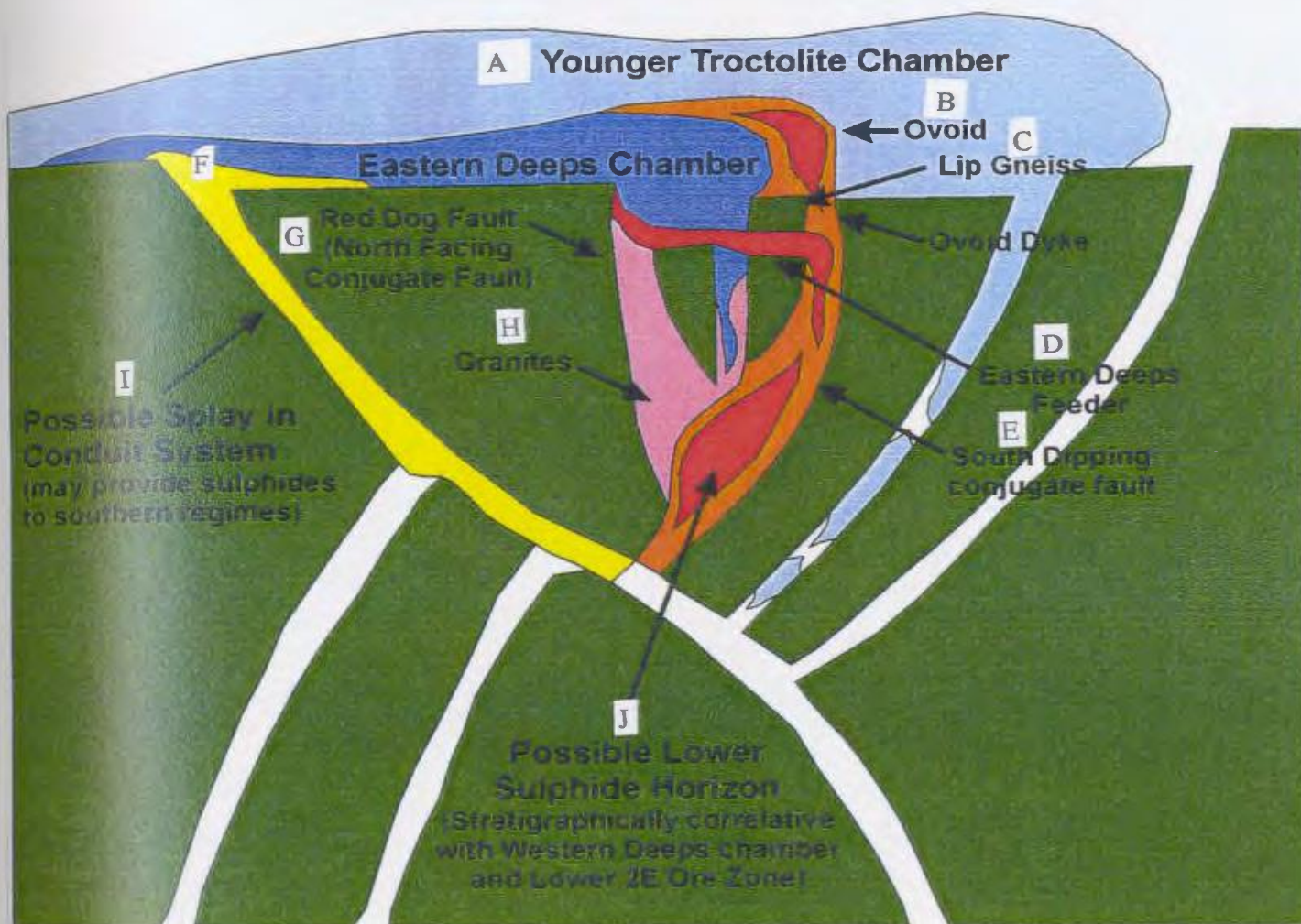


Figure 8.11 A west-facing geological cross-section through L37+00E in the Eastern Deeps: (A) At this site a north-facing conjugate fault is displayed which is thought to define a structural discontinuity at low stratigraphic levels along the south margin of the Eastern Deeps chamber, (B) At this site, a more southern north-facing conjugate fault is thought to define a structural rise or step in the graben structure which may constrain the Eastern Deeps at higher stratigraphic levels.



Interpreted/Drawn by DEL

Figure 8.12 A conceptual three dimensional model for the structures which controlled the emplacement and defined the geometry of the main block: (A) The Ovoid feeder conduit/dyke was emplaced along the south-facing conjugate fault found closest to the core of the graben, (B) The Ovoid trap formed within the dilatency developed adjacent to the Eastern Deeps chamber, (C) The Western Deeps chamber constrained to the core of the graben is interpreted to have been emplaced through the vertical structure (Footwall Depression) found near the base of the north margin of the chamber. The Western Deeps is thought to be constrained to the south at lower stratigraphic levels by a north-facing conjugate fault (i.e. Red Dog fault) to the south. However, at higher stratigraphic levels (above present levels of erosion) the chamber flowed over this structural rise and was constrained by a more southern north-facing conjugate fault, (D) The Eastern Deeps feeder emplaced along horizontal fractures found at the lower contact of the Lip Gneiss, (E) The current level of erosion results in the highest stratigraphy of the Voisey's Bay system being removed, (F) A later magmatic intrusion (i.e. Mushua/Sarah) may have been present above the Voisey's Bay intrusion prior to being removed by erosion.



Interpreted/Drawn by DEL

Figure 8.13 A conceptual west-facing two dimensional model for the structures, geometry and spatial relationships in the Voisey's Bay magmatic Ni sulphide deposit: (A) A possible later magmatic intrusion (i.e. Mushua/Sarah) above the Voisey's Bay intrusion prior to being removed through erosional processes, (B) The Ovoid feeder conduit/dyke is emplaced along the south-facing conjugate fault found closest to the core of the graben, (C) The Lip Gneiss at the north margin of the Eastern Deeps chamber in geometric coincidence with the Footwall Depression. (D) Horizontal fractures controlling the emplacement of the Eastern Deeps feeder, (E) A south dipping limb of a north-facing conjugate fault, (F) The Eastern Deeps chamber constrained to the core of the graben and is interpreted to have been emplaced through the vertical structure (Footwall Depression) found at the base near the north margin of the chamber, (G) The Eastern Deeps is thought to be constrained to the south at lower stratigraphic levels by a north-facing conjugate fault (i.e. Red Dog fault) to the south, (H) Granitic sheets and veins intruding along vacant dilatencies in the graben, (I) The possible existence of other conduits or conduit splays developed along the graben structures, (J) The possible existence of a lower sulphide trap developed at the intersection of the primary east-west fault (i.e. Footwall Depression) with the north and south-facing conjugate faults. Within the Reid Brook zone this space accommodates the Western Deeps chamber, however, to the East this dilatency may be in-filled by the Ovoid feeder conduit. Under such circumstances the feeder conduit could have developed a trap through similar processes as those which produced the Ovoid trap.

8.5. Summary of the Tectonomagmatic History of the Voisey's Bay Deposit

The sequence of geological events that formed and physically shaped the Voisey's Bay deposit, can be condensed into the following lithotectonic events:

1. Deep seated, east/west crustal faults developed in response to the Nain-Churchill collision (ca. 1.8 Ga) during the Torngat Orogeny.
2. A thermal magmatic pulse was introduced (pre 1.3 Ga) into the weak, over-thickened crust that resulted from the collisional events.
3. Uplift and extension were associated with the development of a crustal welt (1.35-1.29 Ga). Syn-magmatic tectonism (i.e. formation of the graben-like structures) developed during the peak of magmatic activity.
4. Contraction of the crustal welt (with abatement in magmatic activity) produced sub-horizontal compressional fractures.
5. On the regional scale, steps 2-4 may have been repeated as other thermal pulses were introduced. Grenvillian deformation caused post-emplacement sinistral transcurrent faulting (ca. 1.1 Ga.) along the pre-existing east/west structures.
6. A Reidel shear system developed in rheologic response to the oblique stresses implied through the strike-slip deformation (post/syn ca. 1.1 Ga.).

Chapter 9: Conclusions and Discussion

9.1 Conclusions

This study has documented the physical processes which affected the transport, distribution and capture of magmatic Ni sulphides in the Voisey's Bay system. Models have also been established for the physical shapes and geometries of the conduits and chambers which host this magmatic system. As well, an attempt was made to resolve the lithotectonic history of the deposit. The significant factors determined in this study are summarized below.

Chapter 3. Theoretically, a magmatic conduit can be divided into two domains, the feeder and trap, where physical processes are analogous to that of a meandering tributary. The processes affecting sulphide propagation and sulphide distribution are as follows:

A. The rapid expansion of a conduit to produce trap-like geometry can be attributed to three physical parameters: flexuring, primary dilation, and inclination.

- Flexures encountered along the flow path can result in voluminous accumulations of magmatic fluids. Subsequently, the conduit may expand through assimilation or the fragmentation of the country rock.
- When the magmatic flow enters a dilatant feature, a drop in fluid pressure will result. The magmatic fluids will pool allowing for more extensive assimilation of the wall rock causing an expansion to the conduit width.
- Changes to the topographic gradient of the conduit will delay magmatic flow, allowing for further assimilation and erosion of the conduit walls.

B. The physical controls that govern conduit swelling can assist in sulphide capture, but do not guarantee the success of sulphide collection. Conversely, changes to the physical environment may favor sulphide collection, but may not contribute to conduit expansion.

- Inflections and changes in the conduit gradient may be discrete and of no advantage to width expansion, however, these changes may be significant enough to hamper the transportation and propagation of heavy suspended sulphides.
- Persistent introduction of fresh magma is required to replenish and reduce the effects of convective heat loss to the country rock through assimilation and the formation of chill margins, without such thermal replenishment the system can quickly reach assimilation limitations and become stagnant.
- A steep gradient within the conduit will require an increase in velocity for flow to compensate and achieve the imposed obstacle. If the velocity does not meet the compensation threshold, the magma can solidify against the adjacent country rock blocking sulphides from plating against the wall rock.

C. Conduits will follow the least resistant path, as created by country rock incompetencies. These weaknesses can be manifested as joint, fracture, or fault systems and to a broader extent, regional dominant fabrics, such as gneissosities.

D. Multiple conduits have the ability to amalgamate and bifurcate.

E. Rock and sulphide textures will provide a record of physical processes and their interactions within the conduit.

-The leopard texture will be developed in a homogeneous environment where even sulphide distribution and batch crystallization is favored. This texture represents the transition from the turbulent environment of early, anterior magmatic pulses, to the more tranquil, laminar flow of trailing magmatic pulses. Such textures signify a restricted and regulated flow regime.

-The breccia texture depicts a noisy transitional zone where the liquid composition is low and the heavy material can no longer be carried in suspension.

-The vein breccia depicts a high velocity and low viscosity event that results in the successful penetration of early material by sulphides. This would be characteristic of zones where the warm, posterior fluids make initial contact with earlier, cooler pulses.

-Chilled textures characterize rapid heat loss as would be expected in any region where the hot magmatic fluid make initial contact with the cool wall rock.

Chapter 4. Preliminary analysis proposed a simple model for the Ovoid where lithological stratification was developed through gravity settling within a rootless chamber, or alternatively, upon the magma being expelled into a magmatic chamber. Current geological interpretations recognize the Ovoid as a magmatic trap, nourished upwards through a stratigraphically lower, but continuous, feeder conduit/dyke.

A. The feeder established a narrow channel for the rapid transport of magmatic and sulphide-bearing fluids. The Ovoid, representing an expanse in this conduit system, channeled ascending magmatic fluids, and also acted dominantly as a trap for the capture of sulphides.

B. The Ovoid is a conduit, a plunging continuum that is not observed to abruptly end at physical margins.

C. The progressive westward changes in the dyke geology do not represent a discontinuity in the system, but stratigraphic changes associated with the plunge of the Ovoid.

D. The Ovoid lithostratigraphy consists of the following sequences: Chilled Troctolite, Leopard Textured Troctolite, semi-massive to massive sulphides, and Basal Breccia Sequence.

-The Chilled Troctolite contains insignificant mineralization consisting of trace to 1% finely disseminated sulphides. The Chilled Troctolite is not only evident in the highest stratigraphic sequences, but can be locally preserved in marginal contact zones.

-Leopard Textured Troctolite consists of a troctolite with or augite oikocrysts enclosing plagioclase and it is intergrown with a sulphide-rich matrix, generally hosting 15-45 % sulphides. This sequence is found in the core of the Ovoid below the Chilled Troctolite.

- The massive and semi-massive sulphides are either in direct contact with the footwall contact or are buffered from the gneiss interface by thin sequences of Chilled Troctolite or Basal Breccia.
- The Basal Breccia can variably host between 1 and 40 % sulphides. It is most apparent proximal to the lower margins of the Ovoid. Basal Breccia, made less evident due to a lower concentration of fragments, is also found in contact with the upper horizons of Chilled Troctolite.

E.. The Ovoid stratigraphy is a result of physical processes acting on magma as it exits a narrow conduit and flows into the wider, stratigraphically higher trap.

F. The Ovoid may not be an isolated system, but the locus for multiple feeders that physically splayed and coalesced (eg. Octopus Model).

Chapter 5. The Mini-Ovoid is established as the western continuation of the Ovoid. It provides documentation for environmental and geometric changes developing as physical processes are altered within the conduit system.

A. Although narrower than the Ovoid, the Mini-Ovoid was a sulphide trap. There is, however, a significant loss to the efficiency of sulphide capture with the contraction of the system.

B. Physical attributes that favor sulphide capture include:

- Footwall irregularities or embayments,
- A wide feeder throat where vast volumes of magma can enter the trap over a relatively short duration of time,
- A flexure in the trap which can act as a shelf for the collection of sulphides,
- An inflection between the trap and feeder domains that disrupts flow and causes dense sulphides to be dumped.

Chapter 6. The Western Extension is broken into two domains, the Reid Brook zone to the west and the Discovery Hill zone to the east. Both zones are continuous with the Ovoid and Mini-Ovoid. These are lower stratigraphic components of the Ovoid feeder conduit/dyke exposed at surface due to the innate plunge of the system:

A. The Reid Brook zone is characterized by several anomalous geological features;

- The conduit in this domain is proximal to, but not in coincidence with, the upper margins of the Western Deeps magma chamber.
- Mineralization is not only hosted within the conduit, but is found as veins in the footwall and hangingwall paragneisses.
- Vein mineralization in the country rock was redistributed along late conjugate faults/off-sets (310° and 030°).

B. Lithological nomenclature for the deposit has been revised based on facies models for the Western Extension. The spatial and temporal relationships of these sequences can be compared to those of a deltaic river system. Lithological groups are divided in three environmental domains, or facies, as follows: the Feeder, the Noisy, and the Quiet domains

- The Feeder succession consists of the Marginal sequence, the Transitional sequence, and the Feeder Melange. This domain is associated with the earliest magmatic pulses that traversed the

conduit. Spatially, these units are found as intermittent relicts lining the conduit wall, elsewhere they are associated with narrow parts of the conduit.

- The Noisy domain documents an interactive, turbulent environment with multiple interrelated geological and physical relationships. It includes intercalated sequences related to the mineralizing event. Sequences in this domain include Original Fragmental Breccia, the Condensed Breccia, the Leopard Textured Breccia and the Vein Breccia.
- The Quiet domain is a non-turbulent flow environment. It is generally associated with widening of the dyke or the formation of micro-traps. Large parcels of sulphides collect in this area with minimal physical or geological interference. Sulphide and silicate minerals grow in an uninhibited forming distinct intergrowth textures. Geological sequences found in this domain include, the Leopard Textured Troctolite and semi-massive to massive sulphides.

C. The physical and temporal relationships of these sequences provide documentation for the kinematics and the relative timing of the mineralizing and non-mineralizing events.

- The Marginal sequence is established as the first magmatic pulse which was then proceeded by the Original Fragmental Breccia. The Transitional sequence, an intermediate sequence linking both the Marginal and Original Fragmental Breccia phases, hosts innate characteristics of both sequences.
- The next magmatic pulse established the Leopard Textured Troctolite and resulted in the veining of the earlier magmatic sequences. Where the Leopard Textured Troctolite interacted with the breccia sequence, a transitional succession (Leopard Textured Breccia) was established.
- This immediate mineralizing event concluded with the intrusion and emplacement of the massive and semi-massive sulphides.

D. The segregation of various magmatic phases (barren and sulphide-bearing) may have been an extensive task performed through several episodes of magmatic separation and differentiation occurring in sub-chambers or traps, at depth. The temporal relationships and chemical compositions of these magmas may deviate at depth due to the extant physical and environmental controls.

Chapter 7. Previous models have suggested the Ovoid represents the base of the Eastern Deeps chamber and provided the plumbing from which the chamber was fed. The discordance in stratigraphic positions between the Ovoid and the Eastern Deeps chamber was postulated to be a result of a late phase of deformation, juxtaposing their relative position.

- A. Evidence suggests that the Ovoid dyke and the Eastern Deeps chamber are related in spatial terms only.
- B. Similar to the Ovoid system, the Eastern Deeps chamber is characterized by a distinct ore zone, namely the Eastern Deeps feeder.
- C. The Eastern Deeps feeder is identified with the following features;
 - A gentle, southeast dip and appears as a sub-horizontal, sill-like body.
 - It intrudes along the footwall contact of the Eastern Deeps chamber.
 - It continues in geometric continuity to the north, beyond the limits of the chamber.
 - The feeder hosts dispersed disseminated sulphides along the base of the chamber with the most significant sulphide concentrations proximal to the chamber entrance.
 - Significant sulphides occur within the constrained feeder, north of the Eastern Deeps chamber.

-Ore-bearing successions within the conduit are lithologically and texturally comparable to those observed in the Ovoid system.

D. The distribution and capture of sulphides from the Eastern Deeps feeder were controlled by physical features, which include:

- The presence of the Entry Line. This axis marks the site at which the constraining surfaces of the feeder were removed as the conduit exited the rigid gneiss medium and enters the chamber. The physical processes occurring at this junction can be compared to those which occur when an expanse in the conduit is encountered.
- The Footwall Depression. This feature is a topographic irregularity and is expressed as a linear trough in the footwall. This structure acted as a trap for the collection of sulphides.
- An inflection or a small off-set proximal to the footwall depression. This element provided a physical obstacle, constraining the distribution of the heaviest sulphide packages.
- The tapering of the conduit/feeder provided by the Lip Gneiss. This feature placed a restriction on conduit width as it passes into the Eastern Deeps chamber causing dense fragment or sulphide bearing magmas to choke the chamber entrance. As a result, thick sulphide sequences collected on the posterior side of this restriction to the north, back within the conduit system.

E. The Eastern Deeps feeder is thought to post-date the emplacement of the Eastern Deeps chamber. The chamber is speculated to not have been solidified when the mineralized feeder intruded, therefore, mixing or mingling of the two magmatic fluids would have occurred. This process involves the integration of several variables including the density, viscosity, and degree of turbulence of the flow.

F. Multiple conduits may have intruded the north wall of the Eastern Deeps. These failed feeders do not host the significant mineralization typical of the ore-bearing conduits elsewhere, but are lithologically similar. These magmatic structures may represent offshoots or bifurcation channels from the ore-bearing conduits (Ovoid feeder conduit or Eastern Deeps Feeder), or alternatively, early sills from which the chamber was originally fed.

Chapter 8. The geometries of the Voisey's Bay system is controlled by five prominent structures:

- East/west lineaments.
- East/west, steeply dipping, north and south facing conjugate normal faults.
- Sub-horizontal brittle fractures.
- East/west strike-slip sinistral faults.
- NW (310°) and NE (030°) brittle conjugate fault sets.

A. The east/west lineaments straddle the Nain/Churchill boundary and are interpreted to be crustal faults developed during the Torngat Orogeny. These structures, therefore, developed long before the intrusion of the Reid Brook Complex.

B. The primary east/west lineaments (ca. 1.8 Ga.) were reactivated through crustal doming, in response to the rise of the magmatic plume during the ca. 1.3 Ga. anorogenic event that produced the Nain Plutonic suite.

-A juvenile extensional event was initiated along these pre-existing structures and focused on the crustal weakness associated with the east/west lineaments (ca. 1.8 Ga.).

- This anorogenic episode produced a series of broad graben-like structures defined by the east/west, steeply dipping, north and south facing conjugate normal faults (ca. 1.3 Ga.). These are syn-magmatic structures which focused and constrained magmatic distribution in the study area.
- A sub-horizontal fracture system is speculated to have been produced in response to the cooling and collapse of the crustal dome as the extensional structures continued to develop and then subside.
- The sub-horizontal structures provided secondary channels for magmatic propagation.

C. A east/west sinistral transcurrent event exploited the pre-existing crustal weaknesses developed through the primary east/west lineaments and the east/west conjugate faults.

-Reactivation of the east-west structures post-dates the emplacement of the Nain Plutonic suite and is interpreted to be a response to Grenvillian deformation (ca.1.1 Ga.).

D. The development of the NW (310°) and NE (030°) brittle conjugate faults sets is thought to mark the last significant episode of deformation.

- These structures are interpreted to be Reidel brittle shears developed in response to the east/west sinistral strike-slip event.
- This event resulted in the structural dislocation of the Voisey's Bay deposit, including both conduits and chambers.

E. The temporal relationship between the magmatic events and the development of the structural system is crucial to resolving the emplacement history of the deposit. Space/dilation must be established to produce large magmatic traps, such as the Ovoid.

Because of this study, the image of the Voisey's Bay deposit becomes one of a diverse and dynamic magmatic system. As with other nickel sulphide deposits, primary igneous events control the petrogenesis of the deposit by providing the environment favorable for initial sulphide formation. The distribution of these magmatic and sulphide bodies, however, are controlled by physical and environmental processes. Petrogenetic studies are of the utmost importance to understanding the original formation of such nickel sulphide systems, but are of limited applicability to the exploration of the systems if not incorporated with studies of temporal and spatial events. Given, through knowledge of the petrogenesis, that a magmatic system is capable of hosting significant sulphides, understanding the physical processes controlling where, why and how these sulphides

were distributed are of equal importance to the successful exploration of economic nickel systems.

9.2 Discussion

9.2.1 Timing and Genesis:

Two magmatic chambers, the Eastern Deeps and Western Deeps chambers, are spatially related to the mineralizing system. The conduits which carried and distributed the sulphides appear to post-date the emplacement of these chambers, as is also suggested by Lightfoot (1998). Both the conduit and the chamber magmas are thought to have been produced from a mantle-derived reservoir at depth in the lower crust. Early contamination and fractionation processes occurred in this parental chamber along with the segregation of immiscible sulphides, as documented to occur within nickel sulphide systems by Naldrett (1989a, 1989b). With the continued influx of new magma (multiple thermal pulses), the earliest fractionated magmas at the top of the chamber were expelled, followed later by the denser sulphide melt (Naldrett *et al.* 1996). The fresh magma could also contribute chalcophile elements to the sulphide liquid before it was expelled from the chamber. If there is a substantial break in the magmatic transfer, the dense, sulphide laden magma would gravity settle and collect at the bottom of the parental chamber. With continuous magmatic transfer, the melts were expelled and ascended through the crust by navigating structural weaknesses. Ascending magmas may have encountered and resided in multiple sub-chambers (i.e. traps) before reaching the site of final deposition. Within the sub-chambers the sulphides were exposed to large transfers of magmas, and, therefore, were able to scavenge chalcophile elements from magmas that passed through (*op.cit.*).

With multiple cycles of chamber discharge and capture, the sulphides could have become considerably upgraded from their initial chalcophile concentrations (i.e. Ni), as stated by Naldrett (1989a, 1989b). As well, individual magmatic surges could serve as a catalyst, pushing earlier, trapped melts from their current traps and causing them to ascend into stratigraphically higher sub-chambers.

Within the upper crust, the magmas which fed the Eastern Deeps and Western Deeps chambers are speculated to have ascended through channels established by the primary normal, east/west faults. The increase in thermal activity may have induced a juvenile extensional event, where strain was accommodated along the pre-existing, east/west normal faults. The dilatency initially produced by this deformation would form the root or core to the basin-like structure.

The earliest, sulphide-poor magmas continued to ascend along the normal faults until a trap or dilatency in the core of the extensional structure impeded their ascent. These interactive events established the Eastern and Western Deeps chambers. During these magmatic episodes, progressive deformation continued and the inherent structures of the graben-like complex were established. Sulphide rich-magmas lingering in sub-traps were expelled into the conduit network by disturbances within the system (i.e. later pulses of magma or deformation). In lower crustal regimes, the sulphide-rich magmas followed the same conduits as did the earlier, sulphide-poor magmas. With continued dilatency the primary conduit may have branched or been coalesced with other magmatic channels when multiple structures were transected (i.e. fault junctions). The continual development of extensional structures would not only benefit the ascent of the dense sulphide fluid

through an increase in the hydraulic pressure (cf. Scarfe *et al.*, 1987), but would also establish new traps for sulphide capture and provide sites for magma transfer that could result in nickel upgrade.

Temporally, the Western Deeps chamber was the site of first magma capture, as it was the nucleus of the earliest dilatency (i.e. in the core below the floor of the graben). During continued extension, the floor of the graben established a basin-like structure which provided a trap (i.e. formation of the Eastern Deeps chamber) for the magma that continued to ascend past the Western Deeps chamber (Figures 9.1 and 9.2).

As the sulphide-rich melts, lingering at depth, began to ascend along the normal faults to higher crustal levels, they would have encountered an obstruction provided by the Western Deeps Chamber. This geological structure lies below the floor in the root of the basin, therefore, with continued deformation (i.e. extension), dilatency would have been accommodated along the margins of the chamber. This space provided a channel or structural weakness for the continued ascent of the sulphide-bearing magmas through the Western Deeps chamber. It is further suggested, that the dilatency continued to expand the core of the graben (i.e. fault triple junction), opening space adjacent to the eastern edge of Western Deeps chamber (Figures 7.13, 8.1 and 8.2) and possibly forming a trap for late sulphide melts that is yet to be disclosed.

As the nickel-rich magma continued to rise past the margin of the Western Deeps chamber, it preferentially navigated the south-facing conduit system as it progressively developed. In this higher stratigraphic regime, the floor of the basin-like structure continued to be deformed through extension, thus creating a void or new dilatency at the

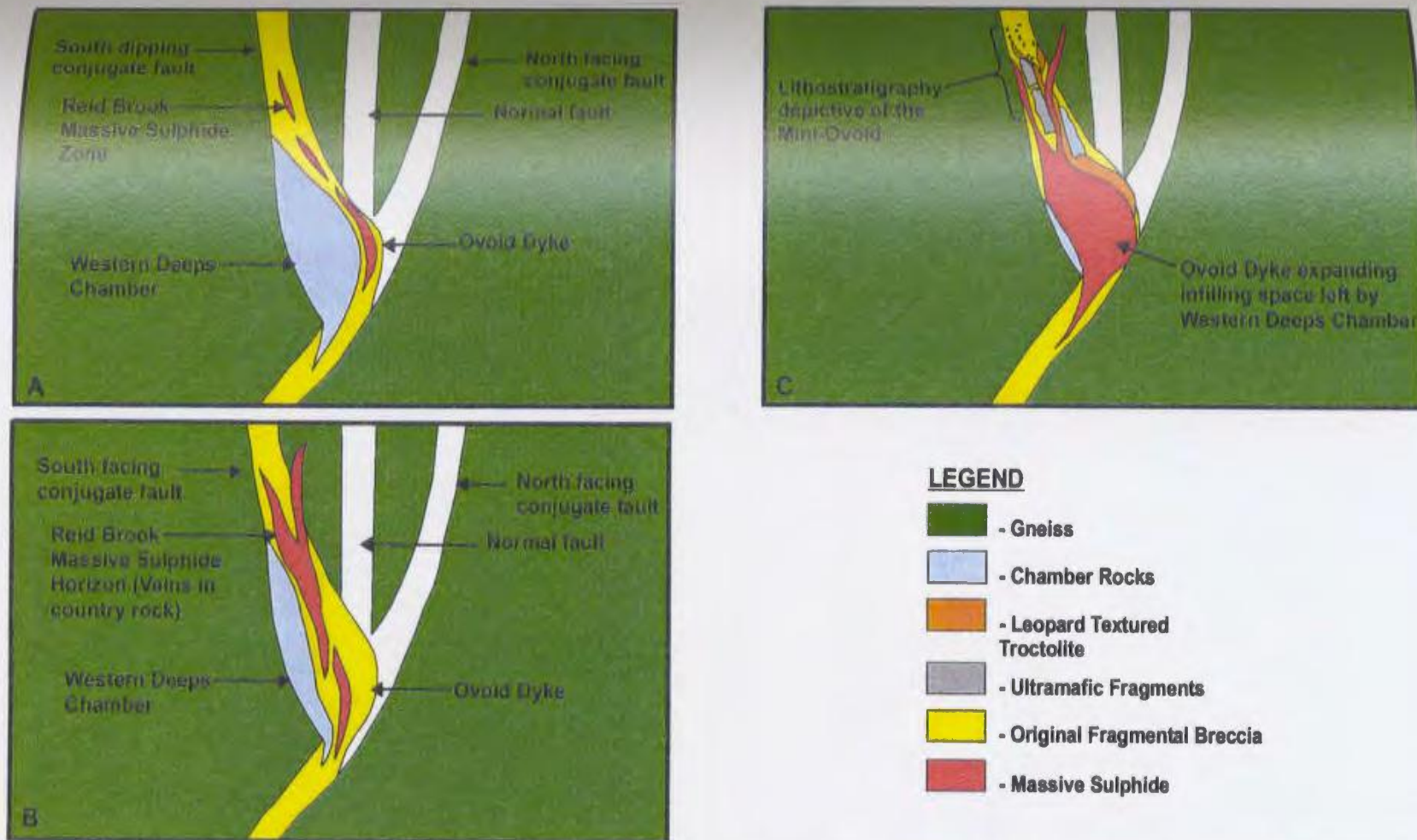


Figure 9.1 Schematic profiles showing the Western Deeps chamber and the Ovoid feeder conduit in-filling the dilatency created at the fault triple junction. The junction is produced by the intersection of the primary normal fault with the north and south-facing conjugate faults. (A) An east-facing section through L7+00W in the Reid Brook zone. The Western Deeps chamber occupies most of the dilatency within the triple junction, while the Ovoid conduit only in-fills space along the margin of the chamber. (B) An east-facing section through L2+00W in the Reid Brook zone. The Western Deeps chamber tapers to the east, while the Ovoid conduit expands. The Ovoid conduit in-fills the space which was originally occupied by the Western Deeps chamber to the west. (C) An east-facing section through L2+00E in the Reid Brook zone. At this site, the Ovoid occupies most of the dilatency within the triple junction and only the tapered eastern margin of the Western Deeps chamber is present. The Ovoid conduit expands within the dilatency to produce a trap that may be comparable to the Mini-Ovoid.

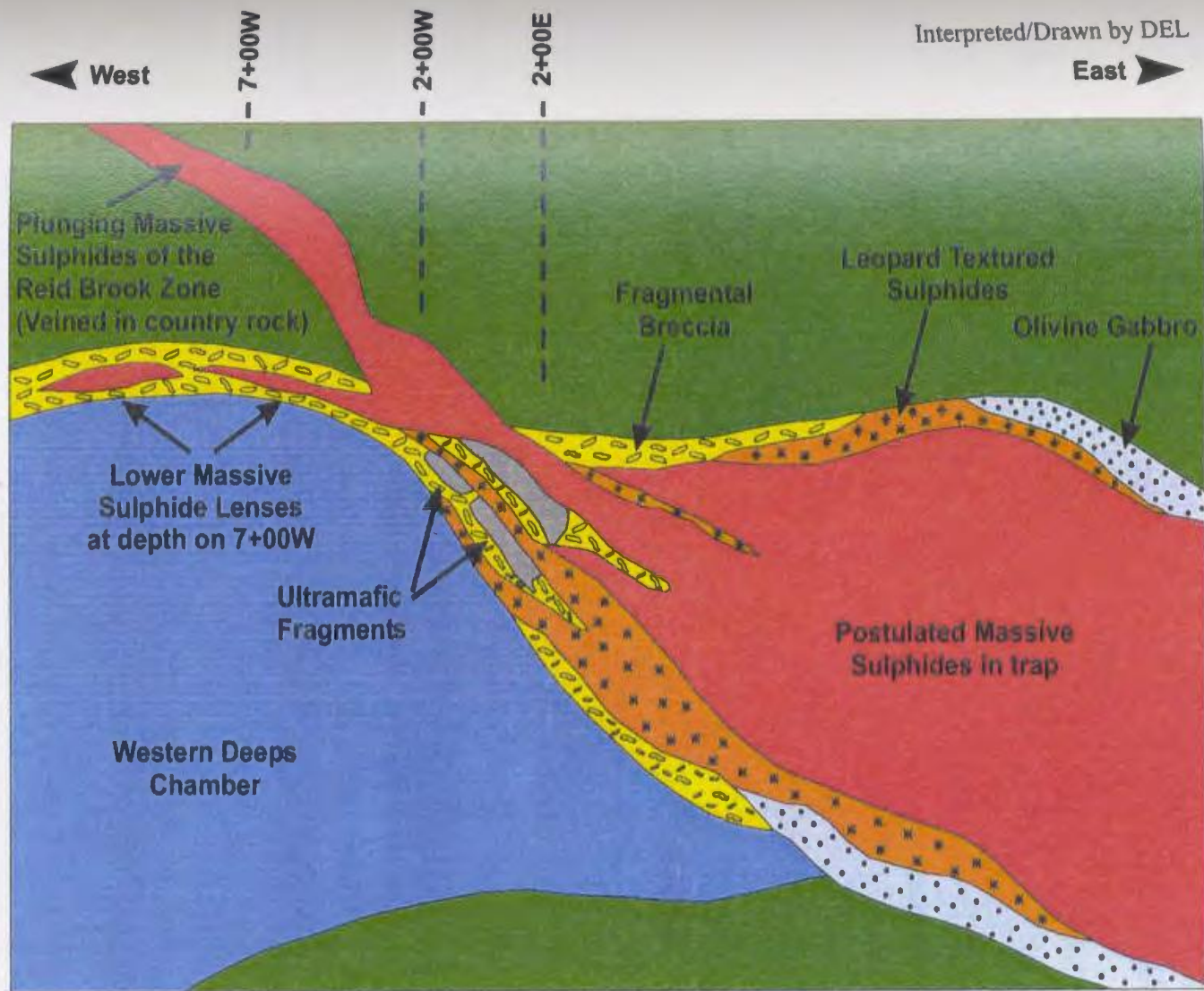


Figure 9.2 A schematic long section showing the Western Deeps chamber and the Ovoid feeder conduit in-filling the dilatency created at the fault triple junction produced by the intersection of the primary normal fault with the north and south-facing conjugate faults. The Western Deeps chamber tapers to the east leaving space (dilatency) for the expansion of the Ovoid conduit. This figure characterizes the geology (i.e. fragments and veined sulphides) from exploration drilling in this area and proposes a model for the presence of a large sulphide trap to the east.

western margin of the Eastern Deeps chamber where the nickel-bearing magma could be captured (Figures 8.2 and 8.3). The skewed character displayed by the extensional system (see chapter 7) indicates that the floor or basin was a tapered feature with west directed dilatency (i.e. less dilatency to the west). The nickel sulphide-bearing magma upon reaching this void, would collect and in-fill this space at the western edge of the Eastern Deeps chamber (Figures 7.8. and 8.3). This activity signifies the formation of the Ovoid trap. Once the Ovoid was filled to capacity, the magma may have either continued to ascend into a now eroded, stratigraphically higher trap or, alternatively, pinched out (Figures 8.7.c., 8.9.b. and 9.3) and ceased propagation.

As the last, trailing magmatic pulses ascended through the system, magmatic activity would be minimal. The bulk of the thermal activity would have coincided with the early emplacement of the large volumes of magma into the two chambers (i.e. Eastern and Western Deeps). As a result, following the intrusion of these large volumes of magma, the uplift or crustal welt would begin to subside, creating sub-horizontal, compressional features. The last surge of the nickel sulphide-bearing magma would continue to ascend towards the Ovoid trap along the south-facing conjugate fault system, as did the preceding magmatic pulses. North of the Eastern Deeps, however, the flow was impeded either through choking or contraction of the conduit (Ovoid feeder conduit/dyke). Magma was then forced to bifurcate along a secondary plane of weakness provided by the horizontal fracture surfaces. This diversion or splay resulted in the development of the Eastern Deeps feeder (Figures 8.7.c. and 8.13). Being transported south along this horizontal fracture set, the nickel-rich melt would have intersected the base of the Eastern Deeps chamber (Figure

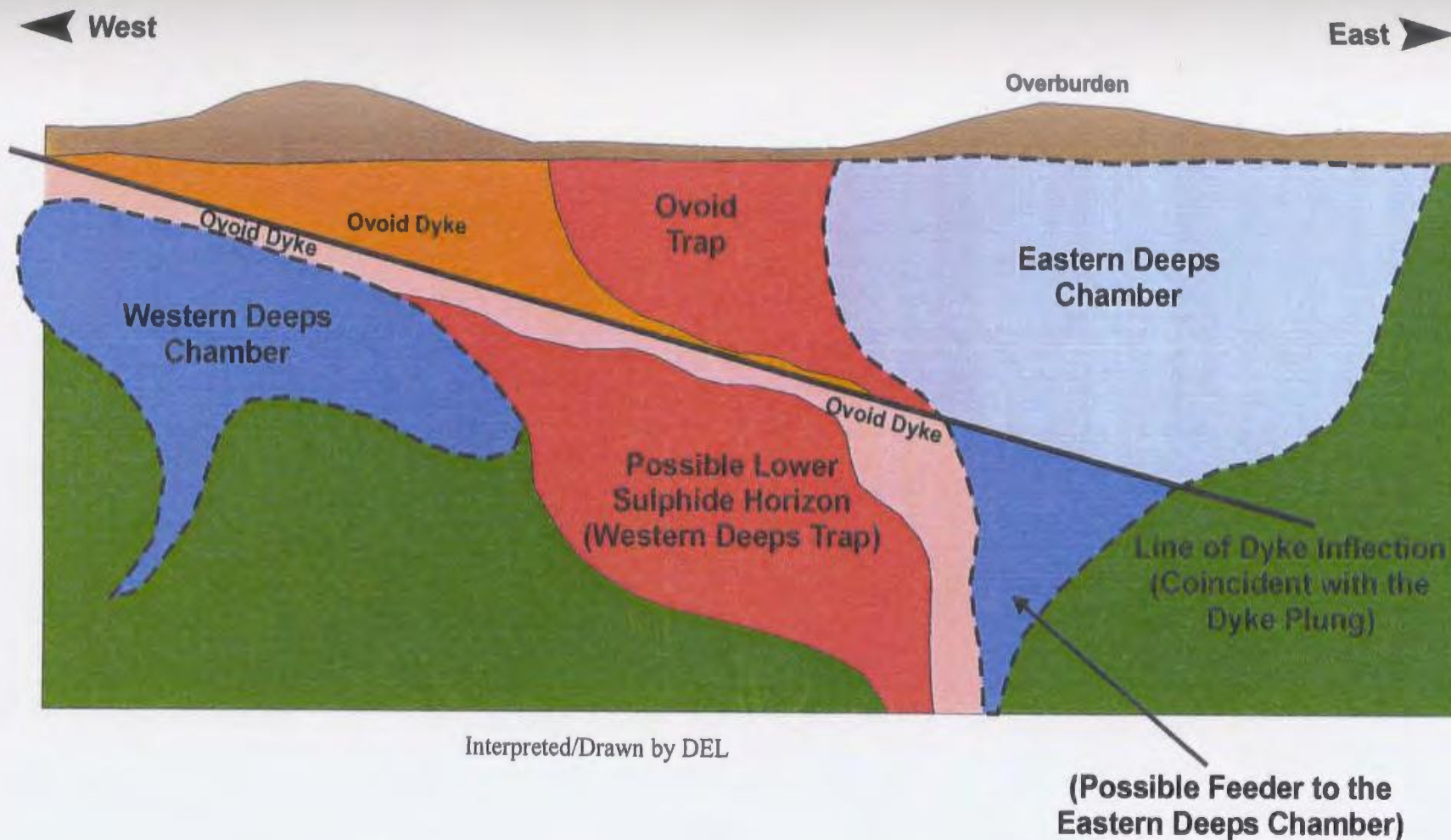


Figure 9.3 A schematic long section showing the chambers and conduits within the Voisey's Bay deposit. The chambers are shown in-filling primary dilatencies while the conduits appear to occupy and expand (i.e. trap) within secondary dilatencies produced through progressive extension/deformation. The line representing the inflection axis of the conduit appears to separate the dilatencies produced above the floor of the graben from those produced below.

8.6.b.). The margins of this magmatic medium would provide a structural weakness and would, therefore, have allowed the sulphide system to intrude along its basal contact. Initially when expelled into the crystalline mush of the chamber, the conduit may have remained as a semi-cohesive package. But with further intrusion into the chamber, the lack of a physical constraint on the upper margin of the feeder could induce a loss in cohesion of the system and initiate mingling between the two magmas.

It has been suggested that the Western Deeps chamber was the parental trap and site for sulphide immiscibility (eg. Naldrett *et al.*, 1996; Li and Naldrett, 1998). To date, however, no ultramafic cumulates have been found in this system that could have provided the ultramafic fragments present in the mineralized conduit sequences (i.e. Basal Breccia). Furthermore, if the Ovoid conduit was generated and then expelled from this chamber, it would not have conformed to gravity forces, as it lies over a less dense, sulphide-poor medium. If such a process did occur in this anomalous (i.e. reverse grading) manner, why are there no fragments from the roof of the chamber scattered about the funnel shaped chamber exit? It therefore, becomes apparent that the true parental chamber must reside undisclosed at depth.

The question also arises as to what is the source for this mantle derived magma? Earlier sections in this text have established that magmatic activity was associated with anorogenic magmatism, magmatism that can not be placed in the time context of orogenic events in the area. Morse and Hamilton (1990) proposed that the magmatism was derived from a mantle plume. Anorthosites phase of the Nain Plutonic suite have been documented to contain anomalously radiogenic Sr isotopes, but do not have increased Rb

concentrations (op.cit.). Morse and Hamilton (1990) further speculate that if this anomalous signature was a product of country rock contamination, then the Rb should have also been proportionately increased. Likewise the radiogenic Sr cannot be explained as a function of the expulsion of volatiles, since volatile xenoliths found in the Kiglapait mafic to ultramafic layered complex (Figure 1.5) have similar low Rb values (op.cit.). Morse and Hamilton, therefore, stated that the high Sr isotopic value is a mantle derived signature.

Theriault and Barnes (1998) suggest that between 1.33-1.11 Ga Laurentia drifted over a stationary mantle plume. With the motion of the moving plates added to the original plume instability, additional disturbances could result, including: diapiric chains, solitary waves, secondary detachment, or large area blooms (c.f. Olsen, 1990). Magmatic events associated with plume activity can be extensive and long lived, since melt from the diapir can be tapped through multiple events over time (op.cit.). Further supporting this process, Li and Naldrett (1998) suggest the Voisey's Bay complex formed through at least two magmatic pulses or events. It therefore, would be valid to conclude that parental magmas for the Nain Plutonic suite, and more specifically the Reid Brook complex, were derived from a mantle plume.

9.2.2 Comparison To Other Ni Sulphide Deposits

Magmatic Ni sulphide deposits are associated with ultramafic to mafic rocks. Such systems require sulphide saturation and subsequent separation of a sulphide phase from the silicate melt (sulphide immiscibility) (eg. Maclean, 1969; Rajamani and Naldrett, 1978;

Naldrett and MacDonald, 1980; Naldrett 1973, 1989a, and 1989b). The sulphide phase can separate from the silicate melt before crystallization, or alternatively, during crystallization of the silicate melt through fractional segregation (Papunen, 1996). Sulphide immiscibility, can be assisted by many processes such as the assimilation of silicic crust (SiO_2 and S activities), temperature and pressure, O_2 fugacity, FeO and TiO_2 activities: as defined by the studies of Maclean (1969), Rajamani and Naldrett (1978), Papunen (1996), Li and Naldrett (1998). As stated by Papunen (1996), sulphur-bearing country rocks can contribute extra sulfur to the system, further encouraging sulphur saturation. Also, interaction with large volumes of magma will allow the sulphides to salvage chalcophile elements, potentially upgrading the Ni sulphide (chalcophile) tenor (Naldrett, 1981, 1989a, 1989b). In order to produce significant sulphide tonnages in these systems, the sulphides have to be concentrated or constrained from an original broad, low grade dispersion (*op. cit.*).

The Voisey's deposit shares several similarities with other magmatic Ni sulphide deposits, however, a number characteristics make Voisey's Bay a unique deposit. The following text will summarize the physical, spatial and temporal characteristics of other magmatic Ni sulphide deposits and how these relate to the Voisey's Bay system. This outline will compare and contrast the physical environments of nickel sulphide bodies hosted within well some known giant ore deposits and others of low economic stature. The deposits characterized below were selected for their geological diversity, including: geological setting, metamorphism, and deformation. Specific deposits were also chosen for their suggested analogies to the Voisey' Bay deposit.

Sally Malay Ni-Cu-Co deposit of the East Kimberley of Western Australia, 5.5 Mt @ 1.75% Ni; the following is summarized from the works of Hoatson et al. (1998), and Shedden and Barnes (1996).

Rationale for Comparison:

-The physical environment hosting the mineralization has been directly suggested to be analogous to the Voisey's Bay deposit by Hoatson et al. (1998).

Similarities to the Voisey's Bay Ni Sulphide System:

- Related to an orogenic event (Halls Creek orogen ca. 1.8 Ga.) that is tectonically comparable to the Torngat Orogeny.
- Thought to be composed of multiple sub-chambers (possibly conduits).
- Hosted in gabbroic to troctolitic rocks.
- Has a history of deformation, including strike-slip faulting.
- Interpreted to be composed of multiple magmatic phases/pulses.
- No metamorphic aureole is detected.
- Sulphides collected in a footwall embayment or "keel".
- Authors interpret the sulphide distribution to be strongly influenced by fluid dynamics and the physical geometry of the deposit.
- The deposit hosts a sulphide-bearing breccia sequence containing country rock xenoliths.
- The magmatic system is constrained by an east-west trend.
- Country rocks consist of garnet-cordierite-sillimanite bearing paragneisses which provide an external source for sulphur.
- A marginal gabbroic phase is recognized.
- Contaminated by country rock assimilation.
- Sulphides are hosted in mafic rocks at the base of the intrusion/intrusions.

Dissimilarities to the Voisey's Bay Ni Sulphide System:

- Magmatism is directly related to orogenic events.
- The geological model infers sulphides were collected and concentrated through gravity settling within a chamber setting.
- Sulphides are not recognized in the channels (conduits?) linking the individual chambers.
- A footwall depression is found at the base, but is thought to have formed through thermal erosion and alternatively, and not thought to be a tectonic expression.
- Chambers are not known to be connected, they are separated by narrow channels of mafic granulites and gneisses (Tickalara Metamorphics), no direct evidence for the presence of feeder conduits has been recognized.
- The deposit is characterized by cyclic horizons of ultramafics and mafic rocks.

Jinchaun Ni Sulphide Deposit, southwest margin of the Sino-Korean Platform, 500 Mt. @ 1.2% Ni Naldrett (1997); the following is summarized from the works of Chai and Naldrett (1992a, 1992b) and Zongli (1993).

Rationale for Comparison:

-The physical similarity of the chambers that host the sulphides with the sulphide-bearing conduits in the Voisey's Bay deposit.

Similarities to the Voisey's Bay Ni Sulphide System:

- Sulphides are hosted by a dyke-like structure.
- Strikes in accordance to regional structural trends (i.e. lineations).
- The deposit has been subjected to post-emplacement structural dislocation.

- Gravity, thermal and flow processes are thought to control lithological distribution and deposition.
- Evidence suggests that the deposit was established through multiple magmatic pulses.
- Magma mingling occur between chambers.
- Upper stratigraphy is eroded at surface.
- Massive sulphides are inclusion-bearing.
- Stratigraphy varies in attitude from sub-vertical to horizontal.
- Magmatic sulphide textures include, net, disseminated and oikocrystic (Leopard textures).

Dissimilarities to the Voisey's Bay Ni Sulphide System:

- Ni sulphides are completely hosted within ultramafic rocks.
- The deposit is thought to have formed in an orogenic intrusion.
- Gravity settling processes are thought to dominate the development of sulphide textures.
- A intensely sheared contact is recognized between the intrusion and the adjacent country rocks.
- Emplacement occurred between 1719-1339 Ma.
- The deposit is thought to be the base of a layered intrusion which has been eroded at surface.
- Hosts PGEs.

Sudbury Ni Camp, 16.5 Bt. @1.2% Ni; the following is summarized from the works of Naldrett (1984a, 1984b, 1989a, 1989c, 1997), Rousell et al. (1997).

Rationale for Comparison:

- Extensive research and documentation of the geology within the Sudbury structure and detailed analysis of the ore-bearing environments.

Similarities to the Voisey's Bay Ni Sulphide System:

- Ultramafic fragments found in the sub-layer (ore-bearing unit).
- Evidence supports the early assimilation of country rock.
- Crustal fractures assisted the ascent of magma through the crust.
- Sulphide traps were created by footwall depressions or irregularities.
- Lenticular ore-bearing protrusions radiate out from the main body (Sudbury off-sets).
- Massive ores contain footwall fragments (South Range).
- The Sudbury structure is proximal, but to the north of the Grenville Front.
- Episodes of extension are recognized.

Dissimilarities to the Voisey's Bay Ni Sulphide System:

- Magmatism is thought to have been induced by a meteorite impact.
- Sudbury magmatism occurred at 1.85 Ga.
- The Sudbury structure is recognized as a layered intrusion (Sudbury Igneous complex).
- The intrusives are hosted at the contact of tonalitic gneisses and quartz monzonites.
- Stratigraphy forms concentric rims dipping toward the center of a basin-like structure.
- Breccias are thought to be impact features and not magmatic in origin.

Noril'sk Ni Camp, 9.0 Bt. @ 2.7%, (Naldrett,1997); the following is summarized from the works of Naldrett et al. (1989a, 1997b), Naldrett and Mac Donald (1980), Naldrett et al.(1995), and Eckstrand (1996).

Rationale for Comparison:

- The size and the economic potential associated with this deposit make it an intriguing world class model for the study of nickel sulphide deposits. As well, the presence of mineralized conduits extending outward from the main magmatic reservoir suggests physical similarities to the mineralized conduits in the Voisey's Bay deposit.

Similarities to the Voisey's Bay Ni Sulphide System:

- Dyke-like protrusions that radiate from chamber host the main mineralization.
- Evidence for crustal contamination.
- Magma is thought to have ascended through a transcrustal fault.
- Hosted in mafic to ultramafic rocks.
- Loop textures recognized within the massive sulphides.

Dissimilarities to the Voisey's Bay Ni Sulphide System:

- No breccia textures.
- Sulphides were collected and concentrated through gravity settling within a large closed reservoir (pond).
- Lenticular protrusions extending out from the magmatic reservoir are thought to represent exit conduits.
- A large metamorphic aureole is recognized.
- Occurrence of PGE enrichment.
- The sulphide-bearing reservoir is thought to be the site of sulphide segregation in opposition to such processes occurring at depth in a deeper chamber.
- This intrusion provides the plumbing for the transport of overlying lavas of Permian-early Triassic flood basalts.

Hirva Ni-Cu deposit Finland, 8.7 Mt. 0.57% Ni; the following is summarized from the works of Papunen and Penttilä, (1996):

Rationale for Comparison:

- Role of metamorphism in the formation of nickel sulphides.

Similarities to the Voisey's Bay Ni Sulphide System:

- The shape of the complex infers fractionation occurred in a conduit-like body, a possible feeder to overlying volcanics.
- The deposit is proximal to graphitic metasediments.
- Lithological and sulphide textures are linked to secondary physical processes.
- Massive sulphides locally extend into the adjacent country rocks.
- It is in physical proximity to sulphidic schists.
- The complex is sub-vertical, funnel shaped structure.

Dissimilarities to the Voisey's Bay Ni Sulphide System:

- Hosted in a ultramafic complex (Serpentinite).
- Deposit hosted by an ultramafic igneous complex.
- Intense metamorphism and alteration are recognized within the system.
- The deposit genesis is associated with 1.9-1.85 Ga. subduction related events.

Hartly Lake complex, part of the Great Dyke, Zimbabwe, 168 Mt. @ 0.16Ni%; the following is summarized from the works of Gellatly (1996):

Rationale for Comparison:

- Association to deep-seated crustal structures.

Similarities to the Voisey's Bay Ni Sulphide System:

- The ore bodies are found within mafic magmatic sequences.
- The emplacement is associated with a transcrustal fault (Great Dyke of Zimbabwe).
- Oikocrystic textures are recognized within Main Sulphide Zone.
- Leopard textures are typical in the disseminated sulphide zones.
- Mafic sequences occur as homogeneous thick layers.

Dissimilarities to the Voisey's Bay Ni Sulphide System:

- Genetically the structure represents a layered intrusion
- The intrusion is hosted within granites.
- Hosts PGEs.
- Cyclic ultramafic sequences underlie the mafic rocks.

Kambalda district, Western Australia

66 Mt. @ 2.9Ni%; the following is summarized from the works of Naldrett (1997), Lesher (1989) and Lesher et al. (1984):

Rationale for Comparison:

- Nickel sulphides are hosted within channel-like flows, and therefore, their distributions will be influenced by physical and environmental processes.

Similarities to the Voisey's Bay Ni Sulphide System:

- Pentlandite displays exsolved textures (i.e. discontinuous bands), as is similarly depicted by the Loop Textures in the Voisey's Bay ore.
- The sulphides did not gravity settle from a stagnant system, but alternatively, were deposited within a dynamic channel-like system.
- Physical processes acting within the system can be compared to those occurring in a river system.
- Basal ores were focussed and constrained by footwall irregularities that are thought to pre-date sulphide emplacement (troughs or footwall depressions).
- Troughs are thought to be bounded by steeply dipping normal or reverse faults (geometry is controlled by structure).
- Magma flow can overflow and deviate from the troughs (branch or bifurcation).
- Magmatic flow is interpreted to have been turbulent and not laminar.
- Sulphides are recognized to intrude the country rock along planes of weakness (i.e. fractures).

Dissimilarities to the Voisey's Bay Ni Sulphide System:

- Hosted in a rift-bounded Archean greenstone belt (mafic to ultramafic volcanics).
- The country rocks are composed of felsic-intermediate volcanics and sediments.
- Contamination occurred through in situ assimilation or thermal erosion of adjacent country rocks.
- Ore is deposited in elongate channels and not within bulbous traps.
- Sulphide and magma distribution is controlled by gravity forces; flow conforms to the topographic gradient.
- Stratiform magmatic sequences are found at the base of the troughs.
- The geometries of the massive sulphide horizons are controlled by deformation.
- Sulphide horizons are not intercalated, but appear to maintain stratiform contacts.
- Collectively, the sulphide horizons grade downwards (normal grading) from less dense, disseminated sulphides into denser, massive sulphide horizons at the base.

Although the Voisey's Bay deposit shares many characteristics with other magmatic nickel systems, it remains an enigma. In the past nickel deposits in similar geological settings to that of Voisey's Bay have not been documented as economic systems, nor have they shown physical processes with comparable dynamics. The

differences between the Voisey's Bay deposit and other Ni deposits are significant: for example, unlike many other Ni deposits (i.e. Noril'sk, Sally Malay, Jinchuan), the Voisey's Bay deposit did not rely on gravity settling to extract and concentrate the sulphide phases. As they are currently found in massive sulphide bodies. To a small extent, settling is recognized within conduit traps, however, the small size of these traps did not allow large accumulations of magmatic material to be contained whereby sulphides could be concentrated through gravitational settling. This process may have played a dominant role in initial sulphur segregation at depth within the parental chamber, but is not a significant control to the collection of sulphide bodies as they are presently preserved in Voisey's Bay.

Unlike other nickel systems, the ore-bearing conduits of the Voisey's Bay deposit are not proven to directly feed an existing magmatic complex (i.e. Hitura). Nor do these conduits represent choked channels exiting (i.e. Noril'sk) a large magmatic reservoir. Alternatively, these are physically dynamic, ore-bearing conduits which were likely to have been derived from a parental chamber at depth. If derived from a common source at depth, the large volumes of magma infilling the chambers could have been focused to the surface coeval with early episodes of deformation. During this early magmatic activity the sulphide-rich conduit fluids may have resided in traps at depth. They were only freed to ascend through the system as new magmatic pulses pushed them from their residential traps. Furthermore, the magmatic intrusions (i.e. chambers) did not appear to produce large volumes of sulphides in situ, as all significant mineralization in the Voisey's Bay system is found within or adjacent to the conduits. There is no direct evidence to suggest

that there was a significant break between these two magmatic events (i.e. chamber emplacement and conduit development). Conversely, the conduit magmas are documented as locally mixing with the chamber magmas (Li and Naldrett, 1998), therefore, establishing that crystallization processes were not evolved when the conduit magmas were introduced to the chamber magmas. Therefore there was no significant break in the two magmatic events and the Voisey's Bay deposit is a dynamic interactive system.

A further distinguishing feature of the Voisey's Bay deposit from other magmatic Ni sulphide systems is the absence of ultramafic rocks. Other deposits are generally hosted within, or in close proximity to ultramafic rocks (i.e. Hartley complex, Noril'sk, Jinchuan, and Hitura). To date, no ultramafic rocks have been found in the Voisey's Bay deposit, except for ultramafic fragments, the source for which have yet to be defined. Furthermore, as opposed to many intrusive magmatic sulphide deposits (i.e. Sudbury and Noril'sk), the Voisey's Bay deposit does not contain PGEs. Finally, the Voisey's Bay system is not anomalous as it is directly associated with metamorphic events, nor does it display a discrete metamorphic aureole, as do the Hitura and Noril'sk deposits.

Collectively the geological attributes of the Voisey's Bay deposit define a unique nickel sulphide system, however, it does have some similarities to other nickel sulphide camps. Whether sulphides collect through gravity settling in a closed reservoir or are captured within a dynamic conduit system, a physical structure is required to restrain and consolidate sulphide masses. Embayments, surface irregularities and structural discontinuities provide physical mediums for the capture of sulphides regardless of the deposit setting (i.e. Sudbury and Sally Malay). In the Voisey's Bay deposit, the

distribution of sulphides was controlled by comparable features, for example: the footwall depression within the Eastern Deeps.

Numerous deposits also contain sulphide bodies that have been dislodged and redistributed along post-emplacement structures. In Voisey's Bay at least one such structure is recognized, the 2E-2W fault panel (Figure 5.4). Similar splays or extensions extending from a main ore body are exhibited by the Sudbury Off-sets and Jinchaun deposits. The presence of these structures indicates that sulphides can be redistributed along late, post-emplacement structures or can be contained within parasitic structures in a broad range of geological settings.

Another geological element common to other nickel sulphide deposits is the influence of crustal contamination. Many deposits including Voisey's Bay, indicate crustal contamination of the primary magma as an important ore-forming component. Furthermore, many magmatic Ni deposits show indications of olivine depletion within the mafic or ultramafic host rocks, and have mineralization associated with fragmental or breccia rocks that contain country rock inclusions (i.e. Sudbury and Jinchaun).

9.2.3 Exploration Significance, Expanding Current Resources within the Voisey's Bay Deposit

With the Ovoid established as a continuous conduit system there is no current evidence to suggest this structure can not continue to the east along its defined trend (Figures 8.12, 9.4 and 9.5). The geological model purposed in this study suggests that the Ovoid (Ovoid feeder conduit/dyke) continues to the east along the north margin of the Eastern Deeps. When so modeled, the Ovoid dyke conforms to a discrete and regular

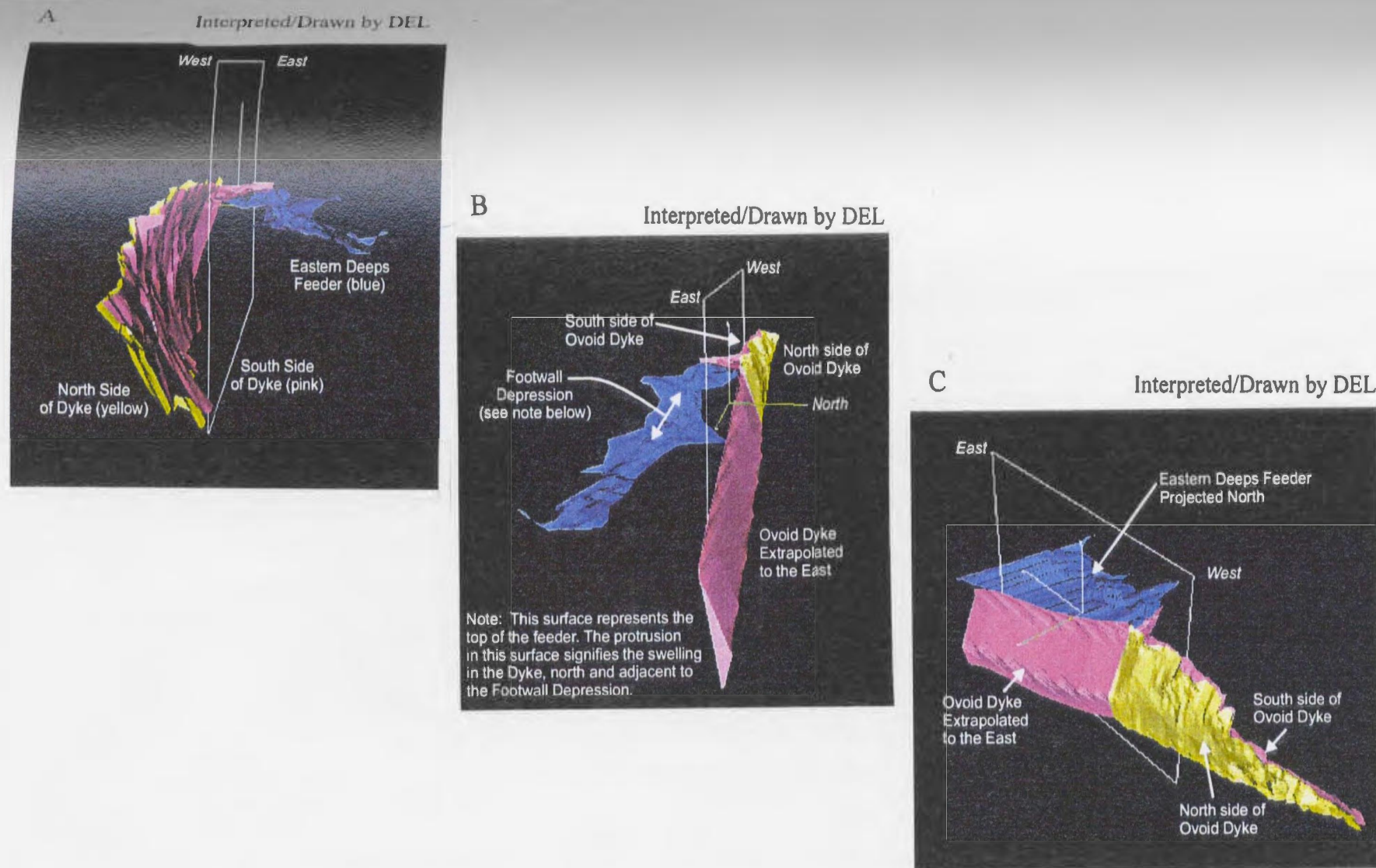
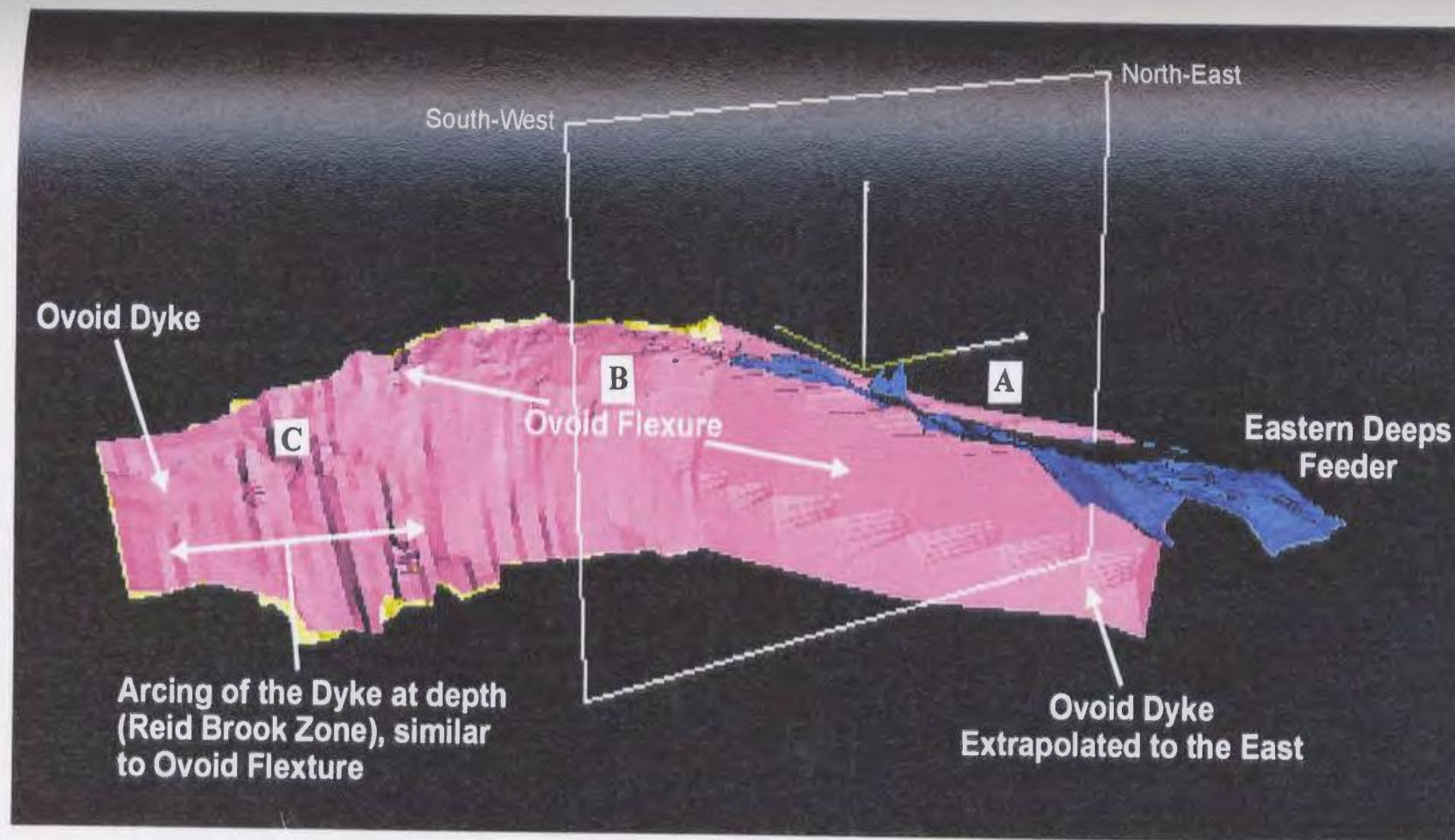


Figure 9.4 Three dimensional models produced from drill hole data, showing the relationships between the Ovoid conduit/dyke and the Eastern Deeps feeder. (A) An east-facing model displaying the Eastern Deeps feeder intersecting the Ovoid conduit/dyke to the north. (B) A west-facing model displaying the Ovoid conduit/dyke extrapolated east along its defined trend through the Eastern Deeps, but north of the Eastern Deeps feeder. (C) A west-facing model displaying the Ovoid conduit/dyke extrapolated east along its defined trend through the Eastern Deeps and the Eastern Deeps feeder extrapolated north (along its trend) to where it appears to intersect and coalesce with the Ovoid conduit/dyke.



Interpreted/Drawn by DEL

Figure 9.5 A three dimensional model produced from drill hole data, showing the relationships between the Ovoid conduit/dyke and the Eastern Deeps feeder: (A) The Ovoid conduit/dyke is extrapolated east along its defined trend through the Eastern Deeps and the Eastern Deeps feeder is extrapolated north (along its trend) to where it appears to intersect and coalesce with the Ovoid conduit/dyke, (B), (C) The inflection axis of the Ovoid Conduit/dyke at depth within the Reid Brook zone appears to be mimicking the inflection axis found below the Ovoid and Mini-Ovoid traps.

geometry (Figures 8.4, 8.5 and 9.5). These geometric controls can be used to extrapolate and predict the occurrence of this sulphide-bearing dyke into areas that currently remain unexplored. This exercise thus provides focus for continued exploration, both proximal and distal to the deposit limits as they are currently defined.

The plunge for the Ovoid dyke is established to be $23^{\circ} \rightarrow 090^{\circ}$. By projecting this plunge past the eastern limits of the dyke as currently delineated (Figures 9.6 and 9.7), the position of the dyke and its potential sulphide traps can be accurately targeted (i.e. proximal to flexures) (Figures 9.6.b. and 9.7.a.). The multiple sulphide traps that are currently delineated (i.e. Discovery Hill and Mini-Ovoid) are speculated to persist and to continue at depth to the east in conformity to the plunge designated by the conduit/dyke.

More specifically, it should be recognized that individual sulphide bodies (i.e. Discovery Hill and Ovoid) display highly variant three dimensional geometry. It is therefore, pertinent to recognize that the sulphides do not necessarily have to plunge in complete coincidence with the plunge/pitch of the conduit/dyke, but alternatively may establish their own internal geometry within this host (Figures 9.6.b. and 9.7.a.). It should not be presumed that the individual sulphide bodies will be constrained to exclusive traps that are defined by the structural contours. Physical processes can result in a single sulphide horizon being dispersed over multiple traps (i.e. velocity and viscosity). As an example, in chapter 5 the Mini-Ovoid and Ovoid sulphides are documented as mingling at the edges of both traps.

As with the Ovoid dyke, the Eastern Deeps feeder can be extrapolated in accordance to its defined trend north of the Eastern Deeps chamber (Figure 9.4).

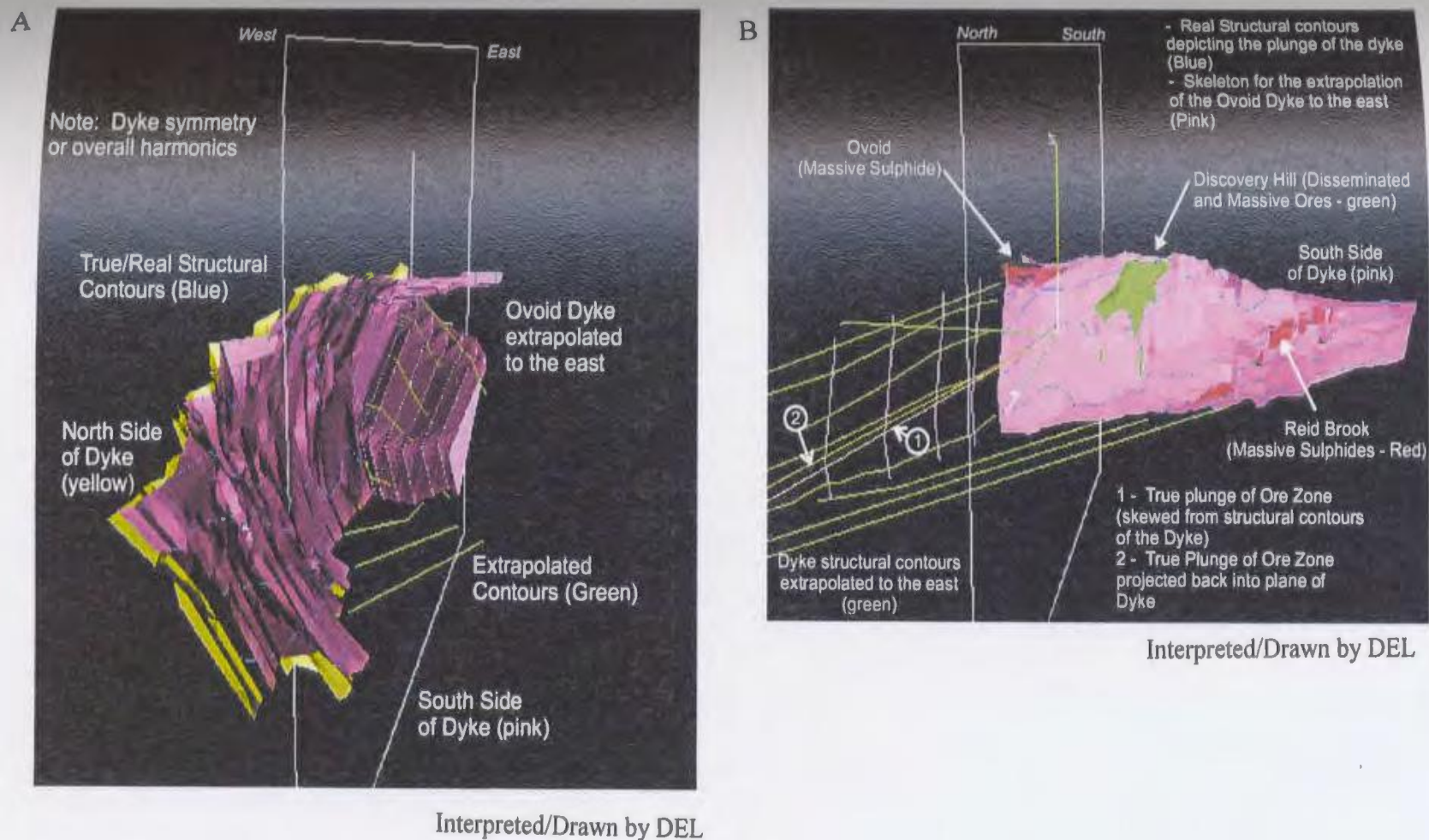
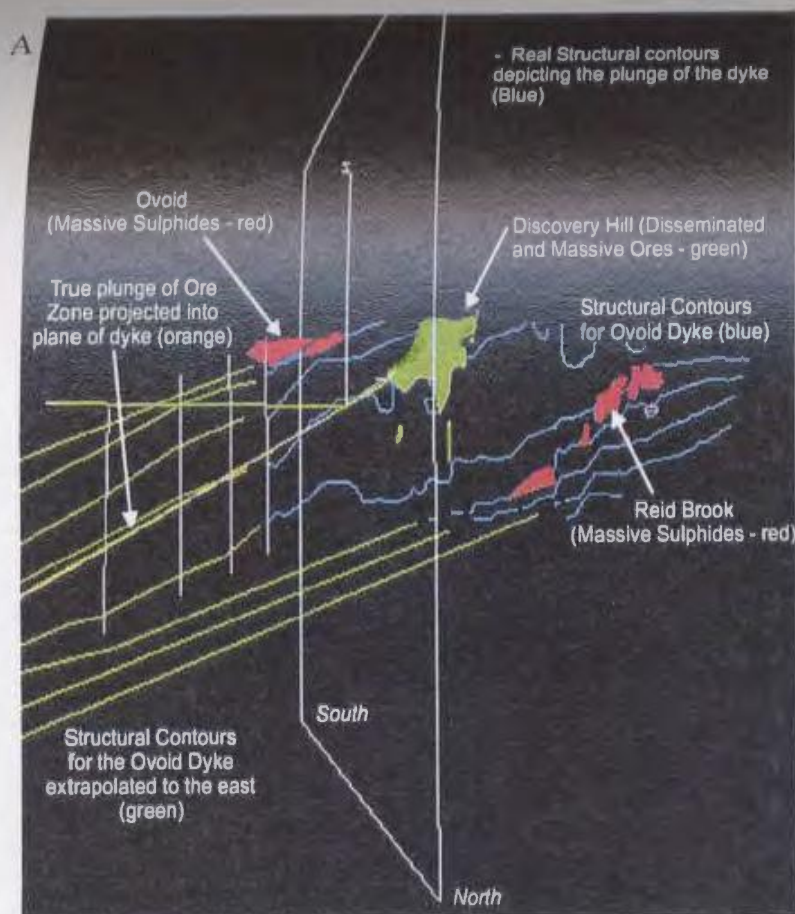
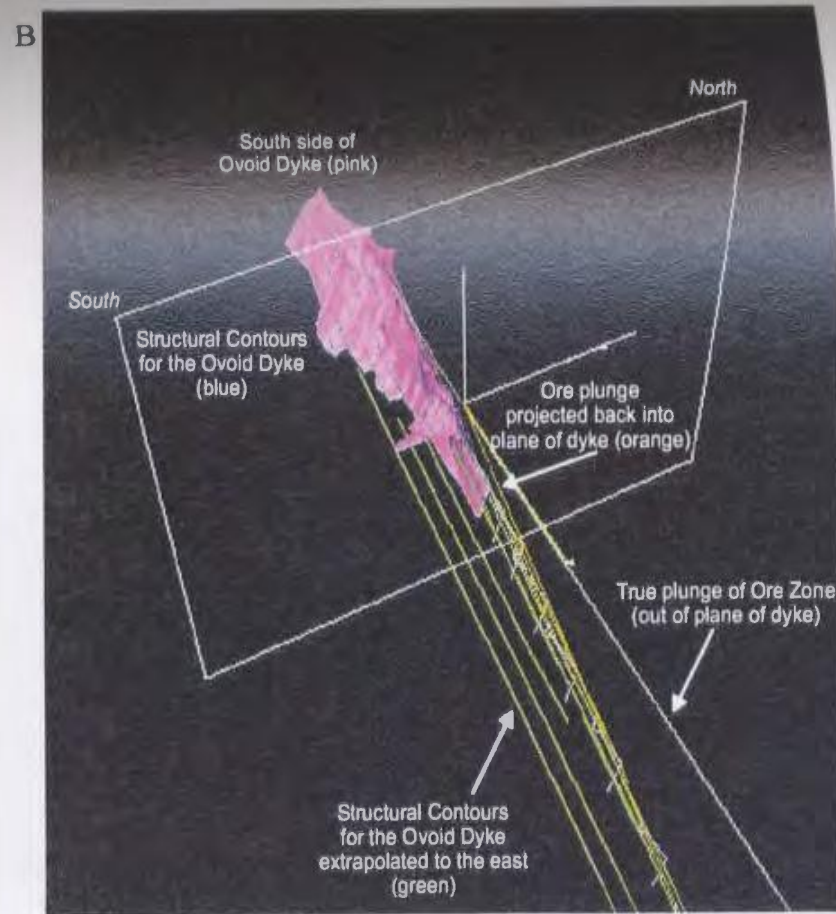


Figure 9.6 A three dimensional model produced from drill hole data, showing the symmetry of the Ovoid conduit/dyke. (A) Structural contours (blue lines) through the Ovoid conduit/dyke appear as a series of geometrically regular, parallel inflection axes. These axes can be extrapolated to the east to predict the occurrence and geometry of the Ovoid conduit/dyke north of the Eastern Deeps. (B) The plunge of the mineralized zones (i.e. Ovoid, Mini-Ovoid, Discovery Hill, and Reid Brook zones) appears skewed to the structural contours. Each mineralized zone, however, appears to be constrained by two structural contours.



Interpreted/Drawn by DEL



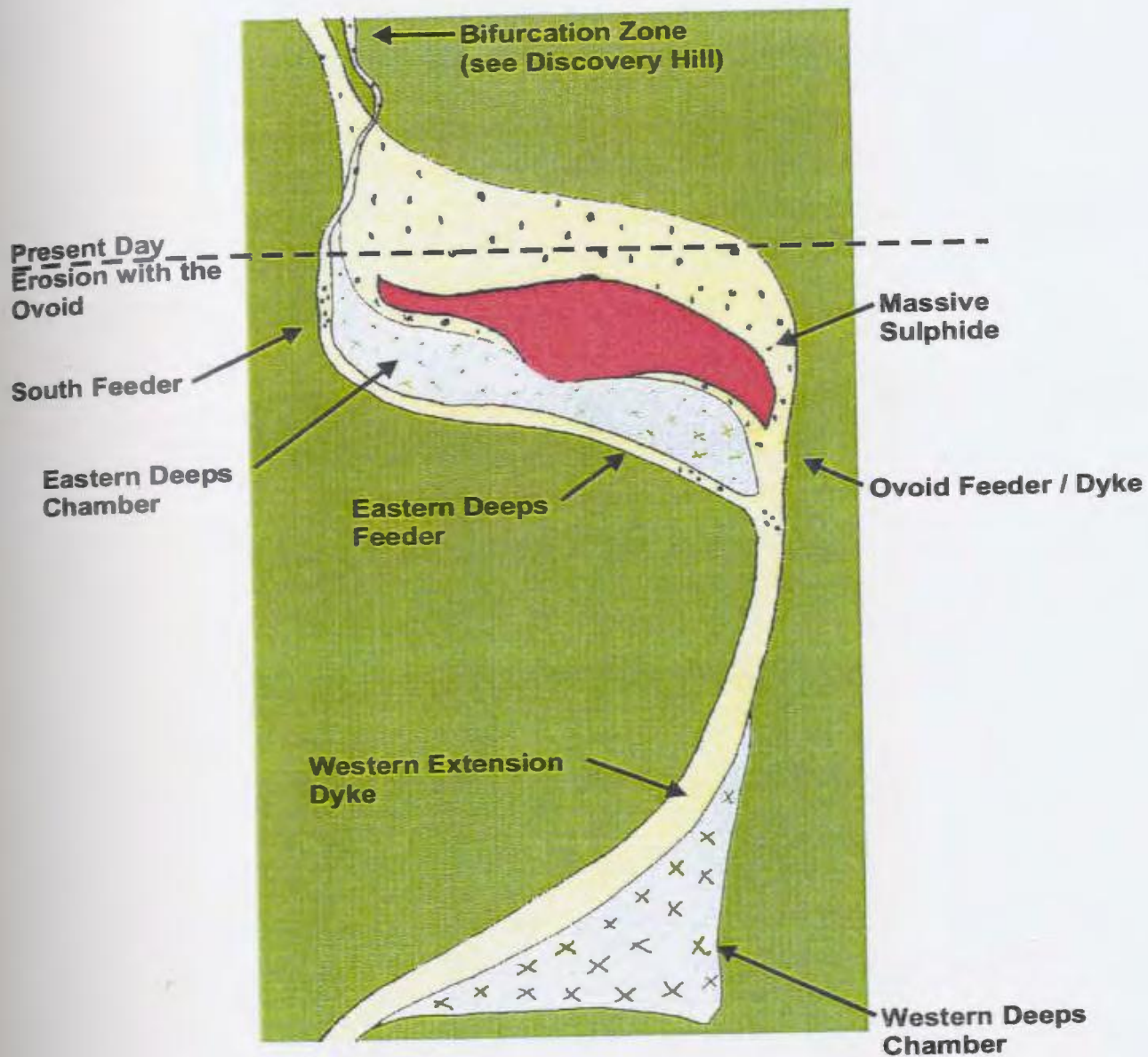
Interpreted/Drawn by DEL

Figure 9.7 Three dimensional models produced from drill hole data, showing the relationship between the plunge of the multiple mineralized zones to the symmetry of the structural contours: (A) The surfaces of the Ovoid conduit/dyke have been removed to more clearly display the geometric relationships between the mineralized zones and the structural contours. The plunge of the mineralized zones (i.e. Ovoid, Mini-Ovoid, Discovery Hill, and Reid Brook zones) appears skewed to the structural contours. Each mineralized zone, however, appears to be constrained by two structural contours, (B) The structural contours for the Ovoid conduit/dyke extrapolated to the east through the Eastern Deeps. The true plunge of the mineralization appears to deviate greatly from that of the structural contours. This feature is related to the frequent changes in the width of the Ovoid conduit/dyke, whereby the mineralization distributed within a three dimensional trap. If this true plunge is projected back to a two dimensional surface (i.e. x and z planes only), it will lie in coincidence with the structural contours.

Geological relationships observed in the Ovoid indicate the coalescence of two unique conduit systems (Figures 4.11 and 8.13) which are both capable of bearing sulphides. It appears these two conduits represent the Ovoid feeder conduit/dyke and the Eastern Deeps feeder, but of most significance, can these systems be expected to intersect north of the Eastern Deeps? Can this be the site where the Eastern Deeps feeder splays from the Ovoid conduit?

To the north, the Eastern Deeps feeder does not only appear to be proximal to the Ovoid conduit/dyke, but appears to intersect the Ovoid conduit (Figures 9.4.c. and 9.5). This relationship, as postulated, can result in two possible scenarios: (1) The Eastern Deeps feeder continues and propagate to the north, after intersecting and penetrating through the Ovoid conduit, remaining true to its current trend. In this model the Eastern Deeps conduit could have an extensive expression to the north, restricted only by the extent of the horizontal fracture system to which it follows, (2) Alternatively, as observed in the Ovoid domain, this conduit may coalesce with the Ovoid dyke at the line of intersection (Figures 4.11, 8.13, and 9.8). If this assumption is correct and both feeders are coeval, there is a significant possibility that a large and proximal sulphide body could be found either, at the junction of both dyke systems, or at depth in the parental/dominant conduit (i.e. Ovoid feeder conduit/dyke) (Figure 8.13).

Besides increasing the local potential for undisclosed sulphide bodies, the idea that conduits can splay and yet still host significant sulphides, suggests further exploration targets outside the current limits of the deposit. Multiple and lateral diverse splays may



Interpreted/Drawn by DEL

Figure 9.8 A schematic west-facing section showing the spatial relationships between the chambers and conduits within the Voisey's Bay deposit. The Ovoid appears to be a trap within the feeder conduit which probably continued to ascend above present erosion levels. The Eastern Deeps feeder is stratigraphically below the Ovoid, and appears to be a branch or bifurcation from the Ovoid feeder conduit/dyke. The Eastern Deeps feeder may coalesce or intersect the Ovoid to the south and, therefore, represent the south feeder and the Bifurcation Zone. To the east after splaying from the Ovoid conduit/dyke, the Eastern Deeps feeder intersects the base of the Eastern Deeps chamber. At depth the Ovoid conduit/dyke intrudes along the margin of the Western Deeps chamber.

exist within many regional domains. The conduits currently known may only be secondary parasitic features to larger primary systems, yet to be discovered.

9.2.4 Finding a new high grade Voisey's Bay type of Ni sulphide deposit

The challenges encountered when exploring for new magmatic Ni sulphide deposits prove diverse and numerous. An index of inherent characteristics can be used as a broad generic template to focus on new, potentially economic Ni sulphide terranes. The list, as provided below, will define characteristics shared by magmatic Ni sulphide (summarized from Maclean, 1969; Cai and Naldrett, 1992a, 1992b; Naldrett and MacDonald, 1980; Naldrett, 1994a, 1994b, 1989c, 1997; Papunen, 1996; and Lightfoot, 1998). These features may not be true of all Ni deposits.

- 1) Ni-depletion within olivines in host rocks.
- 2) Crustal contamination.
- 3) Proximal to an external sulphide source (sulphidic sediments)
- 4) Pre, syn, or post-magmatic tectonism.
- 5) Fragment bearing mafic or ultramafic rocks (breccia).
- 6) Extensive mafic/ultramafic magmatism.
- 7) Tentacle-like protrusions associated with magmatic reservoirs/traps.
- 8) Structures or surface irregularities to concentrate and constrain sulphide distribution.

These attributes will prove useful during the early stages of exploration when trying to isolate prospective terranes. Within terranes that have been previously determined to be favorable Ni hosts, however, these broad characteristics will not be of great assistance and will not provide specific criteria allowing for the sterilization of potential economic ground. These generic features establish a geological setting favorable to host magmatic Ni sulphides, but do not restrict or guarantee the possibility of an economic Ni sulphide occurrence.

It is pertinent to study potentially economic ground (see above) within the context of the local geological environment. For example, the Voisey's Bay deposit has not been directly associated with a layered ultramafic body, however, when analyzed in detail it is found to host ultramafic fragments. Genetic associations may not be initially evident in a particular regime, therefore, close attention has to be made to discrete features. Furthermore, when generic attributes isolate a potential Ni host, the economic viability of the system can not be judged solely on its physical similarity to other deposits, eg. the Voisey's Bay magmatic event is not an immediate product of orogenic processes.

Such suggestions do not infer that obvious magmatic processes are to be disregarded in the exploration process, conversely, such criteria must be applied in immediate geological context. To use Voisey's Bay as a further example, it is recognized that gravity settling processes do not dominate sulphide distribution or their concentrations. This conclusion does not mean this process did not affect sulphide melts at some stage, most likely early in their evolution in the parental chamber. In summary, because a particular body does not conform to known or well documented parameters, does not mean it can not host a significant Ni sulphide body. Conversely, if a particular process or attribute is not evident within a perspective terrane, it does not eliminate the possibility of this feature or features existing, as it can be masked or overprinted by other dominant processes.

In light of the Voisey's Bay deposit, emphasis has been placed on the controls over physical processes in the development of magmatic Ni deposits. Anomalous processes appear to govern the distribution and concentration of sulphides in Voisey's Bay,

however, it in the end these processes may produce geological features similar to those present in other projects. For example, the Sudbury Offsets are sulphide-bearing protrusions radiating out from the base of the intrusion into the country rock. These structures are comparable to the conduits or feeders in the Voisey's Bay deposit. Can these features be choked conduits, feeding sulphides to the basal sequences? Furthermore, as with Noril'sk, can a dyke network proximal to a sulphide reservoir represent original feeder conduits that open at depth into early traps where the known sulphides once resided or where other sulphide concentrations may exist, in opposition to these structures representing exit conduits. Other physical similarities can be documented between deposits as within the Jinchuan system. Can the "*chambers*" described in the Jinchuan deposit actually be large macroscopic traps within the conduit system. Mineralization may have been derived from an intrusion at depth and was subsequently pushed to the surface within a conduit network such that, they collected in a trap through similar physical processes that produced the Ovoid. If such interpretations are applicable, numerous established deposits may have the potential to host sulphides, yet to be disclosed through conventional geological models and, therefore, require reevaluation.

BIBLIOGRAPHY

Abrajano, T.A. and Pasteris, J.D.

1989: Zambaldes ophiolite, Philippines II. Sulphide petrology of the critical zone of the Acoje Massif. *Contributions to Mineralogy and Petrology*, Vol. 103, pp. 64-77.

Abrajano, T.A., Pasteris, J.D., and Bacuta, G.C.

1989: Zambaldes ophiolite, Philippines I. Geology and petrology of the critical zone of the Acoje Massif. *Tectonophysics*, Vol. 1168, pp. 65-100.

Arbaret, L., Diot, H., and Bouchez, J.

1996: Shape fabrics of particles in low concentration suspensions: 2D analogue experiments and applications to tilting in magma. *Journal of Structural Geology*, Vol. 18, No. 7, pp. 941-950.

Barnes, S.J., Zientek, M.L., and Severson, M.J.

1997: Ni, Cu, Au, and Platinum-group element contents of sulphides associated with intraplate magmatism: a synthesis. *Canadian Journal of Earth Sciences*, vol. 34, pp.337-351.

Bridgwater, D., Watson, J. and Windley, B.F.

1973: The Archean craton of the North Atlantic. *Transactions Royal Society of London*, A273, pp.427-437.

Bruce, P., and Huppert, H.E.

1990: Solidification and melting along dykes by the laminar flow of basaltic magma. *Magma Transport and Storage. Edited by M.P. Ryan*, John Wiley and Sons Ltd., pp. 87-101.

Butt, D., and Hayes, J.

1997: Personal Communication 20/07/97, Voisey's Bay Nickel Company, Exploration Department.

Campbell, I.H., Naldrett, A.J., and Barnes, S.J.

1983: A model for the origin of platinum-rich horizons in the Bushveld and Stillwater Complexes. *Journal of Petrology*, Vol. 24, pp. 133-165.

Chai, G., and Naldrett, A.J.

1992a: Petrology and geochemistry of the Jinchaun ultramafic intrusion: cumulate of a high-Mg basalt magma. *Journal of Petrology*, Vol. 33, pp. 1-27.

Chai, G., and Naldrett, A.J.

1992b: PGE mineralization of the Jinchuan Ni-Cu sulphide deposit, N.W. China. *Economic Geology*, Vol. 87, pp. 1475-1495.

Condie, K.

1997: Sources of Proterozoic mafic dyke swarms: constraints from Th/Ta and La/Yb ratios. *Pre-Cambrian Research*, Vol. 81, pp. 3-14.

Corrigan, D., and Hamner, S.

1997: Anorthositic and related granitoids in the Grenville orogen: A product of convective thinning of the lithosphere?, *Geology*, Vol. 2, No.1, pp. 61-64.

Cruden, Alexander, R.

1998: On the emplacement of tabular granites. *Journal of the Geological Society*, London, Vol. 155, pp. 853-862.

Cruden, Alexander, R.

1990: Flow and fabric development during the diapiric rise of magma. *Journal of Geology*, Vol. 98, pp. 681-698.

Diamond Fields Resources Inc.

1996: Report from Voisey's Bay 04/95.

Doglioni, Carlo

1995: Geological remarks on the relationships between extension and convergent geodynamic settings. *Tectonophysics* 252, pp.253-267.

Eckstrand, O.R.

1996: Nickel-copper sulphide. *In* *Geology of Canadian Mineral Deposit Types*. Edited by O.R. Eckstrand, W.D. Sinclair, and R.I. Thorpe. Geological Survey of Canada, *Geology of Canada*, number 8, pp. 584-605.

Emslie, R.F.

1980: Geology and petrology of the Harp Lake Complex, central Labrador: an example of Elsonian magmatism: Geological Survey of Canada, *Bulletin* 293, pp.136.

Ermanovics, I.F., Van Kranendonk, M., Corriveau, L., Mengel, F., Bridgwater, D., and Sherlock, R.

1989: The boundary zone of the Nain -Churchill provinces in the North River-Nutak map areas, Labrador, *in* *Current Research, Part C: Geological Survey of Canada, Paper* 89-1C, pp. 385-394.

Evans-Lamswood, D.

1997a: Reconstruction of the Red Dog Fault Zone, V.B.N.C., Exploration Office, Memorandum

Evans-Lamswood, D.

1997b: Report on Multiple Feeder Zones, VBNC, Exploration Office, Memorandum

Evans-Lamswood, D.

1997c: Report on Southeast Plunging Ore Zone, V.B.N.C., Exploration Office, Memorandum

Evans-Lamswood, D.

1997d: Report: Conceptual Model of Western Deeps Evans-Lamswood, V.B.N.C., Exploration Office, Memorandum

Evans-Lamswood, D.

1997e: Report on Western Extension Reassessment, Evans-Lamswood, V.B.N.C., Exploration Office, Memorandum

Evans-Lamswood, D.

1996a: Isopacs for Eastern Deeps, Archean Resources, Deposit Exploration, Memorandum

Evans-Lamswood, D.

1996b: Report: The Ovoid-a structural synopsis, Archean Resources, Deposit Exploration, Memorandum

Evans-Lamswood, D.

1996c: Report on Eastern Deeps Lip Gneiss, Archean Resources, Exploration Office, Memorandum

Farrow, C.

1997: Most recent geochronological results from Memorial University of Newfoundland., INCO, Field Exploration Office, Copper Cliff, Memorandum

Gellatly, D.C.

1996: PGM and Nickel-Copper mineralization in the Hartley complex, Zimbabwe., Nickel '96, The Australasian Institute of Mining and Metallurgy, Publication Series No. 6/96, Published by The Australasian Institute of Mining and Metallurgy, Carlton Victoria Australia, pp. 139-143.

Golder Associates

1997: Equal area lower hemisphere projections of discontinuity populations based on orientated core; OV9701-07. M.Rougier, Golder Associates, 2180 Meadowvale Boulevard, Mississauga, Ontario, L5N 5S3, Memorandum

Groves, D.I., Korkiakoski, E.A., McNaughton, N.J., Leshner, C.M., and Cowden, A.

1986: Thermal erosion by komatiites at Kamalda and genesis of nickel ores., Nature, Vol. 319, pp. 136-139.

Gower, C.F., James, D.T., Nunn, G.A.G. and Wardle, R.J.
1995: The Eastern Grenville Province. *In* LABRADOR '95: The geology and mineral deposits of Labrador: A guide for the exploration geologist. CERR/NDNR Report, pp.73-101.

Gower, C.F., Rivers, T., and Brewer, T.S.
1990: Middle-Proterozoic mafic magmatism in Labrador, eastern Canada, *in* Gower, C.F., Rivers, T., and Ryan, B., eds., Mid-Proterozoic Laurentia-Baltica: Geological Association of Canada, Special Paper 38, pp. 485-506.

Gower, C.F., Rivers, T., and Ryan, B.
1990: Mid-Proterozoic Laurentia-Baltica: an overview of its geological evolution and a summary of the contributions made by this volume, *in* Gower, C.F., Rivers, T., and Ryan, B., eds., Mid-Proterozoic Laurentia-Baltica Geological Association of Canada, Special Paper 38, pp. 1-20.

Gower, C.F., Flanagan, M.J., Kerr, A. and Bailey, D.G.
1982: Geology of the Kaipokok Bay-Big River area, Central Mineral Belt, Labrador., Newfoundland Department of Mines and Energy, Report 82-87, pp. 87.

Hamilton, M.A., Emslie, R.F., and Roddick, J.C.
1994: Detailed emplacement chronology of the Mid-Proterozoic Nain Plutonic Suite, Labrador: insights from U-Pb systematics in zircon and badelleyite. Eighth International conference on Cosmochronology and Isotope Geology. United States Geological Survey Circular 1107, pp.124.

Hoatson, Dean M., Sproule, Rebecca A., and Lambert, David D.
1998: Are there Voisey's Bay-type Ni-Cu-Co sulphide deposits in the East Kimberley of Western Australia., *in* The Gangue, G.A.C.-Mineral Deposits Division, issue 58, pp. 6-8.

Hoffman, P.F.,
1988: United Plates of America, the birth of a craton: Early Proterozoic assembly and growth of Laurentia. *Annual Review of Earth and Planetary Science*, 16, pp. 543-603.

Horn, R.
Personal communication 05/1997, INCO Exploration, Sheridan Park, Missasaga, Ontario.

Jamison, W. and Calon, T.
1994: Structural Geology of the Ramah Disturbed Belt, Torngat Orogen, Labrador. ECSOOT Transect Meeting, Lithoprobe Report 45, pp. 90-108.

King, S.
1996-4: Partial reconstruction of the Deposit area of the Main Block using potential field geophysics. Internal report, Archean Resources, Geophysics Section

Korstgard, J., Ryan, B., and Wardle, R.

1987: The boundary between Proterozoic and Archean crustal blocks in central West Greenland and Northern Labrador. *In* Evolution of the Lewisian and Comparable High Grade Terrains. *Edited by* R.J. Park and J. Tarney. Geological Society of London, Special Publication No. 27, pp. 247-259.

Koyaguchi, T., and Blake, S.

1991: Origin of mafic enclaves: Constraints on the magma mixing model from fluid dynamic experiments. Enclaves and Granite Petrology, 13 Developments in Petrology. *Edited by* J. Didier and B. Barbarin, pp. 415-429.

Krogh, T.E., and Davis, G.L.

1973: The significance of inherited zircons on the age and origin of igneous rocks-an investigation of the ages of the Labrador adamellites: Carnegie Institute of Washington Yearbook 72, pp. 610-613.

Lambert, D.D., Foster, J.G., Frick, L.R., Li, C., and Naldrett, A.J.

1998: Re-Os isotopic systematics of the Voisey's Bay Ni-Cu-Co magmatic ore system, Labrador, Canada., Preprint of paper for special thematic issue of *LITHOS* "Geodynamics of Giant Magmatic Ore Systems", editors; D.D. Lambert and E.M. Ripley.

Lee, D.

Personal communication, Voisey's Bay Nickel Company, Field Exploration Office, Voisey's Bay, Labrador, May 1997.

Lee, D.

1987: Geothermometry and petrologic history of a contact metamorphosed section of the Tasiuyak gneiss, west of Nain, Labrador., B.Sc. thesis (Honors), Department of Earth Sciences, Memorial University of Newfoundland.

Lee, D., King, S., Evans-Lamswood, D., and Wheeler, R

1995: Second Year Assessment Report, Voisey's Bay Nickel Company Ltd., Voisey's Bay Deposit: Project No. 1100, Licence No. 657

Leshner, C.M.

1989: Komatiite-associated nickel sulphide deposits. *In* Ore Deposition Associated with Magmas. *Edited by* J.A. Whitney and A.J. Naldrett. Society of Economic Geologists, Reviews in Economic Geology, Vol. 4, pp. 43-62.

Leshner, C.M., Arndt, N.T., and Groves, D.I.

1984: Genesis of komatiite-associated nickel sulphide deposits at Kambalda, Western Australia: a distal volcanic model. *In* Sulphide Deposits in Mafic and Ultramafic Rocks. *Edited by* D.L. Buchana and M.J. Jones, Institute of Mining and Metallurgy, London, pp.70-80.

Li, C. and Naldrett, A.J.

1998: Geology and Olivine Stratigraphy of the Voisey's Bay Complex: Evidence for multiple Intrusion. Department of Geology, University of Toronto, Toronto, Ontario, Canada M5S 3B1. Preprint/unpublished distributed as a report to INCO Exploration. June 1998.

Li, C., and Naldrett, A.J.

1997: Voisey's Bay Research Project Progress Report. Dept. of Geology, University of Toronto

Lightfoot, P.

1998: Geological and geochemical Relationships in the Reid Brook Intrusive Complex, Labrador: Exploration Strategies for Magmatic Ni-Cu-Co Ores at Voisey's Bay., INCO, Field Exploration Office, Copper Cliff, Pathways '98.

Lightfoot, P.

1997a: Voisey's Bay: some observations on the sequence of events in the RBIC and the recognition of magmas that have equilibrated with sulphide. INCO, Field Exploration Office, Copper Cliff, Memorandum

Lightfoot, P.

1997b: Voisey's Bay: Exploration implications of Ni-Co variations in minerals, rocks and ores. INCO, Field Exploration Office, Copper Cliff, Memorandum

Maclean, W.H.

1969: Liquidus phase relationships in the FeS-FeO-Fe₃O₄-SiO₂ systems and their application in geology. *Economic Geology*, Vol. 64, pp. 865-884.

Maury, R., and Didier, J.

1991: Xenoliths and the role of assimilation. *Enclaves and Granite Petrology*, 13 *Developments in Petrology*, Edited by J.Didier and B.Barbarin., pp. 529-543.

McClay, K.R.

1987: The mapping of geological structures. *Geological Society of London Handbook*. Open University Press, Milton Keynes and Halsted Press, John Wiley and Sons, New York-Toronto.

Morse, S.A.

1983: p.15., *Science*, 220, pp. 193-195. *In Anorthositic, Granitoid and Related Rocks of the Nain Plutonic Suite*, IGCP #290-#315 Excursion-Nain Area, August 1994.

Morse, S.A., and Hamilton, M.A.

1990: The problem of unsupported Radiogenic Strontium in the Nain Anorthosites, Labrador. *in* Gower, C.F., Rivers, T., and Ryan, B., eds., *Mid-Proterozoic Laurentia-Baltica Geological Association of Canada, Special Paper 38*, pp. 373-385.

Naldrett, A.J.

1997: Key factors in the genesis of Noril'sk, Sudbury, Jinchuan, Voisey's Bay and other world class Ni-Cu-PGE deposits: implications for exploration. *Australian Journal of Earth Sciences*, Vol. 44, pp. 283-315.

Naldrett, A.J.

1989a: Introduction: Magmatic deposits associated with mafic rocks. *In Ore Deposition Associated with Magmas. Edited by J.A. Whiteney and A.J. Naldrett. Society of Economic Geologist, Reviews in Economic Geology Volume 4*, pp. 1-3.

Naldrett, A.J.

1989b: Sulphide melts: crystallization temperatures, solubilities in silicate melts, and Fe, Ni, and Cu partitioning between basaltic magmas and olivine. *In Ore Deposition Associated with Magmas. Edited by J.A. Whiteney and A.J. Naldrett. Society of Economic Geologist, Reviews in Economic Geology Volume 4*, pp. 5-20.

Naldrett, A.J.

1989c: Contamination and origin of the Sudbury structure and its ore. *In Ore Deposition Associated with Magmas. Edited by J.A. Whiteney and A.J. Naldrett. Society of Economic Geologist, Reviews in Economic Geology Volume 4*, pp. 119-134.

Naldrett, A.J.

1984a: Ni-Cu ores of the Sudbury Igneous Complex-Introduction. *In The Geology and Ore Deposits of the Sudbury Structure. Edited by E.G. Pye, A.J. Naldrett and P.E. Giblin. Ontario Geological Survey Special Volume 1*, pp.302-306.

Naldrett, A.J.

1984b: Summary, discussion and synthesis. *In The Geology and Ore Deposits of the Sudbury Structure. Edited by E.G. Pye, A.J. Naldrett and P.E. Giblin. Ontario Geological Survey Special Volume 1*, pp. 523-569.

Naldrett, A.J.

1981: Nickel sulphide deposits: Classification, composition and genesis. *Economic Geology 75th Anniversary Volume*, pp.628-685.

Naldrett, A.J.

1973: Nickel sulphide deposits-their classification and genesis with special emphasis on deposits of volcanic association. *Transactions of the Canadian Institute of Mining and Metallurgy*, Vol. 76, pp. 183-201.

Naldrett, A.J., and MacDonald, A.J

1980: Tectonic setting of Ni-Cu sulphide ores: their importance in genesis and exploration. *In The Continental Crust and Its Mineral Deposits. Edited by D.W. Strangway. Geological Association of Canada Special Paper 20*: pp. 633-657.

- Naldrett, A.J., and von Gruenewaldt, G.
1989: Association of platinum-group elements with chromite in layered intrusions and ophiolite complexes. *Economic Geology*, Vol. 84., pp. 180-187.
- Naldrett, A.J., Keats, H., Sparkes, K., and Moore, R.
1996: Geology of the Voisey's Bay Ni-Cu-Co Deposit, Labrador, Canada. *Exploration and Mining Geology*, Vol. 5, No. 2, pp.169-179.
- Naldrett, A.J., Singh, J., Krstic, S., and Li, C.
1998: The mineralogy of the Voisey's Bay Ni-Cu-Co deposit Northern Labrador, Canada: Influence of oxidation state on textures and mineral compositions. *Economic Geology* (work in progress).
- Naldrett, A.J., Federenko, V.A., Lightfoot, P.C., Kunilov, V.A., Gorbachev, N.S., Doherty, W., and Johan, Z.
1995: Ni-Cu-PGE deposits of the Noril'sk region, Siberia: Their formation as conduits for flood basalt volcanism. *Institute of Mining and Metallurgy Transactions*, Vol. 104, pp. B18-B36.
- Nicolas, A. and Ildefonse, B.
1996: Flow mechanics and viscosity in basaltic magma chambers. *Geophysical Research Letters*, Vol. 23, No. 16, pp. 2013-2016.
- Olsen, Peter
1990: Hot spots, swells and mantle plumes. *In Magma Transport and Storage, Edited by M.P. Ryan*, John Wiley and Sons Ltd., pp. 33-51.
- Papunen, H.
1996: Ni-Cu Deposits in Intrusive Mafic Rocks-A Review. Nickel '96, The Australasian Institute of Mining and Metallurgy, Publication Series No. 6/96, Published by The Australasian Institute of Mining and Metallurgy, Carlton Victoria Australia, pp. 123-127.
- Papunen, H. and Penttila, V.
1996: Mineralogy and Geology of the serpentinite associated Hitura Ni-Cu Deposit, Finland, Nickel '96, The Australasian Institute of Mining and Metallurgy, Publication Series No. 6/96, Published by The Australasian Institute of Mining and Metallurgy, Carlton Victoria Australia, pp. 79-88.
- Peredery, W.V., and geological staff
1982: Geology and nickel sulphide deposits of Thompson belt, Manitoba. *In Precambrian sulphide deposits*, H.S. Robinson Memorial Volume, *Edited by R.W. Hutchinson*, C.D. Spence, and J.M. Franklin. Geological Association of Canada, Special Paper 25, pp. 165-209.

Rajanani, V., and Naldrett, A.J.

1978: Partitioning of Fe, Co, Ni, and Cu between sulphide liquid and basaltic melts and the composition of Ni-Cu sulphide deposits. *Economic Geology*, Vol. 73, pp. 82-93.

Riley, G., and Kohlstedt, D.

1990: An experimental study of melt migration in an olivine-melt system.

Magma Transport and Storage. Edited by M.P. Ryan, John Wiley and Sons Ltd., pp. 77-86.

Ripley, E.M., Park, Y.R., Li, C., and Naldrett, A.J.

1998: Sulphur and oxygen isotope evidence of country rock contamination in the Voisey's Bay Ni-Cu-Co deposit, Labrador, Canada, Preprint of paper for special thematic issue of *LITHOS* "Geodynamics of Giant Magmatic Ore Systems".

Rivers, T.

1995: Lithotectonic elements of the Grenville Province: A review. Ecsoot Transect Meeting, LITHOPROBE Report 45, pp. 159-199.

Rivers, T. and Mengel, F.

1994: A Cross-Section of the Abloviak Shear Zone at Saglek Fiord, and a preliminary tectonic model for Torngat Orogen. In Eastern Canadian Shield On-Shore-Offshore Transect (ECSOOT), Report of Transect Meeting (December 10-11, 1993). Edited by R.J. Wardle and J. Hall. University of British Columbia, LITHOPROBE Secretariat, Report 36, pp.171-184.

Rousell, D.H., Gibson, H. L., and Jonasson, I.R.

1997: The tectonic, magmatic and mineralization history of the Sudbury structure., *Exploration Mining Geology*, Vol. 6, No. 1, pp. 1-22.

Ryan, B.

1996: Commentary on the location of the Nain-Churchill boundary in the Nain Area. Current Research, Newfoundland Department of Natural Resources, Geological Survey, Report 96-1, pp. 109-129.

Ryan, A.B.

1995: Lithotectonic elements of the Grenville Province: A review. ECSOOT Transect Meeting, Lithoprobe Report 45, pp. 159-199.

Ryan, A.B.

1994: Regional Geological Setting of the Nain Plutonic Suite. Anorthositic, Granitoid and Related Rocks of the Nain Plutonic Suite., International Geological Correlation Programme, Projects #290 and #315, pp. 2-5.

Ryan, A.B.

1991: p.14. , Science. 51:pp.193-225. *In* Anorthositic, Granitoid and Related Rocks of the Nain Plutonic Suite, IGCP #290-#315 Excursion-Nain Area, August 1994.

Ryan, A.B.

1984: Regional geology of the central part of the Central Mineral Belt, Labrador. Newfoundland Department of Mines and Energy, Memoir 3, 1985 p.

Ryan, A.B. and Lee, D.

1986: p. 11. Newfoundland department of Mines and Energy, Mineral development Division, Report 86-1, pp.79-88. *In* Anorthositic, Granitoid and Related Rocks of the Nain Plutonic Suite, IGCP #290-#315 Excursion-Nain Area, August 1994.

Ryan, A.B., and Lee, D.

1985: Geological Map of the Reid Brook Area, Labrador North District (NTS 14D/8). Government of Newfoundland Department of Natural Resources, Geological Survey Branch, Map 89-18, Open File 014D/08/0037, scale 1:50 000.

Ryan, B., Wardle, R.J., Gower, C.F. and Nunn, G.A.G.

1995: Nickel-Copper sulphide mineralization in Labrador: The Voisey's Bay Discovery and its Exploration Implications. Current Research, Report 95-1, Geological Survey, Department of Natural Resources, Government of Newfoundland and Labrador, pp. 177-204.

Scarfe, C., Mysen, B., and Virgo, D.

1987: Pressure dependence of the viscosity of silicate melts. *Magmatic Processes: Physiochemical Principles*, The Geochemical Society, Special Publication, No. 1, *Edited* by B. Mysen, pp. 59-67.

Shedden, S.H. and Barnes, G.J.

1996: East Kimberley nickel province-characteristics and Origin of the Sally Malay Ni-Cu-Co deposit, East Kimberley, Western Australia., Nickel '96, The Australasian Institute of Mining and Metallurgy, Publication Series No. 6/96, Published by The Australasian Institute of Mining and Metallurgy, Carlton Victoria Australia, pp. 145-154.

Spence, D., and Turcotte, D.

1990: Buoyancy-driven magma fracture: A mechanism for ascent through the Lithosphere and the emplacement of diamonds. *Journal of Geophysical Research*, Vol. 95, pp. 5133-5139.

Streckeisen, A.

1976: To each plutonic rock its proper name. *Earth Science review*, Vol. 12, pp. 1-33.

Synder, D., Crambes, C., Tait, S., and Wiebe, R.

1997: Magma Mingling in Dykes and Sills. *The Journal of Geology*, Vol. 105, pp. 75-86.

Theriault, Robert D. and Barnes, Sarah-Jane

1998: Speculations on the origin of Proterozoic anorthosite and associated Ni-bearing troctolitic rocks of northeastern America: Traces of a Voisey's Bay-Adirondack mantle plume? Department des sciences Appliquees, Universite du Quebec a Chicoutimi, Chicoutimi, Qc G7H 2B1, rtheriau@uquebec.ca.'

Turcotte, D.

1990: On the role of laminar and turbulent flow in buoyancy driven magma fractures. *Magma Transport and Storage. Edited by M.P. Ryan, John Wiley and Sons Ltd.*, pp. 103-111.

Turcotte, D.

1987: Physics of magma segregation processes. *Magmatic Processes: Physiochemical Principles*, The Geochemical Society, Special Publication, No. 1, *Edited by B. Mysen*, pp. 69-74.

Upton, B.G.J.

1974: The alkaline province of southwest Greenland, in Sørensen, H., ed., *The Alkaline Rocks*: John Wiley and Sons, London, pp. 221-238.

Wardle, R.J. and Wilton, D.H.C.

1995: The geology and mineral deposits of Labrador: A guide for the exploration geologist. CERR/NDNR Report, pp. 232.

Wardle, R.J., Ryan, B. and Ermnovics, I.

1990: Geoscience Canada, 17: 217-221. *In Anorthositic, Granitoid and Related Rocks of the Nain Plutonic Suite*, IGCP #290-#315 Excursion-Nain Area, August 1994. pp.3.

Wardle, R.J., Swinden, S., and James, D.T.

1995: The southeast Churchill Province. *In Labrador '95: The geology and mineral deposits of Labrador: A guide for the exploration geologist*. CERR/NDNR Report, p.p. 26-35.

Warren, R.G. and Ellis, D., J.

1996: Mantle underplating, granite tectonics, and metamorphic P-T-t paths. *Geology*, v. 24, no. 7, pp.663-666.

Whitehead, J., and Helfrich, K.

1990: Magma waves and diapiric dynamics. *Magma Transport and Storage. Edited by M.P. Ryan, John Wiley and Sons Ltd.*, pp.53-76.

Wiebe, R.A.

1985: Proterozoic basalt dikes in the Nain anorthosite complex, Labrador: *Canadian Journal of Earth Sciences*, v. 22, pp.1149-1157.

Wilton, D.H.C.

1996: Metallogenic overview of the Nain Province, northern Labrador.. CIM Bulletin, Vol. 89, pp. 43-52.

Xue, S. and Morse, S.A.

1993: p.11 *Geochim. Cosmochim. Acta*, 57: 3935-3948. *In* Anorthositic, Granitoid and Related Rocks of the Nain Plutonic Suite, IGCP #290-#315 Excursion-Nain Area, August 1994.

Zongli, Tang

1993: *Genetic model of the Jinchuan nickel-copper deposit.*, *in* Kirkham, R.V., Sinclair, W.D., Thorpe, R.I., and Duke, J.M., eds., *Mineral Deposit Modelling: Geological Association of Canada, Special Paper 40*, pp. 389-401.

APPENDIX A:
Quick Logs and Boris Logs

Abbreviation Legends Used For Quick Logs.

CELL #1	
Rxn name	
LT	LEUCOTROCTOLITE
TR	TROCTOLITE
MT	MELATROCTOLITE
LQ	LEUCOGABBRO
OQ	OLIVINE GABBRO
MQ	MELAGABBRO
GR	GABBRO
UM	ULTRAMAFIC
FG	FERROGABBRO/DIORITE
PQ	PARAGNEISS
ON	ORTHOGNEISS
ST	STENITE
GR	GRANITE
MM	Migmatite
OB	OVERBURDEN
MP	MAFIC DYKE
QV	QUARTZ VEIN
QF	QUARTZ FELDSPATHIC VEIN
MR	MASSIVE SULPHIDES
SM	SEMI-MASSIVE SULPHIDES
ST	STRUCTURAL

CELL #2	
%mineralization	
00	BARREN
01	TR-5%
05	5-10%
10	10-15%
15	15-20%
20	20-25%
25	25-30%
30	30-35%
35	35-40%
40	40-45%
45	45-50%
50	50-55%
55	55-60%
60	60-65%
65	65-70%
70	70-75%
75	75-80%
80	80-85%
85	85-90%
90	90-95%
95	95-100%

CELL #3	
amt. Frag	
X	N/A
F	FRAGMENT FREE
R	FRAGMENT RICH (>10%)
P	FRAGMENT POOR (<10%)

CELL #4	
FRAGMENT TYPES	
X	N/A
U	ULTRAMAFIC
F	FERROGABBRO/DIORITE
T	TROCTOLITE
B	SILICATE RICH (INCLUSION)
A	APHRIC & NOT IDENTIFIABLE
P	PARAGNEISS
O	ORTHOGNEISS

CELL #5	
ASPECT RATIOS	
XX	N/A
Q1	ASPECT RATIO (< or =) 2:1
Q2	ASPECT RATIO (< or =) 3:1
Q3	ASPECT RATIO (< or =) 4:1
10	ASPECT RATIO (< or =) 10:1
11	ASPECT RATIO > 10:1

CELL #6	
GRAIN SIZE	
F	FINE GRAINED
M	MEDIUM GRAINED
O	COARSE GRAINED
P	PEGMATOIDAL

CELL #7	
SILICATE TEXTURES	
N	NORMAL
V	VARIABLE
C	CHILLED
L	LAYERED
S	STELLATE

CELL #8A	
UNUSUAL MINERALOGY	
X	N/A
B	BIOTITE
I	ILMENITE
M	MAGNETITE
P	GRAPHITE
G	GARNET
H	HEMATITE
C	CHLORITE
S	SERPENTINE
Q	QUARTZ
T	TALC

CELL #8B	
MODAL % for 8A	
XX	N/A
01	TR-5%
05	5-10%
10	10-15%
15	15-20%
20	20-25%
25	25-30%
30	30-35%
35	35-40%
40	40-45%
45	45-50%
50	50-55%
55	55-60%
60	60-65%
65	65-70%
70	70-75%
75	75-80%
80	80-85%
85	85-90%
90	90-95%
95	95-100%

CELL #9A	
ALTERATION	
X	N/A
I	INTENSE
M	MODERATE
T	TRACED (TRACE)

CELL #9B	
ALTERATION HOST	
X	N/A
S	SHEAR
F	FRACTURE
V	VENNING
P	PERVASIVE

CELL #10	
ORE TEXTURE	
X	N/A
L	LEOPARD
D	DISSEMINATED
B	BERRY
N	NET
V	VEINED
M	MASSIVE
F	FRAG. LADEN MASSIVE

CELL #11	
EXTRAS	
X	N/A
1	HIGHLY FRACTURED ZONE
2	BROKEN CORE
3	LOST CORE
4	COQUE
5	FAULT
6	MYLONITE
7	SUB-MYLONITE
8	BRECCIATED
9	MIXED/CONTAMINATED

An Example of the Revised (Lightfoot, P., Farrow, C., and Evans-
Lamswood, D.) Quick Logs: VB-98-433c.

Point Number	VB-98-4330
UTM Northing	644933.00
UTM Easting	622746.66
UTM Zone	68N
UTM Datum	WGS 84
UTM Spheroid	WGS 84
UTM Projection	UTM
UTM Units	Meters
UTM Datum	WGS 84
UTM Spheroid	WGS 84
UTM Projection	UTM
UTM Units	Meters

VB-98-4330
 WGS 84 (WGS84) from VB-98-4330
 Preliminary UTM Coordinates:

VB-98-4330
 WGS 84 (WGS84) from VB-98-4330
 Preliminary UTM Coordinates:

UTM Northing	644933.00
UTM Easting	622746.66
UTM Zone	68N
UTM Datum	WGS 84
UTM Spheroid	WGS 84
UTM Projection	UTM
UTM Units	Meters
UTM Datum	WGS 84
UTM Spheroid	WGS 84
UTM Projection	UTM
UTM Units	Meters

UTM Northing	644933.00
UTM Easting	622746.66
UTM Zone	68N
UTM Datum	WGS 84
UTM Spheroid	WGS 84
UTM Projection	UTM
UTM Units	Meters
UTM Datum	WGS 84
UTM Spheroid	WGS 84
UTM Projection	UTM
UTM Units	Meters

UTM Northing	644933.00
UTM Easting	622746.66
UTM Zone	68N
UTM Datum	WGS 84
UTM Spheroid	WGS 84
UTM Projection	UTM
UTM Units	Meters
UTM Datum	WGS 84
UTM Spheroid	WGS 84
UTM Projection	UTM
UTM Units	Meters

**An Example of the Early Version of Quick Logs:
VB-95-106.**

VB-95-106

Hole Number	VB-95-106
E/W coordinates	5+00 E
N/S coordinates	0+75 N
Elevation	5167.168
Drilling Angle	-70
Azimuth	175
Commenced Drilling	May 21/95
Set Casing	May 21/95
Ceased drilling	May 24/95
Total Depth (EOH)	311.5

UTM Coordinates
554946.580 / 6243500.720

TROPARI TESTS		
Depth	Dip	Corr. Azimuth
127.10	-68	184
218.50	-68	172
310.00	-66	303

TROPARI TESTS		
Depth	Dip	Corr. Azimuth

Rig #

From (m)	To (m)	Interval	Rock Code	Description of Core	Comments
0.00	4.50	4.50	OB	Overburden	
4.50	113.40	108.90	GN	Gneiss	
113.40	155.40	42.00	TR	Troctolite(trace sulphides-Qz veining)	
155.40	156.50	1.10	TR	Troctolite(5% Diss. Sulphides)	top
156.50	159.40	2.90	TR	Troctolite(15-20% Diss. Sulphides)	
159.40	167.20	7.80	TR	Troctolite(50% Diss. Sulphides)	
167.20	178.00	10.80	TR	Troctolite(Trace Sulphides)	minor pegmatites
178.00	185.20	7.20	TR	Troctolite(35-50% Diss. Sulphides)	
185.20	189.60	4.40	TR	Troctolite(25-30% Diss. Sulphides)	
189.60	193.60	4.00	PG	Pegmatite	
193.60	242.80	49.20	TR	Troctolite(60-75% Diss. Sulphides)	
242.80	244.40	1.60	MS	Massive Sulphide	
244.40	245.10	0.70	TR	Troctolite(5% Diss. Sulphides)	serpentinized
245.10	246.30	1.20	TR	Troctolite(50% Diss. Sulphides)	
246.30	246.70	0.40	MS	Massive Sulphide	
246.70	247.20	0.50	TR	Troctolite(Trace Sulphides)	serpentinized
247.20	247.70	0.50	MS	Massive Sulphide	
247.70	251.30	3.60	TR	Troctolite(75% Diss. Sulphides)	
251.30	258.80	7.50	TR	Troctolite(5% Diss. & Semi-Massive)	serpentinized/sheared
258.80	263.10	4.30	GN	Gneiss(1% Veined Sulphides)	
263.10	268.40	5.30	AD	Aphyric Dyke	
268.40	281.50	13.10	GN	Gneiss	
281.50	281.80	0.30	QZ	Quartz Vein	sheared
281.80	293.60	11.80	AD	Aphyric Dyke	sheared
293.60	295.60	2.00	QZ	Quartz Vein	sheared
295.60	311.50	15.90	GN	Gneiss	
311.50		-311.50		END OF HOLE	
0.00		0.00			
0.00		0.00			
0.00		0.00			
0.00		0.00			

Rock Codes Used for Boris Logs.

```

// BorIS for Windows
// Voisey's Bay Custom Rock Dictionary   October 1997
// Edits made to sulphide percentages on June 24, 1998 by RW
// File Format:
// 1-10 character abbreviation, 1-30 character definition
//*****
//
AD  , aphyric dike
AMPH , amphibole
AMPHT , amphibolite
AN  , anorthosite
ANGB , anorthositic gabbro
ANNR , anorthositic norite
ASP  , arsenopyrite
BBS  , bottom breccia sequence
BBS1 , basal breccia sequence - barren
BBS2 , basal breccia sequence Tr-5% sulphides
BBS3 , basal breccia sequence 5-15% sulphides
BBS4 , basal breccia sequence 15-40% sulphides
BBS5 , basal breccia sequence 40-75% sulphides
BC   , broken core
BDRK , bedrock
BLDR , boulder
BX   , breccia
BX1  , breccia barren
BX2  , breccia Tr-5%
BX3  , breccia 5-15%
BX4  , breccia 15-40%
BX5  , breccia 40-75%
CAS  , casing
CLAY , clay
CLSD , clastic sediment
CORE , core
CP   , chalcopyrite
CPXT , clinopyroxenite
CRAG , clast rich agglomerate
CRDT , cordierite
CT   , contact
CT1  , chilled troctolite - barren
CT2  , chilled troctolite Tr-5% sulphides
CT3  , chilled troctolite 5-15% sulphides
CTCL , cataclasite
CUM  , cumulate
DIA  , diabase
DIKE , dike
DNT  , dunite
ECGL , eclogite
ENGN , enderbitic gneiss
EXT  , extensive

```

FCIN , felsic intrusive
 FDIOR , ferrodiorite
 FEGB , ferrogabbro
 FGB1 , ferrogabbro - barren
 FGB2 , ferrogabbro Tr-5% sulphides
 FGB3 , ferrogabbro 5-15% sulphides
 FGB4 , ferrogabbro 15-40% sulphides
 FGB5 , ferrogabbro 40-75% sulphides
 FLDK , felsic dike
 FLOW , flow
 FLT , fault
 FM1 , feeder melange - barren
 FM2 , feeder melange Tr-5% sulphides
 FM3 , feeder melange 5-15% sulphides
 FM4 , feeder melange 15-40% sulphides
 FM5 , feeder melange 40-75% sulphides
 G , gneiss
 GB , gabbro
 GBAN , gabbroic anorthosite
 GBNR , gabbro norite
 GN , galena
 GOSS , gossan
 GOUG , gouge
 GPGN , garnetiferous paragneiss
 GR , granite
 GRAV , gravel
 GRDR , granodiorite
 GRGN , granite gneiss
 GRNL , granulite
 GRPT , graphite
 GRSC , graphitic schist
 GRTD , granitoid
 GWKE , graywacke
 HARZ , harzburgite
 HEM , hematite
 HFZ , highly fractured zone
 ILMT , ilmenite
 INMD , intermediate dike
 INMI , intermediate intrusive
 INTR , intrusive
 LBX1 , leopard-textured breccia - barren
 LBX2 , leopard-textured breccia Tr-5% sulphides
 LBX3 , leopard-textured breccia 5-15% sulphides
 LBX4 , leopard-textured breccia 15-40% sulphides
 LBX5 , leopard-textured breccia 40-75% sulphides
 LC , lost core
 LCGB , leucogabbro
 LCGN , leucogabbro norite
 LCTR , leucotroctolite

LHER , ilherzolite
 LTT1 , leopard texture troctolite - barren
 LTT2 , leopard texture troctolite Tr-5% sulphides
 LTT3 , leopard texture troctolite 5-15% sulphides
 LTT4 , leopard texture troctolite 15-40% sulphides
 LTT5 , leopard texture troctolite 40-75% sulphides
 MASU , massive sulfide
 MFDK , mafic dike
 MFI , mafic intrusive
 MGMT , migmatite
 MGT1 , marginal troctolite - barren
 MGT2 , marginal troctolite Tr-5% sulphides
 MGT3 , marginal troctolite 5-15% sulphides
 MGT4 , marginal troctolite 15-40% sulphides
 MGT5 , marginal troctolite 40-75% sulphides
 MLGB , melagabbro
 MLGN , melagabbronorite
 MLNR , melanorite
 MLTR , melatroctolite
 MONZ , monzonite
 MT , magnetite
 MTSD , metasediment
 MYKT , myrmekite
 MYL , mylonite
 MZ , mixed zone
 MZD , monzodiorite
 MZGB , monzogabbro
 NR , norite
 NRGB , noritic gabbro
 NT , normal troctolite
 NT1 , normal troctolite - barren
 NT2 , normal troctolite Tr-5% sulphides
 NT3 , normal troctolite 5-15% sulphides
 NT4 , normal troctolite 15-40% sulphides
 NT5 , normal troctolite 40-75% sulphides
 OB , overburden
 OBX1 , original fragmental breccia - barren
 OBX2 , original fragmental breccia Tr-5% sulphides
 OBX3 , original fragmental breccia 5-15% sulphides
 OBX4 , original fragmental breccia 15-40% sulphides
 OBX5 , original fragmental breccia 40-75% sulphides
 OGB1 , olivine gabbro - barren
 OGB2 , olivine gabbro Tr-5% sulphides
 OGB3 , olivine gabbro 5-15% sulphides
 OGB4 , olivine gabbro 15-40% sulphides
 OGB5 , olivine gabbro 40-75% sulphides
 OLGB , olivine gabbro
 OLNR , olivine norite
 OPXT , orthopyroxenite

ORGN , orthogneiss
 PEG , pegmatite
 PO , pyrrhotite
 PRDT , peridotite
 PRGN , paragneiss
 PXT , pyroxenite
 PY , pyrite
 QPGN , quartzo-feldspathic paragneiss
 QTZ , quartz
 QTZT , quartzite
 QV , quartz vein
 QZDK , quartzofeldspathic dike
 QZVN , quartzofeldspathic vein
 RK , rock
 RPGR , rapakivi granite
 SCH , schist
 SED , sediment
 SERP , serpentine
 SHR , shear
 SLMN , sillimanite
 SMAS , semi-massive sulfide
 SP , sphalerite
 SPFX , spinifex textured flow
 SPPD , serpentized peridotite
 SRPT , serpentinite
 STRC , structure
 SULF , sulfide
 SYNT , syenite
 TBX , tectonic Breccias
 TBX1 , troctolite breccia - barren
 TBX2 , troctolite breccia Tr-5% sulphides
 TBX3 , troctolite breccia 5-15% sulphides
 TBX4 , troctolite breccia 15-40% sulphides
 TBX5 , troctolite breccia 40-75% sulphides
 TGM1 , troctolite-gneiss melange - barren
 TGM2 , troctolite-gneiss melange Tr-5% sulphides
 TGM3 , troctolite-gneiss melange 5-15% sulphides
 TGM4 , troctolite-gneiss melange 15-40% sulphides
 TGM5 , troctolite-gneiss melange 40-75% sulphides
 TNLT , tonalite
 TR1 , troctolite - barren
 TR2 , troctolite Tr-5% sulphides
 TR3 , troctolite 5-15% sulphides
 TR4 , troctolite 15-40% sulphides
 TR5 , troctolite 40-75% sulphides
 TROC , troctolite
 TRT1 , transitional troctolite - barren
 TRT2 , transitional troctolite Tr-5% sulphides
 TRT3 , transitional troctolite 5-15% sulphides

TRT4 . transitional troctolite 15-40% sulphides
 TRT5 . transitional troctolite 40-75% sulphides
 UM . ultramafic
 UMIV . ultramafic intrusive
 VBX1 . vein breccia - barren
 VBX2 . vein breccia Tr-5% sulphides
 VBX3 . vein breccia 5-15% sulphides
 VBX4 . vein breccia 15-40% sulphides
 VBX5 . vein breccia 40-75% sulphides
 VN . vein
 VNG . veining
 VT . variable troctolite
 VT1 . variable troctolite - barren
 VT2 . variable troctolite Tr-5% sulphides
 VT3 . variable troctolite 5-15% sulphides
 VT4 . variable troctolite 15-40% sulphides
 VT5 . variable troctolite 40-75% sulphides
 -
 -

An Example (VB-95-018) of a Boris Log Which Includes: Lithology; and
Recorded Assays.

VB95018 **INCO Limited - Exploration Department** VB95018
Standard Log

Borehole	: VB95018	Project	: Voisey Bay
Northing	: 6243207.63	Property	: Diamond Field Block 1
Easting	: 555936.76	Township/County	:
Elevation	: 5080.60 m	Province/State	: Labrador
Hole length	: 198.70 m	Mine	:
		Country	: Canada
Setup name:		NTS/SECT.T.R.	: 14-D-8
No Assays		UTM Coordinates	:
		Date Started	:
Print Date:		Date Completed	:
06-Feb-1999 16:30		Logged By	: Dawn Evans-Lamswood
		Logging Started	:
		Logging Completed	:
		Drilled By	:
		Drill Type	:
		Core Size	: NQ
		Hole Size	:
		Left In Hole	:
		Section	:
		Level	:
		Heading	:
		Inclination	:
		Grid Name	:
		Baseline Azimuth	: 85
		Borehole Bearing	:
		Assayed For	:
		Attitude Test Method	:
		Measurement(M/F)	: M
		Claim #	:
		Anomaly #	:

Survey records

depth	azm	dip	depth	azm	dip
0.00	1.00	-90.00	197.00	1.00	-89.00

COMMENTS: Converted to BorISWin 21-Nov-1997 18:02:49
 GENERATED BY BORIS-VAX 18-JUN-1997 11:06:23.79
 ELEMENTSNI CU CO S FE
 UNITS: % % % % %

GENERATED BY BORIS-VAX 14-MAY-1997 12:54:22.67
 ELEMENTSSG NI CU CO S
 UNITS: GRN % % % %
 GENERATED BY BORIS-VAX 14-MAY-1997 10:11:54.48
 ELEMENTSSG NI CU CO S
 UNITS: GRN % % % %
 GENERATED BY BORIS-VAX 18-FEB-1997 16:38:44.88
 ELEMENTSNI CU CO S FE
 UNITS: % % % % %
 Expl Grid Coords 2+00S/15+00E
 ENG GRID COORDS ARE 5101.0E, 4797.0N

From m	To m	Description
0.00	19.40	OVERBURDEN
		Overburden.

19.40 57.00 MASSIVE SULFIDE

Massive sulphides; pentlandite found in crystal form as well tied up in net vein system in pyrrhotite, magnetite concentrations control general textures in the core; an increase in magnetite masks the net vein texture and gives the core an overall choppy / pitted appearance; down section, pentlandite appears to be weakly aligned; this is a primary settling effect, there is no evidence that this is a secondary structural event; chalcopyrite is associated with interstitial space between pentlandite crystals 19.43-34.0 - 45-50% pyrrhotite, 25-30% pentlandite, 20% chalcopyrite, and 5% magnetite; magnetite is in low abundance, is blebbish (anhedral to subhedral) and has a consistent size with an average of 1.5cm; 5 chalcopyrite has a strong signature consistently associated with pentlandite interstitial space, although it does spread from pentlandite zones into non pentlandite zones (starts off being constrained by pentlandite, but then spreads to surrounding regions; pentlandite is subhedral, in crystal form, and has an average size of 1.7cm ranging from 0.5-2.3cm, although it is fairly consistent in size; pentlandite has strong / intense net veining 34.0-45.0 - 45-50% pyrrhotite, 20-25% pentlandite, 20% chalcopyrite, and 10% magnetite; weak and gradual increase in magnetite content; magnetite is more inconsistent in shape, blebbish, has a strong embayed texture with more of a size variation (inconsistent at 0.1-1.75cm); chalcopyrite appearance is more consistent; chalcopyrite is still associated with pentlandite, but is not totally controlled by pentlandite crystals (i.e., pentlandite crystals with a small quantity of chalcopyrite or a few pentlandite crystals

From m	To m	Description
		and a lot of chalcopyrite diffusing out into non pentlandite interstitial space; pentlandite has strong to intense net veining, but it weakens slightly down section; pentlandite crystal form is euhedral to subhedral, and it has less intergrown boundaries; pentlandite is relatively equigranular (0.5-2.0cm, averaging 1.2cm) 45.0-54.0 - 40-45% pyrrhotite, 25% pentlandite, 15-20% chalcopyrite, and 15% magnetite; the core has taken on a more pitted / choppy appearance, probably due to increase in magnetite (pits are evidently plucked magnetite); there is a weak size variation in magnetite (0.1-0.5cm, averaging 0.15cm) which is anhedral / blebbish; chalcopyrite shows reduction in quantity; where present, chalcopyrite is associated with pentlandite, but not a ubiquitous pentlandite - chalcopyrite association; pentlandite (0.5-1.75cm, averaging 1.5cm) is subhedral; net veining is less prominent 54.0-57.0 - 45-50% pyrrhotite, 25% pentlandite, 15% chalcopyrite, and 10% magnetite; magnetite has a weak alignment parallel to the horizontal plane with a 3:1 length : width ratio where it is aligned (2.5cm average size); chalcopyrite is reduced, still associated with pentlandite (same as above); pentlandite (0.4-1.8cm in size) has a large size variation, frequent intergrown boundaries, strong net veining, and the crystal form is subhedral.

57.00 115.40 TROCTOLITE 15-40% SULPHIDES

Troctolite with semi-massive to disseminated sulphides (varies in abundance); zones of dark prismatic crystals (weak spinex texture) clinopyroxene? or possibly plagioclase, previous diamond drill hole suggests clinopyroxene; the troctolite is feldspar phyric and frequently has a spiney texture; semi-massive zones appear brecciated, probably a primary event as sulphides are being exhaled into basin 57.0-61.72 - 15-20% mineralization; pyrrhotite > pentlandite > chalcopyrite; disseminated to semi-massive in troctolite; no magnetite is present 61.72-76.0 - 5-10% mineralization; pyrrhotite > pentlandite > chalcopyrite; disseminated, but semi-massive appears to follow fractures; spinex texture is still apparent 62.3-63.0 - chloritic slip planes (at 45 degrees to core axis), slicken sides are approximately horizontal 68.7 - 1cm wide chlorite vein (approximately 85 degrees to core axis) 76.0-77.5 - trace to 1% mineralization, pentlandite > pyrrhotite 77.5-79.5 - 5-10% mineralization, pyrrhotite > pentlandite > chalcopyrite; semi-massive; appears to be infilling fracture zones (no consistent orientation) 79.5-81.3 - trace to 1-2% mineralization; pyrrhotite > pentlandite; disseminated; troctolite is strongly feldspar phyric 81.3-85.0 - 5-10% mineralization; pyrrhotite > pentlandite > chalcopyrite; disseminated to semi-massive; consistently oriented late infilled fractures 82.7-82.8 -

From m	To m	Description
		serpentinite / chlorite infilling fractures perpendicular to the wall; fractures are 1.5cm wide, and at 20 degrees to core axis 83.4-83.5 - incompetent, rubbly zone with chlorite along inconsistently oriented fracture surfaces 85.0-86.2 - 2-3% mineralization; pyrrhotite > pentlandite +/- chalcopyrite; disseminated; the troctolite is very fine grained 86.2-90.9 - 5% mineralization; pyrrhotite > pentlandite > chalcopyrite; disseminated to semi-massive 90.4-90.7 - chlorite and serpentinite slip planes (inconsistent orientations) 90.9-104.5 - 15-20% mineralization; pyrrhotite > pentlandite > chalcopyrite; disseminated to semi-massive; semi-massive sulphides appear to enclose brecciated fragments of troctolite 104.5-108.0 - approximately 10% mineralization; disseminated to semi-massive 108.0-109.85 - granitic plug; gradational contact with the troctolite, therefore it was probably caught up as the troctolite was emplaced (pegmatitic); trace to less than 1% chalcopyrite? 109.85-115.4 - pyrrhotite > pentlandite > chalcopyrite; semi-massive to disseminated (the troctolite has a strong brecciated appearance); sulphides are remobilized to infill around fragments 114.3 - chlorite gouge.

115.40 116.30 MASSIVE SULFIDE

Massive sulphides; 50% pyrrhotite, 30% pentlandite, 10% chalcopyrite, and 10% magnetite; pentlandite is subhedral to anhedral (1.0-2.0cm); magnetite is blebbish, less than 0.1cm; chalcopyrite is associated with pentlandite.

116.30 119.25 TROCTOLITE 15-40% SULPHIDES

Troctolite; fine grained; feldspar phyrlic; disseminated to semi-massive sulphides; weak foliation, possibly a result of late movement in pre-troctolite fault zone (old fault zone – passage way for expulsion of magma and sulphides 116.3-117.3 - 15% mineralization; pyrrhotite > pentlandite > chalcopyrite; streaky appearance defining a weak to moderate foliation at approximately 70 degrees to core axis 117.3-119.25 - less than or equal to 5% disseminated to semi-massive sulphides; pyrrhotite > pentlandite > chalcopyrite; very fine grained troctolite (locally very chloritic); semi-massive zone occurs in 117.3-117.8m zone (shear zone) 117.3-117.8 - chlorite - poor core recovery; rubbly.

119.25 135.60 MASSIVE SULFIDE

From m	To m	Description
		Massive sulphides 119.25-135.6 - 40-45% pyrrhotite, 25% pentlandite, 20% chalcopyrite, and 10-15% magnetite; contact is at 60 degrees to core axis (sheared fluidy contact, possibly graphite (hard?); pentlandite (1.8cm is approximate average) is euhedral to subhedral; magnetite (0.1-0.4cm) 130.0-135.0 - moderate to strong alignment of magnetite (approximately 10 degrees to core axis); magnetite increases to an average of 15%; pyrrhotite > pentlandite > chalcopyrite > magnetite

135.60 141.00 TROCTOLITE TR-5% SULPHIDES

Troctolite with disseminated sulphides; feldspar phyrlic 135.0-138.0 - approximately 75% core recovery – intense chloritization (broken / rubbly)
 135.6-138.3 - approximately 2% pyrrhotite > pentlandite > chalcopyrite; disseminated
 138.3-141.0 - 5-10% mineralization; pyrrhotite > pentlandite +/- chalcopyrite; disseminated; fine disseminated material appears to enclose mafic clasts.

141.00 149.90 GRANODIORITE

Granodiorite; melanocratic; medium grained; intense foliation 141.8 - granitic pegmatitic veins (3cm wide); upper contact with the troctolite is mixed (troctolite enclaves in granodiorite).

149.90 153.80 TROCTOLITE TR-5% SULPHIDES

Troctolite; fine grained (feldspar phyrlic); 1-2% sulphides; pyrrhotite +/- pentlandite +/- chalcopyrite, finely disseminated; the contact is interleaved (partial melting) enclaves of troctolite at the bottom of the granodiorite; subhorizontal chlorite slip planes.

153.80 198.70 GRANODIORITE

Granodiorite; melanocratic; medium grained; intense foliation to gneissosity.

VB95018 **INCO Limited - Exploration Department** VB95018
Assay Log

Borehole	: VB95018	Project	: Voisey Bay
Northing	: 6243207.63	Property	: Diamond Field Block 1
Easting	: 555936.76	Township/County	:
Elevation	: 5080.60 m	Province/State	: Labrador
Hole length	: 198.70 m	Mine	:
		Country	: Canada
Setup name:		NTS/SECT.T.R.	: 14-D-8
Assays		UTM Coordinates	:
		Date Started	:
Print Date:		Date Completed	:
06-Feb-1999 16:34		Logged By	: Dawn Evans-Lamswood
		Logging Started	:
		Logging Completed	:
		Drilled By	:
		Drill Type	:
		Core Size	: NQ
		Hole Size	:
		Left In Hole	:
		Section	:
		Level	:
		Heading	:
		Inclination	:
		Grid Name	:
		Baseline Azimuth	: 85
		Borehole Bearing	:
		Assayed For	:
		Attitude Test Method	:
		Measurement(M/F)	: M
		Claim #	:
		Anomaly #	:

Survey records

depth	azm	dip	depth	azm	dip
0.00	1.00	-90.00	197.00	1.00	-89.00

COMMENTS: Converted to BorlSWin 21-Nov-1997 18:02:49
 GENERATED BY BORIS-VAX 18-JUN-1997 11:06:23.79
 ELEMENTSNI CU CO S FE

VB95018

INCO Limited - Exploration Department

Assay Log

VB95018

UNITS: % % % % %
 GENERATED BY BORIS-VAX 14-MAY-1997 12:54:22.67
 ELEMENTSSG NI CU CO S
 UNITS: GRN % % % %
 GENERATED BY BORIS-VAX 14-MAY-1997 10:11:54.48
 ELEMENTSSG NI CU CO S
 UNITS: GRN % % % %
 GENERATED BY BORIS-VAX 18-FEB-1997 16:38:44.88
 ELEMENTSNI CU CO S FE
 UNITS: % % % % %
 Expl Grid Coords 2+00S/15+00E
 ENG GRID COORDS ARE 5101.0E, 4797.0N

From m	To m	Length m	Sample#	CO %	CU %
0.00	19.40	19.40	NS		
19.40	21.00	1.60	DF2773	0.2350	2.1400
21.00	22.00	1.00	DF2774	0.1770	0.6200
22.00	23.00	1.00	DF2775	0.2260	2.3200
23.00	24.00	1.00	DF2776	0.2550	3.0000
24.00	25.00	1.00	DF2777	0.2360	2.7400
25.00	26.00	1.00	DF2778	0.2350	1.7200
26.00	27.00	1.00	DF2779	0.2450	1.6400
27.00	28.00	1.00	DF2780	0.2840	2.4800
28.00	29.00	1.00	DF2781	0.2260	0.9000
29.00	30.00	1.00	DF2782	0.2250	2.0000
30.00	31.00	1.00	DF2783	0.1470	0.4800
31.00	32.00	1.00	DF2784	0.2040	4.8800
32.00	33.00	1.00	DF2785	0.2850	2.2200
33.00	34.00	1.00	DF2786	0.2250	2.7200
34.00	35.00	1.00	DF2787	0.2250	1.3000
35.00	36.00	1.00	DF2788	0.1840	4.7200
36.00	37.00	1.00	DF2789	0.1860	1.9600
37.00	38.00	1.00	DF2790	0.2350	1.1000
38.00	39.00	1.00	DF2791	0.2140	4.3200
39.00	40.00	1.00	DF2792	0.1950	2.3400
40.00	41.00	1.00	DF2793	0.1960	1.2400
41.00	42.00	1.00	DF2794	0.1860	2.0800

VB95018

Page 2

VB95018

VB95018

INCO Limited - Exploration Department

Assay Log

VB95018

From m	To m	Length m	Sample#	CO %	CU %
42.00	43.00	1.00	DF2795	0.2550	1.9800
43.00	44.00	1.00	DF2796	0.2360	1.7200
44.00	45.00	1.00	DF2797	0.1870	1.4200
45.00	46.00	1.00	DF2798	0.1660	1.3800
46.00	47.00	1.00	DF2799	0.1870	1.1400
47.00	48.00	1.00	DF2800	0.1960	1.0200
48.00	49.00	1.00	DF2801	0.1760	1.5600
49.00	50.00	1.00	DF2802	0.1760	1.9800
50.00	51.00	1.00	DF2803	0.2060	1.9400
51.00	52.00	1.00	DF2804	0.2070	1.8800
52.00	53.00	1.00	DF2805	0.1960	1.2400
53.00	54.00	1.00	DF2806	0.2250	2.7200
54.00	55.00	1.00	DF2807	0.2060	1.5200
55.00	56.00	1.00	DF2808	0.1770	1.1600
56.00	57.00	1.00	DF2809	0.2250	1.9800
57.00	58.00	1.00	DF2810	0.0780	0.7400
58.00	59.00	1.00	DF2811	0.0770	0.7000
59.00	60.00	1.00	DF2812	0.0530	0.4200
60.00	61.00	1.00	DF2813	0.0900	0.9000
61.00	62.00	1.00	DF2814	0.1210	0.8800
62.00	63.00	1.00	DF2815	0.0100	0.1800
63.00	64.00	1.00	DF2816	0.1120	0.9600
64.00	65.00	1.00	DF2817	0.0870	0.6200
65.00	66.00	1.00	DF2818	0.0530	0.3800
66.00	67.00	1.00	DF2819	0.0530	0.3600
67.00	68.00	1.00	DF2820	0.0420	0.3800
68.00	69.00	1.00	DF2821	0.0770	0.5600
69.00	70.00	1.00	DF2822	0.0280	0.2000
70.00	71.00	1.00	DF2823	0.0390	0.2800
71.00	72.00	1.00	DF2824	0.0420	0.4800
72.00	73.00	1.00	DF2825	0.0520	0.2600
73.00	74.00	1.00	DF2826	0.1000	0.9000
74.00	75.00	1.00	DF2827	0.0400	0.3200
75.00	76.00	1.00	DF2828	0.0300	0.3600
76.00	77.00	1.00	DF2829	0.0100	0.1000
77.00	78.00	1.00	DF2830	0.0280	0.4200

VB95018

Page 3

VB95018

VB95018 INCO Limited - Exploration Department VB95018
Assay Log

From m	To m	Length m	Sample#	CO %	CU %
78.00	79.00	1.00	DF2831	0.0640	0.5400
79.00	80.00	1.00	DF2832	0.0290	0.2200
80.00	81.00	1.00	DF2833	0.0100	0.0400
81.00	82.00	1.00	DF2834	0.0390	0.3200
82.00	83.00	1.00	DF2835	0.0280	0.2400
83.00	84.00	1.00	DF2836	0.0270	0.1600
84.00	85.00	1.00	DF2837	0.0450	0.6000
85.00	86.00	1.00	DF2838	0.0270	0.0600
86.00	87.00	1.00	DF2839	0.0390	0.2000
87.00	88.00	1.00	DF2840	0.0100	0.1200
88.00	89.00	1.00	DF2841	0.0280	0.2000
89.00	90.00	1.00	DF2842	0.0100	0.1200
90.00	91.00	1.00	DF2843	0.0520	0.5000
91.00	92.00	1.00	DF2844	0.0760	0.9200
92.00	93.00	1.00	DF2845	0.0530	0.6600
93.00	94.00	1.00	DF2846	0.0750	0.6800
94.00	95.00	1.00	DF2847	0.0530	0.6600
95.00	96.00	1.00	DF2848	0.0530	0.6000
96.00	97.00	1.00	DF2849	0.1090	1.1200
97.00	98.00	1.00	DF2850	0.0520	0.4800
98.00	99.00	1.00	DF2851	0.0850	0.6800
99.00	100.00	1.00	DF2852	0.0520	0.7000
100.00	101.00	1.00	DF2853	0.0850	0.6200
101.00	102.00	1.00	DF2854	0.0860	0.6200
102.00	103.00	1.00	DF2855	0.0420	0.4200
103.00	104.00	1.00	DF2856	0.0520	0.4200
104.00	105.00	1.00	DF2857	0.0400	0.3600
105.00	106.00	1.00	DF2858	0.0270	0.1800
106.00	107.00	1.00	DF2859	0.0280	0.2800
107.00	108.00	1.00	DF2860	0.0410	0.4000
108.00	109.00	1.00	DF2861	0.0100	0.1000
109.00	110.00	1.00	DF2862	0.0100	0.1000
110.00	111.00	1.00	DF2863	0.0740	0.5600
111.00	112.00	1.00	DF2864	0.0970	1.5000
112.00	113.00	1.00	DF2865	0.0770	0.7200
113.00	114.00	1.00	DF2866	0.0520	0.4400

VB95018

INCO Limited - Exploration Department

Assay Log

VB95018

From m	To m	Length m	Sample#	CO %	CU %
114.00	115.00	1.00	DF2867	0.0750	0.5400
115.00	116.00	1.00	DF2868	0.1610	0.5000
116.00	117.00	1.00	DF2869	0.1290	0.4800
117.00	118.00	1.00	DF2870	0.0500	0.6800
118.00	119.00	1.00	DF2871	0.0100	0.0400
119.00	120.00	1.00	DF2872	0.1300	0.5000
120.00	121.00	1.00	DF2873	0.1750	1.4600
121.00	122.00	1.00	DF2874	0.1560	1.0200
122.00	123.00	1.00	DF2875	0.1560	0.9400
123.00	124.00	1.00	DF2876	0.1950	1.3200
124.00	125.00	1.00	DF2877	0.1830	3.9400
125.00	126.00	1.00	DF2878	0.1870	1.4400
126.00	127.00	1.00	DF2879	0.1850	1.0600
127.00	128.00	1.00	DF2880	0.1950	2.0600
128.00	129.00	1.00	DF2881	0.2620	2.8600
129.00	130.00	1.00	DF2882	0.2330	3.4800
130.00	131.00	1.00	DF2883	0.1830	0.8800
131.00	132.00	1.00	DF2884	0.2030	1.6400
132.00	133.00	1.00	DF2885	0.2030	1.6200
133.00	134.00	1.00	DF2886	0.2130	2.4000
134.00	135.00	1.00	DF2887	0.1830	1.7800
135.00	136.00	1.00	DF2888	0.1230	0.8800
136.00	137.00	1.00	DF2889	0.0100	0.0200
137.00	138.00	1.00	DF5552	0.0100	0.0800
138.00	139.00	1.00	DF5553	0.0100	0.1200
139.00	140.00	1.00	DF5554	0.0280	0.1400
140.00	141.00	1.00	DF5555	0.0100	0.1000
141.00	142.00	1.00	DF18861	<0.0100	0.0400
142.00	143.00	1.00	DF18862	<0.0100	<0.0200
143.00	144.00	1.00	DF18863	<0.0100	<0.0200
144.00	145.00	1.00	DF18864	<0.0100	<0.0200
145.00	146.00	1.00	DF18865	<0.0100	<0.0200
146.00	147.00	1.00	DF18866	<0.0100	<0.0200
147.00	148.00	1.00	DF18867	<0.0100	<0.0200
148.00	149.00	1.00	DF18868	<0.0100	<0.0200
149.00	150.00	1.00	DF18869	<0.0100	<0.0200

VB95018

Page 5

VB95018

VB95018 **INCO Limited - Exploration Department** VB95018
Assay Log

From m	To m	Length m	Sample#	CO %	CU %
150.00	151.00	1.00	DF18870	<0.0100	<0.0200
151.00	152.00	1.00	DF18871	<0.0100	<0.0200
152.00	153.00	1.00	DF18872	<0.0100	<0.0200
153.00	154.00	1.00	DF18873	<0.0100	<0.0200
154.00	155.00	1.00	DF18874	<0.0100	<0.0200
155.00	156.00	1.00	DF18875	<0.0100	<0.0200
156.00	157.00	1.00	DF18876	<0.0100	<0.0200
157.00	158.00	1.00	DF18877	<0.0100	<0.0200
158.00	159.00	1.00	DF18878	<0.0100	0.0200
159.00	198.70	39.70	NS		

An Example (VB-95-186) of a Boris Log Which Includes: Lithology; and
Magnetic Susceptibility.

VB95186

INCO Limited - Exploration Department

Standard Log

VB95186

Borehole : VB95186
 Northing : 6243545.81
 Easting : 554452.84
 Elevation : 5135.15 m
 Hole length : 166.40 m

Setup name:
 No Assays

Print Date:
 06-Feb-1999 16:43

Project : Voisey Bay
 Property : Voisey Bay Main Grid
 Township/County : -
 Province/State : Labrador
 Mine : -
 Country : Canada
 NTS/SECT.T.R. : 14 D 08
 UTM Coordinates : -
 Date Started : -
 Date Completed : -
 Logged By : Dan Lee, Dawn Evans-Lamswood
 Logging Started : September 16, 1995
 Logging Completed : September 18, 1995
 Drilled By : Petro
 Drill Type : -
 Core Size : NQ
 Hole Size : -
 Left In Hole : -
 Section : 0+00
 Level : -
 Heading : -
 Inclination : -45
 Grid Name : Main Grid
 Baseline Azimuth : 085
 Borehole Bearing : 180
 Assayed For : Cu Ni Co S PMs
 Attitude Test Method : Tropani
 Measurement(M/F) : M
 Claim # : -
 Anomaly # : -

Survey records

depth	azm	dip	depth	azm	dip
0.00	175.00	-45.00	158.50	190.00	-45.00
86.00	182.00	-45.00			

COMMENTS:

Converted to BorISWin 21-Nov-1997 18:03:57
 GENERATED BY BORIS-VAX 18-JUN-1997 11:06:23.79
 ELEMENTSNI CU CO S FE

VB95186

Page 1

VB95186

VB95186

INCO Limited - Exploration Department Standard Log

VB95186

UNITS: % % % % %
 GENERATED BY BORIS-VAX 14-MAY-1997 12:54:22.67
 ELEMENTSSG NI CU CO S
 UNITS: GRN % % % %
 GENERATED BY BORIS-VAX 18-FEB-1997 16:38:44.88
 ELEMENTSNI CU CO S FE
 UNITS: % % % % %
 Expl Grid Coords 1+20N/0+00

From m	To m	Description
0.00	19.70	OVERBURDEN
		Overburden

19.70 28.70 PARAGNEISS

Well developed quartzofeldspathic paragneiss with abundant garnets.

20.00	Magnetic_Suscept	: 0.06
21.00	Magnetic_Suscept	: 0.05
22.00	Magnetic_Suscept	: 0.32
23.00	Magnetic_Suscept	: 0.12
24.00	Magnetic_Suscept	: 0.16
25.00	Magnetic_Suscept	: 0.17
26.00	Magnetic_Suscept	: 0.54
27.00	Magnetic_Suscept	: 0.69
28.00	Magnetic_Suscept	: 0.29

28.70 32.00 MAFIC DIKE

Fine grained mafic dyke contacts in broken core.

29.00	Magnetic_Suscept	: 0.27
30.00	Magnetic_Suscept	: 0.36
31.00	Magnetic_Suscept	: 0.40

32.00 40.10 PARAGNEISS

Garnetiferous paragneiss for most part quartzofeldspathic but screens of biotite rich layers do occur

VB95186

Page 2

VB95186

From m	To m	Description
32.00		Magnetic_Suscept : 0.55
33.00		Magnetic_Suscept : 0.75
34.00		Magnetic_Suscept : 0.14
35.00		Magnetic_Suscept : 0.47
36.00		Magnetic_Suscept : 0.84
37.00		Magnetic_Suscept : 0.33
38.00		Magnetic_Suscept : 0.13
39.00		Magnetic_Suscept : 0.22
40.00		Magnetic_Suscept : 0.48

40.10 41.40 GRANITE

Coarse earlier granitic dyke at 45° to c.a.

41.00 Magnetic_Suscept : 0.04

41.40 82.80 PARAGNEISS

Paragneiss as above 43.5-43.9 - coarse earlier granitic dyke with acicular mineral appears to be biotite 56.3-56.7 - quartzofeldspathic vein (intense sericitic alteration) 61.8-62.7 - quartzofeldspathic gneiss 62.7-82.1 - gametiferous paragneiss 67.6-67.9 - intense shear zone at 15° to c.a. (strike/slip), - paragneiss is mylonitized 68.5-72.2 - core blocky/rubblely not consistent enough to determine fracture orientation, fracture surfaces are chloritic = smeared trace sulphides 72.9-74.3 - lighter grey granular tuffaceous looking material. 82.1-82.8 - fine grained aphyric mafic dyke. Contacts are in broken core.

42.00	Magnetic_Suscept : 0.06
43.00	Magnetic_Suscept : 0.21
44.00	Magnetic_Suscept : 0.06
45.00	Magnetic_Suscept : 0.23
46.00	Magnetic_Suscept : 0.65
47.00	Magnetic_Suscept : 0.25
48.00	Magnetic_Suscept : 0.06
49.00	Magnetic_Suscept : 0.79
50.00	Magnetic_Suscept : 0.39
51.00	Magnetic_Suscept : 0.47
52.00	Magnetic_Suscept : 0.37
53.00	Magnetic_Suscept : 0.08

From m	To m	Description
54.00		Magnetic_Suscept : 0.31
55.00		Magnetic_Suscept : 0.17
56.00		Magnetic_Suscept : 0.26
57.00		Magnetic_Suscept : 0.21
58.00		Magnetic_Suscept : 0.39
59.00		Magnetic_Suscept : 0.22
60.00		Magnetic_Suscept : 0.20
61.00		Magnetic_Suscept : 0.35
62.00		Magnetic_Suscept : 0.19
63.00		Magnetic_Suscept : 0.02
64.00		Magnetic_Suscept : 0.14
65.00		Magnetic_Suscept : 0.06
66.00		Magnetic_Suscept : 0.10
67.00		Magnetic_Suscept : 0.06
68.00		Magnetic_Suscept : 0.96
69.00		Magnetic_Suscept : 1.80
70.00		Magnetic_Suscept : 0.55
71.00		Magnetic_Suscept : 1.24
72.00		Magnetic_Suscept : 1.55
73.00		Magnetic_Suscept : 0.30
74.00		Magnetic_Suscept : 0.74
75.00		Magnetic_Suscept : 1.39
76.00		Magnetic_Suscept : 0.79
77.00		Magnetic_Suscept : 0.63
78.00		Magnetic_Suscept : 0.11
79.00		Magnetic_Suscept : 0.13
80.00		Magnetic_Suscept : 0.18
81.00		Magnetic_Suscept : 0.43
82.00		Magnetic_Suscept : 0.06

82.80 84.10 PEGMATITE

Granitic pegmatite, very minor garnets, and local biotite looks

83.00	Magnetic_Suscept : 2.53
84.00	Magnetic_Suscept : 0.23

84.10 85.60 MASSIVE SULFIDE

From m	To m	Description
		Well developed massive sulphide with abundant chalcopyrite and magnetite droplets. Contact angles are sharp. Top contact at 40° to c.a. bottom contact at 65° to c.a.

85.00 Magnetic_Suscept : 105.00

85.60 93.10 PARAGNEISS

Garnetiferous paragneiss. Lower contact is relatively sharp against the troctolite with some weak shearing locally within the gneiss

86.00	Magnetic_Suscept : 2.19
87.00	Magnetic_Suscept : 0.16
88.00	Magnetic_Suscept : 0.47
89.00	Magnetic_Suscept : 0.05
90.00	Magnetic_Suscept : 0.13
91.00	Magnetic_Suscept : 0.59
92.00	Magnetic_Suscept : 0.32
93.00	Magnetic_Suscept : 1.05

93.10 113.70 TROCTOLITE TR-5% SULPHIDES

Troctolite 93.1-98.2 - lighter grey troctolite, no abrasive shearing along top contact. Possibly could be chilled - hard to say for sure. 93.1-94.5 - 1-2% sulphides 94.5-98.2 - well developed bottom sequence with abundant fragments, 5-8% blotchy sulphides and local dissemination. 98.2-(102.1) - traces of sulphide, troctolite very fine grained with thin chloritic veinlets at 30-35° to c.a. 102.1-104.3 - approximately 2-3% blotchy sulphides, granitic fragments present, local felsic contamination. 102.5-102.7 - chloritic fractures (20-25° to c.a.), oblique dip/slip 104.3-107.4 - 10-15% blotchy sulphides, frequent aphyric fragments 105.9- 106.0 - chloritic fracture at 15° to c.a. (oblique dip/slip) 107.4-109.7 - 5% blotchy sulphides, aphyric and granitic fragments 109.7-112.2 - 10-15% blotchy sulphides, aphyric and granitic fragments 112.2-112.7 - 5% finely disseminated to blotchy sulphides 112.2-112.3 - chloritic fracture at 20° to c.a. (oblique dip/slip to oblique strike slip) 112.2-112.8 - frequent fragments present and sulphides tend to be more blotchy than finely disseminated 112.8-no visible fragments, sulphides finely disseminated (rare blotchy sulphides).

94.00	Magnetic_Suscept : 1.73
95.00	Magnetic_Suscept : 3.16

From m	To m	Description
96.00		Magnetic_Suscept : 2.33
97.00		Magnetic_Suscept : 1.32
98.00		Magnetic_Suscept : 6.49
99.00		Magnetic_Suscept : 7.33
100.00		Magnetic_Suscept : 0.90
101.00		Magnetic_Suscept : 5.43
102.00		Magnetic_Suscept : 7.11
103.00		Magnetic_Suscept : 7.41
104.00		Magnetic_Suscept : 12.50
105.00		Magnetic_Suscept : 4.52
106.00		Magnetic_Suscept : 3.52
107.00		Magnetic_Suscept : 6.23
108.00		Magnetic_Suscept : 1.23
109.00		Magnetic_Suscept : 2.00
110.00		Magnetic_Suscept : 5.56
111.00		Magnetic_Suscept : 10.70
112.00		Magnetic_Suscept : 4.09
113.00		Magnetic_Suscept : 1.77

113.70 116.50 TROCTOLITE 15-40% SULPHIDES

113.70 114.30 - 25-30% disseminated to blotchy sulphides 114.3-115.4 - 60% disseminated sulphides, aphyric fragments present, - local felsic contamination
115.4-116.5 - 75% semi-massive sulphides, felsic contamination, - cpy only associated = felsic material.

114.00	Magnetic_Suscept : 3.40
115.00	Magnetic_Suscept : 8.46
116.00	Magnetic_Suscept : 0.87

116.50 117.20 PARAGNEISS

Paragneiss 40% semi-massive sulphides veins in paragneiss and quartzofeldspathic gneiss, -- veins parallel to paragneiss fabric (45-50° to c.a.)

117.00	Magnetic_Suscept : 0.11
--------	-------------------------

117.20 166.40 PARAGNEISS

Paragneiss, locally gametiferous. 117.2-118.0 - 1-2% veined (stringers)

From m	To m	Description
		<p>sulphides, sulphides also concentrated along foliation 118.0-120.8 - paragneiss with abundant biotite. Core moderately broken, traces of sulphide 120.8-126.5 - zone of garnetiferous paragneiss with strongly broken core and local fault gouge. Gouge from 120.8-120.9. Abundant fractures at 20-30° to c.a. with oblique strike slip movement indicated especially ~ 124.1. Gouge again from 124.9-125.0, 126.2-126.3 at 55° to c.a. Traces of sulphides 129.2-136.8 - trace - 1% sulphides (po+cpy+py) pn?, - sulphides concentrated along schistosity or coarse/blotchy disseminated in less foliated zones. 130.8-131.0 - fault gouge 133.2-136.8 - fine grained tuff coarse looking material granular with abundant quartz grains. 149.7-150.0 - fault gouge, paragneiss brecciated in a siliceous matrix (at 10° to c.a.) 157.5-157.8 - trace - 1% sulphides concentrated along fabric 157.8-166.4 - well developed garnetiferous paragneiss with abundant graphite locally. The garnets are strongly fractured and for the most part are not altered. EOH @ 166.4M.</p>
118.00		Magnetic_Suscept : -0.20
119.00		Magnetic_Suscept : -0.27
120.00		Magnetic_Suscept : 0.01
121.00		Magnetic_Suscept : 0.26
122.00		Magnetic_Suscept : 0.87
123.00		Magnetic_Suscept : 0.52
124.00		Magnetic_Suscept : 0.02
125.00		Magnetic_Suscept : 0.50
126.00		Magnetic_Suscept : 0.08
127.00		Magnetic_Suscept : 0.26
128.00		Magnetic_Suscept : 0.14
129.00		Magnetic_Suscept : 0.30
130.00		Magnetic_Suscept : 1.58
131.00		Magnetic_Suscept : 1.26
132.00		Magnetic_Suscept : 3.49
133.00		Magnetic_Suscept : 2.75
134.00		Magnetic_Suscept : 2.67
135.00		Magnetic_Suscept : 4.50
136.00		Magnetic_Suscept : 0.52
137.00		Magnetic_Suscept : 3.11
138.00		Magnetic_Suscept : 0.44
139.00		Magnetic_Suscept : 0.93
140.00		Magnetic_Suscept : 7.81

VB95186

**INCO Limited - Exploration Department
Standard Log**

VB95186

From m	To m	Description
141.00		Magnetic_Suscept : 0.25
142.00		Magnetic_Suscept : 4.79
143.00		Magnetic_Suscept : 2.75
144.00		Magnetic_Suscept : 1.38
145.00		Magnetic_Suscept : 0.28
146.00		Magnetic_Suscept : 0.40
147.00		Magnetic_Suscept : 0.17
148.00		Magnetic_Suscept : 0.82
149.00		Magnetic_Suscept : 0.20
150.00		Magnetic_Suscept : 0.57
151.00		Magnetic_Suscept : 0.24
152.00		Magnetic_Suscept : 0.47
153.00		Magnetic_Suscept : 0.16
154.00		Magnetic_Suscept : 0.21
155.00		Magnetic_Suscept : 0.08
156.00		Magnetic_Suscept : 0.19
157.00		Magnetic_Suscept : 0.19
158.00		Magnetic_Suscept : 2.47
159.00		Magnetic_Suscept : 0.22
160.00		Magnetic_Suscept : 0.15
161.00		Magnetic_Suscept : 0.26
162.00		Magnetic_Suscept : 0.24
163.00		Magnetic_Suscept : 0.17
164.00		Magnetic_Suscept : 0.19
165.00		Magnetic_Suscept : 0.10
166.00		Magnetic_Suscept : 0.15

VB95186

Page 8

VB95186

An Example (VB-96-321) of a Boris Log Which Includes: Lithology; Percent Mineralization; Core Axis Angles; Recovery; and RQD.

VB96321 **INCO Limited - Exploration Department** VB96321
Standard Log

Borehole	: VB96321	Project	: Voisey's Bay Main Block
Northing	: 6243253.01	Property	: Voisey's Bay
Easting	: 552989.62	Township/County	: -
Elevation	: 5057.74 m	Province/State	: Newfoundland and Labrador
Hole length	: 457.20 m	Mine	: -
		Country	: Canada
Setup name:		NTS/SECT.T.R.	: -
No Assays		UTM Coordinates	: -
		Date Started	: August 20, 1996
Print Date:		Date Completed	: September 16, 1996
06-Feb-1999 17:28		Logged By	: Dawn Evans-Lamswood
		Logging Started	: August 20, 1996
		Logging Completed	: September 16, 1996
		Drilled By	: Petro Drilling Co.
		Drill Type	: -
		Core Size	: NQ
		Hole Size	: 457.2 metres
		Left In Hole	: none
		Section	: L 15+00W
		Level	: surface
		Heading	: -
		Inclination	: -74
		Grid Name	: Western Extension
		Baseline Azimuth	: 085
		Borehole Bearing	: 355
		Assayed For	: Ni, Cu, Co, Au, Pt
		Attitude Test Method	: Gyro Survey
		Measurement(M/F)	: M
		Claim #	: -
		Anomaly #	: -

Survey records

depth	azm	dip	depth	azm	dip
0.00	1.58	-76.17	180.00	2.98	-74.75
30.00	1.66	-74.50	210.00	3.88	-75.03
60.00	1.84	-74.17	240.00	4.25	-75.33
90.00	2.21	-74.00	270.00	4.63	-75.83
120.00	2.50	-74.08	300.00	5.83	-76.75
150.00	3.52	-74.58	330.00	7.94	-76.58

VB96321

INCO Limited - Exploration Department

Standard Log

VB96321

depth	azm	dip	depth	azm	dip
360.00	11.70	-76.17	420.00	14.29	-78.00
390.00	13.37	-77.50	450.00	15.23	-78.00

COMMENTS: Converted to BorlSWin 21-Nov-1997 18:05:25
 GENERATED BY BORIS-VAX 18-JUN-1997 11:06:23.79
 ELEMENTSNI CU CO S FE
 UNITS: % % % % %
 GENERATED BY BORIS-VAX 14-MAY-1997 12:54:22.67
 ELEMENTSSG NI CU CO S
 UNITS: GRN % % % %
 GENERATED BY BORIS-VAX 14-MAY-1997 10:38:12.30
 ELEMENTSSG NI CU CO S
 UNITS: GRN % % % %
 GENERATED BY BORIS-VAX 16-JAN-1997 12:10:35.45
 ELEMENTSSG NI CU CO
 UNITS: GRN % % PPB

From m	To m	Description
0.00	100.30	OVERBURDEN Overburden.

100.30 155.90 PARAGNEISS

Garnetiferous paragneiss; gneissosity at 45 degrees to core axis; rare blotchy veined sulphides 102.6-103.2 - trace to 1% blotchy sulphides; concentrated in mafic chloritized matrix of gneiss; sulphides appear injected and not remobilized (pyrrhotite/pentlandite/chalcopyrite) 109.7-110.2 - rapikivi granite 113.3-113.7 - trace chalcopyrite 113.7-113.8 - aphyric, non magnetic, mafic dyke 114.9-115.2 - rapikivi granite, small (1cm thick); aphyric, non magnetic, dykelet present (less than 1.0cm thick) 115.2-123.8 - garnetiferous paragneiss; garnets weakly reacted; trace sulphides (pyrrhotite/pentlandite/chalcopyrite); (ie: 120.2m); fabric at 60-70 degrees to core axis 123.8-123.9 - fresh (late) quartzofeldspathic vein at 30 degrees to core axis; 3cm wide 123.9-124.3 - quartzofeldspathic contamination; nebulous, garnetiferous paragneiss inclusions 124.3-125.5 - garnetiferous paragneiss; sulphides (pyrrhotite/pentlandite /chalcopyrite) do not appear remobilized, but injected/veined in soft media (ie: surround feldspathic material in softer chlorite matrix; however, some sulphides appear to be starting remobilization and are being

VB96321

Page 2

VB96321

From m	To m	Description
		<p>pulled out along hairline fractures; trace to 1% sulphides (pyrrhotite/pentlandite/chalcopyrite) 125.5-126.1 - paragneiss continues, 35-45% fine grained, disseminated sulphides (pyrrhotite/pentlandite/chalcopyrite), overall sulphides appear amalgamating/cumulative with minor remobilization along steep (0-10 degrees to core axis) hairline fractures, these remobilized zones are chalcopyrite enriched, there also appears to be some mafic mixing /overprinting (sugary texture) 126.1-127.2 - garnetiferous paragneiss; 1-3% fine grained disseminated (pyrrhotite/pentlandite/chalcopyrite) sulphides; sulphides appear concentrated in softer matrix material; chalcopyrite enriched zones of remobilized sulphides along hairline fractures; fabric nebulous in sulphide rich zones; no mafic contamination 127.2-128.6 - garnetiferous paragneiss; trace, fine grained disseminated to blotchy (pyrrhotite/pentlandite/chalcopyrite) sulphides; fabric at 75-80 degrees to core axis 128.6-129.5 - garnetiferous paragneiss; 25-30% fine grained disseminated sulphides (pyrrhotite/pentlandite/chalcopyrite) to semi massive, intense yellow, leafy alteration-leucite? 129.5-131.6 - garnetiferous paragneiss; trace to 1% sulphides (pyrrhotite/pentlandite/chalcopyrite); fine grained, disseminated sulphides, infrequent remobilization along hairline fractures 131.6-132.1 - garnetiferous paragneiss; 30-35% semi massive to fine grained disseminated (pyrrhotite/pentlandite/chalcopyrite) sulphides; sulphides cumulative/amalgamated texture, appears to have troctolitic inclusions 132.1-136.2 - garnetiferous paragneiss; 1-2% (pyrrhotite/pentlandite/ chalcopyrite); blotchy, semi massive sulphides; gneissosity at 60 degrees to core axis 133.5-133.6 - quartzofeldspathic dykelet/vein at 60 degrees to core axis 133.8-133.9 - fabric locally steepens to 45 degrees to core axis; chloritic alteration 135.2-136.2 - biotite and amphibole rich 136.2-154.1 - granitic pegmatite; rare trace sulphides in brittle fractures; upper contact irregular/diffuse (approximately 45 degrees to core axis) 154.1-155.5 - light grey, fine grained granitic orthogneiss; no fabric; local hematite staining 155.1-155.4 - blocky core; hairline fractures in varying orientations (quartz filled trace sulphides) 155.5-155.9 - rapikivi granite; feldspar megacrysts augened (long axis at 25-30 degrees to core axis).</p>
100.30	122.00	21.70 %MIN : tr-1
122.00	123.00	1.00 %MIN : trace
123.00	124.00	1.00 %MIN : barn-tr
124.00	125.00	1.00 %MIN : tr-1
125.00	126.00	1.00 %MIN : 35-45
126.00	127.00	1.00 %MIN : 1-3
127.00	128.00	1.00 %MIN : trace
128.00	128.70	0.70 %MIN : trace

VB96321

INCO Limited - Exploration Department

Standard Log

VB96321

From m	To m	Description	
128.70	129.70	1.00 %MIN	: 25-30
129.70	130.70	1.00 %MIN	: tr-1
130.70	131.60	0.90 %MIN	: tr-1
131.60	132.00	0.40 %MIN	: 30-35
132.00	133.00	1.00 %MIN	: 1-2
133.00	134.00	1.00 %MIN	: 1-2
134.00	135.00	1.00 %MIN	: 1-2
135.00	136.00	1.00 %MIN	: 1-2
136.00	137.00	1.00 %MIN	: trace
137.00	138.00	1.00 %MIN	: trace
138.00	155.90	17.90 %MIN	: trace
100.30	122.00	21.70 CANG	: foln45
122.00	123.00	1.00 CANG	: foln65
123.00	124.00	1.00 CANG	: mass
124.00	125.00	1.00 CANG	: mass
125.00	126.00	1.00 CANG	: mass
126.00	127.00	1.00 CANG	: mass
127.00	128.00	1.00 CANG	: foln75
128.00	128.70	0.70 CANG	: foln75
128.70	129.70	1.00 CANG	: mass
129.70	130.70	1.00 CANG	: mass
130.70	131.60	0.90 CANG	: mass
131.60	132.00	0.40 CANG	: mass
132.00	133.00	1.00 CANG	: foln60
133.00	134.00	1.00 CANG	: foln60
134.00	135.00	1.00 CANG	: foln60
135.00	136.00	1.00 CANG	: foln60
136.00	137.00	1.00 CANG	: mass
137.00	138.00	1.00 CANG	: mass
138.00	155.90	17.90 CANG	: mass
100.30	103.60	3.30 RECOVERY	: 100
103.60	106.70	3.10 RECOVERY	: 100
106.70	109.70	3.00 RECOVERY	: 100
109.70	112.80	3.10 RECOVERY	: 100
112.80	115.80	3.00 RECOVERY	: 100
115.80	118.90	3.10 RECOVERY	: 100
118.90	121.90	3.00 RECOVERY	: 100
121.90	125.00	3.10 RECOVERY	: 100

VB96321

Page 4

VB96321

VB96321

INCO Limited - Exploration Department

Standard Log

VB96321

From m	To m	Description	
125.00	128.00	3.00 RECOVERY	: 100
128.00	131.10	3.10 RECOVERY	: 100
131.10	134.10	3.00 RECOVERY	: 100
134.10	137.10	3.00 RECOVERY	: 100
137.10	140.20	3.10 RECOVERY	: 100
140.20	143.20	3.00 RECOVERY	: 100
143.20	146.30	3.10 RECOVERY	: 100
146.30	149.40	3.10 RECOVERY	: 100
149.40	152.40	3.00 RECOVERY	: 100
152.40	155.40	3.00 RECOVERY	: 100
155.40	158.50	3.10 RECOVERY	: 100
100.30	103.60	3.30 RQD	: 92
103.60	106.70	3.10 RQD	: 98
106.70	109.70	3.00 RQD	: 93
109.70	112.80	3.10 RQD	: 85
112.80	115.80	3.00 RQD	: 82
115.80	118.90	3.10 RQD	: 98
118.90	121.90	3.00 RQD	: 98
121.90	125.00	3.10 RQD	: 97
125.00	128.00	3.00 RQD	: 83
128.00	131.10	3.10 RQD	: 98
131.10	134.10	3.00 RQD	: 96
134.10	137.10	3.00 RQD	: 93
137.10	140.20	3.10 RQD	: 97
140.20	143.20	3.00 RQD	: 100
143.20	146.30	3.10 RQD	: 100
146.30	149.40	3.10 RQD	: 100
149.40	152.40	3.00 RQD	: 100
152.40	155.40	3.00 RQD	: 90
155.40	158.50	3.10 RQD	: 81
123.00	124.00	1.00 TXTR	: neb
125.00	126.00	1.00 TXTR	: sugary
126.00	127.00	1.00 TXTR	: neb
127.00	128.00	1.00 TXTR	: fg
128.00	128.70	0.70 TXTR	: fg
128.70	129.70	1.00 TXTR	: fg
129.70	130.70	1.00 TXTR	: fg
130.70	131.60	0.90 TXTR	: fg

VB96321

Page 5

VB96321

From m	To m	Description	
131.60	132.00	0.40 TXTR	: fg
136.00	137.00	1.00 TXTR	: gmc
137.00	138.00	1.00 TXTR	: gmc
138.00	155.90	17.90 TXTR	: gmc

155.90 156.30 ORTHOGNEISS

Fine grained, granitic orthogneiss; rare phenocrystic felds (maybe remanents of early granitic pegmatites) 156.1-156.3 - granitic pegmatites rotated into fabric.

155.90	156.30	0.40 %MIN	: bam-tr
155.90	156.30	0.40 CANG	: mass
155.90	156.30	0.40 TXTR	: fg-gmc

156.30 159.80 PEGMATITE

Granitic pegmatite.

156.30	159.80	3.50 %MIN	: bam-tr
156.30	159.80	3.50 CANG	: mass
158.50	161.50	3.00 RECOVERY	: 100
158.50	161.50	3.00 RQD	: 100
156.30	159.80	3.50 TXTR	: gmc

159.80 163.20 TROCTOLITE BRECCIA TR-5% SULPHIDES

Basal breccia sequence; 10-15% aphyric mafic fragments; borderline BBS/VT; very difficult to judge amount of fragments, a top of sequence fragments are clearly definable, but become diffuse/injected down sequence 160.5-161.8 - weak fabric at 70 degrees to core axis; defined by biotite and quartzofeldspathic veinlets; long axis of fragments also follow this fabric, probably not a primary flow fabric since later veinlets are incorporated into it and as well hairline lenses of chlorite are concentrated along the fabric Trace, fine to medium grained, disseminated sulphides (pyrrhotite/ pentlandite/chalcopyrite) Moderate to intense biotite alteration locally where fabric is more intense.

159.80	163.20	3.40 %MIN	: trace
159.80	163.20	3.40 CANG	: wk.f70
161.50	164.60	3.10 RECOVERY	: 100
161.50	164.60	3.10 RQD	: 100

From m	To m	Description
-----------	---------	-------------

163.20 165.80 TROCTOLITE TR-5% SULPHIDES

Intercalated variable troctolite and ultramafic; variable troctolite has approximately 5% aphyric fragments which are very diffuse (highly digested) Trace finely disseminated sulphides (pyrrhotite/pentlandite/chalcopryite) Variable troctolite (non magnetic) exhibits thin strongly magnetic, melanocratic lenses, it appears that this maybe weak ultramafic contamination which probably becomes preferentially separated into thin lenses due to induced strain whether it be primary flow or a secondary deformative event? Locally when ultramafic does not exhibit a strong degree of preferential separating, it appears to be weakly/brecciated troctolite Frequent granitic to quartzofelds veinlets present, stayed and in random orientations: 163.2-163.4, 163.7-163.8, 164.0-164.2, 164.4-164.6, 164.9-165.0, 165.7-165.8.

163.20	165.80	2.60	%MIN	: trace
163.20	165.80	2.60	CANG	: mass
164.60	167.60	3.00	RECOVERY	: 100
164.60	167.60	3.00	RQD	: 98

165.80 170.80 TROCTOLITE BRECCIA TR-5% SULPHIDES

Basal breccia sequence; trace to finely disseminated sulphides (pyrrhotite/pentlandite/chalcopryite) Fragments approximately 15-20% aphyric mafic fragments, this zone has intense and highly digested, quartzofeldspathic veinlets (wispy texture), the first time a true correlation of the aphyric mafic fragments can be clearly seen as a protolith, the quartzofeldspathic veinlets are actually fragments (troctolite is interfingering and enclaving the quartzofeldspathic material), the quartzofeldspathic material appears as true fragments (float in troctolite matrix), but other instances appears vein like where edges of fragments expand beyond edges of core and fragments are probably lesoidal in shape 165.8-170.8 - edges of the quartzofeldspathic fragments can be observed gradually diffusing into aphyric mafic/mesocratic material (identical to the aphyric mafic fragments frequently observed), possibly these fragments are totally digested granitic fragments with the mafic materials segregated to margins (ie: frequently the aphyric fragments exhibit aphyric feldspathic cores).

165.80	170.80	5.00	%MIN	: trace
165.80	170.80	5.00	CANG	: mass
167.60	170.70	3.10	RECOVERY	: 100
170.70	173.70	3.00	RECOVERY	: 100

From m	To m	Description	
167.60	170.70	3.10 RQD	: 100
170.70	173.70	3.00 RQD	: 81
165.80	170.80	5.00 TXTR	: wispy

170.80 174.00 TROCTOLITE BRECCIA TR-5% SULPHIDES

Intercalated ultramafic and basal breccia sequence; aphyric fragments (10-15%) in both sequences as well as defined quartzofeldspathic fragments Trace to 1% finely disseminated sulphides (pyrrhotite/pentlandite/ chalcopyrite; no sharp contacts observed between basal breccia sequence and ultramafic, frequently transition interrupted by quartzofeldspathic veins, where visible the contact appears gradational; there appears to be two sequences of quartzofeldspathic material, one as late veins (sharp, fresh contacts, the second are fragments with digested margins and an infrequent fabric (possibly some fragments are gneissic).

170.80	174.00	3.20 %MIN	: tr-1
170.80	174.00	3.20 CANG	: mass
173.70	176.80	3.10 RECOVERY	: 100
173.70	176.80	3.10 RQD	: 96

174.00 197.30 TROCTOLITE TR-5% SULPHIDES

Variable troctolite; rare trace sulphides (pyrrhotite/pentlandite/ chalcopyrite); (weakly hybridized by quartzofeldspathic contamination) 174.0-176.2 - trace to 1% fine to medium grained disseminated sulphides with 5-10% aphyric to feldspathic phyrlic fragments; troctolite is fine grained to massive 176.2 - rare trace sulphides; troctolite has sugary/granular texture, bleached feldspars; biotite rich patches; frequent, fine grained bronzite (basically hybridized due to feldspathic contamination-see below) frequent quartzofeldspathic veins at varying degrees of digestion—aphyrlic to feldspathic phyrlic to weakly altered veinlets) 189.3-195.4 - less contaminated, fine grained, purple plagioclase (less hybridization) 195.4-195.8 - rapikivi granite; grey green colour; megacrystic plagioclase 195.8-197.3 - variable troctolite; trace to fine grained disseminated sulphides (pyrrhotite/pentlandite/chalcopyrite), diffuse patches, possibly injected fragments?.

174.00	197.30	23.30 %MIN	: tr-1
174.00	197.30	23.30 CANG	: mass
176.80	179.80	3.00 RECOVERY	: 100
179.80	182.90	3.10 RECOVERY	: 100

From m	To m	Description	
182.90	185.90	3.00 RECOVERY	: 100
185.90	189.00	3.10 RECOVERY	: 100
189.00	192.00	3.00 RECOVERY	: 100
192.00	195.10	3.10 RECOVERY	: 100
195.10	198.10	3.00 RECOVERY	: 100
176.80	179.80	3.00 RQD	: 100
179.80	182.90	3.10 RQD	: 100
182.90	185.90	3.00 RQD	: 100
185.90	189.00	3.10 RQD	: 100
189.00	192.00	3.00 RQD	: 99
192.00	195.10	3.10 RQD	: 100
195.10	198.10	3.00 RQD	: 100
174.00	197.30	23.30 TXTR	: sugary

197.30 457.20 RAPAKIVI GRANITE

Rapakivi granite; megacrystic feldspars, leucite? (yellow/leafy), alteration; grey, green in colour 225.9-228.1 - enclaved variable troctolite; moderate biotite alteration; grey, green in colour 230.7-232.0 - enclaved variable troctolite; barren; moderate biotite alteration; intensely hematized granitic pegmatites present (231.2-231.3, 231.4-231.5, 231.7-231.8) 233.4-233.6 and 233.9-234.0 - granitic pegmatite 243.5-246.8 - variable troctolite becoming pegmatitic and anorthositic down section 288.6-288.7 - injected quartzofeldspathic vein 323.8-324.1 - aphyric, non magnetic mafic dyke (rubbly) but contacts appear to be approximately 60 degrees to core axis 335.6-335.7 - quartzofeldspathic pegmatite Frequent olivine/leucite Megacrystic enriched zone with frequent pyroxene.

EOH 457.2 metres.

197.30	228.60	31.30	%MIN	: bam-tr
228.60	231.60	3.00	%MIN	: bam-tr
231.60	234.70	3.10	%MIN	: bam-tr
234.70	457.20	222.50	%MIN	: bam-tr
197.30	228.60	31.30	CANG	: mass
228.60	231.60	3.00	CANG	: mass
231.60	234.70	3.10	CANG	: mass
234.70	457.20	222.50	CANG	: mass
198.10	201.20	3.10	RECOVERY	: 100
201.20	204.20	3.00	RECOVERY	: 100

VB96321

INCO Limited - Exploration Department

Standard Log

VB96321

From m	To m	Description	
204.20	207.30	3.10 RECOVERY	: 100
207.30	210.30	3.00 RECOVERY	: 100
210.30	213.40	3.10 RECOVERY	: 100
213.40	216.40	3.00 RECOVERY	: 100
216.40	219.50	3.10 RECOVERY	: 100
219.50	222.50	3.00 RECOVERY	: 100
222.50	225.60	3.10 RECOVERY	: 100
225.60	228.60	3.00 RECOVERY	: 100
228.60	231.60	3.00 RECOVERY	: 100
231.60	234.70	3.10 RECOVERY	: 100
234.70	237.70	3.00 RECOVERY	: 100
237.70	240.80	3.10 RECOVERY	: 100
240.80	243.80	3.00 RECOVERY	: 100
243.80	246.90	3.10 RECOVERY	: 100
246.90	249.90	3.00 RECOVERY	: 100
249.90	253.00	3.10 RECOVERY	: 100
253.00	256.00	3.00 RECOVERY	: 100
256.00	259.10	3.10 RECOVERY	: 100
259.10	262.10	3.00 RECOVERY	: 100
262.10	265.20	3.10 RECOVERY	: 100
265.20	268.20	3.00 RECOVERY	: 100
268.20	271.30	3.10 RECOVERY	: 100
271.30	274.30	3.00 RECOVERY	: 100
274.30	277.40	3.10 RECOVERY	: 100
277.40	280.40	3.00 RECOVERY	: 100
280.40	283.50	3.10 RECOVERY	: 100
283.50	286.50	3.00 RECOVERY	: 100
286.50	289.60	3.10 RECOVERY	: 100
289.60	292.60	3.00 RECOVERY	: 100
292.60	295.70	3.10 RECOVERY	: 100
295.70	298.70	3.00 RECOVERY	: 100
298.70	301.80	3.10 RECOVERY	: 100
301.80	304.80	3.00 RECOVERY	: 100
304.80	307.80	3.00 RECOVERY	: 100
307.80	310.90	3.10 RECOVERY	: 100
310.90	313.90	3.00 RECOVERY	: 100
313.90	317.00	3.10 RECOVERY	: 100
317.00	320.00	3.00 RECOVERY	: 100

VB96321

Page 10

VB96321

VB96321

INCO Limited - Exploration Department

Standard Log

VB96321

From m	To m	Description	
320.00	323.10	3.10 RECOVERY	: 100
323.10	326.10	3.00 RECOVERY	: 100
326.10	329.20	3.10 RECOVERY	: 100
329.20	332.20	3.00 RECOVERY	: 100
332.20	335.30	3.10 RECOVERY	: 100
335.30	338.30	3.00 RECOVERY	: 100
338.30	341.40	3.10 RECOVERY	: 100
341.40	344.40	3.00 RECOVERY	: 100
344.40	347.50	3.10 RECOVERY	: 100
347.50	350.50	3.00 RECOVERY	: 100
350.50	353.60	3.10 RECOVERY	: 100
353.60	356.60	3.00 RECOVERY	: 100
356.60	359.70	3.10 RECOVERY	: 100
359.70	362.70	3.00 RECOVERY	: 100
362.70	365.80	3.10 RECOVERY	: 100
365.80	368.80	3.00 RECOVERY	: 100
368.80	371.90	3.10 RECOVERY	: 100
371.90	374.90	3.00 RECOVERY	: 100
374.90	378.00	3.10 RECOVERY	: 100
378.00	381.00	3.00 RECOVERY	: 100
381.00	384.00	3.00 RECOVERY	: 100
384.00	387.10	3.10 RECOVERY	: 100
387.10	390.10	3.00 RECOVERY	: 100
390.10	393.20	3.10 RECOVERY	: 100
393.20	396.20	3.00 RECOVERY	: 100
396.20	399.30	3.10 RECOVERY	: 100
399.30	402.30	3.00 RECOVERY	: 100
402.30	405.40	3.10 RECOVERY	: 100
405.40	408.40	3.00 RECOVERY	: 100
408.40	411.50	3.10 RECOVERY	: 100
411.50	414.50	3.00 RECOVERY	: 100
414.50	417.60	3.10 RECOVERY	: 100
417.60	420.60	3.00 RECOVERY	: 100
420.60	423.70	3.10 RECOVERY	: 100
423.70	426.70	3.00 RECOVERY	: 100
426.70	429.80	3.10 RECOVERY	: 100
429.80	432.80	3.00 RECOVERY	: 100
432.80	435.90	3.10 RECOVERY	: 100

VB96321

Page 11

VB96321

VB96321

INCO Limited - Exploration Department

Standard Log

VB96321

From m	To m	Description	
435.90	438.90	3.00 RECOVERY	: 100
438.90	442.00	3.10 RECOVERY	: 100
442.00	445.00	3.00 RECOVERY	: 100
445.00	448.10	3.10 RECOVERY	: 100
448.10	451.10	3.00 RECOVERY	: 100
451.10	454.20	3.10 RECOVERY	: 100
454.20	457.20	3.00 RECOVERY	: 100
198.10	201.20	3.10 RQD	: 100
201.20	204.20	3.00 RQD	: 100
204.20	207.30	3.10 RQD	: 100
207.30	210.30	3.00 RQD	: 100
210.30	213.40	3.10 RQD	: 100
213.40	216.40	3.00 RQD	: 100
216.40	219.50	3.10 RQD	: 89
219.50	222.50	3.00 RQD	: 100
222.50	225.60	3.10 RQD	: 94
225.60	228.60	3.00 RQD	: 100
228.60	231.60	3.00 RQD	: 66
231.60	234.70	3.10 RQD	: 41
234.70	237.70	3.00 RQD	: 92
237.70	240.80	3.10 RQD	: 100
240.80	243.80	3.00 RQD	: 99
243.80	246.90	3.10 RQD	: 98
246.90	249.90	3.00 RQD	: 100
249.90	253.00	3.10 RQD	: 100
253.00	256.00	3.00 RQD	: 100
256.00	259.10	3.10 RQD	: 100
259.10	262.10	3.00 RQD	: 100
262.10	265.20	3.10 RQD	: 100
265.20	268.20	3.00 RQD	: 100
268.20	271.30	3.10 RQD	: 100
271.30	274.30	3.00 RQD	: 100
274.30	277.40	3.10 RQD	: 100
277.40	280.40	3.00 RQD	: 100
280.40	283.50	3.10 RQD	: 100
283.50	286.50	3.00 RQD	: 100
286.50	289.60	3.10 RQD	: 100
289.60	292.60	3.00 RQD	: 100

VB96321

VB96321

VB96321

INCO Limited - Exploration Department **Standard Log**

VB96321

From m	To m	Description	
292.60	295.70	3.10 RQD	: 100
295.70	298.70	3.00 RQD	: 100
298.70	301.80	3.10 RQD	: 100
301.80	304.80	3.00 RQD	: 100
304.80	307.80	3.00 RQD	: 100
307.80	310.90	3.10 RQD	: 100
310.90	313.90	3.00 RQD	: 100
313.90	317.00	3.10 RQD	: 100
317.00	320.00	3.00 RQD	: 100
320.00	323.10	3.10 RQD	: 100
323.10	326.10	3.00 RQD	: 87
326.10	329.20	3.10 RQD	: 100
329.20	332.20	3.00 RQD	: 100
332.20	335.30	3.10 RQD	: 100
335.30	338.30	3.00 RQD	: 100
338.30	341.40	3.10 RQD	: 100
341.40	344.40	3.00 RQD	: 100
344.40	347.50	3.10 RQD	: 100
347.50	350.50	3.00 RQD	: 100
350.50	353.60	3.10 RQD	: 100
353.60	356.60	3.00 RQD	: 100
356.60	359.70	3.10 RQD	: 100
359.70	362.70	3.00 RQD	: 100
362.70	365.80	3.10 RQD	: 100
365.80	368.80	3.00 RQD	: 100
368.80	371.90	3.10 RQD	: 100
371.90	374.90	3.00 RQD	: 100
374.90	378.00	3.10 RQD	: 100
378.00	381.00	3.00 RQD	: 100
381.00	384.00	3.00 RQD	: 100
384.00	387.10	3.10 RQD	: 100
387.10	390.10	3.00 RQD	: 100
390.10	393.20	3.10 RQD	: 100
393.20	396.20	3.00 RQD	: 100
396.20	399.30	3.10 RQD	: 100
399.30	402.30	3.00 RQD	: 100
402.30	405.40	3.10 RQD	: 100
405.40	408.40	3.00 RQD	: 100

VB96321

Page 13

VB96321

VB96321

INCO Limited - Exploration Department

Standard Log

VB96321

From m	To m	Description	
408.40	411.50	3.10 RQD	: 100
411.50	414.50	3.00 RQD	: 100
414.50	417.60	3.10 RQD	: 100
417.60	420.60	3.00 RQD	: 100
420.60	423.70	3.10 RQD	: 98
423.70	426.70	3.00 RQD	: 100
426.70	429.80	3.10 RQD	: 100
429.80	432.80	3.00 RQD	: 100
432.80	435.90	3.10 RQD	: 100
435.90	438.90	3.00 RQD	: 100
438.90	442.00	3.10 RQD	: 100
442.00	445.00	3.00 RQD	: 100
445.00	448.10	3.10 RQD	: 95
448.10	451.10	3.00 RQD	: 99
451.10	454.20	3.10 RQD	: 100
454.20	457.20	3.00 RQD	: 100
197.30	228.60	31.30 TXTR	: rap
228.60	231.60	3.00 TXTR	: rap
231.60	234.70	3.10 TXTR	: rap
234.70	457.20	222.50 TXTR	: rap

VB96321

Page 14

VB96321

APPENDIX B:
Digitized Sections

Figure B-3.A An Example (13+00E) of an Interpreted (Digitized) Section with Lithology/Rock Codes (see Appendix A)
Displayed on the Drill Hole Trace .
Scale 1:1000

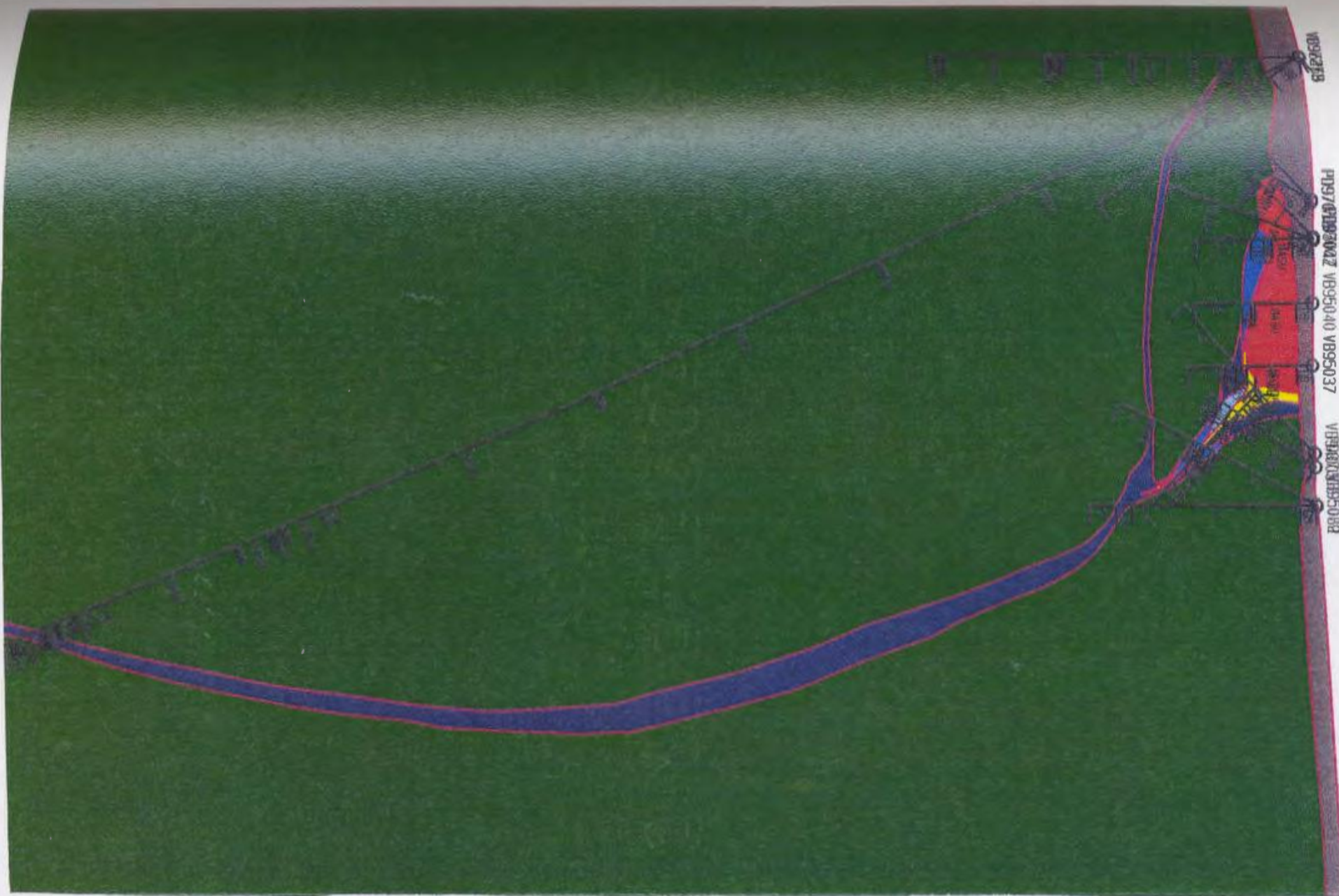


Figure B-4.A An Example (L13+0E) of an Interpreted (Digitized) Section with Lithology/Rock Codes (see Appendix A)
Displayed on the Drill Hole Trace and Color Added.

Scale 1:5000

Scale 1:5000

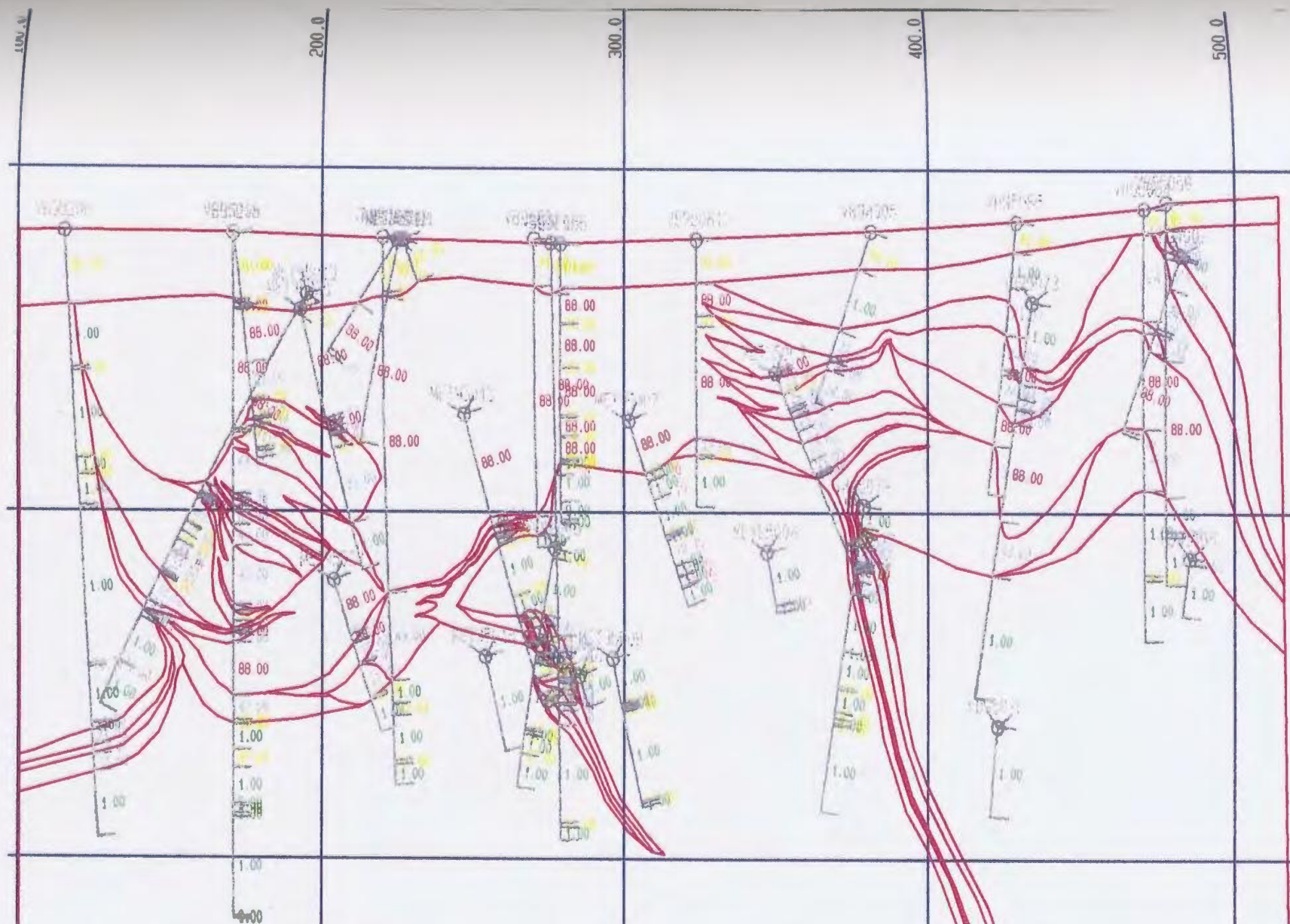


Figure B-6.A An Example (012E) of an Interpreted (Digitized) Long-Section with Lithology/Rock Codes (see Appendix A)
 Displayed on the Drill Hole Trace
 Scale 1:2000

APPENDIX C:
Data Display

Figure C-2.A.: An Example of Lithology Data from Boris (see Appendix A) Displayed on a West Facing Drill Hole Section.

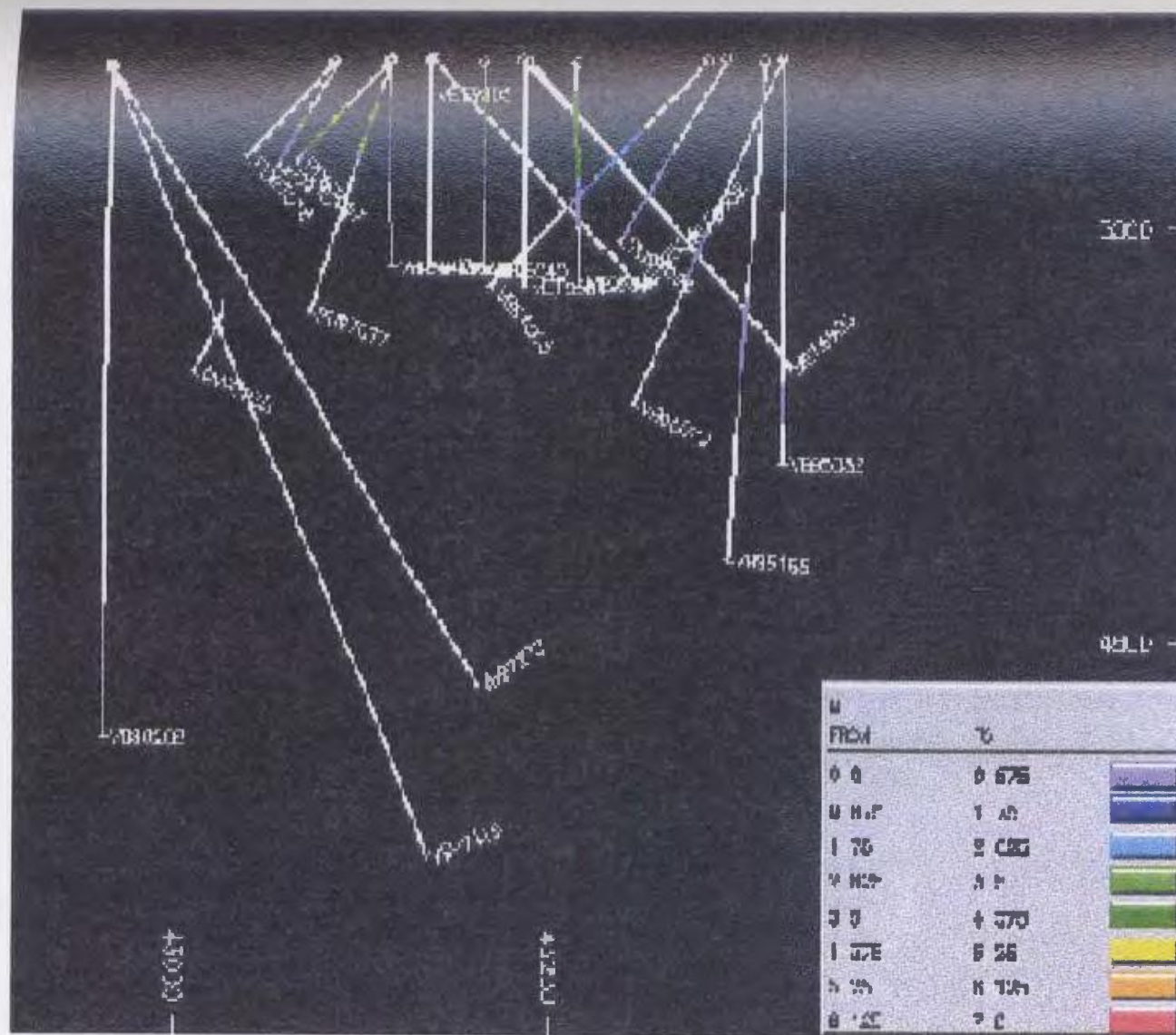


Figure C-3.A.: An Example of Ni Grades (%) from Boris Assay Samples (see Appendix A) Displayed on a West Facing Drill Hole Section.

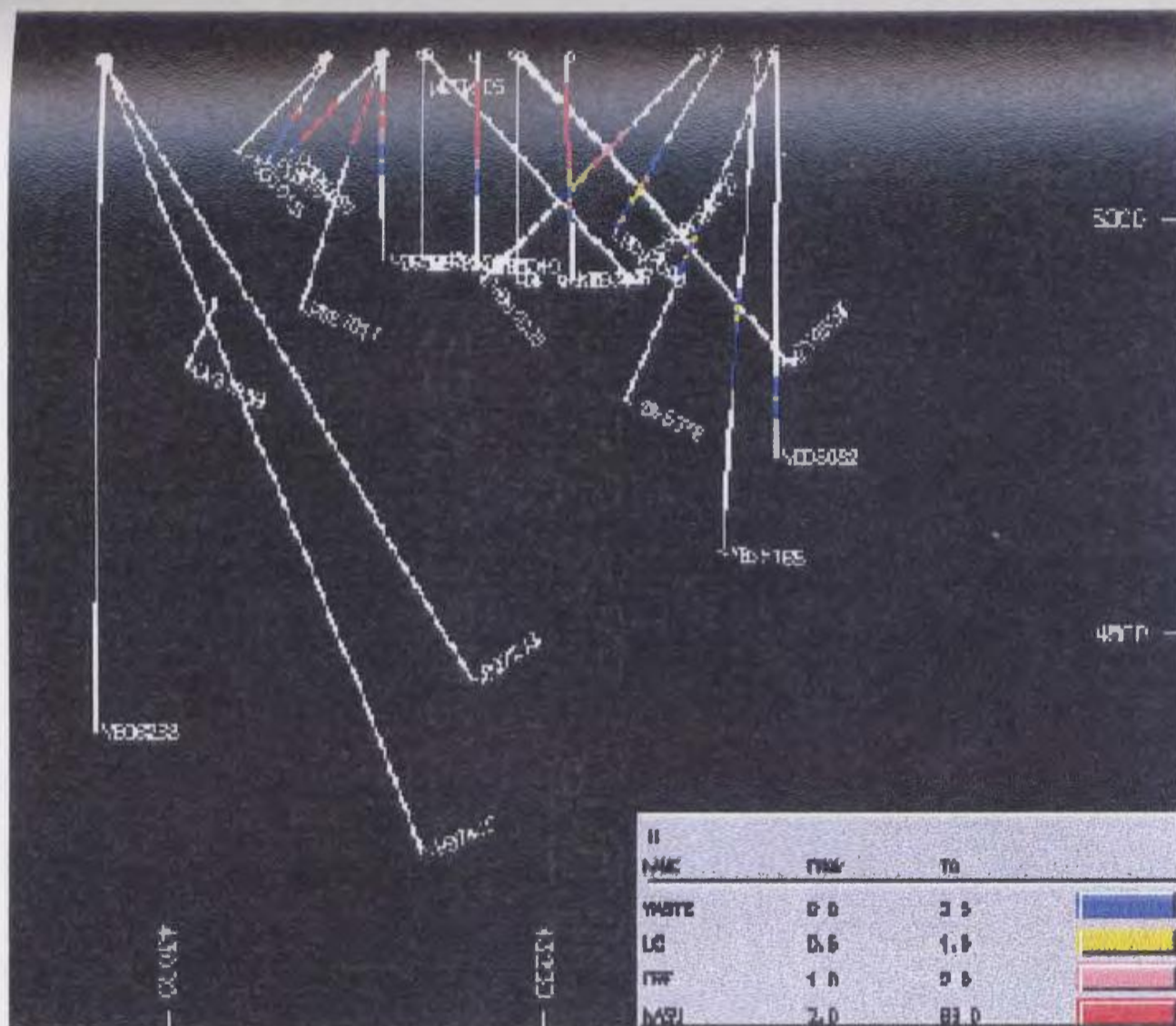
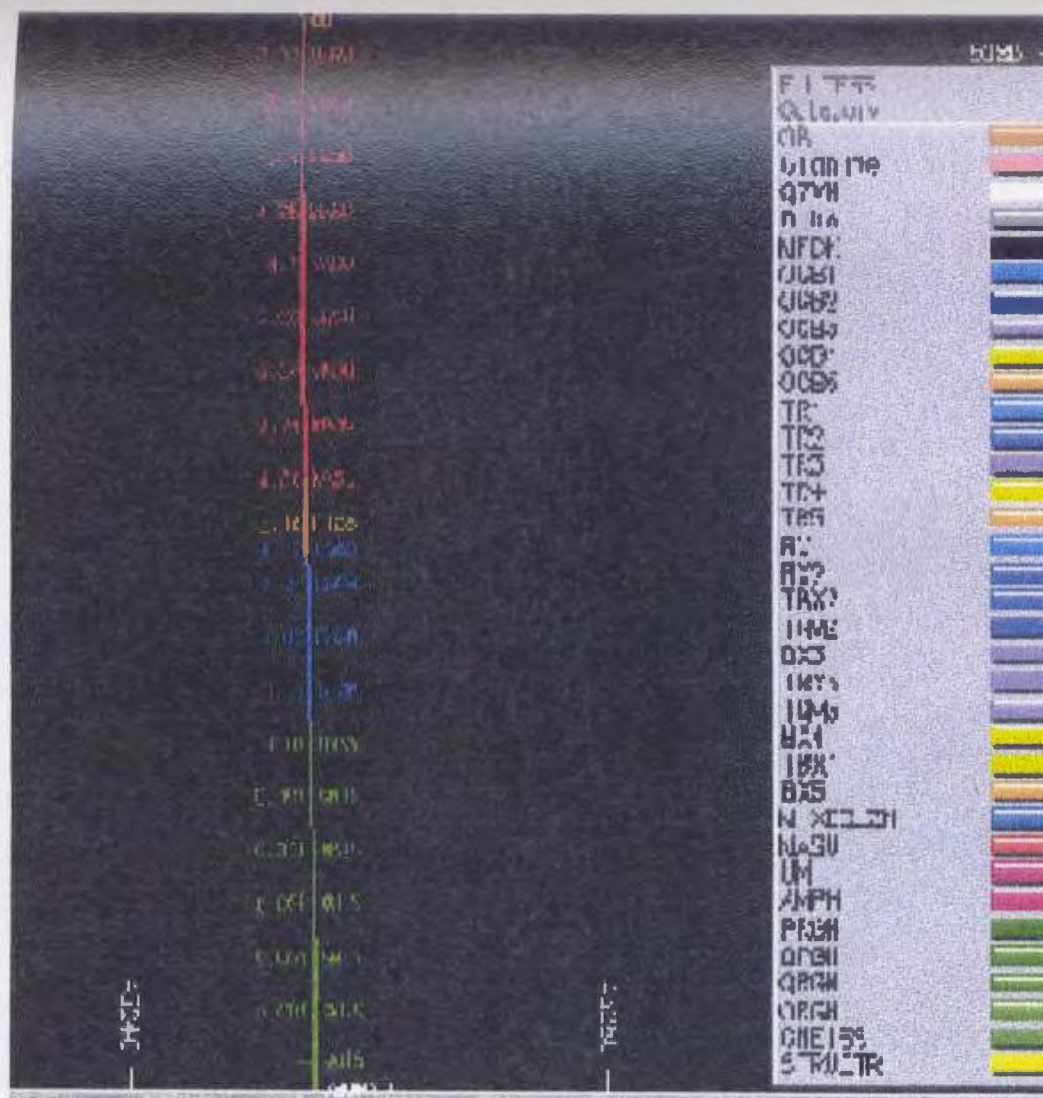


Figure C-4.A.: An Example of Ni (%) Grade Cut-Off Displayed on a West Facing Drill Hole Section (Waste Ni% less than 5%. Low Grade between 0.5-1%Ni, Ore between 1.0-2.0%Ni and Massive at 2%Ni or greater), Based on Assays from Boris (see Appendix A).



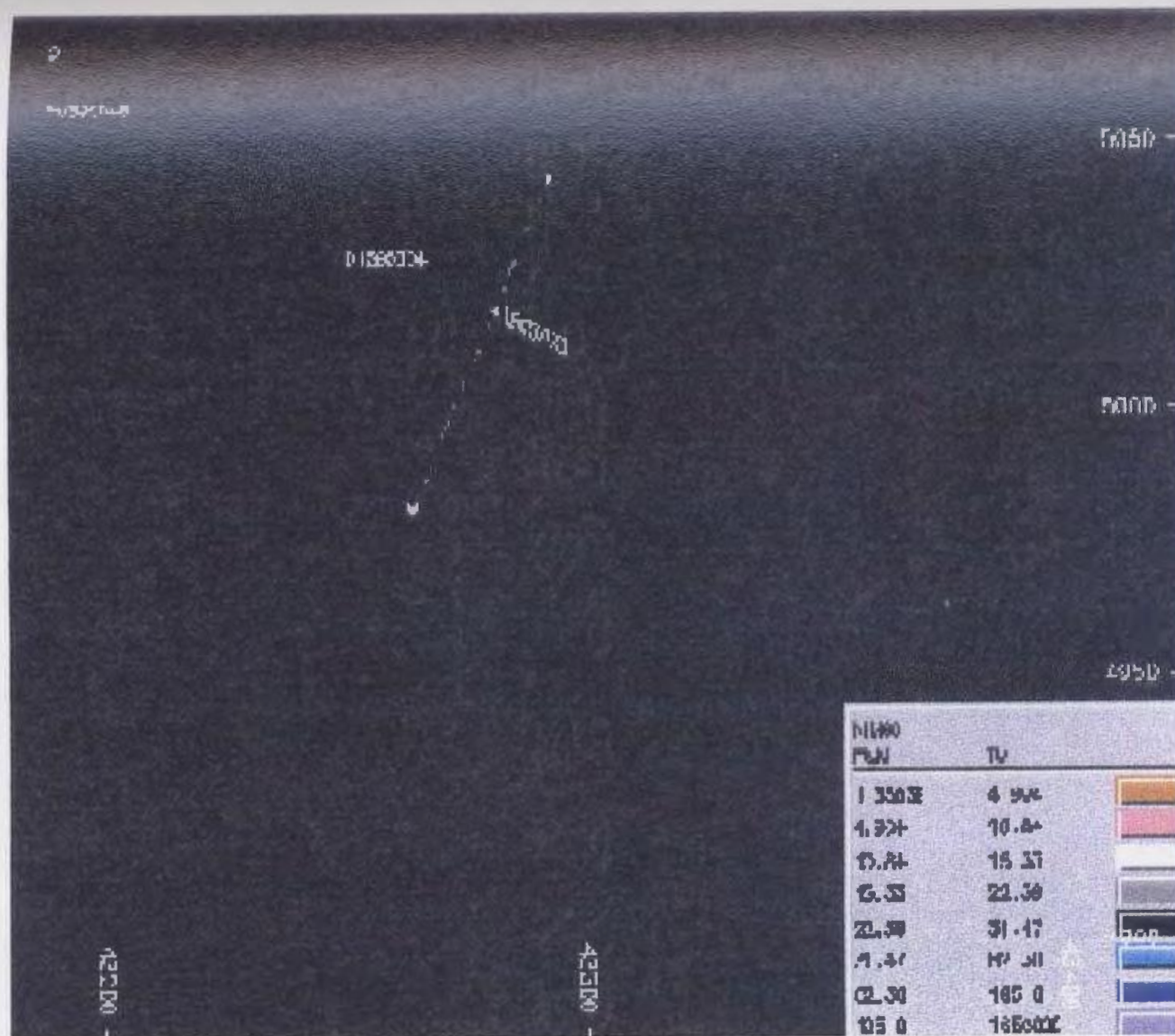


Figure C-6.A.: An Example of the Display of Lithogeochemical Data Sets; Ni /MgO Displayed On a Drill Hole in Plan View.

COORDINATES Z,Y,Z = (35651.25, 43267.15, 4958.03) View plane U.S. - -0.72
 BHID = VED5C71 Total samples : 22
 FROM = 107.50 K,Y,Z = (35691.25, 43237.57, 4950.94)
 TO = 108.50 K,Y,Z = (35691.23, 43237.15, 4958.03)
 LENGTH = 1.00 NC,ZC = (175.00, 45.00)

 ROCK =
 CU = 170.0 ZC = 55.0 STDAT = 3501
 SIO2 = 46.2 AL2O3 = 13.7 CAO = 7.97
 MgO = 7.31 Na2O = 3.45 K2O = 3.5
 FE2O3 = 11.8 MnO = 3.13 TiO2 = 1.04
 P2O5 = 0.40 ZF2O3 = - LOI = 3.0
 SUM = 98.55 ZF = 115.0 S = 3.35
 Y1 = 17.0 LA = 27.65 CT = 25.9
 PR = 11.11 V2O5 = 14.11 BV = 11.71
 EU = 11.33 SE = 3.0 F3 = 3.01
 DV = 0.0 WC = 7.0 F2 = 7.0
 TN = 0.0 XT = 2.71 L3 = 3.03
 TH = 0.6 J = 3.0 CA = -
 RR = 7.0 SF = 574.5 Y3 = 5.0
 DIF = 2.4 FA = -1.0 ZN = 55.3
 CR = 150.0 Z = - JC = 11.3
 CKY4 = 8.81477 372 = 4.14445 91M30 = 14.4548

Figure C-7.A.: An Example of the Data Summary Available for Each Point On a Drill Hole Trace with A Lithogeochemical Sample Taken and Analyzed. Individual or Multiple Data Sets from this List can be Displayed On the Drill Hole Traces, as with NI/MGO (Figure C-6-A).

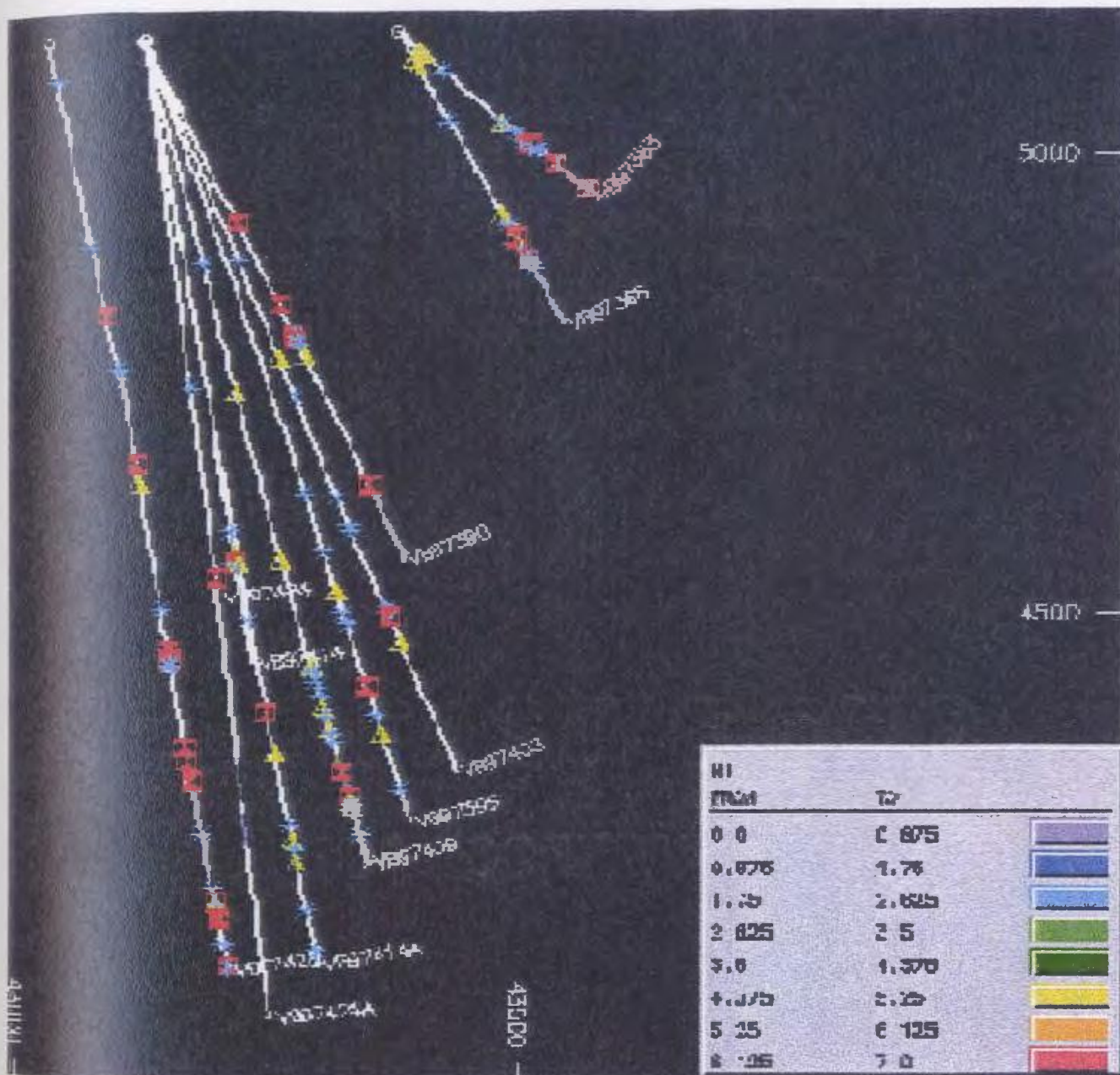


Figure C-8.A.: An Example of Structural Data Displayed On Drill Hole Traces (West Facing Cross Section) with Symbols and Colors Representing Specific Structural Groups.

Coords X,Y,Z = (53823.91, 43010.04, 4990.81)
FILENAME: STER3PT
COLOUR : 17.0 COLOUR17
SYMBOL : 201.0
LSTYLE : 0.0
GROOP :
COMMENTS: cross cut by
ZONE :
TYPE : 0.0
DIPDIRN : 290.0
SDIP : 30.0
DESCRIPT: FRAC-JNTG
STRUCTGP: STR-2

Figure C-9.A.: An Example of the Data Summary Available for Each Point On a Drill Hole Trace with A Recorded Structural Element. Individual or Multiple Data Sets Can be Displayed On the Drill Hole Traces, as with Figure C-8-A..

APPENDIX D:

Relog Data

VB95120

From	To	Original Rock Code
0	0.8	91
0.8	103	1
103	124.5	1.07
124.5	134	32
134	136.1	97
136.1	150.5	32
150.5	151	34
151	154.7	32
154.7	155.6	96
155.6	158.6	32
158.6	160.1	33.5
160.1	173.5	34
173.5	179	32
179	180.8	96
180.8	189.3	1
189.3	218	32
218	227.4	96
227.4	227.8	34
227.8	228.1	96
228.1	229.6	32
229.6	235.1	33
235.1	236.2	34
236.2	238.4	33.5
238.4	240.8	96
240.8	279.5	1

From	To	Relog Rock Code
0	0.8	OB
0.8	124.3	ORGN
124.3	134.5	TRAN
134.5	136.6	MD
136.6	151.1	TRANVN
151.1	153.9	ORGN
153.9	159.3	TRANVN
159.3	173.4	LTTVN
173.4	179.3	TRAN
179.3	180.8	QTZVN
180.8	196	ORGN
196	197.2	TRAN
197.2	204.8	ORGN
204.8	216.1	MARG
216.1	217.7	FBXVN
217.7	227.2	GRDK
227.2	232	FBX
232	234.5	TRAN
234.5	239.8	MARG
239.8	279.5	ORGN

Figure D-2.A.: An Example (VB-95-120) of the Original Lithology Codes (see appendix B for Legend) and the Relog Codes (see Appendix A for legend).

VB95134

From	To	Original Rock Code
0	5.5	91
5.5	56.5	1
56.5	56.55	93
56.55	72.2	1
72.2	82.8	22
82.8	83.5	71
83.5	84.3	22
84.3	92.6	1
92.6	94	88
94	104.8	1
104.8	110.4	21
110.4	111.6	71
111.6	127.3	22
127.3	131.2	97
131.2	135.4	71.7
135.4	157.2	29
157.2	160.1	24
160.1	160.2	96.93
160.2	162.7	24
162.7	163.1	23
163.1	168.5	29
168.5	170.5	71
170.5	171.4	95
171.4	175.9	71
175.9	176.4	43
176.4	176.6	93
176.6	179.3	45
179.3	184.4	44
184.4	191.1	71
191.1	202	24
202	202.05	93
202.05	207.9	24
207.9	208.8	23
208.8	210.5	71
210.5	221.3	22
221.3	221.6	96.93
221.6	222.4	22
222.4	228.8	97
228.8	233.1	93.92
233.1	240.1	71
240.1	242.3	1
242.3	242.9	71
242.9	250.9	1

From	To	Relog Rock Code
0	5.5	OB
5.5	72.2	ORGN
72.2	84.3	MARG
84.3	90	ORGN
90	93.7	VNBX
93.7	105	ORGN
105	117	MARG
117	127.4	TRAN
127.4	131.3	MD
131.3	135.4	GRDK
135.4	162.6	LTT
162.6	163	MARG
163	168.5	LTTVN
168.5	171.6	TRAN
171.6	175.9	GRDK
175.9	184.5	UMVN
184.5	191.1	GRDK
191.1	199.4	TRANVN
199.4	221.5	FBXVN
221.5	222.4	TRAN
222.4	231	MD
231	233	TRAN
233	240.1	QTZVN
240.1	250.9	ORGN

Figure D-3.A.: An Example (VB-95-134) of the Original Lithology Codes (see appendix B for Legend) and the Relog Codes (see Appendix A for legend)

VB95117

From	To	Original Rock Code
0	2.3	91
2.3	50	1
50	53.1	32
53.1	53.2	96
53.2	63.2	1.07
63.2	78.5	32
78.5	79.5	33.5
79.5	90.9	35
90.9	91.5	88
91.5	115.7	35
115.7	117.7	34
117.7	121.9	33.5
121.9	124	35
124	125.2	34
125.2	131.4	88
131.4	133.4	97
133.4	134	35
134	135.3	33.5
135.3	161.5	35
161.5	164	33.5
164	164.2	88
164.2	168.8	33.5
168.8	169.7	88
169.7	172.9	33.5
172.9	185.2	1
185.2	188.1	97
188.1	190.8	1

From	To	Relog Rock Code
0	2.3	OB
2.3	50.3	ORGN
50.3	51.8	MARG
51.8	53.2	TRAN
53.2	63.7	ORGN
63.7	70.2	MARG
70.2	79.6	TRANVN
79.6	95	LTTVN
95	108	LTTBX
108	117.6	LTT
117.6	120.7	TRAN
120.7	125	FBX
125	160.8	LTT
160.8	168	FBXVN
168	172.5	TRANVN
172.5	185.9	ORGN
185.9	188.6	MD
188.6	190.8	ORGN

Figure D-4.A.: An Example (VB-95-117) of the Original Lithology Codes (see appendix B for Legend) and the Relog Codes (see Appendix A for legend).

VB95079

From	To	al Rock Code and Fault Code
0	14.5	91.00 Z
14.5	21.2	1.00 Z
21.2	21.3	1.03 Z
21.3	27.7	1.00 Z
27.7	28	94.03 A
28	29.3	1.00 Z
29.3	29.7	1.03 Z
29.7	58.1	1.00 Z
58.1	58.5	1.03 Z
58.5	59	1.00 Z
59	59.1	97.00 Z
59.1	59.4	1.03 Z
59.4	61.3	1.00 Z
61.3	61.4	1.03 Z
61.4	62.1	1.00 Z
62.1	62.3	1.03 Z
62.3	65.7	1.00 Z
65.7	65.8	1.03 Z
65.8	66.2	1.00 Z
66.2	66.3	1.03 Z
66.3	74.2	1.00 Z
74.2	74.3	95.06 F
74.3	81.3	1.00 Z
81.3	81.9	94.03 F
81.9	96.9	1.00 Z
96.9	99.5	41.00 Z
99.5	102.8	43.00 Z
102.8	107.7	42.00 Z
107.7	107.9	44.00 Z
107.9	108.5	42.00 Z
108.5	108.7	44.00 Z
108.7	109	95.00 F
109	109.5	42.00 Z
109.5	109.7	94.02 F
109.7	110.5	88.00 Z
110.5	114	43.00 Z
114	117.8	42.00 Z
117.8	118.3	1.07 Z
118.3	136.3	1.00 Z
136.3	136.4	1.03 Z
136.4	148	1.00 Z
148	148.6	97.00 Z
148.6	155.3	1.00 Z
155.3	157.9	97.00 Z
157.9	159.6	1.00 Z
159.6	160.1	97.00 Z
160.1	187.8	1.00 Z

Figure D-5 A: An Example (VB-95-079) of the Original Lithology Codes (see appendix B for Legend) and the Fault Relog Codes (A, and F are Individual Intersections from Separate Faults, Z Represents No Fault Intersection).

An Example of an Original Drill Log (VB-95-120) Before being Relogged for
Specific Lithological Relationships.

VB95120 INCO Limited - Exploration Department VB95120
Standard Log

Borehole	: VB95120	Project	: Voisey Bay
Northing	: 6243503.32	Property	: Diamond Field Block 1
Easting	: 554847.83	Township/County	: -
Elevation	: 5178.52 m	Province/State	: Labrador
Hole length	: 279.50 m	Mine	: -
		Country	: Canada
Setup name:		NTS/SECT.T.R.	: 14-D-8
No Assays		UTM Coordinates	: -
		Date Started	: -
Print Date:		Date Completed	: -
08-Feb-1999 20:58		Logged By	: Robert Wheeler
		Logging Started	: June 2, 1995
		Logging Completed	: June 6, 1995
		Drilled By	: Petro
		Drill Type	: -
		Core Size	: NQ
		Hole Size	: -
		Left In Hole	: -
		Section	: 4+00E
		Level	: -
		Heading	: -
		Inclination	: -65
		Grid Name	: -
		Baseline Azimuth	: 85
		Borehole Bearing	: 175
		Assayed For	: -
		Attitude Test Method	: tropani
		Measurement(M/F)	: M
		Claim #	: -
		Anomaly #	: -

VB95120

Page 1

VB95120

VB95120 INCO Limited - Exploration Department VB95120
Standard Log

Survey records

depth	azm	dip	depth	azm	dip
0.00	175.00	-65.00	182.90	177.00	-65.00
91.40	180.00	-65.00	274.30	184.00	-65.00

COMMENTS: Converted to BorlSWin 21-Nov-1997 18:03:28
 GENERATED BY BORIS-VAX 18-JUN-1997 11:06:23.79
 ELEMENTSNI CU CO S FE
 UNITS: % % % % %
 GENERATED BY BORIS-VAX 14-MAY-1997 12:54:22.67
 ELEMENTSSG NI CU CO S
 UNITS: GRN % % % %
 GENERATED BY BORIS-VAX 18-FEB-1997 16:38:44.88
 ELEMENTSNI CU CO S FE
 UNITS: % % % % %
 Expl Grid Coords 0+75N/4+00E
 ENG GRID COORDS ARE 4008.5E, 5073.5N

From m	To m	Description
0.00	0.80	OVERBURDEN
		Overburden

0.80 124.50 GNEISS

Gneiss Quartz-kspars-biotite gneiss. Strongly magnetic with minor cross-cutting felsic pegmatite/veins and quartz veins. 13.7-13.9 - felsic vein

VB95120 INCO Limited - Exploration Department VB95120
Standard Log

From m	To m	Description
		at 45° to c.a. 15.7-15.9 - felsic vein at 80° to c.a. 20.5 - quartz-vein (3cm) with mafic inclusions, 2% cpy 26.3-26.5 - quartz-feldspar vein at 50° c.a. 83.5-83.6 - felsic vein at 50° to c.a. 95.1-95.5 - felsic pegmatite at 20° to c.a. 103.0-124.5 - trace veined cpy in gneiss.

124.50 134.00 TROCTOLITE - BARREN

Troctolite Chilled upper contacts with gneiss barren - trace sulphide

134.00 136.10 MAFIC DIKE

Mafic dyke, aphyric.

136.10 150.50 TROCTOLITE - BARREN

Troctolite as above.

150.50 151.00 TROCTOLITE 15-40% SULPHIDES

Disseminated/semi-massive. Minor quartz veining bottom sequence.

151.00 154.70 TROCTOLITE TR-5% SULPHIDES

Troctolite with trace disseminated, weakly serpentinized and sheared.

VB95120 INCO Limited - Exploration Department VB95120
Standard Log

From m	To m	Description
154.70	155.60	QUARTZ VEIN White quartz vein.
155.60	158.60	TROCTOLITE TR-5% SULPHIDES Troctolite Troctolite with trace disseminated sulphides.
158.60	160.10	TROCTOLITE 5-15% SULPHIDES Troctolite Troctolite with 15% disseminated sulphides.
160.10	169.80	TROCTOLITE 15-40% SULPHIDES Troctolite Troctolite with 50% disseminated sulphides with minor felsic veins.
169.80	173.50	TROCTOLITE 15-40% SULPHIDES Troctolite Troctolite with 30-40% disseminated sulphides.
173.50	179.00	TROCTOLITE TR-5% SULPHIDES Troctolite Troctolite with 2-3% disseminated and semi-massive blebs. Sheared with minor quartz veins (4-5cm) bottom sequence.

VB95120 **INCO Limited - Exploration Department** VB95120
Standard Log

From m	To m	Description
179.00	180.80	QUARTZ VEIN White quartz vein with troctolite inclusions. 5% veined cpy. Contacts at 45° to c.a.
180.80	195.90	GNEISS Gneiss Quartz-kspar-biotite gneiss with minor felsic veins. Trace veined cpy.
195.90	197.20	MAFIC DIKE Mafic dyke, aphyric, weakly magnetic at 50° to c.a.
197.20	204.00	TROCTOLITE-GNEISS MELANGE TR-5% SULPHIDES Mixed zone - (troctolite/gneiss) with trace veined cpy.
204.00	218.00	TROCTOLITE - BARREN Troctolite, sheared and serpentinized with minor quartz-kspar veins, trace sulphide, 217.4 (4cm) semi-massive blebs.
218.00	228.10	PEGMATITE Pegmatite 218.0-227.4 - pegmatite at 50° to c.a. 227.4-227.8 - troctolite

VB95120

Page 5

VB95120

VB95120 INCO Limited - Exploration Department VB95120
Standard Log

From m	To m	Description
		incl? with 25% disseminated sulphides. 227.8-228.1 - felsic pegmatite at 40° to c.a.

228.10 238.40 TROCTOLITE TR-5% SULPHIDES

Troctolite 228.1-229.6 - troctolite with 1-2% disseminated/semi-massive blebs bottom sequence. 229.6-235.1 - troctolite with 5% disseminated/blebby sulphides. Serpentinized with minor felsic veins. 235.1-236.2 - troctolite with 25% disseminated sulphides. 236.2-238.4 - troctolite with 10-15% disseminated sulphides, sheared.

238.40 240.80 PEGMATITE

Felsic pegmatite at 50° to c.a. (239.0 - 239.3) Troctolite inclusions with 10% disseminated sulphides.

240.80 279.50 GNEISS

Gneiss Quartz-biotite-ksp, non-magnetic-weakly magnetic. Minor felsic pegmatites. 247.6 - felsic pegmatite at 55° to c.a. 255.9-256.2 - felsic pegmatite at 50° to c.a. 276.6-276.8 - quartz vein at 20° to c.a. .
 EOH @ 279.50 metres.

An Example of A Relog (VB-95-120) for Specific Lithological Relationships.

VB95120**Relog/97: Dawn Evans**

- 0.0-0.8 Granodioritic orthogneiss. Medium grey with a weak green hue. Medium grained. Nebulous weak fabric at approximately 20° to core axis.
- 0.8-124.3 7.0-7.4 Intense chlorite and quartz veining and sericite. Shared non brecciated appearance.
74.9-119.1 Fabric becomes true gneissosity, Gradational. Fabric still at 10-30° to core axis.
119.1 Contact is brecciated and between rows but fabric at 60° to core axis.
- 124.3-134.5 Fine to medium grained variable (transitional) troctolite. Chill zone from 124.3-124.7. Actual contact is broken, can't get angle. The transitional troctolite is weak to moderately homogeneous with patches of bleached feldspar. Frequent quartzofeldspathic veinlets. Barren to trace sulphides with rare remobilized zones.
128.2-128.3 Quartzofeldspathic vein at 45° to core axis with remobilized sulphides.
128.9-129.0 Cm wide quartzofeldspathic vein with remobilized sulphides.
- 134.5-136.6 Aphyric non-magnetic mafic dyke sharp chilled contacts. Upper contact 65° to core axis. Lower contact 65° to core axis.
- 136.6-151.1 Fine to medium grained variable (transitional) troctolite. Chill zone from 124.3-124.7. Actual contact is broken, can't get angle. The transitional troctolite is weak to moderately homogeneous with patches of bleached feldspar. Frequent quartzofeldspathic veinlets. Barren to trace sulphides with rare remobilized zones.
140.1-10.2 Coarse grained with felsic contamination.
140.2-147.1 More homogeneous. Consistently medium grained. Rare veining but ubiquitous trace fine grained disseminated sulphides.
147.1-147.2 Vein breccia intruding. 3 cm massive sulphide veining at 70° to core axis. Sharp regular contacts and plagioclase inclusions. Other veins of pyroxene rich material and quartzofeldspathic veinlet at top contact. The intermediate area between the veins is mottled. Biotite rich with possible gneissic contamination.

- 148.8-149.1 A sub-horizontal fabric defined. Compositionally looks like troctolite but texturally gneiss. Probably gneiss, very small aphyric digested material. Contacts masked by alteration around quartzofeldspathic vein (20° to core axis) and bleached white feldspars.
- 149.8-149.9 Thin 0.25 cm massive sulphide veinlet along chlorite shear at 50° to core axis.
- 150.4-150.6 Loose irregular semi massive vein (vein breccia with troctite inclusion).
- 150.6-150.8 Brecciated granitic pegmatite. Appears brecciated by vein breccia or early breccia with infilling by vein breccia?
- 150.8-151.1 Marginal zone, mottled, coarse grained. Remobilized sulphides along veinlets of pegmatite granite.
- 151.1-153.9 Intense fabric. Gneiss block at 45° to core axis. Mesocratic. Down section fabric weakens and appears more troctolitic (marginal mixed zone).
- 151.1-152.9 Gneiss block.
- 152.9-153.9 Intercalated gneiss and troctolite (marginal zone).
- 153.9-159.3 153.9-154.9 Transitional troctolite (transitional to chilled). Sharp upper contact at 40° to core axis, distinct from above marginal zone in that it is fine grained, homogenous and no patched zones of bleached felsic material.
- 154.9-155.6 Granitic pegmatite at 10° to core axis.
- 155.6 Homogenous fine to medium grained troctolite. Rare bleached feldspars. Rare quartzofeldspathic veins, Traces to no sulphide.
- 158.5-159.3 1% fine grained disseminated sulphide, net textured, with a 2cm wide vein breccia at 35° to core axis. Appears to be injected along feldspathic vein. Locally honeycomb texture (weak).
- 159.3-173.4 159.3-163.5 Leopard textured troctolite on verge of being leopard breccia. 15% sulphides. Spotty texture resulting from (4 cm) sub-rounded troctolite inclusions (well defined locally) but remnant may be insitu troctolite or early troctolite inclusions?
- 161.8-162.5 Enclaved vein breccia. Disjunctive veins and semi-massive clots with troctolite inclusions. Matrix near clots appears to be leopard breccia with troctolite inclusions but intermediate zones are leopard textured breccia.
- 163.5-173.4 25-30% leopard textured sulphides. Leopard texture is not intensely developed and locally appears as net textured but, when looked at

as a whole, a distinct leopard texture can be observed (homogenous dispersion of sulphides and oikacrysts).

164.6-164.8 Quartzofeldspathic vein (85° to core axis with irregular veined and clotty massive sulphide patches).

167.3-167.5 Quartzofeldspathic vein at 80° to core axis.

167.8-169.7 Leopard texture remains but sulphides have a wavy amalgamated to aligned appearance.

167.8-167.9 2 cm wide semi massive vein of vein breccia. 60° to core axis (intruding leopard textured troctolite).

167.9-173.4 Good leopard textured troctolite (oikocrysts).

173.4-179.3 173.4-173.5 Marginal zone with gneiss block. Upper contact at 35-40° to core axis, very sharp. Strong thin fabric/gneissosity at 15° to core axis.

173.5-174.6 The upper contact is gradational. Barren of sulphide.

Abundant ilmenite. Variable transitional troctolite, no purple plagioclase.

174.6-175.5 Chilled troctolite, no sharp contact except for a rapid grain size deviation over a short interval. Barren of sulphide.

175.5-179.3 Chaotic zone with quartzofeldspathic veins (8cm wide) and intercalated, mottled, highly contaminated troctolite and chilled troctolite and mesocratic material with remnant fabric. Barren of sulphide. It looks like mottled troctolite is enclaved in chilled troctolite.

179.3-180.8 Quartz vein with enclaves of intensely chloritized mafic material with remobilized chalcopryite rich sulphide in loose veins.

180.8-196.0 180.8-190.8 Weakly chloritized granitic orthogneiss. Fabric weak but appears to be at a low angle, approximately 60° to core axis. Mesocratic, medium grey, fine grained, nebulous.

190.8-196.0 Gneiss is very fine grained mesocratic. Only weak remnant fabric left, appearance is showing signs of intercalation of troctolite (but can't call it marginal troctolite yet because compositionally the bulk composition is gneiss).

190.5-190.8 A sharp upper contact 80-70° to core axis with what looks like an inclusion of a quartzofeldspathic rich orthogneiss, lower contact broken.

195.6-195.7 Troctolite dykette at 80° to core axis.

- 196.0-197.2 Chilled aphyric troctolite? Sharp upper contact at 30° to core axis. non-magnetic. lower contact at 50-55° to core axis. Very fine grained. Trace sulphides (chalcopyrite enriched).
- 197.2-204.8 Mesocratic nebulous gneiss again, as above unit.
- 204.8-216.1 204.8-214.7 Good marginal troctolite. upper contact gradational (mixed) not distinct. Good honeycomb texture. Rare trace sulphides. Blotchy appearance. Mottled chlorite down section. Great grain size variation. Fine to coarse grained.
- 214.7-216.1 Ingested gneiss block. Relict fabric at 45° to core axis. Thinly banded, sharp lower contact (irregular) but upper contact is gradational.
- 216.1-217.7 Marginal mottled troctolite. Trace fine grained disseminated sulphides.
- 217.2-217.3 Vein breccia, loose margins. Semi massive with troctolite enclaves does have veined appearance.
- 217.6-217.4 A condensed breccia unit. Highly digested aphyric sub-rounded fragments with 5% sulphides. Cut off by pegmatite.
- 217.7-227.2 217.7-222.2 Granite pegmatite, upper contact at 10° to core axis.
- 222.8-227.2 Chaotic fragmental breccia, highly digested gneiss fragments, aphyric with feldspar phyrlic rims. Elongate to sub-angular (jumbled alignment) (1 - 10 cm in size). 5-10% blotchy sulphide accumulated at sides.
- 227.2-232.0 227.8-228.1 Granitic pegmatite.
- 228.1-229.5 Fine grained, locally aphyric. Rare fine grained to coarse grained blotchy sulphide. Appears to be intercalated with ultramafic. Wispy contacts between ultramafic and troctolite.
- 229.5-232.0 Original fragmental breccia. 3-5% coarse grained blotchy sulphides. 10-15% highly digested gneiss fragments. Elongate sub-rounded to sub-angular. Being condensed in small intervals (not evenly dispersed).
- 232.0 Transitional troctolite. Very fine grained. No fragments. Rare veined sulphides. Rapid transition in fragment occurrence; random in upper zones and condensed over short intervals near lower zones.
- 232.0-234.5 232.0-232.2 Gneiss block, fabric weak at 45° to core axis. Interstitial sulphides.

- 232.0-234.8 Looks like a true variable troctolite (transitional troctolite). Fine grained disseminated sulphide, 1-2%, increasing down section. Weak bleaching of feldspars.
- 234.5-239.8 234.8-235.9 5% fine grained net textured sulphides with a locally wispy alignment. There is a string alignment of the mafic matrix/interstitial material. Locally blotchy sulphides also. Gneissosity at 45° to core axis.
- 235.9-238.9 Marginal zone. Not mottled but strong wispy intercalation of gneissic material (mesocratic) but a strong fabric. Fine grained disseminated (net textured) sulphides along gneissosity at 45° to core axis and locally blotchy coarse grained sulphide patches.
- 238.9-239.6 Granitic pegmatite.
- 239.6-239.8 Chilled troctolite. Blotchy remobilized sulphide (5%).
- 239.8-279.5 239.8-240.8 Granitic pegmatite.
- 240.8-244.7 Light grey granitic gneiss. Weak fabric at 45° to core axis. Fine to medium grained.
- 244.7-247.8 Granitic pegmatite.
- 249.6-250.0 Mylonitic zone with augened early feldspar veins.
- 250.0-250.0 Fabric developed into moderate to intense, thinly banded gneissosity.
- 276.4-277.2 Intense chlorite and sericite alteration.
- 279.5-279.5 End of Hole.

An Example of an Original Drill Log (VB-95-134) Before being Relogged for
Specific Lithological Relationships.

VB95134 **INCO Limited - Exploration Department** VB95134
Standard Log

Borehole	: VB95134	Project	: Voisey Bay
Northing	: 6243478.24	Property	: Diamond Field Block 1
Easting	: 554895.84	Township/County	: -
Elevation	: 5168.23 m	Province/State	: Labrador
Hole length	: 250.90 m	Mine	: -
		Country	: Canada
Setup name:		NTS/SECT.T.R.	: 14-D-8
No Assays		UTM Coordinates	: -
		Date Started	: -
Print Date:		Date Completed	: -
08-Feb-1999 19:40		Logged By	: Dan Lee
		Logging Started	: June 16, 1995
		Logging Completed	: June 20, 1995
		Drilled By	: Petro
		Drill Type	: -
		Core Size	: NQ
		Hole Size	: -
		Left In Hole	: -
		Section	: 4+50E
		Level	: -
		Heading	: -
		Inclination	: -65
		Grid Name	: -
		Baseline Azimuth	: 85
		Borehole Bearing	: 175
		Assayed For	: -
		Attitude Test Method	: tropani
		Measurement(M/F)	: M
		Claim #	: -
		Anomaly #	: -

Survey records

depth	azm	dip	depth	azm	dip
0.00	175.00	-65.00	250.90	183.00	-65.00
128.90	179.00	-64.00			

COMMENTS: Converted to BorlSWin 21-Nov-1997 18:03:33
 GENERATED BY BORIS-VAX 18-JUN-1997 11:06:23.79
 ELEMENTSNI CU CO S FE

UNITS: % % % % %
 GENERATED BY BORIS-VAX 14-MAY-1997 12:54:22.67
 ELEMENTSSG NI CU CO S
 UNITS: GRN % % % %
 GENERATED BY BORIS-VAX 18-FEB-1997 16:38:44.88
 ELEMENTSNI CU CO S FE
 UNITS: % % % % %
 Expl Grid Coords 0+50N/4+50E

From m	To m	Description
0.00	5.50	OVERBURDEN
		Overburden

5.50 72.20 GNEISS

Gneiss Moderately magnetic dioritic gneiss with and Archean mylonite from 23.5 - 24.1 at 45° to c.a. The gneiss has a reddish tinge locally as well as thin granitic veins at variable angles to c.a. Thin granitic veins concentrated from 26.5 - 31.7 at generally low (0-30°) angles to c.a. From 54.0 - 55.7 high strain zone with pinch and swell textures developed. Gougy core at 56.5 with core angles at 50° to c.a. Magnetic nature of the gneiss decreases below 62.1m

72.20 82.80 TROCTOLITE - BARREN

Coarse Troctolite The troctolite has some reduction in grain size but no well developed chill with some gneissic fragments near the contact. Becomes really coarse grained below 73.8m

82.80 83.50 GRANITE

From 82.8 - 83.5 is a coarse white granitic vein with traces of sulphides. Contacts at 20° to c.a.

83.50 84.30 TROCTOLITE TR-5% SULPHIDES

Coarse textured troctolite with a few gneissic fragments

From m	To m	Description
84.30	104.80	GNEISS Gneiss Dioritic gneiss with top contact at 50-55° to c.a. with local white granitic stringers with traces of sulphide. 89.8 - 92.1 - increased chalcopryite below 89.8 along fractures, <1% sulphides 92.1 - 92.2 - mineralized white granitic vein with 5-10% sulphides. The vein is at 65° to c.a. 92.2 - 92.6 - as per 89.8 - 92.1 92.6 - 94.0 - massive sulphide vein at 10° to c.a. The zone intruded has between 60-70% total sulphides 94.0 - 94.4 - < 1% chalcopryite stringers in fractures at 60° to c.a. 94.4 - 104.8 - Dioritic gneiss with barren factures at 50° to c.a.
104.80	110.40	TROCTOLITE - BARREN Troctolite Slight reduction in grainage against the contact but rapidly becomes coarse grained. Traces of sulphide for first 1.0m then barren of sulphides. Several white granitic stringers from 106.8 - 106.9 at 40° to c.a., 110.4 - 111.6 at 60° to c.a., 114.0 - 114.1, 120.1 - 120.2 both at 55° to c.a.
110.40	111.60	GRANITE Granite White granite stringer
111.60	123.10	TROCTOLITE - BARREN Troctolite as above.
123.10	127.30	TROCTOLITE TR-5% SULPHIDES Troctolite as above 1% sulphides.
127.30	131.20	MAFIC DIKE Mafic dyke, irregular bottom but sharp upper contact at 65° to c.a.
131.20	134.50	PEGMATITE White pegmatite grained with local magnetite crystals and rounded troctolite

From m	To m	Description
		clasts.

134.50 168.50 TROCTOLITE 40-75% SULPHIDES

Troctolite 135.4 - 138.7 - top sequence leopard rock with 50 - 55% sulphides
 138.7 - 143.2 - leopard rock with 50-60% sulphides. A slight fabric was noted within
 the sulphides especially the chalcopryrite veins at 45° to c.a. 143.2 - 157.0 - leopard
 rock with 60-70% sulphides 157.0 - 157.2 - granitic stringer at 60° to c.a. 157.2 -
 160.1 - leopard rock with 45-50% sulphides and a slight orientation at 60° to c.a.
 160.1 - 160.2 - quartz vein with small amount of fault gouge. 160.2 - 162.7 leopard
 rock with 50% sulphides 162.7 - 163.1 - reduced sulphide (10-15%) with a few
 chalcopryrite stringers at 45° to c.a. 163.1 - 164.6 - leopard rock with 50-60% sulphide
 with minor gouge at 163.3 164.6 - 165.2 - white granitic vein with contacts at 75° to
 c.a. 165.2 - 168.5 - leopard rock with weak orientation of the sulphides at 50° to c.a.
 Total 50-75% sulphides

Bottom Sequence

168.50 175.90 GRANITE

White/pink granite with 70° to c.a. contacts 170.5 - 171.4 - broken core with
 bottom sequence (fault??) black serpentized ultramafic clasts 10% sulphides 171.4
 - 175.9 - coarse pink granite.

175.90 184.40 TROCTOLITE BRECCIA 15-40% SULPHIDES

Troctolite 175.9 - 176.4 - bottom sequence with black serpentized clasts, and
 gneissic clasts with spinel on margins 10-20% sulphides 176.4 - 176.6 - broken
 gougy core 176.6 - 178.3 - local ultramafic clasts in troctolite with 5-8% sulphides
 178.3 - 179.3 - bottom sequence with serpentized and gneissic clasts 2-4cm veins
 of massive sulphide appear to be brecciating the troctolite. Massive sulphide from
 179.3 - 179.9. Overall the interval has 75% sulphides. 179.9 - 184.4 - bottom
 sequence with massive vein sulphides 2-5cm wide brecciating the troctolite. Local
 ultramafic clasts. 30-40% sulphides

184.40 191.10 GRANITE

From m	To m	Description
		White coarse granite

191.10 208.80 TROCTOLITE 40-75% SULPHIDES

Troctolite 191.1 - 200.9 - leopard rock with some oikocrysts up to 1.0cm. Some sort of banding at 45° to c.a. Total of 50% sulphides. Some exotic fragments. One zone with lesser sulphides 200.5-200.9, 3-5% sulphides. 200.9 - 207.9 - 40% sulphides with a quartz vein from 204.1- 04.3 minor fault gouge at 202.0 207.9 - 208.8 - 10% sulphides

208.80 210.50 PEGMATITE

Pink granite pegmatite

210.50 222.40 TROCTOLITE TR-5% SULPHIDES

Troctolite 210.5 - 217.5 - bottom sequence troctolite with 5% blotchy sulphides. Blocky core with quartz vein from 212.3 - 212.4 at 40° to c.a. 217.5 - 222.4 - troctolite with traces of sulphides becoming blocky with local gouge zones and a quartz vein from 221.3 - 221.6 at 40° to c.a.

222.40 228.80 MAFIC DIKE

Massive fine grained mafic dyke

228.80 233.10 FAULT

Gougy faulty zone

233.10 240.10 GRANITE

Pink granite dyke

240.10 242.30 GNEISS

Dioritic gneiss

VB95134 **INCO Limited - Exploration Department** VB95134
Standard Log

From m	To m	Description
242.30	242.90	GRANITE Pink granite dyke with contacts at 45° to c.a.
242.90	250.90	GNEISS Dioritic Gneiss. EOH 250.90 metres..

An Example of A Relog (VB-95-134) for Specific Lithological Relationships.

VB95134**Relog/97: Dawn Evans**

- 0.0-5.5 Overburden.
- 5.5-72.2 Granitic gneiss. Mesocratic, grey with weak green hue. Altered, baked appearance. Fabric is at approximately 20° to core axis (weak to moderate development - nebulous). Distinct lensoidal biotite zones. Medium grained.
- 26.5-28.3 Submylonitic with weak hematite stains. Fabric at 30° to core axis.
- 29.2-30.0 Submylonitic with epidote and quartz veins (0.5cm wide). Looks like a brittle infilling. Moderate hematite.
- From 30.0 Fabric is more fine grained and better developed. 30° to core axis.
- 52.7-56.0 Mylonitic to submylonitic with augened feldspathic pegmatite.
- 72.2-84.3 Gradational contacts. A gradual increase in mesocratic appearance and loses fabric. Develops into true marginal troctolite with honeycomb textures. Barren to rare trace sulphides, grey blue, locally mottled.
- 75.7-75.8 Granitic pegmatite.
- 80.2-84.3 Rare relict gneiss (moderately developed and honeycomb texture no longer cloudy but distinct crystal outlines from gneiss). Mesocratic.
- 82.7-83.5 Quartzofeldspathic pegmatite (more syenitic with mostly anorthosite plagioclase).
- 83.5-84.3 1% remobilized sulphides in marginal troctolite.
- 84.3-90.0 Granodiorite, thinly and intensely banded at 30-35° to core axis. Upper contact sharp and defined by granite vein. Appears submylonitic. Frequent quartzofeldspathic veins (coarse grained) with troctolite inclusions. Quartzofeldspathic veins at 84.6-84.9, 84.2-84.3, and 85.9-86.3m.
- 90.0-93.7 90.0-92.7 Trace pyrrhotite/pentlandite/chalcopyrite veinlets ≤ 1cm wide at 45-50° to core axis.
- 92.7-93.7 Loose massive sulphide vein at 30° to core axis. Approximately 35-40% silicate rich inclusions. Contacts are parallel to

fabric. Pyrrhotite/pentlandite/ chalcopyrite present. Fine grained sulphide crystals.

- 93.7-105.0 93.7-97.5 Trace stringer veinlets as above, and rare loose semi-massive veins (30% sulphides) 5cm wide and at 45-50° to core axis.
 97.5-105.0 Gneissic fabric shallowing to 45-50° to core axis and more granitic (leucocratic) down section. Still have sulphide stringers and rare chalcopyrite blebs.
- 105.0-117.0 105.0-110.5 Marginal troctolite. Good honeycomb texture. Contact mixed but distinct. Rare trace remobilized chalcopyrite. Frequent quartzofeldspathic veins, 50-80° to core axis, 5-9cm in width. Local mottle zones near veins.
 110.5-111.5 Quartzofeldspathic pegmatite.
 111.5-117.0 Marginal troctolite, as above. Feldspar vein (massive texture at 30-40° to core axis, 8cm wide).
- 117.0-127.4 Transitional troctolite. Quartzofeldspathic vein defines contact. Troctolite is coarse grained to locally pegmatitic. Trace fine to medium grained disseminated sulphides. Frequent feldspar veins with no honeycomb textures or contamination. Very regular grain size - homogeneous (like good variable troctolite). Locally mottled adjacent to veins.
- 127.4-131.3 Aphyric non-magnetic mafic dyke. Upper contact is destroyed, lower contact is intercalated with quartzofeldspathic vein.
- 131.3-135.4 Granitic pegmatite.
- 135.4-162.6 Good leopard textured troctolite with clotting or filter pressing of sulphides at the margins. 35-45% sulphides. No fragments or vein breccia present. Very homogeneous.
 150.5-162.6 A weak wavy alignment of sulphides. Infrequently appears to be a result of oikacrysts pushing out, other times it is ambiguous.
 156.9-157.1 Microgranite vein.
 159.4-160.6 Remobilized chalcopyrite enrichment and weak chlorite and quartzofeldspathic veining.

- 162.6-163.0 Marginal troctolite. Honeycomb, not cloudy, by more feldspar phyrlic (more defined) probably gneissic contamination (a block). Intense sulphide veining in fractures at 50-60° to core axis.
- 163.0-168.5 163.0-163.3 Vein breccia. Net sulphides, 40%, with elongate (3cm long) gneiss (increased digestion, aphyric) fragment. Lower contact is sheared with intense chlorite present.
 163.3-168.5 Leopard textured troctolite. 35-40% sulphides. Wavy alignment again. Good oikacrysts. Infrequent chalcopyrite enrichment.
 164.7-165.3 Quartzofeldspathic veins.
- 168.5-171.6 168.5-170.6 Quartzofeldspathic vein.
 170.6-171.6 Intense chloritic troctolite. Massive with ≤ 15% coarse grained blebby sulphides.
- 171.6-175.9 Granitic pegmatite.
- 175.9-184.5 Highly serpentinized ultramafic intruded by blebby to loose vein breccia. Overall, 15% sulphides. Vein breccia contains ultramafic fragments.
- 184.5-191.1 Granitic pegmatite.
- 191.1-199.4 191.1-192.3 Net textured sulphides, as above. There appears to be troctolite inclusions. Rare vein breccia (blotchy sulphides, sharp contacts). Continues with sequences below.
- 199.4-221.5 199.4-208.7 5-10% small aphyric fragments, subangular. Infrequent gneissic core remains. Approximately 25-30% sulphides.
 200.0-200.1 Vein breccia (massive sulphide). Sharp but irregular contacts. 70% sulphides.
 Frequent quartz veins (204.7-205.0, 208.7-210.5).
 210.5-221.0 Original fragmental breccia continues but with approximately 30% fine to medium grained disseminated sulphides. Subangular fragments, aphyric, no alignment.
 212.3-212.5 Sheared quartzofeldspathic vein at 80° to core axis. Troctolite is intensely chloritized proximal to this zone. Original fragment with coarse grained blotchy sulphides (3-5%) concentrated into horizons. Fragments are rare but consistently aphyric.

- 221.0-221.5 Quartzofeldspathic veins intensely shearing troctolite. Very chloritic.
- 221.5-222.4 Intercalated quartzofeldspathic veins (sheared) and chloritic troctolite? And relict gneiss. No sulphide.
- 222.4-231.0 222.4-230.4 Aphyric, non-magnetic dyke. Brittle feldspar infilling veinlets. Highly fractured.
230.1-231.0 Intercalated quartzofeldspathic vein and mafic dyke.
- 231.0-233.0 Intense chlorite breccia zone. Rubbly, highly fractured, fault gouge.
- 233.0-240.1 Quartzofeldspathic pegmatite. 2 mechanical fractures. Moderate hematite.
- 240.1-250.9 240.1-246.1 Granodiorite. Fine to medium grained. Light grey. Weak fabric development at approximately 45° to core axis.
250.9 End of Hole.

An Example of an Original Drill Log (VB-95-117) Before being Relogged for
Specific Lithological Relationships.

VB95117 **INCO Limited - Exploration Department** VB95117
Standard Log

Borehole	: VB95117	Project	: Voisey Bay
Northing	: 6243451.94	Property	: Diamond Field Block 1
Easting	: 554847.37	Township/County	: -
Elevation	: 5172.96 m	Province/State	: Labrador
Hole length	: 190.80 m	Mine	: -
		Country	: Canada
Setup name:		NTS/SECT.T.R.	: 14-D-8
No Assays		UTM Coordinates	: -
		Date Started	: -
Print Date:		Date Completed	: -
08-Feb-1999 19:51		Logged By	: Robert Wheeler
		Logging Started	: May 31, 1995
		Logging Completed	: June 2, 1995
		Drilled By	: Petro
		Drill Type	: -
		Core Size	: NQ
		Hole Size	: -
		Left In Hole	: -
		Section	: 4+00E
		Level	: -
		Heading	: -
		Inclination	: -65
		Grid Name	: -
		Baseline Azimuth	: 85
		Borehole Bearing	: 175
		Assayed For	: -
		Attitude Test Method	: unknown
		Measurement(M/F)	: M
		Claim #	: -
		Anomaly #	: -

Survey records

depth	azm	dip
0.00	175.00	-65.00

COMMENTS: Converted to BorlSWin 21-Nov-1997 18:03:27
 GENERATED BY BORIS-VAX 18-JUN-1997 11:06:23.79
 ELEMENTSNI CU CO S FE

VB95117

INCO Limited - Exploration Department Standard Log

VB95117

UNITS: % % % % %
 GENERATED BY BORIS-VAX 14-MAY-1997 12:54:22.67
 ELEMENTSSG NI CU CO S
 UNITS: GRN % % % %
 GENERATED BY BORIS-VAX 18-FEB-1997 16:38:44.88
 ELEMENTSNI CU CO S FE
 UNITS: % % % % %
 Expl Grid Coords 0+25N/4+00E
 ENG GRID COORDS ARE 4007.6E, 5020.9N

From m	To m	Description
0.00	2.30	OVERBURDEN Overburden
2.30	30.90	GNEISS Gneiss Quartz-kspars-biotite gneiss strongly magnetic. Cross-cut by felsic pegmatites (2cm-1m)
30.90	32.10	PEGMATITE Felsic pegmatite with mafic inclusions (troctolite) sheared.
32.10	50.00	GNEISS Gneiss as above
50.00	53.20	TROCTOLITE TR-5% SULPHIDES Disseminated Zone (Top) Troctolite with various amounts of disseminated and veined sulphides. 50 - 53.1 - troctolite with trace sulphides. 53.1 - 53.2 - felsic vein
53.20	63.20	GNEISS

VB95117

Page 2

VB95117

VB95117 **INCO Limited - Exploration Department** VB95117
Standard Log

From m	To m	Description
		Gneiss as above (quartz-kspars-biotite) with 1-2% vein sulphides.

63.20 78.50 TROCTOLITE TR-5% SULPHIDES

Troctolite 63.2 - 78.5 - troctolite with 5% vein and disseminated sulphides, sheared.

78.50 131.40 TROCTOLITE 40-75% SULPHIDES

78.5 - 79.5 -

Troctolite with 15-20% disseminated sulphides 79.5 - 90.9 - troctolite with 60-80% disseminated sulphides, locally sheared. 90.9 - 91.5 - massive sulphide 91.5 - 115.7 - troctolite with 75% disseminated sulphides. 115.7 - 117.7 - troctolite with 50% disseminated and veined sulphides. 117.7 - 121.9 - troctolite with 5-10% disseminated and veined sulphides. Sheared with minor fault gouges. Serpentinized. 121.9 - 124.0 - troctolite with 70% disseminated sulphides. 124.0 - 125.2 - troctolite with 25% veined and semi-massive sulphides. 125.2 - 131.4 - troctolite with 80% disseminated sulphides.

131.40 133.40 MAFIC DIKE

Mafic dyke, aphyric, weakly magnetic.
 Contacts at 65° to c.a.

133.40 161.50 TROCTOLITE 40-75% SULPHIDES

Troctolite as above 133.4 - 134.0 - troctolite with 60% disseminated sulphides. 134.0 - 135.3 - troctolite with 10% veined sulphides, serpentinized. 135.3 - 161.5 - troctolite with 70-80% disseminated sulphides.

161.50 164.00 TROCTOLITE 5-15% SULPHIDES

Troctolite with 10-15% veined and disseminated sulphides.

VB95117 **INCO Limited - Exploration Department** VB95117
Standard Log

From m	To m	Description
164.00	169.70	TROCTOLITE 40-75% SULPHIDES 164.0 - 164.2 - massive sulphide. 80% cpy, vein. 164.2 - 168.8 - troctolite with 5-10% veined sulphides. Sheared and strongly serpentinized. 168.8 - 169.7 - massive sulphide
169.70	172.90	TROCTOLITE-GNEISS MELANGE 5-15% SULPHIDES Mixed Zone - Gneiss with minor troctolite. Sheared with quartz veining 5-10% veined sulphides.
172.90	183.10	GNEISS Gneiss Quartz-kspars-biotite with trace veined sulphides (first 3-4m)
183.10	188.10	MAFIC DIKE Mafic dyke, aphyric, strongly magnetic Contacts at 50° to c.a.
188.10	190.80	GNEISS EOH 190.80 metres.

An Example of A Relog (VB-95-117) for Specific Lithological Relationships.

VB95117

Relog/97: Dawn Evans

- 0.0-2.3 Overburden.
- 2.3-50.3 Granodioritic gneiss. Medium grained. Medium to dark grey. Early injected feldspathic pegmatite. Weak to moderate gneissosity at 10° to core axis. Becoming diorite down section and mesocratic dark grey.
- 27.0-27.1 Sheared at 35° to core axis. Weak hematization. Quartz and chlorite veinlets defining shear. Remobilized chalcopyrite (trace to 1%).
- 31.2-32.3 Submylonite. Ribboned and boudinaged pegmatite veins.
- 44.4 Rare sulphide stripes parallel to fabric.
- 50.3-51.8 Marginal zone. Dark grey. Barren. Fine grained chill zones. Frequent quartzofeldspathic pegmatite (irregular). Intercalated troctolite and gneiss. Massive aphyric zones are troctolite then there are coarser mottled zones with a weak fabric (gneiss). Contact broken but approximately 70° to core axis.
- 51.8-53.2 Chilled troctolite. Barren. Massive aphyric lower contact cut by irregular granitic to quartzofeldspathic pegmatite.
- 53.2-63.7 Mesocratic dark grey Dunite. Good fabric at margins, 10-30° to core axis. Trace to 1% sulphide stringers.
- 56.7-56.8 Vein breccia. Semi-massive loose (approximately 10° to core axis) irregular vein with troctolite inclusion.
- 58.0-58.1 Loose semi-massive vein breccia. Irregular with approximately 30% sulphides. Adjacent to granitic pegmatite.
- 58.1-63.7 Disseminated to veined sulphides (remobilized), trace to 1%.
- 63.7-70.2 Marginal troctolite. Trace fine grained disseminated or coarse angular (interstitial) sulphides. Honeycomb textures - feldspathic contamination. Mottled with chlorite, locally pegmatitic. Upper contact is not sharp, just nebulous gneiss which gradually loses all gneissic signatures.
- 70.2-79.6 Gradually loses contaminants and becomes a variable troctolite - transitional troctolite with local variations in grain size. Trace (rare)

- blotchy sulphides. Locally coarse grained to pegmatitic. Purple to medium grey.
- 71.6-71.7 Vein breccia. Semi-massive clot with troctolite inclusion. Irregular margins.
- 75.5-75.6 Vein breccia, as above, with coarse grained interstitial/angular sulphides.
- 79.6-95.0 79.6-84.2 5-7% fine grained disseminated sulphides. Quiet in appearance. No fragments. Looks like the start of a weak leopard textured troctolite. Right now, sulphides are outlining dark spots that may be actual crystals from crystallization. Then, as we go down, sulphides are settling and oikacrysts are actually growing.
- 84.2-90.5 No sharp contact. 35-40% fine grained disseminated sulphides. 10-15% oikacrysts. Remainder is net textured, therefore weak leopard textured troctolite.
- 90.9-91.5 Massive sulphide. Sharp contact at 70° to core axis. Lower contact appears to be irregular with soft sedimentary features, slumping down into troctolite.
- 91.5-95.0 Leopard textured troctolite, as above, but 25-35% sulphides.
- 95.0-108.0 ¼ core all jumbled and out of order, but appears to be leopard textured troctolite, as above, with small intervals of leopard breccia with both aphyric subangular gneiss and troctolite fragments.
- 108.0-117.6 108.0-116.0 Leopard textured troctolite mode. Oikacrysts. Same as above.
- 116.0-116.8 Increased chlorite alteration. Streaky remobilized sulphides (chalcopyrite rich). Transitional troctolite. Splotchy appearance, possibly rare fragment.
- 116.8-117.6 Weak leopard textured troctolite (leopard breccia). Difficult to say, textures masked by increase in leopard textured troctolite (pale green glassy alteration) with dark spots, possible fragments.
- 117.6-120.7 117.6-118.8 Transitional troctolite. Increase chlorite alteration. Fine grained to blotchy coarse grained sulphides (net/random textured). Matrix aphyric troctolite.
- 118.7-118.8 Irregular vein breccia, breccia troctolite into angular blocks. 5% sulphides.

- 118.8-120.7 Shear zone (quartzofeldspathic subvertical veinlets). Increased chlorite alteration. Rubbly but probably transitional troctolite. 1-2% sulphides.
- 120.7-125.0 120.7-121.7 Chilled troctolite with rare medium grained sulphides. Aphyric.
- 121.7-121.8 Contact zone. Gradational with 1-2% very fine grained net textured sulphides and feldspathic fragments.
- 121.8-124.0 Good leopard textured troctolite (35-40% sulphides). First 10cm sulphides are clotty with net textured sulphides – probably an inclusion of original troctolite.
- 124.0-125.0 10% troctolite and digested gneiss fragments. Chaotic. 3-5% net sulphides, fine grained to coarse grained and blotchy. Fragments are sub-rounded (difficult to see - ¼ core and lower contact broken).
- 125.0-160.8 125.0-132.1 Leopard textured troctolite. 35% and increasing to 45-50% down section. Weak intermittent oikacrysts, appears to be some that are irregular, possibly troctolite inclusions.
- 125.0-125.3 Clotty net sulphides with troctolite inclusions.
- 132.1-133.4 Aphyric chilled troctolite. Trace very fine grained disseminated sulphides. Top contact broken, core jumbled and ¼ not insitu. ?Lower contact. Fine grained, not aphyric and sharp, but only because marked by sulphides and not a chill or composite.
- 133.4-133.8 Leopard textured troctolite with 20% sulphides.
- 133.8-135.2 Fine grained chilled troctolite/normal. Dark grey, unaltered. Upper contact broken, lower contact gradational with common vein breccia. 1cm to 3cm thick loose veins or clotty sulphides with troctolite inclusions.
- 135.3-154.3 Good leopard textured troctolite. Gradational contact defined by a gradual increase in sulphides. Some appear irregular in shape (but not as inclusions). This could be some crystallization. A weak wavy alignment as sulphides accumulate around margins of oikacrysts. 35-50% sulphides. A reverse seive effect: oikacrysts squeezing sulphides back and where sulphide percentage is high, the density increases and they amalgamate. As sulphides increase down section, it becomes difficult to tell if oikacrysts or troctolite inclusions.
- 154.3-160.8 25-30% sulphides. No exact contact, but oikacrysts are large, up to 3 or 4cm. May represent crystallization, plus sulphides are

medium grained leopard textured troctolite and not fine grained as is usually seen. Some may be troctolite inclusions.

- 160.8-168.0 Clotty vein breccia present. Poorly digested fragments, cloudy to feldspar phyrlic with reaction rims developed. 3-5% fine to coarse grained disseminated sulphides. No sharp upper contact, only a local decrease in sulphides and a 1cm wide
163.0-168.0 Mottled, locally chilled rare trace sulphides. Core broken/jumbled. Weak feldspar contamination. Zones of relict gneiss fabric.
164.0 Vein breccia. Loose 30% sulphides.
- 168.0-172.5 168.0-168.7 Massive sulphide vein, 90% sulphide. Chalcopyrite depleted. Loop textures. Troctolite inclusions. Upper contact broken but sharp, lower contact broken, approximately 45° to core axis.
168.7-172.5 Marginal troctolite. Prominent chill zones. Vein breccia at 170.4-170.6m. 70% sulphides. Troctolite inclusions. Upper contact broken but at 45° to core axis, lower contact irregular.
170.7 Quartzofeldspathic shear zone (intense with gneiss and troctolite inclusions and remobilized sulphides).
- 172.5-185.9 Granodioritic gneiss. Light to medium grey. Thin bands, but strong gneissosity, 40-45° to core axis. Locally biotite rich bands. Appears weakly baked.
- 185.9-188.6 Aphyric, strongly magnetic dyke – mafic.
- 188.6-190.8 Granodioritic gneiss. Light to medium grey. Thin bands, but strong gneissosity, 40-45° to core axis. Locally biotite rich bands. Appears weakly baked.
190.8 End of Hole.

An Example of an Original Drill Log (VB-95-079) Before being Relogged for
Specific Lithological Relationships.

VB95079

INCO Limited - Exploration Department

Standard Log

VB95079

Borehole	: VB95079	Project	: Voisey Bay
Northing	: 6243324.93	Property	: Diamond Field Block 1
Easting	: 555739.20	Township/County	:
Elevation	: 5082.54 m	Province/State	: Labrador
Hole length	: 187.80 m	Mine	:
		Country	: Canada
Setup name:		NTS/SECT.T.R.	: 14-D-8
No Assays		UTM Coordinates	:
		Date Started	:
Print Date:		Date Completed	:
08-Feb-1999 20:01		Logged By	: Robert Wheeler
		Logging Started	:
		Logging Completed	:
		Drilled By	:
		Drill Type	:
		Core Size	: NQ
		Hole Size	:
		Left In Hole	:
		Section	:
		Level	:
		Heading	:
		Inclination	:
		Grid Name	:
		Baseline Azimuth	: 85
		Borehole Bearing	:
		Assayed For	:
		Attitude Test Method	:
		Measurement(M/F)	: M
		Claim #	:
		Anomaly #	:

Survey records

depth	azm	dip	depth	azm	dip
0.00	175.00	-65.00	185.80	176.00	-65.00
20.40	176.00	-64.00			

COMMENTS:

Converted to BorISWin 21-Nov-1997 18:03:12
 GENERATED BY BORIS-VAX 18-JUN-1997 11:06:23.79

VB95079

Page 1

VB95079

VB95079

INCO Limited - Exploration Department

Standard Log

VB95079

ELEMENTSNI CU CO S FE
 UNITS: % % % % %
 GENERATED BY BORIS-VAX 14-MAY-1997 12:54:22.67
 ELEMENTSSG NI CU CO S
 UNITS: GRN % % % %
 GENERATED BY BORIS-VAX 14-MAY-1997 10:11:54.48
 ELEMENTSSG NI CU CO S
 UNITS: GRN % % % %
 GENERATED BY BORIS-VAX 18-FEB-1997 16:38:44.88
 ELEMENTSNI CU CO S FE
 UNITS: % % % % %
 Expl Grid Coords 0+90S/13+00E
 ENG GRID COORDS ARE 4902.0E, 4910.0N

From m	To m	Description
0.00	14.50	OVERBURDEN
		Overburden.

14.50 95.90 GNEISS

Gneiss; dark grey; medium grained, equigranular; moderately magnetic; strong foliation at 40-50 degrees to core axis; major and minor felsic pegmatites throughout
 22.4-22.5 - felsic pegmatite at 35 degrees to core axis 32.3-33.4 - felsic pegmatite at 40 degrees to core axis; minor mafics chloritized with biotite / magnetite +/- trace sulphides; the pegmatite shows a mylonitic fabric locally 39.6 - 4cm felsic pegmatite at 25 degrees to core axis 57.4-57.6 - felsic pegmatite at 10 degrees to core axis
 59.0-59.1 - mafic dyke at 80 degrees to core axis; fine grained; non-magnetic
 67.6-68.1 - felsic pegmatite at 30 degrees to core axis; minor blotches of chloritized mafic 75.05 - 2cm felsic pegmatite at 40 degrees to core axis 81.6-81.7 - felsic pegmatite at 40 degrees to core axis; highly strained (sub-mylonite) upper contact.

95.90 99.50 TROCTOLITE - BARREN

Troctolite; dark grey / black with pink plagioclase phenocrysts; non-magnetic; 0% to trace sulphides.

VB95079

Page 2

VB95079

From m	To m	Description
99.50	106.40	TROCTOLITE 5-15% SULPHIDES Troctolite with 10-15% disseminated sulphides; locally, sulphide blebs are with visible chalcopryite and pentlandite 103.5-106.5 - blotchy with serpentinized blebs.
106.40	109.70	TROCTOLITE TR-5% SULPHIDES Troctolite with only trace sulphides 107.96-108.05 - massive sulphides bleb with chalcopryite and pentlandite 108.58-108.7 - massive sulphides with 30% chalcopryite.
109.70	110.45	MASSIVE SULFIDE Massive sulphides; massive pyrrhotite with 2-3% magnetite, 2% pentlandite, and 4% chalcopryite.
110.45	113.60	TROCTOLITE 5-15% SULPHIDES Troctolite with 5-10% blebs of sulphides; serpentinized blotches (bottom).
113.60	117.00	TROCTOLITE TR-5% SULPHIDES Troctolite with trace to less than 5% disseminated sulphides.
117.00	117.50	PEGMATITE Quartz - potassium feldspar pegmatite at 40 degrees to core axis with chloritized mafic and minor sulphides.
117.50	117.70	TROCTOLITE - BARREN Troctolite, fine grained (fresh), with only trace sulphides.
117.70	155.90	GNEISS

VB95079 **INCO Limited - Exploration Department** VB95079
Standard Log

From m	To m	Description
		Gneiss; dark grey; medium grained; weakly magnetic; strong foliation at 30 degrees to core axis; minor felsic pegmatites and mafic dykes 134.6 - 2cm felsic pegmatite at 30 degrees to core axis 148.6-149.2 - mafic dyke at 70 degrees to core axis; fine grained; weakly magnetic.

155.90 157.90 MAFIC DIKE

Mafic dyke at 40 degrees to core axis; fine grained; weakly magnetic.

157.90 187.80 GNEISS

Gneiss, as above 177.2-177.5 - felsic pegmatite at 50 degrees to core axis; sulphide blebs (pyrrhotite) 181.3-181.5 - felsic pegmatite at 40 degrees to core axis 187.0-187.4 - felsic pegmatite at 50 degrees to core axis; sulphide blebs.

An Example of A Relog (VB-95-079) for Structural Information.

VB95079**Relog/97: Dawn Evans**

0.0-14.5	Overburden.																												
14.5-95.9	<table><tr><td>21.2-21.3</td><td>Hematite staining. Quartz vein, brecciated gneiss.</td></tr><tr><td>27.7-28.0</td><td>Quartz vein, brecciated gneiss and hematite staining. 20-30° to core axis.</td></tr><tr><td>29.3-29.7</td><td>Hematite staining and rubbly quartz veinlets, brecciated gneiss.</td></tr><tr><td>32.0-33.9</td><td>Granitic pegmatite (annealed), early</td></tr><tr><td>58.1-58.5</td><td>Rare (localized) quartz veinlets, brecciated gneiss, and hematite staining.</td></tr><tr><td>59.0-59.1</td><td>Aphyric non-magnetic (diabasic) mafic dyke.</td></tr><tr><td>59.1-59.4</td><td>Quartz veinlets, brecciated gneiss, and hematite at 50° to core axis.</td></tr><tr><td>61.3-61.4</td><td>Fresh quartz veining and hematite staining at 40° to core axis (minor breccia).</td></tr><tr><td>62.1-62.3</td><td>Quartz veinlets at 40° to core axis. Hematite staining (no breccia) (infilling brittle fractures).</td></tr><tr><td>65.7-65.8</td><td>Hematite and quartz veinlet at 50° to core axis.</td></tr><tr><td>66.2-66.3</td><td>Hematite and quartz veinlet at 30° to core axis.</td></tr><tr><td>67.3-67.9</td><td>granitic pegmatite with quartz recrystallized in tension gashes at 30° to core axis.</td></tr><tr><td>74.2-74.3</td><td>Chlorite? Fractures or shears at 10° to core axis.</td></tr><tr><td>81.6-81.9</td><td>Hematite staining (intense), quartz veins at 30° to core axis (brecciated gneiss).</td></tr></table>	21.2-21.3	Hematite staining. Quartz vein, brecciated gneiss.	27.7-28.0	Quartz vein, brecciated gneiss and hematite staining. 20-30° to core axis.	29.3-29.7	Hematite staining and rubbly quartz veinlets, brecciated gneiss.	32.0-33.9	Granitic pegmatite (annealed), early	58.1-58.5	Rare (localized) quartz veinlets, brecciated gneiss, and hematite staining.	59.0-59.1	Aphyric non-magnetic (diabasic) mafic dyke.	59.1-59.4	Quartz veinlets, brecciated gneiss, and hematite at 50° to core axis.	61.3-61.4	Fresh quartz veining and hematite staining at 40° to core axis (minor breccia).	62.1-62.3	Quartz veinlets at 40° to core axis. Hematite staining (no breccia) (infilling brittle fractures).	65.7-65.8	Hematite and quartz veinlet at 50° to core axis.	66.2-66.3	Hematite and quartz veinlet at 30° to core axis.	67.3-67.9	granitic pegmatite with quartz recrystallized in tension gashes at 30° to core axis.	74.2-74.3	Chlorite? Fractures or shears at 10° to core axis.	81.6-81.9	Hematite staining (intense), quartz veins at 30° to core axis (brecciated gneiss).
21.2-21.3	Hematite staining. Quartz vein, brecciated gneiss.																												
27.7-28.0	Quartz vein, brecciated gneiss and hematite staining. 20-30° to core axis.																												
29.3-29.7	Hematite staining and rubbly quartz veinlets, brecciated gneiss.																												
32.0-33.9	Granitic pegmatite (annealed), early																												
58.1-58.5	Rare (localized) quartz veinlets, brecciated gneiss, and hematite staining.																												
59.0-59.1	Aphyric non-magnetic (diabasic) mafic dyke.																												
59.1-59.4	Quartz veinlets, brecciated gneiss, and hematite at 50° to core axis.																												
61.3-61.4	Fresh quartz veining and hematite staining at 40° to core axis (minor breccia).																												
62.1-62.3	Quartz veinlets at 40° to core axis. Hematite staining (no breccia) (infilling brittle fractures).																												
65.7-65.8	Hematite and quartz veinlet at 50° to core axis.																												
66.2-66.3	Hematite and quartz veinlet at 30° to core axis.																												
67.3-67.9	granitic pegmatite with quartz recrystallized in tension gashes at 30° to core axis.																												
74.2-74.3	Chlorite? Fractures or shears at 10° to core axis.																												
81.6-81.9	Hematite staining (intense), quartz veins at 30° to core axis (brecciated gneiss).																												
95.9-99.5	96.9-99.5 Barren, fine grained troctolite. Contact with gneiss is very ambiguous (not distinct). As a whole, troctolite has a chilled appearance but not a sharp chill at contact.																												
99.5-106.7	<table><tr><td>99.5-102.8</td><td>5-7% fine grained disseminated blotchy sulphides. 10% aphyric fragments with rare granitic fragment present.</td></tr><tr><td>102.8-106.7</td><td>1-3% blotchy sulphide, approximately 25-35% aphyric fragments and granitic fragments.</td></tr></table>	99.5-102.8	5-7% fine grained disseminated blotchy sulphides. 10% aphyric fragments with rare granitic fragment present.	102.8-106.7	1-3% blotchy sulphide, approximately 25-35% aphyric fragments and granitic fragments.																								
99.5-102.8	5-7% fine grained disseminated blotchy sulphides. 10% aphyric fragments with rare granitic fragment present.																												
102.8-106.7	1-3% blotchy sulphide, approximately 25-35% aphyric fragments and granitic fragments.																												
106.7-109.7	Fine grained troctolite, no fragments present. 2-3% sulphide (rare fine grained disseminated and semi massive bands at 107.7-107.9 and 108.5-108.7m.																												

- 108.7-109.0 Appears altered and weakly sheared. Chalcopyrite stringers offset by siliceous veinlets at 60° to core axis (olivine altered).
- 109.5-109.7 Brecciated and sheared by chlorite or serpentinite (at first, looks chilled but is actually brecciated).
- 109.7-110.45 Massive sulphide. Small pentlandite crystals (infrequent).
- 110.45-113.6 110.5-114.0 5-7% blotchy sulphides, 50-55% aphyric granitic fragments.
- 113.6-117.8 114.0-117.8 Fine to medium grained with trace fine to medium grained disseminated sulphides. No fragments visible, variable textured, but exhibits good chill against gneiss.
- 117.0-117.5 Granitic pegmatite.
- 117.8-187.8 Granite to granodioritic gneiss. Moderate to intensely folded remobilized sulphides at 118.3m (trace quantities).
- 136.3-136.4 Hematite and epidote veinlet at 30° to core axis (no breccia).
- 148.0-148.6 aphyric non-magnetic dyke (diabase)
- 155.8-157.9 Aphyric non-magnetic dyke (diabase)
- 169.9-170.9 Granitic pegmatite.
- 172.6-172.9 Granitic pegmatite.
- 176.9-177.2 Granitic pegmatite.
- 181.4-181.6 Granitic pegmatite.
- 187.0-187.3 Granitic pegmatite.
- 187.8-187.8 End of Hole.

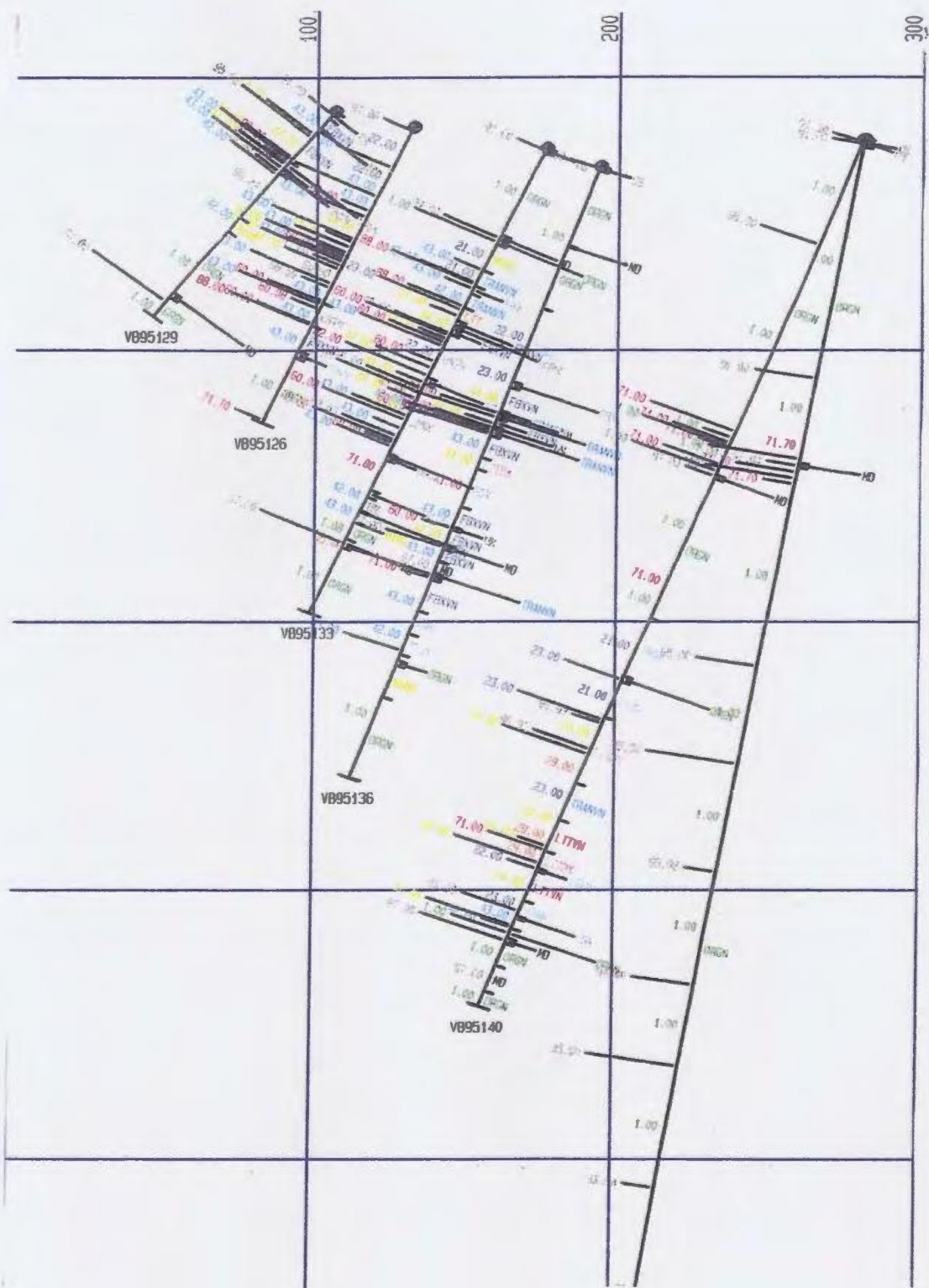
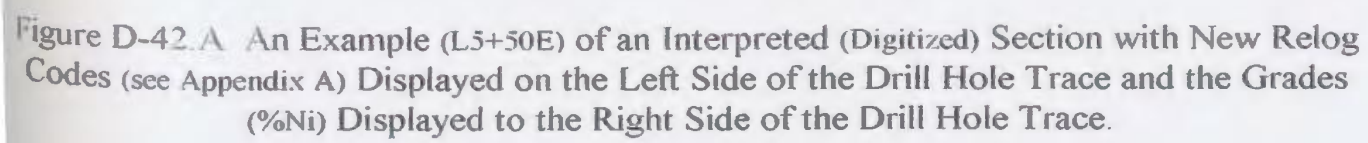
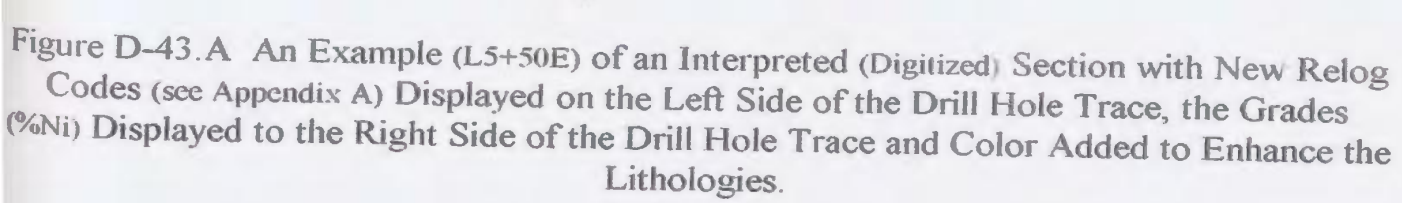


Figure D-41 A An Example (L5+50E) of a Non-Interpreted Section with Old Lithology Codes (see Appendix B) Displayed on the Left Side of the Drill Hole Trace and the New Relog Lithology Codes (see Appendix A) Displayed to the Right Side of the Drill Hole Trace.





APPENDIX E:
Model Generation

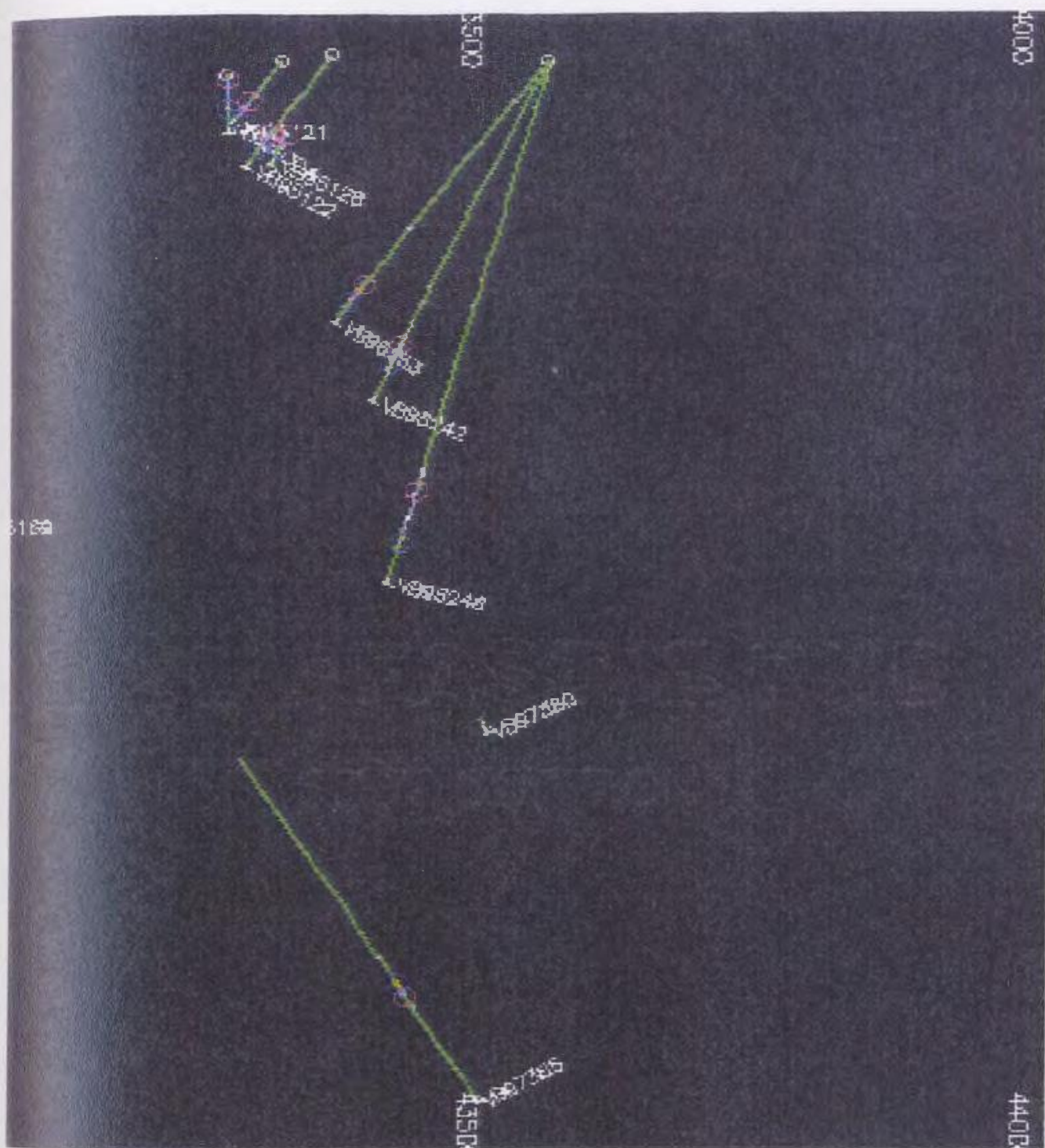


Figure E-2.A An Example of Points Snapped to a Contact on Drill Hole Traces. These Points Can be Used to Create a DTM Surface or Used as Anchors to Digitize a String.

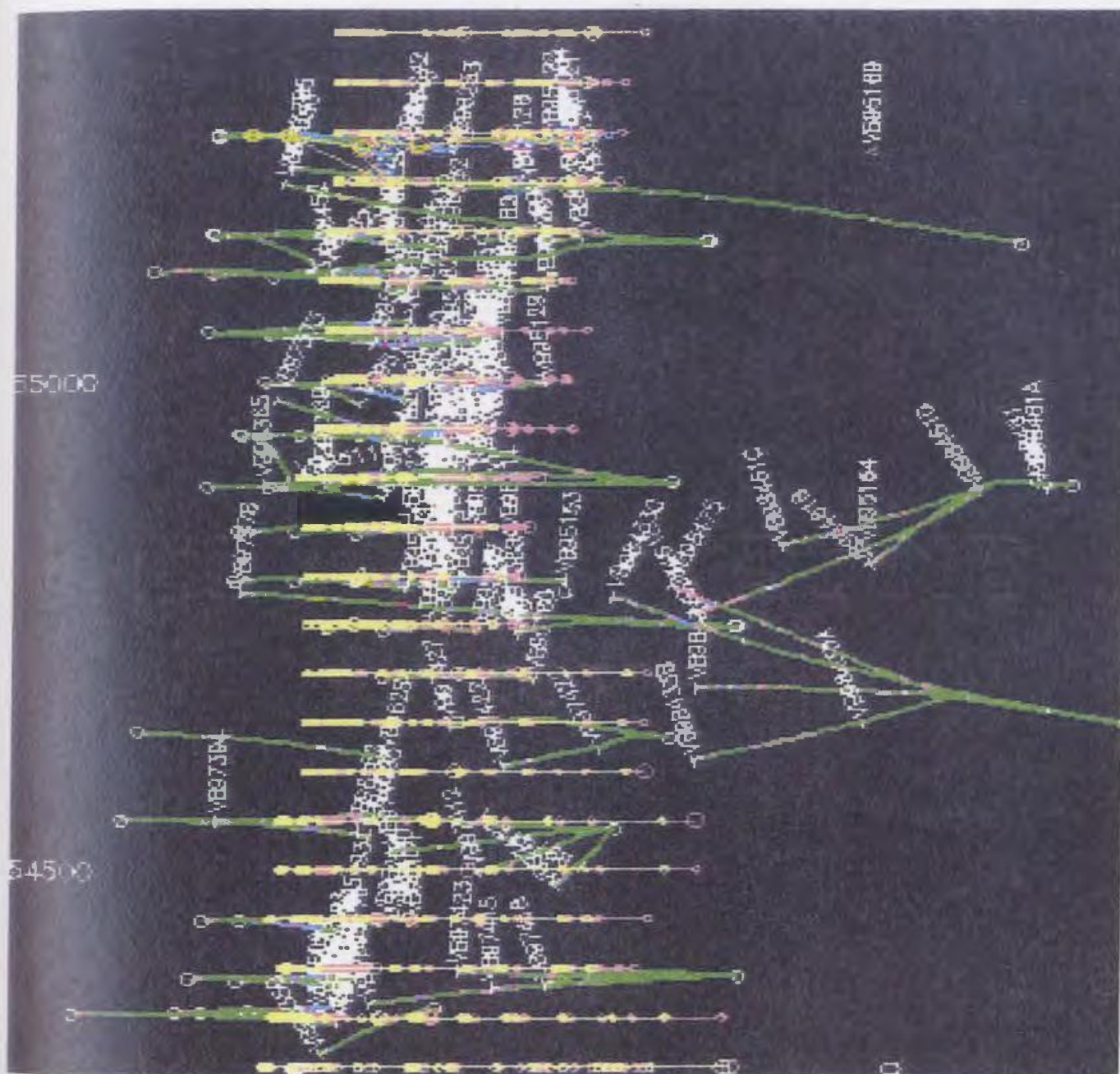


Figure E-4. A An Example (Plan View) of a Wire Frame (DTM Surface) Model Sliced with Slices Converted to Strings.

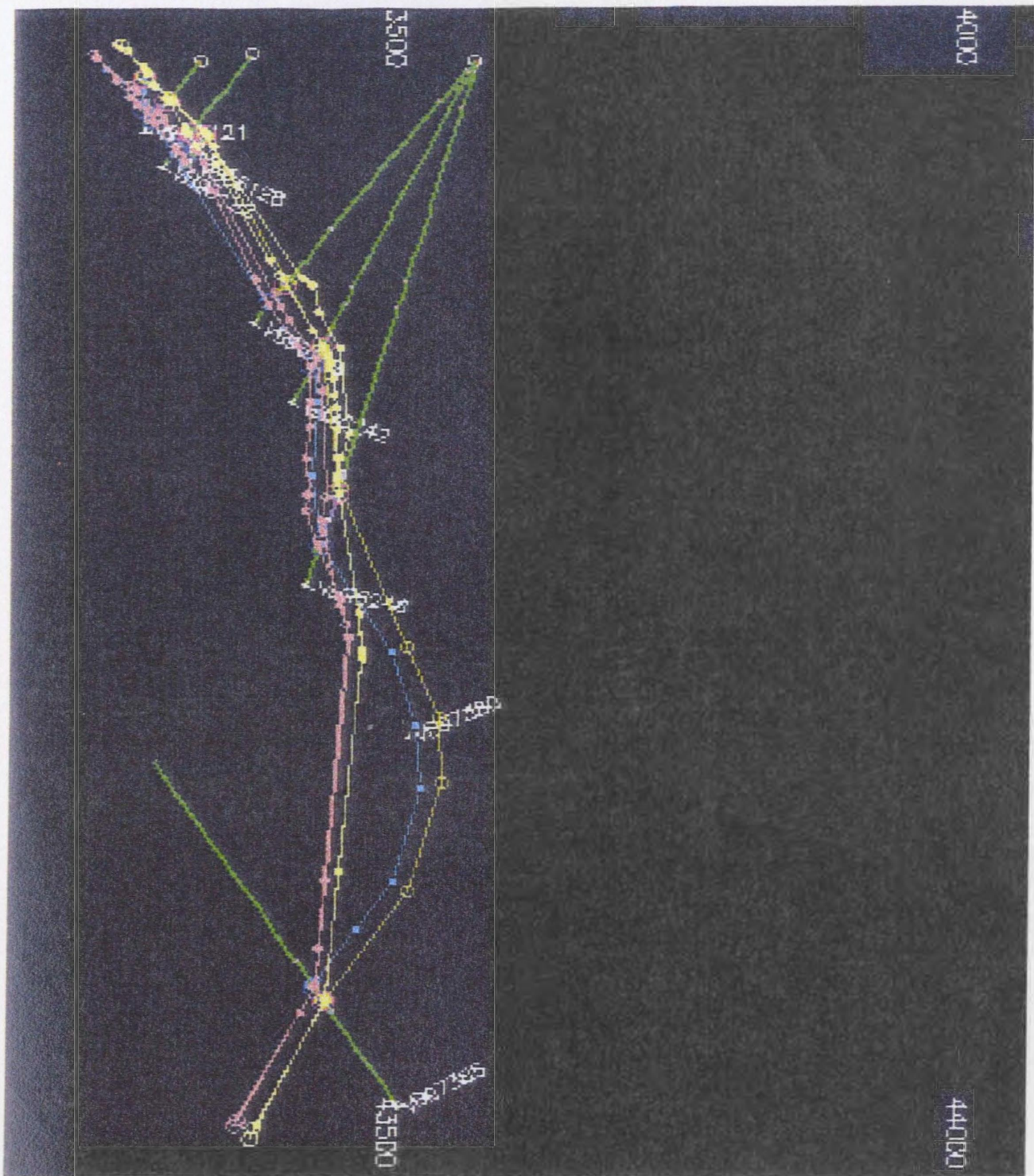


Figure E-5.A An Example of a Wire Frame (DTM Surface) Model Sliced with Slices Converted to Strings. These Strings can then be Modified to Accurately Represent the Detailed Geology or Alternatively, can be Used as a Guide to Create New Strings. The Modified or New Strings are then Used to Generate a New Model (DTM Surface).

Figure 1.2
Main Block Geology Map
(compilation)

Note: This is a solid geology produced through surface mapping and geology obtained through diamond drilling. Outcrop measurements are positioned on the outcrop from GPS co-ordinates obtained during the mapping process, however, infrequency measurements will appear adjacent to the outcrop due to the limited precision of the GPS device. Some of the map symbols have been modified from the legend for the purpose of this text and are as follows: Bodies of water (i.e. lakes and ponds) appear white; ▲ and ■ symbols are comment fields that can only be used with the digital file; ■ solid red fill pattern within the Ovoid and Mini Ovoid represent massive sulphides; solid yellow fill pattern within the Ovoid and Mini Ovoid represent disseminated sulphides; pink open fill patterns within the Eastern Deeps deposit represent massive sulphides; yellow open fill patterns within the Eastern Deeps deposit represent disseminated sulphides; large size sigmoidal fault patterns are faults defined through surface mapping; : medium size sigmoidal fault patterns are faults assumed through surface mapping and diamond drilling; small size sigmoidal fault patterns are faults interpreted through diamond drilling.

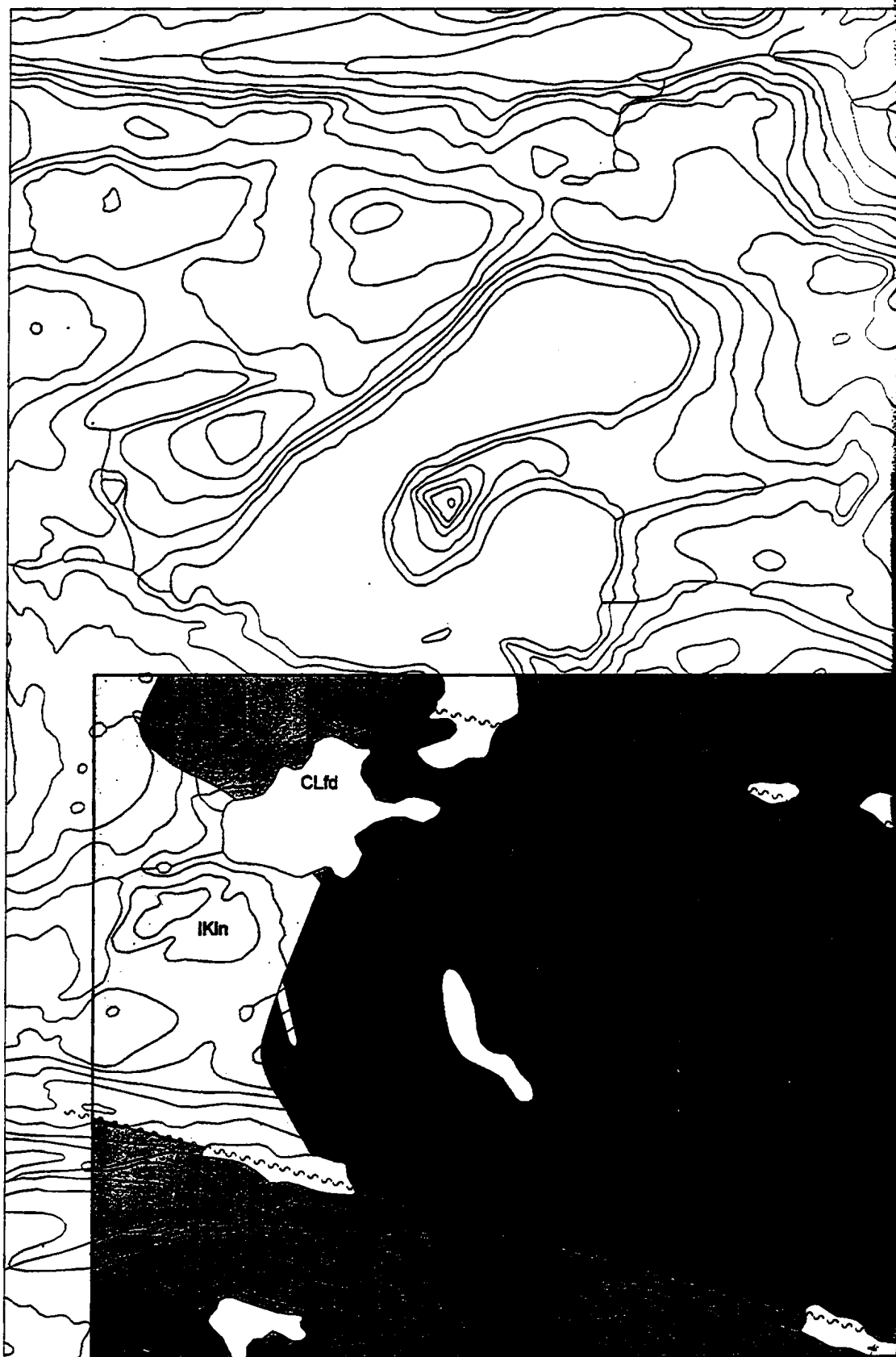
NOTE TO USERS

Oversize maps and charts are microfilmed in sections in the following manner:

LEFT TO RIGHT, TOP TO BOTTOM, WITH SMALL OVERLAPS

This reproduction is the best copy available.

UMI[®]



LEGEND

NAIN PLUTONIC SUITE

GRANITOID INTRUSIONS

MAKHAVINEKH GRANITE



intrusive breccia



medium quartz monzonite



coarse quartz monzonite



granite

VOISEY'S BAY GRANITE



intrusive breccia



monzonite



quartz monzonite



granite

REID BROOK INTRUSIVE COMPLEX

MUSHUAU TROCTOLITE



troctolite



leucotroctolite



olivine gabbro



gabbro

VOISEY'S BAY TROCTOLITE



troctolite



leucotroctolite



olivine gabbro



undivided

ASHLEY TROCTOLITE



troctolite



olivine gabbro



undivided

ANORTHOSITE MASSIFS

IKADLVIK ANORTHOSITE



anorthosite



leuconorite

KANGEKLUALUK ANORTHOSITE



anorthosite







leuconorite

LEGEND


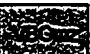
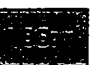

NAIN PLUTONIC SUITE

ANITOID INTRUSIONS

MAKHAVINEKH GRANITE





	intrusive breccia
	medium quartz monzonite
	coarse quartz monzonite
	granite

VOISEY'S BAY GRANITE

	intrusive breccia
	monzonite
	quartz monzonite
	granite

AND BROOK INTRUSIVE COMPLEX




SHUAU TROCTOLITE

	troctolite
	leucotroctolite
	olivine gabbro
	gabbro

VOISEY'S BAY TROCTOLITE

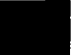


	troctolite
	leucotroctolite
	olivine gabbro
	undivided

ASHLEY TROCTOLITE

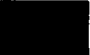


	troctolite
	olivine gabbro
	undivided

NORTHOSITE MASSIFS

IKADLVIK ANORTHOSITE

	anorthosite
	leuconorite
	leuconorite

KANGEKLUALUK ANORTHOSITE

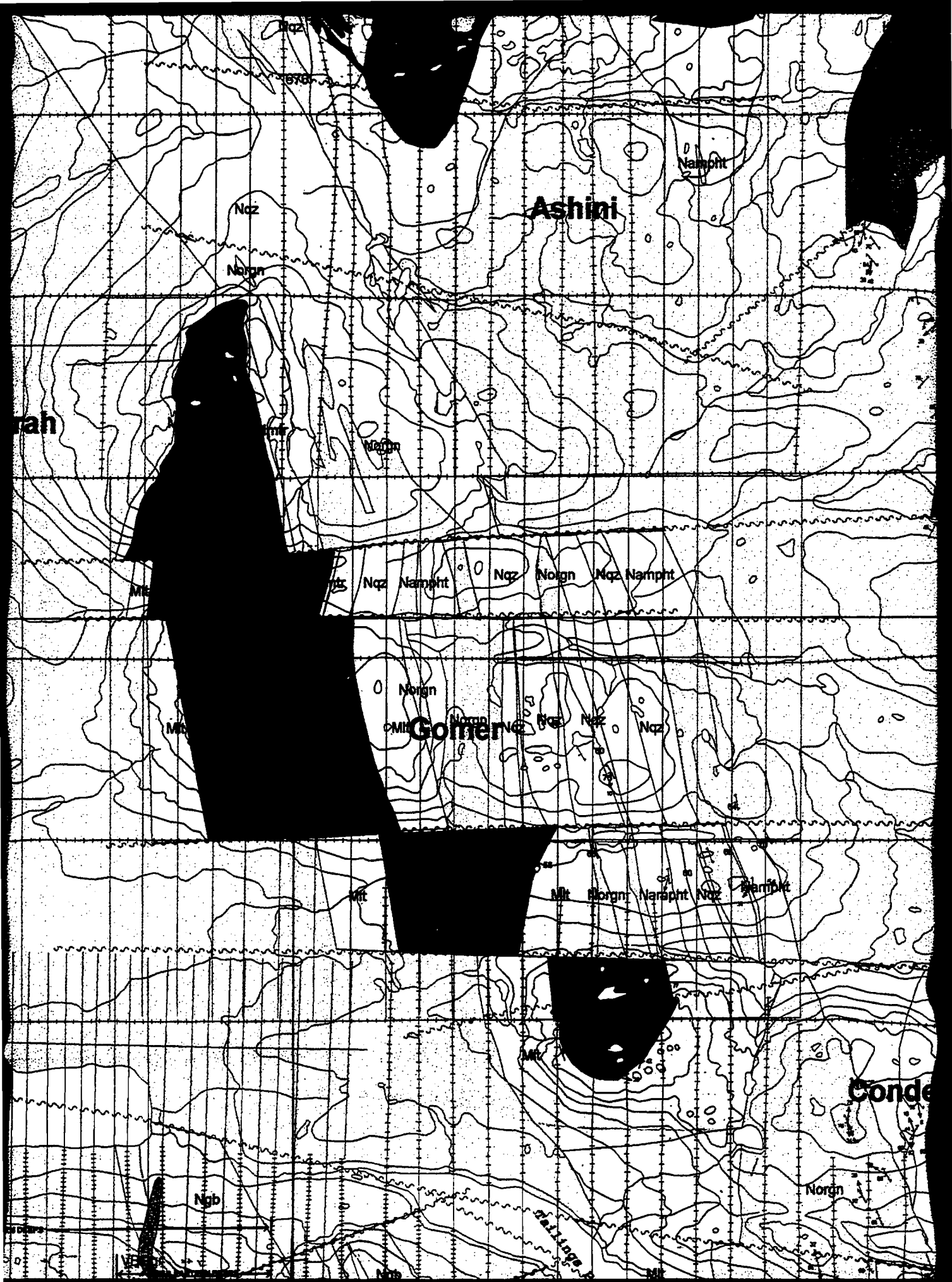
	anorthosite
	leuconorite
	leuconorite

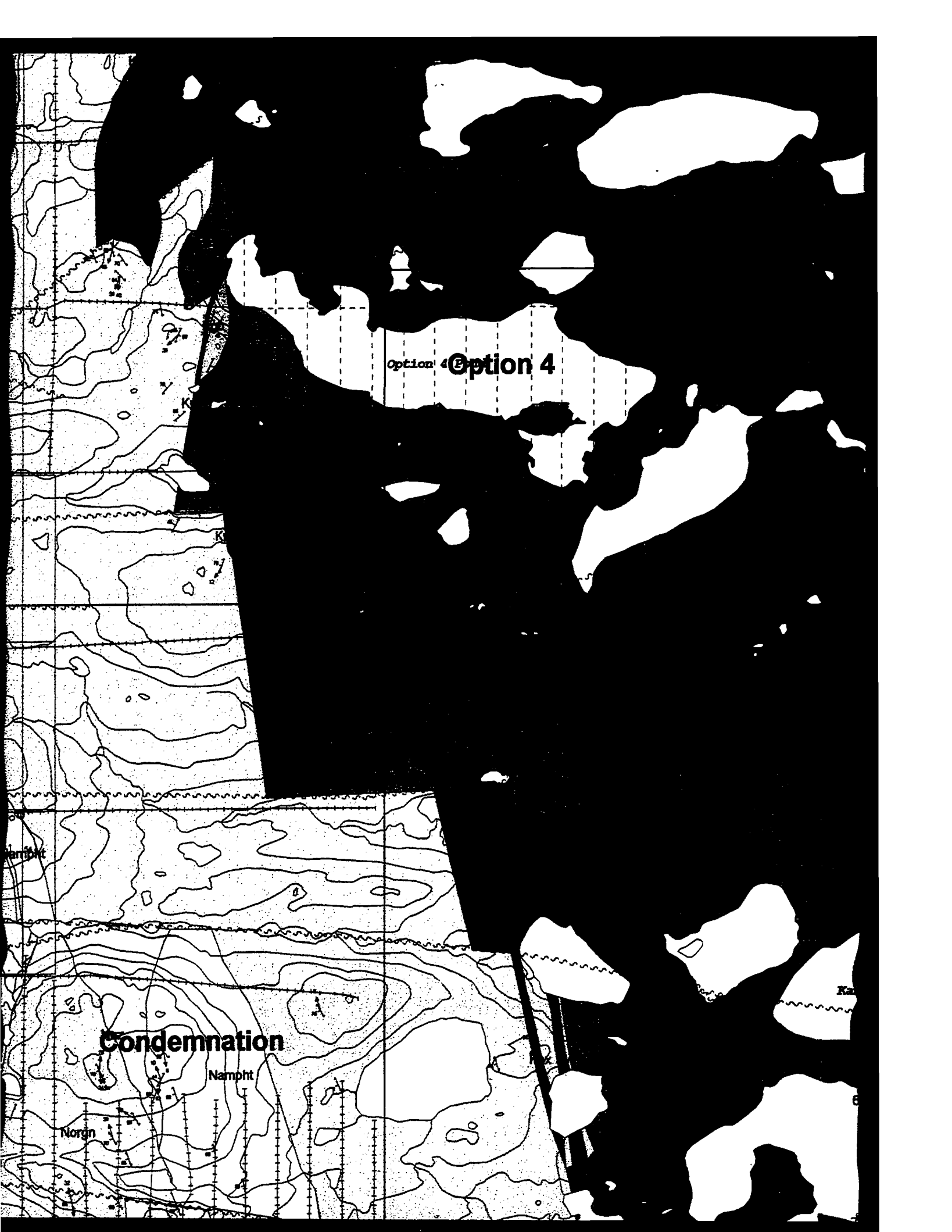












Option 4

Condemnation

Namphit

Norgin

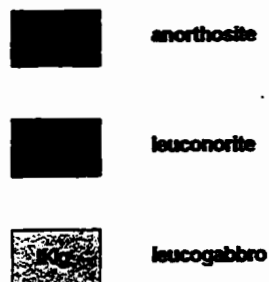


Kangeklualuk Bay

Korgn

690

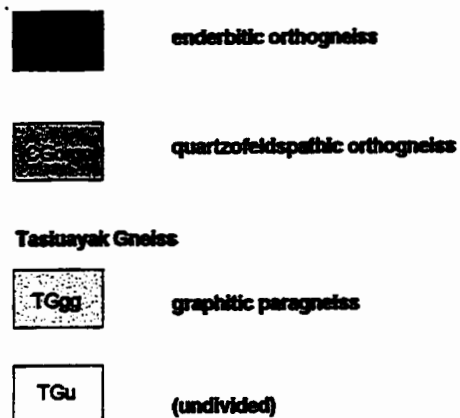
IKADLVIK ANORTHOSITE



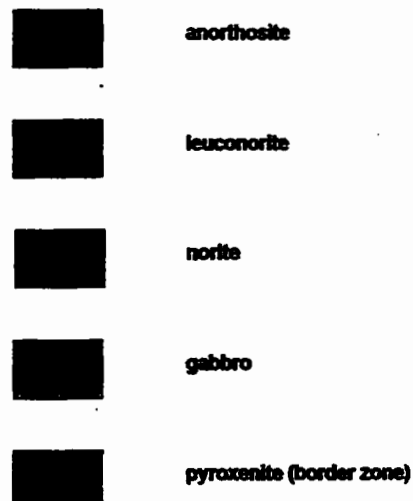
Cabot Lake



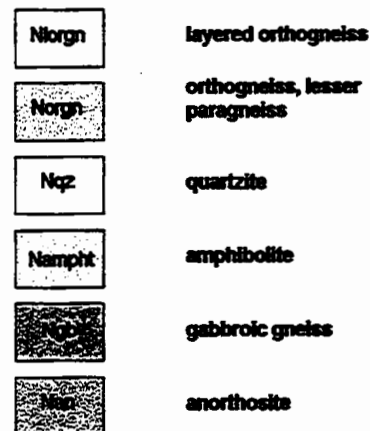
CHURCHILL PROVINCE



KANGEKLUALUK ANORTHOSITE



NAIN PROVINCE (Archean)






SYMBOLS



SURFACE PROJECTION OF DISSEMINATED SULPHIDE





IKADLIVIK ANORTHOSITE

	anorthosite
	leuconorite
	leucogabbro


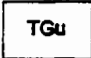
Cabot Lake

	ferro diorite (Cabot Lake)
--	----------------------------

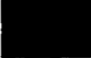



CHURCHILL PROVINCE

	enderbitic orthogneiss
	quartzofeldspathic orthogneiss

Tasiuyak Gneiss



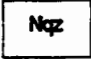



	graphitic paragneiss
	(undivided)

KANGEKLUALUK ANORTHOSITE

	anorthosite
	leuconorite
	norite
	gabbro

	pyroxenite (border zone)
---	--------------------------

NAIN PROVINCE (Archean)

	layered orthogneiss
	orthogneiss, lesser paragneiss
	quartzite
	amphibolite
	gabbroic gneiss
	anorthosite

SYMBOLS

 GEOLOGICAL BOUNDARY / REGIONAL MAPPING

 GEOLOGICAL BOUNDARY
(defined, approximate, assumed)

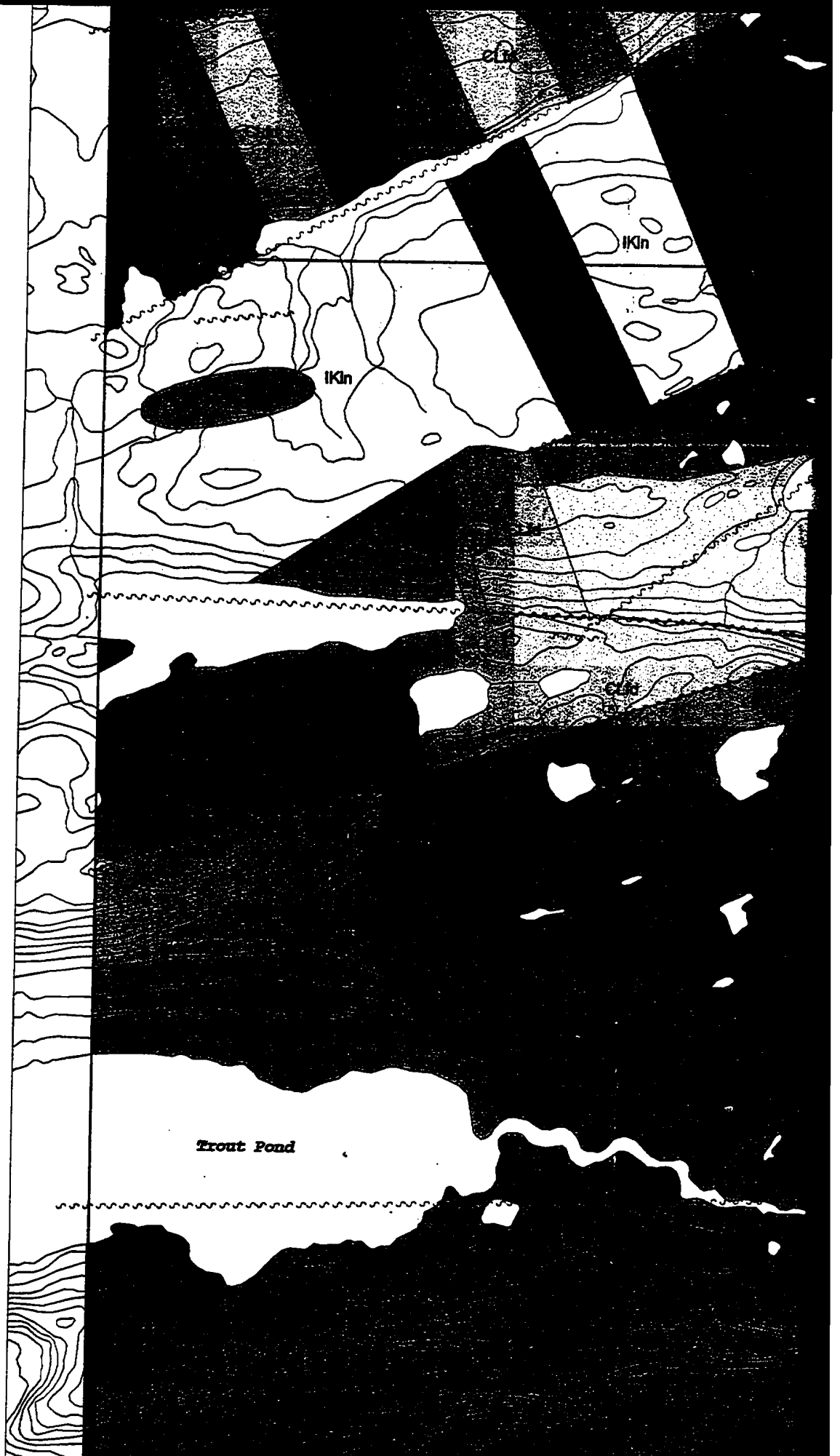
 FAULT
(defined, approximate)

 SURFACE PROJECTION OF MASSIVE SULPHIDE

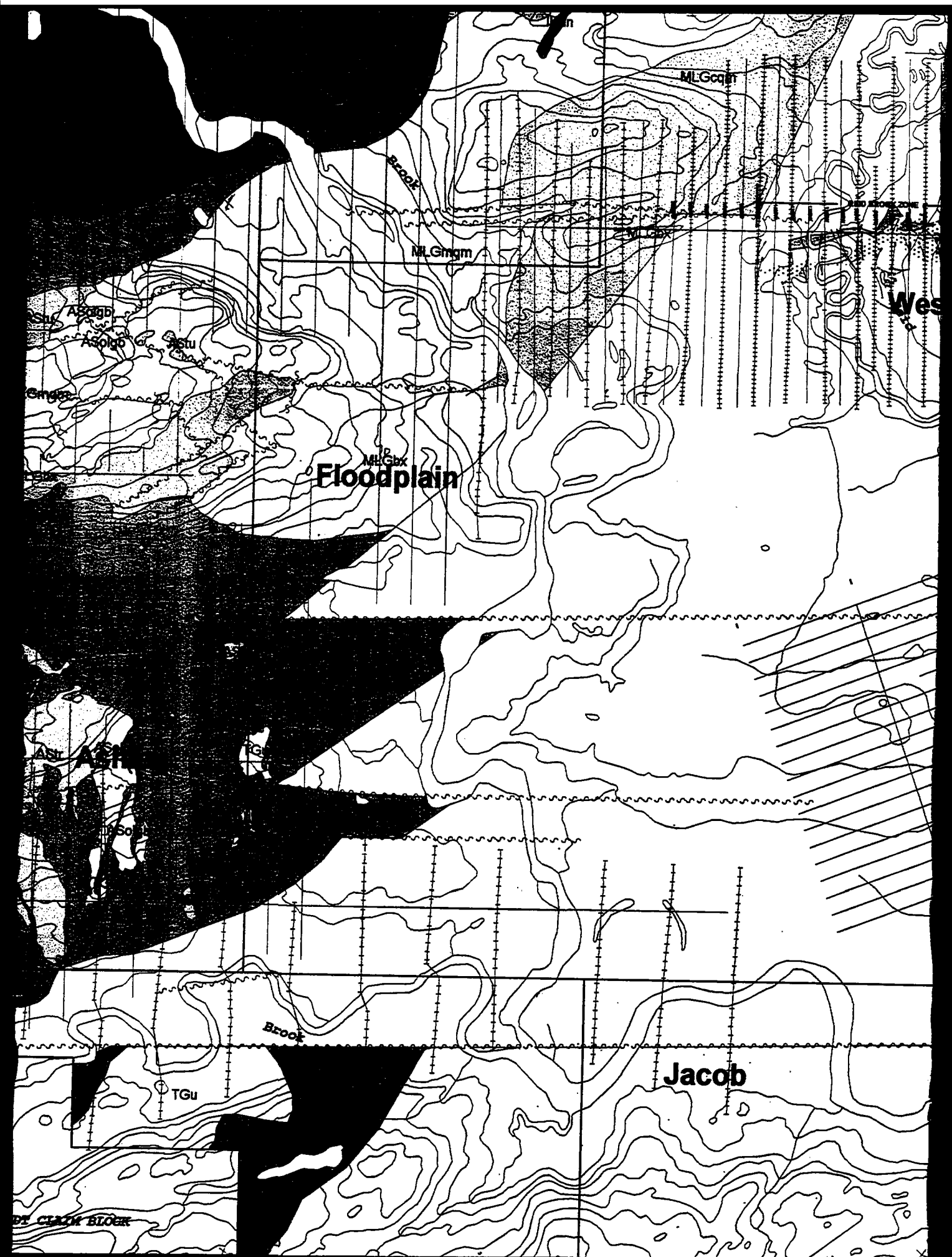
SURFACE PROJECTION OF DISSEMINATED SULPHIDE

 DIAMOND DRILL HOLE

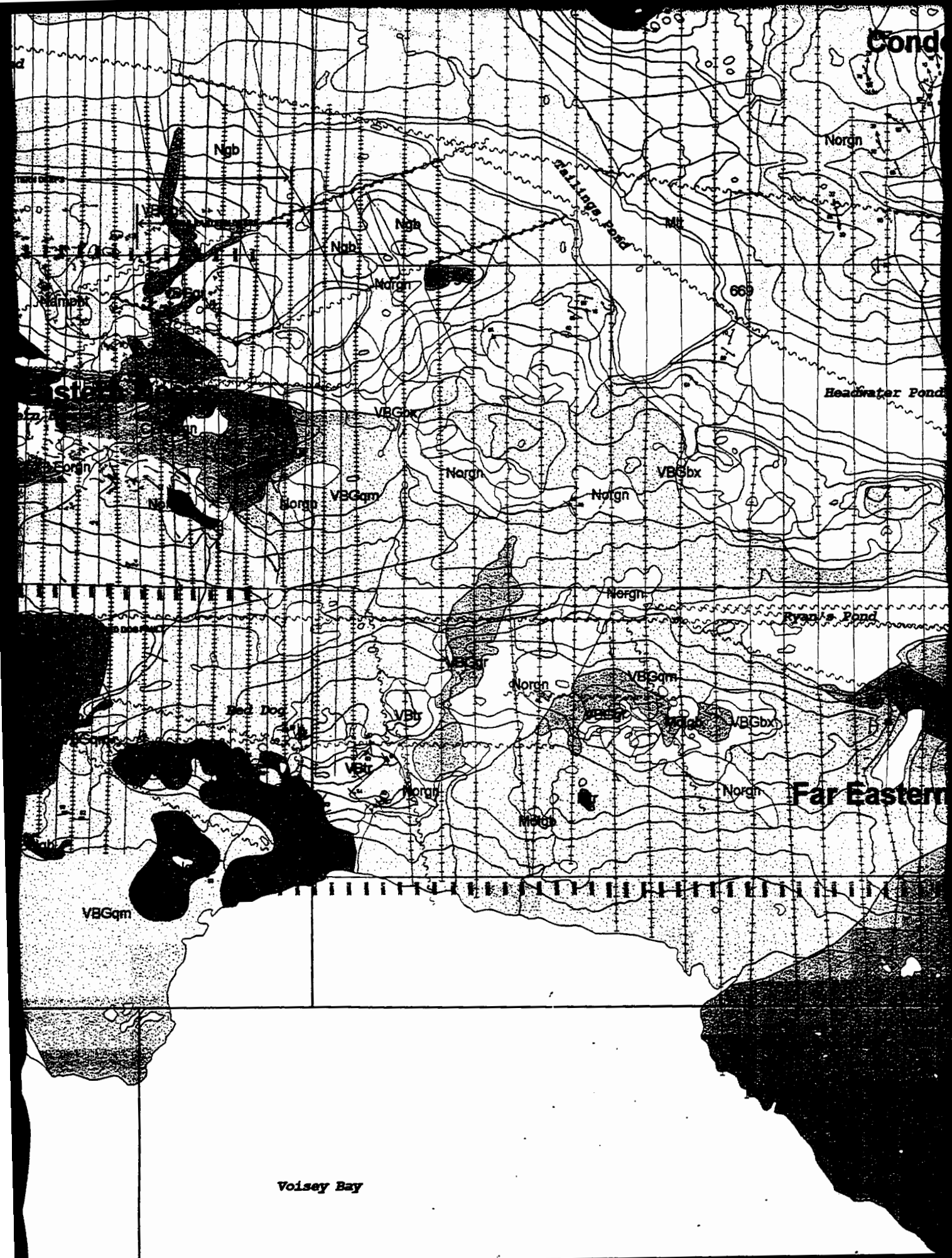
 OUTCROP











Condemnation

Nampht

Norgn

142

36

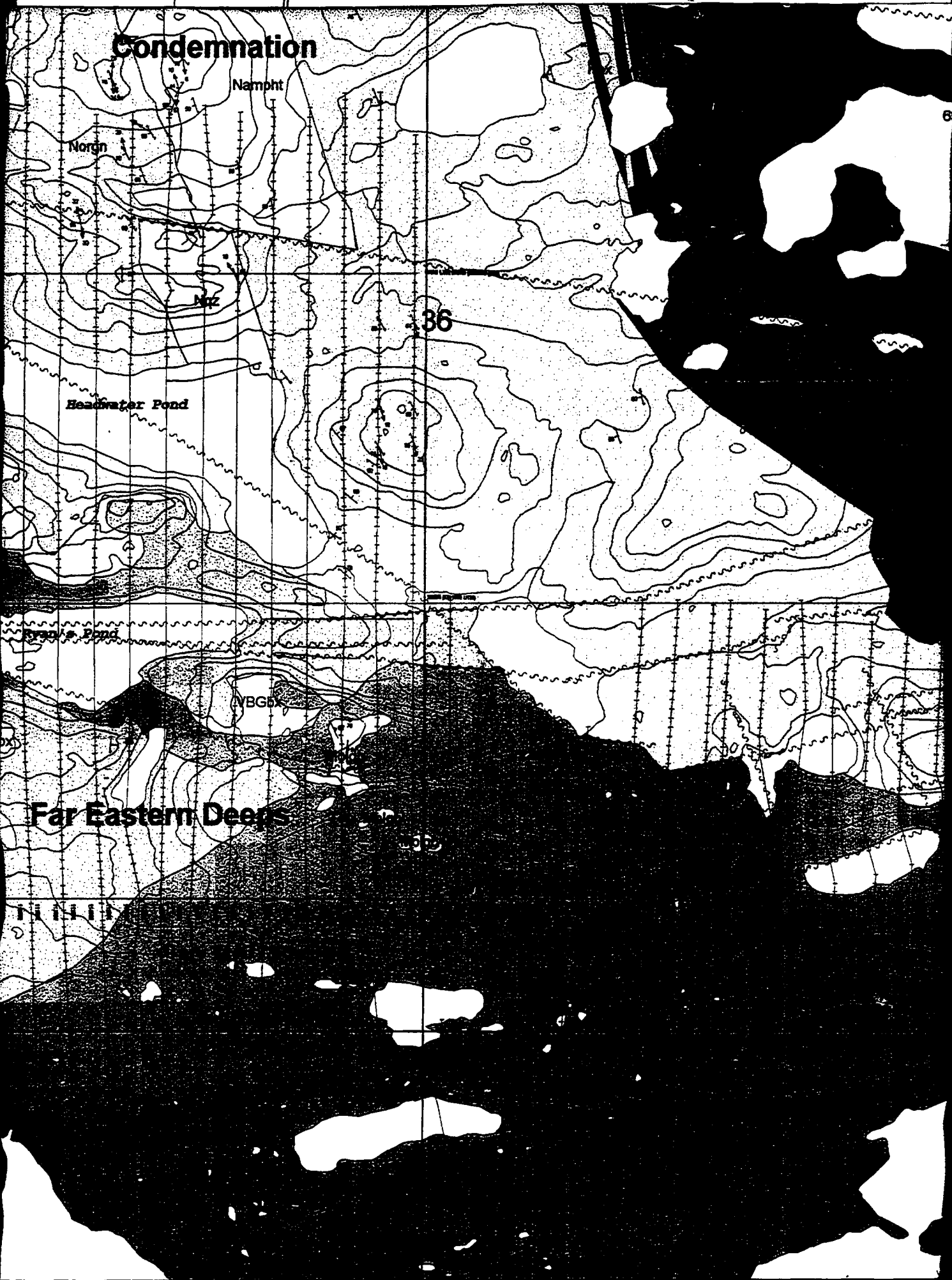
Headwater Pond

Ryan's Pond

VBGbx

Far Eastern Deeps

132



690

VBGmz

VBGmz

(defined, approximate)

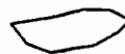


SURFACE PROJECTION OF MASSIVE SULPHIDE

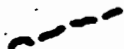
SURFACE PROJECTION OF DISSEMINATED SULPHIDE



DIAMOND DRILL HOLE



OUTCROP



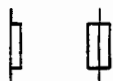
GEOPHYSICAL ANOMALY (MAX-MIN)



**Fault
(dip indicated)**



**Fold Axis
(2nd Generation)**



**Fracture
(inclined, vertical)**



**Axial plane
(2nd generation)**



**Healed Fracture
(inclined, vertical)**



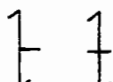
**Granite dyke
(inclined, vertical)**



**Lineation
(1st, 2nd generation)**



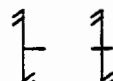
**Mafic dyke
(inclined, vertical)**



**Foliation -1st generation
(inclined, vertical)**



**Igneous layering
(inclined, vertical)**



**Foliation -2nd generation
(inclined, vertical)**



**Observed contact
(dip indicated)**

**THIS IS A COMBINED LEGEND
NOT ALL SYMBOLS APPEAR ON THIS MAP**

Revision Date

Description

Geologist



**VOISEY'S BAY NICKEL
COMPANY LIMITED**

A subsidiary of Inco Limited

MAILING ADDRESS

Suite 700, Baine Johnston Center
10 Fort William Place
St. John's, NF, Canada
A1C 1K4
Tel. 709-758-8888 Fax. 709-758-8888

CONFIDENTIAL

This Document contains confidential information and may not be distributed in whole or in part without the consent of

Voisey's Bay Nickel Company

CONFIDENTIALITY RELEASE

Date

Released By

Initial

(defined, approximate)



SURFACE PROJECTION OF MASSIVE SULPHIDE

SURFACE PROJECTION OF DISSEMINATED SULPHIDE



DIAMOND DRILL HOLE



OUTCROP



GEOPHYSICAL ANOMALY (MAX-MIN)



**Fault
(dip indicated)**



**Fold Axis
(2nd Generation)**



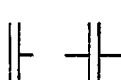
**Fracture
(inclined, vertical)**



**Axial plane
(2nd generation)**



**Healed Fracture
(inclined, vertical)**



**Granite dyke
(inclined, vertical)**



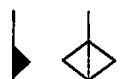
**Lineation
(1st, 2nd generation)**



**Mafic dyke
(inclined, vertical)**



**Foliation -1st generation
(inclined, vertical)**



**Igneous layering
(inclined, vertical)**



**Foliation -2nd generation
(inclined, vertical)**



**Observed contact
(dip indicated)**

**THIS IS A COMBINED LEGEND
NOT ALL SYMBOLS APPEAR ON THIS MAP**

Revision Date

Description

Geologist



**VOISEY'S BAY NICKEL
COMPANY LIMITED**

A subsidiary of Inco Limited

MAILING ADDRESS

Suite 700, Baine Johnston Center
10 Fort William Place
St. John's, NF, Canada
A1C 1K4
Tel. 709-758-8888 Fax. 709-758-8899

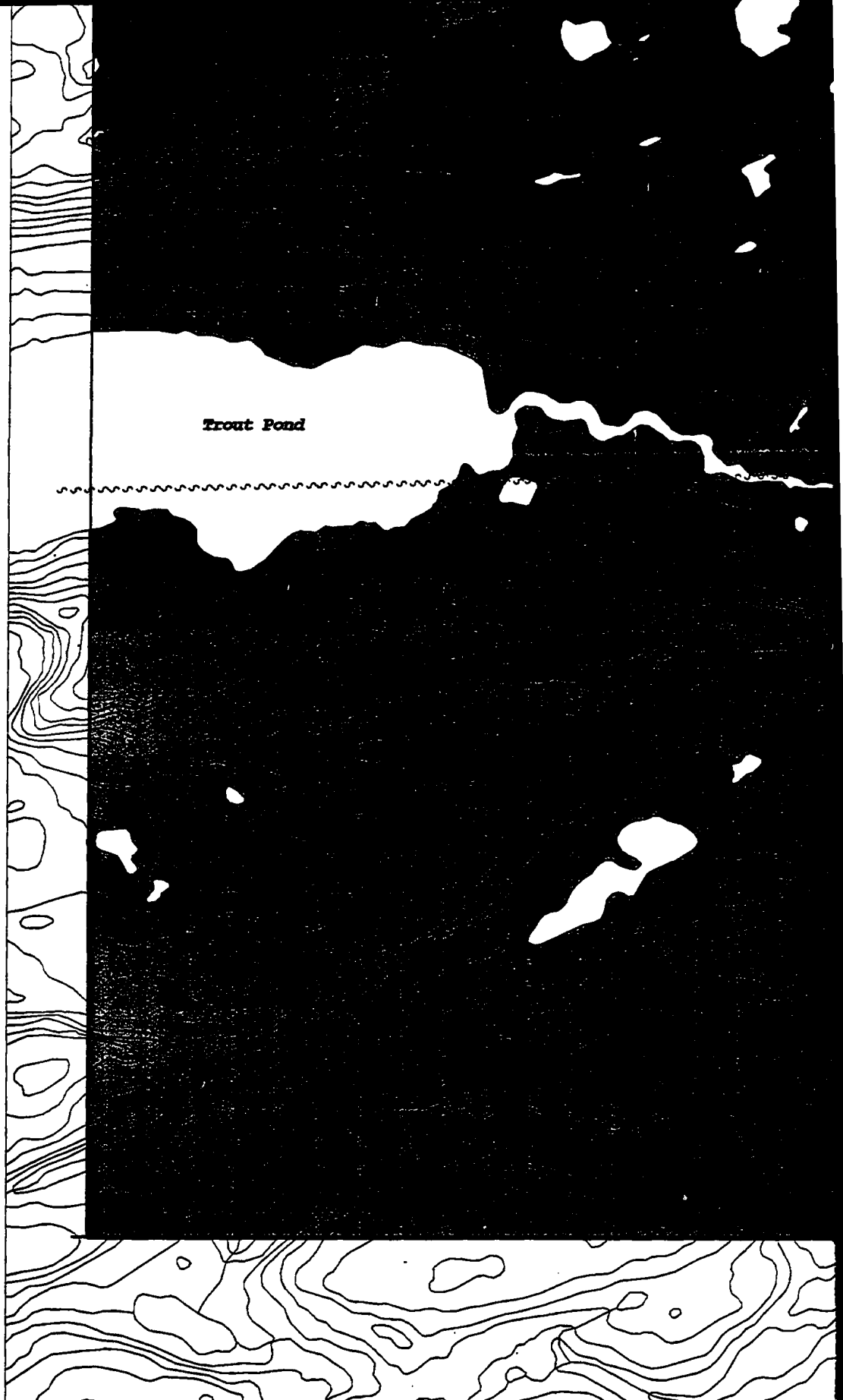
CONFIDENTIAL

This Document contains confidential
information and may not be distributed
in whole or in part without
the consent of

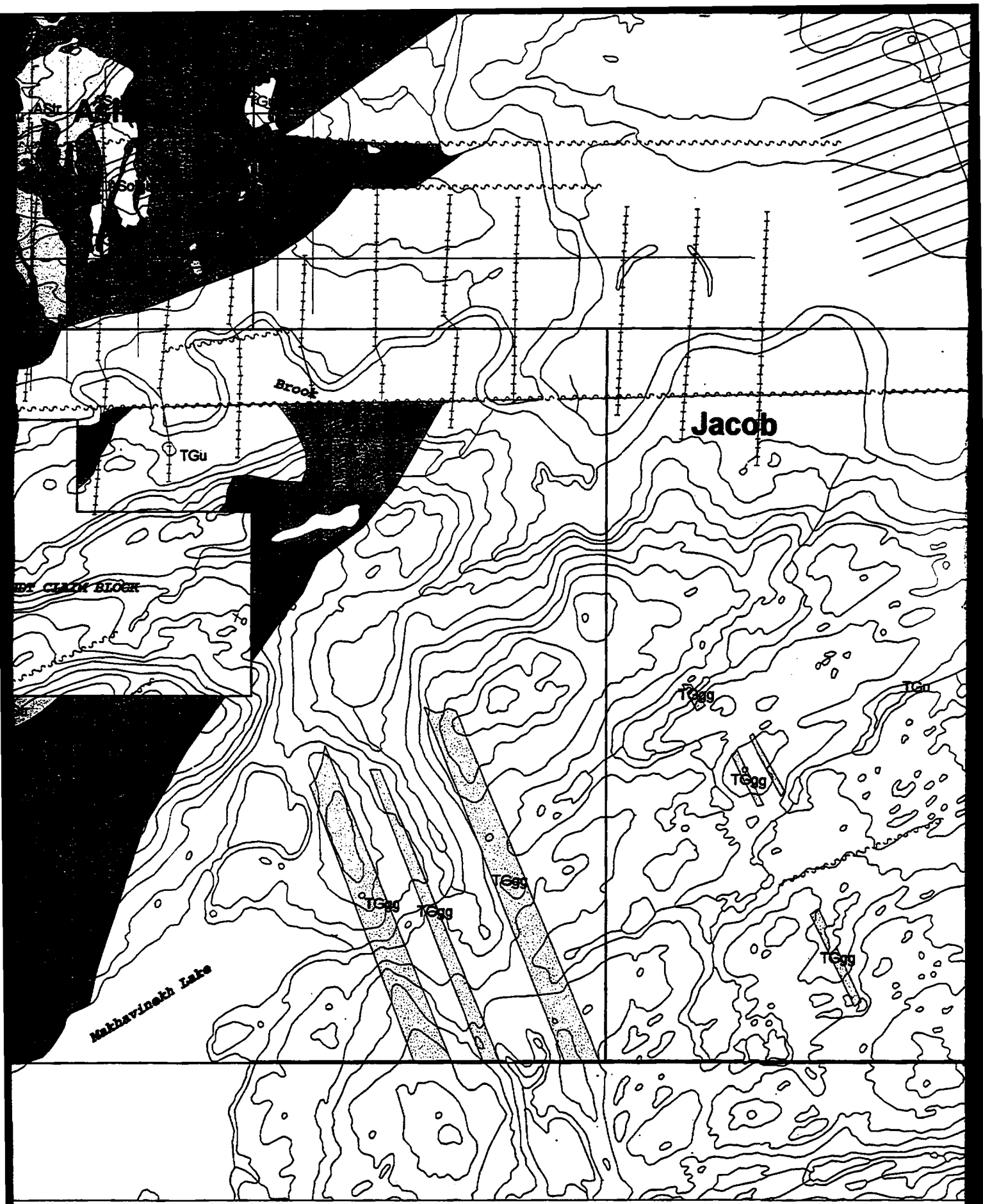
Voisey's Bay Nickel Company Ltd.

CONFIDENTIALITY RELEASE

Trout Pond







Archie

Re

VBGqm

TCu

688

MLgr

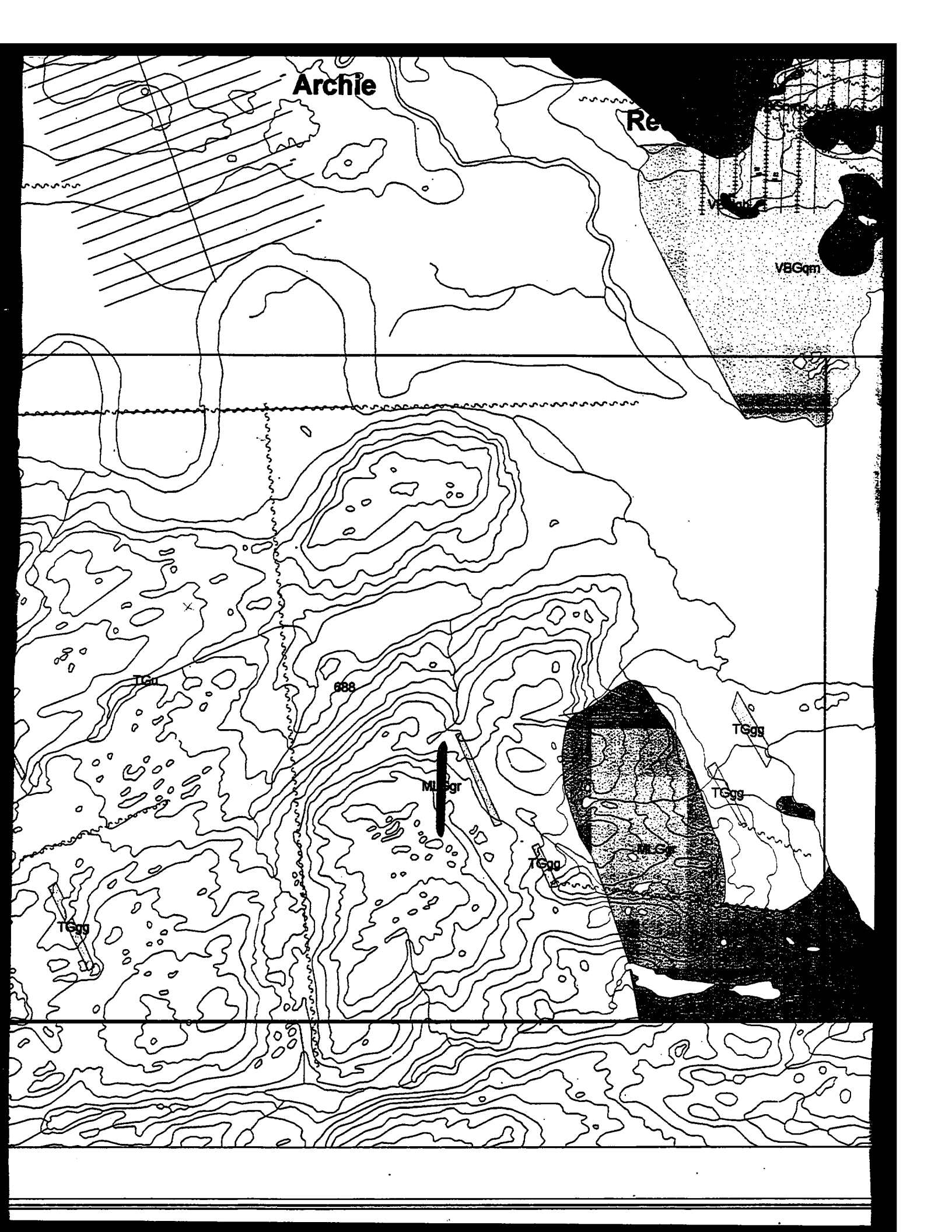
TCgs

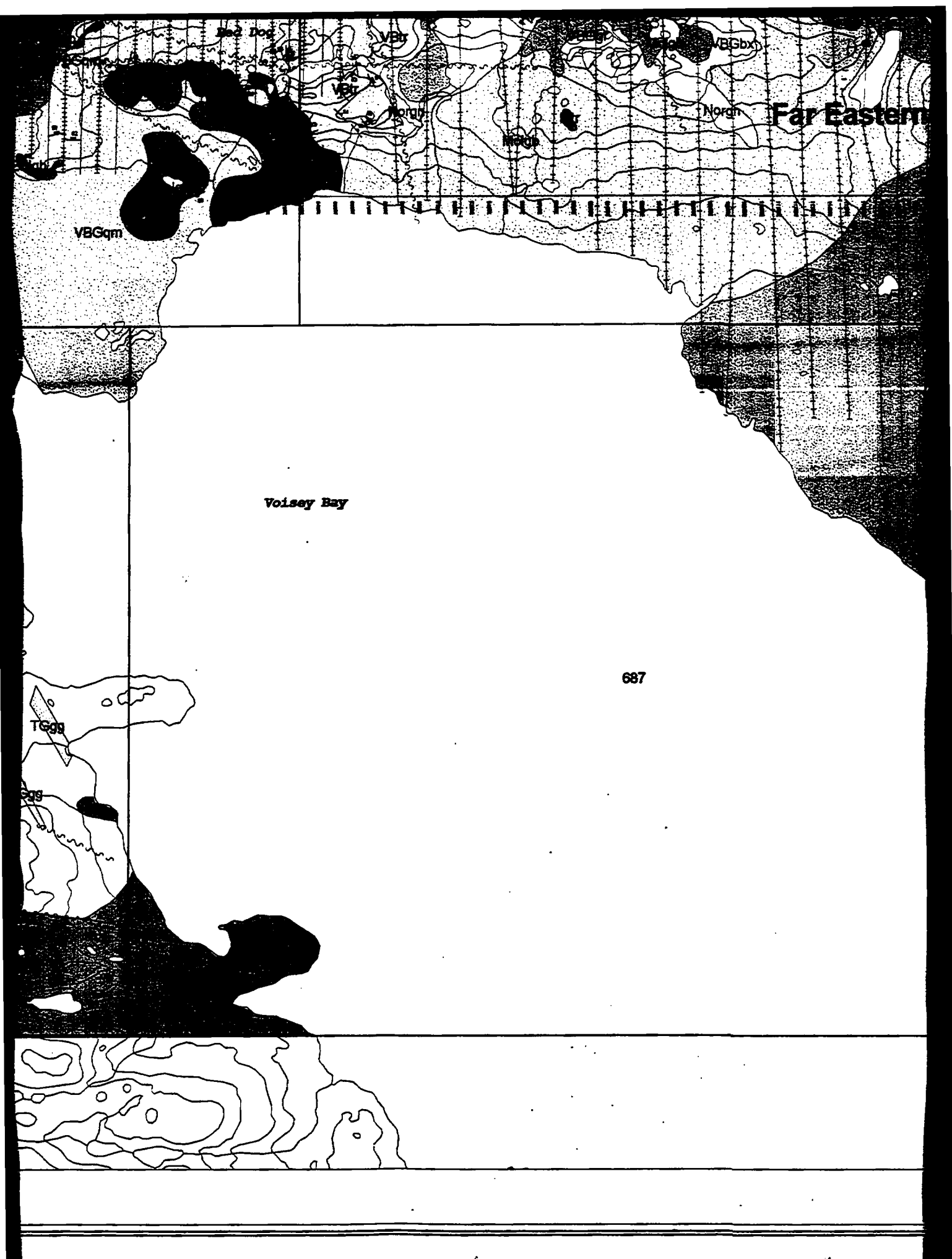
TCgs

MLC

TCgo

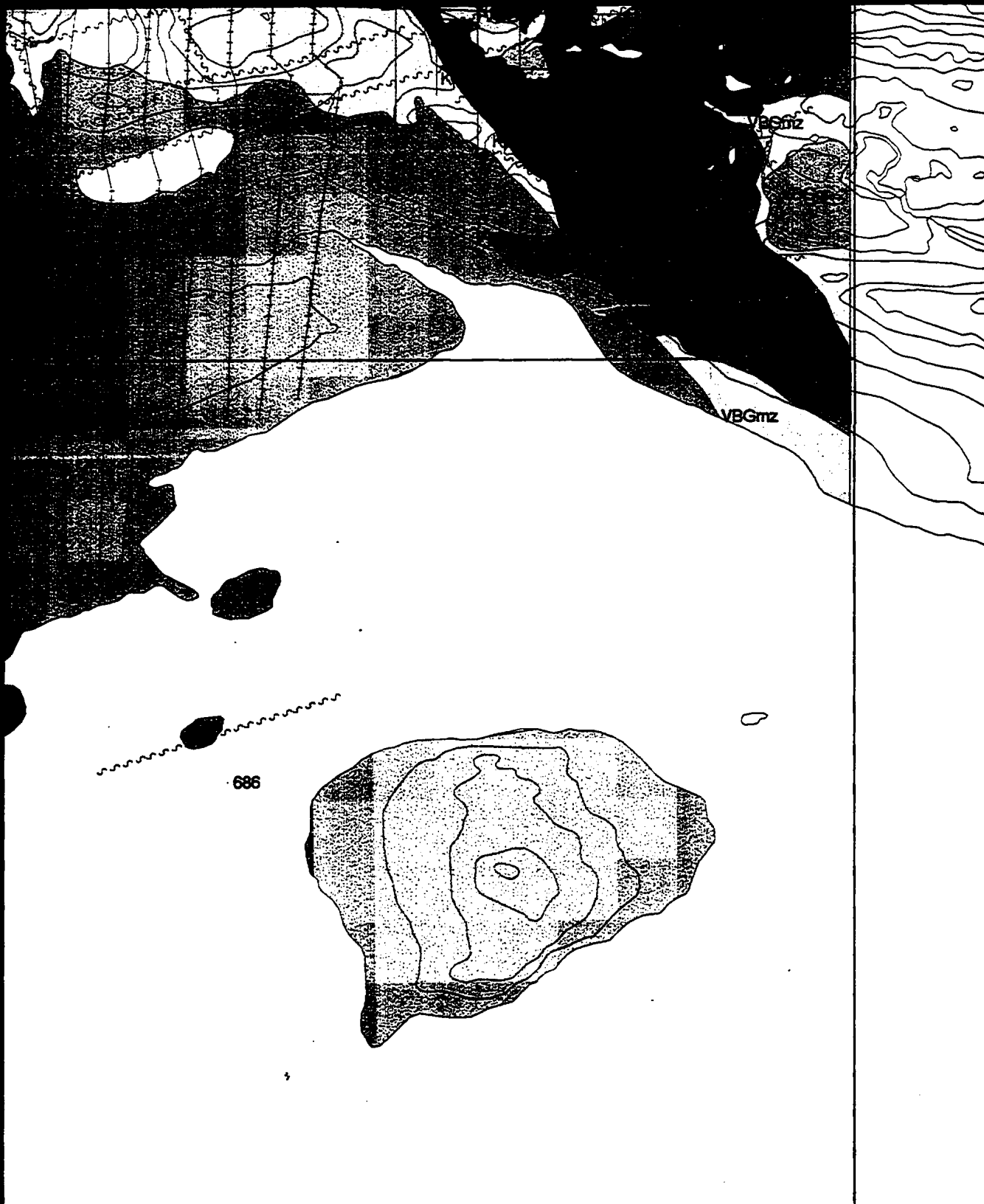
TCgs





Far Eastern Deeps





Revision Date

Description

Geologist



**VOISEY'S BAY NICKEL
COMPANY LIMITED**

A subsidiary of Inco Limited

MAILING ADDRESS

Suite 700, Baine Johnston Center
10 Fort William Place
St. John's, NF, Canada
A1C 1K4
Tel. 709-758-8888 Fax. 709-758-8899

CONFIDENTIAL

This Document contains confidential
information and may not be distributed
in whole or in part without
the consent of
Voisey's Bay Nickel Company Ltd.

CONFIDENTIALITY RELEASE

Date

Released By

Initials

Title :

Preliminary

LABRADOR, VOISEY'S BAY PROJECT

Geology of the Voisey's Bay Main Block

Description :

Compilation of detailed mapping by; Darrell P. Butt
Detailed mapping by; Darrell Butt and John Hayes (1997)
Contributions to mapping project include; S. Dunsworth, D. Fitzpatrick
Includes data from Ryan and Lee (1989), Mackela and Babineau (1995)
Deposit structural interpretation compiled by; D. Evans Lamswood
Massive and disseminated ore zones compiled by; R. Wheeler

Geologist(s) :

Darrell Butt

Scale :

Scale 1: 25,000

Print Date :

May 2, 1998

File Name(s) :

MI Workspace :Mainblock Compmap_97_96
Plotter File (HPGL) :Mainblock Compmap_97_96

License(s)

670

Revision Date

Description

Geologist

**VOISEY'S BAY NICKEL
COMPANY LIMITED**

A subsidiary of Inco Limited

MAILING ADDRESS

Suite 700, Baine Johnston Center
10 Fort William Place
St. John's, NF, Canada
A1C 1K4
Tel. 709-758-8888 Fax. 709-758-8899

CONFIDENTIAL

This Document contains confidential
information and may not be distributed
in whole or in part without
the consent of

Voisey's Bay Nickel Company Ltd.**CONFIDENTIALITY RELEASE**

Date

Released By

Initials

Title :

Preliminary

LABRADOR, VOISEY'S BAY PROJECT

Geology of the Voisey's Bay Main Block

Description :

Compilation of detailed mapping by; Darrell P. Butt
Detailed mapping by; Darrell Butt and John Hayes (1997)
Contributions to mapping project include; S. Dunsworth, D. Fitzpatrick
Includes data from Ryan and Lee (1989), Mackela and Babineau (1995)
Deposit structural interpretation compiled by; D. Evans Lamswood
Massive and disseminated ore zones compiled by; R. Wheeler

Geologist(s) :

Darrell Butt

Scale :

Scale 1: 25,000

Print Date :

May 2, 1998

File Name(s) :

Workspace :Mainblock Compmap_97_96
Plotter File (HPGL) :Mainblock Compmap_97_96

License(s)

670

Figure 4.1
Deposit Geology Map
(compilation)

Note: This is a solid geology produced through surface mapping and geology obtained through diamond drilling. Outcrop measurements are positioned on the outcrop from GPS co-ordinates obtained during the mapping process, however, infrequency measurements will appear adjacent to the outcrop due to the limited precision of the GPS device. Some of the map symbols have been modified from the legend for the purpose of this text and are as follows: Bodies of water (i.e. lakes and ponds) appear white; ▲ and ■ symbols are comment fields that can only be used with the digital file; ■ solid red fill pattern within the Ovoid and Mini Ovoid represent massive sulphides; solid yellow fill pattern within the Ovoid and Mini Ovoid represent disseminated sulphides; pink open fill patterns within the Eastern Deeps deposit represent massive sulphides; yellow open fill patterns within the Eastern Deeps deposit represent disseminated sulphides; large size sigmoidal fault patterns are faults defined through surface mapping; ; medium size sigmoidal fault patterns are faults assumed through surface mapping and diamond drilling; small size sigmoidal fault patterns are faults interpreted through diamond drilling.

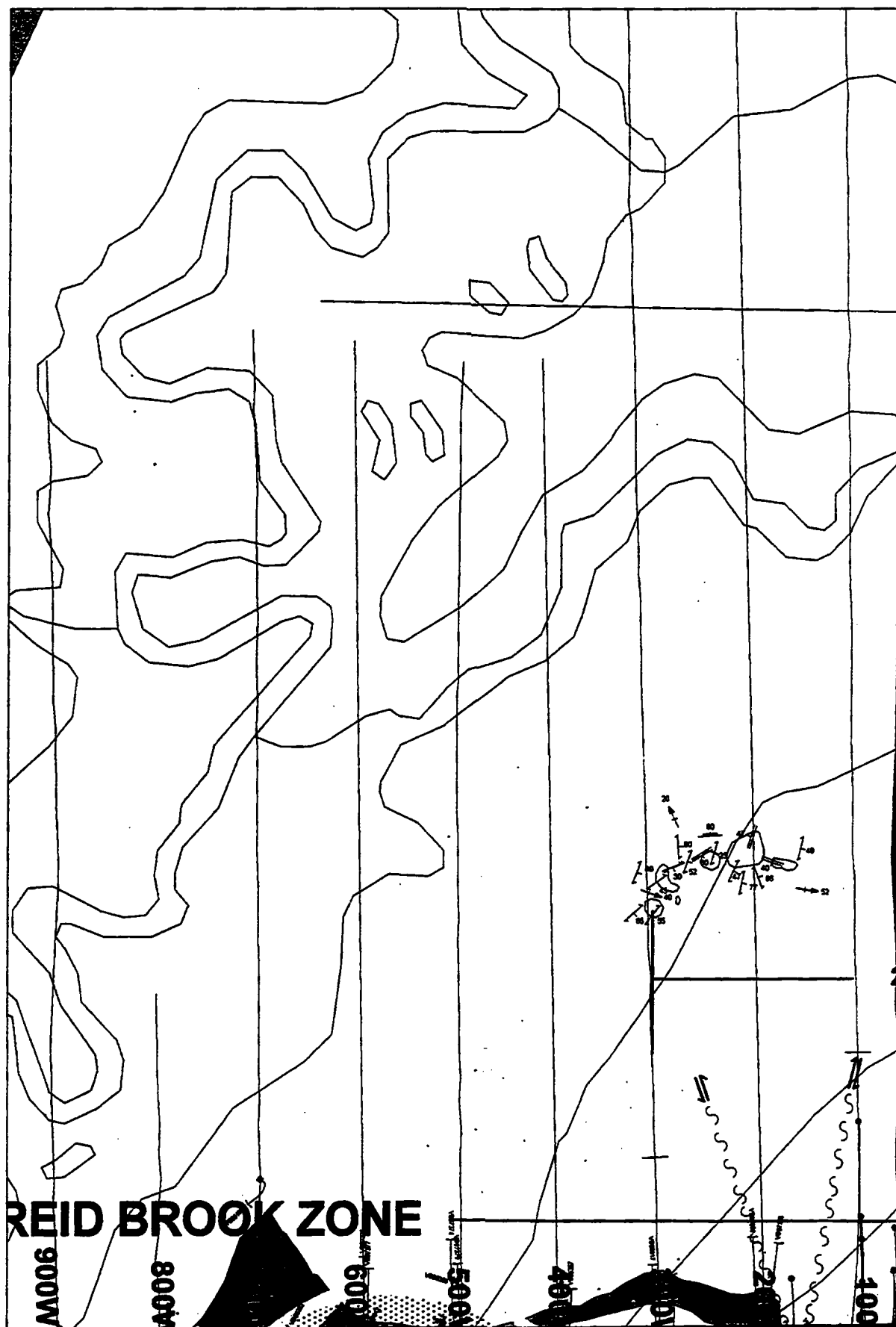
NOTE TO USERS

Oversize maps and charts are microfilmed in sections in the following manner:

LEFT TO RIGHT, TOP TO BOTTOM, WITH SMALL OVERLAPS

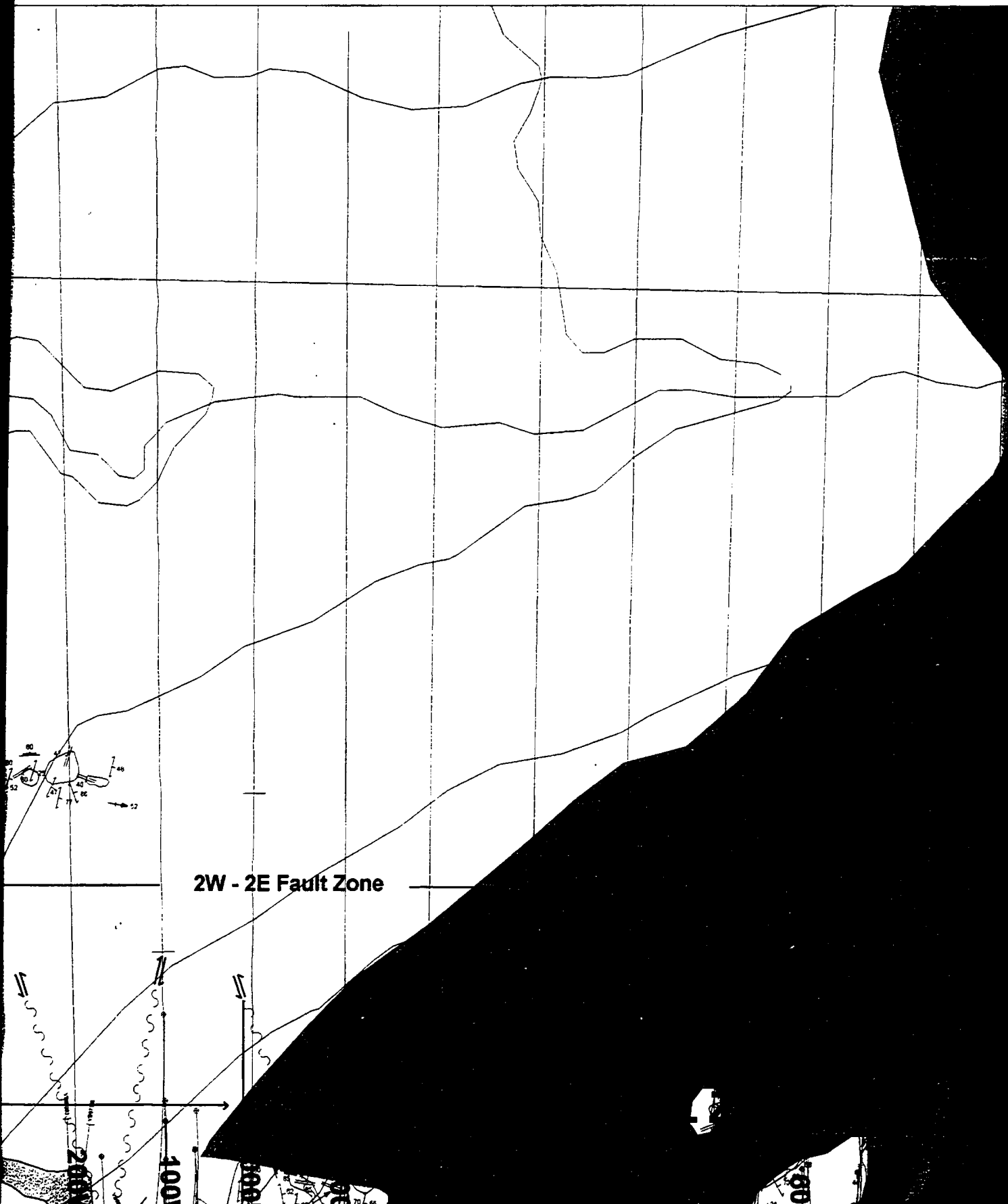
This reproduction is the best copy available.

UMI[®]

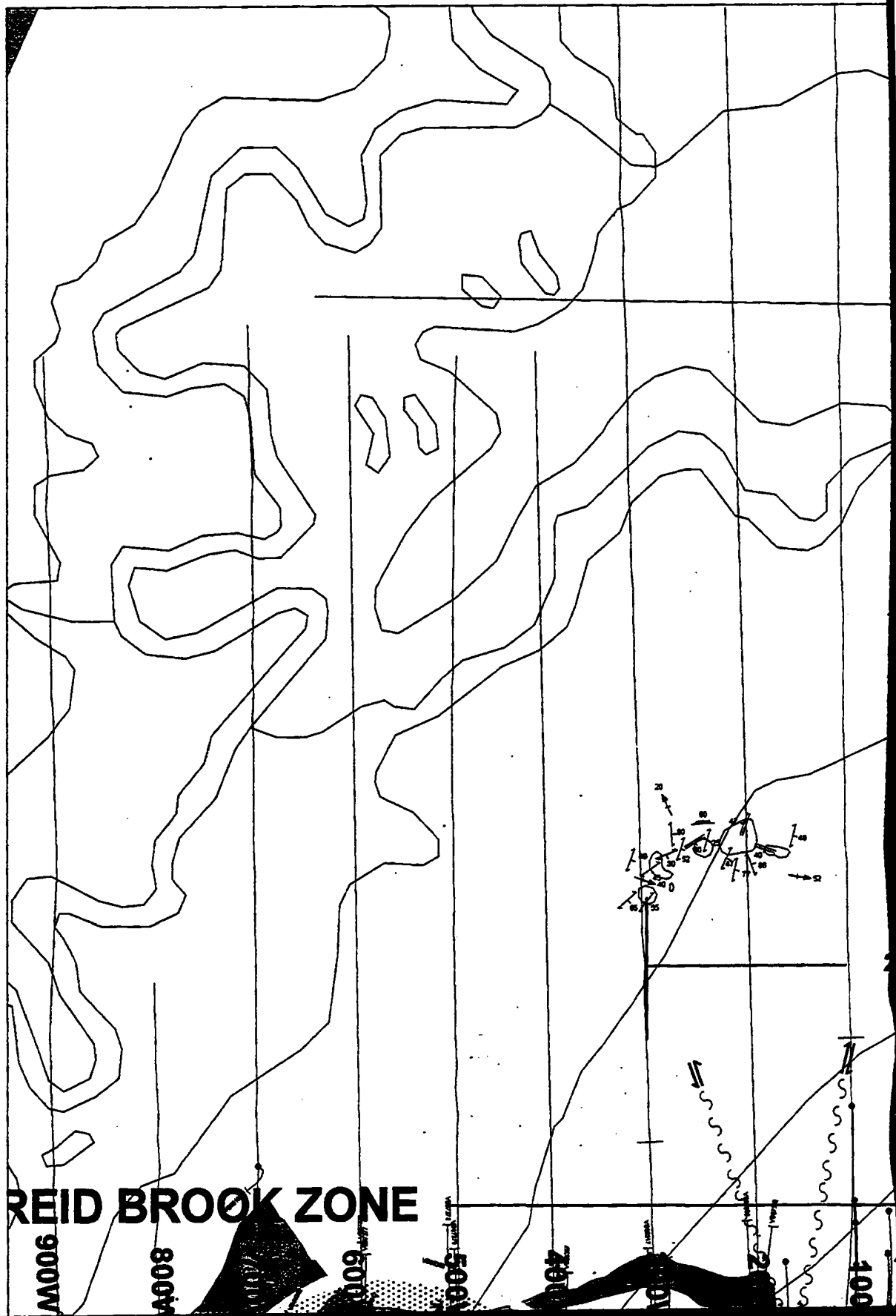


REID BROOK ZONE

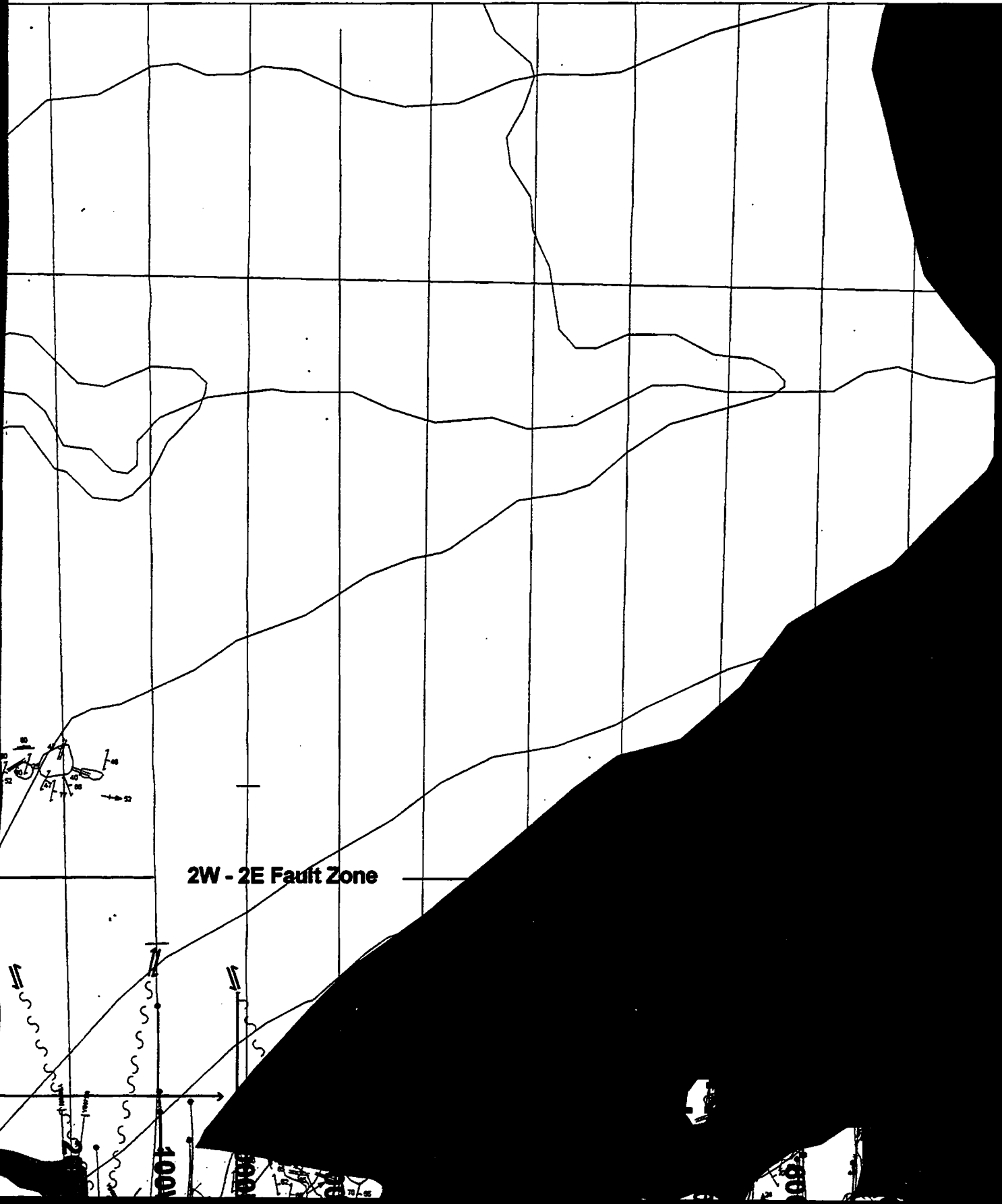
2W - 2E Fault Zone

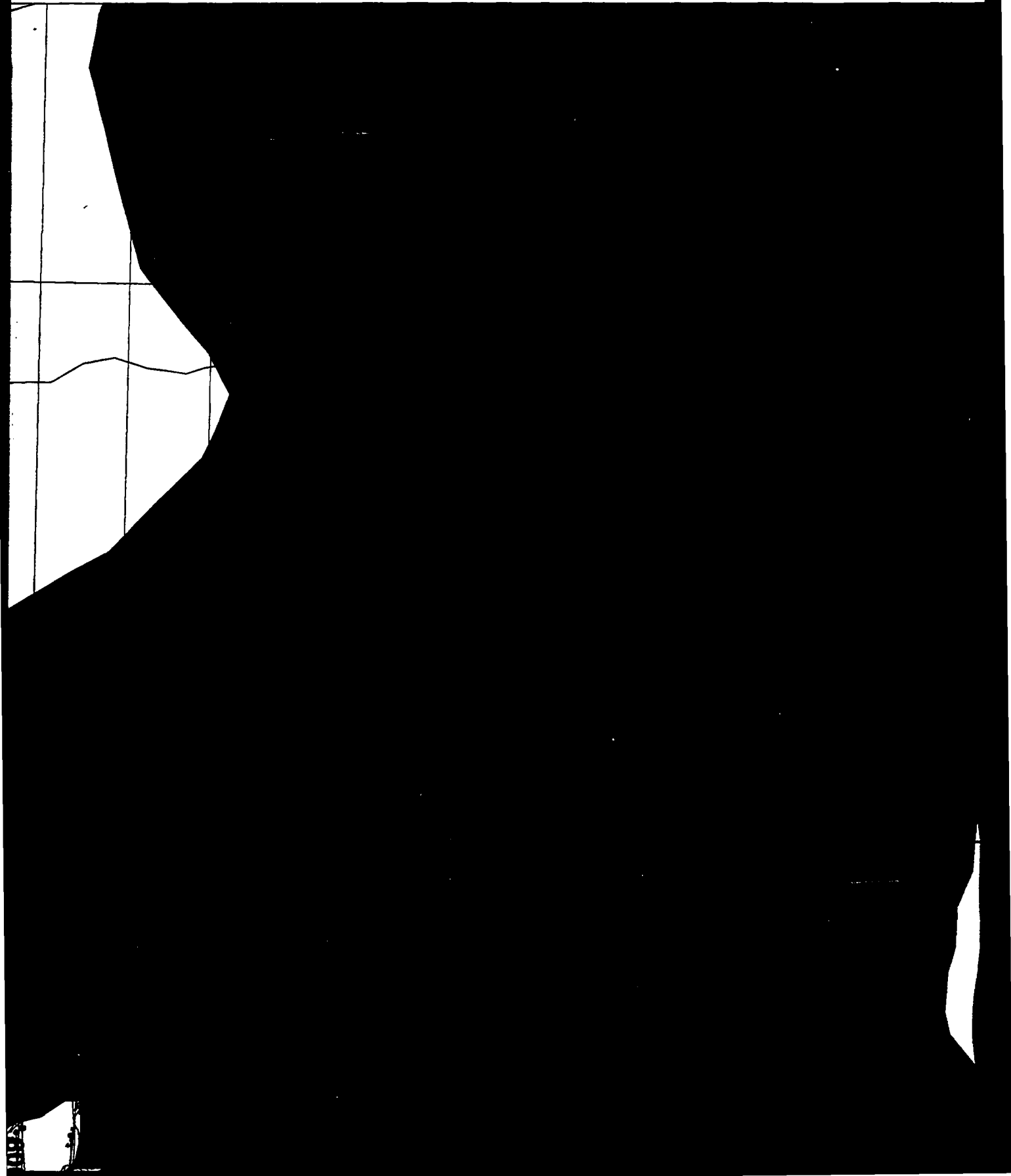


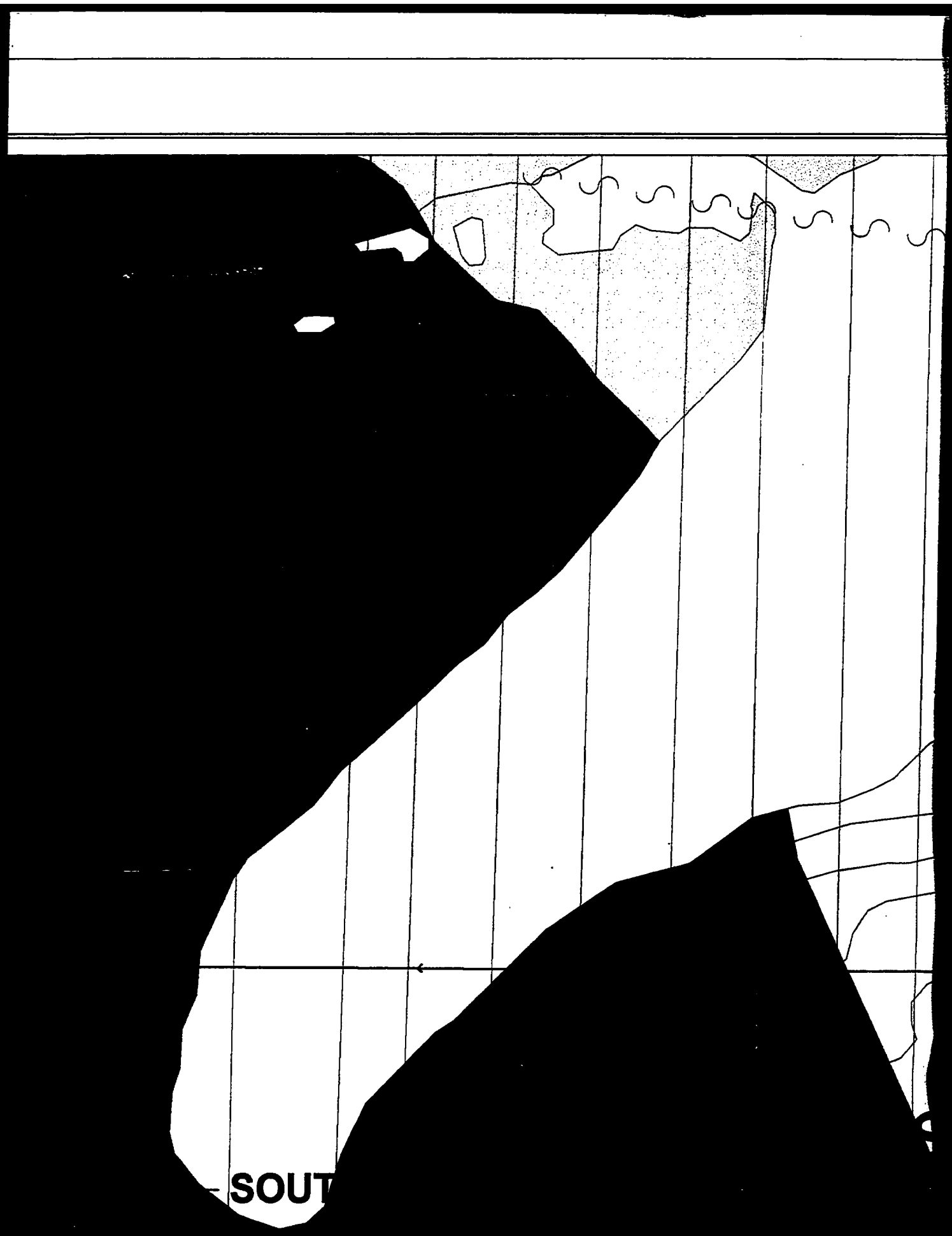
REID BROOK ZONE



2W - 2E Fault Zone







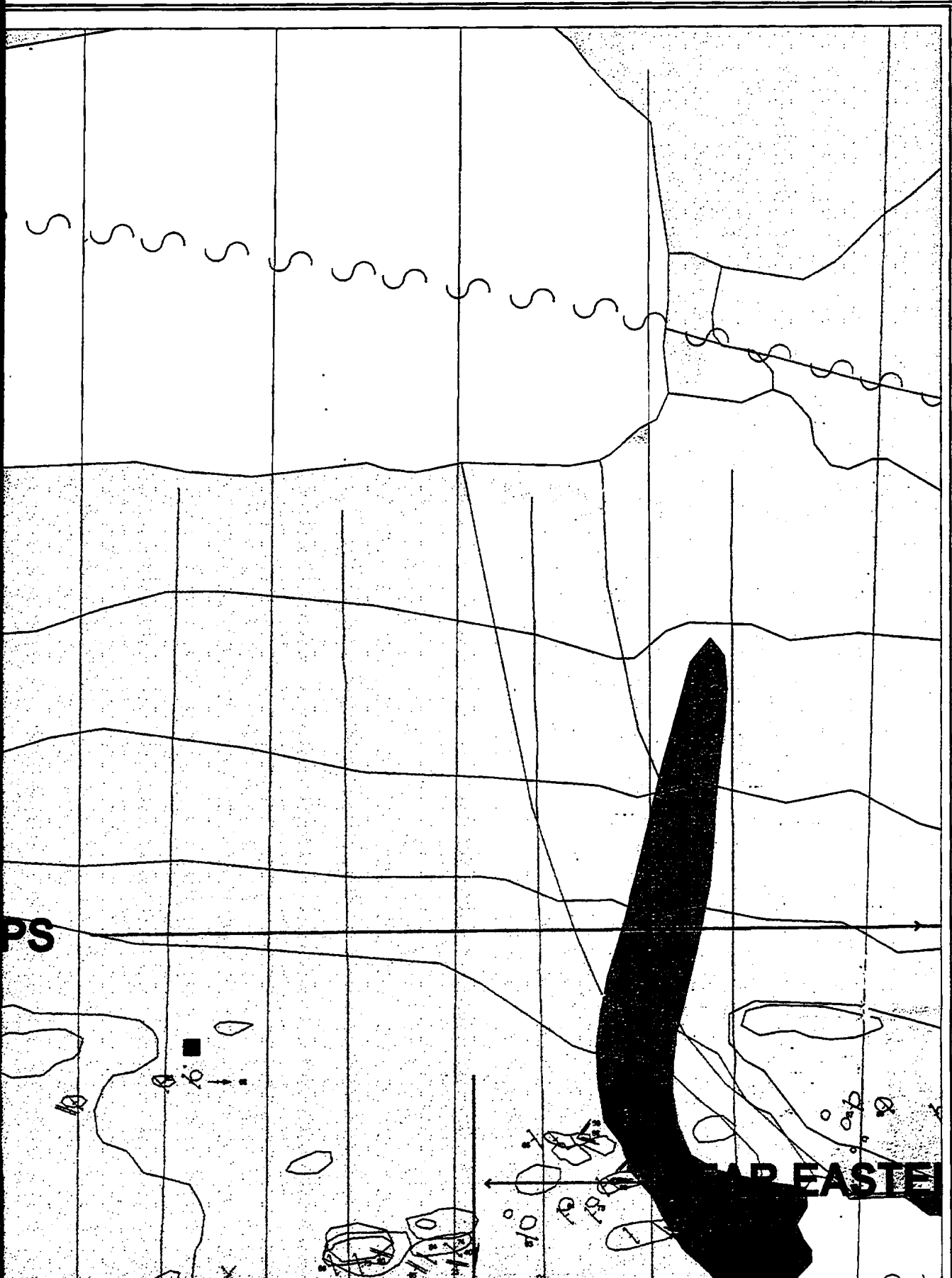


A hand-drawn map on graph paper. The map features a large, irregularly shaped area in the center, possibly representing a pond or a specific terrain. This area is filled with a stippled pattern. Above this area, there is a series of wavy lines, likely representing a shoreline or a boundary. Below the stippled area, there are several smaller, irregular shapes, some of which are also stippled. The map is labeled with 'Camp Pond' in a large, bold, cursive font at the top, 'EASTERN DEEPS' in a bold, sans-serif font in the middle, and 'S Hill' in a bold, sans-serif font at the bottom left. There are also some small, handwritten symbols and numbers scattered throughout the map, particularly in the lower right quadrant.

Camp Pond

EASTERN DEEPS

S Hill



PS

EAST

LEGEND

NAIN PLUTONIC SUITE

GRANITOID INTRUSIONS

MAKHAVINEKH GRANITE



intrusive breccia



medium quartz monzonite



coarse quartz monzonite



granite

VOISEY'S BAY GRANITE



intrusive breccia



monzonite



quartz monzonite



granite

REID BROOK INTRUSIVE COMPLEX

MUSHUAU TROCTOLITE



troctolite



leucotroctolite



olivine gabbro



gabbro

VOISEY'S BAY TROCTOLITE



troctolite



leucotroctolite



olivine gabbro



undivided

ASHLEY TROCTOLITE



troctolite



olivine gabbro



undivided

ANORTHOSITE MASSIFS

IKADLVIK ANORTHOSITE



anorthosite



leuconorite



leucogabbro

KANGEKLUALUK ANORTHOSITE



anorthosite



leuconorite



norite

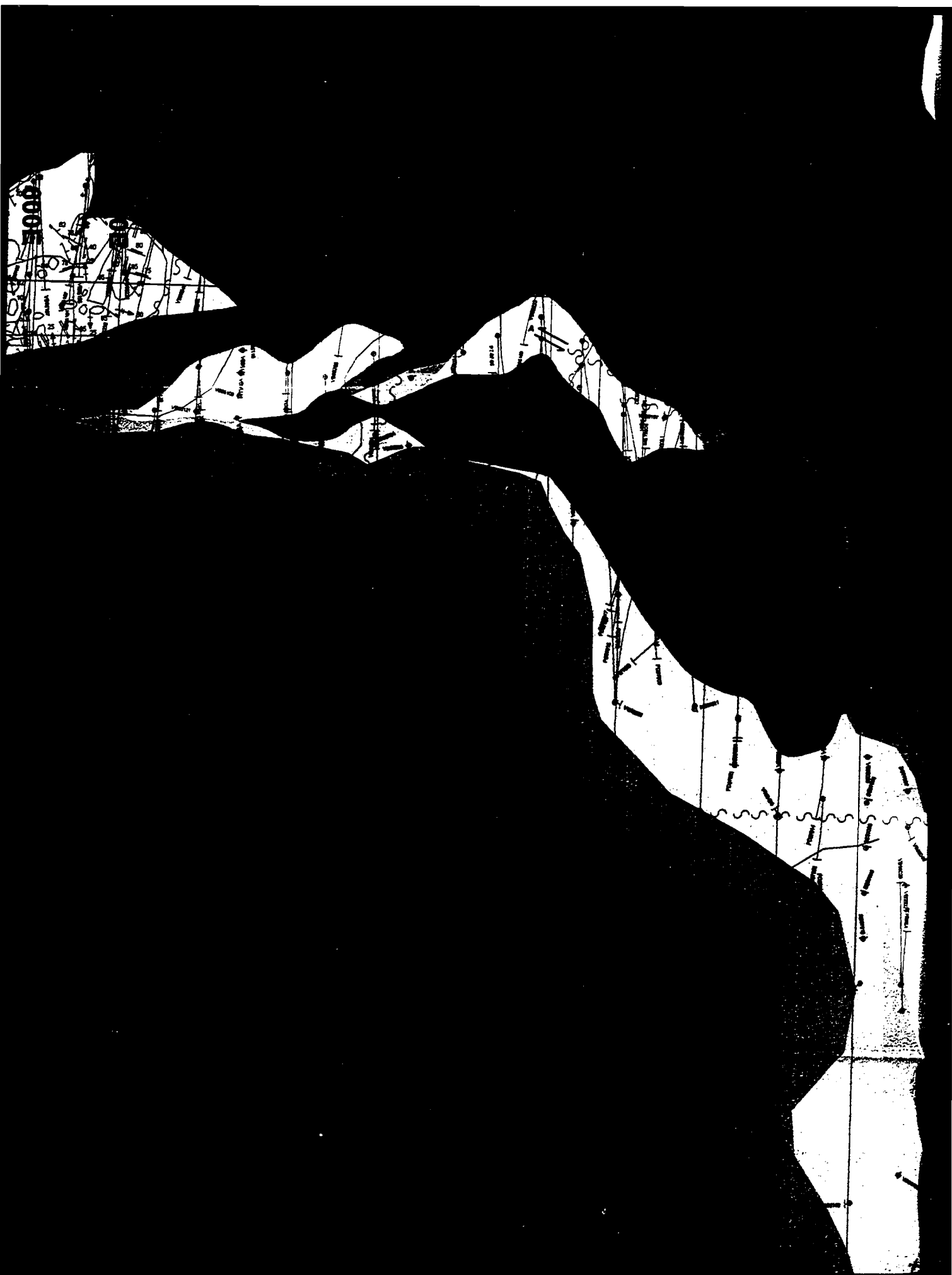
The map displays a complex geological area with several key features:

- Topographic Contours:** Labeled with values 900W, 800W, 700W, 600W, 500W, 400W, 300W, 200W, 100W, and 0W.
- Reid Brook Zone:** A large, irregularly shaped area in the upper right, shaded with a stippled pattern.
- Reid Brook:** A winding line representing the brook, labeled "Reid" in a large, bold, sans-serif font.
- Other Labels:** "TGU" is visible in the lower right corner.
- Geological Features:** Various lines, dots, and symbols representing geological structures and data points.

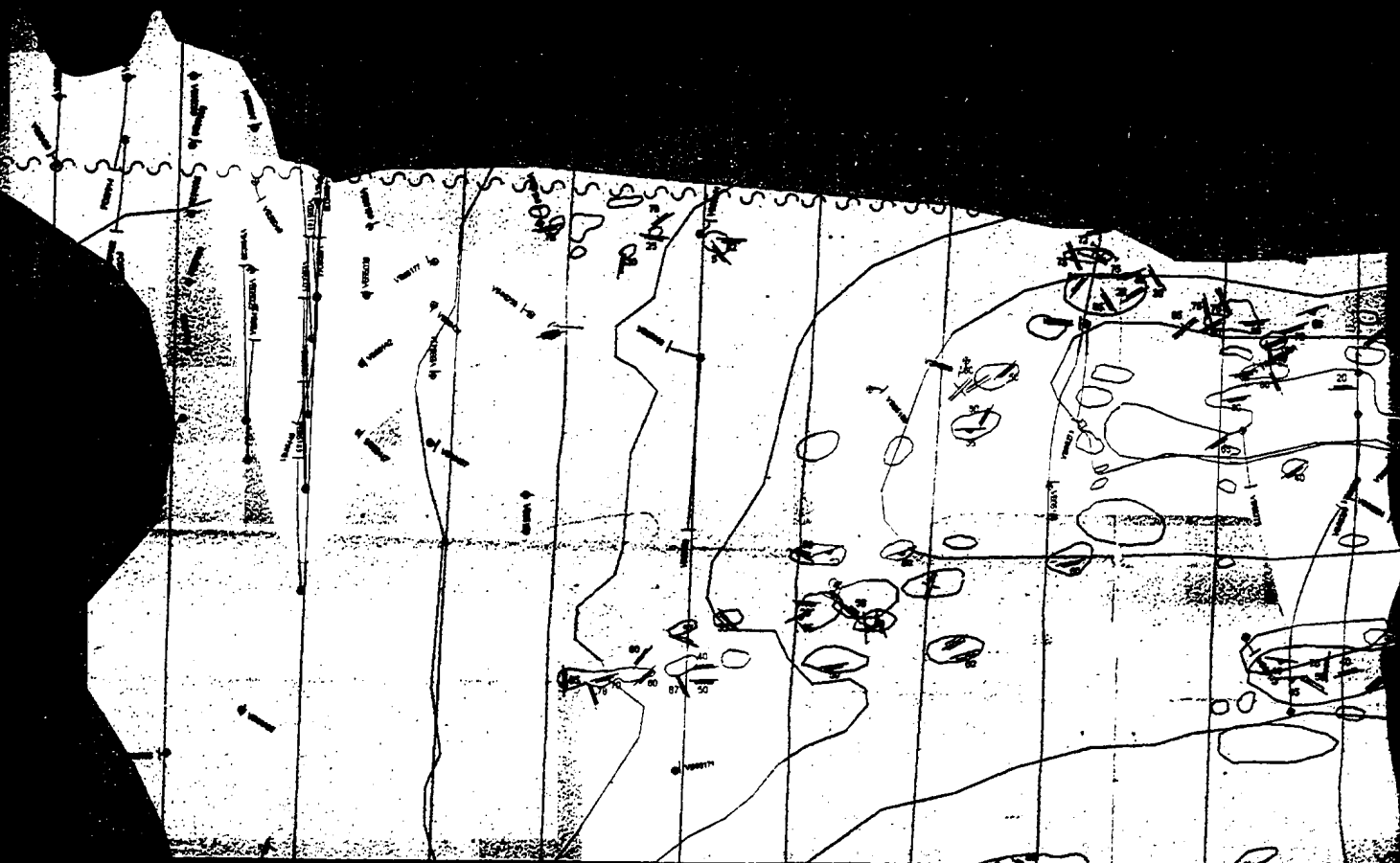
Reit

TGu





SOUT



S Hill

6300E

6400E

6500E

6600E

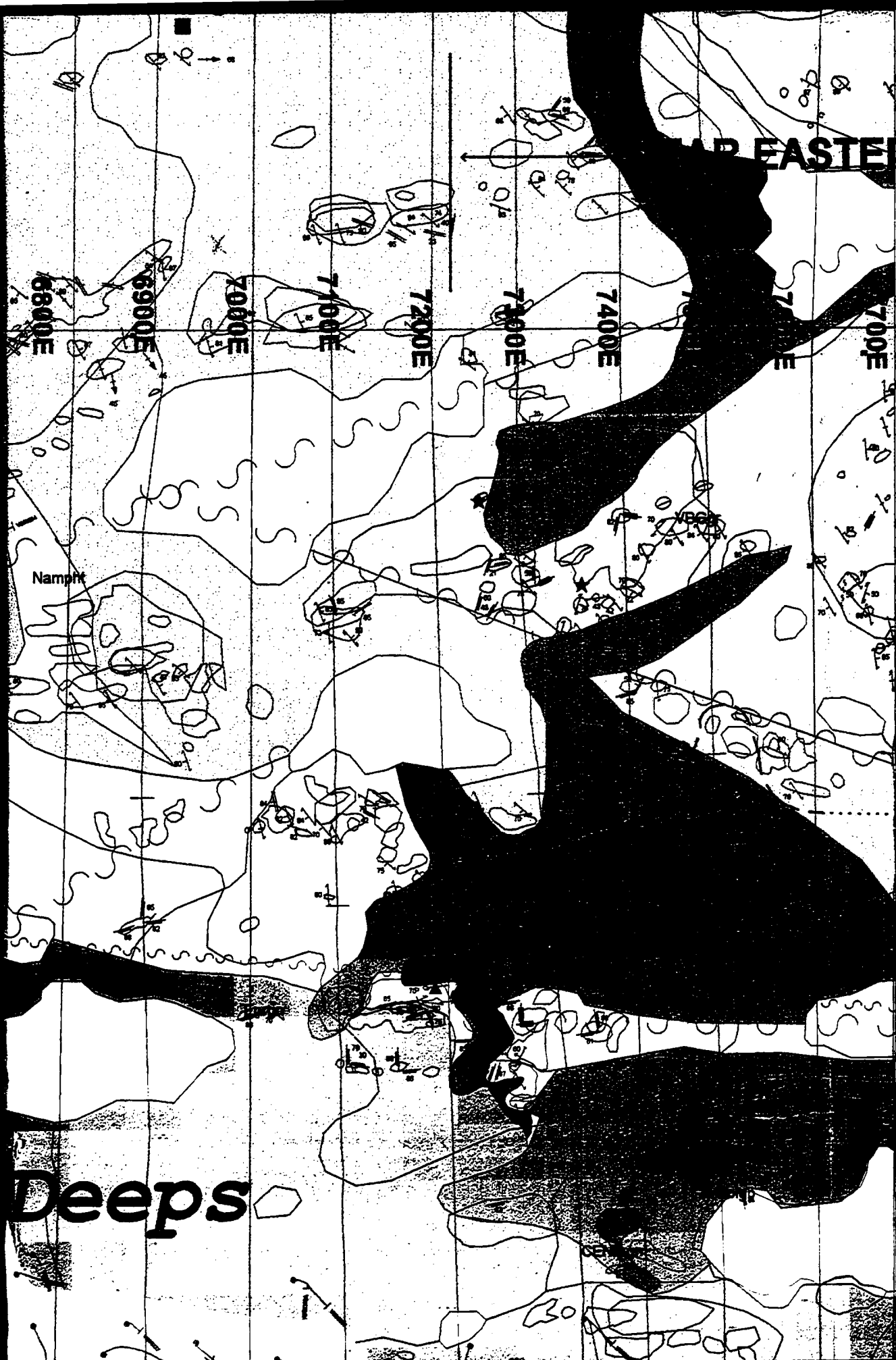
6700E

6800E

6900E

Namphit

Eastern Deep



Deeps

EASTERN

IKADLVIK ANORTHOSITE

 anorthosite

 leuconorite

 leucogabbro

Cabot Lake

 ferro diorite (Cabot Lake)

KANGEKLUALUK ANORTHOSITE

 anorthosite

 leuconorite

 norite

 gabbro

 pyroxenite (border zone)

CHURCHILL PROVINCE

 enderbitic orthogneiss

 quartzofeldspathic orthogneiss

Tasiuyak Gneiss

 graphitic paragneiss

 (undivided)

NAIN PROVINCE (Archean)

 layered orthogneiss

 orthogneiss, lesser paragneiss

 quartzite

 amphibolite

 gabbroic gneiss

 anorthosite

SYMBOLS

 GEOLOGICAL BOUNDARY / REGIONAL MAPPING

 GEOLOGICAL BOUNDARY
(defined, approximate, assumed)

 FAULT
(defined, approximate)

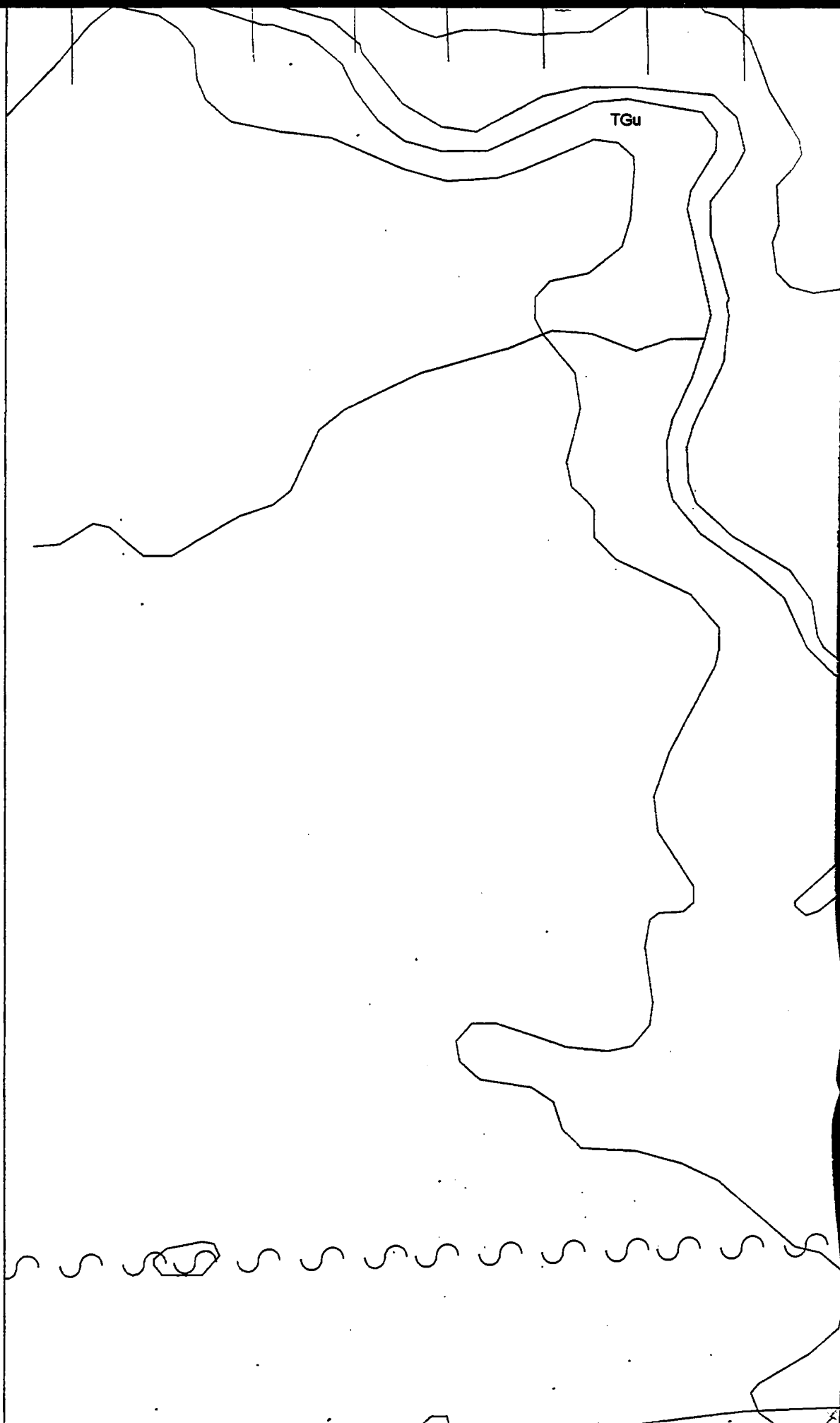
 SURFACE PROJECTION OF MASSIVE SULPHIDE

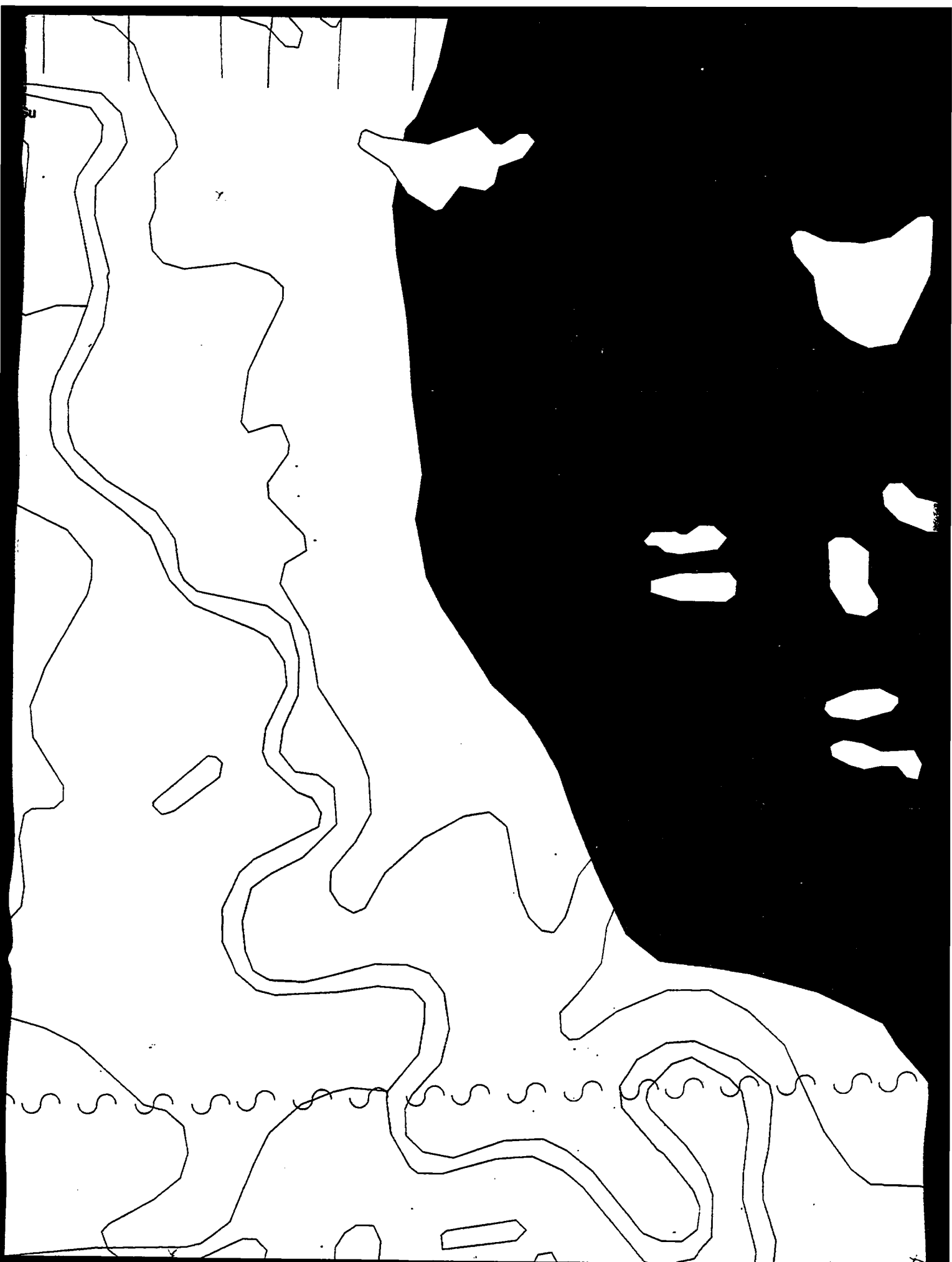
 SURFACE PROJECTION OF DISSEMINATED SULPHIDE

 DIAMOND DRILL HOLE

 OUTCROP

 GEOPHYSICAL ANOMALY (MAX-MIN)



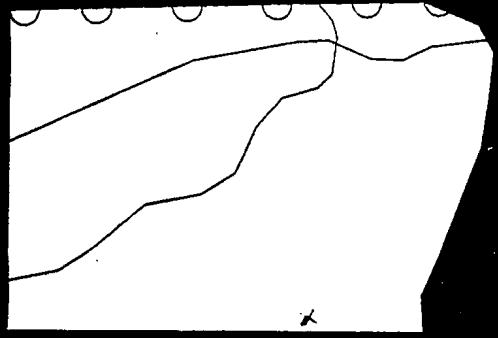


TGu

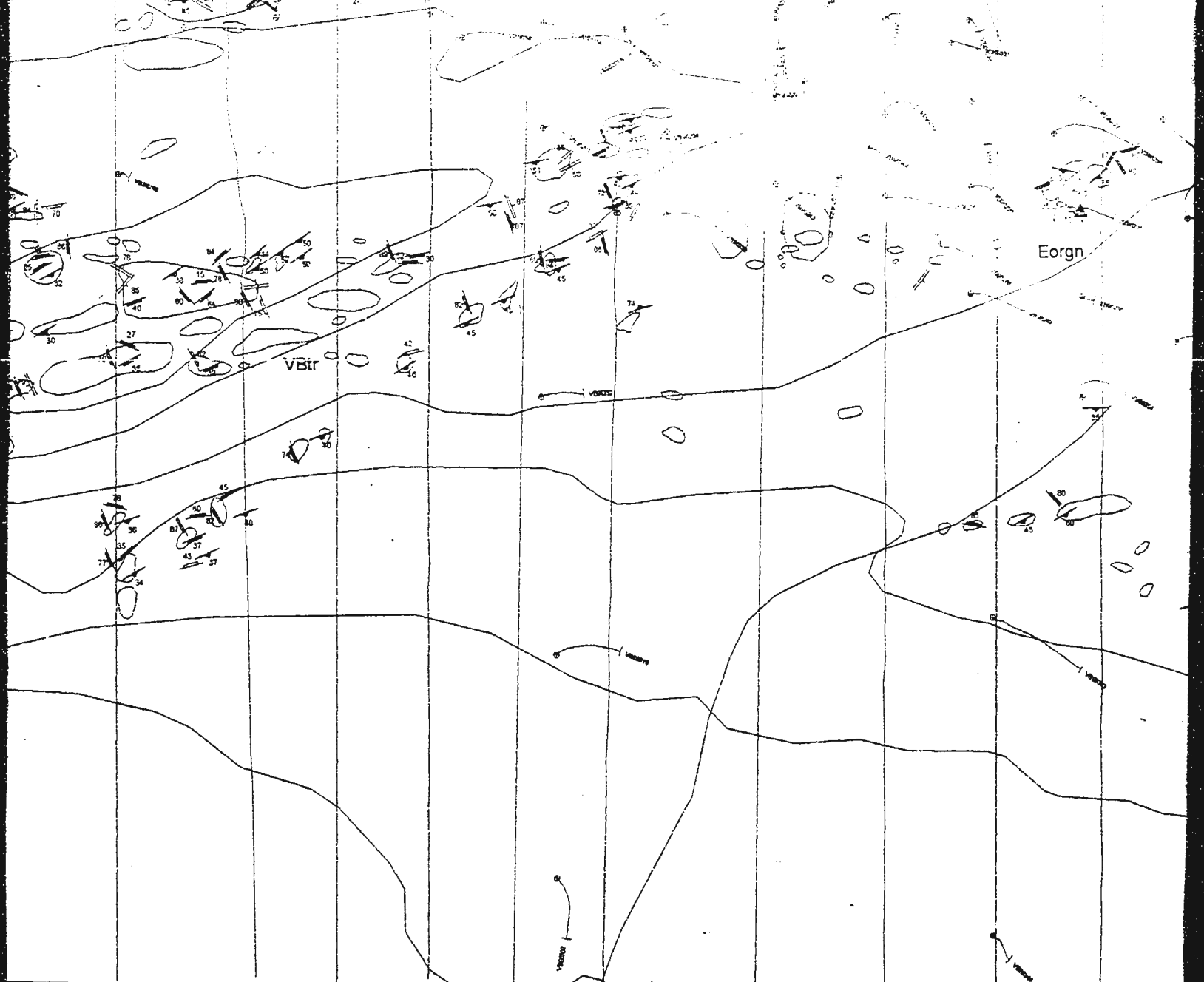
Brood



6100E



Eastern Deep

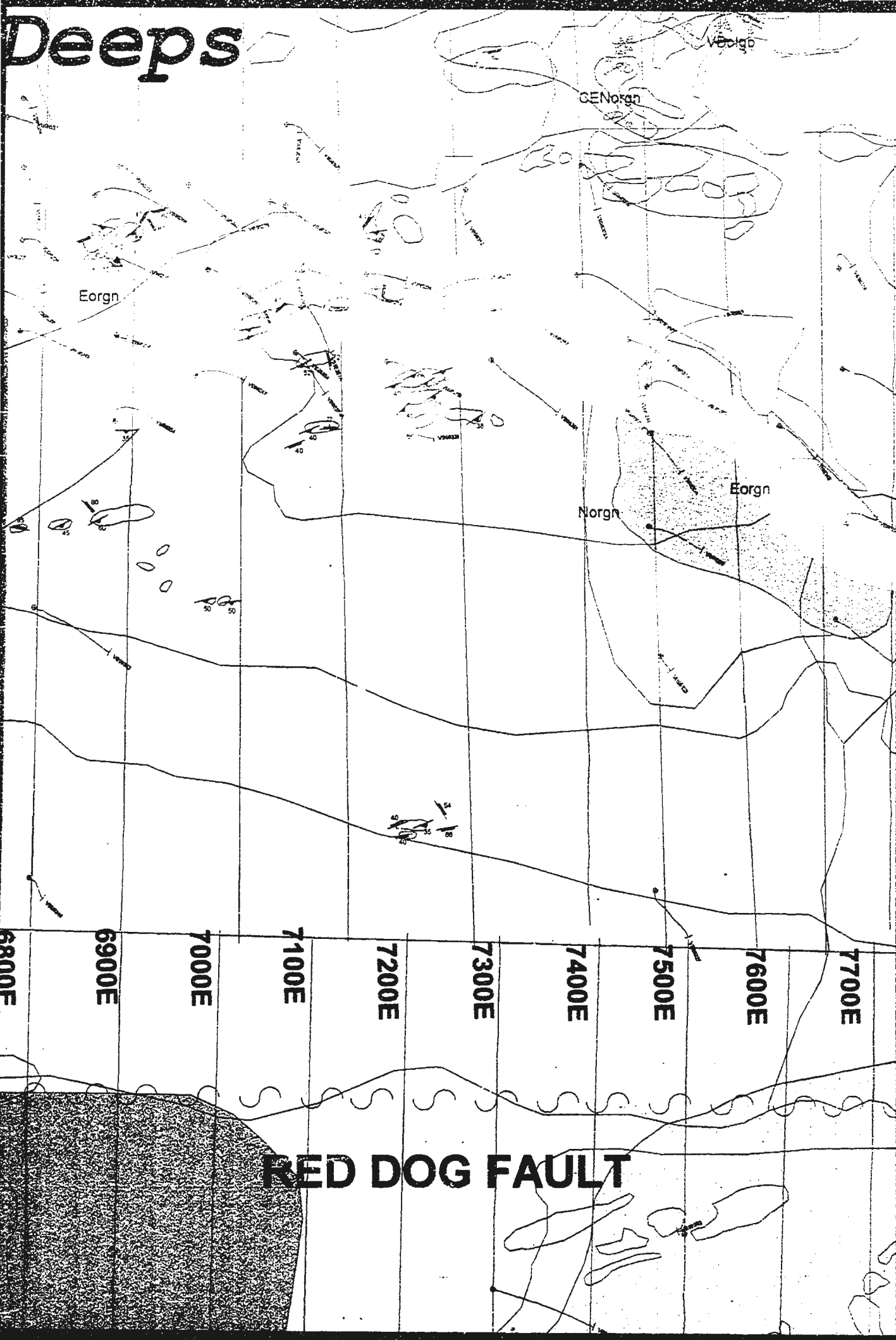


Eorgrn

VBtr

6000E 6100E 6200E 6300E 6400E 6500E 6600E 6700E 6800E 6900E

Deep



Revis

CONF

SURFACE PROJECTION OF MASSIVE SULPHIDE

SURFACE PROJECTION OF DISSEMINATED SULPHIDE



DIAMOND DRILL HOLE

OUTCROP



GEOPHYSICAL ANOMALY (MAX-MIN)

Fault
(dip indicated)

Fold Axis
(2nd Generation)

Fracture
(inclined, vertical)

Axial plane
(2nd generation)

Healed Fracture
(inclined, vertical)

Granite dyke
(inclined, vertical)



Lination
(1st, 2nd generation)



Mafic dyke
(inclined, vertical)

Foliation -1st generation
(inclined, vertical)



Igneous layering
(inclined, vertical)

Foliation -2nd generation
(inclined, vertical)

Observed contact
(dip indicated)

THIS IS A COMBINED LEGEND
NOT ALL SYMBOLS APPEAR ON THIS MAP

Revision Date

Description

Geologist



**VOISEY'S BAY NICKEL
COMPANY LIMITED**

A subsidiary of Inco Limited

MAILING ADDRESS

Suite 700, Baine Johnston Center
10 Fort William Place
St. John's, NF, Canada
A1C 1K4
Tel. 709-758-8888 Fax. 709-758-8899

CONFIDENTIAL

This Document contains confidential
information and may not be distributed
in whole or in part without
the consent of

Voisey's Bay Nickel Company Ltd.

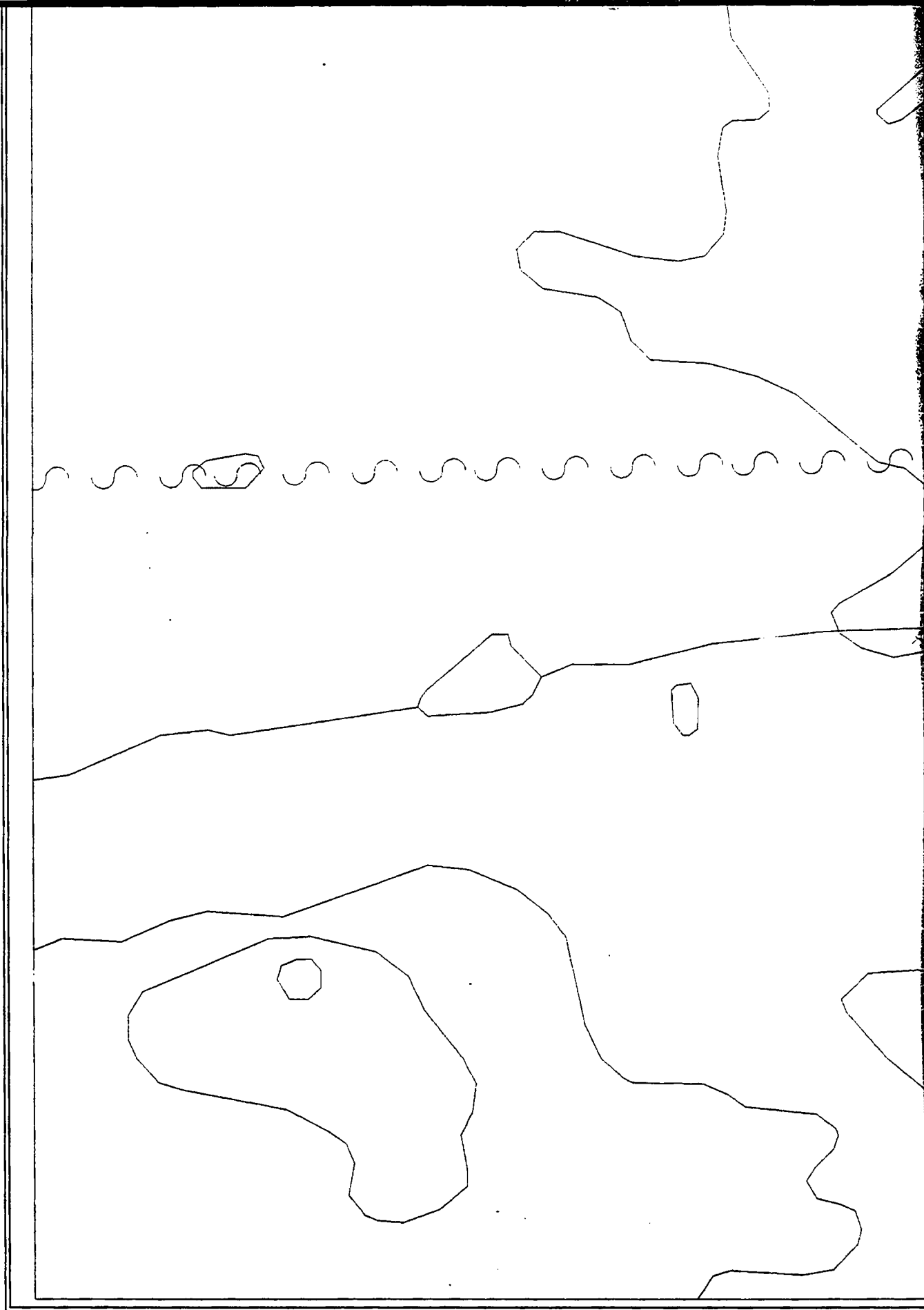
CONFIDENTIALITY RELEASE

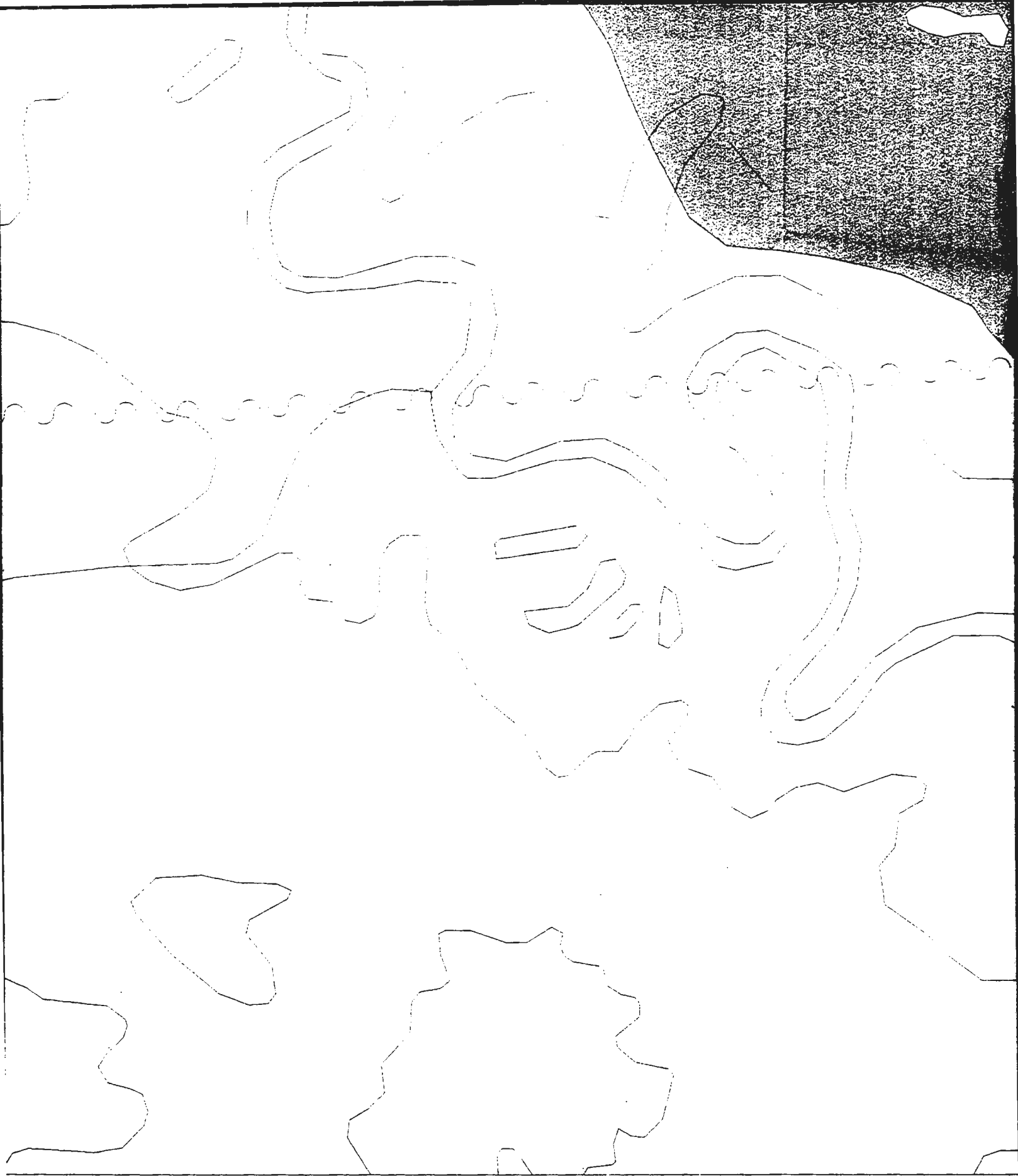
Date

Released By

Initial

7700E





Brook

TGu

6200E

6100E

6000E

5900E

5800E

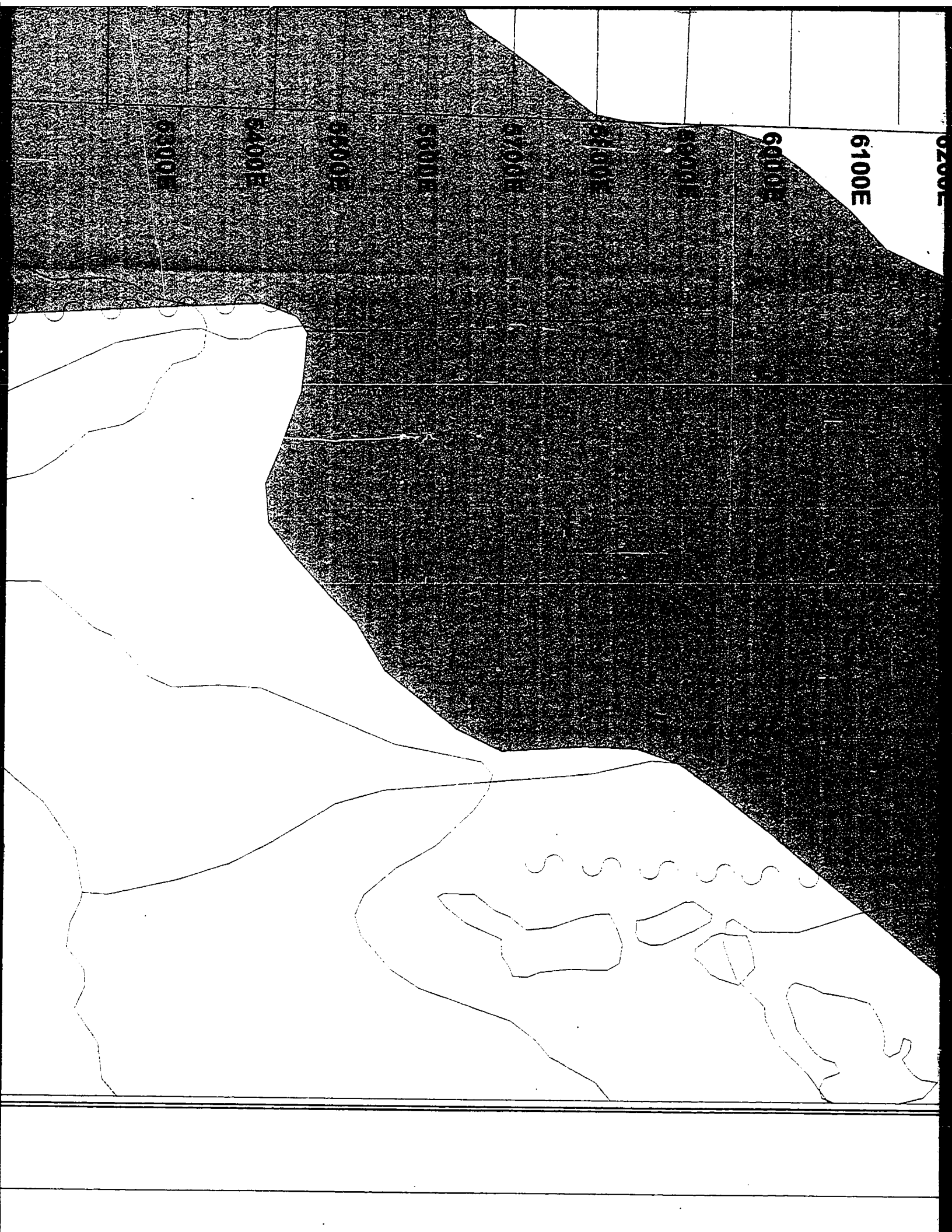
5700E

5600E

5500E

5400E

5300E



6900E

6800E

6700E

6600E

6500E

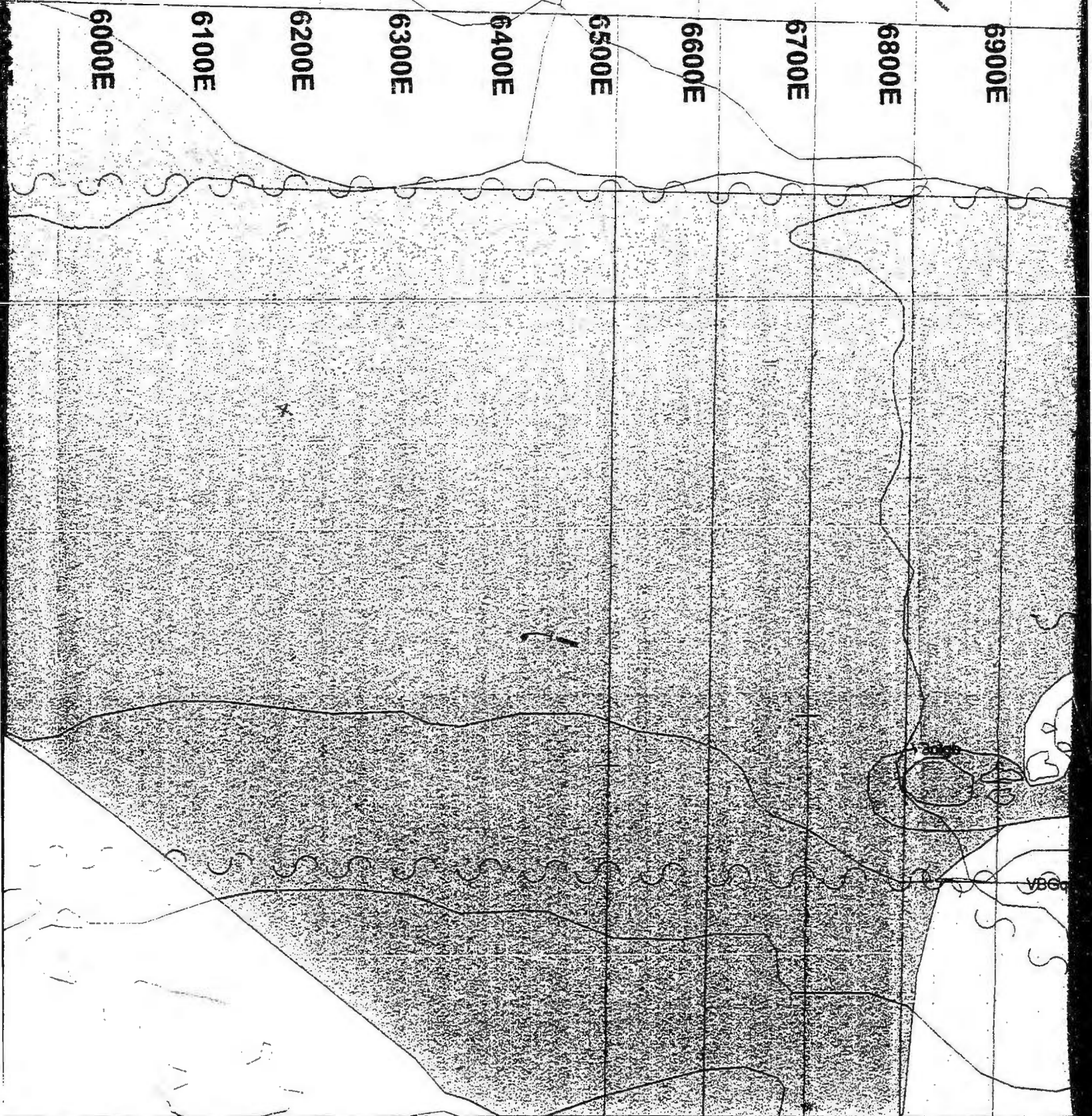
6400E

6300E

6200E

6100E

6000E



Rev

CON

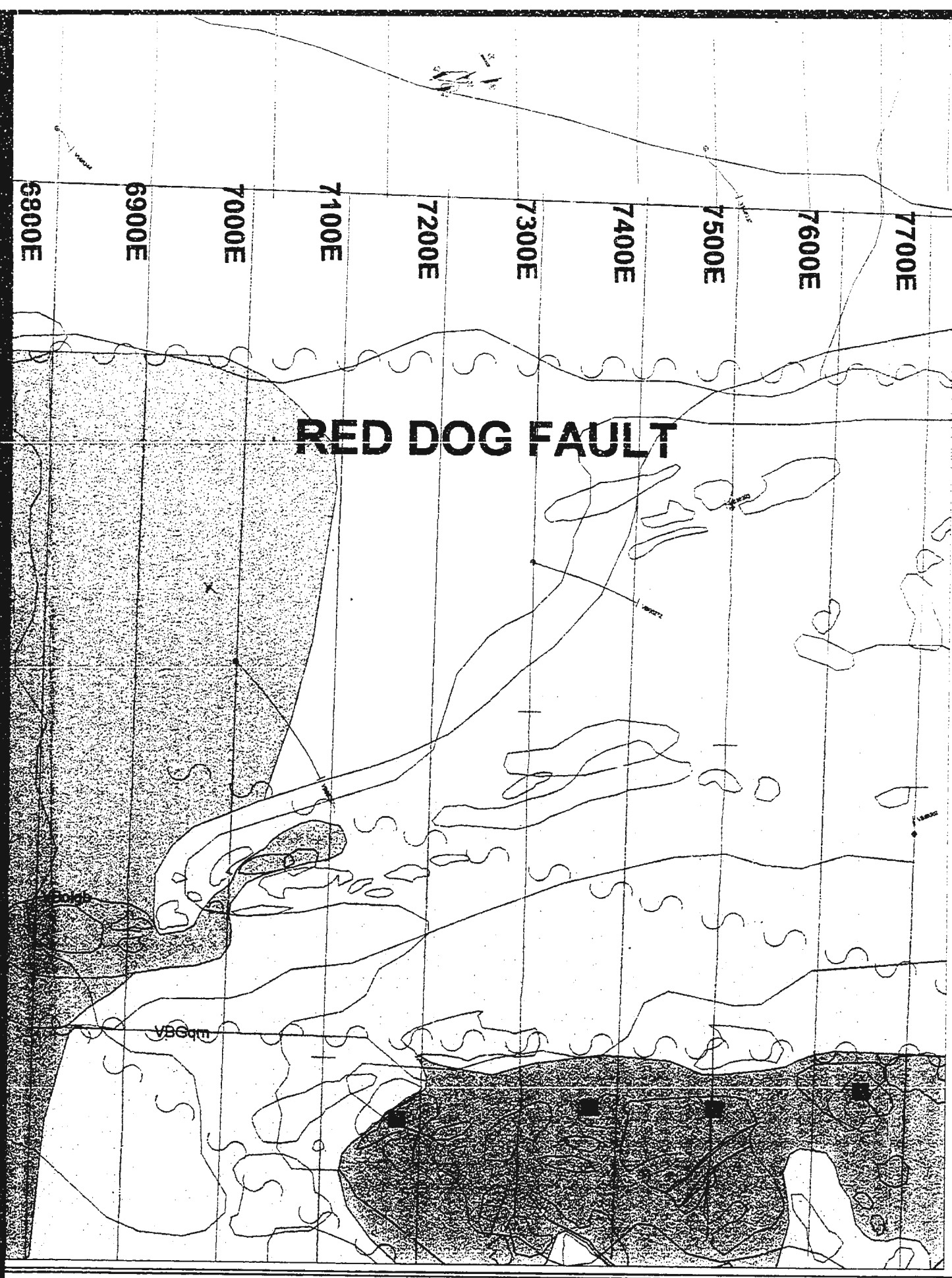
Title :

Desc

Geolo

Darre

File N
MI W
Plotte





**VOISEY'S BAY NICKEL
COMPANY LIMITED**

A subsidiary of Inco Limited

MAILING ADDRESS

Suite 700, Baine Johnston Center
10 Fort William Place
St. John's, NF, Canada
A1C 1K4
Tel. 709-758-8888 Fax. 709-758-8899

CONFIDENTIAL

This Document contains confidential
information and may not be distributed
in whole or in part without
the consent of

Voisey's Bay Nickel Company Ltd.

CONFIDENTIALITY RELEASE

Date

Released By

Initial

Title :

Preliminary

LABRADOR, VOISEY'S BAY PROJECT

Geology and Strucure of the Voisey's Bay Ni, Cu, Co Deposits

Description :

**Compilation of detailed mapping by; Darrell P. Butt
Detailed mapping by; Darrell Butt and John Hayes (1997)
Contributions to mapping project include; S. Dunsworth, D. Fitzpatrick
Includes data from Ryan and Lee (1989), Mackela and Babineau (1995)
Deposit structural interpretation compiled by: D. Evans Lamswood
Massive and disseminated ore zones compiled by; R. Wheeler**

Geologist(s) :

Darrell Butt

Scale :

Scale 1: 5,000

Print Date :

May 2, 1998

File Name(s) :

**MI Workspace :Dawn_Thesis1
Plotter File (HPGL) :Dawn_Thesis**

License(s)

670

7700E

